

**SSC-437**

**MODELING LONGITUDINAL  
DAMAGE IN SHIP COLLISION**



This document has been approved  
For public release and sale; its  
Distribution is unlimited

**SHIP STRUCTURE COMMITTEE**  
**2005**

**SHIP STRUCTURE COMMITTEE**

RADM Thomas H. Gilmour  
U. S. Coast Guard Assistant Commandant,  
Marine Safety and Environmental Protection  
Chairman, Ship Structure Committee

Mr. W. Thomas Packard  
Director,  
Survivability and Structural Integrity Group  
Naval Sea Systems Command

Dr. Jack Spencer  
Senior Vice President  
American Bureau of Shipping

Mr. Joseph Byrne  
Director, Office of Ship Construction  
Maritime Administration

Mr. Gerard A. McDonald  
Director General, Marine Safety,  
Safety & Security  
Transport Canada

Mr. Thomas Connors  
Director of Engineering  
Military Sealift Command

Dr. Neil Pegg  
Group Leader – Structural Mechanics  
Defence Research & Development Canada – Atlantic

**CONTRACTING OFFICER TECHNICAL REP.**

Chao Lin / MARAD  
Natale Nappi / NAVSEA  
Robert Sedat / USCG

**EXECUTIVE DIRECTOR**  
Lieutenant Eric M. Cooper  
U. S. Coast Guard

**SHIP STRUCTURE SUB-COMMITTEE**

**AMERICAN BUREAU OF SHIPPING**

Mr. Glenn Ashe  
Mr. Yung Shin  
Mr. Phil Rynn  
Mr. William Hanzalek

**DEFENCE RESEARCH & DEVELOPMENT ATLANTIC**

Dr David Stredulinsky  
Mr. John Porter

**MARITIME ADMINISTRATION**

Mr. Chao Lin  
Mr. Carlos Setterstrom  
Mr. Richard Sonnenschein

**MILITARY SEALIFT COMMAND**

Mr. Joseph Bohr  
Mr. Rick A. Anderson  
Mr. Michael W. Touma

**NAVAL SEA SYSTEMS COMMAND**

Mr. Jeffery E. Beach  
Mr. Edward E. Kadala  
Mr. Allen H. Engle  
Mr. Charles L. Null

**TRANSPORT CANADA**

Mr. Jacek Dubiel

**UNITED STATES COAST GUARD**

Mr. Rubin Sheinberg  
Mr. Robert Sedat  
Commander Ray Petow

**CANADIAN COAST GUARD**

Mr. Daniel Gauvin

Member Agencies:

*American Bureau of Shipping  
Defence Research Development Canada  
Maritime Administration  
Military Sealift Command  
Naval Sea Systems Command  
Society of Naval Architects & Marine Engineers  
Transport Canada  
United States Coast Guard*



**Ship  
Structure  
Committee**

Address Correspondence to:

Executive Director  
Ship Structure Committee  
U.S. Coast Guard (G-MSE/SSC)  
2100 Second Street, SW  
Washington, D.C. 20593-0001  
Web site: <http://www.shipstructure.org>

**SSC - 437  
SR - 1426**

**December 2004**

**MODELING LONGITUDINAL DAMAGE IN SHIP COLLISIONS**

The primary objective of this project is to improve, validate and assess the simplified collision damage model SIMCOL. This project focuses on predicting the longitudinal extent of damage in cases where both ships have forward speed, and at oblique collision angles. Longitudinal damage is particularly important in oil outflow and damage stability calculations.

In 1979, the Ship Structure Committee (SSC) conducted a review of collision research and design methodologies. They concluded that the most promising simplified collision analysis alternative was to extend Minorsky's original analysis of high-energy collisions by including consideration of shell membrane energy absorption. The approach taken in this project is to progressively increase the complexity of SIMCOL starting with a modified Minorsky approach until results with sufficient accuracy and sensitivity to design characteristics is obtained.

This study takes the second step in predicting side damage and oil outflow in ship collisions. It provides a rational probabilistic method for defining collision cases, provides a validation of a simplified collision model both deterministically and probabilistically, and provides results comparing damage for single hull and double hull tankers. The most significant products of this study are the demonstration of a rational process and the development of a method for determining longitudinal extent of damage through transverse structure.

A handwritten signature in black ink that reads "T. H. Gilmour".

T. H. GILMOUR

Rear Admiral, U.S. Coast Guard  
Chairman, Ship Structure Committee

## Technical Report Documentation Page

1. Report No. SSC Report SR-1426	2. Government Accession No.	3. Recipient's Catalog No.	
4. Title and Subtitle Modeling Longitudinal Damage in Ship Collisions		5. Report Date October 2004	
		6. Performing Organization Code	
7. Author(s) Sajdak, J.A.W., Brown, A.J.		8. Performing Organization Report No. SR-1426	
9. Performing Organization Name and Address Department of Aerospace and Ocean Engineering. Virginia Polytechnic Institute and State University Blacksburg, VA 24061-0203		10. Work Unit No. (TRAIS)	
		11. Contract or Grant No. DTCG32-02-C-R00002	
12. Sponsoring Agency Name and Address Ship Structure Committee      US Coast Guard C/O US Coast Guard          Research & Development Ctr. 2100 Second Street, SW      1082 Shennecossett Road Washington, DC 20593      Groton, Connecticut 06340		13. Type of Report and Period Covered by Report 01/08/02-10/15/04	
		14. Sponsoring Agency Code G-M	
15. Supplementary Notes			
<p><b>16. Abstract</b></p> <p>The primary objective of this project is to improve, validate and assess the simplified collision damage model, SIMCOL, to support continuing work by SNAME Ad Hoc Panel #6 and IMO working groups. Work accomplished under prior SSC and SNAME sponsorship made excellent progress towards predicting damage penetration in ship collisions. This project focuses on predicting the <b>longitudinal</b> extent of damage in cases where both ships have forward speed, and at oblique collision angles. Longitudinal damage is particularly important in oil outflow and damage stability calculations. Current models do not provide adequate predictions of longitudinal damage, particularly in way of transverse bulkheads. The specific tasks completed in this project are:</p> <ul style="list-style-type: none"> <li>• Developed SIMCOL Version 3.0 including: <ul style="list-style-type: none"> <li>1) Deformable Bow sub model</li> <li>2) Implementation and validation of theory for the determination of energy absorbed in longitudinal extent of damage.</li> </ul> </li> <li>• Developed the capability to model collision events using LSDYNA – used in simplified model development and validation.</li> <li>• Validated Virginia Tech LSDYNA ship collision modeling procedure.</li> <li>• Validated SIMCOL using real collision data, and probabilistic collision data for penetrating collisions.</li> </ul>			
17. Key Words ship collisions, longitudinal ship damage		18. Distribution Statement Distribution is available to the public through: National Technical Information Service U.S. Department of Commerce Springfield, VA 22151 Ph. (703) 487-4650	
19. Security Classification (of this report) Unclassified	20. Security Classification (of this page) Unclassified	21. No. of Pages 389	22. Price

**CONVERSION FACTORS**  
(Approximate conversions to metric measures)

To convert from	to	Function	Value
<b>LENGTH</b>			
inches	meters	divide	39.3701
inches	millimeters	multiply by	25.4000
feet	meters	divide by	3.2808
<b>VOLUME</b>			
cubic feet	cubic meters	divide by	35.3149
cubic inches	cubic meters	divide by	61,024
<b>SECTION MODULUS</b>			
inches <sup>2</sup> feet <sup>2</sup>	centimeters <sup>2</sup> meters <sup>2</sup>	multiply by	1.9665
inches <sup>2</sup> feet <sup>2</sup>	centimeters <sup>3</sup>	multiply by	196.6448
inches <sup>4</sup>	centimeters <sup>3</sup>	multiply by	16.3871
<b>MOMENT OF INERTIA</b>			
inches <sup>2</sup> feet <sup>2</sup>	centimeters <sup>2</sup> meters	divide by	1.6684
inches <sup>2</sup> feet <sup>2</sup>	centimeters <sup>4</sup>	multiply by	5993.73
inches <sup>4</sup>	centimeters <sup>4</sup>	multiply by	41.623
<b>FORCE OR MASS</b>			
long tons	tonne	multiply by	1.0160
long tons	kilograms	multiply by	1016.047
pounds	tonnes	divide by	2204.62
pounds	kilograms	divide by	2.2046
pounds	Newtons	multiply by	4.4482
<b>PRESSURE OR STRESS</b>			
pounds/inch <sup>2</sup>	Newtons/meter <sup>2</sup> (Pascals)	multiply by	6894.757
kilo pounds/inch <sup>2</sup>	mega Newtons/meter <sup>2</sup> (mega Pascals)	multiply by	6.8947
<b>BENDING OR TORQUE</b>			
foot tons	meter tons	divide by	3.2291
foot pounds	kilogram meters	divide by	7.23285
foot pounds	Newton meters	multiply by	1.35582
<b>ENERGY</b>			
foot pounds	Joules	multiply by	1.355826
<b>STRESS INTENSITY</b>			
kilo pound/inch <sup>2</sup> inch <sup>3/2</sup> (ksi <sup>1/2</sup> /in)	mega Newton MNm <sup>3/2</sup>	multiply by	1.0998
<b>J-INTEGRAL</b>			
kilo pound/inch	Joules/mm <sup>2</sup>	multiply by	0.1753
kilo pound/inch	kilo Joules/m <sup>2</sup>	multiply by	175.3

## TABLE OF CONTENTS

<b>CHAIRMAN OF SSC LETTER</b>	<b>III</b>
<b>TECHNICAL REPORT DOCUMENTATION PAGE</b>	<b>V</b>
<b>CONVERSION FACTORS</b>	<b>VI</b>
<b>TABLE OF CONTENTS</b>	<b>VII</b>
<b>LIST OF FIGURES</b>	<b>X</b>
<b>LIST OF TABLES</b>	<b>XV</b>
<b>CHAPTER 1 MOTIVATION AND INTRODUCTION</b>	<b>1</b>
<b>CHAPTER 2 COLLISION BASICS</b>	<b>4</b>
2.1 Ship-to-Ship Collisions	4
2.2 Collision Physics	5
2.3 Vessel Motion	8
2.4 Energy Absorbing Structure	9
<b>CHAPTER 3 FINITE ELEMENT MODELING OF SHIP COLLISIONS</b>	<b>14</b>
3.1 Overview of FE Modeling	14
3.2 Structural Geometry	14
3.3 Element Types	20
3.4 Finite Element Mesh	20
3.5 Smearing Techniques	20
3.6 External Dynamics and Constraints	25
3.7 LSDYNA Analysis Parameters	26
3.7.1 Contact and Friction	26
3.7.2 Material Properties	28
3.7.3 Element Failure	31
3.7.3.1 Determination of Failure Strain	31
3.7.4 Strain Rate	38
3.8 Typical Results	39
3.9 Calibration	42
3.9.1 David E. Day - Marine Flier Collision	43
3.10 Summary of Finite Element Analysis in Ship-to-Ship Collisions	52

<b>CHAPTER 4</b>	<b>SIMPLIFIED MODELING METHODS</b>	<b>53</b>
<b>4.1</b>	<b>Methods for Determining Energy Absorbed by the Struck Ship</b>	<b>54</b>
4.1.1	<i>Minorsky (Energy Coefficient) Method</i>	54
4.1.2	<i>Pedersen and Zhang Energy Coefficient</i>	57
4.1.3	<i>Paik and Pedersen Energy Coefficient</i>	58
4.1.4	<i>ALPS/SCOL</i>	58
4.1.5	<i>DAMAGE</i>	59
<b>4.2</b>	<b>Methods for Determining Energy Absorbed by the Striking Ship Bow</b>	<b>61</b>
4.2.1	<i>Amdahl's Method</i>	61
4.2.2	<i>Pedersen's Method</i>	61
<b>4.3</b>	<b>Methods for Determining Energy Absorbed by Striking and Struck Ships</b>	<b>62</b>
4.3.1	<i>DTU Collision Model</i>	62
4.3.2	<i>SIMCOL Version 2.1</i>	64
4.3.2.1	<i>SIMCOL Version 2.1 External Dynamics Sub-Model</i>	65
4.3.2.2	<i>SIMCOL Version 2.1 Internal Sub-Module</i>	69
4.3.2.3	<i>SIMCOL Probabilistic Damage Assessment</i>	80
4.3.2.4	<i>SIMCOL Simplified Probabilistic Oil Outflow Calculation</i>	80
<b>4.4</b>	<b>Summary of Simplified Methods</b>	<b>82</b>
<b>CHAPTER 5</b>	<b>SIMCOL VERSION 3.0</b>	<b>84</b>
<b>5.1</b>	<b>Energy Coefficient Method for use with Structural Decks and Stringers</b>	<b>84</b>
<b>5.2</b>	<b>Energy Coefficient Method for use with Longitudinal and Transverse Bulkheads and Longitudinal Crushing of Side Shell</b>	<b>92</b>
<b>5.3</b>	<b>Deformable Bow Model</b>	<b>97</b>
<b>5.4</b>	<b>Longitudinal Deflection of Transverse Bulkheads and Webs</b>	<b>98</b>
5.4.1	<i>Flow Theory of Plasticity</i>	111
5.4.2	<i>Energy Absorption in Rectangular Region</i>	113
5.4.3	<i>Energy Absorption in Triangular Region</i>	116
5.4.4	<i>The Energy Absorbed from an Eight-Region Plate</i>	119
5.4.5	<i>The Energy Absorbed from a Twenty-Five-Region Plate</i>	122
5.4.5.1	<i>Determination of Deflections in CS 1 with a Z-Direction Initial Step</i>	136
5.4.5.2	<i>Determination of Deflections in CS 1 with a X-Direction Initial Step</i>	140
5.4.5.3	<i>Determination of Deflections in CS 2 with a Z-Direction Initial Step</i>	143
5.4.5.4	<i>Determination of Deflections in CS 2 with a X-Direction Initial Step</i>	144
5.4.5.5	<i>Determination of Deflections in CS 3 with a Z-Direction Initial Step</i>	146
5.4.5.6	<i>Determination of Deflections in CS 3 with a X-Direction Initial Step</i>	150
5.4.5.7	<i>Determination of Deflections in CS 4 with a Z-Direction Initial Step</i>	156
5.4.5.8	<i>Determination of Deflections in CS 4 with a X-Direction Initial Step</i>	157
5.4.6	<i>Validation of Energy Absorption of Twenty-Five-Region Plate</i>	159
<b>CHAPTER 6</b>	<b>SIMCOL VERSION 3.0 VALIDATION</b>	<b>179</b>
<b>6.1</b>	<b>David E. Day Marine Flier Collision</b>	<b>179</b>
<b>6.2</b>	<b>P&amp;T Adventurer Tullahoma Collision</b>	<b>180</b>
<b>6.3</b>	<b>SIMCOL Probabilistic Validation</b>	<b>181</b>
6.3.1	<i>Collision Probability</i>	182

6.3.2	<i>Collision Event Random Variables</i>	183
6.3.2.1	Striking Ship Type and Displacement	184
6.3.2.2	Striking Ship Characteristics	188
6.3.2.3	Struck Ship Variables	200
6.3.2.4	Collision Scenario Variables	201
6.3.3	<i>Validation</i>	201
<b>CHAPTER 7 CONCLUSIONS AND FUTURE WORK</b>		<b>206</b>
<b>REFERENCES</b>		<b>207</b>
<b>APPENDICES</b>		<b>215</b>

# LIST OF FIGURES

FIGURE 1 FIGURE OF DAMAGE DEFINITION .....	4
FIGURE 2 - COLLISION OF M/V ALEXIA AND M/V ENIF .....	6
FIGURE 3 - DAMAGE TO M/V ENIF .....	6
FIGURE 4 - COLLISION OF M/T GAS ROMAN AND M/V SPRINGBOK.....	7
FIGURE 5 - BOW PENETRATION OF COLLISION OF M/T GAS ROMAN AND M/V SPRINGOK.....	7
FIGURE 6 - BOW DAMAGE OF COLLISION OF M/T GAS ROMAN AND M/V SPRINGBOK.....	8
FIGURE 7 - ILLUSTRATION OF CONSTRAINED VESSEL YAW .....	9
FIGURE 8 - ACTUAL COLLISION BOW DAMAGE.....	12
FIGURE 9 - BOW DAMAGE TO NORWEGIAN DREAM.....	13
FIGURE 10 - KARISA BOW DAMAGE.....	13
FIGURE 11 - SHIP-TO-SHIP COLLISION AS MODELED IN LSDYNA .....	15
FIGURE 12 - DETAILED LSDYNA BOW MODEL.....	16
FIGURE 13 - STRUCK SHIP LSDYNA MODEL.....	17
FIGURE 14 - STRUCK SHIP CARGO SECTION MESH .....	18
FIGURE 15 STRUCK SHIP CARGO SECTION GEOMETRY VIEW FROM OUTBOARD.....	19
FIGURE 16 STRUCK SHIP CARGO SECTION GEOMETRY VIEW FROM CENTERLINE.....	19
FIGURE 17 - RIGID BOW COLLISION WITH DOUBLE-SIDED TEST SECTION .....	21
FIGURE 18 - SMEARING TEST RESULT COMPARISON OF ENERGY VS. PENETRATION .....	23
FIGURE 19 - SMEARING CASES 1, 2 AND 6 RESULT COMPARISON OF ENERGY VS. PENETRATION.....	24
FIGURE 20 - SMEARING CASES 1 AND 2 HOURGLASS ENERGY VS. TIME.....	24
FIGURE 21 - CONTACT NODAL REQUIREMENT .....	26
FIGURE 22 - FRICTION AND KINETIC ENERGY VS. PENETRATION [70] .....	27
FIGURE 23 - COULOMB FRICTION VS. RELATIVE VELOCITY OF CONTACT SURFACES.....	28
FIGURE 24 - KINEMATIC/ISOTROPIC ELASTIC PLASTIC MATERIAL STRESS STRAIN CURVE .....	29
FIGURE 25 - MATERIAL TYPES 3 AND 24 STRESS/STRAIN CURVES .....	30
FIGURE 26 - COMPARISON OF ELEMENT FAILURE CRITERIA CB AND CM .....	31
FIGURE 27 - ILLUSTRATION OF DUCTILE AND BRITTLE FRACTURES.....	32
FIGURE 28 - REPORTED FAILURE STRAINS VS. ELEMENT LENGTH SIZE [29,57,59,60,61,69,72,73,74,75].....	33
FIGURE 29 KITAMURA NECESSARY FAILURE STRAIN RESULTS [57] .....	34
FIGURE 30 - CHARPY-V-NOTCH (CVN) TEST .....	34
FIGURE 31 - CHARPY-V-NOTCH (CVN) SAMPLE DIMENSION.....	35
FIGURE 32 - SAMPLE CHARPY TEST DATA OF ABS GRADE B STEEL [76].....	35
FIGURE 33 - CVN FEM MESH .....	36
FIGURE 34 - CVN FEM ANALYSIS.....	36
FIGURE 35 - FEA CHARPY ENERGY VS. SAMPLE THICKNESS.....	37
FIGURE 36 - FEA CHARPY ENERGY VS. L/T RATIO.....	37
FIGURE 37 - FEA CHARPY ENERGY (DIVIDED BY 10) VS. FAILURE STRAIN (FS).....	38
FIGURE 38 - FOLDING-DOWN UPPER BOW OF CONVENTIONAL BOW MODEL.....	39
FIGURE 39 - SHIP TO SHIP COLLISION SIMULATION.....	40
FIGURE 40 - DAMAGED OUTER SHELL AND DECK FOR DOUBLE HULL TANKER.....	40
FIGURE 41 - BULB OF STRIKING SHIP PENETRATING OUTER SHELL OF STRUCK SHIP .....	41
FIGURE 42 - DAMAGED WEB AND SHELL OF DH150.....	41
FIGURE 43 - DAMAGED WEB AND SHELL OF DH150.....	42
FIGURE 44 - DAMAGED WEB AND SHELL OF DH150.....	42
FIGURE 45 - DAVID E. DAY - MARINE FLIER COLLISION ANALYSIS FEA MODEL .....	43
FIGURE 46 - DAVID E. DAY MARINE FLIER FEA DAMAGE AT 0.5 SECONDS.....	44
FIGURE 47 - DAVID E. DAY FEA HULL DAMAGE AT 0.5 SECONDS.....	44
FIGURE 48 - MARINE FLIER FEA BOW DAMAGE AT 0.5 SECONDS.....	44
FIGURE 49 - DAVID E. DAY - MARINE FLIER DAMAGE AT 1.0 SECONDS.....	45
FIGURE 50 - DAVID E. DAY FEA HULL DAMAGE AT 1.0 SECONDS.....	45
FIGURE 51 - MARINE FLIER FEA BOW DAMAGE AT 1.0 SECONDS.....	45
FIGURE 52 - DAVID E. DAY - MARINE FLIER FEA DAMAGE AT 1.5 SECONDS .....	46
FIGURE 53 - DAVID E. DAY FEA HULL DAMAGE AT 1.5 SECONDS.....	46

FIGURE 54 - MARINE FLIER FEA BOW DAMAGE AT 1.5 SECONDS.....	46
FIGURE 55 - DAVID E. DAY - MARINE FLIER FEA DAMAGE AT 2.0 SECONDS.....	47
FIGURE 56 - DAVID E. DAY FEA HULL DAMAGE AT 2.0 SECONDS.....	47
FIGURE 57 - MARINE FLIER FEA BOW DAMAGE AT 2.0 SECONDS.....	47
FIGURE 58 - DAVID E. DAY - MARINE FLIER FEA DAMAGE AT 2.5 SECONDS.....	48
FIGURE 59 - DAVID E. DAY FEA HULL DAMAGE AT 2.5 SECONDS.....	48
FIGURE 60 - MARINE FLIER FEA BOW DAMAGE AT 2.5 SECONDS.....	48
FIGURE 61 - DAVID E. DAY - MARINE FLIER FEA DAMAGE AT 3.0 SECONDS.....	49
FIGURE 62 - DAVID E. DAY FEA HULL DAMAGE AT 3.5 SECONDS.....	49
FIGURE 63 - MARINE FLIER FEA BOW DAMAGE AT 3.0 SECONDS.....	49
FIGURE 64 - DAVID E. DAY - MARINE FLIER FEA DAMAGE AT 3.5 SECONDS.....	50
FIGURE 65 - DAVID E. DAY FEA HULL DAMAGE AT 3.5 SECONDS.....	50
FIGURE 66 - MARINE FLIER FEA BOW DAMAGE AT 3.5 SECONDS.....	50
FIGURE 67 - DAVID E. DAY - MARINE FLIER FEA DAMAGE AT 4.0 SECONDS.....	51
FIGURE 68 - DAVID E. DAY FEA HULL DAMAGE AT 4.0 SECONDS.....	51
FIGURE 69 - MARINE FLIER FEA BOW DAMAGE AT 4.0 SECONDS.....	51
FIGURE 70 - REARDON AND SPRUNG ABSORBED ENERGY VS. DAMAGED VOLUME.....	56
FIGURE 71 - PAIK, CHOE AND THAYAMBALLI ABSORBED ENERGY VS. DAMAGED VOLUME.....	56
FIGURE 72 - PEDERSEN AND ZHANG ABSORBED ENERGY VS. DAMAGED VOLUME.....	57
FIGURE 73 - DAMAGE FROM ALPS/SCOL SIMULATION.....	59
FIGURE 74 DTU SHIP DYNAMICS MODEL.....	63
FIGURE 75 - SIMCOL SIMULATION PROCESS.....	65
FIGURE 76 - SIMCOL EXTERNAL SHIP DYNAMICS.....	66
FIGURE 77 - WEB DEFORMATION IN SIMCOL.....	70
FIGURE 78 - MEMBRANE GEOMETRY.....	71
FIGURE 79 - FORCE DIAGRAM FOR AN OBLIQUE ANGLE COLLISION.....	72
FIGURE 80 DEFLECTION AND FORCES IN DISTORTED WEB FRAMES.....	73
FIGURE 81 - SWEEPING SEGMENT METHOD.....	76
FIGURE 82 - SWEEPING SEGMENT GEOMETRY.....	78
FIGURE 83 - DECK CRUSHING SHOWING ACCORDION FOLDING [21].....	85
FIGURE 84 - DECK CRUSHING SHOWING BOW IMPINGEMENT [21].....	85
FIGURE 85 - PLATE CRUSHING VS. TEARING (CUTTING) [21].....	85
FIGURE 86 - RIGID WEDGE CUTTING AND CRUSHING DECK IN DROP TEST [89].....	85
FIGURE 87 - FEA DECK CUTTING AND CRUSHING.....	86
FIGURE 88 FEA SIMPLIFIED DECK CRUSHING AND CUTTING TEST MODEL.....	86
FIGURE 89 - FEA DECK CRUSHING AND TEARING WITH HEA = 30 DEGREES AT 0.5 SECONDS.....	88
FIGURE 90 - DECK CRUSHING AND TEARING WITH HEA = 30 DEGREES AT 1.0 SECONDS.....	88
FIGURE 91 - DECK CRUSHING AND TEARING WITH HEA = 30 DEGREES AT 1.5 SECONDS.....	89
FIGURE 92 - DECK CRUSHING AND TEARING WITH HEA = 30 DEGREES AT 2.0 SECONDS.....	89
FIGURE 93 FEA PLATE MESH SHOWING CRUSHING AND TEARING AT 2.0 SECONDS FROM HEA = 30 DEGREES.....	90
FIGURE 94 - ABSORBED ENERGY VS. PENETRATION AT HEA = 30 DEGREES.....	90
FIGURE 95 - ABSORBED ENERGY VS. PENETRATION AT HEA = 45 DEGREES.....	90
FIGURE 96 - ABSORBED ENERGY VS. PENETRATION AT HEA = 60 DEGREES.....	91
FIGURE 97 - ACTUAL LONGITUDINAL BULKHEAD CRUSHING.....	92
FIGURE 98 - FEA EXAMPLE OF LONGITUDINAL BULKHEAD CRUSHING.....	92
FIGURE 99 SIMPLIFIED LONGITUDINAL/TRANSVERSE BULKHEAD CRUSHING MODEL.....	93
FIGURE 100 - BULKHEAD CRUSHING AT 0.5 SECONDS.....	94
FIGURE 101 - BULKHEAD CRUSHING AT 1.0 SECONDS.....	94
FIGURE 102 - BULKHEAD CRUSHING AT 1.5 SECONDS.....	95
FIGURE 103 - BULKHEAD MESH CRUSHING AT 1.5 SECONDS.....	95
FIGURE 104 - ABSORBED ENERGY VS. TIME FOR CRUSHING OF BULKHEADS.....	95
FIGURE 105 - DAMAGE EXTENT VS. TIME FOR BULKHEAD CRUSHING.....	96
FIGURE 106 - ABSORBED ENERGY VS. DAMAGE EXTENT FOR BULKHEAD CRUSHING.....	96
FIGURE 107 - CRUSHING FORCE VS. PENETRATION FOR BULK CARRIER STRIKING WALL AT 90 DEGREES.....	97
FIGURE 108 - ACTUAL LONGITUDINALLY DEFORMED WEB [89].....	99
FIGURE 109 - DAMAGE SHOWING LONGITUDINALLY DEFLECTED BULKHEAD AND STRIKING BOW SHAPE.....	100

FIGURE 110 - FEA SHOWING LONGITUDINAL DEFORMATION OF TRANSVERSE BULKHEAD (LOOKING VERTICALLY UP)	100
.....	100
FIGURE 111 - IDEALIZED TRANSVERSE PLATE MODEL	101
FIGURE 112 - SIMCOL WEDGE MODEL	102
FIGURE 113 - CONTACT SCENARIO 1 GEOMETRY	102
FIGURE 114 - CONTACT SCENARIO 1 FEA TEST CASE AT 0.1 SECONDS	103
FIGURE 115 - CONTACT SCENARIO 1 FEA TEST CASE AT 0.2 SECONDS	103
FIGURE 116 - CONTACT SCENARIO 1 FEA TEST CASE AT 0.3 SECONDS	103
FIGURE 117 - CONTACT SCENARIO 1 FEA TEST CASE AT 0.8 SECONDS	103
FIGURE 118 - CONTACT SCENARIO 2 GEOMETRY	104
FIGURE 119 - CONTACT SCENARIO 2 FEA TEST CASE AT 0.2 SECONDS	104
FIGURE 120 - CONTACT SCENARIO 2 FEA TEST CASE AT 0.25 SECONDS	104
FIGURE 121 - CONTACT SCENARIO 2 FEA PLATE MESH DEFLECTION AT 0.25 SECONDS WITH 8 REGION MODEL OVERLAY	105
FIGURE 122 - CONTACT SCENARIO 3 GEOMETRY	105
FIGURE 123 - CONTACT SCENARIO 3 FEA TEST CASE AT 0.1 SECONDS	106
FIGURE 124 - CONTACT SCENARIO 3 FEA TEST CASE AT 0.2 SECONDS	106
FIGURE 125 - CONTACT SCENARIO 3 FEA TEST CASE AT 0.3 SECONDS	106
FIGURE 126 - CONTACT SCENARIO 3 PLATE MESH DEFORMATION AT 0.3 SECONDS	106
FIGURE 127 - CONTACT SCENARIO 4 GEOMETRY	107
FIGURE 128 - CONTACT SCENARIO 4 FEA TEST CASE AT 0.1 SECONDS	107
FIGURE 129 - CONTACT SCENARIO 4 FEA TEST CASE AT 0.2 SECONDS	107
FIGURE 130 - CONTACT SCENARIO 4 PLATE MESH DEFLECTION AT 0.2 SECONDS	107
FIGURE 131 - LONGITUDINAL DEFLECTION SIMPLIFIED ARGUMENT EXAMPLE GEOMETRY	108
FIGURE 132 - IDEALIZED PLATE GEOMETRY DEFINITIONS FOR SIMPLIFIED ARGUMENT	108
FIGURE 133 - CENTERED VERTICAL POSITION OF WEDGE STRIKING PLATE	109
FIGURE 134 - LOWER VERTICAL POSITION OF WEDGE STRIKING PLATE	109
FIGURE 135 - UPPER VERTICAL POSITION OF WEDGE STRIKING PLATE	109
FIGURE 136 - SIMPLIFIED PLATE DEFLECTION AND SIMILAR FEA PLATE MESH DEFLECTION	110
FIGURE 137 - EIGHT-REGION PLATE MODEL	111
FIGURE 138 - RECTANGULAR REGION GEOMETRY AND NOMENCLATURE	114
FIGURE 139 - TRIANGULAR REGION GEOMETRY AND NOMENCLATURE	116
FIGURE 140 - EIGHT REGION PLATE ABSORBED ENERGY VS. TIME COMPARISON TO FEA	121
FIGURE 141 - TWENTY-FIVE REGION PLATE OVERLAYING FEA PLATE MESH DEFORMATION	122
FIGURE 142 - TWENTY-FIVE REGION PLATE GEOMETRY	123
FIGURE 143 - STRIKING WEDGE VARIABLE DEFINITIONS	134
FIGURE 144 - COLLISION ANGLE DEFINITION	135
FIGURE 145 - TEST CASE 4 TWENTY-FIVE REGION PLATE DEFLECTION AT 0.1 SECONDS	161
FIGURE 146 - TEST CASE 4 FEA DEFLECTION AT 0.1 SECONDS	161
FIGURE 147 - TEST CASE 4 TWENTY-FIVE REGION PLATE DEFLECTION AT 0.2 SECONDS	161
FIGURE 148 - TEST CASE 4 FEA DEFLECTION AT 0.2 SECONDS	161
FIGURE 149 - TEST CASE 4 TWENTY-FIVE REGION PLATE DEFLECTION AT 0.3 SECONDS	162
FIGURE 150 - TEST CASE 4 FEA DEFLECTION AT 0.3 SECONDS	162
FIGURE 151 - TEST CASE 4 TWENTY-FIVE REGION PLATE DEFLECTION AT 0.35 SECONDS	162
FIGURE 152 - TEST CASE 4 FEA DEFLECTION AT 0.35 SECONDS	162
FIGURE 153 - TEST CASE 4 FEA PLATE MESH DEFLECTION AT 0.35 SECONDS	163
FIGURE 154 - CASE 1 SIMPLIFIED METHOD AND FEA ABSORBED ENERGY VS. TIME COMPARISON	163
FIGURE 155 - CASE 2 SIMPLIFIED METHOD AND FEA ABSORBED ENERGY VS. TIME COMPARISON	164
FIGURE 156 - CASE 3 SIMPLIFIED METHOD AND FEA ABSORBED ENERGY VS. TIME COMPARISON	164
FIGURE 157 - CASE 4 SIMPLIFIED METHOD AND FEA ABSORBED ENERGY VS. TIME COMPARISON	165
FIGURE 158 - CASE 5 SIMPLIFIED METHOD AND FEA ABSORBED ENERGY VS. TIME COMPARISON	165
FIGURE 159 - CASE 6 SIMPLIFIED METHOD AND FEA ABSORBED ENERGY VS. TIME COMPARISON	166
FIGURE 160 - CASE 7 SIMPLIFIED METHOD AND FEA ABSORBED ENERGY VS. TIME COMPARISON	166
FIGURE 161 - CASE 8 SIMPLIFIED METHOD AND FEA ABSORBED ENERGY VS. TIME COMPARISON	167
FIGURE 162 - CASE 9 SIMPLIFIED METHOD AND FEA ABSORBED ENERGY VS. TIME	167
FIGURE 163 - CASE 10 SIMPLIFIED METHOD AND FEA ABSORBED ENERGY VS. TIME	168

FIGURE 164 - CASE 11 SIMPLIFIED METHOD AND FEA ABSORBED ENERGY VS. TIME.....	168
FIGURE 165 - CASE 12 SIMPLIFIED METHOD AND FEA ABSORBED ENERGY VS. TIME.....	169
FIGURE 166 - CASE 13 SIMPLIFIED METHOD AND FEA ABSORBED ENERGY VS. TIME.....	169
FIGURE 167 - CASE 14 SIMPLIFIED METHOD AND FEA ABSORBED ENERGY VS. TIME.....	170
FIGURE 168 - CASE 15 SIMPLIFIED METHOD AND FEA ABSORBED ENERGY VS. TIME.....	170
FIGURE 169 - CASE 16 SIMPLIFIED METHOD AND FEA ABSORBED ENERGY VS. TIME.....	171
FIGURE 170 - CASE 17 SIMPLIFIED METHOD AND FEA ABSORBED ENERGY VS. TIME.....	171
FIGURE 171 - CASE 18 SIMPLIFIED METHOD AND FEA ABSORBED ENERGY VS. TIME.....	172
FIGURE 172 - CASE 19 SIMPLIFIED METHOD AND FEA ABSORBED ENERGY VS. TIME.....	172
FIGURE 173 - CASE 20 SIMPLIFIED METHOD AND FEA ABSORBED ENERGY VS. TIME.....	173
FIGURE 174 - FEA PLATE CRUSHING.....	173
FIGURE 175 - FEA BENDING VS. SIMPLIFIED METHOD DEFORMATION.....	174
FIGURE 176 - CASE 2 SIMPLIFIED METHOD (WITH AND WITHOUT CRUSHING) AND FEA .....	174
FIGURE 177 - CASE 7 SIMPLIFIED METHOD (WITH AND WITHOUT CRUSHING) AND FEA .....	175
FIGURE 178 - CASE 8 SIMPLIFIED METHOD (WITH AND WITHOUT CRUSHING) AND FEA .....	175
FIGURE 179 - CASE 12 SIMPLIFIED METHOD (WITH AND WITHOUT CRUSHING) AND FEA .....	176
FIGURE 180 - CASE 15 SIMPLIFIED METHOD (WITH AND WITHOUT CRUSHING) AND FEA .....	176
FIGURE 181 - CASE 18 SIMPLIFIED METHOD (WITH AND WITHOUT CRUSHING) AND FEA .....	177
FIGURE 182 - CASE 19 SIMPLIFIED METHOD (WITH AND WITHOUT CRUSHING) AND FEA .....	177
FIGURE 183 - COLLISIONS, 1973-1993 ALL SHIPS WORLDWIDE [78].....	182
FIGURE 184 - ACCIDENT LOCATION [78] – WORLDWIDE TANKER DATA, 1969-1974 .....	182
FIGURE 185 – COLLISION EVENT VARIABLES.....	184
FIGURE 186 – SHIP TYPE PROBABILITY [79].....	185
FIGURE 187 - STRIKING SHIP DISPLACEMENT , WORLDWIDE DISTRIBUTION.....	185
FIGURE 188 – DISPLACEMENT OF SHIPS STRIKING BULK CARRIERS [78] .....	185
FIGURE 189 - STRIKING SHIP DISPLACEMENT - ALL TANKERS.....	186
FIGURE 190 - STRIKING SHIP DISPLACEMENT - BULK CARGO SHIPS.....	186
FIGURE 191 - STRIKING SHIP DISPLACEMENT - FREIGHTERS.....	187
FIGURE 192 - STRIKING SHIP DISPLACEMENT - PASSENGER SHIPS.....	187
FIGURE 193 - STRIKING SHIP DISPLACEMENT - CONTAINER SHIPS.....	187
FIGURE 194 – STRIKING SHIP SPEED [80,82] .....	188
FIGURE 195 - BOW HALF ENTRANCE ANGLE (ALL SHIPS BY TYPE, DESIGN PRACTICE ) [78] .....	189
FIGURE 196 – ALL SHIPS LENGTH VS. DISPLACEMENT [79].....	190
FIGURE 197 – ALL TANKERS LENGTH VS. DISPLACEMENT [79] .....	190
FIGURE 198 – BULK CARGO SHIPS LENGTH VS. DISPLACEMENT [79] .....	191
FIGURE 199 – FREIGHTER LENGTH VS. DISPLACEMENT .....	191
FIGURE 200 – PASSENGER SHIP LENGTH VS. DISPLACEMENT [79].....	192
FIGURE 201 – CONTAINER SHIP LENGTH VS. DISPLACEMENT [79] .....	192
FIGURE 202 – ALL-TANKERS FULL LOAD DRAFT VS. DISPLACEMENT [79].....	193
FIGURE 203 – BULK CARGO SHIP FULL LOAD DRAFT VS. DISPLACEMENT [79] .....	193
FIGURE 204 – FREIGHTER FULL LOAD DRAFT VS. DISPLACEMENT [79] .....	194
FIGURE 205 – PASSENGER SHIP FULL LOAD DRAFT VS. DISPLACEMENT [79].....	194
FIGURE 206 – CONTAINER SHIP FULL LOAD DRAFT VS. DISPLACEMENT [79] .....	195
FIGURE 207 – ALL TANKERS BEAM VS. DISPLACEMENT [79] .....	195
FIGURE 208 – BULK CARGO SHIP BEAM VS. DISPLACEMENT [79] .....	196
FIGURE 209 – FREIGHTER BEAM VS. DISPLACEMENT [79] .....	196
FIGURE 210 – PASSENGER SHIP BEAM VS. DISPLACEMENT [79].....	197
FIGURE 211 – CONTAINER SHIP BEAM VS. DISPLACEMENT [79] .....	197
FIGURE 212 – ALL TANKERS BOW HEIGHT VS. DISPLACEMENT [79] .....	198
FIGURE 213 – BULK CARGO SHIP BOW HEIGHT VS. DISPLACEMENT [79] .....	198
FIGURE 214 – FREIGHTER BOW HEIGHT VS. DISPLACEMENT [70].....	199
FIGURE 215 – PASSENGER SHIP BOW HEIGHT VS. DISPLACEMENT [79].....	199
FIGURE 216 – CONTAINER SHIP BOW HEIGHT VS. DISPLACEMENT [79].....	200
FIGURE 217 - STRUCK SHIP SPEED [82] .....	201
FIGURE 218 – COLLISION ANGLE PDF.....	202
FIGURE 219 - LONGITUDINAL SIDE DAMAGE PROBABILITIES [78].....	202

FIGURE 220 - SIMCOL, MARPOL & HARDER SH100 PENETRATION COMPARISON.....	203
FIGURE 221 - SIMCOL, MARPOL & HARDER DH150 PENETRATION COMPARISON.....	203
FIGURE 222 - SIMCOL, MARPOL & HARDER SH100 LED COMPARISON.....	204
FIGURE 223 - SIMCOL, MARPOL & HARDER DH150 LED COMPARISON.....	204

## LIST OF TABLES

TABLE 1 - COLLISION ENERGY ABSORBING STRUCTURE .....	10
TABLE 2 - COLLISION DESCRIPTIONS .....	10
TABLE 3 - PERCENTAGE OF ENERGY ABSORBED BY STRIKING SHIP BOW [15,36] .....	11
TABLE 4 - PERCENTAGE OF ENERGY ABSORBED BY STRIKING BOW IN COLLISIONS [47] .....	12
TABLE 5 - DOUBLE-SIDED TEST SECTION PARAMETERS.....	22
TABLE 6 - SMEARING TEST CASE NOMENCLATURE.....	23
TABLE 7 - MATERIAL TYPE 3 DEFINITIONS.....	29
TABLE 8 - MATERIAL TYPE 24 DEFINITIONS.....	30
TABLE 9 - ENERGY ABSORBING STRUCTURE METHOD SUMMARY FOR SIMCOL.....	80
TABLE 10 - SIMPLIFIED METHOD SUMMARY .....	82
TABLE 11 - FEA SIMPLIFIED DECK CRUSHING AND CUTTING TEST PARAMETERS .....	87
TABLE 12 - CORRELATION OF ENERGY COEFFICIENT METHODS TO FEA AT HEA = 30 DEGREES .....	91
TABLE 13 - SIMPLIFIED LONGITUDINAL/TRANSVERSE CRUSHING PARAMETERS .....	93
TABLE 14 - CORRELATION RESULTS OF ENERGY COEFFICIENT METHODS FOR BULKHEAD CRUSHING.....	97
TABLE 15 EIGHT REGION PLATE ANALYSIS INITIAL CONDITIONS.....	121
TABLE 16 - CONSTANT PARAMETERS FOR TWENTY-FIVE REGION PLATE TEST CASES.....	160
TABLE 17 - TWENTY-FIVE REGION PLATE TEST CASE VARIABLE VALUES.....	160
TABLE 18 - CORRELATION COEFFICIENT OF SIMPLIFIED METHOD TO FEA ENERGY VS. TIME CURVES .....	178
TABLE 19 - FEA - SIMCOL VALIDATION PERCENT DIFFERENCE.....	180
TABLE 20 - SIMCOL VALIDATION PERCENT DIFFERENCE .....	180
TABLE 21 - STRIKING SHIP TYPE AND DISPLACEMENT .....	188
TABLE 22 - BOW HALF ENTRANCE ANGLE (ALL SHIPS).....	189
TABLE 23 - STRIKING SHIP CHARACTERISTICS.....	200

## CHAPTER 1 Motivation and Introduction

The primary objective of this project is to improve, validate and assess the simplified collision damage model SIMCOL, as part of the continuing work of SNAME Ad Hoc Panel #6 (Structural Design and Response in Collision and Grounding) and IMO working groups. Work accomplished under prior SSC and SNAME sponsorship made excellent progress towards predicting damage penetration in ship collisions. This project focuses on predicting the **longitudinal** extent of damage in cases where both ships have forward speed, and at oblique collision angles. Longitudinal damage is particularly important in oil outflow and damage stability calculations. Current models do not provide adequate predictions of longitudinal damage, particularly in way of transverse bulkheads.

The serious consequences of ship grounding and collision necessitate the development of regulations and requirements for the subdivision and structural design of ships to reduce damage and environmental pollution, and improve safety. The International Maritime Organization (IMO) is responsible for regulating the design of oil tankers and other ships to provide for ship safety and environmental protection. Their ongoing transition to probabilistic performance-based standards requires the ability to predict the environmental performance and safety of specific ship designs. This is a difficult problem requiring the application of fundamental engineering principles and risk analysis [1,2,3,4].

IMO's first attempt at probabilistic performance-based standards for oil tankers was in response to the U.S. Oil Pollution Act of 1990 (OPA 90). In OPA 90, the U.S. requires that all oil tankers entering the U.S. waters must have double hulls. IMO responded to this unilateral action by requiring double hulls or their equivalent. Equivalency is determined based on probabilistic oil outflow calculations specified in the "Interim Guidelines for the Approval of Alternative Methods of Design and Construction of Oil Tankers Under Regulation 13F(5) of Annex I of MARPOL 73/78" [4], hereunder referred to as the Interim Guidelines.

The Interim Guidelines are an excellent beginning, but they have a number of significant shortcomings:

- They use a single set of damage extent probability density functions (pdfs) from limited single-hull accident data applied to all ships, independent of structural design.
- IMO damage pdfs consider only damage significant enough to breach the outer hull. This penalizes structures able to resist rupture.
- Damage extents are treated as independent random variables when they are actually dependent variables, and ideally should be described using a joint pdf.
- Damage pdfs are normalized with respect to ship length, breadth and depth when damage may depend largely on local structural features and scantlings vice global ship dimensions.

It is generally agreed that structural design has a major influence on tanker oil outflow and damaged stability in grounding and collision, but crashworthiness is not considered in present regulations. Recent work by SNAME Ad Hoc Panel #6 for the SSC [83] has made excellent progress in developing and benchmarking collision models that are able to predict collision penetration with reasonable accuracy, however, these models do not provide reliable damage estimates in the longitudinal direction, particularly near transverse bulkheads. Once watertight

or oil boundaries are penetrated, longitudinal damage becomes extremely important in determining the extent of oil outflow and flooding. Therefore, it is essential that current collision models be improved and extended to provide reasonable predictions of longitudinal damage.

The methodology and tools developed in this project provide a practical means of considering structural design in a regulatory framework, and when implemented would improve the safety and environmental performance of ships.

Specific objectives are:

- To support ongoing work by SNAME Ad Hoc Panel #6 (Structural Design and Response in Collision and Grounding).
- To assess and integrate existing simplified collision-damage models and mechanisms into a single Simplified Collision Model (SIMCOL). This model will be used to predict probabilistic collision damage extents given a probabilistic description of collision scenarios. This requires that sub-model physics be sufficiently simple to support overall computational efficiency in probabilistic applications where thousands of runs are required.
- Investigate collisions longitudinally impacting transverse bulkheads and deep webs using finite element analysis (LSDYNA) and actual data where available.
- Creation of a simplified collision model for the determination of longitudinal extent of damage. (Chapter 5)
- Creation of a simplified collision model for the determination of striking ship bow damage. (Chapter 5)
- To validate SIMCOL in the context of a realistic collision simulation using real and finite element model data. (Chapter 6)
- To demonstrate the process and predict probabilistic structural damage for oil tankers. (Chapter 6)
- To achieve international acceptance of this validation by publishing results and making all data and aspects of the research open for discussion and collaboration through SNAME and the Ship Structure Committee.
- To provide the basis for further work in which a parametric analysis of probabilistic results would be incorporated in IMO oil outflow and damage stability regulations.

In 1979, the Ship Structure Committee (SSC) conducted a review of collision research and design methodologies [5,6,7]. They concluded that the most promising simplified collision analysis alternative was to extend Minorsky's original analysis of high-energy collisions by including consideration of shell membrane energy absorption.

A more recent review of the literature and of the applicability of available methods for predicting structural performance in collision and grounding was made at the 1997 International Ship and Offshore Structures Congress (ISSC 97) by Specialist Panel V.4 [8]. Their report states: "Knowledge of behavior on a global level only (i.e., total energy characteristics like the pioneering Minorsky formula) is not sufficient. The designer needs detailed knowledge on the

component behavior (bulkheads, girders, plating, etc.) in order to optimize the design for accident loads.”

The approach taken in this project is to progressively increase the complexity of SIMCOL starting with a modified Minorsky approach until results with sufficient accuracy and sensitivity to design characteristics is obtained. SIMCOL Version 3.0 represents the most recent product of this evolution.

Determination of the energy absorbed through longitudinal damage has often been neglected, treated as minimal compared to the energy absorbed through penetration. However, with oblique angle collisions (as occur more often than T-bone collisions) the energy absorbed in longitudinal damage may be greater than the energy absorbed due to penetration. Additionally, absorption of energy in the longitudinal direction removes energy from the entire system leaving less energy available for penetration.

The determination of the energy absorbed through longitudinal damage is additionally often neglected because of the complexity of: the additional degrees of freedom necessary for the system equations, the additional structural geometry that must be modeled and accounted for as energy absorbing structure and the formulation for the coupled solution of internal and external dynamics that properly considers longitudinal damage. Considering only the additional degrees of freedom necessary for the system equations, Pedersen and Zhang [14] derived expressions for both the longitudinal and transverse energy absorbed in ship-to-ship collisions. Pedersen and Zhang’s expressions are uncoupled from the internal deformation mechanics of the problem and do not explicitly consider the longitudinal damage of the transverse structure of the struck vessel [100]. The determination of energy absorbed through longitudinal damage and the development of a simplified longitudinal damage model is the primary original contribution of this report.

## CHAPTER 2 Collision Basics

Models for analyzing ship collisions were initially developed in the 1950s for ships transporting radioactive materials, and later were applied to other types of ships, including barges, tankers and LPG/LNG carriers. SSC Reports 283, 284 and 285 provide an excellent summary of collision models developed before 1979 [5,6,7]. A more recent review was conducted by the 1997 International Ship and Offshore Structures Congress (ISSC 97), Specialist Panel V.4 [8]. SSC Report 442, produced under SNAME Ad Hoc Panel #6, provides the most recent update [83].

Existing models make different assumptions, and use different sub-models and coupling approaches. The high variability and complexity of damage behavior in ship-to-ship collisions precludes the ability to predict the exact behavior of the vessels during a collision event. However, as with most complex systems, various simplifications and assumptions based upon general behavior collected from multiple events can be made yielding a less complex and definable system. This Chapter is a collection and description of discovered and defined general behaviors, and the simplifications to which they lead.

### 2.1 Ship-to-Ship Collisions

A ship-to-ship collision is a high energy event occurring over a short period of time, often described mathematically through energy and momentum balance equations. Generally, from the time a collision between two vessels is determined imminent until the time of contact, several seconds or a few minutes pass. During this “pre-contact” time each vessel may attempt maneuvers to avoid contact. If successful, then the two vessels are involved in either a near miss or a light contact. If unsuccessful the vessels are involved in a collision. A near miss is the most desirable result of the pre-contact time where the vessels do not contact at all but miss each other. A light contact is an event where the vessels collide but either at such an oblique angle that penetration of one ship into the other does not occur or at such a low speed that again penetration does not occur. A light contact is best described as a collision in which neither of the hulls of the two vessels is compromised (ruptured or torn below the waterline).

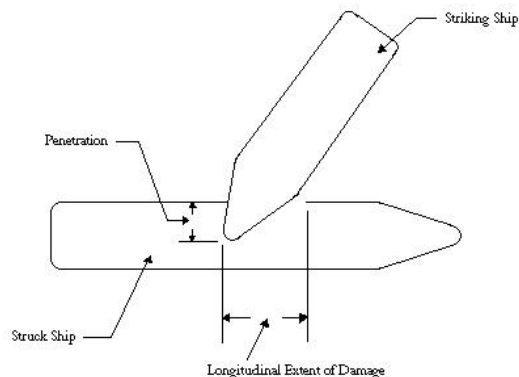


Figure 1 - Collision Damage Definition

A collision is defined as any contact between two vessels resulting in the hull of one or both vessels being compromised (ruptured or torn below the waterline). For the duration of this report, a collision will refer to the contact between two vessels where significant rupture and penetration of one vessel into the hull of the other vessel occurs. This definition of collision is illustrated in Figure 1 where the striking ship has penetrated the struck ship. Note that the referring of the two vessels as the striking ship and struck ship does not imply fault of the collision on either vessel. As with automobile collisions, the fault of the accident is not always on the driver whose forward end is damaged.

This definition of a collision narrows the study of ship-to-ship collisions to only the high energy less oblique “T” collisions, leaving the light contact and below waterline raking collisions for another investigation. Additionally, from the above definition of collision, the definition of damage extent follows directly as an indication of hull rupture with the following characteristics or metrics: 1) Extent of transverse penetration of striking ship into struck ship, 2) Longitudinal extent of outer hull opening, 3) Vertical extent of outer hull opening and 4) Tankage volume opened to sea. For clarity, the definitions of a collision and collision damage are restated as:

Collision: the contact between two vessels (striking and struck) where the penetration of one vessel (striking) into the hull of the other vessel (struck) occurs at an angle at which raking and sharp puncture are minimal energy absorbing components of the total energy balance.

Damage: an indication of hull rupture and if rupture then the measure of: 1) Extent of transverse penetration of striking ship into struck ship, 2) Longitudinal extent of outer hull opening 3) Vertical extent of outer hull opening and 4) Tankage volume opened to sea

## 2.2 Collision Physics

A collision between two vessels is modeled as an inelastic collision [9,10,13,15]. An inelastic collision is formally defined as a collision in which part of the initial kinetic energy of the colliding vessels changes to another form of energy (i.e. damage work and heat). For this report, an inelastic collision is specifically defined as a collision between two vessels that act and move as one body after damage penetration, and where a significant part of the initial kinetic energy of the colliding vessels is converted to mechanical (deformation) energy.

For an inelastic collision the balance of momentum and energy is described by Equations 2.1 and 2.2.

$$M_1V_1 + M_2V_2 = (M_1 + M_2)V_3 \quad (2.1)$$

$$\frac{1}{2}(M_1V_1^2 + M_2V_2^2) = \frac{1}{2}(M_1 + M_2)V_3^2 + E_A + E_F \quad (2.2)$$

Where:

$M_1$  is the mass (plus added mass) tensor of the striking vessel

$M_2$  is the mass (plus added mass) tensor of the struck vessel

$V_1$  is the velocity vector of the striking vessel

$V_2$  is the velocity vector of the struck vessel

$V_3$  is the velocity vector of the combined striking and struck vessels after contact

$E_A$  is the energy absorbed through structural deformation and damage

$E_F$  is the energy imparted to the fluid (wave-making energy) during the collision

As with inelastic automobile collisions, the damage to the struck vessel is often of the shape and form of the bow of the impinging striking vessel (i.e. local damage vice global damage). While damage is sustained to the striking vessel bow, this damage is often the result of heavy and dense cargo or relatively substantial longitudinal structure and weight of the struck ship. These generalities are supported by the realization that most vessel bows comprise additional strengthening structure designed to limit the deteriorative effects of slamming. As such, the bow of the striking vessel is treated as rigid in many analyses, while the damage sustained by the struck vessel is assumed to assume the shape and form of the penetrating rigid bow. These assumptions are supported by Figure 2 through Figure 6 and the works of Simonsen [10], Rosenblatt & Son, Inc. [18] and Chen [35].



Figure 2 - Collision of M/V Alexia and M/V Enif



Figure 3 - Damage to M/V Enif



Figure 4 - Collision of M/T Gas Roman and M/V Springbok

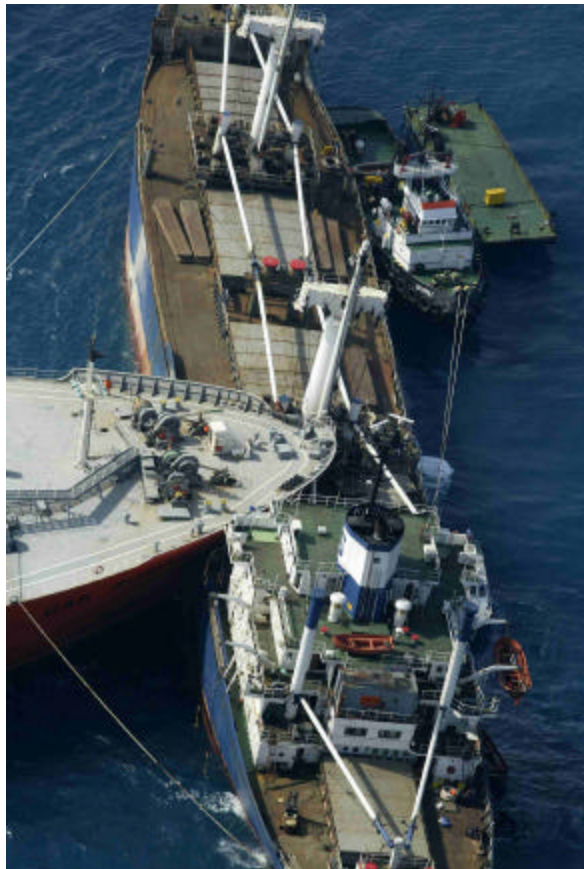


Figure 5 - Bow Penetration of Collision of M/T Gas Roman and M/V Springok



Figure 6 - Bow Damage of Collision of M/T Gas Roman and M/V Springbok

### **2.3 Vessel Motion**

The motion of any vessel treated as a buoyant rigid body may be defined using a six degree of freedom system (surge, sway, heave, pitch, roll and yaw). However, as in maneuvering, a vessel involved in a collision event may be described using only three degrees of freedom (surge sway and yaw) where the motions of heave, pitch and roll may be neglected because the motion, and thus the energy, translated into these degrees of freedom are minimal compared to the motions in the surge, sway and yaw directions [9,10,13,14,16].

A vessel in a collision is induced to roll when a force is applied in the sway direction above or below the vessels vertical center of buoyancy. This statement is only true if the vessel is not bound or constrained by other forces. As previously discussed, a collision is an inelastic event and as such, for most collisions, the roll of one vessel requires the pitch of the additional vessel about the combined center of buoyancy of the joined vessels. This coupling of the two vessels about the combined center of buoyancy limits the ability for either vessel to roll or pitch as the restoring forces in these directions are high and therefore the only motions generally unconstrained are the in planar motions of surge, sway and yaw.

Often vessels involved in a collision continue to maneuver after contact occurs. The maneuvers are either from the attempt to pull away from the collision or from the continuation of a vessel's momentum due to maneuvers performed prior to the contact. Because of the complicated dynamics involved during a collision these post-contact maneuvers are often neglected [9,10,15] and the forces involved in the contact are assumed to include only those forces that are derived from each vessels respective forward momentum at the time of contact.

During an inelastic collision, the yaw of the struck vessel about its own centroid is damped by the requirement to additionally sway and yaw the striking vessel about the struck vessels center of buoyancy (similar to the argument for a three degree of freedom system). A similar argument is made for the yaw of the striking vessel where the damping is provided by the requirement to surge and yaw the struck vessel. With this logical argument the continuation of the yaw momentums of either vessel are effectively damped by the addition of the second vessels mass (i.e. the two ships constrain each others motion). Figure 7 illustrates this phenomenon. The above logical argument does not however eliminate the ability of the combined vessels to yaw about the combine center of buoyancy nor does it preclude the yaw induced from non-amidships contacts, which are due to the initial forward momentum of the striking vessel and the contact location.

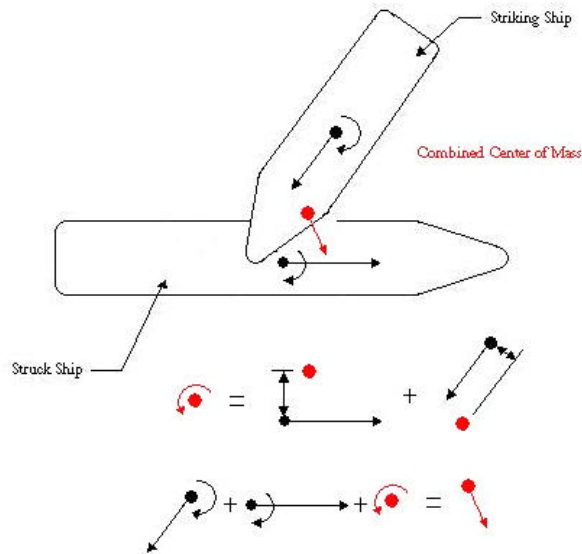


Figure 7 - Illustration of Constrained Vessel Yaw

The argument for neglecting the propulsion forces of each vessel during a collision event is justified through the multitude of collision reports [84] where the vessels involved in collisions often attempt to limit the damage by shutting down the engines or clutching out the shaft and propeller near the time of contact. For those collisions where this does not occur, often the vessels are placed in full astern sometime near the time of contact [84]. In these situations the time at which the propulsion system of the vessel to change the propeller force direction (approximately 100 seconds) is often greater than the time of the entire collision event (less than ten seconds) and therefore the effect is similar to shutting down the engines or clutching out the shaft and propeller.

## 2.4 Energy Absorbing Structure

Recalling the energy balance of Equation 2.2, the energy absorbed through damage term ( $E_A$ ) consists of all the energy absorbed through each structural and non-structural member of the vessel. For the duration of this report, the energy absorbed through damage will only refer to the energy absorbed through the structural components of the vessel, as such; the effects of cargo, ballast and outfit are neglected and saved for future investigations.

Examination of multiple collisions of varying speeds, collision angles, vessel types and collision locations relative to amidships on the struck vessel allows the general statement that the majority of the energy absorbed by damage to structure in a ship-to-ship collision is absorbed by the following eight structural members; side shell, longitudinal bulkheads, decks, stringers, web frames, transverse bulkheads, longitudinal girders and transverse girders.

Table 1 presents the energy absorbed by each of the above structural components for multiple collisions where the struck ship is a tanker. The ships were modeled using finite element analysis as discussed in Chapter 3. Information regarding the structure of each vessel is provided in Appendices A through G.

The average percentage of the total energy absorbed in the collisions by the eight structural members is approximately 95% or simply stated; the majority of the energy absorbed in a ship-to-ship collision is absorbed by the deformation and damage of the side shell, longitudinal bulkheads, decks, stringers, web frames, transverse bulkheads, longitudinal girders and transverse girders. Thus the energy absorbed by additional structure such as struts, columns and brackets may be neglected. While this is generally true, some non-standard structure or structural arrangements may need additional investigation to determine the relevance of the energy absorbing capacity in any individual collision.

Table 1 - Collision Energy Absorbing Structure

	Collision 1	Collision 2	Collision 3	Collision 4
<b>Total Energy in Collision (J)</b>	1.88E+08	6.32E+08	2.27E+08	3.83E+08
<b>Total Energy Absorbed by Structural Damage</b>	4.98E+07	1.93E+08	3.95E+07	1.76E+08
<b>Energy Absorbed By Striking Ship Bow</b>	1.34E+07	5.89E+07	1.45E+07	8.11E+07
<b>Energy Absorbed by Struck Ship</b>	3.65E+07	1.34E+08	2.50E+07	9.49E+07
<b>1 Side Shell</b>	2.43E+07	4.17E+07	8.39E+06	3.66E+07
<b>2 Longitudinal Bulkheads</b>	2.37E+05	1.56E+07	4.95E+05	1.75E+07
<b>3 Decks</b>	4.04E+06	7.81E+06	9.45E+06	7.88E+06
<b>4 Stringers</b>		1.19E+07	4.74E+05	1.12E+07
<b>5 Webs</b>	3.78E+06	8.99E+06	3.90E+06	1.42E+07
<b>6 Transverse Bulkheads</b>	2.51E+06	4.04E+07	1.19E+05	2.77E+04
<b>7 Longitudinal Girders</b>		2.55E+05	1.80E+04	2.26E+05
<b>8 Transverse Girders</b>	8.80E+05	2.32E+05	1.76E+05	2.37E+06
<b>Total Energy from Parts 1 - 8</b>	3.57E+07	1.27E+08	2.30E+07	8.99E+07
<b>% Energy 8 Parts of Struck Ship Energy Absorbed</b>	97.96%	94.89%	92.12%	94.73%
<b>% Energy Bow of Total Energy Absorbed</b>	26.83%	30.57%	36.68%	46.08%

The collisions in Table 1 are described in Table 2.

Table 2 - Collision Descriptions

Collision #	Striking Vessel	Struck Vessel	Collision Angle (Degrees)	Striking Ship Speed (knots)	Struck Ship Speed (knots)	Collision Location
1	C4 Cargo Vessel	T2 Tanker	55	5.5	6.81	9.923 m fwd amidships
2	150k dwt Bulk Carrier	150k dwt Double Hull Tanker	90	5	0	20 m fwd amidships
3	150k dwt Bulk Carrier	150k dwt Double Hull Tanker	45	3	0	20 m fwd amidships
4	40k dwt Container Ship	150k dwt Double Hull Tanker	90	7	0	3.5 m fwd amidships

Although the striking ship bow is often considered rigid as discussed in Section 2.4, this assumption is not always accurate as presented in Table 1 and Table 3. The damaged bow may absorb a large percentage of the total energy of the collision. The energy absorbed through damage to a striking vessel bow is discussed and summarized by Vakkalanka [55]. Woison [17],

Amdahl [23] and Pedersen [22] have also investigated the energy absorbed through damage of the striking vessel bow where it is shown that:

“The almost universal assumption of a rigid striking ship bow in ship collision analysis is not valid. Differences in striking ship bow stiffness, draft, bow height and shape have an important influence on the allocation of absorbed energy between striking and struck ships and the extent of damage in the struck ship. The energy absorbed by the striking ship can be significant and varies in different collision scenarios.” [83]

A reanalysis of Minorsky’s [9] results discussed in Section 4.1.1 and presented in Table 3 shows that the percentage of energy absorbed by the striking ship in real collision cases is significant and is not constant. Using finite element analysis, Valsgard and Pettersen modeled a collision with a double hull struck ship and deformable striking bow that absorbed 55% of the total absorbed energy. Table 1 shows bow energy absorption of up to 46%. Using closed-form equations for bow stiffness, Lutzen., Simonsen, and Pedersen [47] show that bow energy absorption for a large striking ship with a longitudinally-stiffened bow is small. Bow energy absorption for smaller striking ships and for striking ships with transversely-stiffened bows is significant and variable (Table 4).

Table 3 - Percentage of Energy Absorbed by Striking Ship Bow [15,36]

MINORSKY COLLISION CASE		Displacement (tton) [15,36]	n	t (in) [15,36]	V (knots) [15,36]	q (deg) [15,36]	width (ft) [15,36]	penetration (ft) [15,36]	Struck Ship R <sub>T</sub> (ft <sup>2</sup> in)	Minirsky Total R <sub>T</sub> (ft <sup>2</sup> in) [9]	Bow R <sub>T</sub> (ft <sup>2</sup> in)	% Energy Absorbed in Bow
10	Esso Greensboro	21800	1	0.83	15	90	60	60	2988	3250	262	8.1
	Esso Suez	19500			15							
11	Tullahoma	21900	2	0.8	10	90	20	25	800	1100	300	27.3
	P&T Adventurer	8900			14							
21	Gulf Glow	21900	2	0.8	0	65	20	38	1216	1700	484	28.5
	Imperial Toronto	16000			14							
22	Mojave	5600	2	0.5	10	70	28	23	644	900	256	28.4
	Prometed	16000			14							
38	Catawba Ford	21800	1	0.8	10	90	27	10	216	250	34	13.6
	Hoegh Clair	6600			8							
46	David EDay	8700	2	0.7	16.3	55	35	17	833	1300	467	35.9
	Marine Flyer	20400			16.5							
B	Andria Doria	20900	6	0.375	15	90	50	30	3375	3800	425	11.2
	Stockholm	16200			18							

Table 4 - Percentage of Energy Absorbed by Striking Bow in Collisions [47]

Striking Vessel \ Struck Vessel	Bulk Carrier 150,000 DWT	Container Vessel 40,000 DWT	General Cargo 3,000 DWT	Tanker 2,000 DWT	Coaster 500 DWT
Tanker L = 103m	0	0	0	24	97
Tanker L=198m	0	0	36	95	89
Tanker L=317m	0	0	52	99	94
RoRo L=58m	0	0	0	98	91
RoRo L=150m	0	0	20	48	82
RoRo L=180m	0	0	0.4	46	86

Often a collision analysis is evaluated assuming either a rigid striking or a rigid struck vessel. A more appropriate approach is that for a single time step the vessel that is treated as the rigid vessel is the one that would absorb more energy given the same amount of relative deformation. This method is equivalent to a path of least resistance method where the damage is applied to the vessel which absorbs less energy in a given displacement or penetration in a given time step. Figure 8, Figure 9 and Figure 10 illustrate cases of significant bow damage.

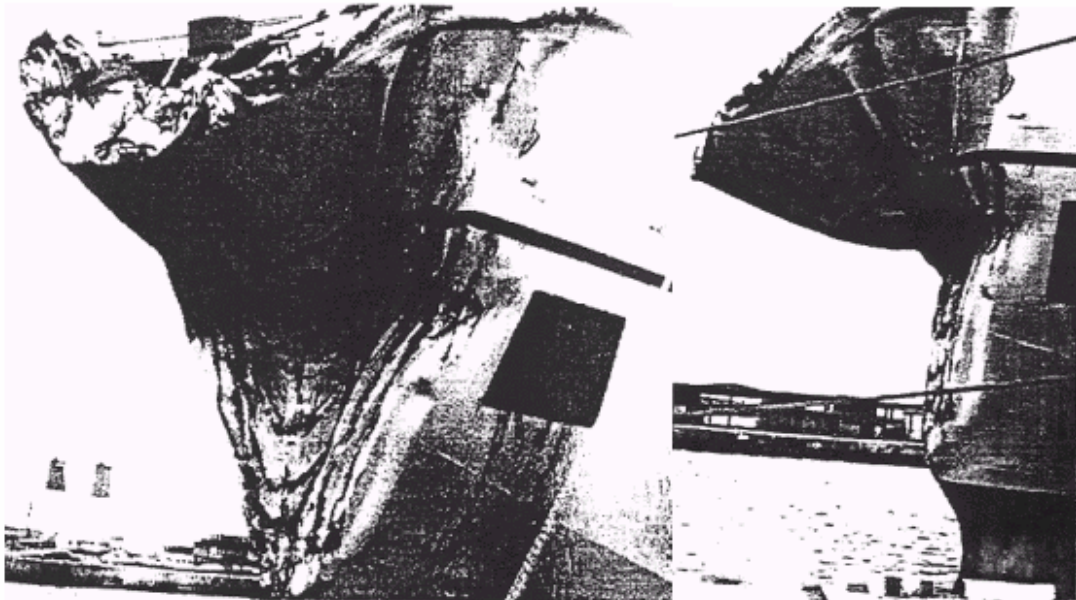


Figure 8 - Actual Collision Bow Damage



Figure 9 - Bow Damage to Norwegian Dream



Figure 10 - Karisa Bow Damage

Thus, a ship-to-ship collision is a high energy event occurring over a short time that can be modeled as an inelastic collision considering only the motions of surge, sway and yaw for each vessel. The initial kinetic energy is imparted to: 1) the remaining kinetic energy of the combined vessels, 2) radiation or wave making energy and 3) deformation energy. The deformation energy is suitably approximated by the summation of energy absorbed by 1) the striking ship bow and 2) the struck ship's side shell, longitudinal bulkheads, decks, stringers, webs, transverse bulkheads, longitudinal girders and transverse girders.

## **CHAPTER 3     Finite Element Modeling of Ship Collisions**

One of the important tools used in this research is finite element analysis (FEA). FEA is used throughout this report for developing and evaluating simplified methods. As discussed in Chapter 2, the cost of full scale collision testing and the inability to properly capture true collision behavior with physical scale modeling precludes live experimentation. The remaining methods of accident investigation and FEA must therefore be used to show and support the theories and simplified analysis described in this report.

LSDYNA is the primary FEA code used in this research, but many of the same issues that must be resolved to effectively use LSDYNA must also be resolved for the efficient application of any FEA code. Other codes in common use for collision modeling include: ABAQUS-EXPLICIT, DYNA3D, and MSC-DYNA.

### **3.1     *Overview of FE Modeling***

Finite element modeling of ship collisions cannot be performed with confidence without significant research, experimentation and validation of modeling techniques, element and material models, and careful model parameter value selection. The casual and undisciplined application of commercial software may produce impressive pictures, but be entirely wrong. The open literature and even detailed technical reports on the subject do not provide sufficient detail, analysis and validation to reproduce or defend many analyses, and “Calibration” of model parameters to one or two validation cases may only provide valid results for a very narrow range of problems.

LSDYNA is a general-purpose, explicit finite element program used to analyze the nonlinear dynamic response of three-dimensional inelastic structures. It was developed primarily for automotive collision applications, but can also be used for ship-to-ship collisions. It performs a fully dynamic analysis, not quasi-static. Crash behavior has large displacements, and is very non-linear with multiple point contact and rupture. Explicit time integration is best for these problems. The use of small time-steps is required for stability, but explicit integration does not require inversion of a large stiffness matrix as is required with implicit methods. Explicit integration also allows discontinuous failure criteria such as rupture strain. The run time required for an explicit code is approximately proportional to the number of nodes vice the square of the number of nodes as with implicit codes.

Case studies in this Chapter use LSDYNA to model collisions between a striking ship and a struck oil tanker, and a striking ship and a double hull wall section. In some cases the striking ship bow is assumed to be rigid and in other cases the bow is deformable.

### **3.2     *Structural Geometry***

There are a number of important objectives to be considered when FEA modeling struck and striking ship structures:

- Minimize the number of nodes and elements to reduce computation time consistent with sufficient computational accuracy
- Minimize complexity
- Minimize ratio of triangular to quadrature elements
- Minimize numerical instabilities through the use of global parameterization controls
- Minimize numerical instabilities by modeling with a consistent, uniform mesh
- Have a minimum of 3 elements per side of any section in the entire vehicle and a minimum of 6 elements per buckle in the energy absorbing parts of the structure
- Have a time step sufficiently small to capture proper behavior and sufficiently large to minimize computational cost
- Minimize element warpage, but limit warpage to  $10^\circ$
- Avoid edge-to-edge contacts
- Avoid initial penetration

Figure 11 shows a striking ship to struck ship collision as modeled in LSDYNA. The striking ship geometry is developed from an AutoCAD model. It includes a detailed bow model forward of the collision bulkhead and lumped beam elements aft of the collision bulkhead. The detailed portion of the bow model is shown in Figure 12 with side-shell, deck, stem, stringers, and primary girder components modeled using meshed shell elements. Stiffeners are smeared into plates as discussed in Section 3.5.

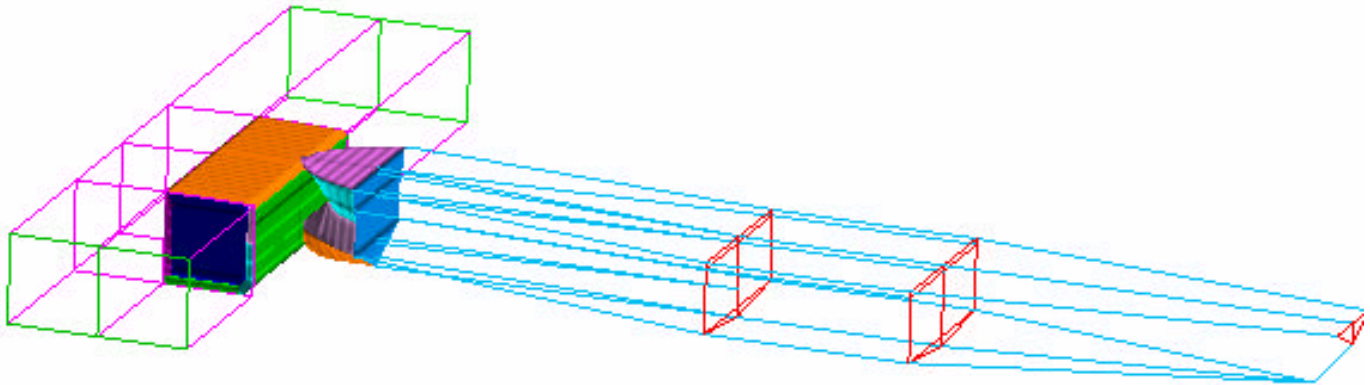


Figure 11 - Ship-to-Ship Collision as Modeled in LSDYNA

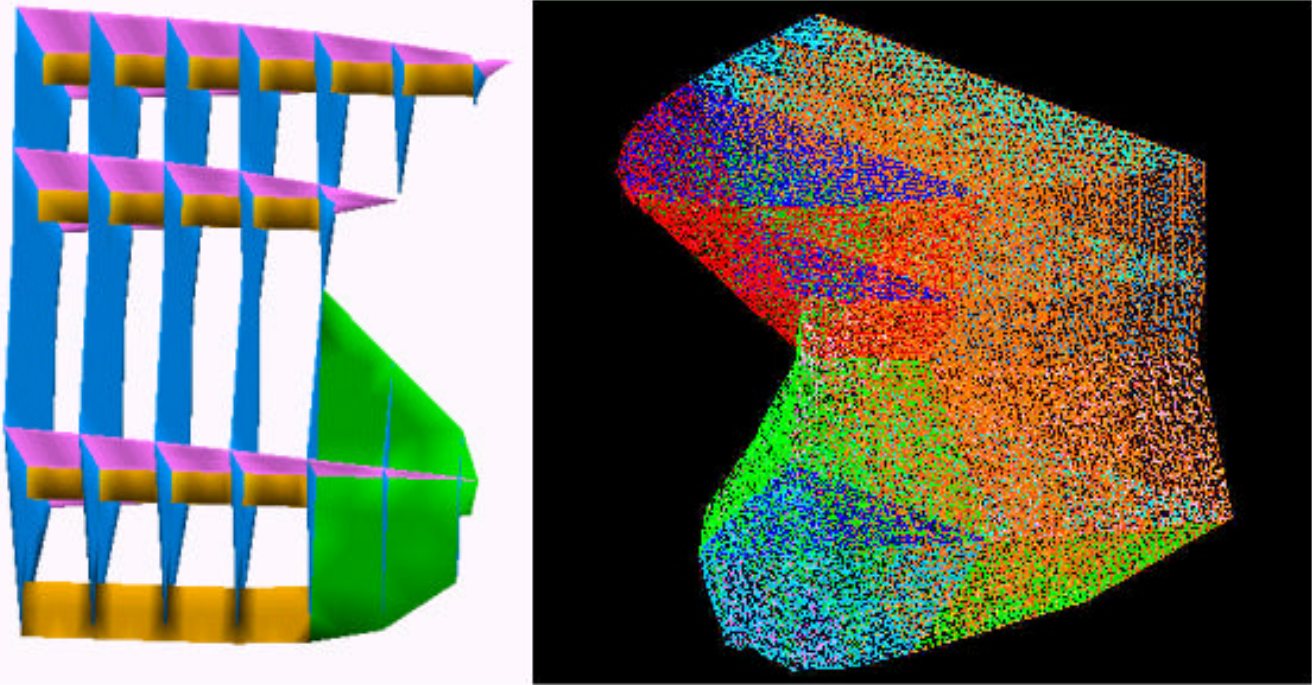


Figure 12 - Detailed LSDYNA Bow Model

In order to simplify the bow model geometry of transverse frames, they are modeled as “stiff” transverse bulkheads using panel elements. “Stiff” is quantified as having increased element thickness or increased material density an order of magnitude beyond the actual structural or material value. Collision results using “stiff” transverse frames compare well with results using detailed transverse frame models. The collision bulkhead is the boundary between the detailed portion of the bow and the remainder of the striking ship. It is also modeled as a “stiff” transverse bulkhead. Fully rigid transverse frames and bulkheads were found to cause very high stresses and premature failure at their interface with the side shell and deck panel elements. They are not used. The remainder of the striking ship aft of the collision bulkhead is modeled using “stiff” Hughes-Liu beam elements and concentrated masses such that the total mass and mass moment of inertia are the same as in the actual ship (including actual mass and added mass in the surge direction). The total cross sectional area of the longitudinal beam elements in this part of the model is determined such their sum is equal to the total longitudinal structure sectional area aft of the collision bulkhead in the real ship. Again, fully rigid beams were found to cause very high stresses and premature failure at their interface with the panel elements so stiff deformable beam elements are used.

The struck ship is usually modeled with only one side of the struck cargo tank, or tanks, in detail. Figure 13 and Figure 14 show the struck cargo tank section. The struck section includes shells, webs, girders, transverse and longitudinal bulkheads and stringers modeled as panel elements. Stiffeners are smeared into the plate thickness.

The remainder of the struck ship is modeled using “stiff” Hughes-Liu beam elements and concentrated masses, as with the bow model. This is based on the assumption that in ship collision cases local structural response dominates the collision results as determined through the results shown in Table 1. Dimensions of the longitudinal lumped beam elements are selected to model the horizontal moment of inertia at amidships. This allows some flexibility for hull girder

horizontal bending (HGHB), although with a large struck ship, horizontal bending in collision is usually small [57]. Forward and aft transverse bulkheads are at the boundaries between the detailed cargo section model and the remainder of the struck ship. In order to simplify the geometry of the boundary transverse bulkheads, they are modeled as “stiff” transverse bulkheads using panel elements only. When a transverse bulkhead is in the way of or close to the collision contact, detailed tank structure is modeled on both sides of a detailed transverse bulkhead and the stiff bulkhead boundary is moved to the opposite end of an additional tank, shown in Figure 15. The centerline bulkhead model is also modeled using a “stiff” bulkhead unless it is in way of or close to the collision contact. When close to the collision contact the centerline bulkhead model is based on ship scantlings and geometry, supported with stiff beam elements that connect to nodes on the opposite deck edge at each frame, deck and stringer as shown in Figure 16. Again, fully rigid beams were found to cause very high stresses and premature failure at their interface with the panel elements so “stiff” deformable beam elements are used.

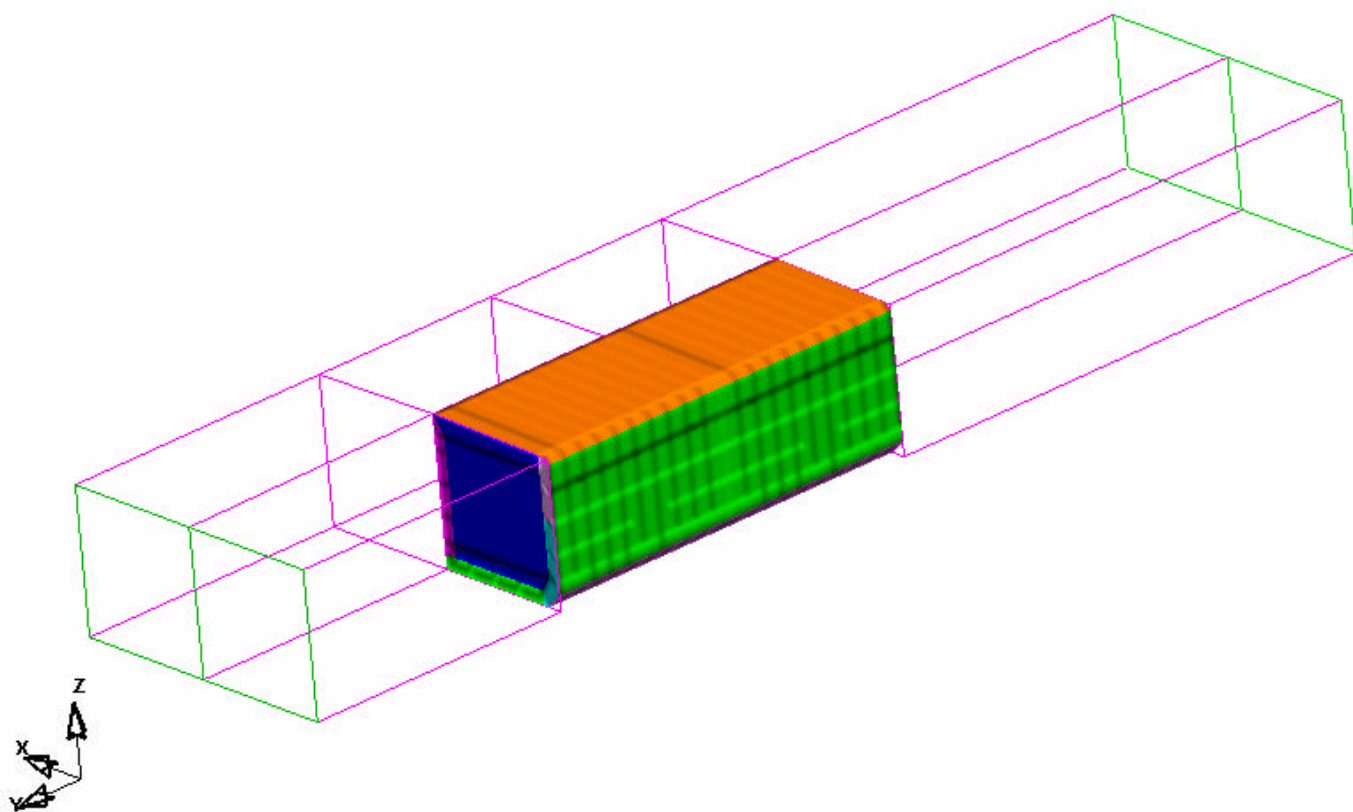


Figure 13 - Struck Ship LSDYNA Model

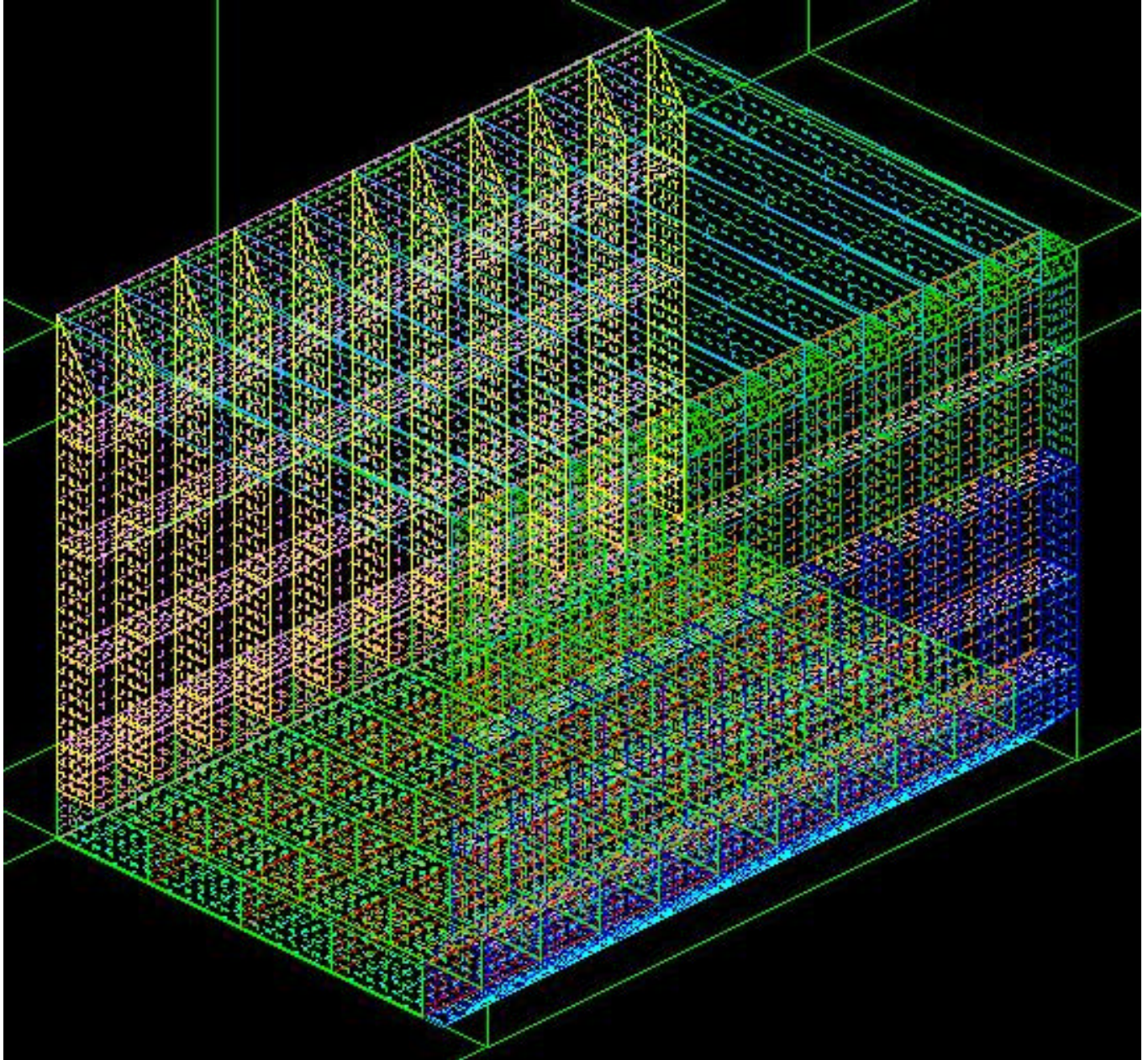


Figure 14 - Struck Ship Cargo Section Mesh

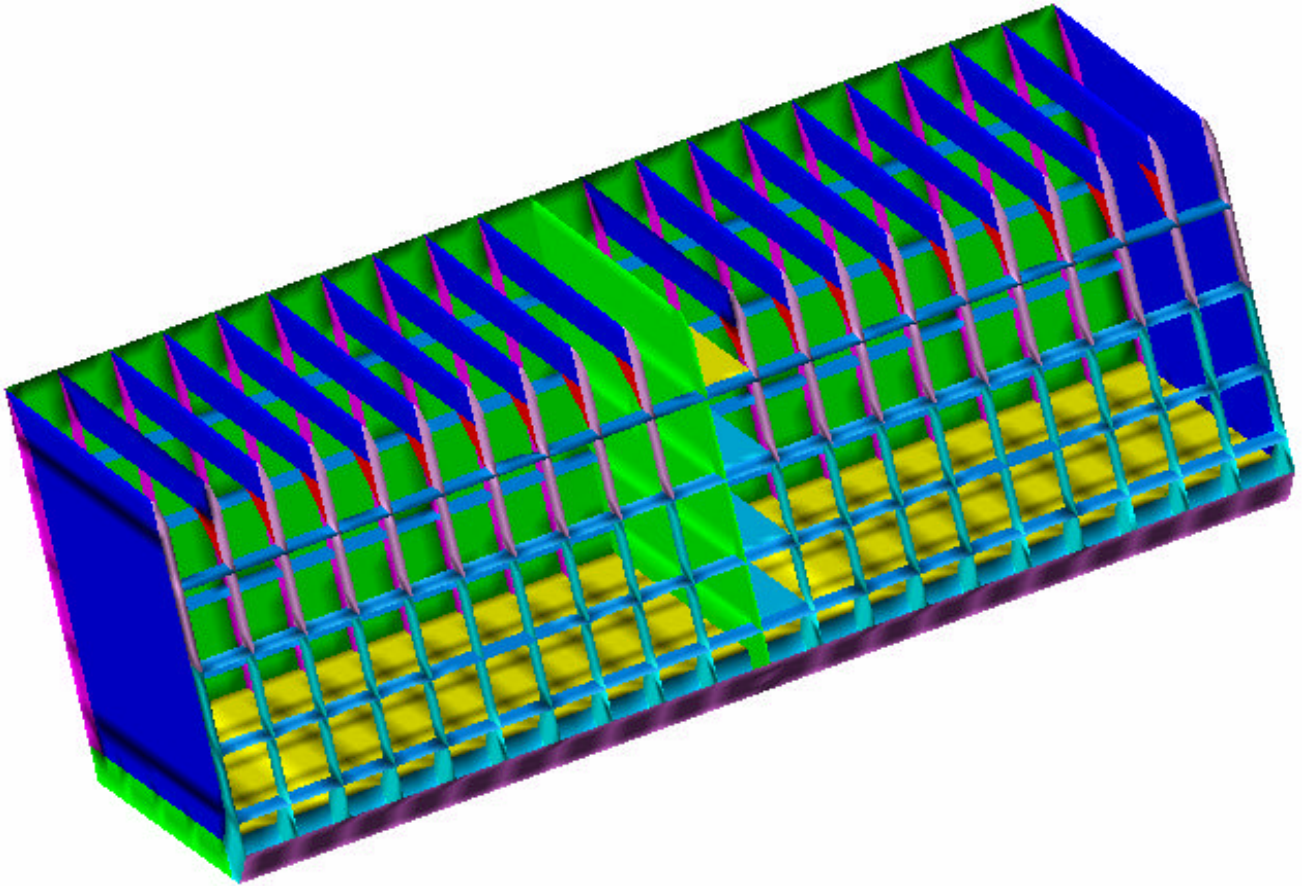


Figure 15 Struck Ship Cargo Section Geometry View from Outboard

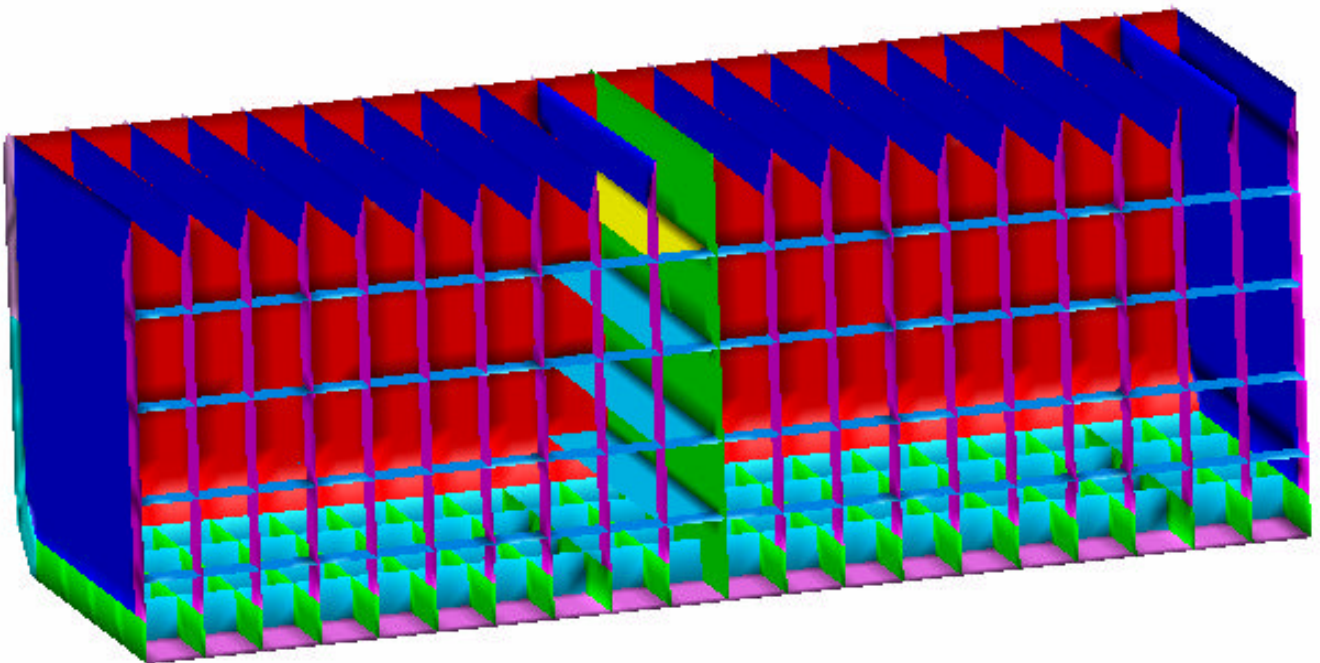


Figure 16 Struck Ship Cargo Section Geometry View from Centerline

### **3.3 Element Types**

LSDYNA has many element types to choose from. In order to save CPU time, solid modeling and a fine mesh are avoided in favor of shell and beam elements and a more coarse mesh. The Hughes-Liu beam element is used for all struck and striking ship model beam elements. Hughes-Liu elements are designed not to fracture and provide out of plane bending not provided by truss elements. Belytschko-Tsay shell elements are used for all plate panels in both the struck and striking ship models. This element uses a local coordinate system that deforms with the element and provides a higher degree of numerical accuracy than a standard shell element at a lower time cost. Numerous runs with other element types available in LSDYNA were not as computationally efficient. Single point (reduced), standard Gauss integration is used and the panel reference location is taken at mid-plane.

Lemmen and Vredeveldt [72] found that two or three integration points through the thickness of a belytschko-tsay element were sufficient. Hourglassing<sup>1</sup> was not a problem with their small mesh (80x80mm). The LSDYNA manual recommends that hourglass energy be less than 10% of the internal energy. Otherwise, other methods should be used, such as triangle-elements instead of quadrilateral-elements or fully integrated elements instead of reduced integration elements. To reduce hourglassing while using the coarse elements, 5 integration points were found to be necessary to maintain the hourglass energy below 10% of the internal energy for most analysis.

### **3.4 Finite Element Mesh**

Starting with an AutoCAD line model of the ship hull geometry, surfaces are created over the lines in the finite element model builder program (FEMB). Next, surfaces are partitioned and joined consistent with major energy absorbing structural members discussed in Chapter 2. The surfaces are auto-meshed with a minimum element dimension of 0.20 meters and a maximum element dimension of .3 meters. Element dimensions less than 0.5 meters are processing time prohibitive (3 to 5 days on a Pentium IV Desktop for the simplified models discussed in Section 3.9), however to obtain a true physical description of the deformed geometry of parts in the struck ship, elements of these sizes are required. Hourglassing is also an important concern with large mesh sizes and must be monitored closely. Finally, mesh problems are repaired manually. The resulting element length to thickness (L/t) ratio is typically 8:1 to 12:1. A uniform mesh throughout both the struck and striking ships detailed sections must be used to eliminate possible numerical errors in the contact due to translation of forces from element to element.

### **3.5 Smearing Techniques**

To reduce computational time and to allow the use of a larger shell element mesh in the bow and cargo section models, plate stiffeners, flanges, and structural holes are smeared into plate panels. This is a common practice, but various methods can be used. Though smearing is not ideal, it is

---

<sup>1</sup> Numerical deformation modes other than rigid body that do not contribute to strains at the integration points

essential as a method to reduce the finite element computational time requirement. As such, the following smearing methods were compared:

- No smearing
- Equivalent Tensile Strength (Area) Smearing
- Equivalent Compression Strength Smearing
- Equivalent Membrane Strength Smearing
- Equivalent Moment of Inertia Smearing

This comparison is performed using an LSDYNA test case of a simple struck ship double-side configuration as shown in Figure 17. Table 5 provides details for the struck double-sided section.

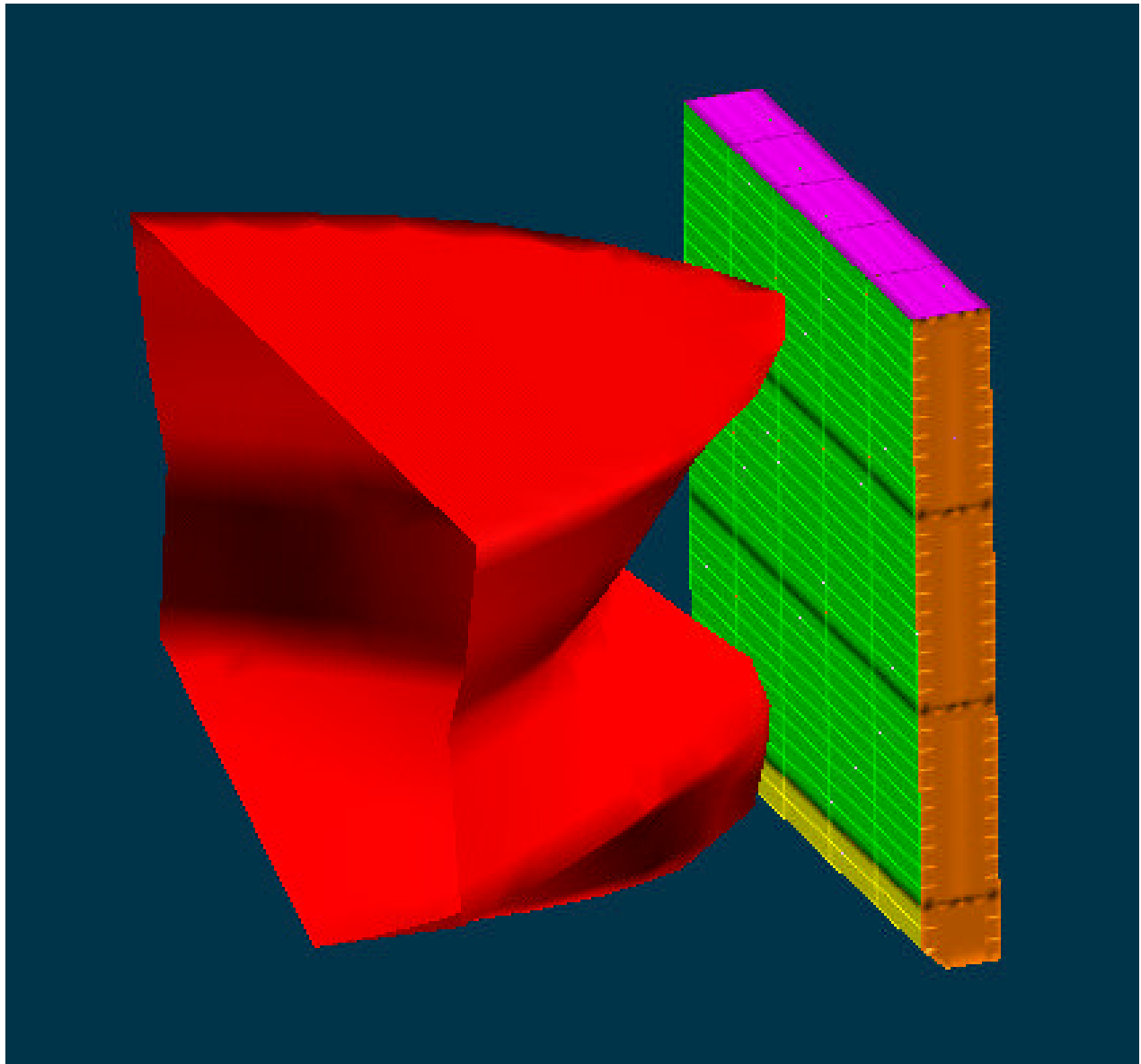


Figure 17 - Rigid Bow Collision with Double-Sided Test Section

Table 5 - Double-Sided Test Section Parameters

Global Dimensions	
Stringer Spacing	9 m
Double Bottom Height	3 m
Double Side Width	3.4m
Struck Section Depth	30 m
Struck Section Length	25 m
Web Spacing	5 m
Sideshell	
Thickness (3 m to 30 m)	20 mm
Stiffener Spacing (3 m to 30 m)	0.9 m
Stiffener Dimensions (3 m to 30 m)	T500,10,200,25
Innershell	
Thickness (0 m to 30 m)	16 mm
Stiffener Spacing (0 m to 3 m)	1 m
Stiffener Spacing (3 m to 30 m)	0.9 m
Stiffener Dimensions (0 m to 30 m)	T500,10,200,25 mm
Stringers and Deck	(3, 12, 21, 30 m)
Thickness	15 mm
Stiffener Spacing	0.875 m
Stiffener Dimensions	T250,10,100,15 mm
Bottom and Bilge Keel	
Thickness	21 mm
Stiffener Spacing	0.7 m
Stiffener Dimensions	600,25 mm
Webs	
Thickness	15 mm
Vertical Stiffener Spacing	1.7 m
Stiffener Dimensions	1000,20 mm

The traditional smearing method [56] provides equivalent tensile strength under longitudinal tension loading using area smearing. The equivalent plate (only) thickness,  $T_t$ , is calculated using Equation 3.1.

$$T_t = \frac{N_s \cdot (A_f + A_w) + A_p}{B} \quad (3.1)$$

$N_s$  is the number of stiffeners and  $A_f$ ,  $A_w$  and  $A_p$  are the stiffener flange, web and plate sectional areas, and  $B$  is the plate span.

Equivalent compressive strength smearing provides equivalent strength under a longitudinal compressive buckling loading. The equivalent compressive strength plate (only) thickness,  $T_c$ , is calculated using Equation 3.2.

$$T_c = b \cdot \sqrt{\frac{p^2}{3.62 \cdot (\frac{L}{r})^2}} \quad (3.2)$$

The variable  $b$  is the stiffener spacing,  $a$  is the plate length, and  $a/b$  is the plate slenderness parameter [85].

The equivalent membrane strength smearing provides equivalent strength under transverse tension (perpendicular to stiffener direction) loading. Because the stiffeners do not provide any support in the transverse direction of the plate, the equivalent membrane strength thickness,  $T_m$ , is equal to the original plate thickness  $T_p$ . Thus the equivalent membrane strength plate has the dimensions of  $a$  and  $B$  with a thickness of  $T_m$  or  $T_p$ .

The equivalent Moment of Inertia smearing is based on plates under an out of plane loading. To develop the equivalent inertial thickness,  $T_i$ , the moment of inertia for the stiffened plate is set equal to that of an equivalent non-stiffened plate and the thickness,  $T_i$ , is solved. Equation 3.3 provides the value of  $T_i$ .

$$T_i = \sqrt[3]{\frac{12 \cdot I_x}{b}} \quad (3.3)$$

Smearing test cases and a combination smearing case where the sideshell and innershell were tension-smearred and the remaining parts were membrane-smearred are summarized in Table 6. Figure 18 and Figure 19 compare absorbed energy vs. penetration results for each smearing method.

Table 6 - Smearing Test Case Nomenclature

Case	Smearing Method
C1	NO SMEARING (AS BUILT)
C2	EQUIVALENT TENSILE STRENGTH (AREA) SMEARING
C3	EQUIVALENT COMPRESSION STRENGTH SMEARING
C4	EQUIVALENT MEMBRANE STRENGTH SMEARING
C5	EQUIVALENT MOMENT OF INERTIA SMEARING
C6	COMBINATION SMEARING

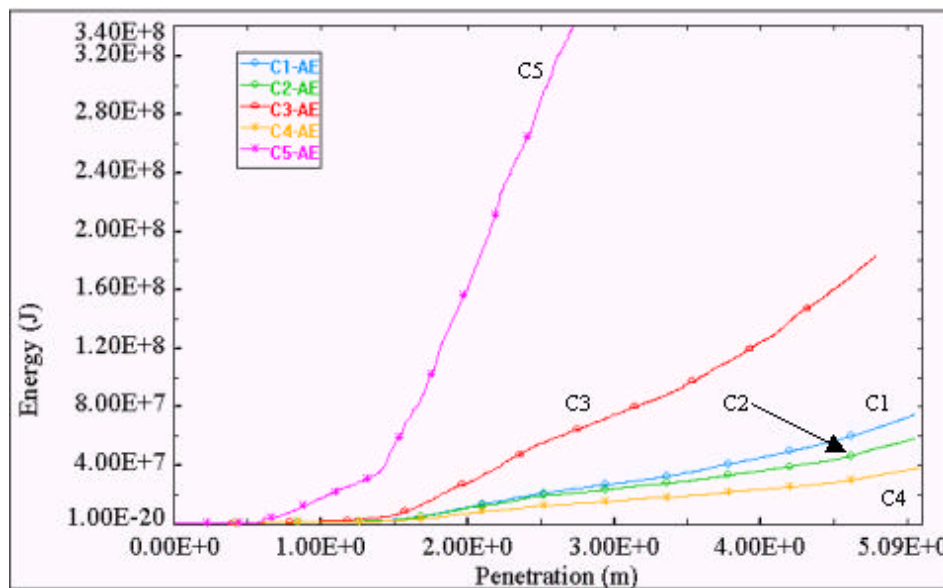


Figure 18 - Smearing Test Result Comparison of Energy vs. Penetration

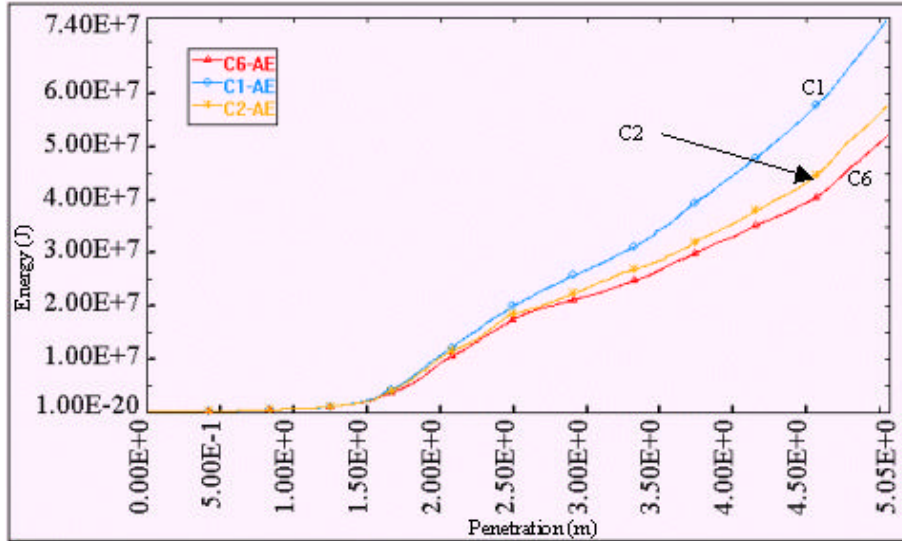


Figure 19 - Smearing Cases 1, 2 and 6 Result Comparison of Energy vs. Penetration

Comparison of smearing results to the unsmear detailed structural model results indicates the following:

- Compression and Moment of Inertia smearing (C3 and C5 respectively) provide too stiff a structure resulting in an under-prediction of penetration and over-prediction of absorbed energy.
- Tension and membrane smearing (Cases C2 and C4 respectively) under predict the energy absorbed and over predict the penetration.
- The average percent difference on penetration between C1 and C2 is less than one half of one percent. The average percent difference on Absorbed Energy between C1 and C2 is 22.00%. The variation in Absorbed Energy between C1 and C2 is due to the increase of Hourglass energy in C2 over C1 as shown in Figure 20 where the hourglass energy for C2 is approximately 27% higher than the hourglass energy at 0.3 seconds or 5.05 meters of penetration.

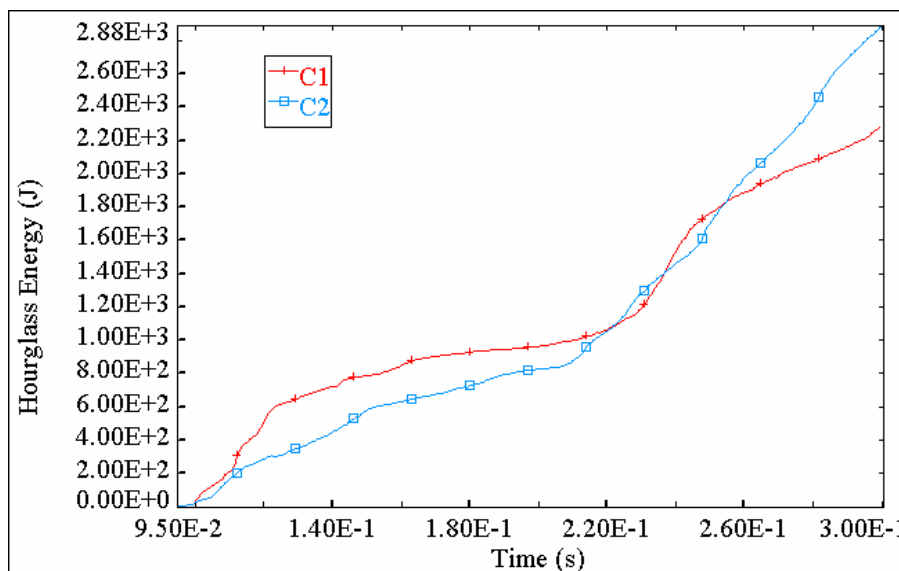


Figure 20 - Smearing Cases 1 and 2 Hourglass Energy vs. Time

Equivalent tension strength smearing provides the best method for modelling ship structures in collision compared to the other smearing methods considered. Tension strength smearing is used in all subsequent analysis.

### 3.6 External Dynamics and Constraints

An LSDYNA simulation is used to model both the internal structural response in collision and the external ship dynamics including hydrodynamics. To save CPU time, an inertia-equivalent method is used vice an explicit calculation of the fluid-structure interaction [58]. Masses and mass moments of inertia in surge, sway and yaw represent the virtual masses (actual plus added mass) for each ship. The masses of the striking ship outside of the bow section are assumed to be concentrated in three transverse section parts shown in Figure 11 in red. The masses of the bow parts are summed and the remaining mass is adjusted by assigning an appropriate mass density to the transverse section parts so that the total mass of the striking ship model is equivalent to the mass of the actual ship, plus its added mass in surge. The locations of the forward two transverse section masses are determined by matching the required added mass moment of inertia in yaw. A similar procedure is followed for the struck ship when the vessel is anchored, moored or still at the time of collision, where the model mass is equivalent to the mass of the actual ship plus the added mass in sway. When the struck ship has forward velocity at the time of the collision, the inertia-equivalent method begins to break down as the mass of the vessel may only be adjusted in the model for a single degree of freedom. To overcome this problem, an equivalent momentum method is applied to the struck ship.

The equivalent momentum method requires that the actual mass ( $M_a$ ) of the vessel times the actual forward velocity ( $V_a$ ) of the vessel is equal to the model mass ( $M_m$ ) times the model forward velocity ( $V_m$ ). Defining the model mass as equivalent to the actual mass of the vessel plus the added mass in sway, then the forward velocity of the struck ship model is calculated using Equation 3.4.

$$V_m = \frac{M_a}{M_m} V_a \quad (3.4)$$

Alternatively, an equivalent energy method may be used where:

$$V_m = \sqrt{\frac{M_a}{M_m} \cdot V_a^2} \quad (3.5)$$

The equivalent momentum method provides the best results based on comparison of method results to the validation case study discussed in Section 3.9.

Added mass values vary over the duration of the collision and depend on hull form [13]. For model simplicity, average added mass coefficients are used where:

$$\begin{aligned} a_{11} &= c_{11} m_s \\ a_{22} &= c_{22} m_s \\ a_{33} &= c_{33} I_{s33} \end{aligned} \quad (3.6)$$

Coefficients values used in this report are selected to standardize results when compared to other published model results, specifically Pedersen [14], Simonsen [10] and Paik [29]. Assumed added mass coefficients are 0.05 in surge ( $c_{11}$ ), 0.85 in sway ( $c_{22}$ ) and 0.21 in yaw ( $c_{33}$ ).

The motion of the striking ship is prevented in the 3, 4 and 5 directions (translation in the Z-axis, rotation around the X-axis and Y-axis or heave, pitch, and roll) by constraining the nodes in the collision bulkhead in these directions. These constraints allow the striking ship model to be very simple and provide for a faster FEA solution. The striking ship motions in heave, pitch, and roll are relatively small and less significant in a collision event as discussed in Chapter 2. The motions of the struck ship are also constrained in these directions, allowing only sway, surge and yaw by constraining the nodes in the boundary transverse bulkheads and beam elements in these directions. This effectively limits ship global motion to the horizontal plane, but allows the deformable sections a full six degrees of freedom.

### 3.7 LSDYNA Analysis Parameters

Other FEM parameters requiring particular consideration include: contact types, failure strain, strain rate dependency, friction and other material properties. A very coarse finite element mesh using primarily panel elements to save CPU time also requires close attention to hour-glassing.

Lemmen and Vredeveldt [59] also use LSDYNA to model full-scale collision tests. Their report identifies variable values that provide results consistent with their test results. Servis et. al. [60] and Naar [61] also provide some excellent general guidance. These are discussed in the following sections.

#### 3.7.1 Contact and Friction

For the ship-to-ship collision analysis the NODES\_TO\_SURFACE and SINGLE\_SURFACE contact types are used, allowing the master segments of the striking ship to penetrate into the struck ship, while ensuring deformation through the nodal requirement (i.e. compatibility). Figure 21 illustrates the nodal requirement where the red slave nodes are not allowed to penetrate through the blue master surface but must remain on the positive side (indicated by normal arrows) of the master segments.

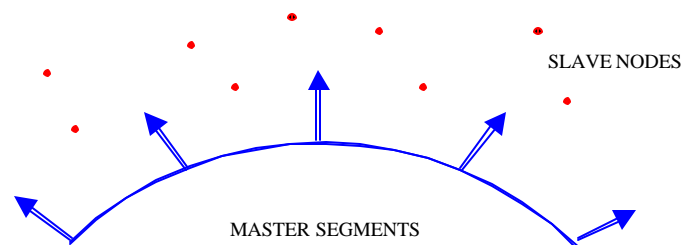


Figure 21 - Contact Nodal Requirement

In NODES\_TO\_SURFACE contacts, nodes in the struck ship are assigned as slave nodes and surfaces in the striking ship are defined as master segments. The contact interface does not allow the slave nodes to penetrate the master segments. If the striking ship is defined as master segments then the penetration of the striking ship into the struck ship may occur and both are enabled to deform. If however, the struck ship is defined as the master segments then the striking

ship cannot penetrate into the struck ship because slave nodes are not allowed to penetrate a master segment as defined by the compatibility requirement. Multiple NODES\_TO\_SURFACE contacts are defined in a single analysis.

Parts in the striking or struck ship are also defined as master segments over other parts in the same ship. As an example, the side shell is defined as a master surface while slave nodes define a web. Each contact is an independent interface such that a part defined by slave nodes in one contact interface may be defined by master segments in another contact interface.

In SINGLE\_SURFACE contacts, a part in the striking and/or struck ship acts as both master surface and slave nodes to itself. This contact ensures proper physical behavior when the side shell is peeled back and contacts itself. Again SINGLE\_SURFACE contact uses a similar approach as the NODES\_TO\_SURFACE contact where the part nodes are constrained to stay on the original side of the contact surface.

Care should be taken to ensure that all possible part-to-part contacts have been considered and accounted for as failure to properly define contacts where contacts exist will allow non-physical violations (i.e. striking ship passing through struck ship without resistance or deformation).

The correct consideration of friction in a ship-ship collision model is also important. As friction is increased the penetration of the striking ship into the struck ship is decreased or the absorbed energy per unit penetration is increased. Several considerations of friction and various static and dynamic friction coefficient values are reported in the literature. The most common value found in the literature for the dynamic friction coefficient is 0.3 [22,59,62,63,64,65]. Reported dynamic coefficients of friction vary from 0.0 to as high as 0.6 and static coefficients are reported at values between 0.5 and 0.8 [28,66,67,68,69]. Wisniewski et al [70] modeled collisions with a 40K dwt container ship striking a 105K dwt double hull crude oil carrier using ABAQUS-EXPLICIT. The dynamic coefficient of friction was varied from 0.0 to 0.6 in a parametric study. Plots of Wisniewski's results are provided in Figure 22 where it is shown that the higher the friction coefficient the faster the loss of kinetic energy of the striking ship. The difference between the friction curves for 0.3 and 0.6 is much smaller than between the curves for 0.0 and 0.3. As a result Wisniewski states, "The effect of friction will not increase significantly for larger values (greater than .6) of the coefficient."

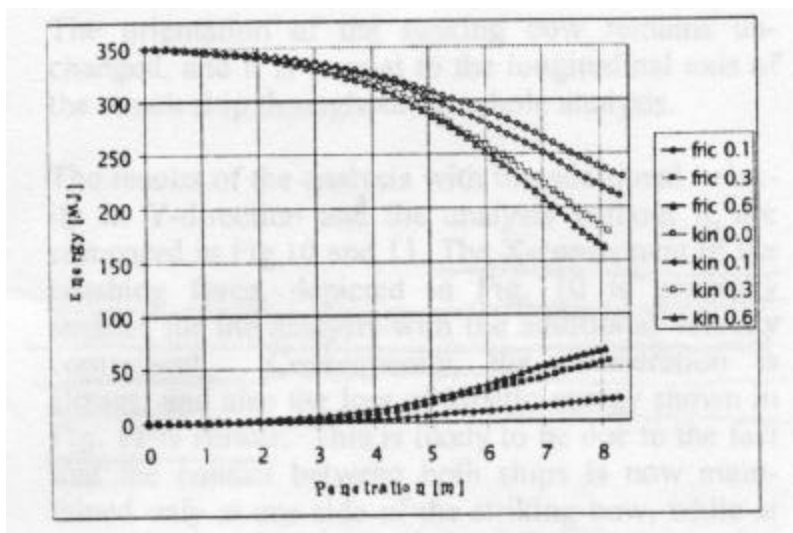


Figure 22 - Friction and Kinetic Energy vs. Penetration [70]

The friction model in LSDYNA is based on the Coulomb friction relation given by Equation 3.7.

$$\mathbf{m}_c = FD + (FS - FD)e^{-DC \cdot ABS(V_{rel})} \quad (3.7)$$

Where:

- $\mu_c$     coulomb friction coefficient
- FS**    static coefficient of friction for mild steel on steel
- FD**    dynamic coefficient of friction for mild steel on steel
- V<sub>rel</sub>**    relative velocity of contact surfaces
- DC**    exponential friction decay coefficient

The LSDYNA User's Manual [71] suggests a value of 0.74 for the static friction coefficient (FS) of dry mild steel on steel. An average value from the literature for FS of wet mild steel on steel is 0.7. The LSDYNA User's Manual suggests a value of 0.57 for the dynamic friction coefficient (FD) of dry mild steel on steel. An average value from the literature for FD is 0.3, for wetted, mild steel on steel. Figure 23 shows the Coulomb Friction value as a function of the change in relative velocity of the contact surfaces in meters per second with a DC value of 7.0. By increasing the value of DC the value of the relative velocity at which the steel on steel contact acts in a dynamic manner is decreased, i.e. the rate of change from the static friction coefficient to the dynamic is increased. Values selected for these coefficients in this report are FS = 0.7, FD = 0.3 and DC = 7.0.

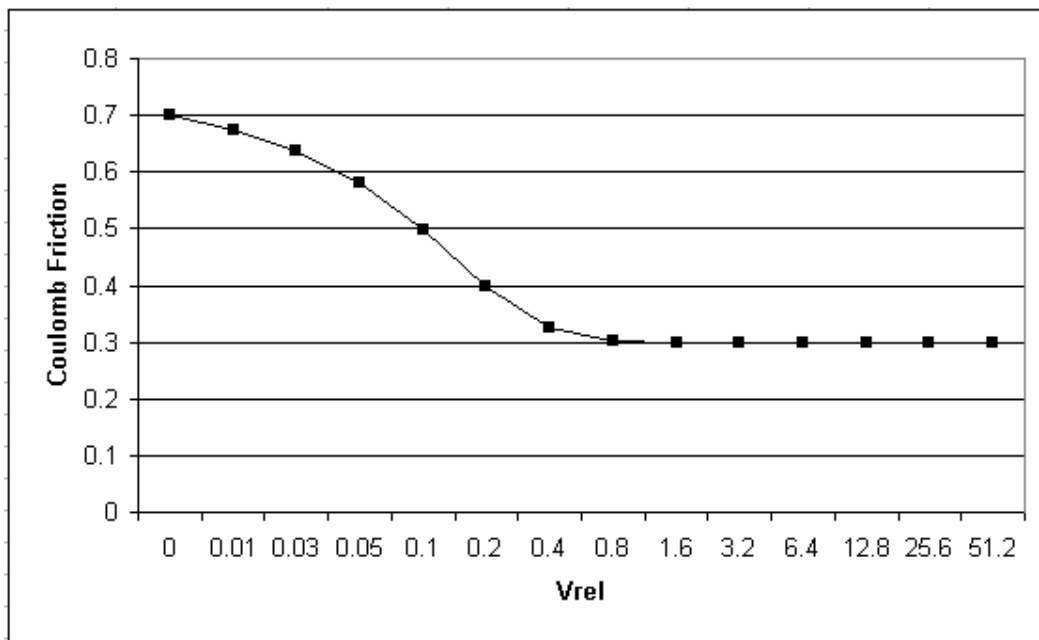


Figure 23 - Coulomb Friction vs. Relative Velocity of Contact Surfaces

### 3.7.2 Material Properties

Only three of many (nearly 100) material types available in LSDYNA were found to be suitable or necessary for ship collision analyses:

- Type 24 – Elastic/Plastic Isotropic with Piecewise Linear Plasticity – This material type allows strain rate effects and complete material fracture. All panels in the struck ship are modeled using LSDYNA Material Type 24. Material behavior is specified using the following parameters: Young’s modulus, yield stress, tangent modulus, failure strain and Cowper and Symonds strain rate parameters.
- Type 3 – Elastic/Plastic Isotropic with Kinematic Plastic Hardening - All transverse beams in the struck and striking ship and panels in the striking ship are modeled using LSDYNA Material Type 3. Material Type 3 is used in the striking ship because of the “No Fracture” behavior in its stress-strain curve shown in Figure 24. It was found that Master Elements modeled with Material Type 24 confuse the contact algorithm in the rare cases when these elements fracture. Model elements away from damaged areas must remain intact for model integrity. The use of Type 3 material avoids these problems.

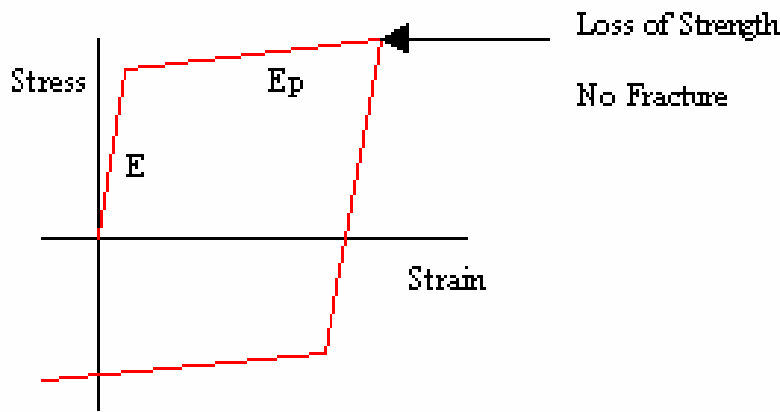


Figure 24 - Kinematic/Isotropic Elastic Plastic Material Stress Strain Curve

- Type 20 – Rigid – Material Type 20 is used in special model cases specifying a rigid bow. Rigid elements are bypassed in deformation processing and are very time efficient.

Parameter values for modeling ABS materials Grade B, AH32 and AH36 using Material Types 3 and 24 are listed in Table 7 and Table 8. Figure 25 shows the resulting stress versus strain curves for Type 3 and Type 24 Material at each grade.

Table 7 - Material Type 3 Definitions

<b>MATERIAL TYPE 3</b>				
NAME	(Material Name)	M3GB	M3GAH32	M3GAH36
TYPE	(Material Type)	3	3	3
MID	(Material Identification Number)	601	602	603
RO	(Material Density)	7.78E+03	7.83E+03	7.85E+03
E	(Material Modulus of Elasticity)	1.90E+11	2.00E+11	2.10E+11
PR	(Material Poissons Ratio)	0.281	0.292	0.303
SIGY	(Material Tension Yeild Stress)	2.35E+08	3.15E+08	3.55E+08
ETAN	(Material Tangent Modulus)	3.75E+09	3.05E+09	3.22E+09
BETA	(Material Hardening Parameter)	0	0	0
SRC	(Cowper-Symmonds Strain Rate Parameter C)	40.4	40.4	40.4
SRP	(Cowper-Symmonds Strain Rate Parameter P)	5	5	5
FS	(Material Failure Strain)	0	0	0
VP	(Material Formulation for rate effects)	0	0	0

Table 8 - Material Type 24 Definitions

<b>MATERIAL TYPE 24</b>				
NAME	(Material Name)	M24GB	M24GAH32	M24GAH36
TYPE	(Material Type)	24	24	24
MID	(Material Identification Number)	701	702	703
RO	(Material Density)	7.78E+03	7.83E+03	7.85E+03
E	(Material Modulus of Elasticity)	1.90E+11	2.00E+11	2.10E+11
PR	(Material Poissons Ratio)	0.281	0.292	0.303
SIGY	(Material Tension Yeild Stress)	2.35E+08	3.15E+08	3.55E+08
ETAN	(Material Tangent Modulus)	3.75E+09	3.05E+09	3.22E+09
FAIL	(Plastic Strain to Failure)	0.1	0.1	0.1
TDEL	(Minimum Time Step Size for Automatic Deletion)	0	0	0
C	(Cowper-Symmonds Strain Rate Parameter C)	40.4	40.4	40.4
P	(Cowper-Symmonds Strain Rate Parameter P)	5	5	5
LCSS	(Load Curve Identification Number for Effective Stress verses Plastic Strain)	0	0	0
LCSR	(Load Curve Identification Number for Strain Rate Scaling Effect on Yeild Stress)	0	0	0
VP	(Material Formulation for rate effects)	1	1	1
EPS1	(Effective Plastic Strain Value 1)	0	0	0
EPS2	(Effective Plastic Strain Value 2)	0	0	0
EPS3	(Effective Plastic Strain Value 3)	0	0	0
EPS4	(Effective Plastic Strain Value 4)	0	0	0
EPS5	(Effective Plastic Strain Value 5)	0	0	0
EPS6	(Effective Plastic Strain Value 6)	0	0	0
EPS7	(Effective Plastic Strain Value 7)	0	0	0
EPS8	(Effective Plastic Strain Value 8)	0	0	0
ES1	(Corresponding Yeild Stress Value to EPS1)	0	0	0
ES2	(Corresponding Yeild Stress Value to EPS2)	0	0	0
ES3	(Corresponding Yeild Stress Value to EPS3)	0	0	0
ES4	(Corresponding Yeild Stress Value to EPS4)	0	0	0
ES5	(Corresponding Yeild Stress Value to EPS5)	0	0	0
ES6	(Corresponding Yeild Stress Value to EPS6)	0	0	0
ES7	(Corresponding Yeild Stress Value to EPS7)	0	0	0
ES8	(Corresponding Yeild Stress Value to EPS8)	0	0	0

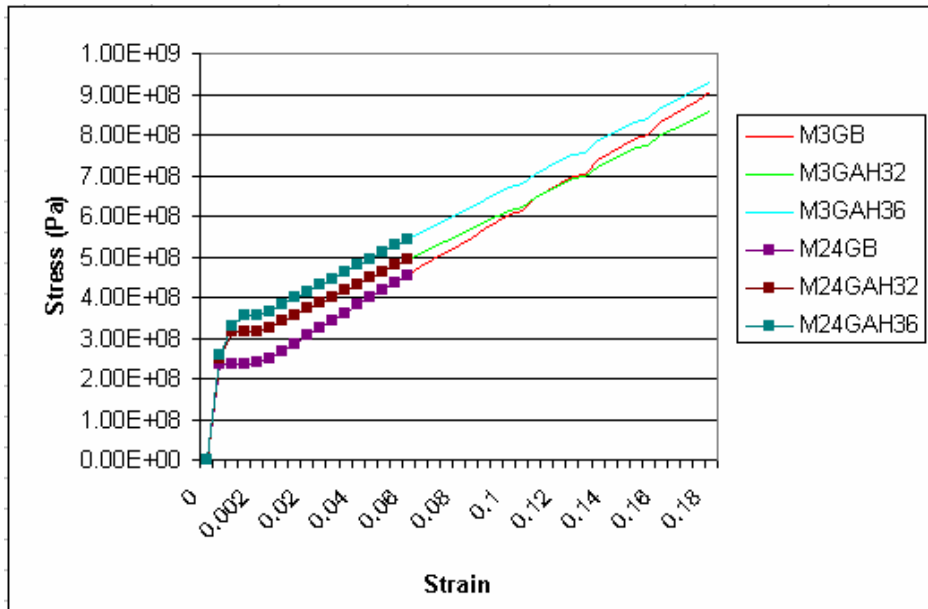


Figure 25 - Material Types 3 and 24 Stress/Strain Curves

### 3.7.3 Element Failure

The difficulty in material modeling in finite elements is the determination of the plastic strain at which the element fails, fractures or ruptures (effectively losing strength and the ability to maintain a stress loading). In this report, the point at which an element is no longer able to provide resistance to loading is referred to as failure. At failure, the element is eliminated from the analysis providing no further resistance to the global deformation.

Lemmen and Vredeveldt [59] used Material Type 24 as discussed in Section 3.7.2 and considered two element failure criteria: 1) criteria with bending (CB) - elements fail at specific integration points (stress then set to zero) when specific integration point equivalent plastic strain reaches the failure value - fails layer by layer; and 2) criteria with membrane strains only (CM) - stresses at all element integration points are set to zero when equivalent plastic strain reaches the failure value in the central layer – the element fails over its full thickness. CB was found to provide results more consistent with their tests and is used throughout this report. Figure 26 illustrates the differences between CB and CM.

Element failure strain has a significant effect on collision model results. A fundamental approach to determining its value is much preferred to the typical “model calibration” approach. This is discussed in the following section.

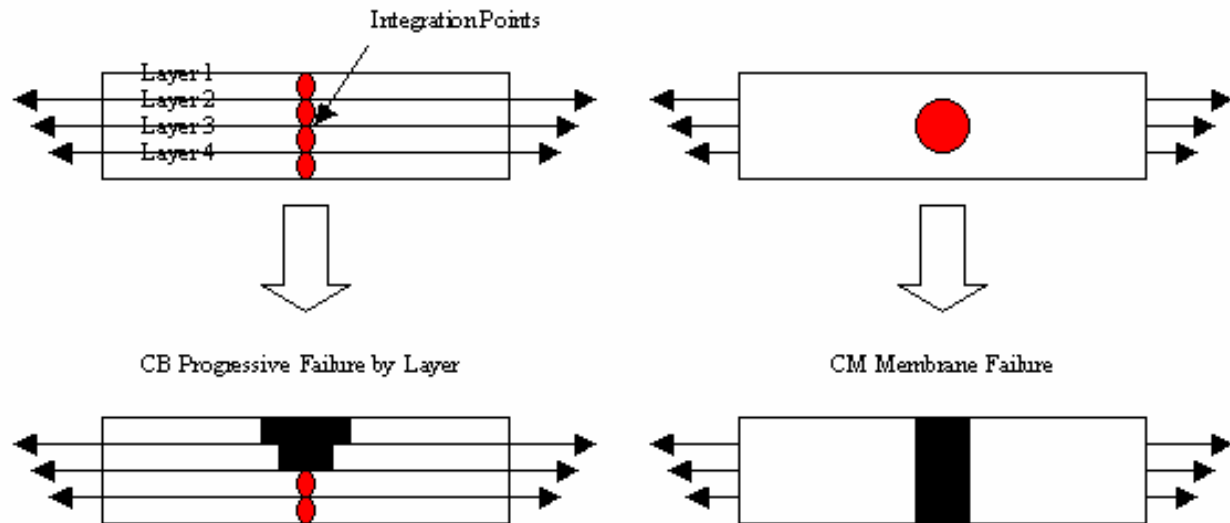


Figure 26 - Comparison of Element Failure Criteria CB and CM

#### 3.7.3.1 Determination of Failure Strain

Failure of a material may be either ductile or brittle. Ductile failure is defined as failure that occurs after significant material thinning and is illustrated Figure 27. Brittle failure is defined as failure that occurs without significant material thinning and is also shown in Figure 27.

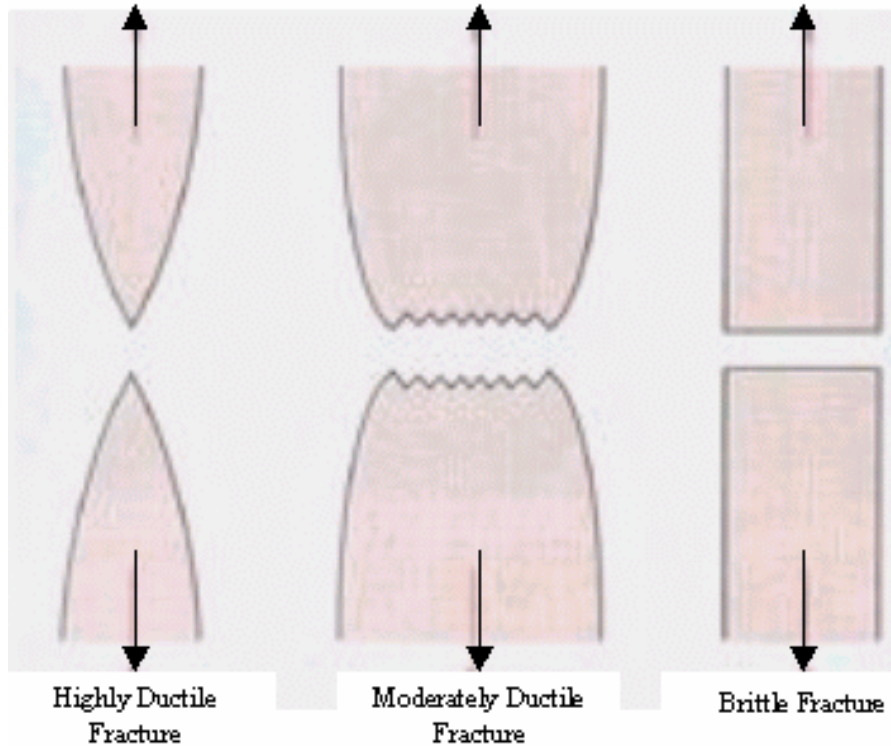


Figure 27 - Illustration of Ductile and Brittle Fractures

In ship-to-ship collisions either ductile or brittle failure may occur. The type of failure is dependant on many variables including temperature, loading, homogeneity, welds, and eccentricity. Because of the complexity of failure, most research has concentrated on the development of a single parameter value (failure strain) that accounts for both ductile and brittle fracture on a global scale (i.e. applicable to all material in a vessel).

Failure strain is the value of effective plastic strain at which a material fails and is based on the St. Venant theory of fracture mechanics [86]. Effective plastic strain  $E_{eff}^p$  is calculated using Equation 3.8 for each element, where  $E_p$  is the plastic strain rate given as the difference between the total strain rate and the elastic strain rate.

$$E_{eff}^p = \int_0^t \left( \frac{2}{3} \dot{E}_p \dot{E}_p \right) \cdot dt \quad (3.8)$$

In the initial phases of using the finite element method, the material failure strain as determined by static tension tests or their equivalent was used in the models. Various material tests performed to determine an appropriate FEA failure strain include the mild steel static tension tests performed by Naar et al [61] yielding a failure strain of 18%, and agreeing with the value of Lehmann et al [46]. Wisniewski et al [70] report a material failure strain of 17% for both mild steel and high tensile steel. Simonsen and Lauridsen [73] report a material failure strain of 19% determined via a tension test on mild steel. Kitamura [57] reports “a lot of material tests have shown that [failure strain] of ordinary mild steel is about 30%.” Finally, Servis et al [60] report a tested material failure strain for mild steel at 46.1%.

Comparison of finite element models to experiment shows that numerical failure strain (the value used in a FEA model) is a function of element size [29,57,59,60,61,69,72,73,74,75], and therefore is not purely a material property. Much research has been performed to determine the proper value of the failure strain. Agreement as to the proper value or relation has yet to be shown though it is generally agreed that the larger the element size the smaller the numerical failure strain value should be. Figure 28 shows a collection of reported failure strains verses element size as used by various authors [29,57,59,60,61,69,72,73,74,75].

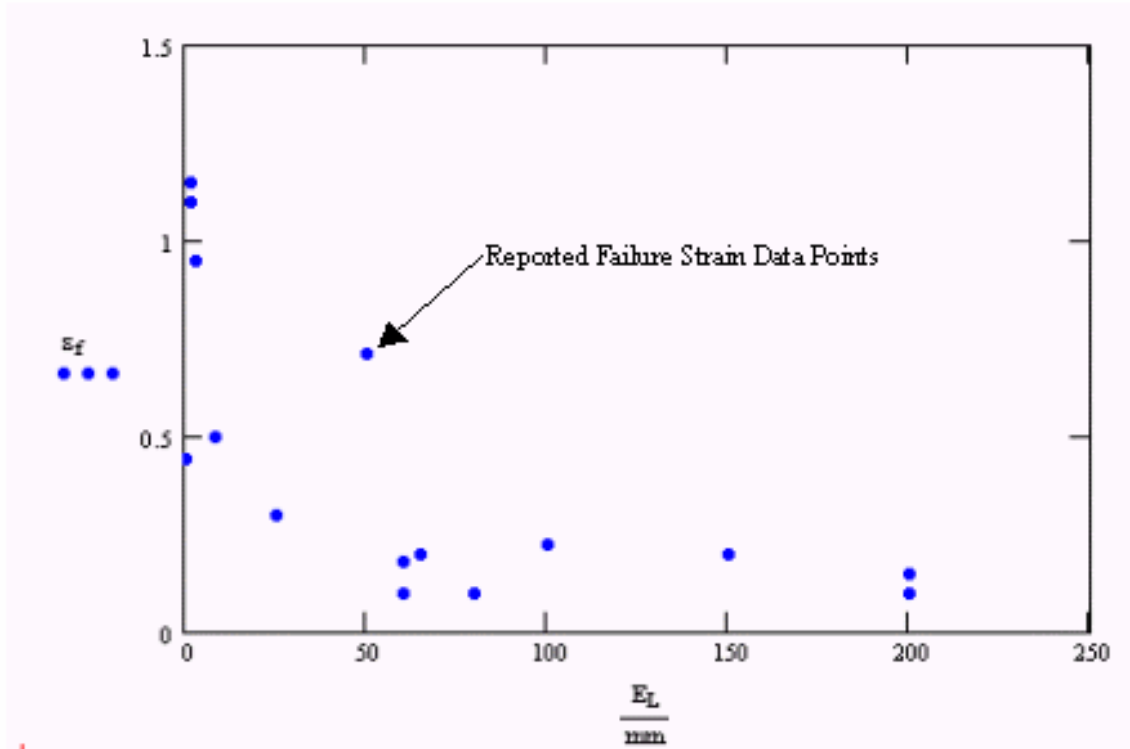


Figure 28 - Reported Failure Strains vs. Element Length Size [29,57,59,60,61,69,72,73,74,75]

Paik and Pederson [29] and Kitamura [57] explain that the lower values of failure strain are used with larger element sizes to numerically account for stress concentration factors such as cracks, corrosion and impact loadings etc... in the model that larger size elements do not properly capture. For this reason, the use of small material samples for the determination of the failure strain is invalid as small material samples do not provide a true representation of actual distributions of imperfections, stress concentrations or provide information as to an average stress state which occurs in larger elements. Paik and Pederson also state, “ship collisions are essentially dynamic problems and dynamic effects may not be neglected.” For this reason, the use of static or quasi-static experiments to validate the numerical failure strain to be used in a dynamic model is also invalid.

Kitamura [57] performed a series of dynamic drop tests and quasi-static penetrations where either scale models were struck repeatedly by a free falling rigid bow model of 8.44 tons or slowly indented by the same rigid bow. Modeling these tests by finite elements, a relation as shown in Figure 29 for failure strain verses average element edge length was determined. However it is unclear whether this relation was developed based on the dynamic tests or the quasi-static.

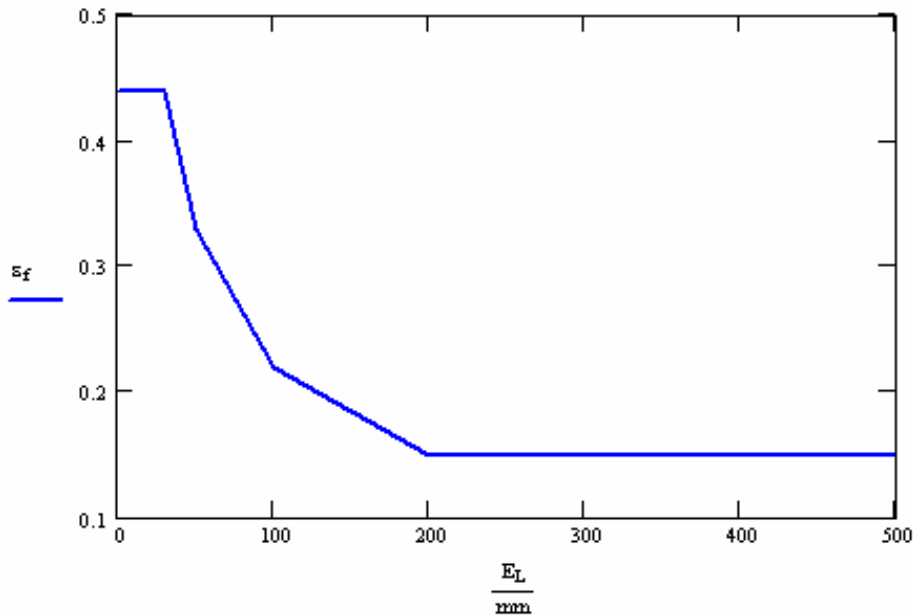


Figure 29 Kitamura Necessary Failure Strain Results [57]

To further examine the relationship between the element edge length and the numerical failure strain while incorporating strain rate effects, a solely dynamic yet simplified test is desired. The simplest dynamic test to which a finite element model is easily implemented with little computational and modeling effort is the Charpy-V-Notch (CVN) test which measures the total material absorbed energy (Charpy energy) prior to fracture. The disadvantage of using the CVN test is that the material sample is small and the distributions of imperfections; stress concentrations or average stress state is not considered.

The Charpy energy, often called the impact energy, is determined by impacting a material sample using a pendulum device as shown in Figure 30. A Pendulum of a known mass is released from a known height and allowed to swing into the material sample located at the bottom of the pendulum's arc. The absorbed energy is calculated by measuring the height to which the pendulum swings after the impact.

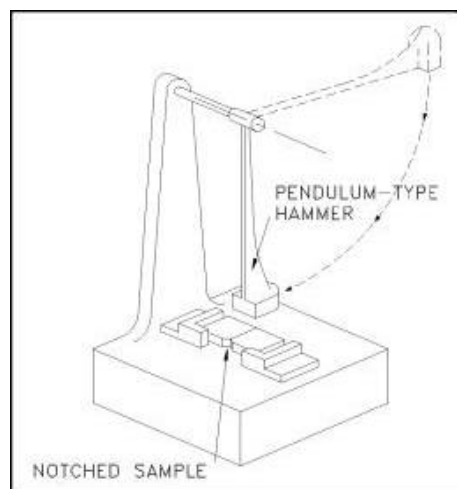


Figure 30 - Charpy-V-Notch (CVN) Test

The standard size of a CVN test specimen is set by ASTM E23 and has dimensions as shown in Figure 31. The long dimension of the sample (55-mm) is cut parallel to the rolling direction of the steel.

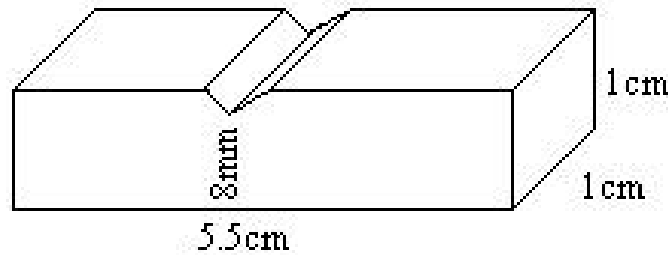


Figure 31 - Charpy-V-Notch (CVN) Sample Dimension

CVN impact tests conducted on ABS GR. B materials at various temperatures by Francis, Cook and Nagy as reported in SSC Report 276 [76] yield an impact energy versus temperature plot (Figure 32) where the transition from brittle to ductile behavior of the material occurs at 0 degrees Fahrenheit and the upper shelf impact energy (absorbed energy in full ductile behavior range) is approximately 57 ft-lb (77 Joules). However, the CVN test is not the most accurate measure of the energy required to fracture a material sample. A large statistical error is present in most tests, and reproducibility is a common problem between facilities. (SSC Report no. 235 [77] reports a CVN upper-shelf impact energy of 112 ft-lb for the ABS GR. B material.)

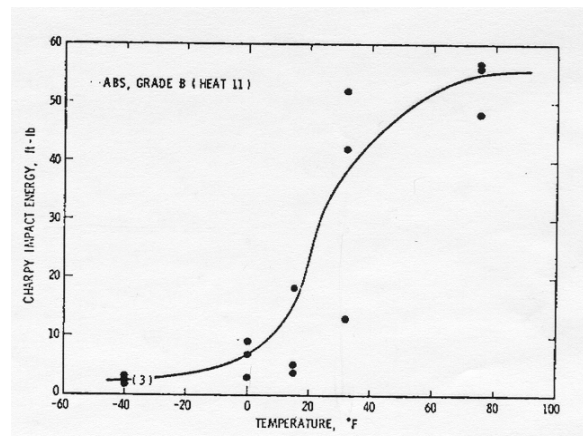


Figure 32 - Sample Charpy Test Data of ABS Grade B Steel [76]

Although statistically abhorrent with a low number of samples, the CVN test is still a very affordable way to determine a statistical impact energy for a specified material and temperature, and is still used by many steel manufacturer's and ship building firms to classify the reliability of specific materials for designed tasks such as ice-breaking, cold-weather transport, and recently collision survivability and damage prediction.

To correlate the FEM to the CVN test data, FEA absorbed energy is compared to the absorbed energy from the actual material (ABS GR. B) at an average service temperature of 60°F. The finite element model of the CVN test specimen consists of a flat plate comprised of varying number of elements and fixed on either end with a constant width of 10 mm and length of 55 mm (an example model shown in Figure 33). This model is developed for application to deck fracture, and uses the Belytschko-Tsay shell element vice a solid element formulation. The shell element is used in the global ship-to-ship finite element model. The use of the shell element in

this case is valid because the stresses developed in the model are all planar and do not vary through the thickness.

The finite element model of the pendulum impactor is modeled by a rigid structure matching the dimensions as specified by ASTM E23. The test specimen is modeled having the material properties of ABS Grade B mild steel as provided in Table 8, where the plastic strain to failure (failure strain) is varied.

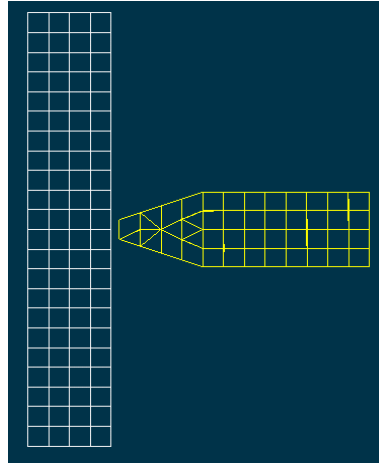


Figure 33 - CVN FEM Mesh

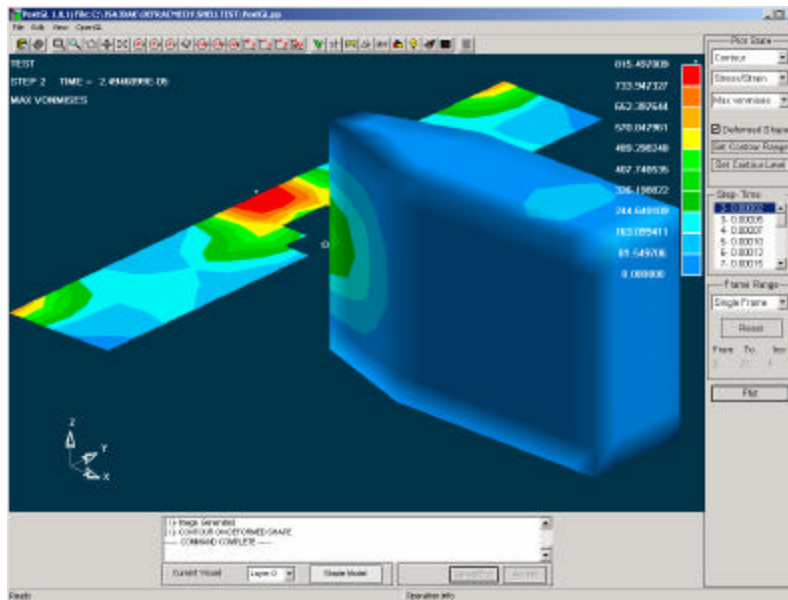


Figure 34 - CVN FEM Analysis

Figure 34 shows that the material sample does not have a uniform planar state of stress and supports the conclusions that the failure strain is not a pure material property but is sensitive to the test configuration and geometry in finite element analysis.

The average computational time on a standard Pentium III Desktop computer for the CVN model was under a minute. After several variations of failure strain (FS), element thickness ( $t$ ) and average element edge length ( $L$ ) the absorbed energy (AE) was found to be a function of  $t$ ,  $L$ , element type and material properties. By maintaining constant element type (Belytschko-Tsay

shell element) and all material properties except failure strain, the absorbed energy is a function of  $t$ ,  $L$  and  $FS$  only. Noting that the absorbed energy is a linear function of element thickness as shown by Figure 35 the effects of element thickness may be eliminated such that the dimensional parameter  $AE/t$  becomes only a function of the dimensionless parameters  $L/t$  and  $FS$  as in Equation 3.9.

$$AE/t = F(L/t, FS) \tag{3.9}$$

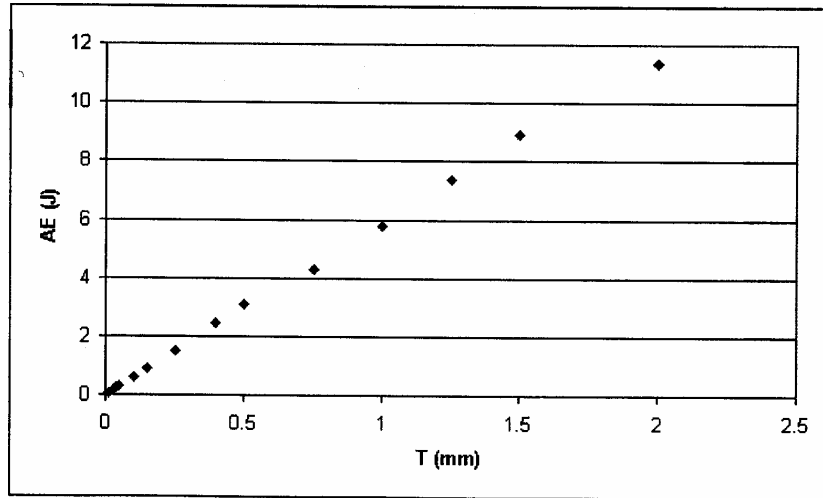


Figure 35 - FEA Charpy Energy vs. Sample Thickness

Maintaining a constant failure strain of 5% (for simplicity) and varying the average element edge length and thickness of the elements in the test specimen, numerical convergence of the  $AE/t$  parameter is shown to occur in Figure 36 for  $L/t$  ratios greater than 2.5.

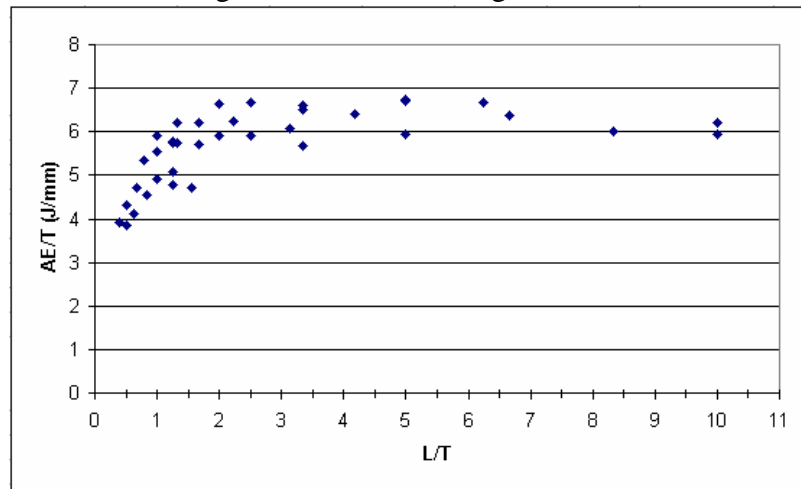


Figure 36 - FEA Charpy Energy vs. L/T Ratio

Thus, the functional dependence of the absorbed energy on  $L$  of elements whose average element edge length is greater than 2.5 times the element thickness may be neglected. At some  $L/T$  ratio much greater than 2.5 the element size will not capture the physics of the material sample used in the CVN test and this approximation method will break down. Therefore, as long as the above conditions are true,  $L/t = 2.5$  and  $L/t$  not  $\gg 2.5$ , then the absorbed energy is only a function of the failure strain and the element thickness as in Equation 3.10.

$$AE = F(FS) \text{ if } L/t=2.5 \text{ and not } \gg 2.5 \quad (3.10)$$

Examination of the effect of failure strain on the absorbed energy in the Charpy-V-Notch model, for the ABS GR. B material shows that the absorbed energy is linearly related to the failure strain (Figure 37), where AE is the absorbed energy in Joules divided by 10 and FS is the failure strain).

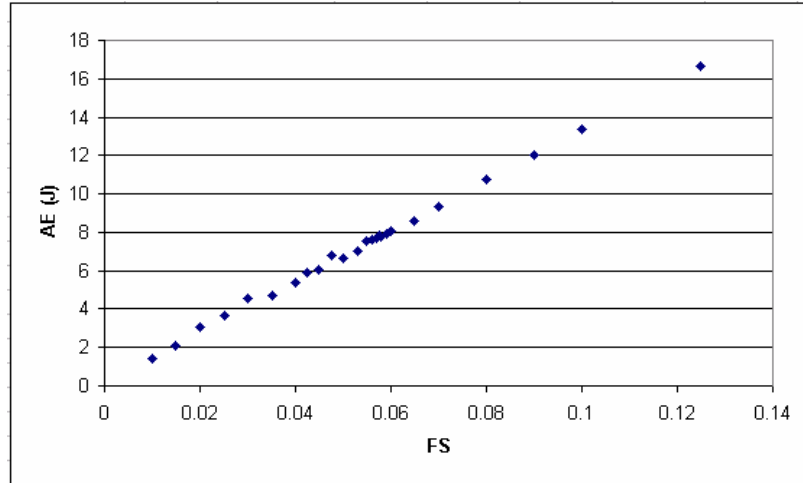


Figure 37 - FEA Charpy Energy (divided by 10) vs. Failure Strain (FS)

By matching the average of reported Charpy energy for mild steel at 60°F [76,77] to Figure 37 where the thickness of both test specimens (numerical and actual) is equal to 10 mm, the numerical failure strain to properly model ABS Gr. B mild steel using Belytchko-tsay elements with material model and properties as given by Table 8 and Figure 25 is approximately 10% (between 6 and 14% to match the actual material test values of [76 and 77]), as long as the  $L/t = 2.5$  condition is met. For ship-to-ship collision analysis a failure strain of 10% will therefore be used for most analyses.

### 3.7.4 Strain Rate

The Cowper and Symonds strain rate model accounts for the effect of strain rate on yield strength. Lemmen and Vredeveldt [59] found this model to give good results. The influence of material inertia forces was found to be negligible, i.e. other than the effect of strain rate, material properties are not sensitive to velocity.

The Cowper-Symonds constitutive equation, Equation 3.11, is widely used and has been found adequate for many theoretical and numerical calculations [29]:

$$s_D = s_y [1 + (\frac{e_r}{C})]^{\frac{1}{P}} \quad (3.11)$$

Where:

$s_D$  dynamic yield stress

$s_y$  material static yield stress

$e_r$  plastic strain rate when the LSDYNA viscous-plasticity option flag is set at 1

$C, P$  material constants

The plastic strain rate,  $e_r$ , is calculated using Equation 3.12. The material properties C and P are most often taken as  $40.4 \text{ sec}^{-1}$  and 5.0 respectively for mild steel [28,29,72]. Paik et al. [28] used C equal to  $3200 \text{ sec}^{-1}$  and P equal to 5.0 for high tensile steel materials based on unidentified test data. These values of C and P for mild steel and high strength steel are used in the collision analysis presented here. Ship to ship collision strain rates in this project reach maximum values of approximately  $0.1 \text{ sec}^{-1}$ . These result in a dynamic yield stress that is 1.3 times the static yield stress in mild steel and can have a significant effect on the results.

$$e_r = \frac{\Delta e_p}{\Delta t} \quad (3.12)$$

Where:

$\Delta e_p$  is the change in plastic strain;

$\Delta t$  is the time step.

### 3.8 Typical Results

Numerical results for the LSDYNA collision simulation runs are provided and discussed in Section 3.9. Figure 38 shows typical upper bow deformation consistent with the photographs in Figure 8. Figure 39 through Figure 41 show typical shell damage results predicted by the model. Figure 42 through Figure 44 show bow penetration into the double side with damage to adjacent webs.

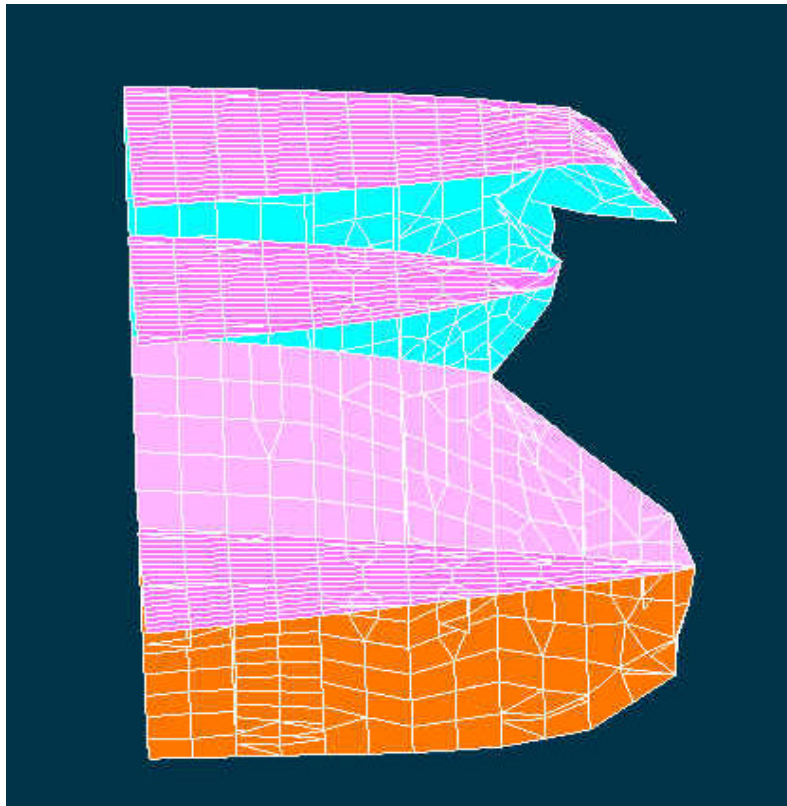


Figure 38 - Folding-Down Upper Bow of Conventional Bow Model

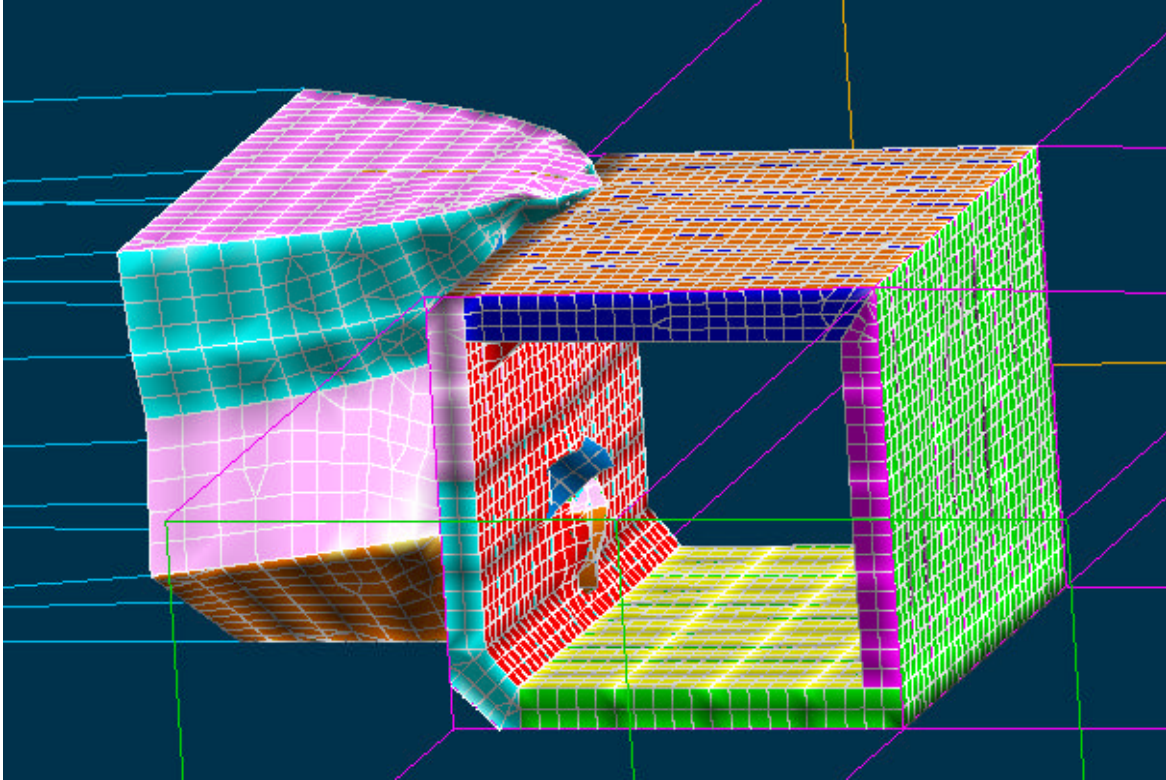


Figure 39 - Ship to Ship Collision Simulation

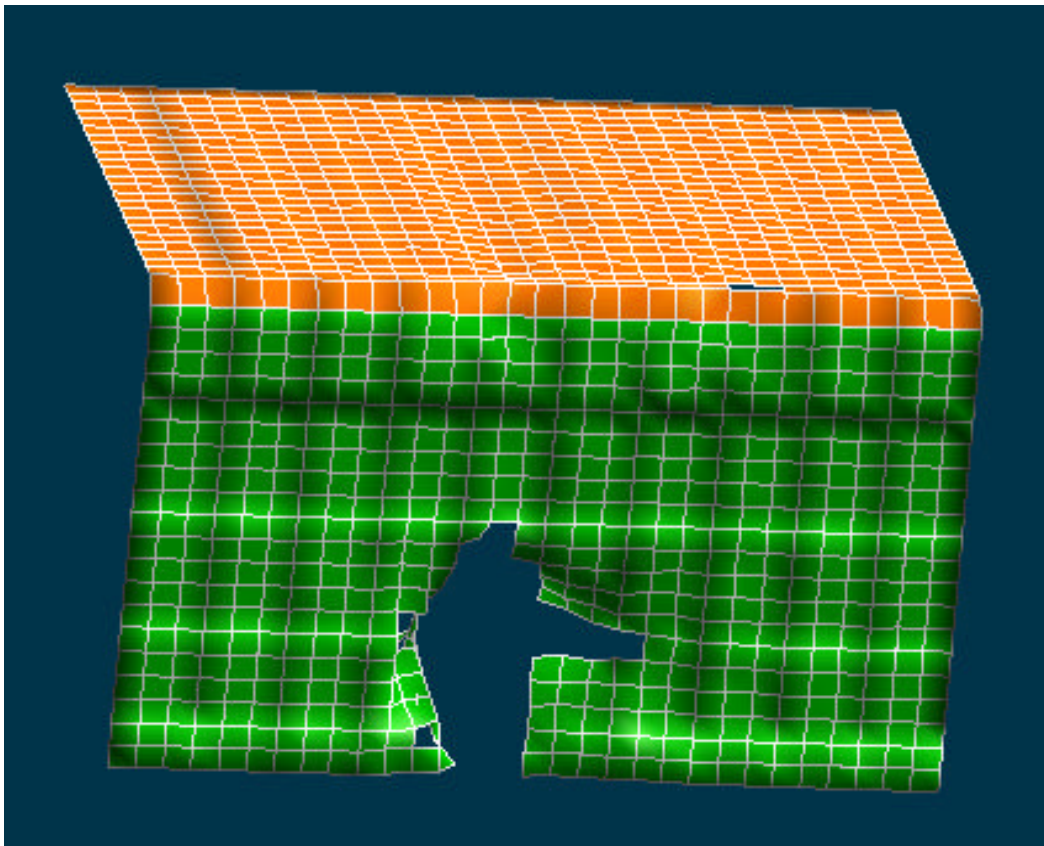


Figure 40 - Damaged Outer Shell and Deck for Double Hull Tanker

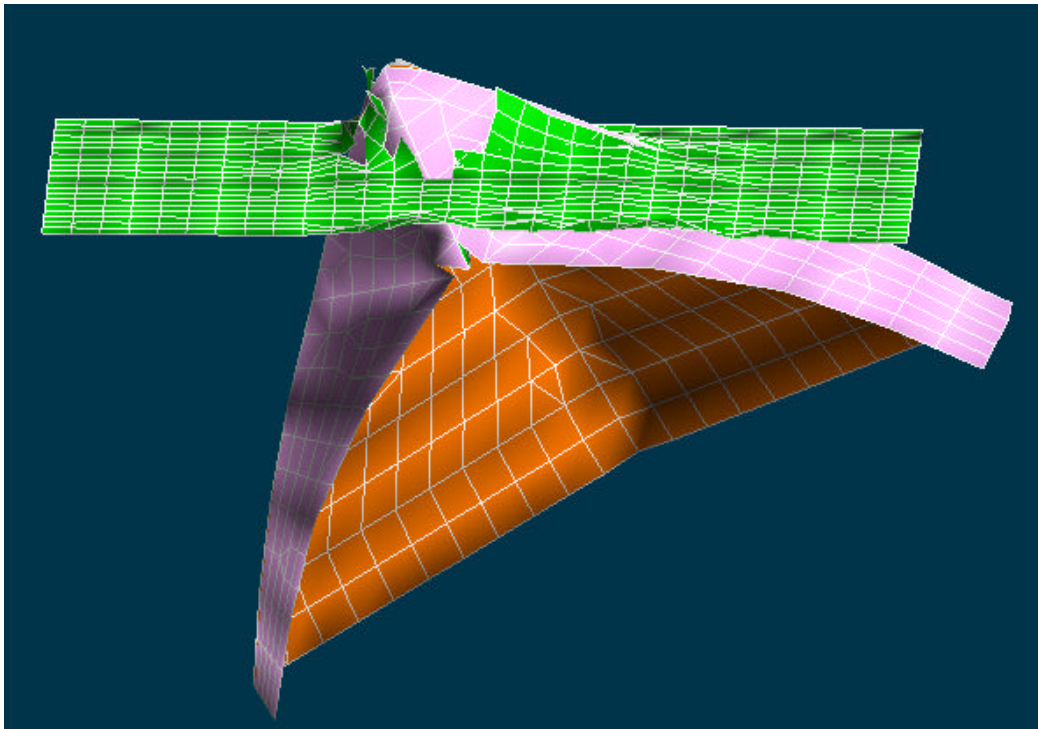


Figure 41 - Bulb of Striking Ship Penetrating Outer Shell of Struck Ship

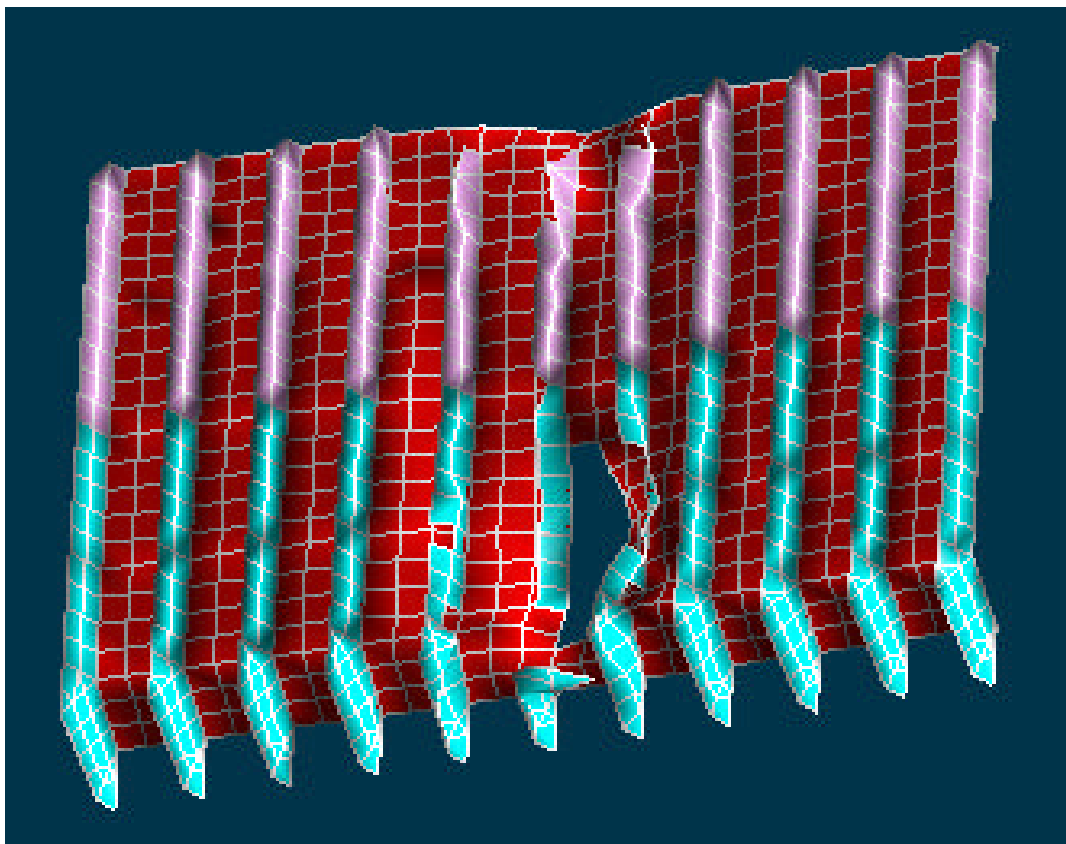


Figure 42 - Damaged Web and Shell of DH150

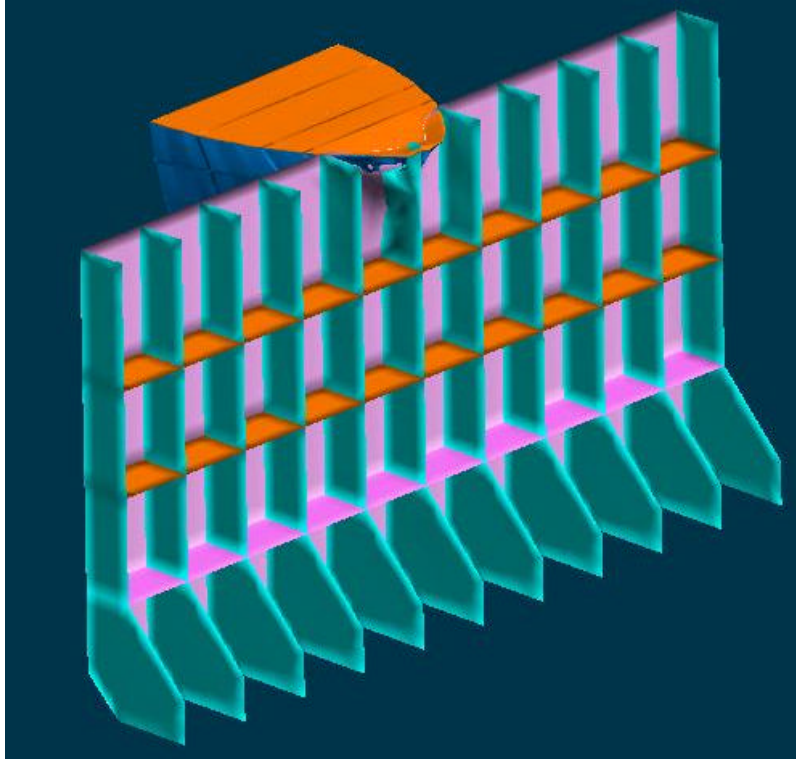


Figure 43 - Damaged Web and Shell of DH150

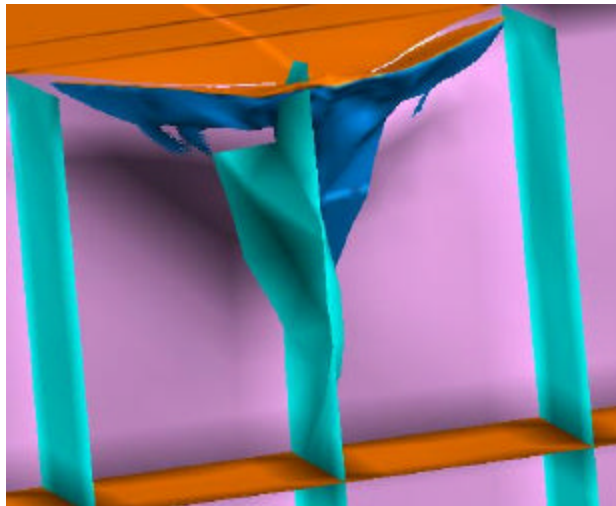


Figure 44 - Damaged Web and Shell of DH150

### 3.9 Calibration

The LSDYNA methodology presented above is calibrated (time step, damping factors and analysis control parameters adjusted) using a real collision case described by Minorsky's [9] original collision data, and additional data and drawings obtained at the National Archives. This was the only near-complete set of data found after nearly two years of search. The calibration case is the collision between the David E. Day and the Marine Flier [84] in the Pacific Ocean on May 17, 1952.

### 3.9.1 David E. Day - Marine Flier Collision

On May 17, 1952 the C4 cargo vessel “Marine Flier” struck the T2 tanker “David E. Day” at a reported 55-degree collision angle between frames 59 and 62 of the David E. Day, approximately 9 meters forward of amidships. The reported vessel speeds at the time of the collision were 16.3 knots for the David E. Day and 16.5 knots for the Marine Flier causing a reported 17 ft of penetration and 35 ft of damage length. However, extensive examination of documents related to the collision revealed that the actual speeds of the Marine Flier and David E. Day at the time of the collision were closer to 5 to 7 knots and the collision angle was in actuality between 50 and 55 degrees. In part these changes were due to last minute “Full Astern” and “Hard Right Rudder” orders given by the masters of each vessel in an effort to avoid the collision.

Structural drawings for both ships were obtained through the National Archives and Records Administration and specific data was used in the LSDYNA FEM model shown in Figure 45. Appendix C provides information on the “Marine Flier” and Appendix F provides information on the “David E. Day”. The collision angle used in the simulation is 51 degrees with a collision location of 10 meters forward of amidships. The initial striking vessel speed is 5.5 knots, and the struck vessel speed is 7 knots. The FEM results are 5.09 meters or 16.7 ft of penetration, and 10 meters or 32.8 ft of damage length. The FEM results are non-conservative by approximately 1.8% in penetration and 6.3% in damage length compared to Minorsky’s [9] reported penetration and damage length values.

Figure 46 through Figure 68 provide a visual record of the David E. Day – Marine Flier collision at half-second intervals until the end of the collision event occurring at 4 seconds. The sustained damage in the finite element analysis is similar to the description of the damage reported in [84].

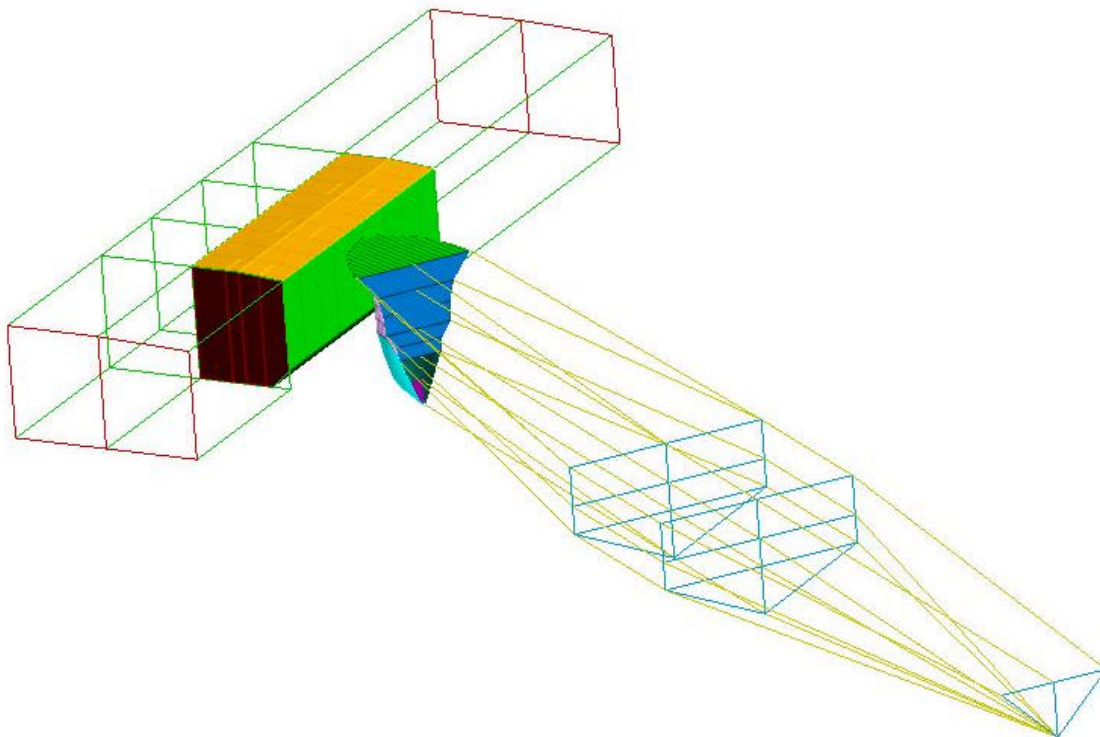


Figure 45 - David E. Day - Marine Flier Collision Analysis FEA Model

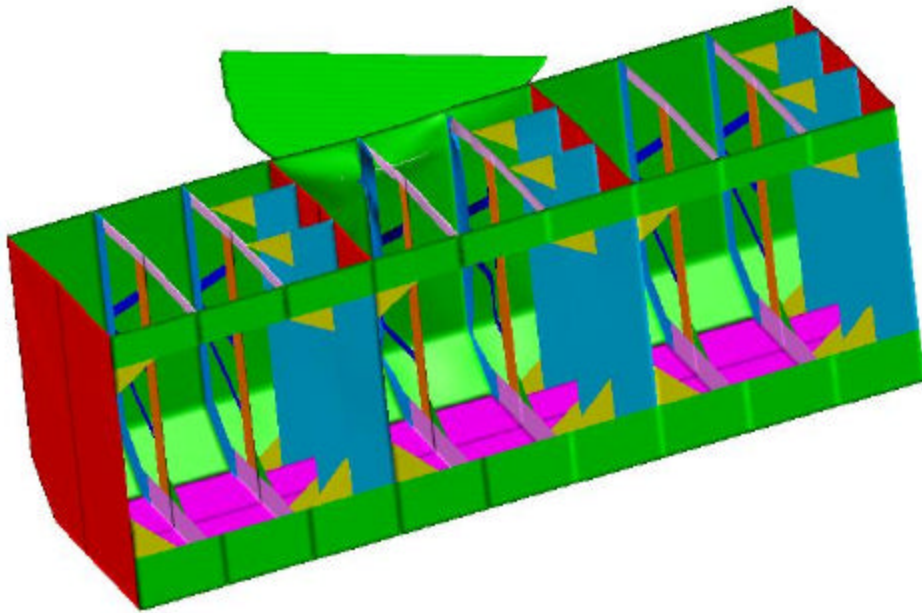


Figure 46 - David E. Day Marine Flier FEA Damage at 0.5 Seconds

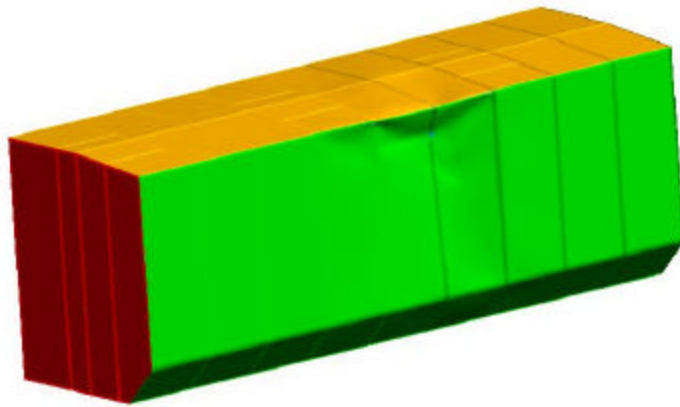


Figure 47 - David E. Day FEA Hull Damage at 0.5 Seconds

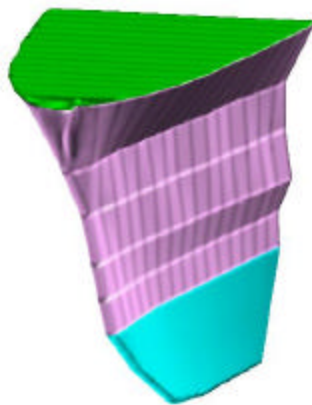


Figure 48 - Marine Flier FEA Bow Damage at 0.5 Seconds

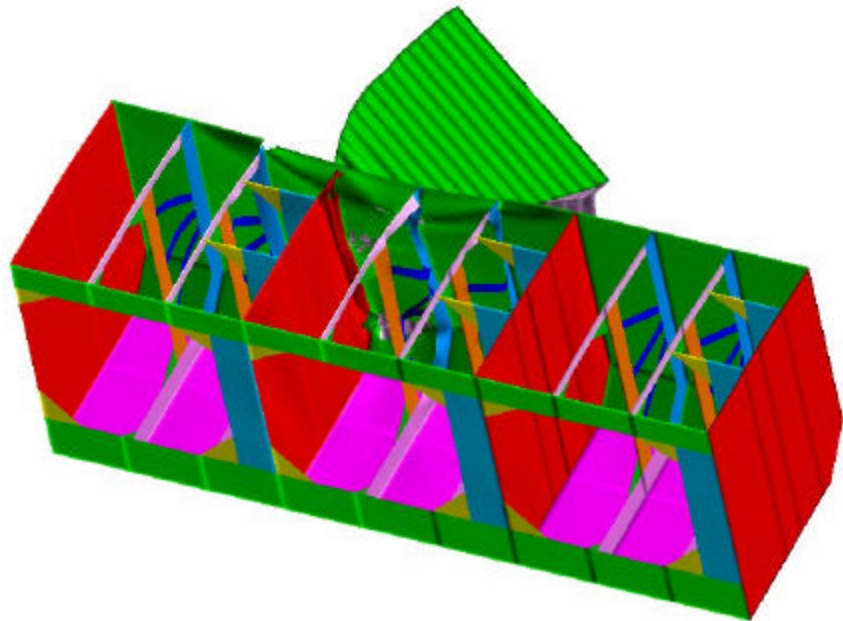


Figure 49 - David E. Day - Marine Flier Damage at 1.0 Seconds

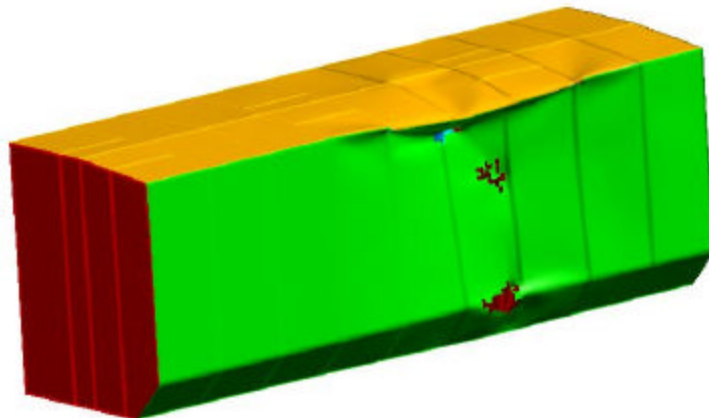


Figure 50 - David E. Day FEA Hull Damage at 1.0 Seconds

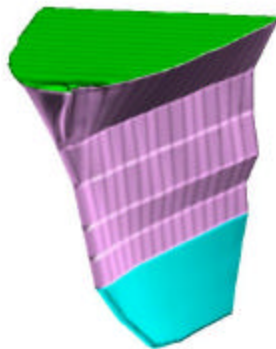


Figure 51 - Marine Flier FEA Bow Damage at 1.0 Seconds

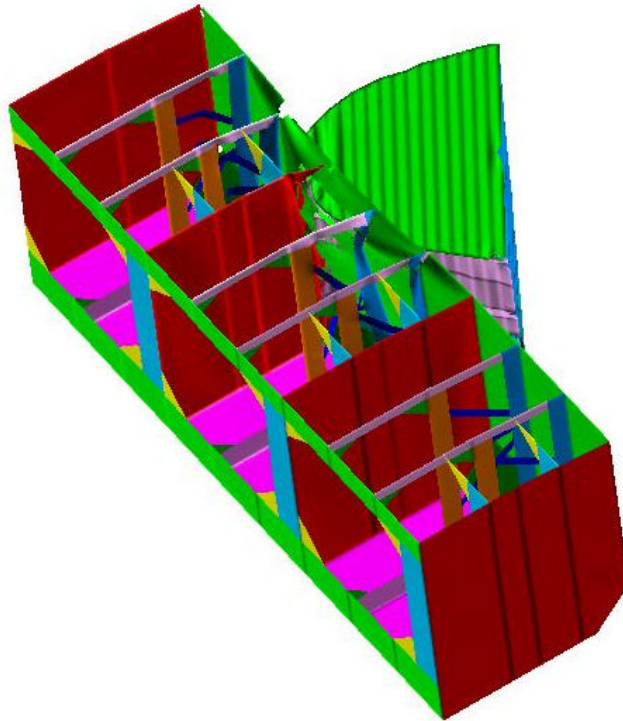


Figure 52 - David E. Day - Marine Flier FEA Damage at 1.5 Seconds

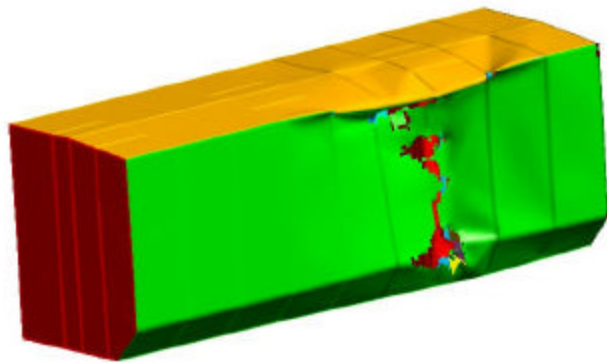


Figure 53 - David E. Day FEA Hull Damage at 1.5 Seconds

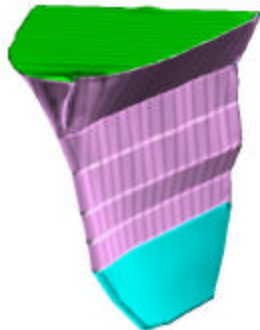


Figure 54 - Marine Flier FEA Bow Damage at 1.5 Seconds

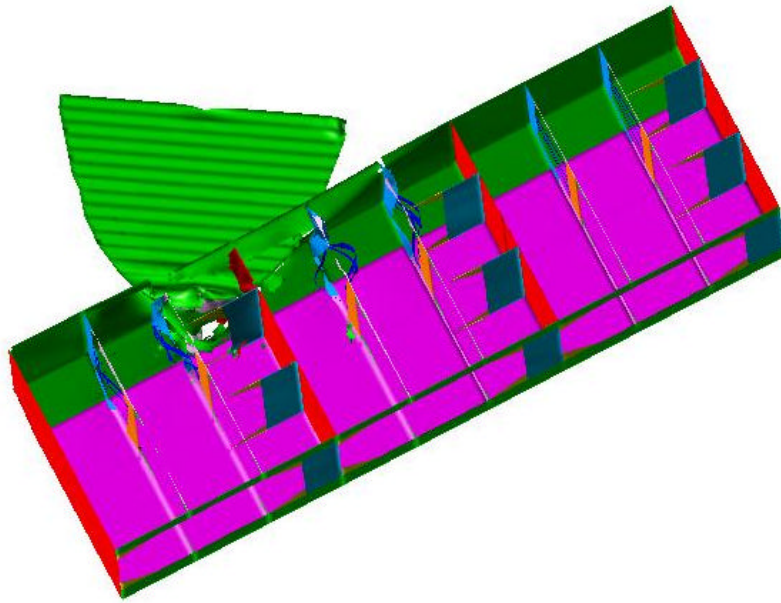


Figure 55 - David E. Day - Marine Flier FEA Damage at 2.0 seconds

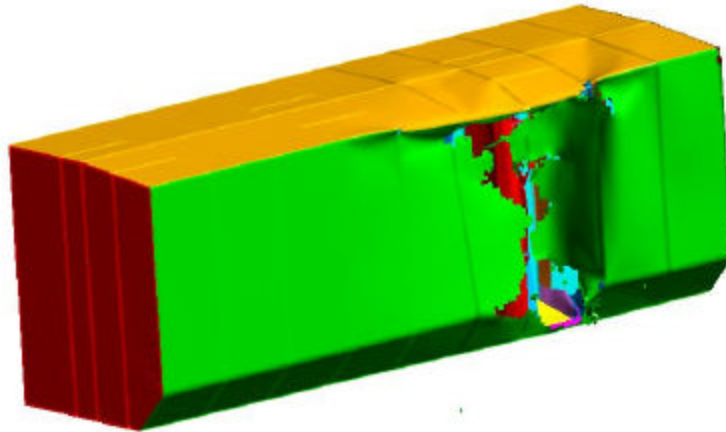


Figure 56 - David E. Day FEA Hull Damage at 2.0 seconds

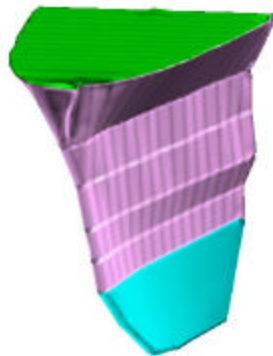


Figure 57 - Marine Flier FEA Bow Damage at 2.0 Seconds

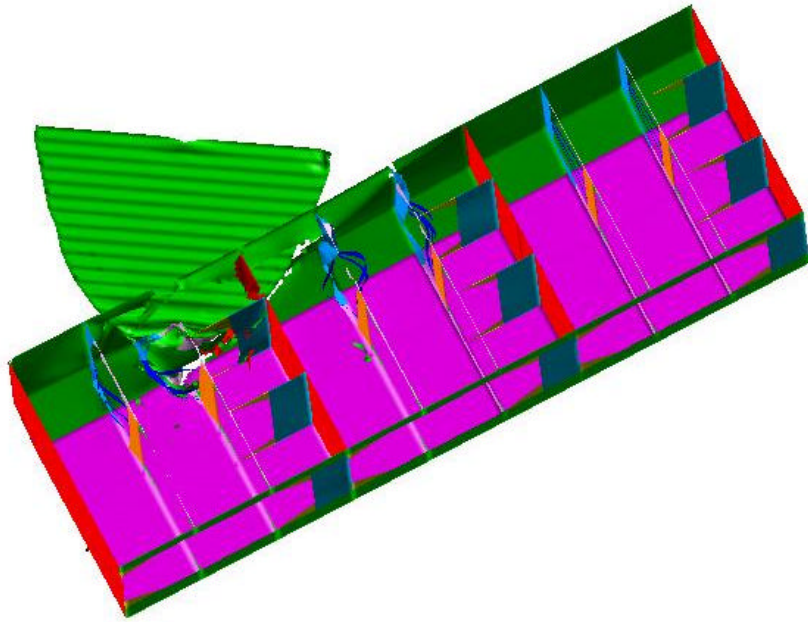


Figure 58 - David E. Day - Marine Flier FEA Damage at 2.5 Seconds

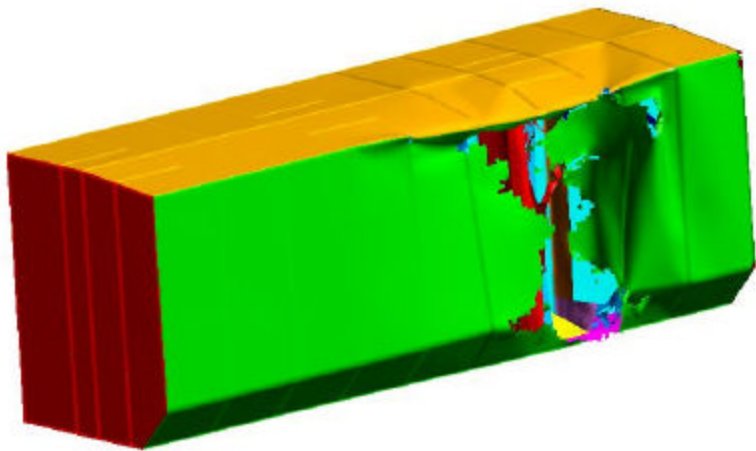


Figure 59 - David E. Day FEA Hull Damage at 2.5 Seconds

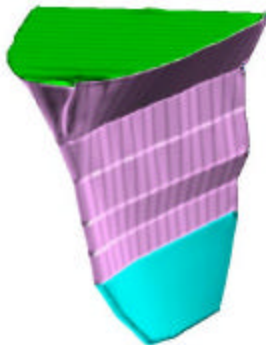


Figure 60 - Marine Flier FEA Bow Damage at 2.5 Seconds

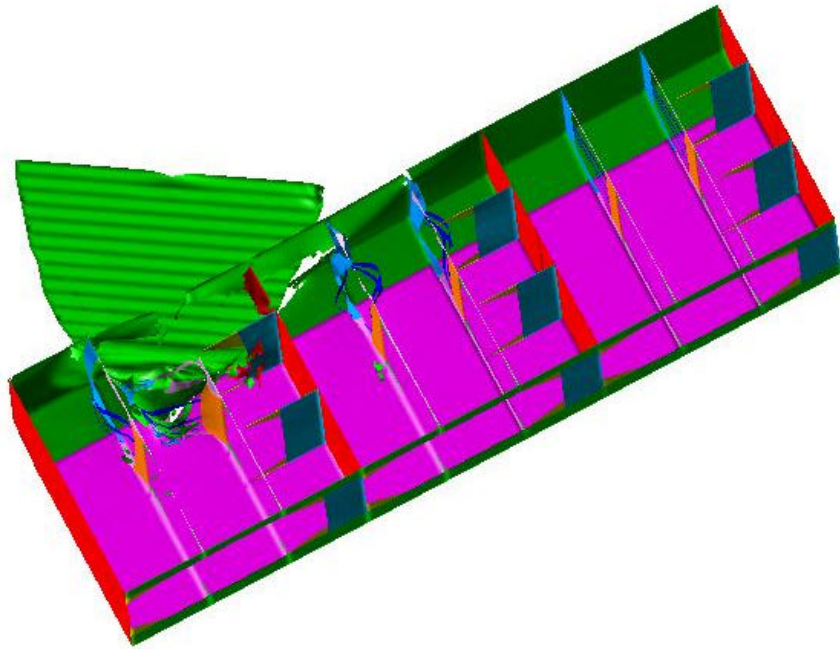


Figure 61 - David E. Day - Marine Flier FEA Damage at 3.0 Seconds

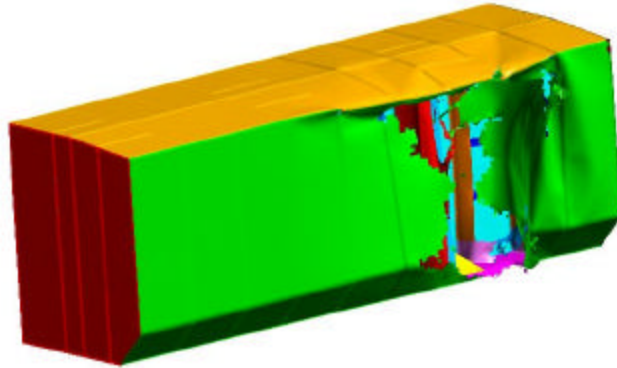


Figure 62 - David E. Day FEA Hull Damage at 3.5 Seconds

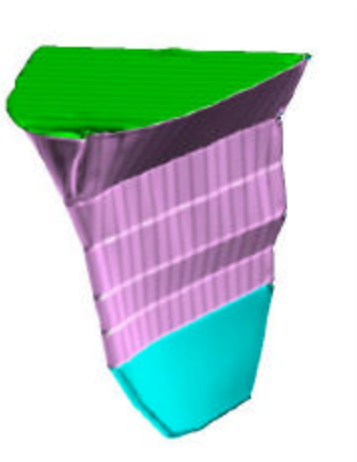


Figure 63 - Marine Flier FEA Bow Damage at 3.0 Seconds

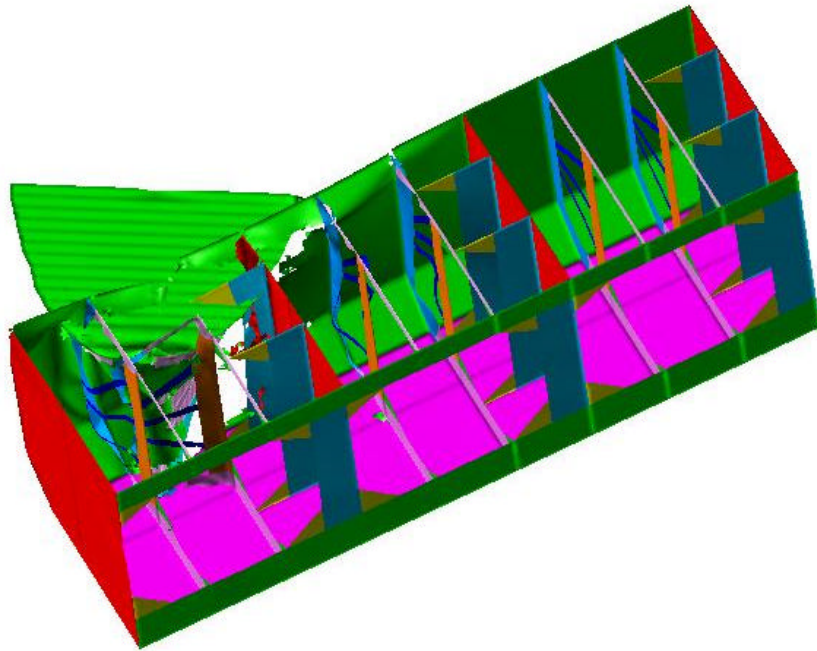


Figure 64 - David E. Day - Marine Flier FEA Damage at 3.5 Seconds

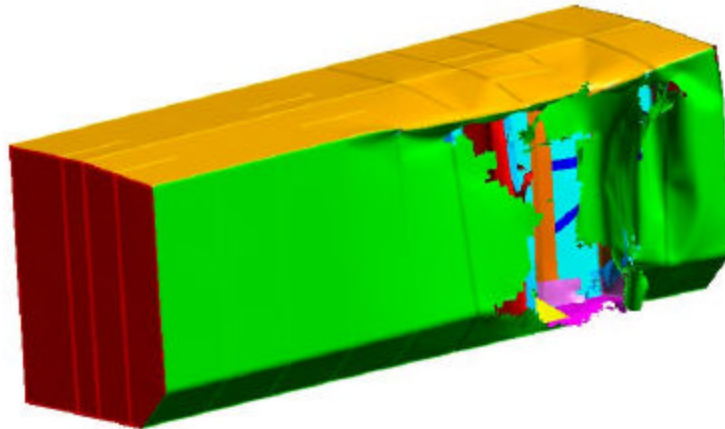


Figure 65 - David E. Day FEA Hull Damage at 3.5 Seconds

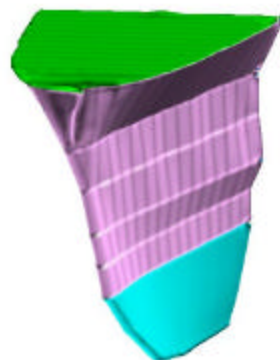


Figure 66 - Marine Flier FEA Bow Damage at 3.5 Seconds

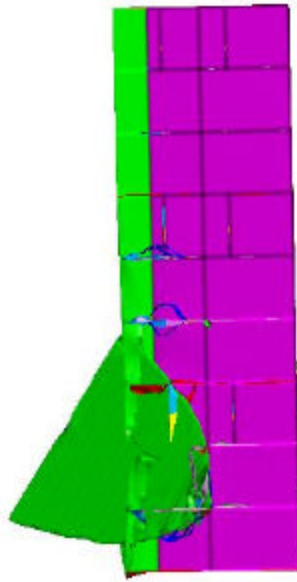


Figure 67 - David E. Day - Marine Flier FEA Damage at 4.0 Seconds

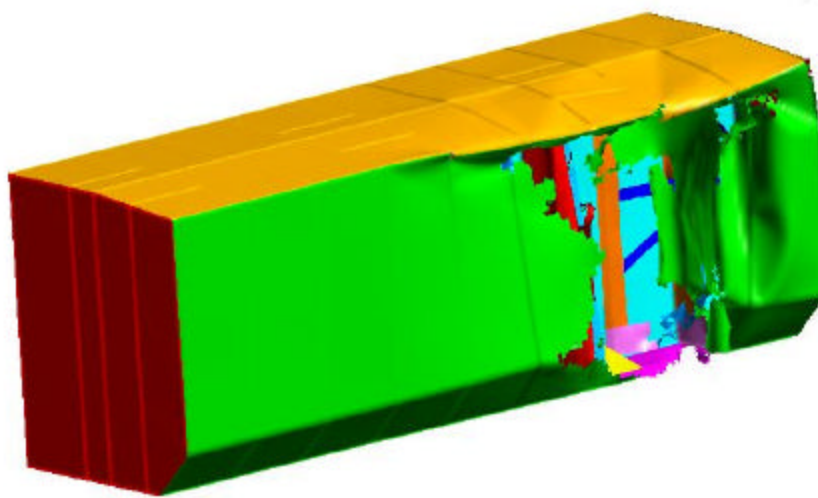


Figure 68 - David E. Day FEA Hull Damage at 4.0 Seconds

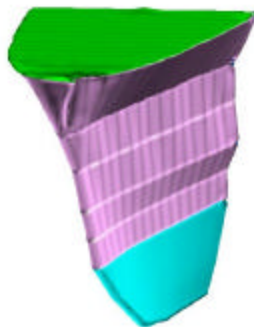


Figure 69 - Marine Flier FEA Bow Damage at 4.0 Seconds

### **3.10 Summary of Finite Element Analysis in Ship-to-Ship Collisions**

While the FEA methods discussed above provide reasonable results as shown in Section 3.9.1, the use of finite element analysis for design optimization or the development of variable response surfaces is currently impractical due to the computational requirements of the finite element methods. A practical example is the use of a small Monte Carlo optimization [35] scheme where 1000 analysis are used varying a set number of design parameters for a single collision scenario. Being conservative and using only one fourth of the average ship-to-ship finite element analysis time on a Pentium IV desktop yields a single analysis time of 22 hours. Thus, 1000 analysis requires at minimum 22000 hours or precisely 2 ½ years. If four collision scenarios are examined, then a full decade of computational time is required. The use of finite element analysis in the remainder of this report is limited to the application of a virtual laboratory assisting in the development and proof of theories and arguments as discussed in later Chapters. It is a development and assessment tool for more simplified modeling methods.

## CHAPTER 4 Simplified Methods for Modeling Ship Collisions

With the high computational cost of finite element analysis, other methods of determining the damage sustained during ship-to-ship collisions were evaluated. Many authors and institutions have investigated aspects of ship-to-ship collisions. A short summary of the methods is provided in the following section with the more applicable methods to this report discussed in detail in Sections 4.1 through 4.3.

Models for analyzing ship collisions were initially developed in the 1950s for ships transporting radioactive materials, and later were applied to other types of ships, including barges, tankers and LPG/LNG carriers. SSC Reports 283, 284 and 285 provide an excellent summary of collision models developed before 1979 [5,6,7]. A more recent review was conducted by the 1997 International Ship and Offshore Structures Congress (ISSC 97), Specialist Panel V.4 [8]. SSC Report 442, produced under SNAME Ad Hoc Panel #6, provides the most recent update [83].

From details of Chapters 2 through 3 the following list of characteristics necessary for any analytical ship-to-ship collision method is provided. This list can be used to determine the completeness of any method and provides a way to compare each of the methods referenced in Section 4.4 and discussed in Sections 4.1 through 4.3.

- Post Collision Momentum – Any collision analysis method should include the determination of each of the energy components of Equation 2.2 including the energy remaining in the system as kinetic energy due to the post collision motion of the combined vessels as occurs in inelastic collisions.
- Struck Ship Forward Velocity – The collision analysis method must consider struck ship forward velocity and its contribution to the initial kinetic energy of the system.
- Oblique Angle Collisions – The collision analysis method must consider collisions which are not ninety degree T-bone collisions, but occur at varying oblique angles. Few actual collisions occur at exactly a ninety-degree collision angle.
- Determination of Energy from Eight Energy Absorbing Structures – The collision analysis method must consider the energy absorbed from the eight critical energy absorbing structures as found in Chapter 2.
- Deformable Bow – The collision analysis method should consider a deformable or energy absorbing striking ship bow structure as some bow structures may not properly be treated as rigid as discussed in Section 2.4.
- Longitudinal Extent of Damage – The collision analysis method must consider not only the penetration of the striking ship into the struck ship, but also the length of damage along the struck ship known as the longitudinal extent of damage for the determination of the full extent of damage which occurs to the vessel during the collision.
- Low Computational Cost – As discussed in Section 3.10, the collision analysis method must encompass a low computational cost while maintaining high solution fidelity. The method must allow for the implementation in an optimization scheme or be used to create response surface curves for use in vessel design phases.

- Coupling of Internal Mechanics and External Dynamics – The collision analysis must consider the effect of the interaction between the global behavior of the vessels and the local deformation and resulting forces.

Prior to discussion of various methods, it is worthy to note that collision analysis models include three primary elements:

- External ship dynamics sub-model;
- Internal sub-model of structural mechanics for the struck and striking ships; and
- Simulation approach that couples the internal and external sub-models.

And collision analysis models may also be categorized by function as:

- Methods suited for determining energy absorbed by struck ship.
- Methods suited for determining energy absorbed by striking ship bow.
- Methods for Determining Energy Absorbed by Both the Striking and Struck Ships

SSC 422 [83] discusses each collision analysis model as categorized by primary elements where here discussion is formatted around the function of each collision analysis model.

#### **4.1 Methods for Determining Energy Absorbed by the Struck Ship**

##### **4.1.1 Minorsky (Energy Coefficient) Method**

Minorsky's correlation between the volume of ship structure damaged in a collision and the collisions kinetic energy is based upon the following three assumptions:

- Only the component of the striking ship speed normal to the course of the struck ship contributes to the kinetic energy available to cause damage;
- The mass of the water entrained during the collision in the sway of the struck ship is equal to forty percent of the displacement of the struck ship;
- The collision is an inelastic event.

Using these assumptions the kinetic energy absorbed in damaging the ship structures during the collision is given by Equation 4.1.

$$\Delta KE = \frac{1}{2} \cdot \left[ \frac{M_{sis} \cdot (M_{sus} + c_{m22} \cdot M_{sus})}{M_{sis} + M_{sus} + c_{m22} \cdot M_{sus}} \right] \cdot (V_{sis} \cdot \sin(\theta))^2 \quad (4.1)$$

where:

**ΔKE** is the energy absorbed due to damaging structure in the collision

**M<sub>sis</sub>** is the displaced mass of the striking ship

**M<sub>sus</sub>** is the displaced mass of the struck ship

**c<sub>m22</sub>** is the added mass coefficient in sway

**V<sub>sis</sub>** is the velocity of the striking ship

**q** is the collision angle

By plotting the kinetic energy absorbed in damaging ship structures during the collision versus the volume of damaged steel material for several collisions as reported by Minorsky [9], and fitting the data points through a linear least squares fit, the correlation between the kinetic energy and the damaged volume is given by Equation 4.2.

$$\Delta KE = 47.2 \cdot R_T + 32.7 \quad (4.2)$$

Where  $R_T$  is the volume of damaged steel, the coefficient multiplying  $R_T$  is the energy coefficient and the intercept term represents the energy absorbed in puncturing and tearing through the shell of the struck ship. Reardon and Sprung [15] reevaluated Minorsky's correlation adding new collision cases after Minorsky's original 1959 data and estimated the intercept term based upon the average of shell damage energy from seven collisions. Based on the new data, Reardon and Sprung [15] reported an updated Minorsky correlation given by Equation 4.3.

$$\Delta KE = 47.1 \cdot R_T + 28.4 \quad (4.3)$$

Minorsky's assumptions are conservative, not considering the energy due to the motion of the struck vessel and only considering a forty percent increase of the mass of the struck vessel in sway motion. Paik, Choe and Thayamballi [28] neglect Minorsky's first assumption and allowed the kinetic energy available in the collision to be a function of the relative velocity between the two ships, the  $\Delta KE$  function reported is:

$$\Delta KE = \frac{1}{2} \cdot \frac{(1 + c_{a1}) \cdot (1 + c_{a2}) \cdot M_1 \cdot M_2}{(1 + c_{a1}) \cdot M_1 + (1 + c_{a2}) \cdot M_2} \cdot V_r^2 \quad (4.4)$$

Where  $c_{a1}$  and  $c_{a2}$  are the added mass coefficients for the striking and struck ships in surge and sway respectively,  $M_1$  and  $M_2$  are the displaced masses of the striking and struck ships respectively, and  $V_r$  is the relative velocity between the two vessels as given by Equation 4.5.

$$V_r = V_1 + V_2 \cdot \cos(\mathbf{q}) \quad (4.5)$$

$V_1$  and  $V_2$  are the forward velocities of the striking and struck ships respectively. Applying Equation 4.4 to the collision data of Reardon and Sprung yields an empirical relation for  $\Delta KE$  as given by Equation 4.6.

$$\Delta KE = 33 \times R_T + 28.4 \quad (4.6)$$

The results of Reardon and Sprung, and Paik, Choe, and Thayamballi's empirical approximations are shown Figure 70 and Figure 71. The high scatter of the results in Paik, Choe, and Thayamballi's empirical approximations becomes more prominent with the use of additional data points.

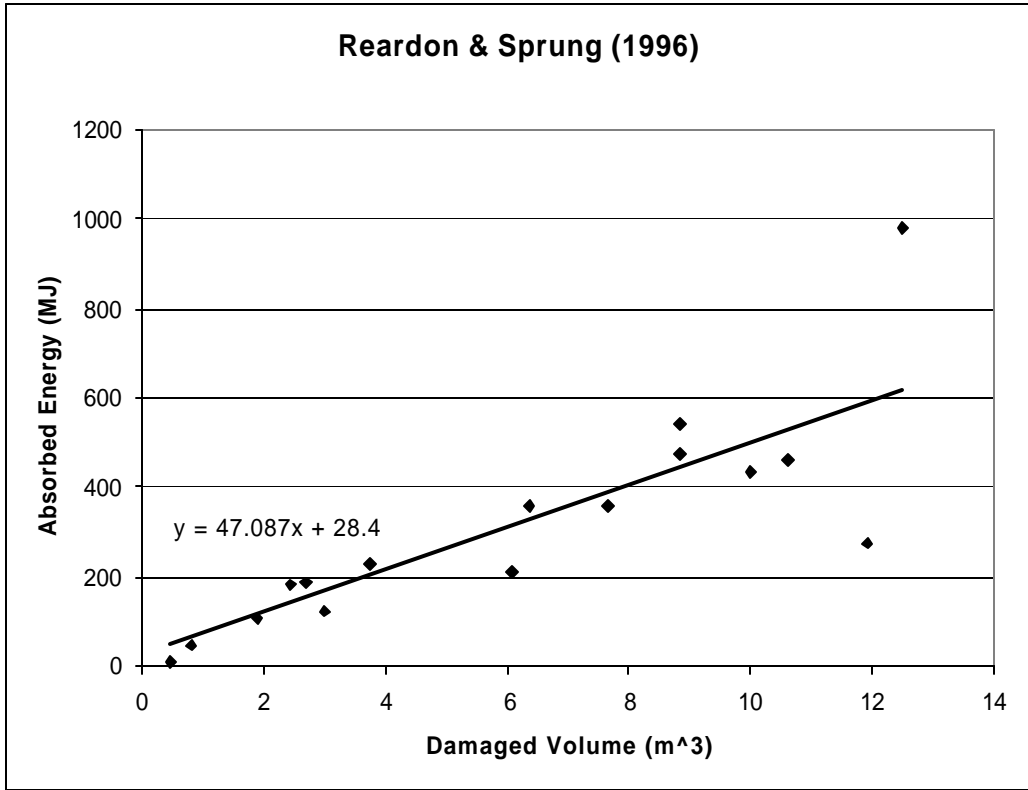


Figure 70 - Reardon and Sprung Absorbed Energy vs. Damaged Volume

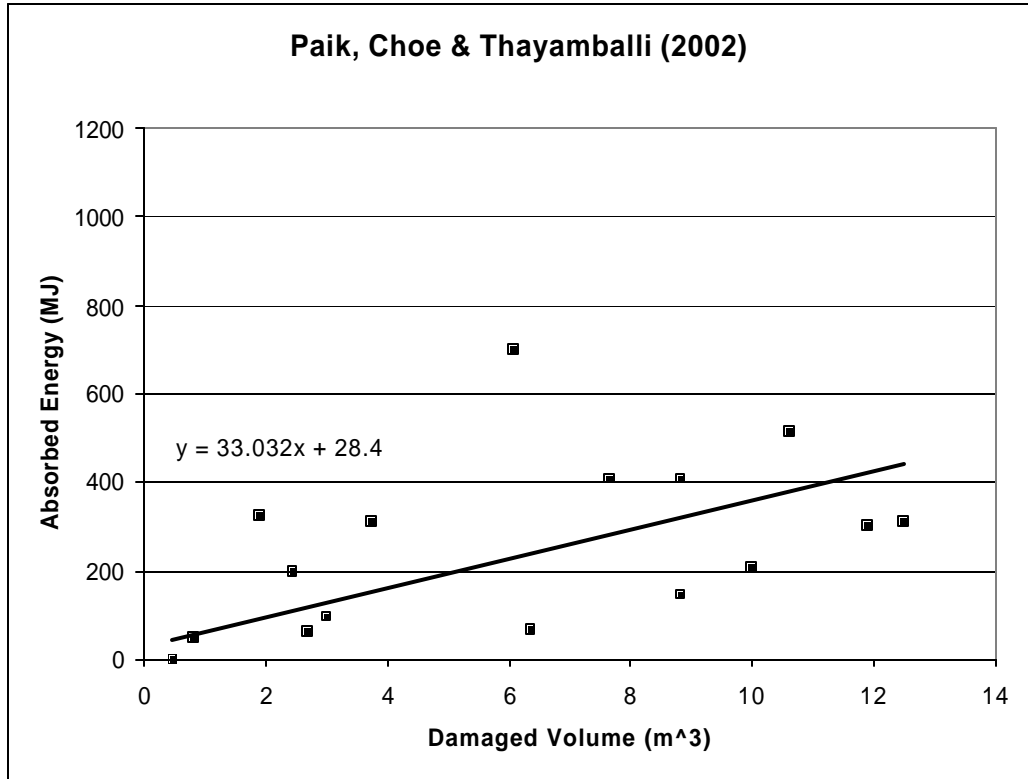


Figure 71 - Paik, Choe and Thayamballi Absorbed Energy vs. Damaged Volume

Several authors have investigated the Minorsky energy coefficient attempting to determine a less empirical approach to the value. Of these, Pedersen and Zhang [14] and Paik and Pedersen [29] approaches are discussed here.

#### 4.1.2 Pedersen and Zhang Energy Coefficient

Pedersen and Zhang developed a relation for the energy absorbed per volume of damaged steel material from the work of Amdahl [23] and Wierzbicki and Abramowicz [87]. The method is based on the crushing, folding and denting modes of L, T or X shaped cross sections. The developed formulation of the Energy Coefficient ( $E_{coef}$ ) is given by Equation 4.7. Where K is a coefficient that depends on the geometrical shape of the crushed structure, the authors proposed an average value of 3.5 for K.

$$E_{coef} = K \cdot s_o \cdot \left(\frac{t}{b}\right)^2 \quad (4.7)$$

$s_o$  is the flow stress,  $t$  is the average thickness and  $b$  is the span of the crushed material. Figure 72 shows the comparison of a fitted line (Minorsky approach) to data points evaluated using Pedersen and Zhangs method of Equation 4.7 on Minorky's original data [9].

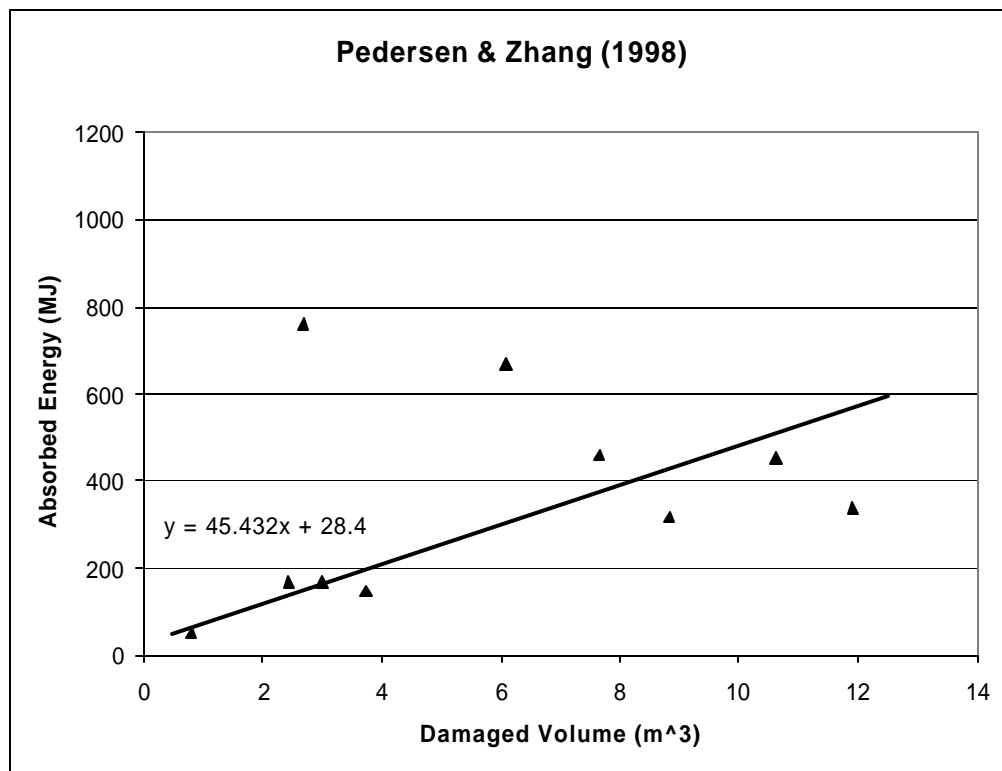


Figure 72 - Pedersen and Zhang Absorbed Energy vs. Damaged Volume

Pedersen and Zhang also developed a relation for the cutting and tearing of bare plate that is given by Equation 4.8.  $G$  is the width of the tearing object (often rigid wedge width) if steady state tearing has been reached otherwise  $G$  is the torn length of the plate.

$$E_{coef} = 3.21 \cdot s_o \cdot \left(\frac{t}{G}\right)^{0.6} \quad (4.8)$$

### 4.1.3 Paik and Pedersen Energy Coefficient

Paik and Pedersen developed two relations for the energy coefficient based on the crushing and folding, cutting and tearing damage modes of plated structures (with and without material strain rate effects). These formulations are derived from Amdahl [23] and are well formulated in [29]. Equation 4.9 is the formulation of  $E_{coef}$  without strain rate effects and Equation 4.10 includes the effect of strain rate.

$$E_{coef} = (1.9514 \cdot (\frac{t}{b})^{0.5} + 0.3661 \cdot \frac{t}{b}) \cdot S_o \quad (4.9)$$

$$E_{coef} = (1 + (\frac{V_m}{1.1026404 \cdot \sqrt{b \cdot t}})^{0.2}) \cdot (1.9514 \cdot (\frac{t}{b})^{0.5} + 0.3661 \cdot \frac{t}{b}) \cdot S_o \quad (4.10)$$

$V_m$  is the mean impact speed that is determined by Equation 4.11.

$$V_m = \frac{\partial d}{\partial t} \quad (4.11)$$

Where  $d(t)$  is the relative motion between the striking and struck vessels.

### 4.1.4 ALPS/SCOL

ALPS/SCOL is a coarse-mesh 3-D non-linear finite element code using super-elements based on the Idealized Structural Unit Method (ISUM) [28,29]. The geometry of the striking and the struck ships is described in a global (three-dimensional) rectangular coordinate system. The stress in an ISUM unit is described in a local element coordinate system. ALPS/SCOL considers sway and yaw of the struck ship with the following assumptions:

- The added masses of the striking and the struck ships are calculated based on ships of similar type and size using a linear strip theory-based computer program.
- The striking ship is assumed to be rigid.
- The analysis of the external and the internal dynamics is undertaken separately.
- The longitudinal velocity of the struck ship is not considered.

Since ALPS/SCOL is based on a simplified 3-D nonlinear finite element approach, damage in three directions (penetration, vertical and horizontal damage) is considered.

The geometry of the striking ship bow shape is described by gap/contact elements. One cargo hold of the struck ship is taken as the extent of the struck ship analysis. ISUM stiffened panel units are used to model the struck vessel structure.

The geometry of the struck ship is described using rectangular or triangular ISUM units. If the deformation of the struck ship is symmetric, the total degrees of freedom in the numerical model are reduced by half. Each node has 3 degrees of freedom. Figure 73 shows damage calculated in a typical ALPS/SCOL simulation.

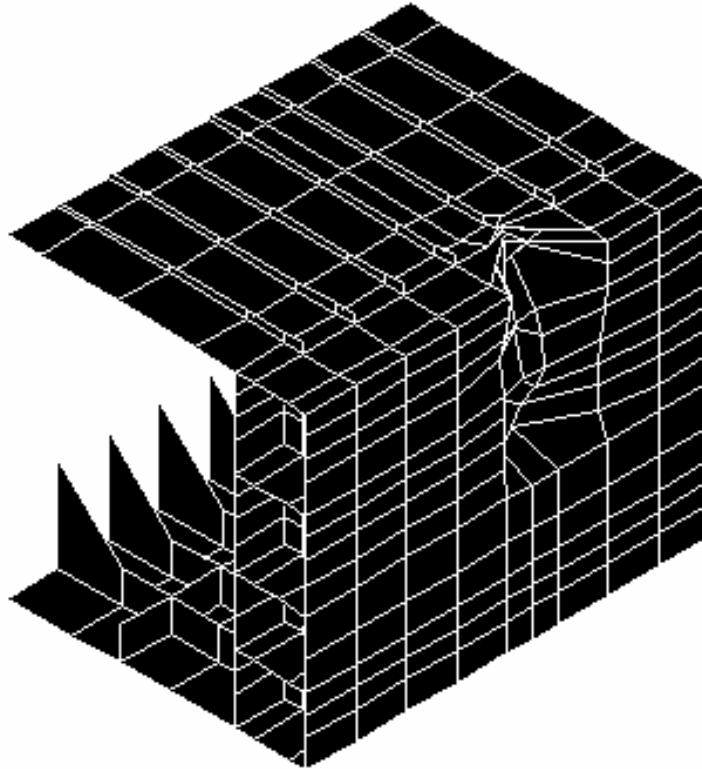


Figure 73 - Damage from ALPS/SCOL Simulation

Design data required for the striking ship includes a detailed bow geometry description, length, beam, depth, draft and displacement. Design data for the struck ship includes, length, beam, depth, draft and displacement, transverse bulkhead location, COG, and detailed structural design and scantlings. Scenario data required includes striking ship velocity and longitudinal location of impact in the struck ship.

#### 4.1.5 DAMAGE

The computer program DAMAGE was developed at MIT under the Joint MIT-Industry Program on Tanker Safety. This project, lead by Professor Tomasz Wierzbicki, was initiated in 1991, and in addition to the program DAMAGE, the project produced more than 70 technical reports about prediction of grounding and collision damage. The program DAMAGE Version 5.0 can be used to predict structural damage in the following accident scenarios [10]:

- Ship grounding on a conical rock with a rounded tip (rigid rock, deformable bottom)
- Right angle ship-ship collisions (deformable side, deformable bow)

Compared to previous models for prediction of grounding and collision damage, a major advantage of DAMAGE is that the theoretical models are hidden behind a modern graphical user interface (GUI). The program has been developed with the objective of making crash analysis of ship structures feasible for engineers that do not have any particular experience in the field of crashworthiness.

The DAMAGE Collision Module calculates velocities and lost kinetic energy after impact using conservation of linear momentum, angular momentum and energy as shown in Equations 4.12 and 4.13:

$$\begin{aligned}
M_{1y}v_1^a + M_{2x}v_2^a &= M_{2x}v_2 \\
I_{1z}\mathbf{w}_1^a + M_{2x}x_1v_2^a &= M_{2x}x_1v_2 \\
v_2^a &= v_1^a + x_1\mathbf{w}_1^a \\
v_1^a &= v_2 \frac{1}{1 + M_{1y}x_1^2/I_{1z} + M_{1y}/M_{2x}} \\
\mathbf{w}_1^a &= v_2 \frac{M_{1y}x_1/I_{1z}}{1 + M_{1y}x_1^2/I_{1z} + M_{1y}/M_{2x}}
\end{aligned} \tag{4.12}$$

where:

- |                  |   |
|------------------|---|
| $M_{1y}$         | virtual mass of the struck ship including added mass in sway;                                     |
| $M_{2x}$         | virtual mass of the striking ship including added mass in surge;                                  |
| $I_{1z}$         | virtual moment of inertia in yaw of the struck ship including yaw added mass (moment of inertia); |
| $v_1^a$          | final velocity of struck ship in the sway direction;  |
| $\mathbf{w}_1^a$ | final angular velocity of struck ship;  |
| $v_2$            | initial velocity of striking ship;  |
| $v_2^a$          | final velocity of striking ship in the sway direction of the struck ship; and                     |
| $x_1$            | impact point to the midship point of struck ship.   |

The kinetic energy absorbed in the collision is then:

$$\Delta KE = \frac{1}{2}M_{1y}v_1^{a2} + \frac{1}{2}M_{2x}v_2^{a2} + \frac{1}{2}I_{1z}\mathbf{w}_1^{a2} - \frac{1}{2}M_{2x}v_2^2 \tag{4.13}$$

Deformation of the bow and the side are calculated separately by moving the striking ship into the struck ship in small increments. In each increment, the total resistance forces from crushing of the bow and penetration into the side are compared. The actual crushing/penetration increment takes place in the ship with lowest resistance. Absorbed energy is calculated. This process continues until absorbed structural energy equals the lost kinetic energy calculated previously. DAMAGE cannot analyze collisions with an oblique striking angle or an initial struck ship velocity. DAMAGE considers the material and structural scantlings of all major structural components of the side structure. The model for the internal mechanics is based on the direct contact deformation of super-elements. The super-elements used to model the side in DAMAGE are:

- Shell and inner side plating panels (laterally loaded plastic membranes)
- Deck panels and girders (crushing)
- Beams (loaded by a concentrated load)
- X-, L- and T-form intersections crushed in the axial direction

## 4.2 Methods for Determining Energy Absorbed by the Striking Ship Bow

### 4.2.1 Amdahl's Method

Amdahl's model for the energy absorption of a striking ship bow is based on theoretical considerations and is correlated against model test results [23]. The model considers the energy dissipated during plastic deformation of basic structural elements such as angles, T-sections and cruciforms. The total crushing load of a specific structure is obtained by adding up all basic element crushing-loads. Amdahl's method leads to the following equation for average crushing length.

$$\sigma_c(\sigma_0, n_{AT}, \tau, DA, n_C, n_T) := 2.42 \cdot \sigma_0 \cdot \left( \frac{n_{AT} \cdot \tau^2}{DA} \right)^{\frac{2}{3}} \cdot \left[ 0.87 + 1.27 \cdot \frac{n_C + 0.31 \cdot n_T}{n_{AT}} \cdot \left[ \frac{DA}{(n_C + 0.31 \cdot n_T) \cdot \tau^2} \right]^{\frac{1}{4}} \right]^{\frac{2}{3}} \quad (4.14)$$

The total crushing load is then found by Equation 4.15.

$$P_{AV}(DA, \sigma_c) := DA \cdot \sigma_c \quad (4.15)$$

Where:

- $s_c$  is the average crushing strength of the bow;
- $s_0$  is the ultimate strength of steel;
- $t$  is the average thickness of the cross section under consideration;
- $DA$  is the cross sectional area of the deformed steel material;
- $n_C$  is the number of cruciforms in the cross section;
- $n_T$  is the number of T-sections in the cross section;
- $n_{AT}$  is the number of angle and T-sections in the cross section.

Appendix H provides a detailed calculation using Amdahl's method for the 150K DWT Bulk Carrier Bow Model described in Appendix A.

### 4.2.2 Pedersen's Method

Pederson [22] proposed a simplified method that consists of an empirical expression to estimate the maximum bow collision load. The maximum bow collision load is given by Equation 4.16.

$$P_{bow} := \begin{cases} \left[ P_0 \cdot L_{bar} \cdot \left[ E_{bar} + (5 - L_{bar}) \cdot L_{bar}^{1.6} \right]^{0.5} \right] & \text{if } E_{bar} \geq L_{bar}^{2.6} \\ \left[ 2.24 \cdot P_0 \cdot (E_{bar} \cdot L_{bar})^{0.5} \right] & \text{otherwise} \end{cases} \quad (4.16)$$

Where:

- $P_{bow}$  is the maximum bow collision load in MN;

$P_0$  is Pederson's reference load equal to 210 MN;

$L_{bar}$  is non-dimensional length given as  $LBP/275$ ;

$E_{bar}$  is the non-dimensional energy given as the initial energy divided by 1425 MN-m.

The total penetration or crush length of the bow of the striking vessel is given by Equation 4.17 and the total duration of the impact is given by Equation 4.18.

$$s_{max} := \frac{\pi}{2} \cdot \frac{E_0}{P_{bow}} \quad (4.17)$$

$$T_0 := 1.67 \cdot \frac{s_{max}}{V_s} \quad (4.18)$$

Where:

$E_0$  is the initial kinetic energy of the striking ship;

$s_{max}$  is the total crush distance of the bow;

$V_s$  is the maximum service speed of the striking ship.

Appendix I provides a detailed calculation using Pedersen's method for the 150K DWT Bulk Carrier Bow Model described in Appendix A.

### **4.3 Methods for Determining Energy Absorbed by Both the Striking and Struck Ships**

#### **4.3.1 DTU Collision Model**

The Technical University of Denmark (DTU) ship collision model solves the external ship dynamics problem uncoupled from the internal mechanics problem and applies the calculated absorbed energy to plastic deformation of the struck ship. Solution of the external dynamics is accomplished based on an analytical method developed by Pederson and Zhang. [14]

Pederson and Zhang apply three local coordinate systems to the striking ship, the struck ship and the impact point separately as shown in Figure 74. By analyzing the motions and impulses around the impact point, the absorbed kinetic energy is derived in both the longitudinal and transverse directions relative to the struck ship. Important assumptions in this analysis include: 1) small rotation during the collision (the angles  $\alpha$  and  $\beta$  in Figure 74 are considered constant); and 2) a constant ratio of absorbed plastic deformation energy for the transverse and longitudinal directions is assumed for the entire collision event. The absorbed energy is calculated uncoupled from the internal mechanics problem.

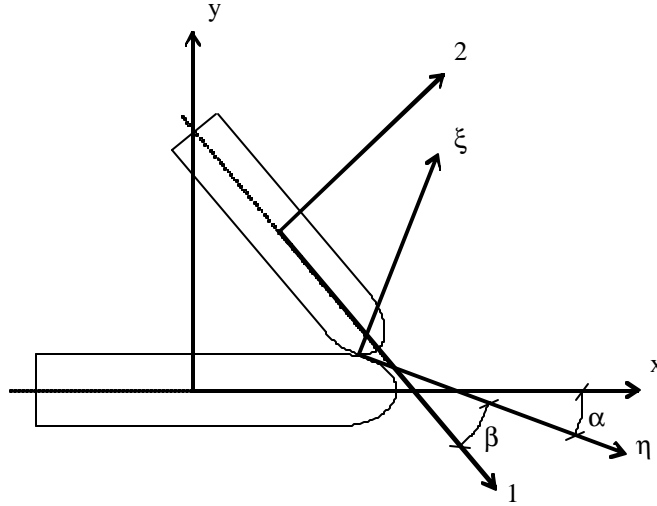


Figure 74 DTU Ship Dynamics Model

Collision absorbed energies in the  $\xi$  (transverse) and  $\eta$  (longitudinal) directions are:

$$E_x = \int_0^{x_{\max}} F_x d\mathbf{x} = \frac{1}{2} \frac{1}{D_x + mD_h} \dot{\mathbf{x}}(0)^2$$

$$E_h = \int_0^{h_{\max}} F_h d\mathbf{h} = \frac{1}{2} \frac{1}{\frac{1}{m}K_x + K_h} \mathbf{h}(0)^2 \quad (4.19)$$

$$E_{total} = E_x + E_h$$

where the coefficients  $D_\xi$ ,  $D_\eta$ ,  $K_\xi$ ,  $K_\eta$  are algebraic expressions that are a function of the ship masses, strike location, collision angle, and added mass coefficients. Added mass coefficients are assumed to be 0.05 in surge, 0.85 in sway and 0.21 in yaw.  $\mathbf{h}(0)$  and  $\dot{\mathbf{x}}(0)$  are the relative longitudinal and transverse velocities between the two ships just prior to impact. Equation 4.19 assumes that the two ships stick together on impact. Whether the two ships slide or stick is determined by the ratio of transverse to longitudinal force-impulses at impact. If this ratio exceeds the coefficient of static friction, it is assumed that the two ships slide. The impulse ratio at impact is assumed constant for the entire process.

This method separately estimates the fraction of the kinetic energy that is available for deformation of the ship structure in the transverse and longitudinal directions. Where the largest assumption of the method is that the ratio of the energy dissipation in the longitudinal direction to the transverse direction is constant over the entire collision. The energy loss for dissipation by structural deformation is expressed in closed form expressions. The procedure is based on a rigid body mechanism, where it is assumed that there is negligible strain energy for deformation outside the contact region, and that the contact region is local and small. This implies that the collision can be considered instantaneous as each body is assumed to exert an impulsive force on the other at the point of contact. The model includes friction between the impacting surfaces so those situations with glancing blows can be identified. Both ships have three degrees of freedom: surge, sway and yaw. The interaction between the ships and the surrounding water is

approximated by simple added mass coefficients, which are assumed to remain constant during the collision. The loss in kinetic energy by the method is determined in two directions, perpendicular and parallel to the side of the struck ship. Both the right and oblique angle collisions are considered and both vessels may have velocity before the collision. The model for the internal mechanics is based on a set of super-elements, where each element represents a structural component. The calculation method is based on the principle that the area of the struck vessel affected by the collision is restricted to the area touched by the striking vessel. The super-elements and mechanisms are:

- Lateral plate deflection and rupture. Large deflections are assumed; this implies that the bending resistance can be neglected
- Crushing of structure intersection elements (Cruciform or T-Section elements)
- In plane crushing and tearing of plates
- Beam deflection and rupture

The design data for the struck vessel includes length, beam, depth, draft, displacement, center of gravity (COG) and detailed structural design and scantlings. The bow of the striking vessel is assumed to be deformable through Amdahl's [23] approach for longitudinally stiffened bows or Lehmann and Yu [46] for transversely stiffened bows however, only the striking ship bow or the struck ship side structure may deform in any one time-step. By a comparison of the crushing energies for the bow and side of the struck vessel it can be determined which structure deforms during the considered time step. If the striking vessel is equipped with a bulbous bow, the analysis of the crushing forces is separated into a bulb analysis and an analysis of the top of the bow above the bulb. The design data for the striking vessel includes stem angle, breadth, bow height, and structural details and scantlings. If the bow is equipped with a bulb, this is assumed to have the form of an elliptic parabola. Scenario data required includes striking and struck ship velocity, collision angle and longitudinal location of impact at the struck vessel. Further details on DTU's collision model can be found in [88].

#### **4.3.2 SIMCOL Version 2.1**

SIMCOL Version 0.0 was developed as part of the work of SNAME Ad Hoc Panel #3 [2,11] where a probabilistic approach to the determination of damage extents was employed. Based on further research, test runs and the need to make the model sensitive to a broader range of design and scenario variables, improvements were progressively made at Virginia Tech [35]. A sweeping segment method was added to the model in SIMCOL Version 1.0 to improve the calculation of damage volume and the direction of damage forces. Models from Rosenblatt [16,18] were applied in Version 1.1 assuming rigid web frames. In Version 2.0, the lateral deformation of web frames was included. In Version 2.1, the vertical extent of the striking ship bow is considered. Version 2.1 is described in this section.

SIMCOL uses a forward difference time-domain simultaneous solution of external ship dynamics and internal deformation mechanics similar to that originally proposed by Hutchison [12].

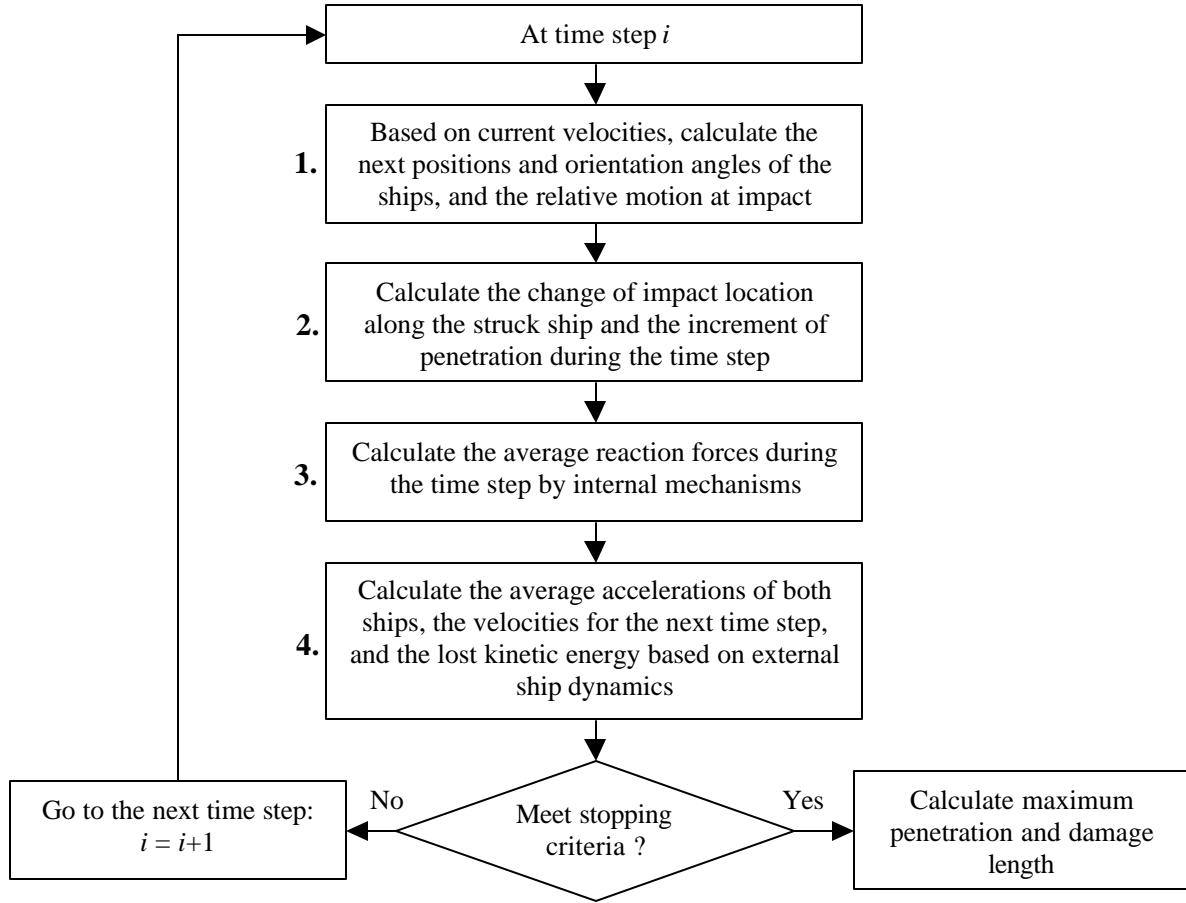


Figure 75 - SIMCOL Simulation Process

Figure 75 shows the SIMCOL simulation process. The Internal Sub-Model performs Steps 2 and 3 in this process. It calculates internal deformation due to the relative motion of the two ships and the internal reaction forces resulting from this deformation. The External Sub-Model performs Steps 1 and 4 in this process. It applies the internal forces to the global motion of the two ships and calculates the resulting accelerations, velocities and motions of the two ships during a time step.

#### 4.3.2.1 SIMCOL Version 2.1 External Dynamics Sub-Model

The External Dynamics Sub-Model uses a global coordinate system shown in Figure 76. Its origin is at the initial (time of strike) center of gravity of the struck ship with the  $x$ -axis towards the bow of the struck ship. The initial locations and orientations of the struck and striking ships in the global coordinate system are:

$$\begin{aligned}
 x_{1,0} &= 0 & y_{1,0} &= 0 & \mathbf{q}_{1,0} &= \mathbf{0} \\
 x_{2,0} &= -l_0 + \frac{L_{BP2}}{2} \cos \mathbf{f}_0 \\
 y_{2,0} &= \frac{B_1}{2} + \frac{L_{BP2}}{2} \sin \mathbf{f}_0 \\
 \mathbf{q}_{2,0} &= \mathbf{f}_0 - \mathbf{p}
 \end{aligned} \tag{4.20}$$

where:

- $x_1, y_1$  center of gravity of the struck ship (m), assumed at amidships;
- $q_1$  heading of the struck ship;
- $x_2, y_2$  center of gravity of the striking ship (m), assumed at amidships;
- $q_2$  heading of the striking ship;
- $LBP_2$  length between perpendiculars of the striking ship (m);
- $B_1$  breadth of the struck ship (m); and
- $f$  collision angle.

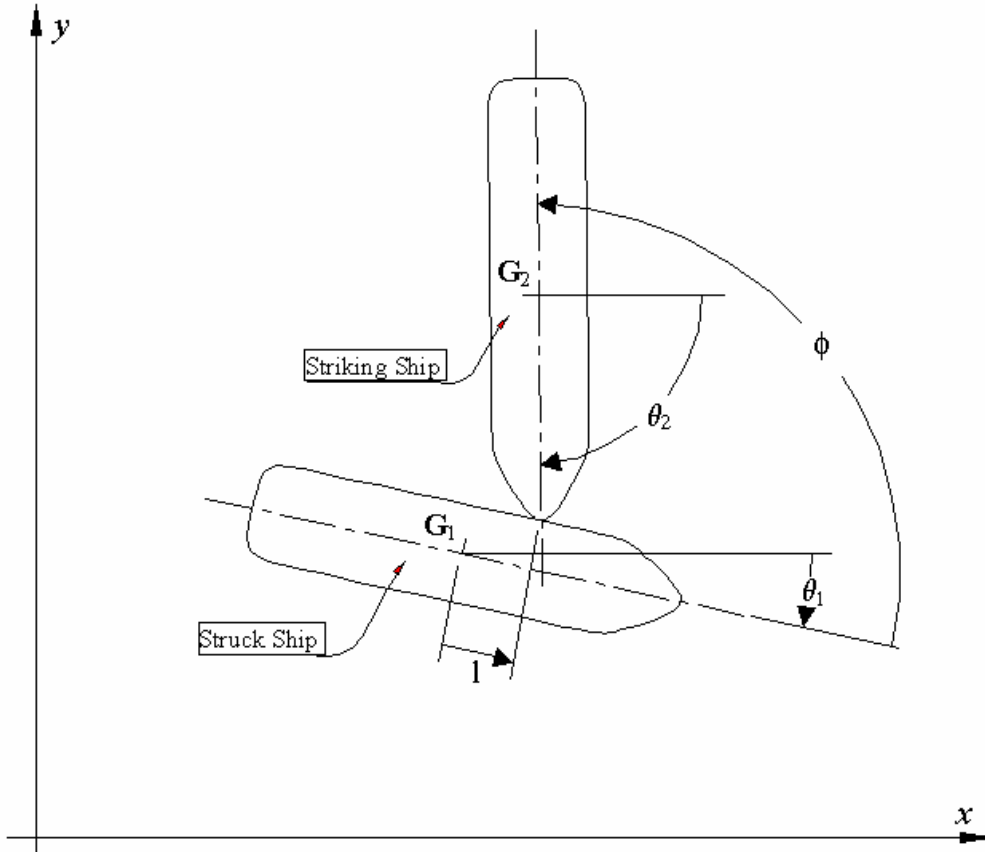


Figure 76 - SIMCOL External Ship Dynamics

A local damage coordinate system,  $\xi$ - $\eta$ , is established on the struck ship to calculate relative movement and collision forces. The origin of this system is set at amidships on the shell plate of the damaged side of the struck ship. Axes  $\xi$  and  $\eta$  point aft and inboard relative to the struck ship. Local coordinate systems are also established at the centers of gravity of both struck and striking ships. Forces and moments in the local systems are transformed to the global  $x$ - $y$  system for solution of the ship dynamics. In the local ship systems, the hydrodynamic added mass for each ship is a tensor in the form:

$$\mathbf{A} = \begin{bmatrix} a_{11} & a_{12} & a_{13} \\ a_{21} & a_{22} & a_{23} \\ a_{31} & a_{32} & a_{33} \end{bmatrix} \quad (4.21)$$

Considering the approximate symmetry of the ships, and with the center of gravity of the ships assumed to be at amidships, the off-diagonal terms of the added mass tensor for each ship are zeros:

$$\mathbf{A}_s = \begin{bmatrix} a_{11} & 0 & 0 \\ 0 & a_{22} & 0 \\ 0 & 0 & a_{33} \end{bmatrix} \quad (4.22)$$

Where:

- $a_{11}$  added mass in the surge direction (kg);
- $a_{22}$  added mass in the sway direction (kg); and
- $a_{33}$  added mass in the yaw direction (kg·m<sup>2</sup>).

The added mass tensor is transformed in accordance with the orientation of each ship to the global coordinate system. The transformed tensor,  $\mathbf{A}_q$ , for each ship is:

$$\mathbf{A}_q = \begin{bmatrix} a_{11} \cos^2 \mathbf{q} + a_{22} \sin^2 \mathbf{q} & (a_{11} - a_{22}) \cos \mathbf{q} \sin \mathbf{q} & 0 \\ (a_{11} - a_{22}) \cos \mathbf{q} \sin \mathbf{q} & a_{11} \sin^2 \mathbf{q} + a_{22} \cos^2 \mathbf{q} & 0 \\ 0 & 0 & a_{33} \end{bmatrix} \quad (4.23)$$

The added mass in surge is approximated by the added mass of a circumscribed cylinder [12]. The added mass in surge,  $a_{11}$ , for each ship is:

$$a_{11} = \frac{4}{3} \mathbf{r} \mathbf{p} \left( \frac{\mathbf{B} \mathbf{T}}{\mathbf{p}} \right)^2 = 0.75225 \mathbf{r} (\mathbf{B} \mathbf{T})^2 \quad (4.24)$$

Where:

- $\mathbf{r}$  density of sea water, 1025 kg/m<sup>3</sup>;
- $\mathbf{B}$  breadth of the ship (m); and
- $\mathbf{T}$  draft of the ship (m).

The added mass in sway is approximated assuming that the cross sections of ships are rectangular [12]. The added mass in sway,  $a_{22}$ , for each ship is:

$$a_{22} = 1.189 \mathbf{r} \mathbf{T}^2 L_{BP} \quad (4.25)$$

Similarly, by assuming that the water planes are rectangular, the added mass in yaw,  $a_{33}$ , is [12]:

$$a_{33} = \frac{2.378 \mathbf{r} \mathbf{T}^2 L_{BP}^3}{24} = 0.0991 \mathbf{r} \mathbf{T}^2 L_{BP}^3 \quad (4.26)$$

Instead of calculating added mass directly, added mass coefficients may be used where:

$$\begin{aligned} a_{11} &= c_{11} m_s \\ a_{22} &= c_{22} m_s \\ a_{33} &= c_{33} I_{s33} \end{aligned} \quad (4.27)$$

Coefficients are used in this report to standardize results when compared to other models. Assumed added mass coefficients are 0.05 in surge ( $c_{11}$ ), 0.85 in sway ( $c_{22}$ ) and 0.21 in yaw ( $c_{33}$ ).

The actual mass for each ship is also represented by a tensor:

$$\mathbf{M}_{ship} = \begin{bmatrix} m_s & 0 & 0 \\ 0 & m_s & 0 \\ 0 & 0 & I_{s33} \end{bmatrix} \quad (4.28)$$

where:

$m_s$  ship mass (kg); and

$I_{s33}$  mass moment of inertia about the yaw axes of each ship ( $\text{kg}\cdot\text{m}^2$ ).

The virtual mass,  $\mathbf{M}_V$ , for each ship is then:

$$\begin{aligned} \mathbf{M}_{Vq} &= \mathbf{M}_{ship} + \mathbf{A}_q = \begin{bmatrix} m_{V11} & m_{V12} & 0 \\ m_{V21} & m_{V22} & 0 \\ 0 & 0 & I_{V33} \end{bmatrix} \\ &= \begin{bmatrix} m_s + a_{11} \cos^2 \mathbf{q} + a_{22} \sin^2 \mathbf{q} & (a_{11} - a_{22}) \cos \mathbf{q} \sin \mathbf{q} & 0 \\ (a_{11} - a_{22}) \cos \mathbf{q} \sin \mathbf{q} & m_s + a_{11} \sin^2 \mathbf{q} + a_{22} \cos^2 \mathbf{q} & 0 \\ 0 & 0 & I_{s33} + a_{33} \end{bmatrix} \end{aligned} \quad (4.29)$$

In Steps 2 and 3 of Figure 75, the Internal Model calculates the resulting deformation, and the average forces and moments generated by this deformation over the time step as discussed in Section 4.3.2.2. In Step 4 of Figure 75, these forces and moments are applied to each ship. The new acceleration for each ship is:

$$\mathbf{V}_s' = \frac{\mathbf{F}}{\mathbf{M}_{VJ}} \quad (4.30)$$

or:

$$\begin{aligned} u' &= \frac{F_x m_{V22} - F_y m_{V12}}{m_{V11} m_{V22} - m_{V12}^2} \\ v' &= \frac{F_y m_{V11} - F_x m_{V12}}{m_{V11} m_{V22} - m_{V12}^2} \\ w' &= \frac{M}{I_{V33}} \end{aligned} \quad (4.31)$$

Where:

$\mathbf{F}$  forces exerted on each ship in the global system,  $\mathbf{F} = \{F_x, F_y, M\}^T$ ;

$F_x$  force in the X direction in the global coordinate system (N);

$F_y$  force in the Y direction in the global coordinate system (N);

$M$  moment about the center of gravity of each ship (N-m);

$\mathbf{V}_s \zeta$  ship acceleration,  $\mathbf{V}_s' = \{u', v', \omega'\}^T$ ;

$u \zeta$  acceleration in the X direction in the global coordinate system ( $\text{m}/\text{s}^2$ );

$v\ddot{\zeta}$  acceleration in the  $Y$  direction in the global coordinate system ( $m/s^2$ ); and  
 $w\ddot{\zeta}$  angular acceleration of each ship in yaw ( $degree/s^2$ ).

The new velocities for each ship at the end of the time step are:

$$\mathbf{V}_{s,n+1} = \mathbf{V}_{s,n} + \mathbf{V}'_s t \quad (4.32)$$

Where:

$n$  time step number; and  
 $t$  length of the time step (second).

Referring to Figure 75, step 1, the velocities from the previous time step are applied to the ships to calculate their positions at the end of the current time step:

$$\mathbf{X}_{n+1} = \mathbf{X}_n + \mathbf{V}_{s,t} t \quad (4.33)$$

Where:

$\mathbf{X}$  location and orientation of each ship in the global system,  $\mathbf{X} = \{x, y, \theta\}^T$ .

#### 4.3.2.2 SIMCOL Version 2.1 Internal Sub-Module

Referring to Figure 75, Steps 2 and 3, the Internal Sub-Model calculates the struck ship deformation resulting from the ships' relative motion, and the average internal forces and moments generated by this deformation over the time step. The Internal Sub-Model determines reacting forces from side and bulkhead (vertical) structures using detailed mechanisms adapted from Rosenblatt [16,18] and discussed in detail in this section. It determines absorbed energy and forces from the crushing and tearing of decks, bottoms and stringers (horizontal structures) using the Minorsky correlation [9] as modified by Reardon and Sprung [15], Equation 4.3. Total forces are the sum of these two mechanisms. In SIMCOL Version 2.1, the striking ship bow is assumed to be wedge-shaped with upper and lower extents determined by the bow height of the striking ship and the relative drafts of the two ships. Deformation is only considered in the struck ship. The striking ship is assumed to be rigid.

Penetration of the struck ship begins with the side shell plating and webs (vertical structures). Figure 77 illustrates the two basic types of strike determined by the strike location relative to the webs. The following assumptions are made consistent with Rosenblatt [18]:

- Plastic bending of shell plating is not considered - The contribution of plastic bending in the transverse deformation of longitudinally stiffened hull plates is negligible. The sample calculation sheets in Rosenblatt [18] support this argument. In six test cases, the energy absorbed in plastic bending never exceeds 0.55% of the total absorbed energy when the cargo boundary is ruptured. It is a good assumption that the plastic membrane tension phase starts from the beginning of collision penetration and is the primary shell energy-absorption mechanism.
- Rupture of stiffened hull plates starting in the stiffeners is not considered - As suggested in McDermott [16], this mechanism is unlikely for most structures except for flat-bar stiffened plates. It is a standard practice to use angles instead of flat bar for longitudinal stiffeners of side shell and longitudinal bulkheads, therefore, this option is not considered in SIMCOL.

- Web frames do not yield or buckle before plates load in membrane tension - McDermott demonstrates that this mechanism is unlikely and does not contribute significantly to absorbed energy in any case. This mechanism requires very weak web frames that would not be sufficient to satisfy normal sea and operational loads.

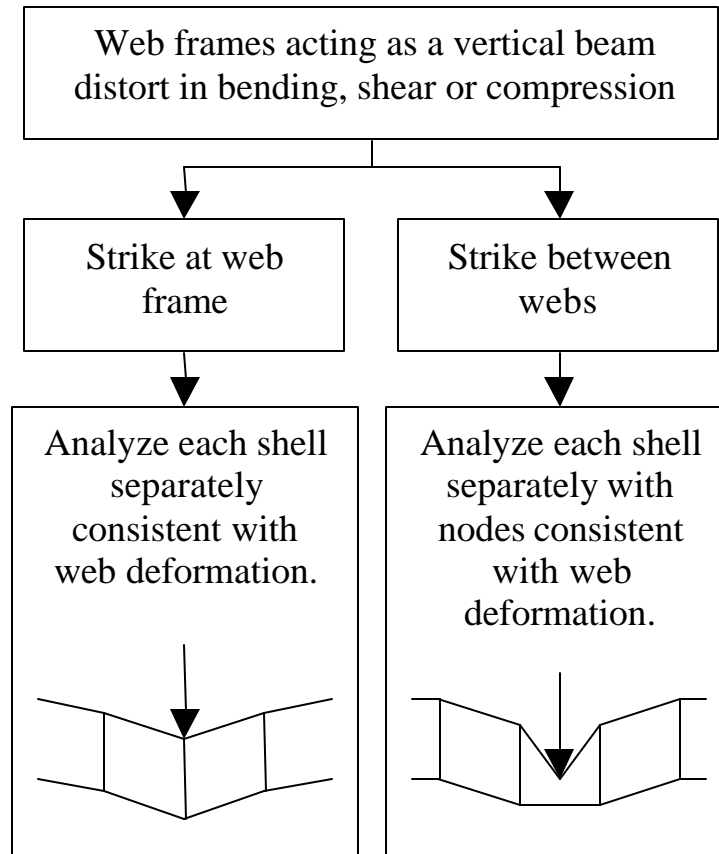


Figure 77 - Web Deformation in SIMCOL

SIMCOL Version 1.1 assumes that flanking web frames are rigid. Version 2.0 and subsequent versions consider the transverse deformation of webs.

In a right-angle collision case, Equation 4.34 gives the total plastic energy absorbed in membrane tension in time step  $n$ . This assumes that the plate is not ruptured, that flanking webs do not deflect in the longitudinal direction, and that compression in the side shell caused by longitudinal bending of ship hull girder is small.

$$\begin{aligned}
 E_n &= T_m e_m \\
 T_m &= s_m t B_e
 \end{aligned}
 \tag{4.34}$$

Where:

- $E_n$  plastic energy absorbed by side shell or longitudinal bulkhead (J);
- $T_m$  membrane tension (N);
- $s_m$  yield stress of side shell or bulkhead adjusted for strain rate (Pa);

- $e_m$  total elongation of shell or bulkhead structure in the web spacing;  
 $t$  smeared thickness of side shell or bulkhead (m);  
 $B_e$  effective breadth (height) of side shell or bulkhead (m);

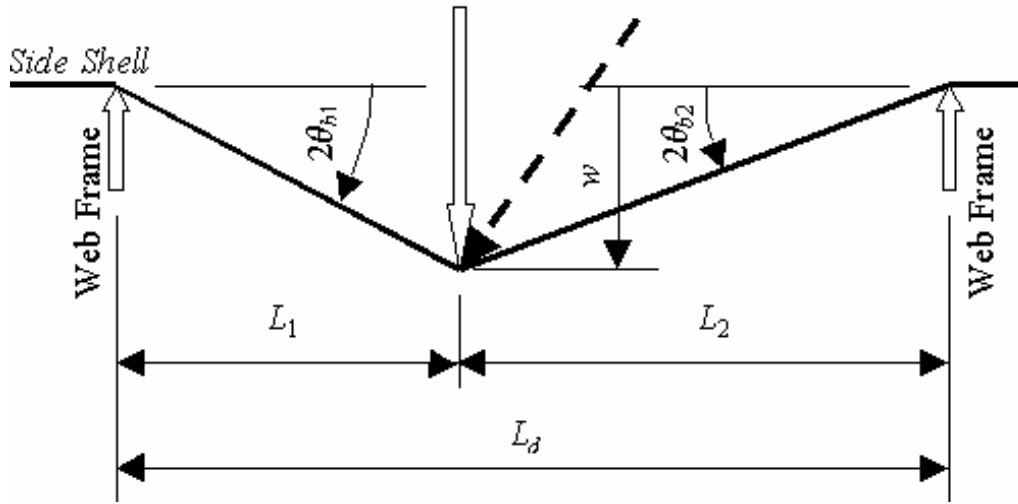


Figure 78 - Membrane Geometry

Figure 78 illustrates the membrane geometry for calculation of elongation where  $e_1$  and  $e_2$  are the elongation of legs  $L_1$  and  $L_2$  respectively:

$$e_i = \sqrt{L_i^2 + w^2} - L_i \cong \frac{w^2}{2L_i} \quad (4.35)$$

$$e_t = e_1 + e_2 = \frac{L_d}{2L_1L_2} w^2$$

Where:

- $L_d$  damage length, or distance between adjacent webs (m)  
 $w_n$  deflection of side shell or bulkhead at time step  $n$  (m)

Side shell rupture due to membrane tension is determined using the following criteria:

- The strain in the side shell reaches the rupture strain,  $\epsilon_r$ , which is taken as 10% in ABS steel;
- The bending angle at a support reaches the critical value as defined in Equation 4.36 [18]:

$$e_m = \frac{4}{3} \frac{s_m}{s_u - s_m \cos q_c} \sin q_c \tan q_c = 1.5D \quad (4.36)$$

Where:

- $e_m$  maximum bending and membrane-tension strain at hull rupture;  
 $s_m$  in-plate stress under membrane-tension (MPa);  
 $s_u$  ultimate stress of the plate (MPa);  
 $q_c$  critical bending angle; and  
 $D$  tension test ductility in a 2-in gage length, 32% for ABS steel.

The criteria for rupture is then:

$$\begin{aligned} e_i &= \frac{e_i}{L_i} \leq e_r \\ q_{bi} &= \frac{1}{2} \arctan \frac{w}{L_i} \cong \frac{w}{2L_i} \leq q_c \end{aligned} \quad (4.37)$$

where:

$e_i$  strain in leg  $i$ ; and  
 $q_{bi}$  bending angle at flanking web frames of leg  $i$ .

Since the striking bow normally has a generous radius, the bending angle at the impact location is not considered in the rupture criteria. From these equations, it can be seen that only the strain and bending angle in the shorter leg need be considered for right angle collisions. Based on material properties of ABS steel, the critical bending angle  $\theta_c$  from Equation 4.37 is 19.896, 17.318 or 16.812 degrees for ABS grade B (mild steel), AH32 or AH36 grades respectively. Once either of the rupture criteria is reached, the side shell or longitudinal bulkhead is considered ruptured and does not continue to contribute to the reacting force.

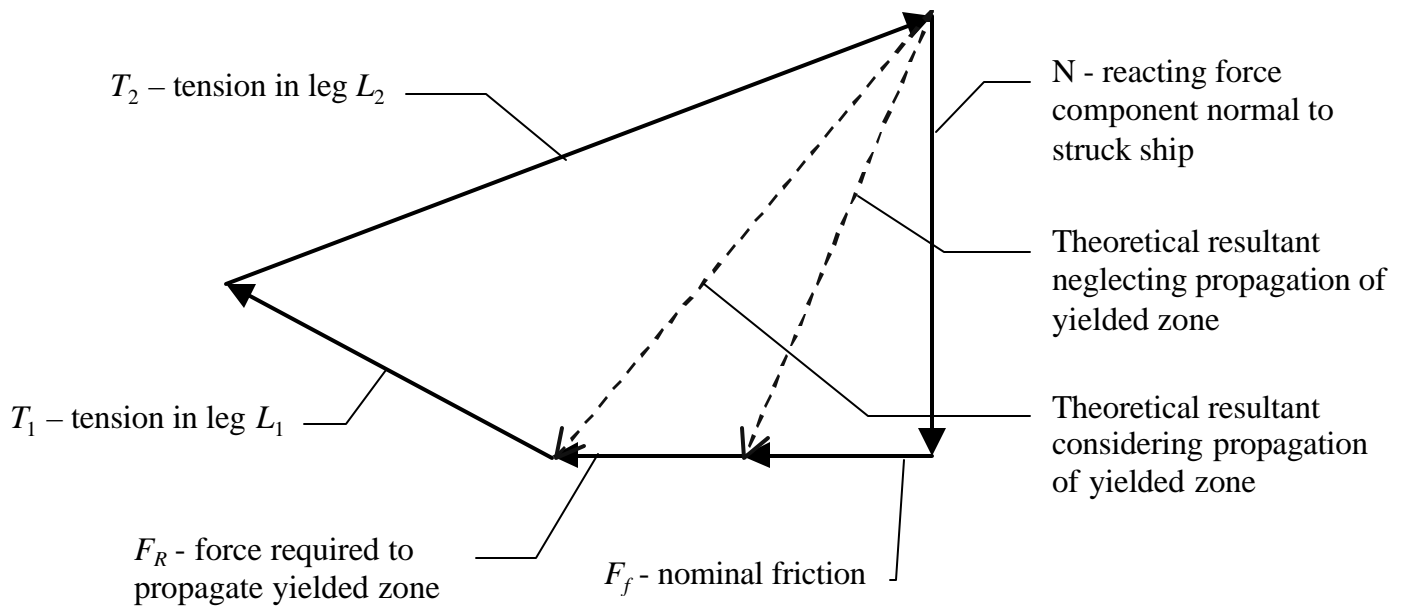


Figure 79 – Force Diagram for an Oblique Angle Collision

For collisions at an oblique angle, the membrane tension is only fully developed in the leg behind the strike,  $L_2$  in Figure 78. This is demonstrated in the force diagram shown in Figure 79, where  $T_1$  is much smaller than  $T_2$ . It is also assumed that all the plastic strain developed from membrane tension is behind the striking point.

The first rupture criterion in Equation 4.37 becomes:

$$e_b = \frac{e_t}{L_b} \leq e_r \quad (4.38)$$

Where  $\epsilon_b$  and  $L_b$  represent the strain and length of the leg behind the strike.

In SIMCOL Version 2.0 and later, transverse deformation of web frames is also considered. Web failure modes include bending, shear, and compression. Web frames are allowed transverse deformation while keeping their longitudinal locations. The resisting force is assumed constant (plastic) at a distorted flanking web frame, and the transverse deformation of the web frame is assumed uniform from top to bottom. The magnitude of this force is its maximum elastic capacity. From Figure 79, the applied force on a rigid flanking web frame is:

$$P_i = T_i \frac{w}{L_i} \quad (4.39)$$

Where  $P_i$  and  $T_i$  are referred to the particular leg  $L_i$ . If the applied force,  $P_i$ , is greater than the maximum elastic capacity of the flanking web frame,  $P_{wf}$ , the particular web frame is deformed as in Figure 80. The change of angle,  $\gamma_c$ , at the distorted web is:

$$g_{ci} \cong \frac{P_{wf}}{T_i} \quad (4.40)$$

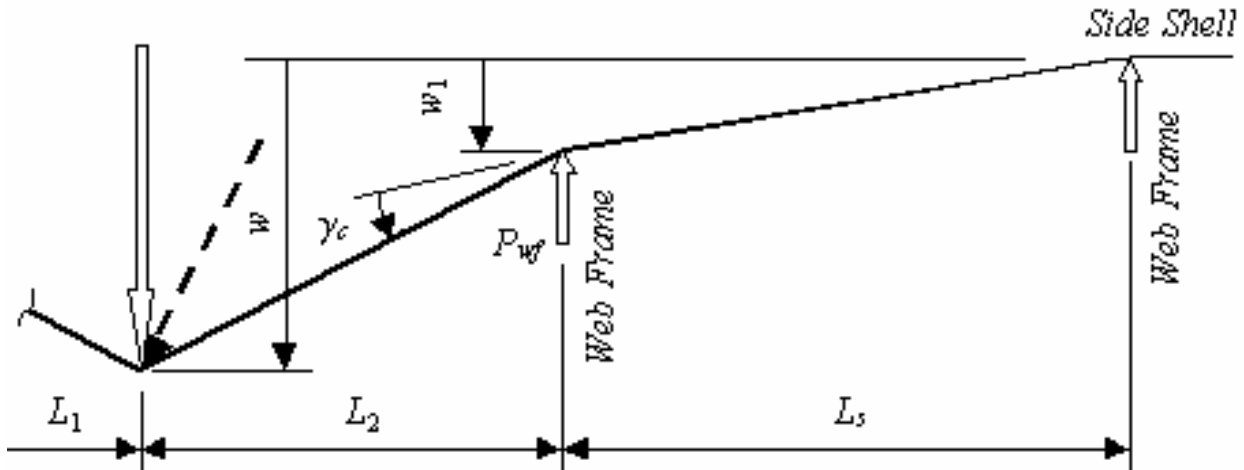


Figure 80 Deflection and Forces in Distorted Web Frames

Rosenblatt [18] proposes an approach to determine whether  $P_i$  exceeds the capacity  $P_{wf}$ , and to estimate the value of  $P_{wf}$ . First, the allowable bending moment and shear force of the web frame at each support, the crushing load of the web, and the buckling force of supporting struts are calculated. Then, the load,  $P_i$ , is applied to the web frame, and the induced moments, shear forces and compression of the web frame and struts are calculated, considering the web frame as a beam with clamped ends. The ratios of the induced loads to the allowable loads are determined using Equation 4.41. If the maximum ratio,  $R_m$ , is greater than unity, the load,  $P$ , exceeds the capacity, and the web frame deforms.

$$R_m = \frac{P}{P_{wf}} \quad (4.41)$$

The deflection at the outermost distorted web frame is:

$$w_n = \frac{L_s}{L_i + nL_s} \left\{ w - g_{c2} \left[ nL_i + \frac{1}{2} (n-1)nL_s \right] \right\} \quad (4.42)$$

Where:

$n$  total number of deformed web frames on the  $L_i$  side; and  
 $L_s$  web frame spacing (m).

The deflection at other deformed web frames is:

$$w_j = (n - j + 1)w_n + \frac{1}{2}(n - j)(n - j + 1)g_{c2}L_s \quad (4.43)$$

Where  $j$  is the number of web frames counted from the striking point. The elongation in adjacent webs is:

$$e_j = \sqrt{(w_j - w_{j+1})^2 + L_s^2} - L_s \quad (4.44)$$

And the elongation in the struck web is:

$$e_{0i} = \sqrt{(w - w_1)^2 + L_i^2} - L_i \quad (4.45)$$

With these elongation and deformation results, the same rupture criteria given in Equations 4.44 and 4.45 are applied to all deformed webs. The total elongation on the  $L_i$  side is:

$$e_{ti} = e_{0i} + \sum_{j=1}^n e_{ji} \quad (4.46)$$

And the energy absorbed in membrane tension and web deformation is:

$$E_i = T_i e_{ti} + P_{wf} \sum_{j=1}^n w_{ji} \quad (4.47)$$

For right angle collisions,  $T_i$  always equals  $T_m$  as calculated in Equation 4.34. In oblique angle collisions,  $T_i$  equals  $T_m$  if  $L_i$  is on the side behind the strike. Based on experimental data, Rosenblatt [18] suggests using  $1/2 T_m$  ahead of the strike and this is used in SIMCOL 2.1.

For double hull ships, if the web frames are distorted because of bending, shearing and buckling of supporting struts, the deformed web frames push the inner skin into membrane tension as shown in Figure 77, and the right angle collision mechanism is applied to the inner hull. Inner skin integrity is checked using Equations 4.37 and 4.38, and the energy absorbed in inner skin membrane tension is calculated using Equation 4.34.

In the simulation, the energy absorbed in membrane tension and web deformation during a time step is:

$$\Delta KE_n = (E_{1,n+1} + E_{2,n+1}) - (E_{1n} + E_{2,n}) \quad (4.48)$$

Considering the friction force,  $F_f$ , in Figure 79, and assuming the dynamic coefficient of friction has a constant value of 0.15, the reacting forces and moments are calculated:

$$\begin{aligned}
\Delta KE_n &= N_n (w_{n+1} - w_n) + F_{fn} |l_{n+1} - l_n| = N_n [(w_{n+1} - w_n) + 0.15 |l_{n+1} - l_n|] \\
F_{fn} &= N_n = \frac{(E_{1,n+1} + E_{2,n+1}) - (E_{1n} + E_{2,n})}{(w_{n+1} - w_n) + 0.15 |l_{n+1} - l_n|} \\
F_{xn} &= F_f \frac{(l_{n+1} - l_n)}{|l_{n+1} - l_n|} = 0.15 F_{fn} \frac{(l_{n+1} - l_n)}{|l_{n+1} - l_n|} \\
M_n &= -F_{xn} d_n + F_{fn} l_n
\end{aligned} \tag{4.49}$$

Where:

- $N_n = F_{fn}$  Force on struck ship normal (transverse) to centerline (N)  
 $F_{xn}$  Force on struck ship parallel (longitudinal) to centerline (N)  
 $M_n$  Yaw moment on struck ship (N m)  
 $d_n$  Distance of longitudinal line of force from centerline (m)  
 $l_n$  Distance of transverse line of force from midship (m)

In addition to the friction force, another longitudinal force,  $F_R$ , the force to propagate the yielding zone, is considered, as shown in Figure 79. McDermott provides an expression for this force [16]:

$$F_R = \frac{s_y d'}{R} \left[ d' t_w \left( 1 - \frac{s_y R}{d' E} \right)^2 + t_f (b - t_w) \left( \frac{d' - 0.5 t_f}{d'} - \frac{s_y R}{d' E} \right) \right] \tag{4.50}$$

Where:

- $d\zeta$  depth of side shell longitudinal stiffeners;  
 $R$  radius of the striking bow;  
 $t_w$  thickness of side shell stiffener webs;  
 $t_f$  thickness of side shell stiffener flanges;  
 $b$  width of side shell stiffener flanges; and  
 $E$  modulus of elasticity.

Or when simplified:

$$\begin{aligned}
c_F &= \frac{F_R}{s_y A_{stiff}} \\
c_A &= \frac{A_{stiff}}{A_{total}} \\
F_R &= c_F c_A s_y t B
\end{aligned} \tag{4.51}$$

Where:

- $c_F$  force coefficient;  
 $c_A$  ratio of sectional areas;  
 $A_{stiff}$  sectional area of stiffeners; and  
 $A_{total}$  total sectional area of stiffeners and their attached plate.

The full implementation of this equation requires structural details that are not appropriate for a simplified analysis. In this study, based on a sampling of typical side shell scantlings, a simplified calculation is used where  $c_{FCA}$  is assumed to have a constant value of 0.025.

Since  $F_R$  also affects membrane tension energy, Equation 4.49 become:

$$\Delta KE_n = F_{hn} [(w_{n+1} - w_n) + 0.15 |l_{n+1} - l_n|] + F_R (l_{n+1} - l_n)$$

$$F_{hn} = \frac{(E_{1,n+1} + E_{2,n+1}) - (E_{1n} + E_{2,n}) - F_R (l_{n+1} - l_n)}{(w_{n+1} - w_n) + 0.15 |l_{n+1} - l_n|} \quad (4.52)$$

$$F_{xn} = (F_R + 0.15 F_{hn}) \frac{(l_{n+1} - l_n)}{|l_{n+1} - l_n|}$$

$$M_n = -F_{xn} d_n + F_{hn} l_n$$

The Internal Sub-Model determines absorbed energy and forces from the crushing and tearing of decks, bottoms and stringers (horizontal structures) in a much more simplified manner using the Minorsky correlation [9] as modified by Reardon and Sprung [15] provided by Equation 4.3.

Step 2, of Figure 75, in the SIMCOL collision simulation process calculates damaged area and volume in the struck ship given the relative motion of the two ships calculated in Step 1 by the External Sub-Model. Figure 81 illustrates the geometry of the sweeping segment method used for this calculation in SIMCOL Version 2.1.

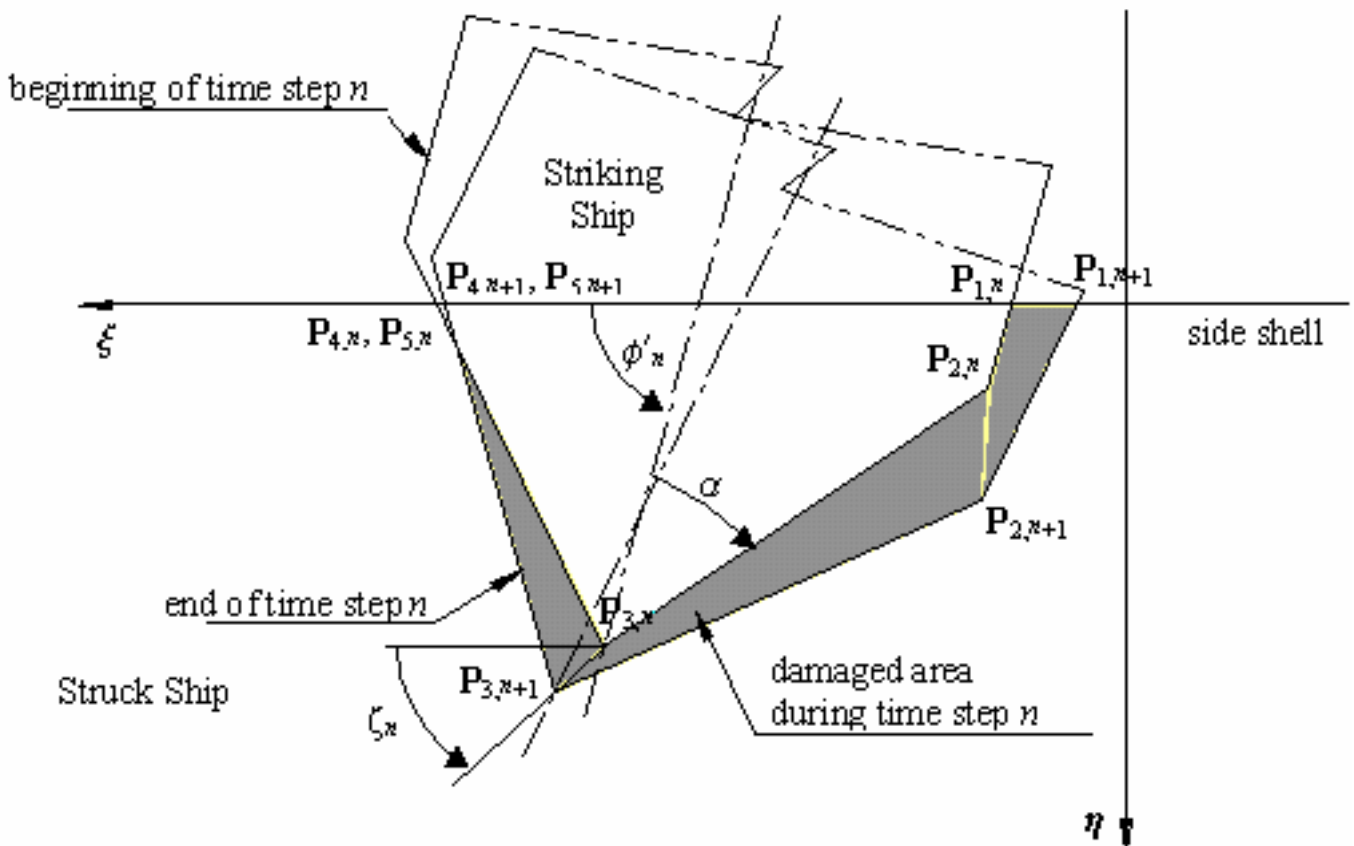


Figure 81 - Sweeping Segment Method

The intrusion portion of the bow is described with five nodes, as shown in Figure 81. The shaded area in Figure 81 is the new damaged area of decks and/or bottoms during the time step. Coordinates of the five nodes in the  $\xi$ - $\eta$  system at each time step are derived from the penetration and location of the impact, the collision angle,  $\phi$ , and the half entrance angle,  $\alpha$ , of the striking bow.

$\mathbf{P}_3$  is specified by the penetration and location of the striking ship relative to the struck ship:

$$\begin{aligned} \mathbf{P}_3 &= \{\mathbf{x}_3, \mathbf{h}_3\} = \{l, d\} \\ \mathbf{f}' &= \mathbf{p} - \mathbf{f} \end{aligned} \quad (4.53)$$

If the parallel body of the striking ship has not penetrated into the struck ship then:

$$\begin{aligned} \overline{\mathbf{P}_2\mathbf{P}_3} &\leq \frac{B_2}{2 \sin \alpha} \quad \text{or} \quad \overline{\mathbf{P}_3\mathbf{P}_4} \leq \frac{B_2}{2 \sin \alpha}, \quad \text{and} \\ \mathbf{P}_2 &= \{\xi_2, \eta_2\} = \left\{ \xi_3 - \frac{\eta_3}{\tan(-\alpha + \phi')}, 0 \right\} \\ \mathbf{P}_1 &= \{\xi_1, \eta_1\} = \mathbf{P}_2 \\ \mathbf{P}_4 &= \{\xi_4, \eta_4\} = \left\{ \xi_3 - \frac{\eta_3}{\tan(\alpha + \phi')}, 0 \right\} \\ \mathbf{P}_5 &= \{\xi_5, \eta_5\} = \mathbf{P}_4 \end{aligned} \quad (4.54)$$

If the parallel body of the striking ship has penetrated into the struck ship then:

$$\begin{aligned} \overline{\mathbf{P}_2\mathbf{P}_3} &> \frac{B_2}{2 \sin \alpha} \quad \text{or} \quad \overline{\mathbf{P}_3\mathbf{P}_4} > \frac{B_2}{2 \sin \alpha}, \quad \text{and} \\ \mathbf{P}_2 &= \{\xi_2, \eta_2\} = \left\{ \xi_3 - \frac{B_2}{2 \sin \alpha} \cos(-\alpha + \phi'), \eta_3 - \frac{B_2}{2 \sin \alpha} \sin(-\alpha + \phi') \right\} \\ \mathbf{P}_1 &= \{\xi_1, \eta_1\} = \left\{ \xi_2 - \frac{\eta_2}{\tan \phi'}, 0 \right\} \\ \mathbf{P}_4 &= \{\xi_4, \eta_4\} = \left\{ \xi_3 - \frac{B_2}{2 \sin \alpha} \cos(\alpha + \phi'), \eta_3 - \frac{B_2}{2 \sin \alpha} \sin(\alpha + \phi') \right\} \\ \mathbf{P}_5 &= \{\xi_5, \eta_5\} = \left\{ \xi_4 - \frac{\eta_4}{\tan \phi'}, 0 \right\} \end{aligned} \quad (4.55)$$

Where:

- $\mathbf{P}_i$  node of penetrated bow;
- $\mathbf{x}_i, \mathbf{h}_i$  coordinates of node in  $\xi$ - $\eta$  system (m); and
- $B_2$  breadth of the striking ship (m).

Once the node coordinates before and after the time step are calculated, the segment of the bow plan that has caused further damage during the time step and the area swept by a specific segment are determined. In the case of the segment  $P_1P_2$  in Figure 81, the out-sweeping area,  $A_1$ , during time step  $n$  is calculated as follows:

$$A_{1,n} = \frac{1}{2} \left( \begin{vmatrix} \mathbf{x}_{2,n} & \mathbf{x}_{1,n} \\ \mathbf{h}_{2,n} & \mathbf{h}_{1,n} \end{vmatrix} + \begin{vmatrix} \mathbf{x}_{2,n+1} & \mathbf{x}_{2,n} \\ \mathbf{h}_{2,n+1} & \mathbf{h}_{2,n} \end{vmatrix} + \begin{vmatrix} \mathbf{x}_{1,n+1} & \mathbf{x}_{2,n+1} \\ \mathbf{h}_{1,n+1} & \mathbf{h}_{2,n+1} \end{vmatrix} + \begin{vmatrix} \mathbf{x}_{1,n} & \mathbf{x}_{1,n+1} \\ \mathbf{h}_{1,n} & \mathbf{h}_{1,n+1} \end{vmatrix} \right) \quad (4.56)$$

The damaged plating thickness  $t$  is the sum thickness of deck, stringer and/or bottom structures that are in the upper and lower extents of the striking bow. Given the damaged material volume (area times thickness), the Minorsky force is calculated based on the following assumptions:

- The resistant force acting on each out-sweeping segment is in the opposite direction of the average movement of the segment. The force exerted on the struck ship is in the direction of this average movement.
- The work of the resistant force is done over the distance of this average movement.
- The total force on each segment acts through the geometric center of the sweeping area.

Using the Minorsky relation as modified by Reardon and Sprung, the energy absorbed by the sweeping segment  $P_1P_2$  is then:

$$\Delta KE_{1,n} = 47.1 \times 10^6 R_{T1,n} = 47.1 \times 10^6 A_{1,n} t \quad (4.57)$$

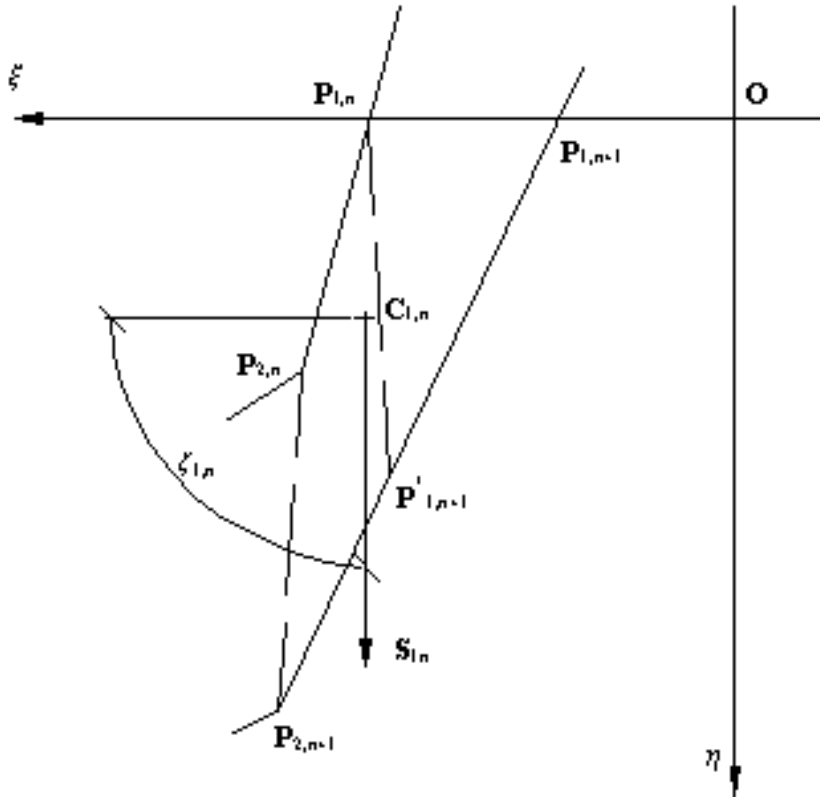


Figure 82 - Sweeping Segment Geometry

The average motion,  $\mathbf{S}_1$ , and the geometric center of the sweeping area,  $\mathbf{C}_1$ , for the segment  $\mathbf{P}_1\mathbf{P}_2$  in time step  $n$  are approximated as follows (Figure 81 and Figure 82):

Select  $\mathbf{P}_{1,n+1}^*$  on  $\mathbf{P}_{1,n+1}\mathbf{P}_{2,n+1}$ , so that  $\overline{\mathbf{P}_{1,n+1}^*\mathbf{P}_{2,n+1}} = \overline{\mathbf{P}_{1,n}\mathbf{P}_{2,n}}$

$$\begin{aligned}\mathbf{S}_{1,n} &= \frac{1}{2}(\mathbf{P}_{2,n}\mathbf{P}_{2,n+1} + \mathbf{P}_{1,n}\mathbf{P}_{1,n+1}^*) \\ &= \frac{1}{2}[\mathbf{P}_{2,n+1} - \mathbf{P}_{2,n} + (\mathbf{P}_{2,n+1} - \mathbf{P}_{1,n+1}) \frac{\overline{\mathbf{P}_{1,n}\mathbf{P}_{2,n}}}{\overline{\mathbf{P}_{1,n+1}\mathbf{P}_{2,n+1}}} - \mathbf{P}_{1,n}]\end{aligned}\quad (4.58)$$

$$\mathbf{C}_{1,n} = \frac{1}{4}(\mathbf{P}_{1,n} + \mathbf{P}_{2,n} + \mathbf{P}_{1,n+1} + \mathbf{P}_{2,n+1})$$

The force exerted through the segment  $\mathbf{P}_1\mathbf{P}_2$  on the struck ship,  $\mathbf{F}_{1,n}$ , and the moment to the origin of the local coordinate system,  $M_{1,n}$ , are then:

$$\begin{aligned}F_{1,n} &= |\mathbf{F}_{1,n}| = \frac{\Delta KE_{1,n}}{s_{1,n}} \\ \mathbf{F}_{1,n} &= \begin{pmatrix} F_{x1,n} \\ F_{h1,n} \end{pmatrix} = \begin{pmatrix} F_{1,n} \cos z_{1,n} \\ F_{1,n} \sin z_{1,n} \end{pmatrix} \\ M_{1,n} &= \mathbf{OC}_{1,n} \times \mathbf{F}_{1,n}\end{aligned}\quad (4.59)$$

Where  $s_{1,n} = |\mathbf{S}_{1,n}|$  and  $\zeta_{1,n}$  is the direction of  $\mathbf{S}_{1,n}$ .

Forces and moments acting on other segments are calculated similarly. The total exerted force,  $\mathbf{F}_n$ , is the sum of the forces and moments on each segment:

$$\mathbf{F}_n = \sum_{i=1}^4 \{F_{xi,n}, F_{hi,n}, M_{i,n}\} \quad (4.60)$$

These forces are added to the side shell, bulkhead and web forces.

Internal forces and moments are calculated for the struck ship in the local coordinate system, i.e. the  $\xi$ - $\eta$  system, and converted to the global system. The forces and moments on the striking ship have the same magnitude and the opposite direction from those on the struck ship.

The damage length,  $L_D$ , is:

$$L_D = \max(\mathbf{x}_{i,j}) - \min(\mathbf{x}_{i,j}) \quad i = 1, \dots, 5 \quad j = 1, \dots, m \quad (4.61)$$

Where  $m$  is the time step and the penetration is given by:

$$P_D = \max(\mathbf{h}_{i,j}) \quad i = 1, \dots, 5 \quad j = 1, \dots, m \quad (4.62)$$

Table 9 provides a summary of the modeling method used in SIMCOL Version 2.1 for each energy absorbing structure discussed in Section 2.4.

Table 9 - Energy Absorbing Structure Method Summary for SIMCOL

<b>Energy Absorbing Structure</b>	<b>Modelling Method</b>
Sideshell	Adapted Rosenblatt Method
Decks	Reardon and Sprung Energy Correlation with Sweeping Segment Method
Stringers	Reardon and Sprung Energy Correlation with Sweeping Segment Method
Longitudinal Bulkheads	Adapted Rosenblatt Method
Transverse Bulkheads	Treated as Rigid
Longitudinal Girders	Reardon and Sprung Energy Correlation
Transverse Girders	Reardon and Sprung Energy Correlation
Webs	Adapted Rosenblatt Method

#### 4.3.2.3 SIMCOL Probabilistic Damage Assessment

SIMCOL calculates probabilistic structural damage using a Monte Carlo simulation [35] with a probabilistic description of the accident scenarios as the primary input. This method uses a simplified collision scenario and striking ship input consistent with available collision scenario and world fleet data. The striking ship is described using a simplified wedge bow geometry [83] shown in Figure 81. SIMCOL also calculates a mean value of penetration, longitudinal extent of damage and oil outflow (discussed in Section 4.3.2.4).

#### 4.3.2.4 SIMCOL Simplified Probabilistic Oil Outflow Calculation

Current hypothetical outflow and tank size requirements for oil tankers are found in Regulations 22-24 of Annex I of MARPOL 73/78. Recognizing that these regulations do not actually assess the environmental performance of tankers, IMO instructed its BLG (Bulk Liquids and Gases) Sub-Committee to develop a new accidental oil outflow regulation modeled after the probabilistic methodology contained in the IMO Guidelines [4]. This new regulation will still not consider the crashworthiness of the structural design. One of the primary objectives of the SIMCOL project is to provide a methodology and model that does consider crashworthiness for potential application in future IMO regulations. The IMO Guidelines provide a probabilistic-based procedure for assessing the oil outflow performance of an alternative tanker design. The alternative design is compared to selected reference double hull design based on a pollution prevention index.

The IMO Guidelines present two procedures for evaluating the oil outflow. The “conceptual” method, applicable for conceptual design approval, assumes the ship survives the damage. For bottom damage, the ship is assumed to rest on the ground at its initial intact drafts, with zero trim and heel. The “survivability” method, applicable to final designs, requires damage stability calculations. For damage cases that fail to satisfy the specified survivability criterion, it is assumed that the ship is lost and 100% of all cargo oil onboard outflows to the sea.

A fully probabilistic evaluation of a specific vessel on a specific route would require development of the following probabilities:

- The probability that the ship will have a grounding or collision accident
- The conditional probability density function for damage location and extent;
- The expected consequences (i.e. quantity of outflow).

The IMO Guidelines do not specifically deal with the probability of whether the ship will have an accident. Rather, it is acknowledged that the risk exists, and it is assumed that the vessel is involved in a grounding or collision event significant enough to breach the outer hull. This is because data for accidents where the outer hull is not breached is rarely recorded. The resulting oil outflow is therefore conditional on an accident significant enough to breach the outer hull. The SIMCOL methodology is conditional only on a collision accident occurring. SIMCOL considers accidents that do not breach the outer hull. This better reflects the true crashworthiness of a structural design.

Rigorous application of the probabilistic oil outflow methodology contained in the IMO Guidelines is a calculation intensive effort based on an empirical description of damage extent and location. SIMCOL follows the basic steps of the IMO methodology, but assembles the damage cases using a Monte Carlo simulation with a probabilistic description of the accident scenarios as the primary input. The following steps are followed in the SIMCOL process:

#### Step 1: Assemble Damage Cases

For each collision case in the Monte Carlo simulation, SIMCOL calculates damage extent. Once collision damage calculations are completed, SIMCOL determines which cargo tanks have been penetrated and ruptured by comparing damage extents to cargo tank subdivision boundaries specified in the SIMCOL input. In addition to depth and length of penetration, SIMCOL also flags when a tank boundary is ruptured. It is assumed in side damage that if a tank is penetrated and ruptured, its entire contents are spilled. The volume of oil in each tank is specified in the SIMCOL input. For a specified collision case, SIMCOL sums the outflow from all ruptured tanks to determine the total outflow for the case.

#### Step 2: Calculate Oil Outflow

Consistent with the IMO analysis approach, 100% outflow for all cargo tanks sustaining side damage is assumed.

#### Step 3: Calculate Oil Outflow Parameters

- The *probability of zero outflow*,  $P_0$ , represents the likelihood that no oil will be released into the environment, given a collision or grounding accident.  $P_0$  equals the cumulative probability of all damage cases without outflow.
- The *mean outflow parameter*,  $O_M$ , is the non-dimensionalized mean or expected outflow, and provides an indication of a design's overall effectiveness in limiting oil outflow. The mean outflow equals the sum of the products of each damage case probability and the associated outflow.  $O_M$  equals the mean outflow divided by the total quantity of oil onboard the vessel.
- The *extreme outflow parameter*,  $O_E$ , is the non-dimensionalized extreme outflow, and provides an indication of the expected oil outflow from particularly severe casualties. The extreme outflow is the weighted average of the upper 10% of all casualties (i.e. all damage cases in the cumulative probability range from 0.9 to 1.0).

#### Step 4: Compute the Pollution Prevention Index

The Pollution Prevention Index is calculated as in the IMO Guidelines.

Alternative designs are compared to reference double hull designs by substituting the outflow parameters for the reference design and the alternative design into the following formula:

$$E = \frac{(0.5)(P_0)}{P_{OR}} + \frac{(0.4)(0.01 + O_{MR})}{0.01 + O_M} + \frac{(0.1)(0.025 + O_{ER})}{0.025 + O_E} \quad (4.63)$$

$P_0$ ,  $O_M$ , and  $O_E$  are the oil outflow parameters for the alternative design, and  $P_{OR}$ ,  $O_{MR}$ , and  $O_{ER}$  are the oil outflow parameters for the IMO reference ship of equivalent size.

#### 4.4 Summary of Simplified Methods

Table 10 provides a summary of the applicability of each simplified method discussed in Chapter 4 with respect to the criteria set forth in Section 2.4.

Table 10 - Simplified Method Summary

	Method	Energy Coefficient	Ahmdahl (cruciform)	Pedersen Empiracle	DAMAGE	DTU	SIMCOL version 2.1
	Post Collision Momentum	No	No	No	No	Yes	Yes
	Struck Ship Forward Velocity	No	No	No	No	Yes	Yes
	Oblique Angle Collisions	No	No	No	No	Yes	Yes
	Deformable Bow	No	Yes	Yes	No	Yes	No
	Longitudinal Extent of Damage	No	No	No	No	Limited	Limited
	Low Computational Cost	Yes	No	Yes	Yes	Yes	Yes
	Coupled Internal Mechanics and External Dynamics	No	No	No	No	No	Yes
8 Critical Energy Absorbing Structures	Sideshell	Yes	Yes	Yes	Yes	Yes	Yes
	Longitudinal Bulkheads	Yes	Yes	Yes	Yes	Yes	Yes
	Structural Decks	Yes	Yes	Yes	Yes	Yes	Yes
	Stringers	Yes	Yes	Yes	Yes	Yes	Yes
	Web Frames	Yes	No	No	Yes	Yes	Yes
	Transverse Bulkheads	Yes	No	No	No	No	No
	Longitudinal Girders	Yes	Yes	Yes	Yes	Yes	Yes
	Transverse Girders	Yes	No	No	Yes	Yes	Yes

As Table 10 shows, the two most promising simplified analysis methods for ship-to-ship collisions are the DTU model discussed in Section 4.3.1 and SIMCOL Version 2.1 discussed in Section 4.3.2. The DTU model is based on a super element formulation that has the advantages of the cruciform approximations and experiments performed by Amdahl [23] and Wierzbicki [20]. However, the internal mechanics and the external dynamics of the analysis are uncoupled and the formulation of the structural input does not allow for an easy manipulation of the method for use in optimization or response surface generation, as does SIMCOL.

SIMCOL, as it is in Version 2.1, is limited in its application necessitating several updates and corrections in order to achieve the desired level of performance as set out in Section 2.4 or as required to fulfill the objectives of the IMO as discussed in Chapter 1. These improvements include a complete method of determining the longitudinal extent of damage through bulkheads and transverse structure and a method for evaluating a deformable bow. Chapter 5 discusses these improvements and inclusions in SIMCOL while creating SIMCOL Version 3.0.

## CHAPTER 5 SIMCOL Version 3.0

SIMCOL Version 3.0 includes four minor and one major improvement from Version 2.1. The minor improvements are as follows and are discussed thoroughly in Sections 5.1 through 5.4. The minor improvements are:

- Modification of the energy coefficient method used for the treatment of structural decks and stringers.
- Treatment of longitudinal crushing of longitudinal bulkheads through the use of an energy coefficient method
- Treatment of transverse crushing of transverse bulkheads through the use of an energy coefficient method
- Inclusion of a deformable wedge bow model through the use of Pedersen's empirical bow crushing model

The major improvement to SIMCOL is the inclusion of a method for the determination of the energy absorbed through the non-uniform longitudinal deflection of transverse bulkheads and webs, which is a necessity whenever the longitudinal extent of damage is to be accurately determined. The method of determining of the energy absorbed through the non-uniform longitudinal deflection of transverse bulkheads and webs is discussed in Section 5.4.

Again, from Section 2.4, the majority of the energy absorbed by damage to structure in a ship-to-ship collision is absorbed by the following eight structural members; side shell, longitudinal bulkheads, decks, stringers, web frames, transverse bulkheads, longitudinal girders and transverse girders. Section 5.1 discusses methods of energy absorption by the decks and stringers and Sections 5.2 and 5.4 discuss methods of energy absorption by the side shell, longitudinal bulkheads, web frames and transverse bulkheads. The energy absorbed by longitudinal and transverse girders is calculated and determined through the methods of SIMCOL 2.1 (Section 4.3.2).

### **5.1 Energy Coefficient Method for use with Structural Decks and Stringers**

SIMCOL Version 2.1 makes use of the Reardon and Sprung [15] energy coefficient as described in Section 4.1 by Equation 4.3. However, the Reardon and Sprung energy coefficient formulation was developed for a T-bone collision with a statistical damage volume method of determining energy absorption. With this method, the mode of damage (i.e. crushing and folding or cutting and tearing) is not important. The Reardon and Sprung energy coefficient (Equation 4.3) is not sensitive to specific structure or the damage modes of the structure such as crushing shown in Figure 83 and combined modes of crushing, folding and tearing as seen with decks and stringers in actual collisions or finite element simulations, Figure 84 through Figure 87.

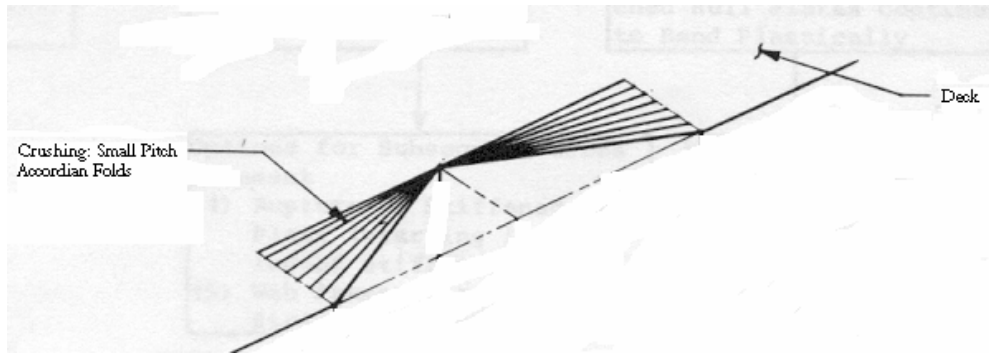


Figure 83 - Deck Crushing Showing Accordion Folding [21]

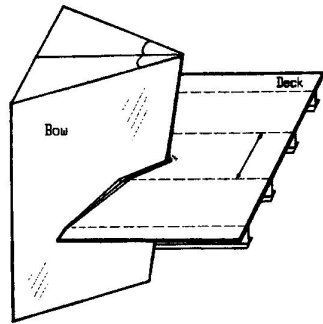


Figure 84 - Deck Crushing Showing Bow Impingement [21]

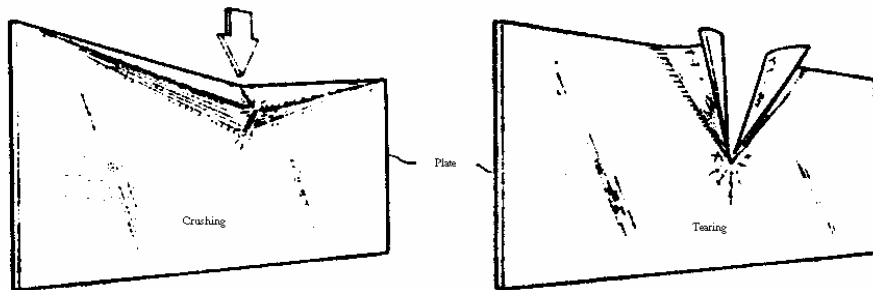


Figure 85 - Plate Crushing vs. Tearing (Cutting) [21]

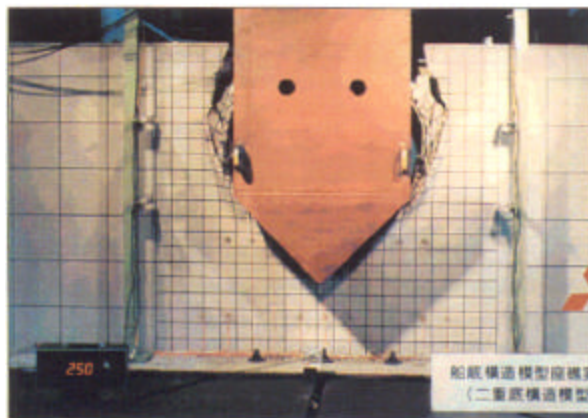


Figure 86 - Rigid Wedge Cutting and Crushing Deck in Drop Test [89]

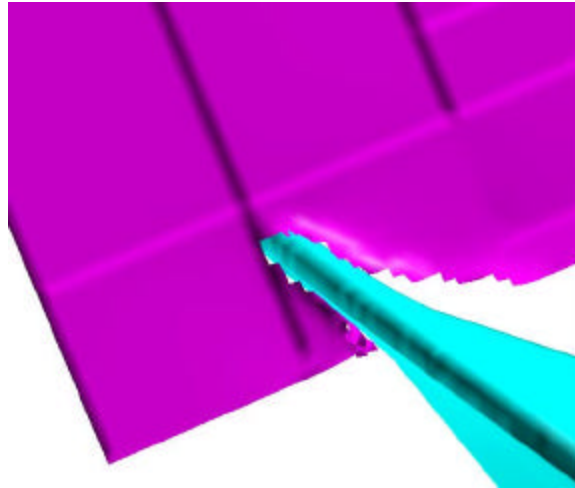


Figure 87 - FEA Deck Cutting and Crushing

An investigation of the Reardon and Sprung and Paik and Pedersen [29] energy coefficient methods, Equations 4.9 and 4.10, was performed to determine which method most accurately captures the energy absorption of decks and stringers when involved in collision. Paik and Pedersen's methods separate the differing types of structure (decks, bulkheads etc.) and modes of damage (crushing, tearing, etc.) and thus may be more applicable for the determination of energy absorption by different structural designs.

The theory of Reardon and Sprung and Paik and Pedersen for crushing, folding or tearing of deck structure is compared to finite element results for a rigid wedge striking the top deck structure of a 150k dwt double hull oil tanker, where the deck, the supporting transverse deck frames, and longitudinal girders are included as shown in Figure 88. The rigid wedge has a mass of  $1.0E+06$  kg and is given a forward velocity of 5 m/s. The deck structure is described in Table 11.

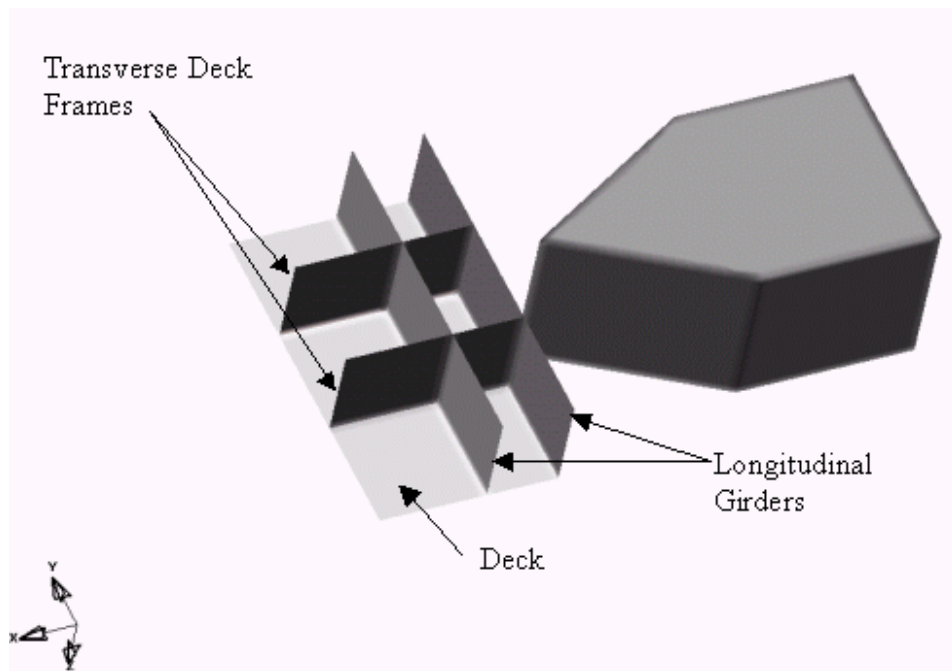


Figure 88 FEA Simplified Deck Crushing and Cutting Test Model

Table 11 - FEA Simplified Deck Crushing and Cutting Test Parameters

Deck Length	9.9 m
Deck Width	5.0 m
Deck Thknss (stiffeners smeared)	31.4 mm
Tr. Deck Frame Depth	3.0 m
Tr. Deck Frame Thknss (flange smeared)	15.0 mm
Outer Long. Girder Depth	3.0 m
Outer Long. Girder Thknss (stiffeners smeared)	23.3 mm
Inner Long. Girder Depth	3.0 m
Inner Long. Girder Thknss (stiffeners smeared)	23.0 mm
Tr. Deck Frame Spacing	3.3 m
Long. Girder Spacing	2.0 m

The forward and aft most edges of the deck structure are simply supported (free only to rotate) while the edge opposite of the impacted edge is clamped (no translation and no rotation). The finite element model uses Belytschko-Tsay shell elements with a uniform mesh size of 250 mm. The deck material is modeled with a Piecewise Linear Plasticity model for steel representing ABS Gr. B with parameters given in Table 8. Analysis with the Finite Element model is performed by substituting nodal constraints on the deck in the z translation and the rotation about the y axis at the intersection for the transverse webs. Additionally, the longitudinal girders are replaced with nodal constraints on the deck in the z translation and rotation about the x axis along the intersection. Replacing the physical structure of the transverse deck frames and longitudinal girders with nodal constraints allows an independent determination of the energy absorbed through the deck plate alone to be evaluated. This is necessary for consistent application with the other models in SIMCOL. The nodal constraints avoid double counting the deformation energy of the webs and longitudinal supports. Friction is assessed through the use of coulomb friction, Equation 3.7 and is representative of mild steel on steel.

The finite element model is run three times. Each iteration uses a different rigid wedge half entrance angle (HEA) specifically HEA = 30, 45 and 60 degrees. Representative deformation of the deck structure is shown in Figure 89 through Figure 93 for the analysis with HEA = 30 degrees.

Comparative results between the theory for crushing or tearing of deck structure using the Reardon and Sprung formulation (Equation 4.3) and the finite element analysis are provided in Figure 94. Comparative results between the theory for crushing or tearing of deck structure using the Paik and Pedersen formulation without strain rate effects (Equation 4.9) and the finite element analysis are provided in Figure 94 through Figure 96. Finally, comparative results between the theory for crushing or tearing of deck structure using the Paik and Pedersen formulation with strain rate effects (Equation 4.10) and the finite element analysis are again provided in Figure 94.

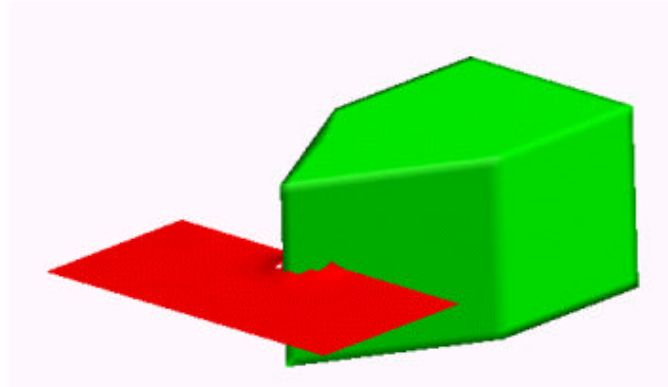
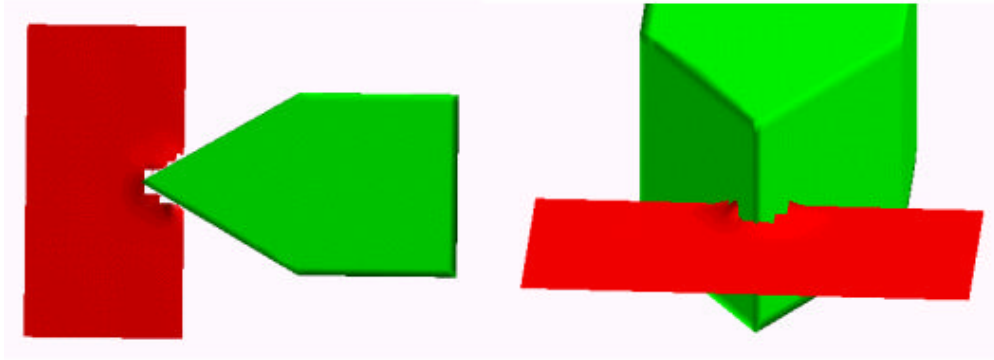


Figure 89 - FEA Deck Crushing and Tearing with HEA = 30 Degrees at 0.5 Seconds

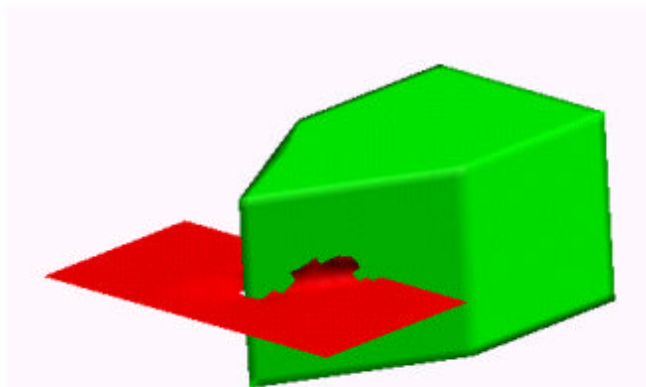
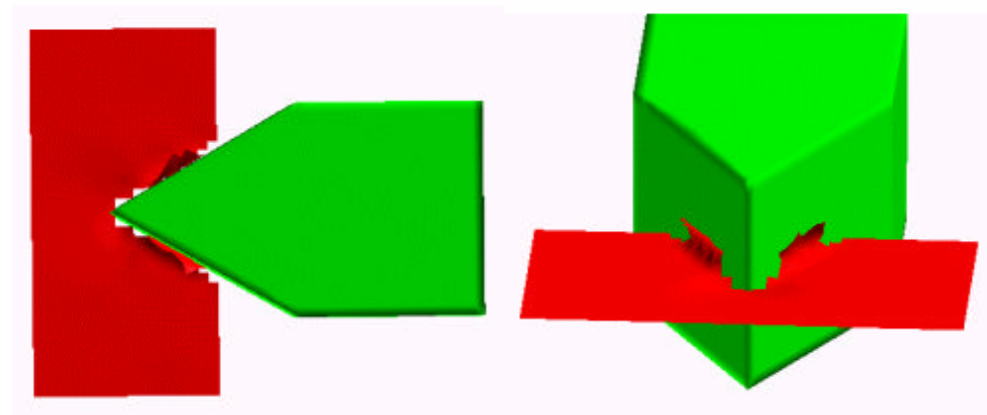


Figure 90 - Deck Crushing and Tearing with HEA = 30 Degrees at 1.0 Seconds

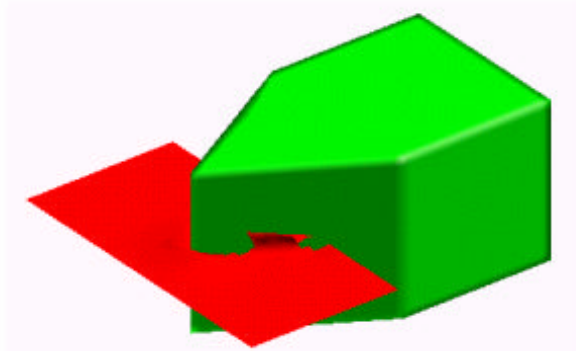
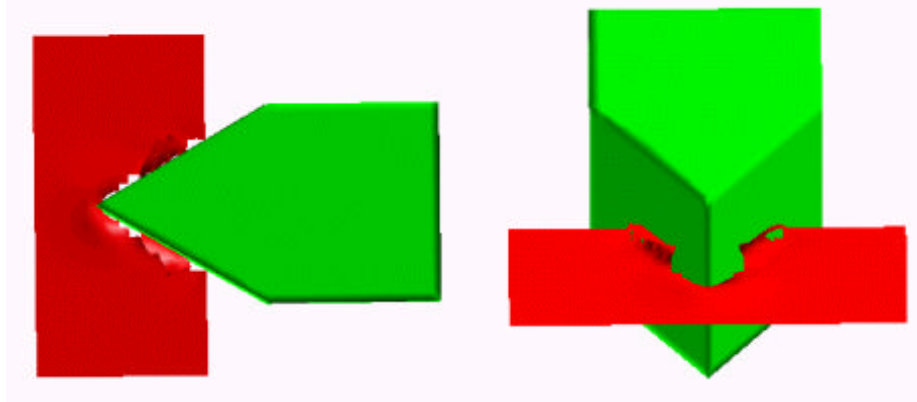


Figure 91 - Deck Crushing and Tearing with HEA = 30 Degrees at 1.5 Seconds

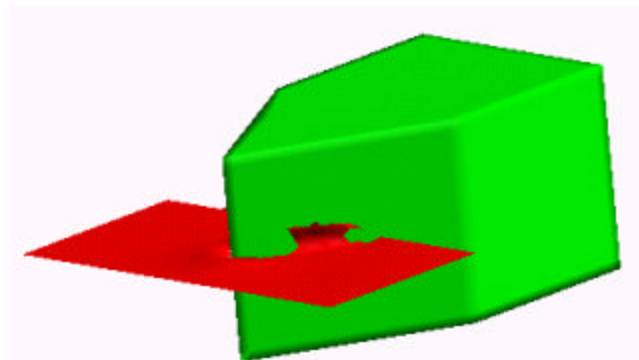
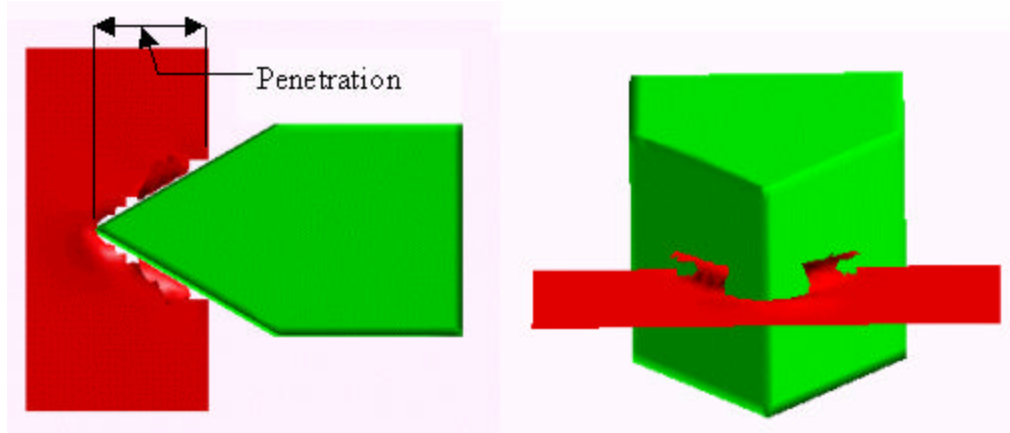


Figure 92 - Deck Crushing and Tearing with HEA = 30 Degrees at 2.0 Seconds

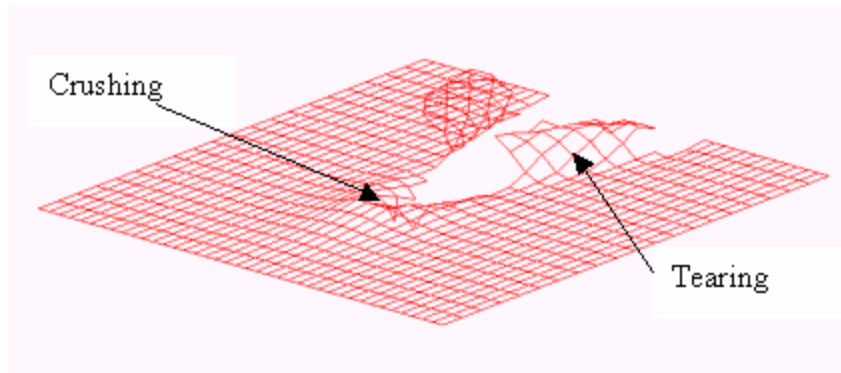


Figure 93 FEA Plate Mesh Showing Crushing and Tearing at 2.0 Seconds from HEA = 30 Degrees

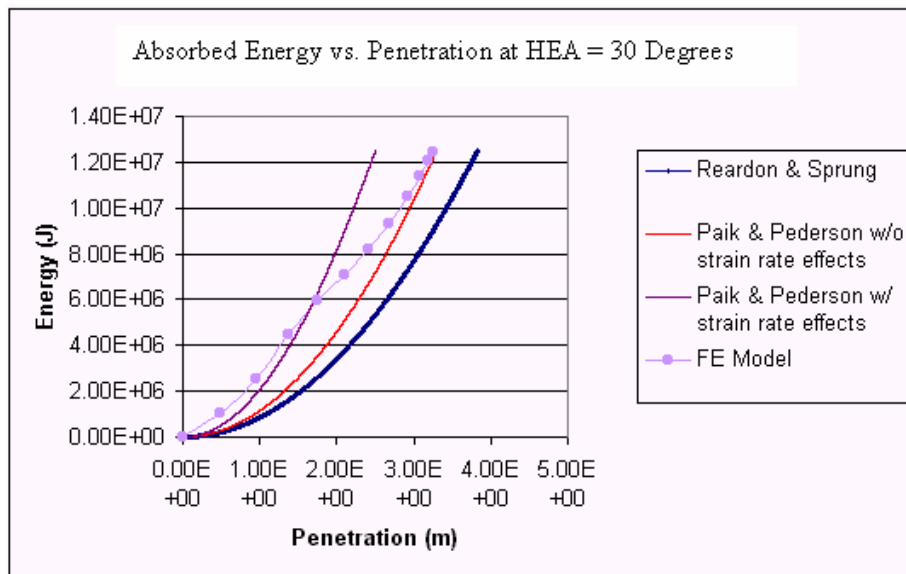


Figure 94 - Absorbed Energy vs. Penetration at HEA = 30 Degrees

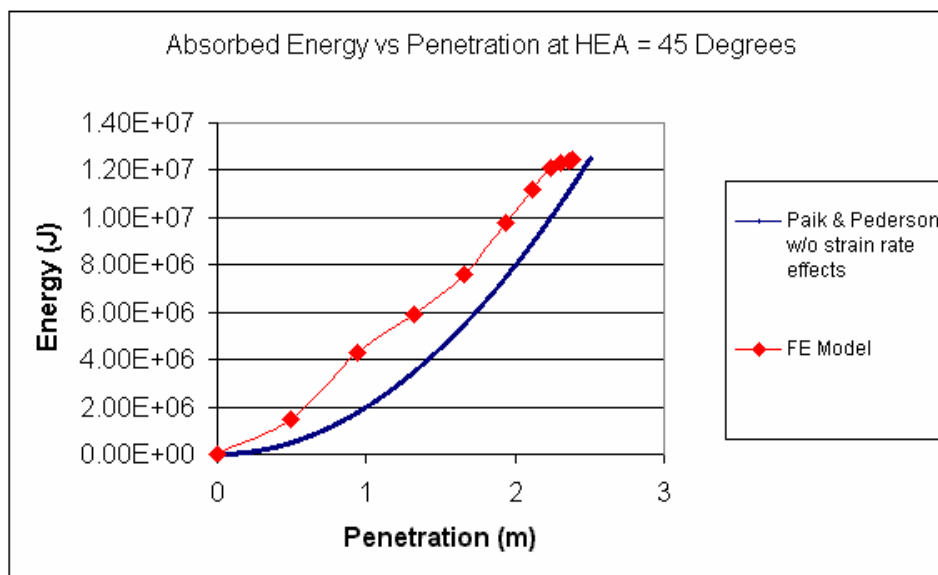


Figure 95 - Absorbed Energy vs. Penetration at HEA = 45 Degrees

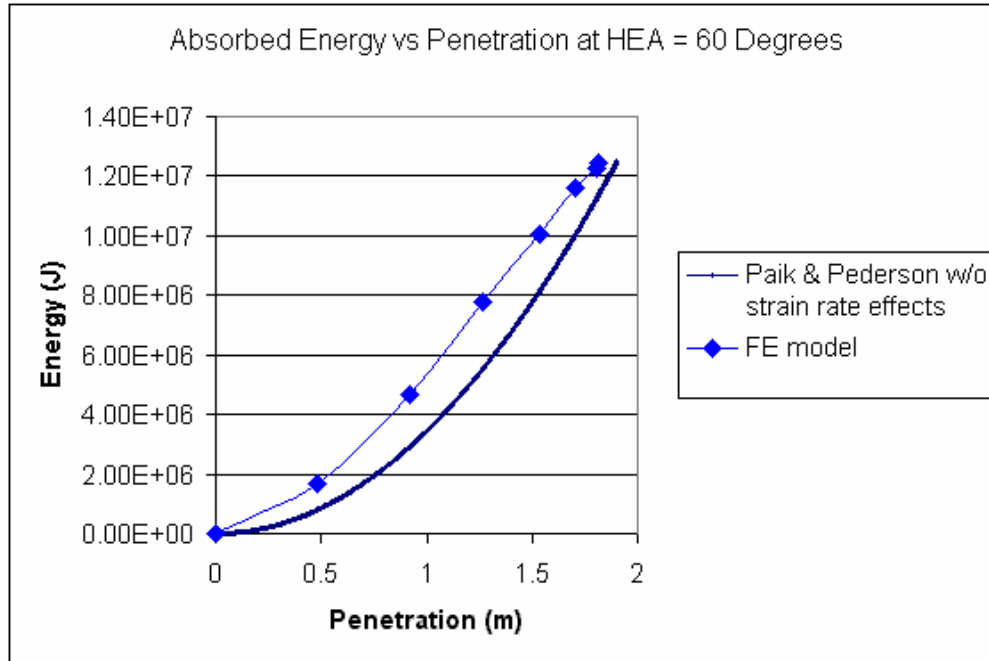


Figure 96 - Absorbed Energy vs. Penetration at HEA = 60 Degrees

All analyses are run until the initial kinetic energy of the striking rigid bow is absorbed (1.25E+07 Joules). Therefore, the determination of the best method is based on a correlation coefficient between the finite element results and the energy coefficient method. Determination of the correlation coefficient (or average error) is calculated in Equation 5.1 where a correlation coefficient of 1 means perfect correlation.

$$R = \frac{\sum_{i=1}^N \left( 1 - \frac{FE_i - T_i}{FE_i} \right)}{N} \quad (5.1)$$

Where:

**FE<sub>i</sub>** value of finite element ordinate

**T<sub>i</sub>** value of energy coefficient (or other method) ordinate

**N** number of abscissa data points

Table 12 provides the correlation results of all tests at HEA = 30 degrees.

Table 12 - Correlation of Energy Coefficient Methods to FEA at HEA = 30 Degrees

Method	R (HEA = 30)
Reardon & Sprung	0.683
Paik & Pedersen w/o strain rate effects	0.779
Paik & Pedersen w/ strain rate effects	0.658

At an HEA of 45 and 60 degrees the correlation coefficients for the Paik and Pedersen formulation without strain rate are 0.77 and 0.82 respectively. As shown by Table 12 the most appropriate energy coefficient method (of those tested) for use in SIMCOL Version 3.0 for the

determination of the energy absorbed by structural decks and stingers is Paik and Pedersen's formulation without strain rate effects as given by Equation 4.9. Additionally, Paik and Pedersen's formulation without strain rate effects is more conservative than the Paik and Pedersen's formulation with strain rate effects.

## **5.2 Energy Coefficient Method for use with Longitudinal and Transverse Bulkheads and Longitudinal Crushing of Side Shell**

Because of the simplicity of the energy coefficient methods, the use of one of these methods for the damage sustained to longitudinal bulkheads subject to an axial or longitudinal force and to transverse bulkheads subject to a transverse force is desired. As shown by Figure 97 and Figure 98 of actual and finite element simulation damage to transverse and longitudinal bulkheads subjected to an axial (parallel to bulkhead) load the use of a crushing energy coefficient mechanism is most appropriate.

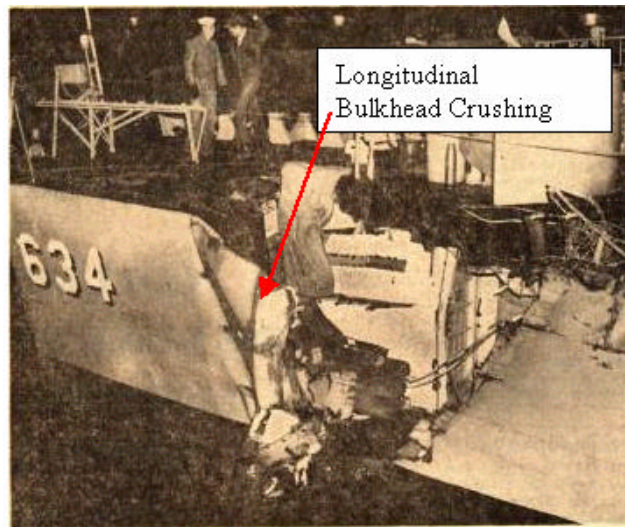


Figure 97 - Actual Longitudinal Bulkhead Crushing

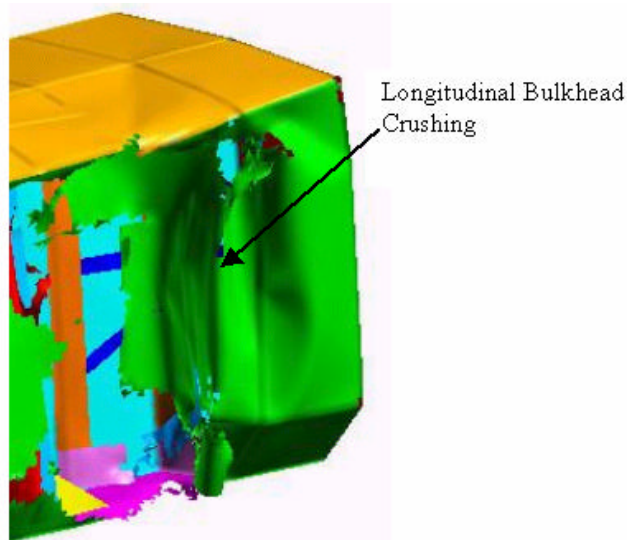


Figure 98 - FEA Example of Longitudinal Bulkhead Crushing

An investigation of the Reardon and Sprung and Pedersen and Zhang [14] energy coefficient methods is performed to determine which method most accurately captures the energy absorption of crushed bulkheads in ship collisions.

The models for crushing of longitudinal and transverse bulkheads are compared to finite element results of a rigid box striking the side shell structure of a 150k dwt double hull oil tanker, where the side shell, the supporting web frames, and stringers are included as shown in Figure 99. The rigid box has a mass of  $3.0E+06$  kg, a height of 17.475 m and is given a forward velocity of 5 m/s. The side shell structure is described Table 13.

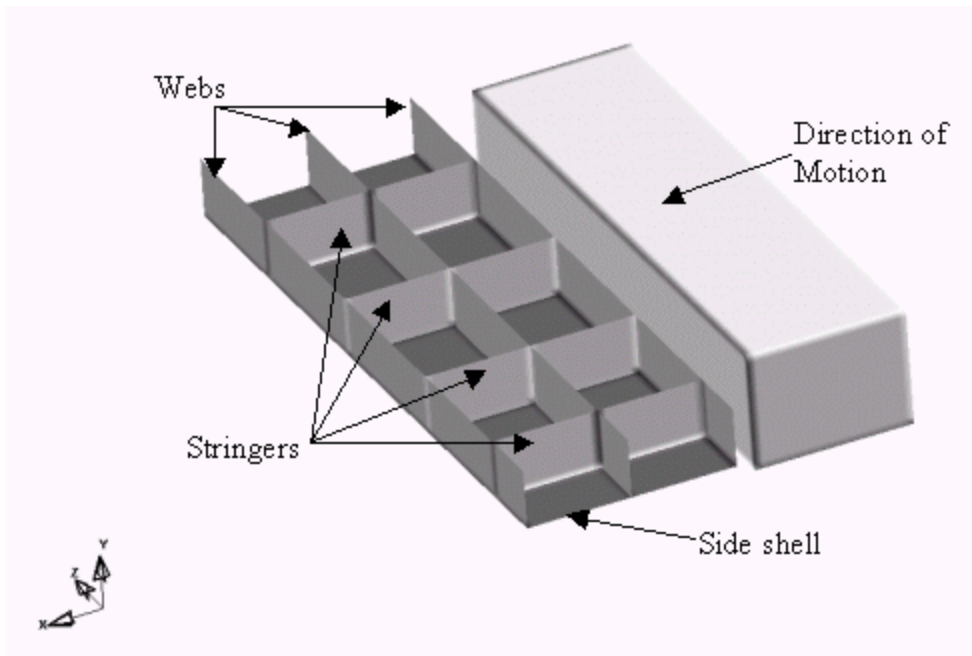


Figure 99 Simplified Longitudinal/Transverse Bulkhead Crushing Model

Table 13 - Simplified Longitudinal/Transverse Crushing Parameters

Sideshell Height	20.50 m
Sideshell Length	6.60 m
Sideshell Thknss (stiffeners smeared)	23.25 mm
Web Frame Depth	2.00 m
Web Frame Thknss	15.00 mm
Stringer Depth	2.00 m
Stringer Thknss	11.70 mm
Web Frame Spacing	3.30 m
First Stringer Height above bottom of Sideshell	1.95 m
Second Stringer Height above bottom of Sideshell	6.20 m
Third Stringer Height above bottom of Sideshell	11.30 m
Fourth Stringer Height above bottom of Sideshell	16.40 m

The upper and lower most edges of the side shell structure are simply supported while the edge opposite of the impacted edge is fixed. The finite element model uses Belytschko-Tsay shell elements with a uniform mesh size of 250 mm. The material of the deck structure is modeled with a Piecewise Linear Plasticity model for steel representing ABS Gr. B with parameters given in Table 8. Analysis of the Finite Element model is performed by eliminating the web frames and

substituting the structure with nodal constraints on the sideshell in the y translation and the rotation about the x axis at the intersection. Additionally, the stringers are replaced with nodal constraints on the deck in the y translation and rotation about the z axis along the intersection. Again, the purpose for replacing the physical structure of the webs and stringers is to independantly determine the energy absorbed only through the side shell plate. Friction is assessed through the use of coulomb friction, Equation 3.7 and is representative of mild steel on steel.

The finite element model is run once. Representative damage is shown in Figure 100 through Figure 103.

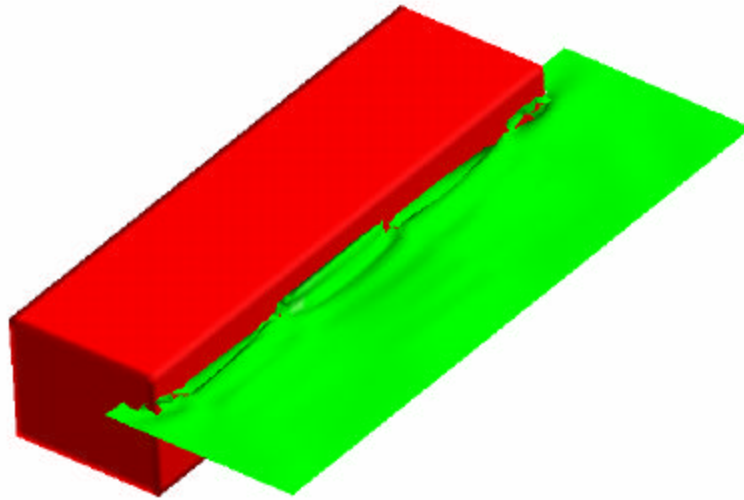


Figure 100 - Bulkhead Crushing at 0.5 Seconds

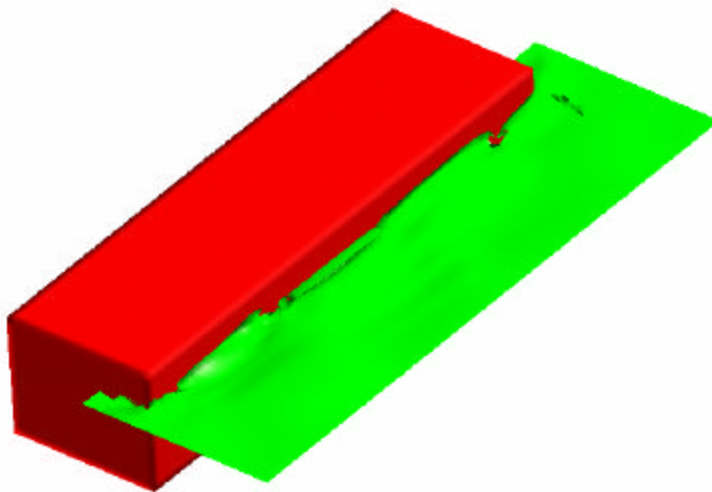


Figure 101 - Bulkhead Crushing at 1.0 Seconds

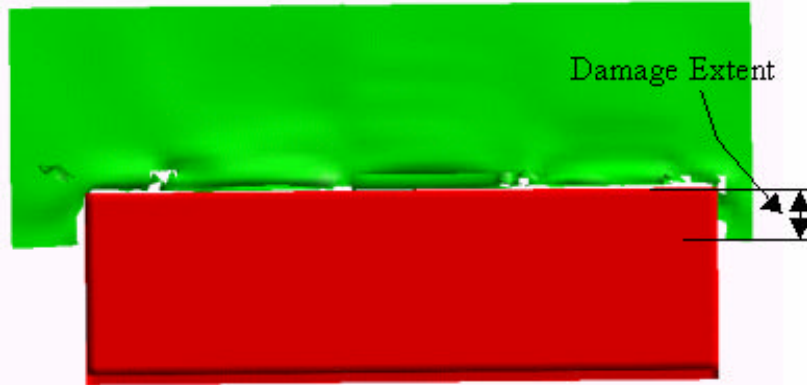


Figure 102 - Bulkhead Crushing at 1.5 Seconds

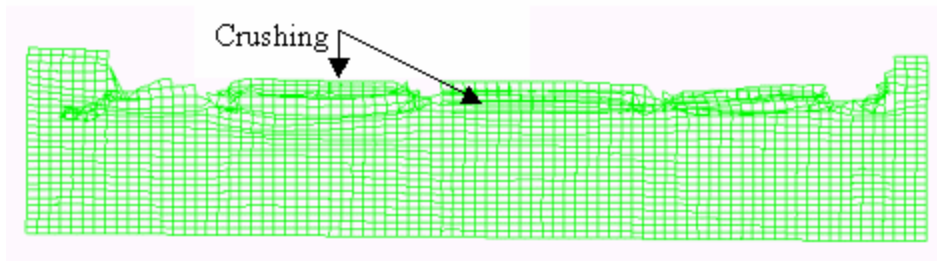


Figure 103 - Bulkhead Mesh Crushing at 1.5 Seconds

Comparative results between the theory for crushing bulkheads using the Reardon and Sprung formulation (Equation 4.3) and the finite element analysis are provided in Figure 104 through Figure 106. Comparative results between the theory for crushing bulkheads using the Pedersen and Zhang formulation (Equation 4.7) and the finite element analysis are also provided in Figure 104 through Figure 106.

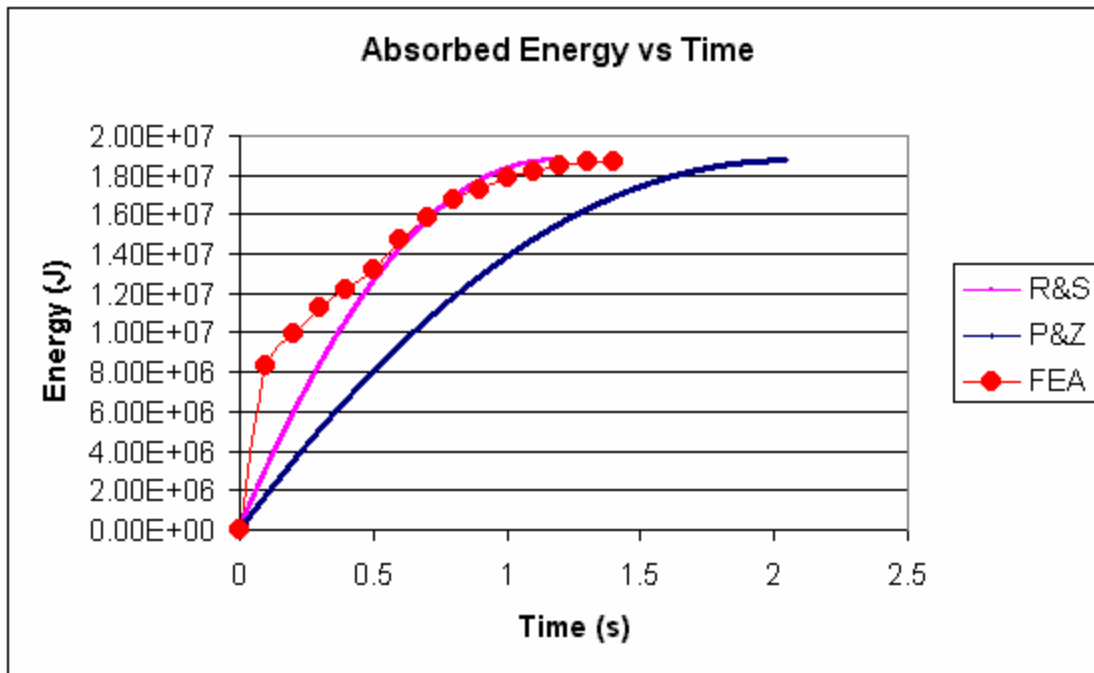


Figure 104 - Absorbed Energy vs. Time for Crushing of Bulkheads

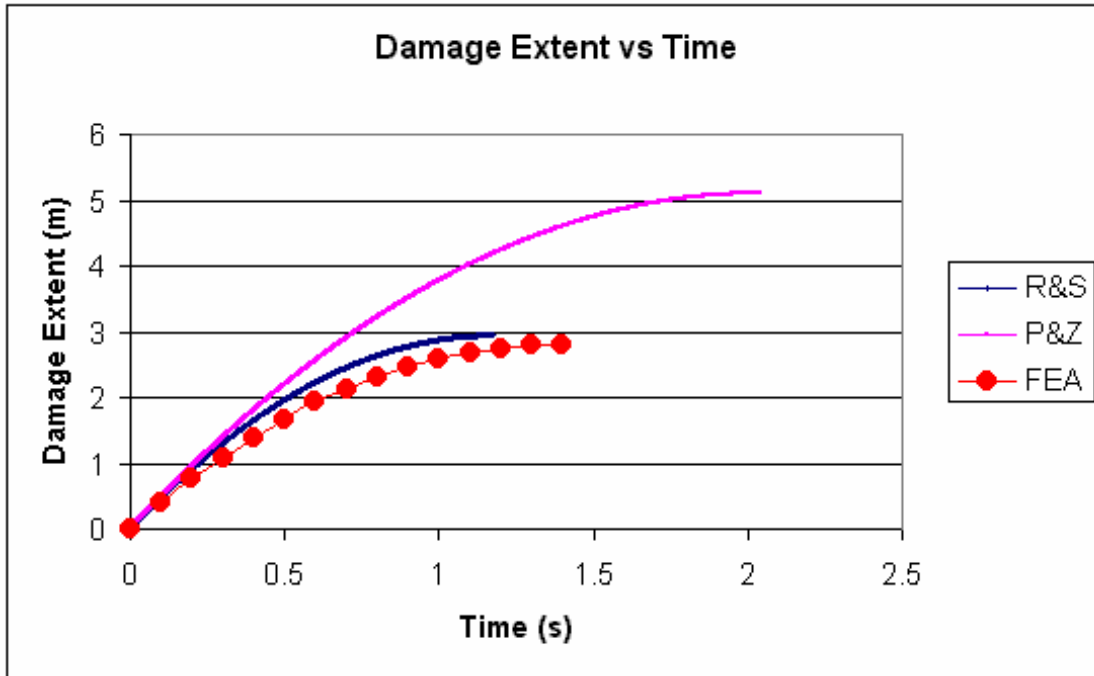


Figure 105 - Damage Extent vs. Time for Bulkhead Crushing

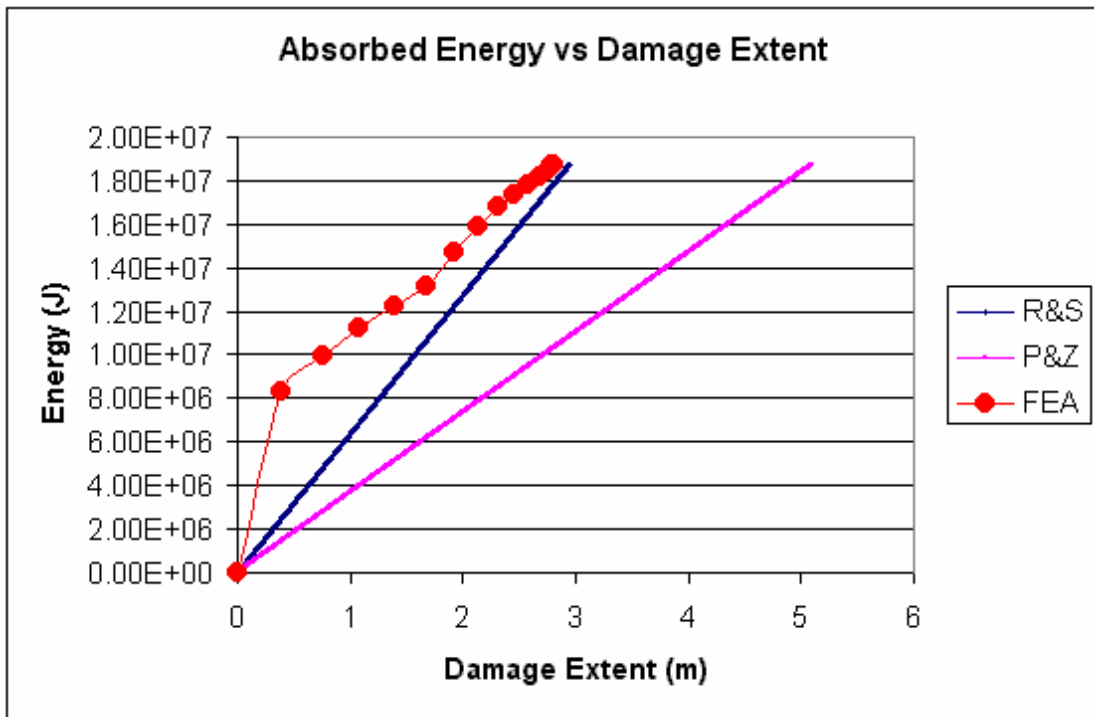


Figure 106 - Absorbed Energy vs. Damage Extent for Bulkhead Crushing

All analyses are run until the initial kinetic energy of the striking rigid box structure is absorbed ( $1.91E+07$  Joules). The determination of the best method is again based on a correlation coefficient of the absorbed energy between the finite element results and the energy coefficient methods. The correlation coefficient is calculated using Equation 5.1. Table 14 provides the correlation results for all tests.

Table 14 - Correlation Results of Energy Coefficient Methods for Bulkhead Crushing

Method	R
Reardon & Sprung	0.869
Pedersen & Zhang	0.459

As shown by Table 14 the most appropriate energy coefficient method (of those tested) for use in SIMCOL Version 3.0 in the determination of energy absorbed by crushing longitudinal and transverse bulkheads is the Reardon and Sprung formulation as given by Equation 4.3.

### 5.3 Deformable Bow Model

SIMCOL Version 3.0 incorporates a deformable bow sub-module that is based on a comparative energy and force method. The energy required to crush the bow normal to the course of the struck ship is compared to the lateral resistive absorbed energy (normal to the side shell of the struck ship) due to the penetration of the striking ship into the struck ship. The lesser energy determines which vessel will sustain damage in the amount of the relative bow motion in the time step (as discussed in Section 2.4). If the energy to crush the bow is less, then the striking ship is not moved or geometrically deformed in the time step. The force due to crushing the bow is applied to both vessels and the energy due to crushing the bow in the time step is added to the total energy absorbed in the collision. The time step is then cycled. The force and energy required to crush the bow is determined using Pedersen's method as discussed in Section 4.2.2 because of its relative simplicity in application while maintaining a reasonable degree of accuracy as shown in Figure 107. Figure 107 compares Pedersen's method (Appendix I) to that of Amdahl's method (Appendix H) for the bow of a 150k dwt bulk carrier described in Appendix A. The initial kinetic energy of the striking ship ( $E_0$ ) is given by Equation 5.2. SIMCOL assumes a maximum service vessel speed ( $V_s$ ) of 16 knots in the Pedersen equation for all striking ships. The crush force per damage length of the bow is given by Equation 5.3 where a simple half sine wave is assumed.

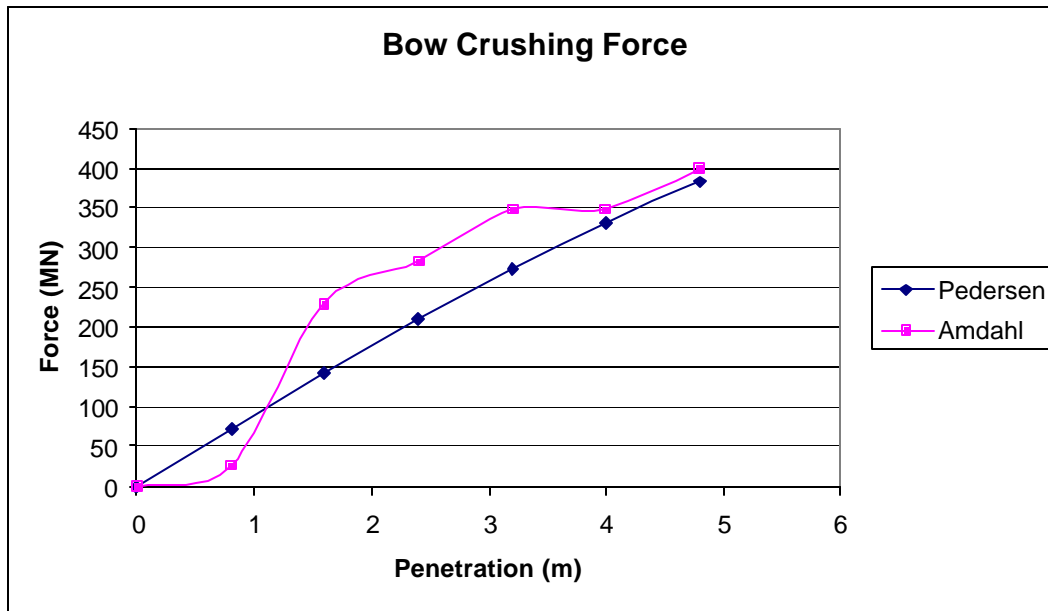


Figure 107 - Crushing Force vs. Penetration for Bulk Carrier Striking Wall at 90 Degrees

$$E_0 = \frac{1}{2} \cdot (1 + c_{11}) \cdot M_{sis} \cdot V_s^2 \quad (5.2)$$

$$F_{bow} = \sin\left(\frac{\pi \cdot x}{2 \cdot s_{max}}\right) \cdot P_{bow} \quad (5.3)$$

Where:

- $E_0$  is the assumed kinetic energy of the striking ship;
- $c_{11}$  is the added mass coefficient in surge (0.05);
- $M_{sis}$  is the displaced mass of the striking ship;
- $V_s$  is the maximum service speed of the striking vessel (16 knots);
- $F_{bow}$  is the crushing force of the bow;
- $x$  is the crush distance parallel to the striking ships centerline;
- $s_{max}$  is the maximum crush distance of the bow (Equation 4.16);
- $P_{bow}$  is the maximum crushing force of the bow (Equation 4.15).

Pederson's method accounts for the effect of strain rate, impact velocity, vessel loading condition, and vessel size for merchant vessels between 500 DWT and 300,000 DWT. Not included in Pederson's method are the effects of eccentric impacts (oblique angle impacts). In SIMCOL, only the right angle components of the forces are compared retaining the applicability of Pederson's method to the oblique angle cases in SIMCOL.

#### **5.4 Longitudinal Deflection of Transverse Bulkheads and Webs**

This section presents the most significant and substantial contribution of this report. A definitive theory does not exist for the determination of the energy absorbed through the longitudinal deflection of transverse bulkheads or webs. However, in a ship-to-ship collision, where the struck ship has forward speed or the collision occurs at an oblique angle, the striking ship both penetrates into the struck ship and crushes transverse structure longitudinally, parallel to the struck ship centerline and at a right angle to the transverse structure. This damage along the length of the struck ship increases the longitudinal extent of damage while absorbing additional energy and providing a resistive force on the striking ship. In this longitudinal damage, energy is absorbed via two mechanisms; 1) the longitudinal crushing of longitudinal bulkheads as discussed in Section 5.2 and 2) the longitudinal deformation of webs and transverse bulkheads. The non-uniform longitudinal or lateral deflection of transverse bulkheads and webs is shown in Figure 108 through Figure 110 where the deformation of the bulkheads and webs is seen to match the geometry of the striking vessel as discussed in Section 2.4.

The energy absorbed through the lateral deformation of webs and/or transverse bulkheads is determined using a plastic membrane energy approach that is derived in detail in Sections 5.4.1 through 5.4.5. The following simplified description is provided as an introduction to the method. This simple example assumes that the striking ship does not contact the internal plate boundaries.

Any transverse bulkhead or web (or primary transverse structure such as transverse girders) may be idealized as a plate of uniform properties with the edges bound by some constraints, (simply supported or free) as shown in Figure 111. The outboard shell of the ship (RS) is considered a longitudinal bulkhead in this analysis.



Figure 108 - Actual Longitudinally Deformed Web [89]

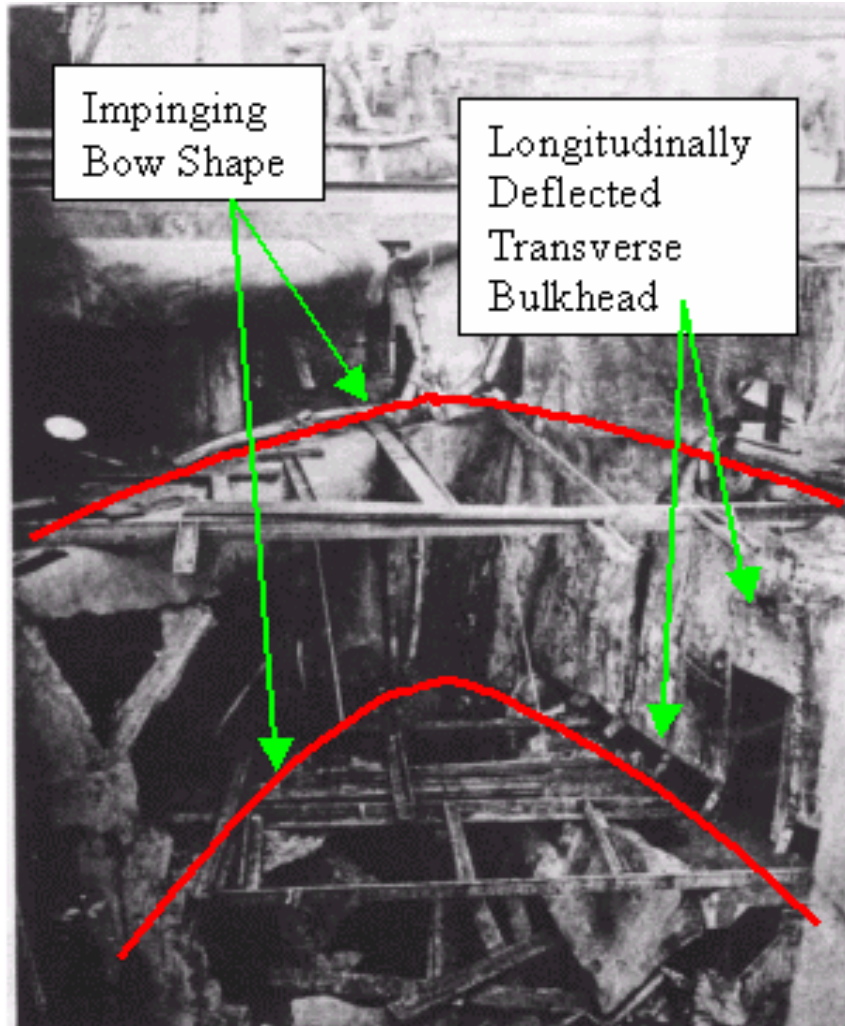


Figure 109 - Damage Showing Longitudinally Deflected Bulkhead and Striking Bow Shape

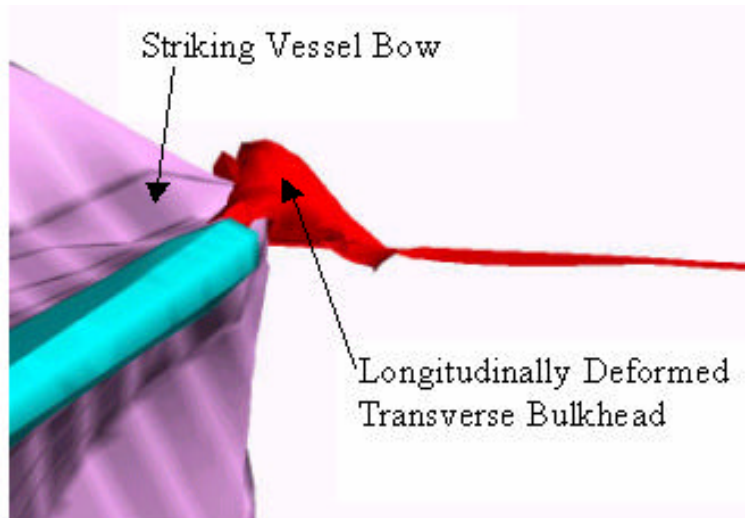


Figure 110 - FEA Showing Longitudinal Deformation of Transverse Bulkhead (looking vertically up)

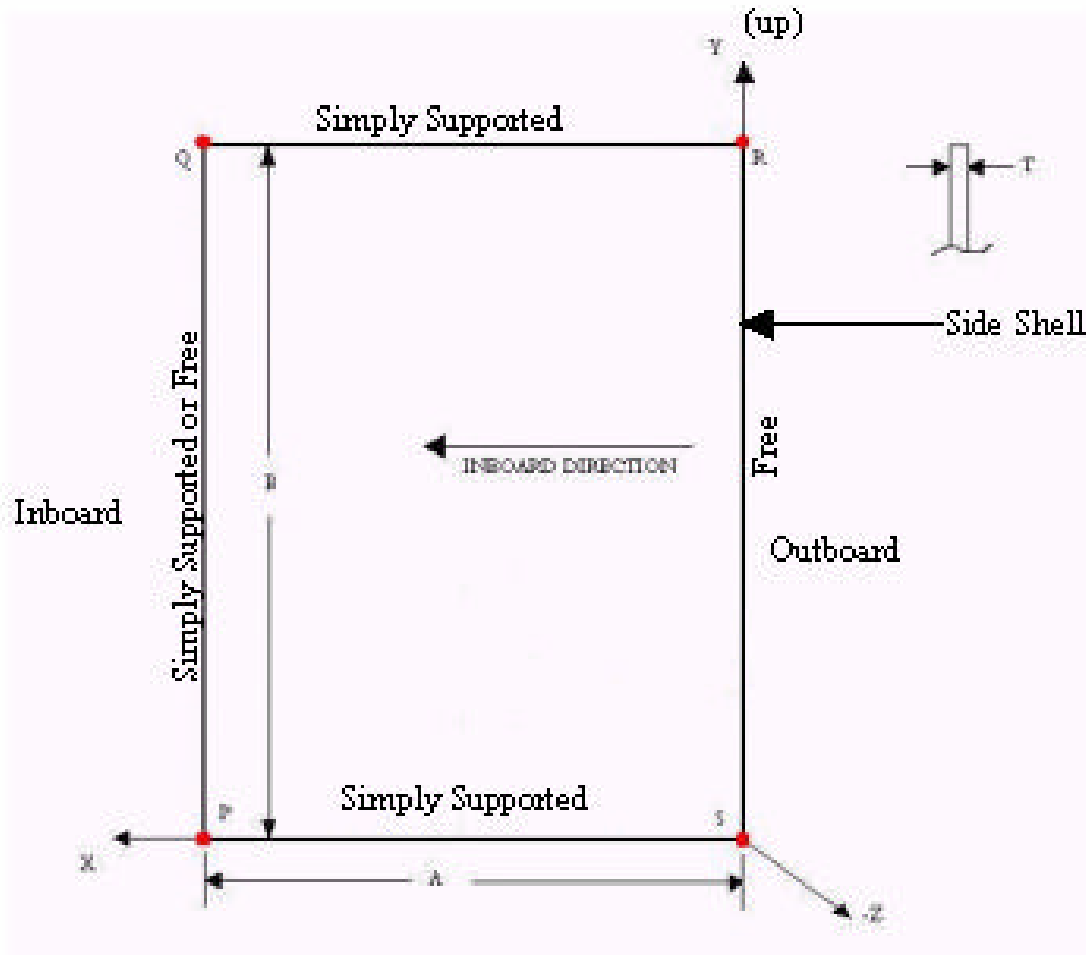


Figure 111 - Idealized Transverse Plate Model

The span ( $A$ ) is either the web depth or represents a transverse bulkhead bounded by longitudinal bulkheads and the height ( $B$ ) is bounded either by decks or by stringers ( $PS$  and  $QR$ ). The upper and lower edges ( $PS$  and  $QR$ ) are thus always simply supported ( $z = 0$ ) so as to not double count energy absorbed by other mechanisms such as deck or stringer crushing discussed in Section 5.1.  $PS$  or  $QR$  being the intersection of the bulkhead or web and a deck or stringer the edges are translationally fixed while rotationally free. The inboard most edge ( $QP$ ) is free only if the plate is a web not bounded by two longitudinal bulkheads. Otherwise the inboard edge is simply supported being the intersection of the transverse structure (bulkhead or web) and a longitudinal bulkhead. The outboard most edge of the plate ( $RS$ ) is always considered free, neglecting any interaction with the longitudinal bulkhead supporting this edge by making the assumption that the energy absorbed via the crushing of the longitudinal bulkhead along this edge is considered by the method of Section 5.2 (i.e. avoids double-counting the energy absorbed in the longitudinal bulkhead at the outer edge).

The transverse plate of Figure 111 can then be assumed to absorb energy independent of other contacted structure. Making use of this independence, the plate is laterally deformed by the striking ship represented in SIMCOL as a wedge model shown in Figure 112.

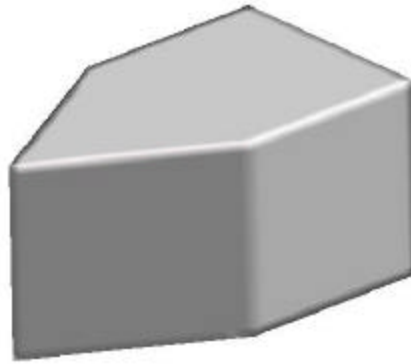


Figure 112 - SIMCOL Wedge Model

For this derivation the wedge is assumed to be rigid, considering only the energy absorbed in the plate. This wedge model allows for four contact scenarios by which the wedge may strike the plate. These contact scenarios are:

- Contact Scenario 1 - Port or starboard bow section contacts the plate at any angle ( $f$ ) less than ninety degrees and greater than zero degrees (illustrated Figure 113 and shown finite element time step progression in Figure 114 through Figure 117).
- Contact Scenario 2 - Port or starboard bow section contacts the plate at any angle ( $f$ ) less than or equal to zero degrees (illustrated in Figure 118 and shown finite element time step progression in Figure 119 through Figure 121).
- Contact Scenario 3 - Port or starboard after body contacts the plate at any angle ( $a$ ) less than ninety degrees and greater than zero degrees (illustrated in Figure 122 and shown finite element time step progression in Figure 123 through Figure 126).
- Contact Scenario 4 - Port or starboard bow section and after body contact the plate where the angle ( $f$ ) is less than ninety degrees and greater than zero degrees and the angle ( $a$ ) is less than or equal to zero degrees (illustrated in Figure 127 and shown finite element time step progression in Figure 128 through Figure 130).

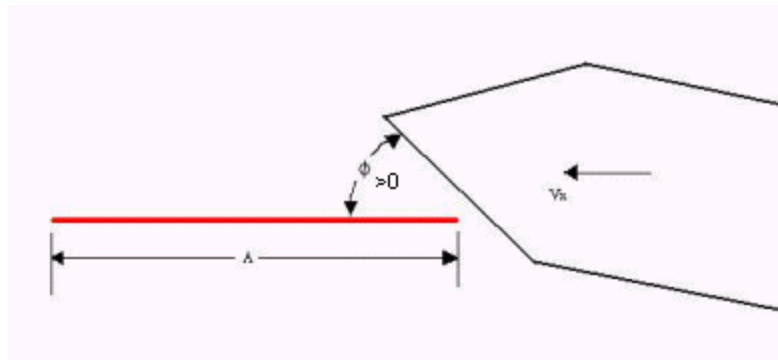


Figure 113 - Contact Scenario 1 Geometry

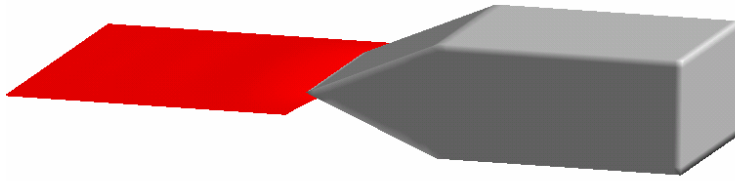


Figure 114 - Contact Scenario 1 FEA Test Case at 0.1 Seconds

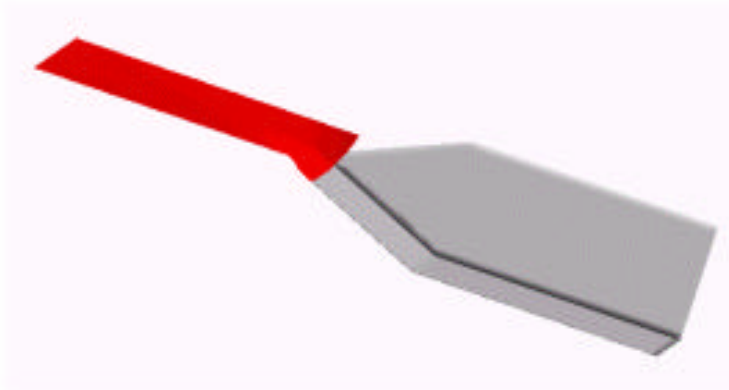


Figure 115 - Contact Scenario 1 FEA Test Case at 0.2 Seconds

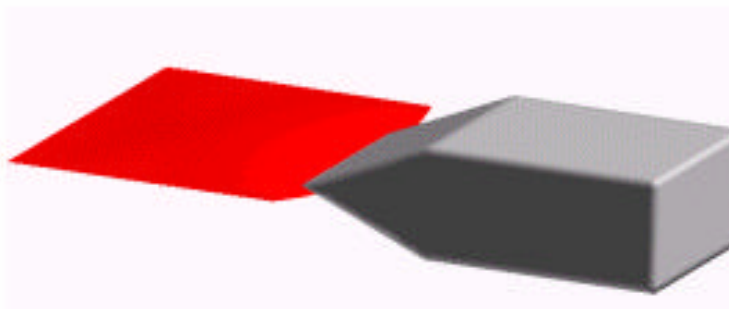


Figure 116 - Contact Scenario 1 FEA Test Case at 0.3 Seconds

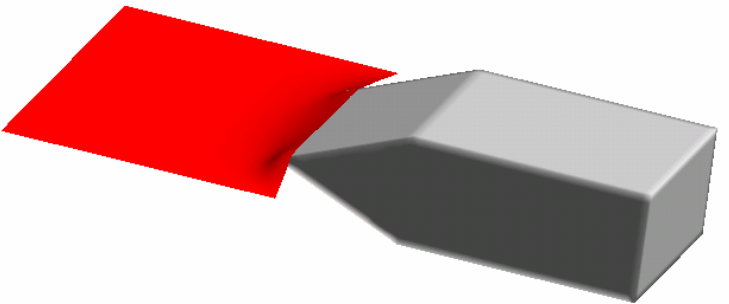


Figure 117 - Contact Scenario 1 FEA Test Case at 0.8 Seconds

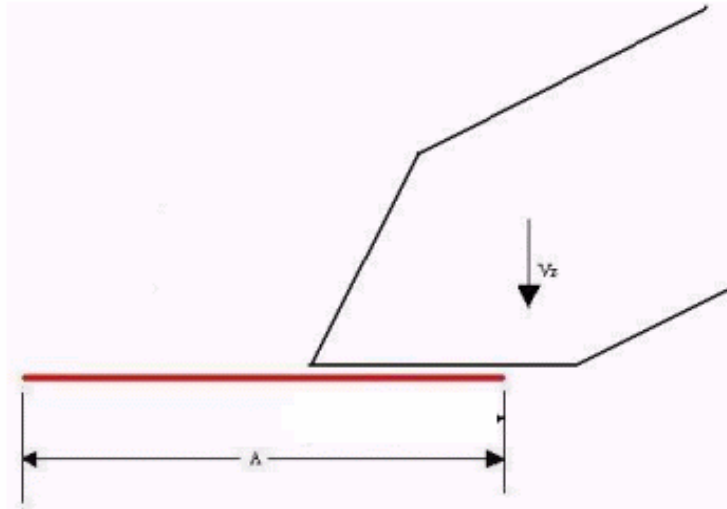


Figure 118 - Contact Scenario 2 Geometry

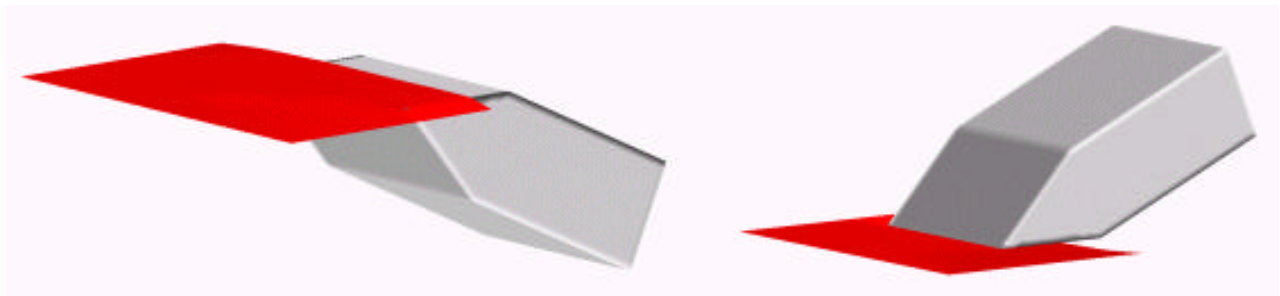


Figure 119 - Contact Scenario 2 FEA Test Case at 0.2 Seconds

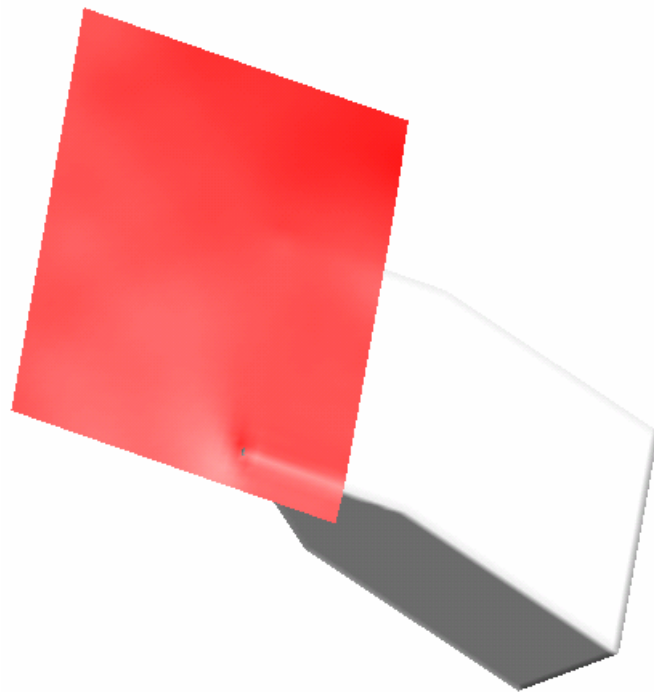


Figure 120 - Contact Scenario 2 FEA Test Case at 0.25 Seconds

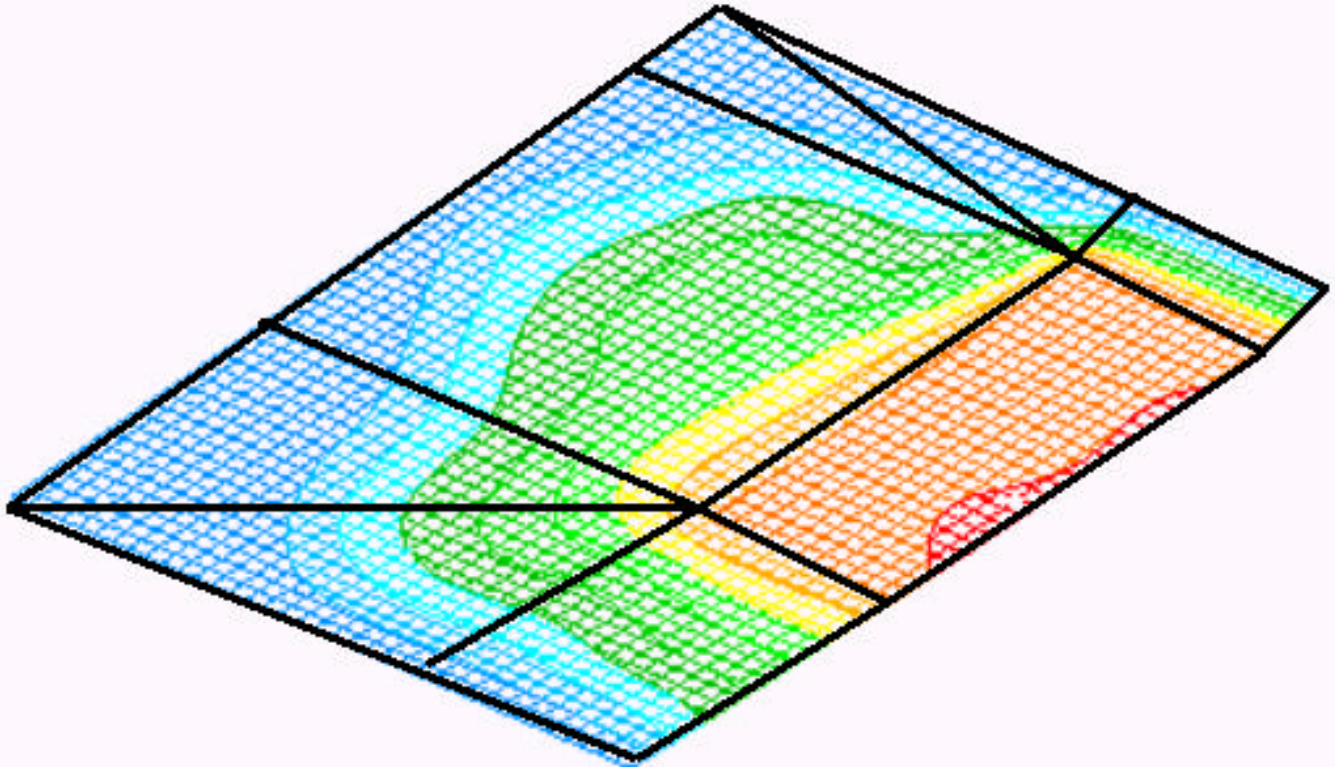


Figure 121 - Contact Scenario 2 FEA Plate Mesh Deflection at 0.25 Seconds with 8 region model overlay

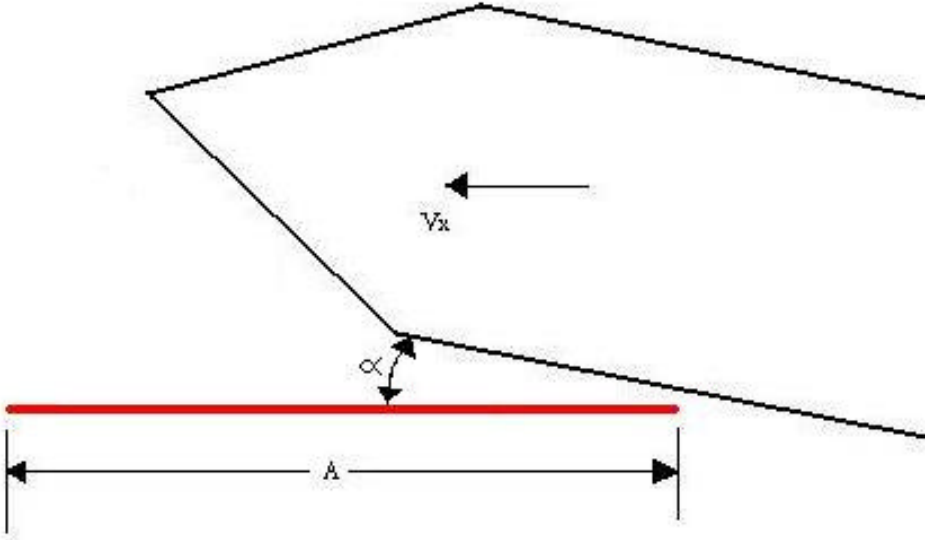


Figure 122 - Contact Scenario 3 Geometry

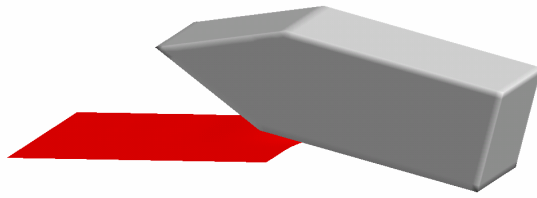


Figure 123 - Contact Scenario 3 FEA Test Case at 0.1 Seconds

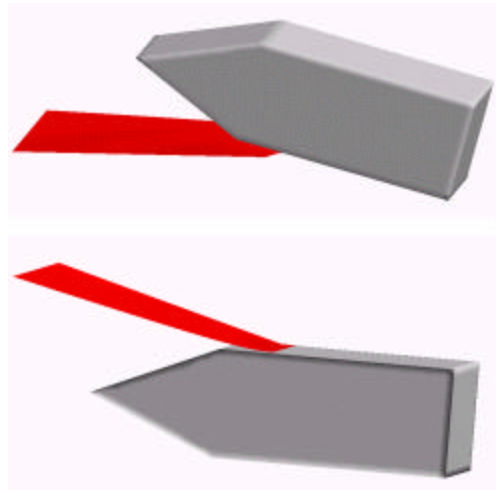


Figure 124 - Contact Scenario 3 FEA Test Case at 0.2 Seconds

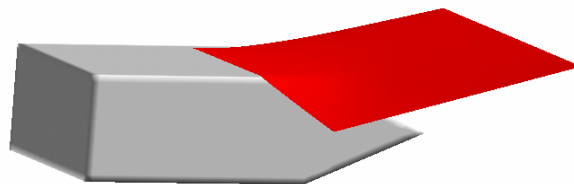


Figure 125 - Contact Scenario 3 FEA Test Case at 0.3 Seconds

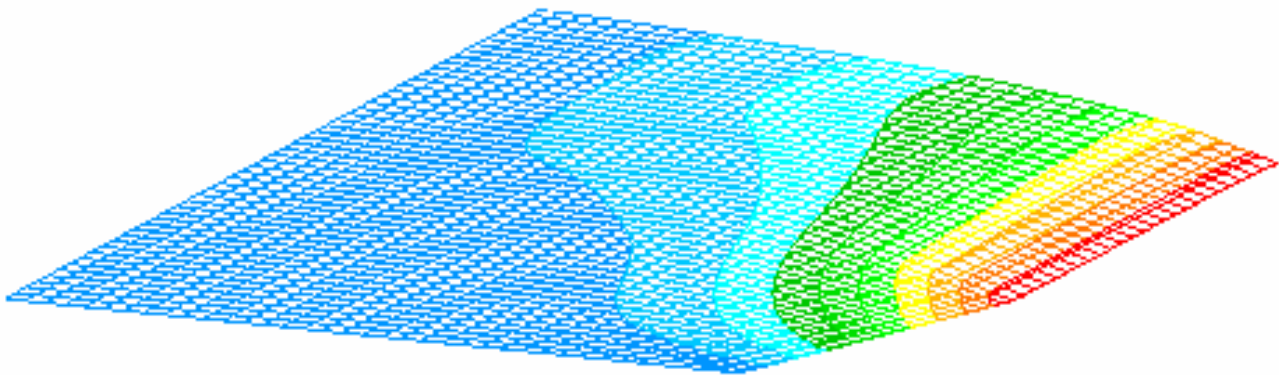


Figure 126 - Contact Scenario 3 Plate Mesh Deformation at 0.3 Seconds

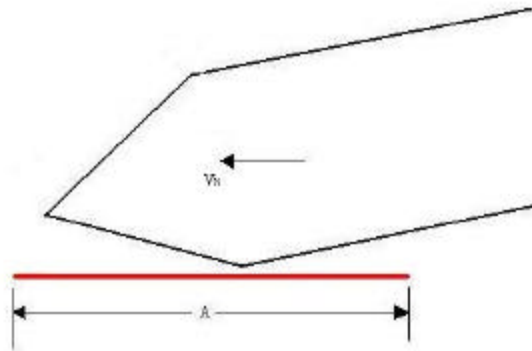


Figure 127 - Contact Scenario 4 Geometry

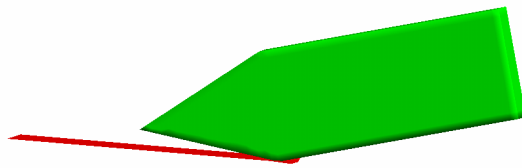


Figure 128 - Contact Scenario 4 FEA Test Case at 0.1 Seconds

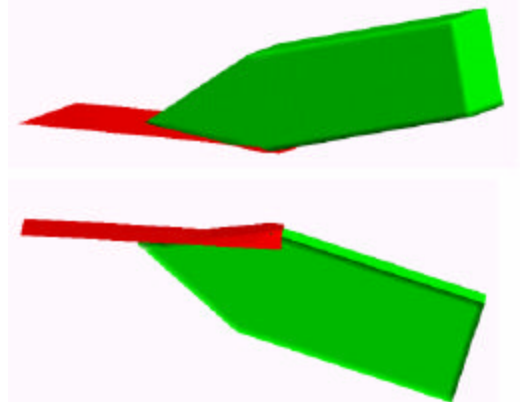


Figure 129 - Contact Scenario 4 FEA Test Case at 0.2 Seconds

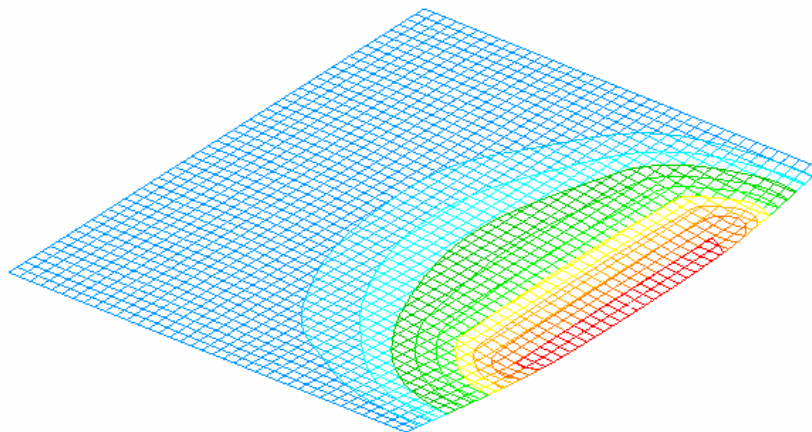


Figure 130 - Contact Scenario 4 Plate Mesh Deflection at 0.2 Seconds

As an example, assume the rigid wedge strikes the plate in Contact Scenario 2 (Figure 118 through Figure 121), where the angle ( $f$ ) equals zero degrees and the wedge model has the initial component velocity zero m/s in the direction parallel to the plate but greater than zero in the direction normal to the plate as described by Figure 131.

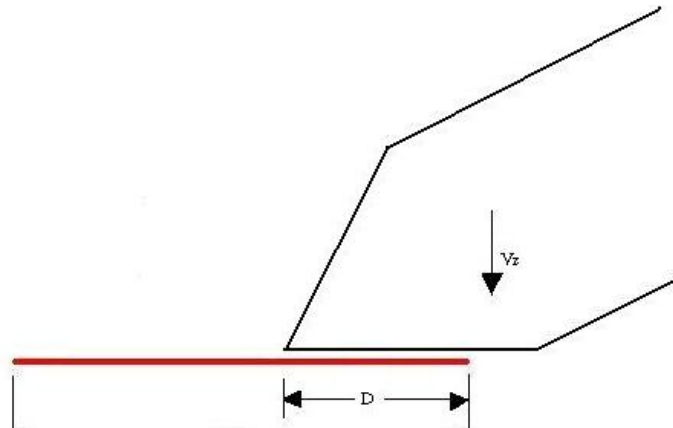


Figure 131 - Longitudinal Deflection Simplified Argument Example Geometry

The plate is struck by the rigid wedge over the shaded region (DF) of Figure 132 in the  $z$  direction with an initial velocity  $V_0$  at the time  $t = 0$  seconds (the moment of contact).

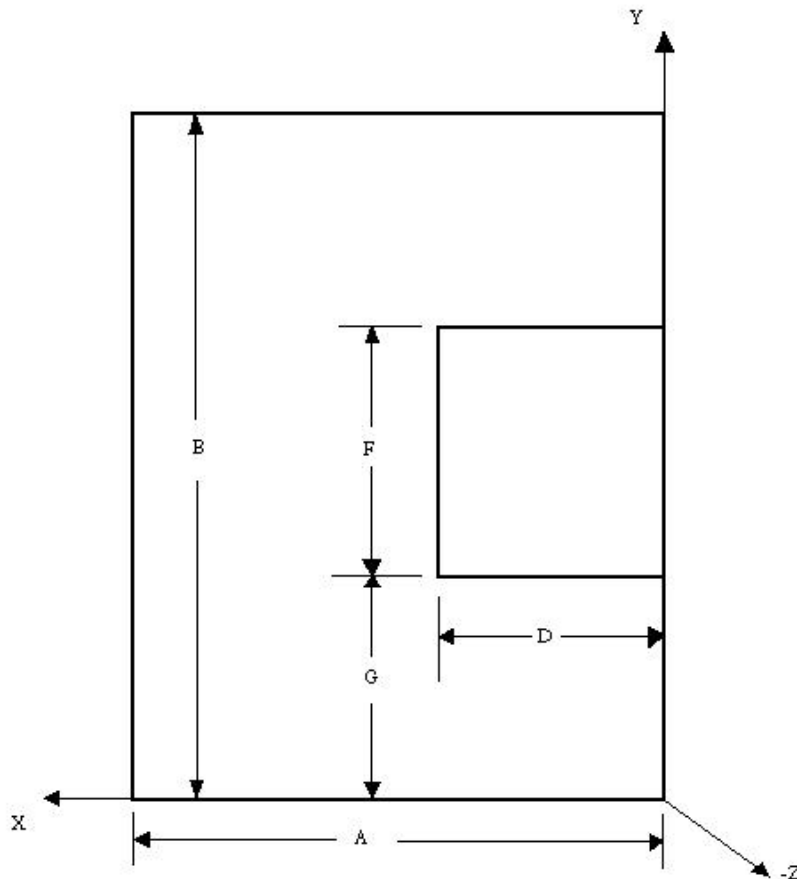


Figure 132 - Idealized Plate Geometry Definitions for Simplified Argument

In this example, the rigid wedge strikes between the upper and lower edges of the plate. Using the nomenclature of Figure 132,  $G=0$  and  $G+F=B$ . Figure 133 through Figure 135 show all possible vertical positions of the wedge relative to the plate. These will be considered in the final 25 region model discussed in Section 5.4.5.

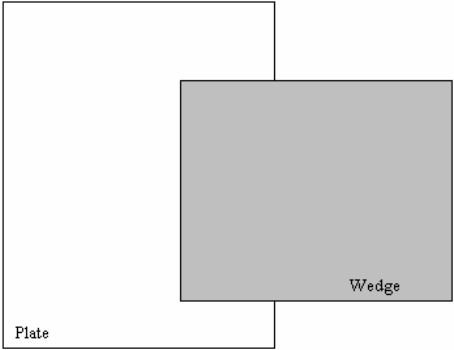


Figure 133 - Centered Vertical Position of Wedge Striking Plate

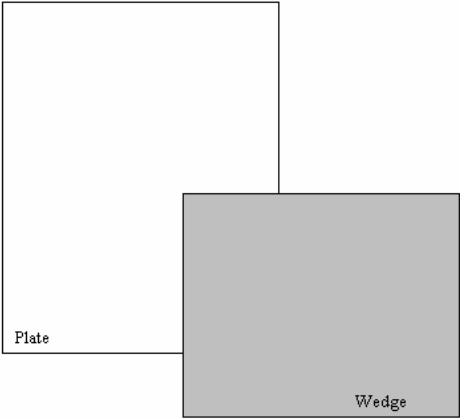


Figure 134 - Lower Vertical Position of Wedge Striking Plate

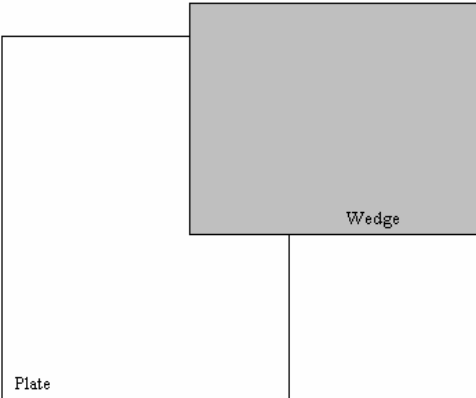


Figure 135 - Upper Vertical Position of Wedge Striking Plate

For the current contact problem of Figure 131, the inboard edge of the plate is assumed to be simply supported. In contact scenario two with the angle ( $f$ ) equal to zero degrees, then the

deflections at  $(X,Y) = (0,G)$ ;  $(X,Y) = (0,G+F)$ ;  $(X,Y) = (D,G)$  and  $(X,Y) = (D,G+F)$  are equal at any time  $t$ . After a small time  $t$  a linear form of the deflection of the plate maybe drawn as shown in Figure 121. Note that the deformed shape in Figure 121 is similar to the deformation of the finite element analysis of contact scenario 2 shown in Figure 119 through Figure 120 and provided again in Figure 136 for side-by-side comparison.

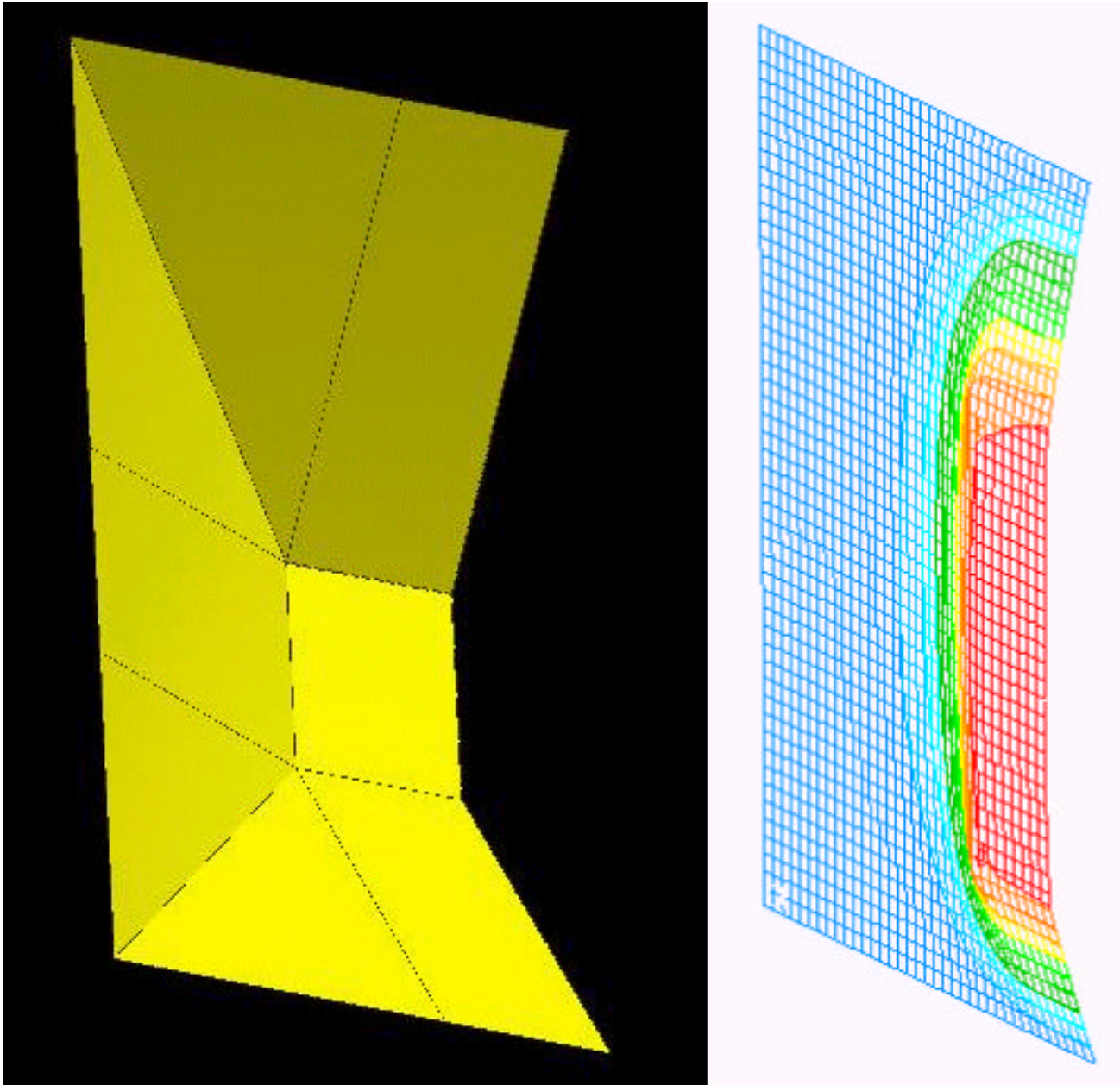


Figure 136 - Simplified Plate Deflection and Similar FEA Plate Mesh Deflection  
The plate is divided into eight energy-absorbing regions defined as shown in Figure 137.

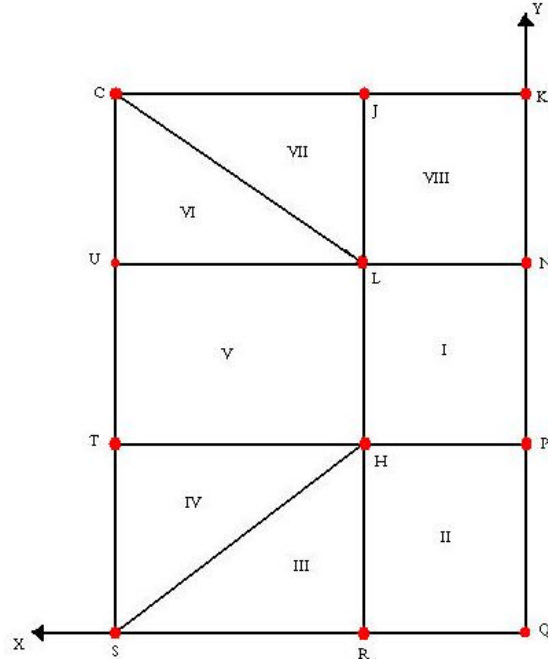


Figure 137 – Eight-Region Plate Model

The energy absorbed through the plastic membrane stretching of each region is calculated over each time step and summed to provide the energy absorbed through the lateral deflection of the plate in each time step. The more complicated but required twenty-five-region plate Figure 142 replaces the simple eight-region plate of Figure 137 to properly capture the deformation of the plate using a linear approximation for the more complicated contact scenarios. Development of the energy absorbing rectangular and triangular regions is discussed in Sections 5.4.2 and 5.4.3 while the super positioning and assembly of the full energy absorbed by the plate is discussed in Section 5.4.4.

### 5.4.1 Flow Theory of Plasticity

Prior to discussion of the energy absorbed by the rectangular and triangular regions presented in Section 5.4.2, a brief review of the flow theory of plasticity is presented. The basic assumptions of flow theory are 1) that the strain of any material may be represented as the sum of an elastic strain and a plastic strain (Equation 5.4) and 2) there exists a loading function (F) at every stage of plastic deformation that prevents the relaxation of the elastic portion of the deformation.

$$\epsilon_{ij} = \epsilon_{ij}^e + \epsilon_{ij}^p \quad (5.4)$$

The second assumption yields the condition that plastic deformation exists and is definable based upon a yield condition. Making use of Von Mises yield function the yield criterion for plastic deformation is given by Equation 5.5.

$$F = \frac{1}{2} \cdot S_{ij} \cdot S_{ij} - \frac{1}{3} \cdot \sigma_y^2 = 0 \quad (5.5)$$

Where:

$$s_{ij} = \sigma_{ij} - \frac{\sigma_{11} + \sigma_{22} + \sigma_{33}}{3} \cdot \delta_{ij} \quad (5.6)$$

Additionally, by making use of the Drucker Postulates [90]:

- During loading, positive work is performed
- The net work performed through a loading and unloading cycle cannot be negative
- During unloading, the limit of the elastic strain is zero

Then an incremental change in work (positive) is equivalent to an applied stress times an incremental change in the plastic strain ( $d\varepsilon_{ij}^P$ ) as shown by Equation 5.7.

$$dE = \sigma_{ij} \cdot d\varepsilon_{ij}^P \quad (5.7)$$

For plastic deformation to occur the incremental change in the loading must be positive and the load function must have a positive slope. Assuming that the strain is linearly related to the stress in infinitesimal changes then Equations 5.4 through 5.7 may be written yielding Equation 5.8 known as the associative flow rule.

$$d\varepsilon_{ij} = d\varepsilon_{ij}^P = D_{ijkl} \cdot d\sigma_{kl} \quad (5.8)$$

$$d\varepsilon_{ij}^P = d\lambda \frac{d}{d\sigma_{ij}}(F) \quad (5.9)$$

$$d\sigma_{kl} = d\gamma \frac{d}{d\sigma_{kl}}(F) \quad (5.10)$$

Where  $d?$  is the incremental linearity constant which is greater than zero.

The associative flow rule of Equation 5.8 states that the increment of plastic strain is normal to the increment of the yield surface where the strain is in the direction of the applied stress.

Returning to Equation 5.7, the incremental change in work can be written as a function of the effective strain ( $d\varepsilon^P$ ) and effective stress ( $s$ ) as:

$$dE = \sigma \cdot d\varepsilon^P \quad (5.11)$$

Where the effective stress is given through Von Misses yield criterion as:

$$\sigma = \sqrt{\frac{3}{2} \cdot S_{ij} \cdot S_{ij}} \quad (5.12)$$

From the associative flow rule the increment of plastic strain may be written as:

$$d\varepsilon_{ij}^P = d\lambda \frac{3}{2} \frac{S_{ij}}{\sqrt{\frac{3}{2} \cdot S_{kl} \cdot S_{kl}}} \quad (5.13)$$

Equation 5.13 yields an effective plastic strain increment relation given by:

$$d\epsilon^P = d\lambda \cdot S_{ij} = \sqrt{\frac{2}{3} \cdot d\epsilon_{ij}^P \cdot d\epsilon_{ij}^P} \quad (5.14)$$

Equation 5.14 states that the effective incremental plastic strain is equivalent to the incremental linearity constant times the deviatoric stress, which reaffirms the relation given by Equation 5.8.

Thus, using the associative flow rule, the plastic strain rate may be written as:

$$\frac{d}{dt} \epsilon_{ij}^P = \left( \frac{d}{dt} \lambda \right) \frac{d}{d\sigma_{ij}} F \quad (5.15)$$

Where the loading function (F) is given by Equation 5.5.

In Equation 5.11 a constant material flow stress (s) equal to the yield stress is used implying a perfectly plastic material law and allowing the determination of the deviatoric stresses to be neglected. Using the above relations the effective plastic strain rate and the rate of energy absorption are given by Equations 5.16 and 5.17.

$$\dot{\epsilon}_e^P = \sqrt{\frac{2}{3} \cdot \dot{\epsilon}_{ij}^P \cdot \dot{\epsilon}_{ij}^P} \quad (5.16)$$

$$\dot{E} = \sigma \cdot \dot{\epsilon}_e^P \quad (5.17)$$

Finally, the determination of the plastic strain rate ( $\dot{\epsilon}_{ij}^P$ ) is provided through the strain-displacement relation given by Equation 5.18.

$$\dot{\epsilon}_{ij}^P = \frac{1}{2} \cdot (\dot{v}_{i,j} + \dot{v}_{j,i}) \quad (5.18)$$

Where the velocity flow field vector (?) describes the vector velocity of any material point at a given time.

The above formulation has the following limitations:

- It is valid for only modest plastic strains (<= 10%)
- It will not predict plastic strains correctly if the principle axes of stress rotate significantly during inelastic deformation

Neither of these limitations provide difficulty with the use of this method as long as the following assumptions are made:

- At plastic strains >=10% the material is assumed to rupture providing no additional energy absorbing capability
- An analysis time step is chosen which limits the rotation of the principle axis of stress for each evaluation

#### 5.4.2 Energy Absorption in Rectangular Region

Given any rectangular region as represented by Figure 138, the points Q, R, S and V are only allowed to move in the z direction. The deflections of point Q are equal to the deflections of

point R at any time and the deflections of point V are equal to the deflections of point S at any time (i.e. segments QR and VS must always remain parallel to the xy plane). If the deflections of S do not equal the deflections of V, or if the deflections of Q do not equal the deflections of R, then the rectangular region must be evaluated as two triangular regions as discussed in Section 5.4.3.

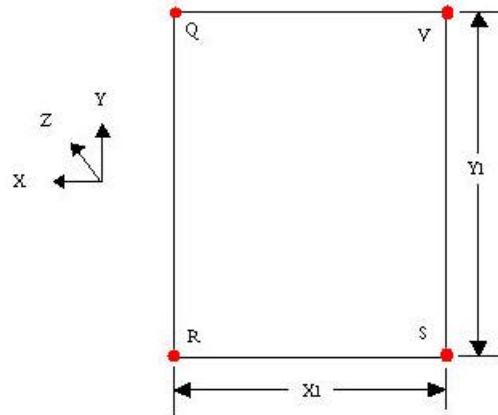


Figure 138 - Rectangular Region Geometry and Nomenclature

The deflections of points V and Q at time  $t = i$  and  $t = f$  from the initial  $V_0$  and  $Q_0$  geometry are represented by  $WV_i$ ,  $WV_f$ ,  $WQ_i$  and  $WQ_f$  respectively. Because the deflections of S equal the deflections of V and the deflections of R equal the deflections of Q at any time then:

$$WS_i = WV_i \quad (5.19)$$

$$WR_i = WQ_i \quad (5.20)$$

$$WS_f = WV_f \quad (5.21)$$

$$WR_f = WQ_f \quad (5.22)$$

The segment lengths between points at any time are given by:

$$V_0 \cdot S_0 = V_i \cdot S_i = V_f \cdot S_f = Q_0 \cdot R_0 = Q_i \cdot R_i = Q_f \cdot R_f = Y_1 \quad (5.23)$$

$$Q_0 \cdot V_0 = R_0 \cdot S_0 = X_1 \quad (5.24)$$

$$Q_i \cdot V_i = R_i \cdot S_i = \left[ X_1^2 + (WV_i - WQ_i)^2 \right]^{\frac{1}{2}} \quad (5.26)$$

Assuming small displacements, then the velocity field vector of any point P bounded by the rectangular region QRSV may be approximated by Equation 5.27.

$$v = \frac{P_f - P_i}{\tau} = \frac{f(x,y)}{\tau} \eta + \frac{g(x,y)}{\tau} \xi + \frac{h(x,y)}{\tau} \kappa \quad (5.27)$$

Where the time step ( $t$ ) is defined by Equation 5.28.

$$\tau = t_f - t_i \quad (5.28)$$

The unit vector (?) is parallel to the segment SR at any time, (?) is parallel to the segment SV at any time and (?) is orthogonal to both (?) and (?) at any time. The extension of any point P, bounded by the region QRSV in the (?) direction over the time step ( $t$ ), and assuming small motions can be approximated using Equation 5.29.

$$f(x,y) = \max \left[ 0, \left( 1 - \frac{x}{X_1} \right) \cdot (Q_f \cdot V_f - Q_i \cdot V_i) \right] \quad (5.29)$$

Where  $X$  is defined as less than or equal to  $X_1$  and greater or equal to 0. Similarly, the extension of any point P in the (?) can be given by Equation 5.30, and assuming only membrane deflections then the extension in the (?) direction is given by Equation 5.31.

$$g(x,y) = 0 \quad (5.30)$$

$$h(x,y) = 0 \quad (5.31)$$

Substitution of Equations 5.25 and 5.26 into Equation 5.29 yields:

$$f(x,y) = \max \left[ 0, \left( 1 - \frac{x}{X_1} \right) \cdot \left[ \left[ X_1^2 + (wV_f - wQ_f)^2 \right]^{\frac{1}{2}} - \left[ X_1^2 + (wV_i - wQ_i)^2 \right]^{\frac{1}{2}} \right] \right] \quad (5.32)$$

Substitution of Equations 5.30, 5.31 and 5.32 into Equation 5.27 yields the velocity flow field for the rectangular region QRSV given by Equation 5.33.

$$v = v_1 \cdot \eta \quad (5.33)$$

$$v_1 = \frac{\alpha_1}{\tau} \cdot \left( 1 - \frac{x}{X_1} \right) \quad (5.34)$$

$$\alpha_1 = \max \left[ 0, \left[ \left[ X_1^2 + (wV_f - wQ_f)^2 \right]^{\frac{1}{2}} - \left[ X_1^2 + (wV_i - wQ_i)^2 \right]^{\frac{1}{2}} \right] \right] \quad (5.35)$$

Using Equations 5.16 and 5.17 then the effective plastic strain rate and rate of energy dissipation over the time step are given by Equations 5.36 and 5.37 respectively.

$$\varepsilon_e = \left( \frac{2}{3} \right)^{\frac{1}{2}} \cdot \left( \frac{\alpha_1}{X_1 \cdot \tau} \right) \quad (5.36)$$

$$E = \sigma_y \cdot \int \varepsilon_e dv \quad (5.37)$$

Integrating Equation 5.37 over the time step ( $t$ ) yields the energy absorbed by the deflection of the rectangular region over the time step as given by Equation 5.38 where  $T$  is the uniform thickness of region QRSV.

$$E = \sigma_y \cdot T \cdot Y_1 \cdot \alpha_1 \cdot \sqrt{\frac{2}{3}} \quad (5.38)$$

To determine when the rectangular region QRSV fails (ruptures) and no longer absorbs energy, a rupture criterion is developed based upon Equation 5.5. Assume that rupture occurs when the total effective strain (insert symbol) is greater than some value of failure (rupture) strain ( $\psi = 10\%$ ) at any point P in the region QRSV. The total effective strain (the strain of the region from time  $t = 0$  to  $t = f$ ) can be given by Equation 5.39 derived in a similar method to Equation 5.36.

$$\epsilon_{\text{eff}} = \left( \frac{1}{X_1} \right) \cdot \left[ \left[ X_1^2 + (WV_f - WQ_f)^2 \right]^{\frac{1}{2}} - X_1 \right] \cdot \sqrt{\frac{2}{3}} \quad (5.39)$$

Thus, for the rectangular region QRSV, the conditional statement of Equation 5.40 gives the energy dissipation over the time step.

$$E = \begin{cases} \sigma_y \cdot T \cdot Y_1 \cdot \alpha_1 \cdot \sqrt{\frac{2}{3}} & \text{if } \epsilon_e < \psi \\ 0 & \text{otherwise} \end{cases} \quad (5.40)$$

### 5.4.3 Energy Absorption in Triangular Region

Similar to the development of the rectangular region energy absorption discussed in Section 5.4.2, the energy absorbed in the triangular region shown in Figure 139 is derived here. For the triangular region NRV of Figure 139, Point N is pinned and points R and V are only allowed movement in the z direction.

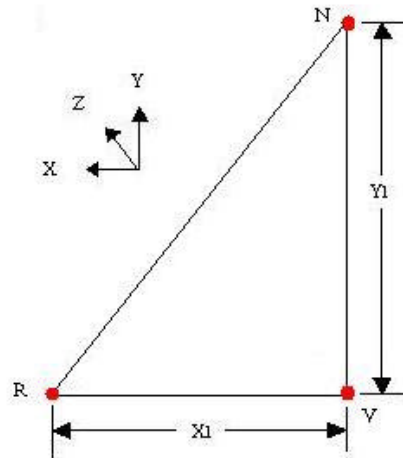


Figure 139 - Triangular Region Geometry and Nomenclature

Again, the deflections of points V and R at time  $t = i$  and  $t = f$  from the initial  $V_0$  and  $R_0$  geometry are represented by  $WV_i$ ,  $WV_f$ ,  $WR_i$  and  $WR_f$  respectively, and the segment lengths between points at any time are given by:

$$R_0 \cdot V_0 = X_1 \quad (5.41)$$

$$N \cdot R_0 = \sqrt{X_1^2 + Y_1^2} \quad (5.42)$$

$$R_i \cdot V_i = \sqrt{X_1^2 + (WV_i - WR_i)^2} \quad (5.43)$$

$$N \cdot R_f = \sqrt{WR_f^2 + X_1^2 + Y_1^2} \quad (5.44)$$

$$N \cdot V_f = \sqrt{WV_f^2 + Y_1^2} \quad (5.45)$$

$$N \cdot V_i = \sqrt{WV_i^2 + Y_1^2} \quad (5.46)$$

$$N \cdot R_i = \sqrt{WR_i^2 + X_1^2 + Y_1^2} \quad (5.47)$$

$$R_f \cdot V_f = \sqrt{X_1^2 + (WV_f - WR_f)^2} \quad (5.48)$$

$$N \cdot V_0 = Y_1 \quad (5.49)$$

Again the vector velocity field may be approximated using Equation 5.27 where here the unit vector (?) is parallel to the segment RV at any time, (?) is parallel to the segment VN at any time and (?) is orthogonal to both (?) and (?) at any time. The extension of any point P, bounded by the region NRV in the (?) direction over the time step (t), and assuming small motions can be approximated using Equation 5.50.

$$f(x,y) = \left(1 - \frac{y}{Y_1}\right) \left(\frac{x}{X_1}\right) \cdot \max[0, (R_f \cdot V_f - R_i \cdot V_i)] \quad (5.50)$$

Similarly, the extension of any point P in the (?) direction can be given by Equation 5.51, and assuming only membrane deflections then the extension in the (?) direction is given by Equation 5.54.

$$g(x,y) = \left(1 - \frac{y}{Y_1}\right) \left(\frac{x}{X_1}\right) \cdot \max\left[0, \left[\sqrt{(R_f \cdot V_f)^2 + (\Omega_1)} - \sqrt{(R_i \cdot V_i)^2 + (\Omega_2)}\right]\right] \quad (5.51)$$

$$\Omega_2 = \frac{Y_1^2 \cdot (R_i \cdot V_i)^2}{(N \cdot R_0)^2 \cdot (R_i \cdot V_i)^2 - \left[(R_i \cdot V_i)^2 - WV_i \cdot (WV_i - WR_i)\right]^2} \quad (5.52)$$

$$\Omega_1 = \frac{Y_1^2 \cdot (R_f \cdot V_f)^2}{(N \cdot R_0)^2 \cdot (R_f \cdot V_f)^2 - \left[(R_f \cdot V_f)^2 - WV_f \cdot (WV_f - WR_f)\right]^2} \quad (5.53)$$

$$h(x,y) = 0 \quad (5.54)$$

Substitution of Equations 5.50, 5.51 and 5.54 into Equation 5.27 yields the velocity flow field for the triangular region NRV given by Equations 5.55 through 5.61.

$$v = V_1 \cdot \eta + V_2 \cdot \xi \quad (5.55)$$

$$V_1 = \frac{\alpha_1}{\tau} \cdot \left( \frac{x}{X_1} \right) \cdot \left( 1 - \frac{y}{Y_1} \right) \quad (5.56)$$

$$V_2 = \frac{\alpha_2}{\tau} \cdot \left( \frac{x}{X_1} \right) \cdot \left( 1 - \frac{y}{Y_1} \right) \quad (5.57)$$

$$\alpha_1 = \max \left[ 0, \left[ \sqrt{X_1^2 + (WV_f - WR_f)^2} - \sqrt{X_1^2 + (WV_i - WR_i)^2} \right] \right] \quad (5.58)$$

$$\alpha_2 = \max \left[ 0, \left[ \sqrt{X_1^2 + (WV_f - WR_f)^2} + \Psi_1 - \sqrt{X_1^2 + (WV_i - WR_i)^2} + \Psi_2 \right] \right] \quad (5.59)$$

$$\Psi_1 = \frac{Y_1^2 \cdot \left[ X_1^2 + (WV_f - WR_f)^2 \right]}{\left( Y_1^2 + X_1^2 \right) \cdot \left[ X_1^2 + (WV_f - WR_f)^2 \right] - \left[ \left[ X_1^2 + (WV_f - WR_f)^2 \right] - WV_f \cdot (WV_f - WR_f) \right]^2} \quad (5.60)$$

$$\Psi_2 = \frac{Y_1^2 \cdot \left[ X_1^2 + (WV_i - WR_i)^2 \right]}{\left( Y_1^2 + X_1^2 \right) \cdot \left[ X_1^2 + (WV_i - WR_i)^2 \right] - \left[ \left[ X_1^2 + (WV_i - WR_i)^2 \right] - WV_i \cdot (WV_i - WR_i) \right]^2} \quad (5.61)$$

To reduce the number of independent variables in Equations 5.56 and 5.57, the independent variable X is replaced with the constant  $X_{ave}$  given by Equation 5.62.

$$X_{ave} = \frac{1}{Y_1} \cdot \int_0^{Y_1} \left( \frac{1}{X_1} \cdot \int_0^{X_1} x dx \right) dy = \frac{X_1}{4} \quad (5.62)$$

Using Equation 5.62 then Equations 5.56 and 5.57 simplify to:

$$V_1 = \frac{\alpha_1}{4\tau} \cdot \left( 1 - \frac{y}{Y_1} \right) \quad (5.63)$$

$$V_2 = \frac{\alpha_2}{4\tau} \cdot \left( 1 - \frac{y}{Y_1} \right) \quad (5.64)$$

Using Equations 5.16 and 5.17 then the effective plastic strain rate and rate of energy dissipation over the time step are given by Equations 5.65 and 5.66 respectively.

$$\varepsilon_e = \frac{1}{4\tau \cdot Y_1} \cdot \sqrt{\frac{2}{3} \cdot \left( \alpha_2^2 + \frac{\alpha_1^2}{2} \right)} \quad (5.65)$$

$$E = \frac{\sigma_y \cdot T \cdot X_1}{8 \cdot \tau} \cdot \sqrt{\frac{2}{3} \cdot \left( \alpha_2^2 + \frac{\alpha_1^2}{2} \right)} \quad (5.66)$$

Integrating Equation 5.66 over the time step (t) yields the energy absorbed by the deflection of the rectangular region over the time step as given by Equation 5.67.

$$E = \frac{\sigma_y \cdot T \cdot X_1}{8} \cdot \sqrt{\frac{2}{3} \cdot \left( \alpha_2^2 + \frac{\alpha_1^2}{2} \right)} \quad (5.67)$$

To determine when the triangular region NRV fails (ruptures) and no longer absorbs energy, a rupture criterion is developed based upon Equation 5.5. Again, assume that rupture occurs when the total effective strain ( $\epsilon_{\text{eff}}$ ) is greater than some value of failure (rupture) strain ( $\Psi = 10\%$ ) at any point P in the region NRV. The total effective strain (the strain of the region from time  $t = 0$  to  $t = f$ ) can be given by Equation 5.68 derived in a similar method to Equation 5.65.

$$\epsilon_{\text{eff}} = \frac{1}{4 \cdot Y_1} \cdot \sqrt{\frac{2}{3} \cdot \left( \Gamma_2^2 + \frac{\Gamma_1^2}{2} \right)} \quad (5.68)$$

$$\Gamma_2 = \sqrt{X_1^2 + (WV_f - WR_f)^2 + \Psi_1} - \sqrt{X_1^2 + 1} \quad (5.69)$$

$$\Gamma_1 = \left[ (WV_f - WR_f)^2 + X_1^2 \right]^2 - X_1 \quad (5.70)$$

Thus, for the triangular region NRV, the conditional statement of Equation 5.71 gives the energy dissipation over the time step.

$$E = \begin{cases} \frac{\sigma_y \cdot T \cdot X_1}{8} \cdot \sqrt{\frac{2}{3} \cdot \left( \alpha_2^2 + \frac{\alpha_1^2}{2} \right)} & \text{if } \epsilon_{\text{eff}} < \Psi \\ 0 & \text{otherwise} \end{cases} \quad (5.71)$$

#### 5.4.4 The Energy Absorbed from an Eight-Region Plate

Returning the example of Section 5.4 relating to Figure 137, the eight-region plate, and using the derivations of the energy absorbed in rectangular and triangular regions in Sections 5.4.2 and 5.4.3 respectively, then the energy absorbed by the plate of Figure 111 over the time step (t) is given by Equation 5.72.

$$E_{P\tau} = E_I + E_{II} + E_{III} + E_{IV} + E_V + E_{VI} + E_{VII} + E_{VIII} \quad (5.72)$$

Examination of the plate of Figure 137 the following conditional statements as to the strength of the plate are expressed in Equation 5.73.

$$E_{P\tau} = \begin{cases} 0 & \text{if } \lambda_I = 0 \\ \frac{E_I}{2} + E_{IV} + E_V + E_{VI} + E_{VII} + E_{VIII} & \text{if } \lambda_{II} = 0 \\ \frac{E_I}{2} + E_{IV} + E_V + E_{VI} + E_{VII} + E_{VIII} & \text{if } \lambda_{III} = 0 \\ E_I + E_{II} + E_{III} + E_{VII} + E_{VIII} & \text{if } \lambda_{IV} = 0 \\ E_I + E_{II} + E_{III} + E_{VII} + E_{VIII} & \text{if } \lambda_V = 0 \\ E_I + E_{II} + E_{III} + E_{VII} + E_{VIII} & \text{if } \lambda_{VI} = 0 \\ \frac{E_I}{2} + E_{II} + E_{III} + E_{IV} + E_V + E_{VI} & \text{if } \lambda_{VII} = 0 \\ \frac{E_I}{2} + E_{II} + E_{III} + E_{IV} + E_V + E_{VI} & \text{if } \lambda_{VIII} = 0 \end{cases} \quad (5.73)$$

Where ( $\lambda_i$ ) is a rupture indicator for each region ( $i = I, II, III, IV, V, VI, VII$  and  $VIII$ ) expressed by Equation 5.74.

$$\lambda_i = \begin{cases} 1 & \text{if } \varepsilon_{\text{eff}} < \Psi \\ 0 & \text{otherwise} \end{cases} \quad (5.74)$$

Using the conditional statements of Equation 5.73 then:

$$\lambda_{II} = \lambda_{III} \quad (5.75)$$

$$\lambda_{VII} = \lambda_{VIII} \quad (5.76)$$

$$\lambda_{IV} = \lambda_V = \lambda_{VI} \quad (5.77)$$

Using the four independent rupture indicators ( $\lambda_I, \lambda_{II}, \lambda_{IV}$  and  $\lambda_{VII}$ ) and the conditional statements of Equation 5.73 then the energy absorbed by the eight-region plate Figure 137 over the time step ( $t$ ) is:

$$E_{P\tau} = \lambda_I \left[ \frac{\lambda_{II} \lambda_{III} + \lambda_{VII} \lambda_{VIII}}{2} \cdot E_I + \lambda_{II} \lambda_{III} (E_{II} + E_{III}) + \lambda_{IV} \lambda_V \lambda_{VI} (E_{IV} + E_V + E_{VI}) + \lambda_{VII} \lambda_{VIII} (E_{VII} + E_{VIII}) \right] \dots \\ \dots \min \left[ 1, (\lambda_{II} \lambda_{III} + \lambda_{IV} \lambda_V \lambda_{VI}) \cdot (\lambda_{II} \lambda_{III} + \lambda_{VII} \lambda_{VIII}) \cdot (\lambda_{VII} \lambda_{VIII} + \lambda_{IV} \lambda_V \lambda_{VI}) \right] \quad (5.78)$$

Summation of the energy absorbed per time step over all time steps between time equal to zero seconds to some time ( $T$ ) seconds yields the total absorbed energy at any time given by Equation 5.79.

$$E_T = \sum_{\tau=1}^T E_{P\tau} \quad (5.79)$$

Using the external dynamics model of SIMCOL and using initial conditions Table 15, Figure 140 provides results for the eight-region plate model as compared to a finite element solution of the same plate subject to the same boundary conditions using an element mesh size of 250 mm.

Table 15 Eight Region Plate Analysis Initial Conditions

<b><i>Initial Conditions</i></b>		
<b>Variable</b>	<b>Value</b>	<b>Unit</b>
Initial Velocity in Z Direction	3	m/s
Analysis Time Step	0.0001	s
Rigid Wedge Mass	50228.4	kg
A	7.5	m
B	10	m
F	5.5	m
G	1.5	m
D	0.75	m

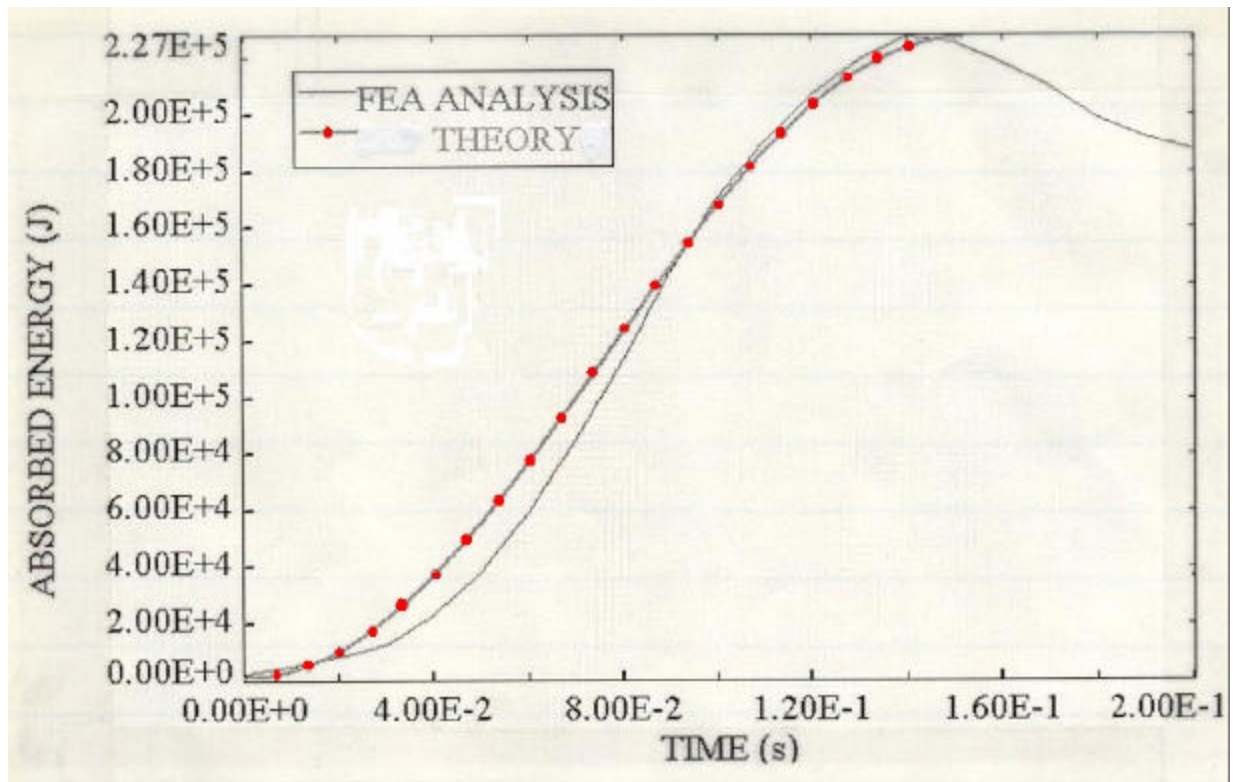


Figure 140 - Eight Region Plate Absorbed Energy vs. Time Comparison to FEA

The results of the analysis in Figure 140 compare well with the finite element solution having a correlation coefficient as calculated by Equation 5.1 of 0.893. The largest difference in the results occurs between  $t = 0.02$  and  $t = 0.085$  seconds due to elastic bending of the plate in the finite element method which is not accounted for in the simplified theory.

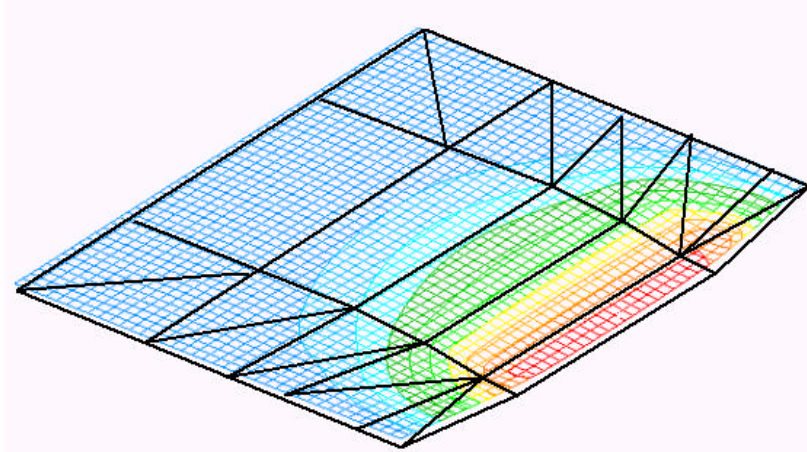


Figure 141 - Twenty-five Region Plate Overlaying FEA Plate Mesh Deformation

While the preceding eight region plate example shows the applicability of the plastic membrane approach to the determination of the energy absorbed from the lateral deflection of transverse bulkheads and plates, to properly use the theory in SIMCOL a new formulation of Equation 5.78 based on twenty five regions is required to accommodate all the possible contact scenarios and an initial velocity vector  $V_0$  which has components both parallel and orthogonal to the plate.

#### 5.4.5 The Energy Absorbed from a Twenty-Five-Region Plate

The eight-panel model of Figure 137 is not applicable for contact scenarios 1, 3 or 4 or for contact scenario 2 with both  $V_x$  and  $V_z$  initial velocity. For these scenarios a minimum of twenty-five regions is necessary to accurately capture the deformation patterns shown in Figure 114 through Figure 117, Figure 123 through Figure 126, Figure 128 through Figure 130 or Figure 141 where the twenty five regions overlay Figure 130.

To simplify the task of developing a general Equation for the determination of the total energy absorbed over a time step ( $t$ ) the following two additional assumptions are made for convenience:

- For contact scenario 2, the angle ( $f$ ) always equals zero degrees, i.e. if the angle ( $f$ ) is less than zero degrees then treat the analysis as if ( $f$ ) equals zero degrees.
- For contact scenario 4, the angle ( $a$ ) always equals zero degrees, i.e. if the angle ( $a$ ) is less than zero degrees then treat the analysis as if ( $a$ ) equals zero degrees.

Using these two assumptions, the deflections at the outboard edge of the plate of Figure 142 (segment HP) will always be equal to the maximum deflection of the plate. Accounting for all four contact scenarios, then after a small time step, a linear form of the deflection of the plate of Figure 111 may be represented with twenty five regions as shown Figure 142.

In Figure 142, regions I, VI and XI represent the initial contact area between the plate and the striking wedge at time  $t = i$  and the deflections of points H, I, J, K and L are equal to the deflections of points P, Q, R, S and T respectively at any time.

With the plate formulation of Figure 142, then the total energy absorbed by the plate over a time step may be written as the sum of the energy absorbed due to the translation in the  $z$  direction

and the energy absorbed due to the motion of the hinge lines in the x direction as is given by Equation 5.80.

$$E_{P\tau} = E_{Z\tau} + E_{X\tau} \quad (5.80)$$

Equation 5.80 effectively decouples the energy absorbed by the plate such that the motion of the rigid wedge over a small time step may be characterized as either an incremental step in the z direction followed by an incremental step in the x direction or as an incremental step in the x direction followed by an incremental step in the z direction. The choice of the initial step direction (x or z) is based on the greater of the available kinetic energy in either the x or z directions, which simplifies to the greater velocity component in the x or z direction. Thus if the component of the velocity in the x direction ( $V_x$ ) is greater than the component of the velocity in the z direction ( $V_z$ ) then the incremental step in the x direction is followed by an incremental step in the z direction. If, however,  $V_z$  is greater than  $V_x$  then the incremental step in the z direction is followed by an incremental step in the x direction. The total energy absorbed by the plate of Figure 142 is much more complicated than the plate of Figure 137 as previously determined in Section 5.4.4, however, the same method as used in Section 5.4.4 applies to the twenty five region plate of Figure 142.

Using the method of rupture indicators, as discussed in Section 5.4.4, the following conditional statements for the twenty-five-region plate can be made:

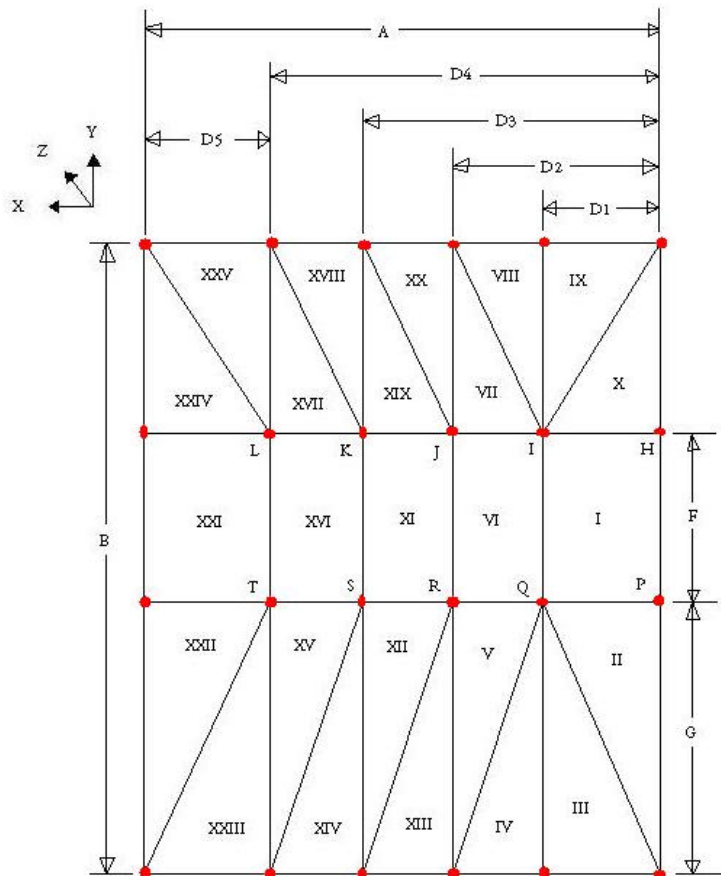


Figure 142 - Twenty-five Region Plate Geometry

$$\begin{aligned}
E_{Z\tau} = E_{X\tau} = & \sum_{i=III}^{IX} E_i + \sum_{i=XI}^{XXV} E_i \text{ if } \lambda_I = 0 \\
& \frac{E_I}{2} + E_{III} + \sum_{i=IV}^{XXV} E_i \text{ if } \lambda_{II} = 0 \\
& E_I + E_{II} + \sum_{i=V}^{XXV} E_i \text{ if } \lambda_{III} = 0 \\
& E_I + E_{II} + \sum_{i=V}^{XXV} E_i \text{ if } \lambda_{IV} = 0 \\
& \sum_{i=I}^{IV} E_i + \sum_{i=VI}^{XXV} E_i \text{ if } \lambda_V = 0 \\
& \sum_{i=I}^{IV} E_i + \sum_{i=VIII}^{XXV} E_i \text{ if } \lambda_{VI} = 0 \\
& \sum_{i=I}^{VI} E_i + \sum_{i=VIII}^{XXV} E_i \text{ if } \lambda_{VII} = 0 \\
& \sum_{i=I}^{VII} E_i + \sum_{i=X}^{XXV} E_i \text{ if } \lambda_{VIII} = 0 \\
& \sum_{i=I}^{VII} E_i + \sum_{i=X}^{XXV} E_i \text{ if } \lambda_{IX} = 0 \\
& \frac{E_I}{2} + \sum_{i=II}^{IX} E_i + \sum_{i=XI}^{XXV} E_i \text{ if } \lambda_X = 0 \\
& \sum_{i=I}^X E_i + \sum_{i=XIII}^{XVIII} E_i + \sum_{i=XX}^{XXV} E_i \text{ if } \lambda_{XI} = 0 \\
& \sum_{i=I}^{XI} E_i + \sum_{i=XIII}^{XXV} E_i \text{ if } \lambda_{XII} = 0 \\
& \sum_{i=I}^{IV} E_i + \sum_{i=VI}^{XII} E_i + \sum_{i=XIV}^{XXV} E_i \text{ if } \lambda_{XIII} = 0 \\
& \sum_{i=I}^{XI} E_i + E_{XIII} + \sum_{i=XV}^{XXV} E_i \text{ if } \lambda_{XIV} = 0 \\
& \sum_{i=I}^{XIV} E_i + \sum_{i=XVI}^{XXV} E_i \text{ if } \lambda_{XV} = 0 \\
& \sum_{i=I}^{XIV} E_i + \sum_{i=XVIII}^{XXV} E_i \text{ if } \lambda_{XVI} = 0 \\
& \sum_{i=I}^{XVI} E_i + \sum_{i=XVIII}^{XXV} E_i \text{ if } \lambda_{XVII} = 0 \\
& \sum_{i=I}^{XVII} E_i + \sum_{i=XX}^{XXV} E_i \text{ if } \lambda_{XVIII} = 0 \\
& \sum_{i=I}^{XVIII} E_i + \sum_{i=XX}^{XXV} E_i \text{ if } \lambda_{XIX} = 0 \\
& \sum_{i=I}^{VI} E_i + \sum_{i=VIII}^{XIX} E_i + \sum_{i=XXI}^{XXV} E_i \text{ if } \lambda_{XX} = 0 \\
& E_{XXIII} + E_{XXV} + \sum_{i=I}^{VI} E_i \text{ if } \lambda_{XXI} = 0 \\
& \sum_{i=I}^{XXI} E_i + \sum_{i=XXIII}^{XXV} E_i \text{ if } \lambda_{XXII} = 0 \\
& E_{XXIV} + E_{XXV} + \sum_{i=I}^{XIV} E_i + \sum_{i=XVI}^{XXII} E_i \text{ if } \lambda_{XXIII} = 0 \\
& E_{XXV} + \sum_{i=I}^{XXIII} E_i \text{ if } \lambda_{XIV} = 0 \\
& \sum_{i=I}^{XVI} E_i + \sum_{i=XVIII}^{XXIV} E_i \text{ if } \lambda_{XV} = 0
\end{aligned}$$

(5.81)

Using the conditional statements of Equation 5.81 then the relations of Equations 5.82 and 5.83 are true.

$$\lambda_{III} = \lambda_{IV} \quad (5.82)$$

$$\lambda_{VIII} = \lambda_{IX} \quad (5.83)$$

Additionally, critical combinations of the rupture indicators lead to the following additional conditional statements:

$$(\lambda_{IV} = 0) \text{ if } \lambda_{III} = 0 \quad (5.84)$$

$$(\lambda_{IX} = 0) \text{ if } \lambda_{VIII} = 0 \quad (5.85)$$

$$(\lambda_{II} = \lambda_X = 0) \text{ if } \lambda_I = 0 \quad (5.86)$$

$$(\lambda_{XII} = \lambda_{XIX} = 0) \text{ if } \lambda_{XI} = 0 \quad (5.87)$$

$$(\lambda_{XXII} = \lambda_{XXIV} = 0) \text{ if } \lambda_{XXI} = 0 \quad (5.88)$$

$$(\lambda_{XVII} = \lambda_{XV} = 0) \text{ if } \lambda_{XVI} = 0 \quad (5.89)$$

$$(\lambda_{III} = 0) \text{ if } \lambda_{IV} = 0 \quad (5.90)$$

$$(\lambda_{VII} = \lambda_V = 0) \text{ if } \lambda_{VI} = 0 \quad (5.91)$$

$$(\lambda_{XVII} = \lambda_{XV} = 0) \text{ if } \lambda_{XVI} = 0 \quad (5.92)$$

$$(\lambda_V = 0) \text{ if } \lambda_{XIII} = 0 \quad (5.93)$$

$$(\lambda_{XV} = 0) \text{ if } \lambda_{XXIII} = 0 \quad (5.94)$$

$$(\lambda_{XIX} = 0) \text{ if } \lambda_{XVIII} = 0 \quad (5.95)$$

$$(\lambda_V = 0) \text{ if } \lambda_{XIII} = 0 \quad (5.96)$$

$$(\lambda_{VII} = 0) \text{ if } \lambda_{XX} = 0 \quad (5.97)$$

$$(\lambda_{XIX} = 0) \text{ if } \lambda_{XVIII} = 0 \quad (5.98)$$

$$(\lambda_{VI} = \lambda_{VII} = 0) \text{ if } \begin{cases} \lambda_V = 0 \\ \lambda_{XIII} = 1 \end{cases} \quad (5.99)$$

$$(\lambda_{XI} = \lambda_{XIX} = 0) \text{ if } \begin{cases} \lambda_{XII} = 0 \\ \lambda_{XIV} = 1 \end{cases} \quad (5.100)$$

$$(\lambda_{XVI} = \lambda_{XVII} = 0) \text{ if } \begin{cases} \lambda_{XV} = 0 \\ \lambda_{XXIII} = 1 \end{cases} \quad (5.101)$$

$$(\lambda_{XI} = \lambda_{XII} = 0) \text{ if } \begin{cases} \lambda_{XIX} = 0 \\ \lambda_{XVIII} = 1 \end{cases} \quad (5.102)$$

$$(\lambda_{XI} = \lambda_{XII} = 0) \text{ if } \begin{cases} \lambda_{XIX} = 0 \\ \lambda_{XVIII} = 1 \end{cases} \quad (5.103)$$

$$(\lambda_{XV} = \lambda_{XVI} = 0) \text{ if } \begin{cases} \lambda_{XVII} = 0 \\ \lambda_{XXV} = 1 \end{cases} \quad (5.104)$$

Using all the above conditional statements, Equations 5.84 through 5.104, then for each region the following conditional equations apply.

$$E_I = \begin{cases} 0 \text{ if } \begin{cases} \lambda_I = 0 \\ \text{or}(\lambda_{II} = \lambda_X = 0) \\ \text{or}(\lambda_{II} = \lambda_{III} = \lambda_{VI} = 0) \\ \text{or}(\lambda_X = \lambda_{IX} = \lambda_{VI} = 0) \\ \text{or}(\lambda_{II} = \lambda_{III} = \lambda_{XIII} = \lambda_{XI} = 0) \\ \text{or}(\lambda_X = \lambda_{IX} = \lambda_{XX} = \lambda_{XI} = 0) \\ \text{or}(\lambda_{II} = \lambda_{III} = \lambda_V = 0) \text{ and } (\lambda_{XIII} = 1) \\ \text{or}(\lambda_X = \lambda_{IX} = \lambda_{VII} = 0) \text{ and } (\lambda_{XX} = 1) \\ \text{or}(\lambda_{II} = \lambda_{III} = \lambda_{XIII} = \lambda_{XIV} = \lambda_{XVI} = 0) \\ \text{or}(\lambda_X = \lambda_{IX} = \lambda_{XX} = \lambda_{XVIII} = \lambda_{XVI} = 0) \\ \text{or}(\lambda_{II} = \lambda_{III} = \lambda_{XIII} = \lambda_{XII} = 0) \text{ and } (\lambda_{XIV} = 1) \\ \text{or}(\lambda_X = \lambda_{IX} = \lambda_{XX} = \lambda_{XIX} = 0) \text{ and } (\lambda_{XVIII} = 1) \\ \text{or}(\lambda_{II} = \lambda_{III} = \lambda_{XIII} = \lambda_{XIV} = \lambda_{XV} = 0) \text{ and } (\lambda_{XXIII} = 1) \\ \text{or}(\lambda_X = \lambda_{IX} = \lambda_{XX} = \lambda_{XVIII} = \lambda_{XVII} = 0) \text{ and } (\lambda_{XXV} = 1) \\ \text{or}(\lambda_{II} = \lambda_{III} = \lambda_{XIII} = \lambda_{XIV} = \lambda_{XXIII} = \lambda_{XXI} = 0) \\ \text{or}(\lambda_X = \lambda_{IX} = \lambda_{XX} = \lambda_{XVIII} = \lambda_{XXV} = \lambda_{XXI} = 0) \end{cases} \\ \frac{E_I}{2} \text{ if } \begin{cases} \lambda_X = 0 \\ \text{or}(\lambda_{II} = 0) \end{cases} \end{cases} \quad (5.105)$$

$$E_{II} = 0 \text{ if } \left| \begin{array}{l} \lambda_{II} = 0 \\ \text{or}(\lambda_X = 0) \end{array} \right. \quad (5.106)$$

$$E_{III} = 0 \text{ if } \left| \begin{array}{l} \lambda_{III} = 0 \\ \text{or}(\lambda_{IV} = 0) \end{array} \right. \quad (5.107)$$

$$E_{IV} = 0 \text{ if } \left| \begin{array}{l} \lambda_{IV} = 0 \\ \text{or}(\lambda_{III} = 0) \end{array} \right. \quad (5.108)$$

$$E_V = 0 \text{ if } \left| \begin{array}{l} \lambda_V = 0 \\ \text{or}(\lambda_{VI} = 0) \\ \text{or}(\lambda_{XIII} = 0) \end{array} \right. \quad (5.109)$$

$$E_{VI} = \left| \begin{array}{l} 0 \text{ if } \left| \begin{array}{l} \lambda_{VI} = 0 \\ \text{or}(\lambda_V = 0) \text{ and } (\lambda_{XIII} = 1) \\ \text{or}(\lambda_{VII} = 0) \text{ and } (\lambda_{XX} = 1) \\ \text{or}(\lambda_{II} = \lambda_{III} = \lambda_{XIII} = \lambda_{XI} = 0) \\ \text{or}(\lambda_X = \lambda_{IX} = \lambda_{XX} = \lambda_{XI} = 0) \\ \text{or}(\lambda_{II} = \lambda_{III} = \lambda_{XIII} = \lambda_{XIV} = \lambda_{XVI} = 0) \\ \text{or}(\lambda_X = \lambda_{IX} = \lambda_{XX} = \lambda_{XVIII} = \lambda_{XVI} = 0) \\ \text{or}(\lambda_X = \lambda_{IX} = \lambda_{VII} = 0) \text{ and } (\lambda_{XX} = 1) \\ \text{or}(\lambda_{II} = \lambda_{III} = \lambda_{XIII} = \lambda_{XII} = 0) \text{ and } (\lambda_{XIV} = 1) \\ \text{or}(\lambda_X = \lambda_{IX} = \lambda_{XX} = \lambda_{XIX} = 0) \text{ and } (\lambda_{XVIII} = 1) \\ \text{or}(\lambda_{II} = \lambda_{III} = \lambda_{XIII} = \lambda_{XIV} = \lambda_{XV} = 0) \text{ and } (\lambda_{XXIII} = 1) \\ \text{or}(\lambda_X = \lambda_{IX} = \lambda_{XX} = \lambda_{XVIII} = \lambda_{XVII} = 0) \text{ and } (\lambda_{XXV} = 1) \\ \text{or}(\lambda_{II} = \lambda_{III} = \lambda_{XIII} = \lambda_{XIV} = \lambda_{XXIII} = \lambda_{XXI} = 0) \\ \text{or}(\lambda_X = \lambda_{IX} = \lambda_{XX} = \lambda_{XVIII} = \lambda_{XXV} = \lambda_{XXI} = 0) \end{array} \right. \\ \frac{E_{VI}}{2} \text{ if } \left| \begin{array}{l} \lambda_I = \lambda_{III} = \lambda_{XX} = 0 \\ \text{or}(\lambda_I = \lambda_{IX} = \lambda_{XX} = 0) \\ \text{or}(\lambda_{XX} = \lambda_{XI} = 0) \\ \text{or}(\lambda_{XIII} = \lambda_{XI} = 0) \end{array} \right. \end{array} \right. \quad (5.110)$$

$$E_{VII} = 0 \text{ if } \left| \begin{array}{l} \lambda_{VII} = 0 \\ \text{or}(\lambda_{XX} = 0) \\ \text{or}(\lambda_{VI} = 0) \end{array} \right. \quad (5.111)$$

$$E_{VIII} = 0 \text{ if } \begin{cases} \lambda_{VIII} = 0 \\ \text{or}(\lambda_{IX} = 0) \end{cases} \quad (5.112)$$

$$E_{IX} = 0 \text{ if } \begin{cases} \lambda_{IX} = 0 \\ \text{or}(\lambda_{VIII} = 0) \end{cases} \quad (5.113)$$

$$E_X = 0 \text{ if } \begin{cases} \lambda_X = 0 \\ \text{or}(\lambda_I = 0) \end{cases} \quad (5.114)$$

$$E_{XI} = \begin{cases} 0 \text{ if } \begin{cases} \lambda_{XI} = 0 \\ \text{or}(\lambda_{XII} = 0) \text{ and } (\lambda_{XIV} = 1) \\ \text{or}(\lambda_{XIX} = 0) \text{ and } (\lambda_{XVIII} = 1) \\ \text{or}(\lambda_{II} = \lambda_{III} = \lambda_{XIII} = \lambda_{XIV} = \lambda_{XVI} = 0) \\ \text{or}(\lambda_X = \lambda_{IX} = \lambda_{XX} = \lambda_{XVIII} = \lambda_{XVI} = 0) \\ \text{or}(\lambda_{II} = \lambda_{III} = \lambda_{XIII} = \lambda_{XIV} = \lambda_{XV} = 0) \text{ and } (\lambda_{XXIII} = 1) \\ \text{or}(\lambda_X = \lambda_{IX} = \lambda_{XX} = \lambda_{XVIII} = \lambda_{XVII} = 0) \text{ and } (\lambda_{XXV} = 1) \\ \text{or}(\lambda_{II} = \lambda_{III} = \lambda_{XIII} = \lambda_{XIV} = \lambda_{XXIII} = \lambda_{XXI} = 0) \\ \text{or}(\lambda_X = \lambda_{IX} = \lambda_{XX} = \lambda_{XVIII} = \lambda_{XXV} = \lambda_{XXI} = 0) \end{cases} \\ \frac{E_{XI}}{2} \text{ if } \begin{cases} \lambda_I = \lambda_{III} = \lambda_{VI} = \lambda_{XIII} = \lambda_{XIV} = 0 \\ \text{or}(\lambda_I = \lambda_{IX} = \lambda_{VI} = \lambda_{XX} = \lambda_{XVIII} = 0) \\ \text{or}(\lambda_{XVIII} = \lambda_{XVI} = 0) \\ \text{or}(\lambda_{XIV} = \lambda_{XVI} = 0) \end{cases} \end{cases} \quad (5.115)$$

$$E_{XII} = 0 \text{ if } \begin{cases} \lambda_{XII} = 0 \\ \text{or}(\lambda_{XI} = 0) \\ \text{or}(\lambda_{XIV} = 0) \end{cases} \quad (5.116)$$

$$E_{XIII} = 0 \text{ if } \lambda_{XIII} = 0 \quad (5.117)$$

$$E_{XIV} = 0 \text{ if } \lambda_{XIV} = 0 \quad (5.118)$$

$$E_{XV} = 0 \text{ if } \begin{cases} \lambda_{XV} = 0 \\ \text{or}(\lambda_{XXIII} = 0) \\ \text{or}(\lambda_{XVI} = 0) \end{cases} \quad (5.119)$$

$$E_{XVI} = \begin{cases} 0 & \text{if } \left| \begin{array}{l} \lambda_{XVI} = 0 \\ \text{or}(\lambda_{XV} = 0) \text{ and } (\lambda_{XXIII} = 1) \\ \text{or}(\lambda_{XVII} = 0) \text{ and } (\lambda_{XXV} = 1) \\ \text{or}(\lambda_{II} = \lambda_{III} = \lambda_{XIII} = \lambda_{XIV} = \lambda_{XXIII} = \lambda_{XXI} = 0) \\ \text{or}(\lambda_X = \lambda_{IX} = \lambda_{XX} = \lambda_{XVIII} = \lambda_{XXV} = \lambda_{XXI} = 0) \end{array} \right. \\ \frac{E_{XVI}}{2} & \text{if } \left| \begin{array}{l} \lambda_I = \lambda_{III} = \lambda_{VI} = \lambda_{XI} = \lambda_{XIV} = \lambda_{XXIII} = 0 \\ \text{or}(\lambda_I = \lambda_{III} = \lambda_{VI} = \lambda_{XI} = \lambda_{XVIII} = \lambda_{XXV} = 0) \\ \text{or}(\lambda_{XXI} = \lambda_{XXV} = 0) \\ \text{or}(\lambda_{XXI} = \lambda_{XXIII} = 0) \end{array} \right. \end{cases} \quad (5.120)$$

$$E_{XVII} = 0 \text{ if } \left| \begin{array}{l} \lambda_{XVII} = 0 \\ \text{or}(\lambda_{XVI} = 0) \\ \text{or}(\lambda_{XXV} = 0) \end{array} \right. \quad (5.121)$$

$$E_{XVIII} = 0 \text{ if } \lambda_{XVIII} = 0 \quad (5.122)$$

$$E_{XIX} = 0 \text{ if } \left| \begin{array}{l} \lambda_{XIX} = 0 \\ \text{or}(\lambda_{XVIII} = 0) \\ \text{or}(\lambda_{XI} = 0) \end{array} \right. \quad (5.123)$$

$$E_{XX} = 0 \text{ if } \lambda_{XX} = 0 \quad (5.124)$$

$$E_{XXI} = 0 \text{ if } \lambda_{XXI} = 0 \quad (5.125)$$

$$E_{XXII} = 0 \text{ if } \left| \begin{array}{l} \lambda_{XXII} = 0 \\ \text{or}(\lambda_{XXI} = 0) \end{array} \right. \quad (5.126)$$

$$E_{XXIII} = 0 \text{ if } \lambda_{XXIII} = 0 \quad (5.127)$$

$$E_{XXIV} = 0 \text{ if } \left| \begin{array}{l} \lambda_{XXIV} = 0 \\ \text{or}(\lambda_{XXI} = 0) \end{array} \right. \quad (5.128)$$

$$E_{XXV} = 0 \text{ if } \lambda_{XXV} = 0 \quad (5.129)$$

Using Equations 5.105 through 5.129 then the formulation of  $(E_{xt})$  or  $(E_{zt})$  may be given by Equation 5.130.

$$\begin{aligned}
E_{X\tau} = E_{Z\tau} = & \lambda_0 \cdot (\lambda_1 \cdot E_I + \lambda_6 \cdot E_{VI} + \lambda_{11} \cdot E_{XI} + \lambda_{16} \cdot E_{XVI} + \lambda_{21} \cdot E_{XXI}) + \dots \\
& \dots + \lambda_0 \cdot \lambda_{YL} \cdot (\lambda_2 \cdot E_{II} + \lambda_3 \cdot E_{III} + \lambda_4 \cdot E_{IV} + \lambda_5 \cdot E_V + \lambda_{13} \cdot E_{XIII}) + \dots \\
& \dots + \lambda_0 \cdot \lambda_{YL} \cdot (\lambda_{12} \cdot E_{XII} + \lambda_{14} \cdot E_{XIV} + \lambda_{15} \cdot E_{XV} + \lambda_{23} \cdot E_{XXIII} + \lambda_{22} \cdot E_{XXII}) + \dots \\
& \dots + \lambda_0 \cdot \lambda_{YU} \cdot (\lambda_{10} \cdot E_X + \lambda_9 \cdot E_{IX} + \lambda_8 \cdot E_{VIII} + \lambda_7 \cdot E_{VII} + \lambda_{20} \cdot E_{XX}) + \dots \\
& \dots + \lambda_0 \cdot \lambda_{YU} \cdot (\lambda_{19} \cdot E_{XIX} + \lambda_{18} \cdot E_{XVIII} + \lambda_{17} \cdot E_{XVII} + \lambda_{25} \cdot E_{XXV} + \lambda_{24} \cdot E_{XXIV})
\end{aligned} \tag{5.130}$$

All of the rupture indicator terms of Equation 5.130 are defined by Equations 5.131 through 5.187.

$$\lambda_1 = \left( \frac{\lambda_{II} + \lambda_X}{2} \right) \cdot \min[1, \lambda_I \cdot \lambda_A \cdot [(\lambda_{II} + \lambda_{III} + \lambda_{VI}) \cdot (\lambda_X + \lambda_{VI} + \lambda_{IX}) \cdot (\lambda_{II} + \lambda_{III} + \lambda_{XIII} + \lambda_{XI}) \cdot \lambda_{Z1}]] \tag{5.131}$$

$$\lambda_{Z1} = (\lambda_X + \lambda_{IX} + \lambda_{XX} + \lambda_{XI}) (\lambda_{II} + \lambda_{III} + \lambda_{XIII} + \lambda_{XIV} + \lambda_{XVI}) (\lambda_X + \lambda_{IX} + \lambda_{XX} + \lambda_{XVIII} + \lambda_{XVI}) (\lambda_{Z2}) \tag{5.132}$$

$$\lambda_{Z2} = (\lambda_{II} + \lambda_{III} + \lambda_{XIII} + \lambda_{XIV} + \lambda_{XXIII} + \lambda_{XXI}) \cdot (\lambda_X + \lambda_{IX} + \lambda_{XX} + \lambda_{XVIII} + \lambda_{XXV} + \lambda_{XXI}) \tag{5.133}$$

$$\lambda_{Z3} = [\lambda_X + \lambda_{IX} + \lambda_{XX} + \lambda_{XIX} + (1 - \lambda_{XVIII})] [\lambda_{II} + \lambda_{III} + \lambda_{XIII} + \lambda_{XIV} + \lambda_{XV} + (1 - \lambda_{XXIII})] (\lambda_{Z4}) \tag{5.134}$$

$$\lambda_A = [\lambda_{II} + \lambda_{III} + \lambda_V + (1 - \lambda_{XIII})] [\lambda_X + \lambda_{IX} + \lambda_{VII} + (1 - \lambda_{XX})] [\lambda_{II} + \lambda_{III} + \lambda_{XIII} + \lambda_{XII} + (1 - \lambda_{XIV})] \cdot \lambda_{Z3} \tag{5.135}$$

$$\lambda_{Z4} = \lambda_X + \lambda_{IX} + \lambda_{XX} + \lambda_{XVIII} + \lambda_{XVII} + (1 - \lambda_{XXV}) \tag{5.136}$$

$$\lambda_2 = \lambda_I \cdot \lambda_{II} \tag{5.137}$$

$$\lambda_3 = \lambda_{III} \cdot \lambda_{IV} \tag{5.138}$$

$$\lambda_4 = \lambda_3 \tag{5.139}$$

$$\lambda_5 = \lambda_V \cdot \lambda_{VI} \cdot \lambda_{XIII} \tag{5.140}$$

$$\lambda_6 = \lambda_B \cdot \min[1, \lambda_{VI} \cdot \lambda_C \cdot (\lambda_{II} + \lambda_{III} + \lambda_{XIII} + \lambda_{XI}) (\lambda_X + \lambda_{IX} + \lambda_{XX} + \lambda_{XI}) (\lambda_{II} + \lambda_{III} + \lambda_{XIII} + \lambda_{XIV} + \lambda_{XVI}) \cdot \lambda_{Z5}] \tag{5.141}$$

$$\lambda_{Z5} = (\lambda_X + \lambda_{IX} + \lambda_{XX} + \lambda_{XVIII} + \lambda_{XVI}) (\lambda_{II} + \lambda_{III} + \lambda_{XIII} + \lambda_{XIV} + \lambda_{XXIII} + \lambda_{XXI}) (\lambda_{Z6}) \tag{5.142}$$

$$\lambda_{Z6} = \lambda_X + \lambda_{IX} + \lambda_{XX} + \lambda_{XVIII} + \lambda_{XXV} + \lambda_{XXI} \quad (5.143)$$

$$\lambda_D = \min[1, (\lambda_I + \lambda_{III} + \lambda_{XIII})] \quad (5.144)$$

$$\lambda_E = \min[1, (\lambda_I + \lambda_{IX} + \lambda_{XX})] \quad (5.145)$$

$$\lambda_F = \min[1, (\lambda_{XX} + \lambda_{XI})] \quad (5.146)$$

$$\lambda_G = \min[1, (\lambda_{XIII} + \lambda_{XI})] \quad (5.147)$$

$$\lambda_B = 8 \cdot \left( \frac{\lambda_D + \lambda_E \cdot \lambda_F \cdot \lambda_G}{2} \right) \left( \frac{\lambda_E + \lambda_D \cdot \lambda_F \cdot \lambda_G}{2} \right) \left( \frac{\lambda_F + \lambda_E \cdot \lambda_D \cdot \lambda_G}{2} \right) \left( \frac{\lambda_G + \lambda_E \cdot \lambda_F \cdot \lambda_D}{2} \right) \quad (5.148)$$

$$\lambda_C = [\lambda_V + (1 - \lambda_{XIII})][\lambda_{VII} + (1 - \lambda_{XX})][\lambda_{II} + \lambda_{III} + \lambda_{XIII} + \lambda_{XII} + (1 - \lambda_{XIV})](\lambda_{Z7}) \quad (5.149)$$

$$\lambda_{Z7} = [\lambda_X + \lambda_{IX} + \lambda_{XX} + \lambda_{XIX} + (1 - \lambda_{XVIII})][\lambda_{II} + \lambda_{III} + \lambda_{XIII} + \lambda_{XIV} + \lambda_{XV} + (1 - \lambda_{XXIII})](\lambda_{Z8}) \quad (5.150)$$

$$\lambda_{Z8} = \lambda_X + \lambda_{IX} + \lambda_{XX} + \lambda_{XVIII} + \lambda_{XVII} + (1 - \lambda_{XXV}) \quad (5.151)$$

$$\lambda_7 = \lambda_{VII} \cdot \lambda_{XX} \cdot \lambda_{VI} \quad (5.152)$$

$$\lambda_8 = \lambda_{VIII} \cdot \lambda_{IX} \quad (5.153)$$

$$\lambda_9 = \lambda_8 \quad (5.154)$$

$$\lambda_{10} = \lambda_I \cdot \lambda_X \quad (5.155)$$

$$\lambda_{11} = \lambda_H \cdot \min[1, \lambda_{XI} \cdot \lambda_J \cdot [(\lambda_{II} + \lambda_{III} + \lambda_{XIII} + \lambda_{XIV} + \lambda_{XVI})(\lambda_X + \lambda_{IX} + \lambda_{XX} + \lambda_{XVIII} + \lambda_{XVI})(\lambda_{Z9})]] \quad (5.156)$$

$$\lambda_{Z9} = (\lambda_{II} + \lambda_{III} + \lambda_{XIII} + \lambda_{XIV} + \lambda_{XXIII} + \lambda_{XXI})(\lambda_X + \lambda_{IX} + \lambda_{XX} + \lambda_{XVIII} + \lambda_{XXV} + \lambda_{XXI}) \quad (5.157)$$

$$\lambda_K = \min[1, (\lambda_I + \lambda_{III} + \lambda_{VI} + \lambda_{XIII} + \lambda_{XIV})] \quad (5.158)$$

$$\lambda_L = \min[1, (\lambda_I + \lambda_{IX} + \lambda_{VI} + \lambda_{XX} + \lambda_{XVIII})] \quad (5.159)$$

$$\lambda_M = \min[1, (\lambda_{XVIII} + \lambda_{XVI})] \quad (5.160)$$

$$\lambda_N = \min[1, (\lambda_{XIV} + \lambda_{XVI})] \quad (5.161)$$

$$\lambda_H = 8 \cdot \left( \frac{\lambda_K + \lambda_L \cdot \lambda_M \cdot \lambda_N}{2} \right) \left( \frac{\lambda_L + \lambda_K \cdot \lambda_M \cdot \lambda_N}{2} \right) \left( \frac{\lambda_M + \lambda_L \cdot \lambda_K \cdot \lambda_N}{2} \right) \left( \frac{\lambda_N + \lambda_L \cdot \lambda_M \cdot \lambda_K}{2} \right) \quad (5.162)$$

$$\lambda_J = [\lambda_{XII} + (1 - \lambda_{XIV})][\lambda_{XIX} + (1 - \lambda_{XVIII})][\lambda_{II} + \lambda_{III} + \lambda_{XIII} + \lambda_{XIV} + \lambda_{XV} + (1 - \lambda_{XXIII})](\lambda_{Z10}) \quad (5.163)$$

$$\lambda_{Z10} = \lambda_X + \lambda_{IX} + \lambda_{XX} + \lambda_{XVIII} + \lambda_{XVII} + (1 - \lambda_{XXV}) \quad (5.164)$$

$$\lambda_{12} = \lambda_{XII} \cdot \lambda_{XI} \cdot \lambda_{XIV} \quad (5.165)$$

$$\lambda_{13} = \lambda_{XIII} \quad (5.166)$$

$$\lambda_{14} = \lambda_{XIV} \quad (5.167)$$

$$\lambda_{15} = \lambda_{XV} \cdot \lambda_{XXIII} \cdot \lambda_{XVI} \quad (5.168)$$

$$\lambda_{16} = \lambda_P \cdot \min[1, \lambda_{XVI}[(\lambda_{II} + \lambda_{III} + \lambda_{XIII} + \lambda_{XIV} + \lambda_{XXIII} + \lambda_{XXI})[\lambda_{XV} + (1 - \lambda_{XXII})](\lambda_{Z11})]] \quad (5.169)$$

$$\lambda_{Z11} = [\lambda_{XVII} + (1 - \lambda_{XXV})] \cdot (\lambda_X + \lambda_{IX} + \lambda_{XX} + \lambda_{XVIII} + \lambda_{XXV} + \lambda_{XXI}) \quad (5.170)$$

$$\lambda_Q = \min[1, (\lambda_I + \lambda_{III} + \lambda_{VI} + \lambda_{XI} + \lambda_{XIV} + \lambda_{XXIII})] \quad (5.171)$$

$$\lambda_R = \min[1, (\lambda_I + \lambda_{IX} + \lambda_{VI} + \lambda_{XI} + \lambda_{XVIII} + \lambda_{XXV})] \quad (5.172)$$

$$\lambda_S = \min[1, (\lambda_{XXI} + \lambda_{XXV})] \quad (5.173)$$

$$\lambda_T = \min[1, (\lambda_{XXI} + \lambda_{XXIII})] \quad (5.174)$$

$$\lambda_P = 8 \cdot \left( \frac{\lambda_Q + \lambda_R \cdot \lambda_S \cdot \lambda_T}{2} \right) \left( \frac{\lambda_R + \lambda_Q \cdot \lambda_S \cdot \lambda_T}{2} \right) \left( \frac{\lambda_S + \lambda_R \cdot \lambda_Q \cdot \lambda_T}{2} \right) \left( \frac{\lambda_T + \lambda_R \cdot \lambda_S \cdot \lambda_Q}{2} \right) \quad (5.175)$$

$$\lambda_{17} = \lambda_{XVII} \cdot \lambda_{XVI} \cdot \lambda_{XXV} \quad (5.176)$$

$$\lambda_{18} = \lambda_{XVIII} \quad (5.177)$$

$$\lambda_{19} = \lambda_{XIX} \cdot \lambda_{XVIII} \cdot \lambda_{XI} \quad (5.178)$$

$$\lambda_{20} = \lambda_{XX} \quad (5.179)$$

$$\lambda_{21} = \lambda_{XXI} \quad (5.180)$$

$$\lambda_{22} = \lambda_{XXI} \cdot \lambda_{XXII} \quad (5.181)$$

$$\lambda_{23} = \lambda_{XXIII} \quad (5.182)$$

$$\lambda_{24} = \lambda_{XXI} \cdot \lambda_{XXIV} \quad (5.183)$$

$$\lambda_{25} = \lambda_{XXV} \quad (5.184)$$

$$\lambda_{YL} = \begin{cases} 1 & \text{if } G > 0 \\ 0 & \text{otherwise} \end{cases} \quad (5.185)$$

$$\lambda_{YU} = \begin{cases} 1 & \text{if } B - (G + F) > 0 \\ 0 & \text{otherwise} \end{cases} \quad (5.186)$$

$$\lambda_0 = \min[1, (\lambda_{YL} + \lambda_{YU})] \quad (5.187)$$

To enable the treatment of transverse bulkheads and webs between double hulls to be similar to the treatment of single hull webs, where the inboard edge is free, the assumption that the inboard edge is simply supported until contacted by the rigid wedge is necessary. The assumption is only practical because a flange located on the free edge stiffens most free webs. Thus, with this assumption there is no mathematical difference in the treatment of either transverse bulkheads or webs.

In an analysis where  $V_x$  is greater than zero then the points I, Q, J, R, K, S, L and T of Figure 142 will move from time step to time step in the x direction and thus  $D_1$ ,  $D_2$ ,  $D_3$  and  $D_4$  will increase in magnitude while  $D_5$  will decrease. At some time  $D_5$  will equal zero and  $D_4$  will equal the span (A). At later times the  $D_3$  will equal (A) followed by  $D_2$  and then  $D_1$ , should the analysis permit. Noting that  $D_1$ ,  $D_2$ ,  $D_3$  and  $D_4$  must always be less than or equal to the plate span, and that the energy absorbed in each region is dependant upon having some x dimension, then Equation 5.130 becomes:

$$\begin{aligned}
E_{X\tau} = E_{Z\tau} = & \lambda_0 \cdot (\lambda_1 \cdot E_I + \lambda_{D1} \cdot \lambda_6 \cdot E_{V1} + \lambda_{D2} \cdot \lambda_{11} \cdot E_{X1} + \lambda_{D3} \cdot \lambda_{16} \cdot E_{XV1} + \lambda_{D4} \cdot \lambda_{21} \cdot E_{XX1}) + \dots \\
& \dots + \lambda_0 \cdot \lambda_{YL} \cdot [\lambda_2 \cdot E_{II} + \lambda_3 \cdot E_{III} + \lambda_{D1} \cdot (\lambda_4 \cdot E_{IV} + \lambda_5 \cdot E_V) + \lambda_{D2} \cdot (\lambda_{12} \cdot E_{XII} + \lambda_{13} \cdot E_{XIII})] + \dots \\
& \dots + \lambda_0 \cdot \lambda_{YL} \cdot [\lambda_{D3} (\lambda_{14} \cdot E_{XIV} + \lambda_{15} \cdot E_{XV}) + \lambda_{D4} \cdot (\lambda_{22} \cdot E_{XXII} + \lambda_{23} \cdot E_{XXIII})] + \dots \\
& \dots + \lambda_0 \cdot \lambda_{YU} \cdot [\lambda_9 \cdot E_{IX} + \lambda_{10} \cdot E_X + \lambda_{D1} \cdot (\lambda_7 \cdot E_{VII} + \lambda_8 \cdot E_{VIII}) + \lambda_{D2} \cdot (\lambda_{19} \cdot E_{XIX} + \lambda_{20} \cdot E_{XX})] + \dots \\
& \dots + \lambda_0 \cdot \lambda_{YU} \cdot [\lambda_{D3} (\lambda_{17} \cdot E_{XVII} + \lambda_{18} \cdot E_{XVIII}) + \lambda_{D4} \cdot (\lambda_{25} \cdot E_{XXV} + \lambda_{24} \cdot E_{XXIV})]
\end{aligned} \tag{5.188}$$

Where the new rupture indicators of Equation 5.188 ( $\lambda_{D1}$ ,  $\lambda_{D2}$ ,  $\lambda_{D3}$  and  $\lambda_{D4}$ ) are given by Equations 5.189 through 5.192.

$$\lambda_{D1} = \begin{cases} 1 & \text{if } D_1 < A \\ 0 & \text{otherwise} \end{cases} \tag{5.189}$$

$$\lambda_{D2} = \begin{cases} 1 & \text{if } D_2 < A \\ 0 & \text{otherwise} \end{cases} \tag{5.190}$$

$$\lambda_{D3} = \begin{cases} 1 & \text{if } D_3 < A \\ 0 & \text{otherwise} \end{cases} \tag{5.191}$$

$$\lambda_{D4} = \begin{cases} 1 & \text{if } D_4 < A \\ 0 & \text{otherwise} \end{cases} \tag{5.192}$$

For each contact scenario the deflections in the z direction of points P, Q, R, S, and T may differ and will definitely change depending upon which motion (x or z) is the initial incremental step direction. A similar statement may also be made for the values of  $D_1$ ,  $D_2$ ,  $D_3$  and  $D_4$ . To continue the analysis and to enable the determination of the points P, Q, R, S and T, the initial position (relative to the plate) and the geometry of the striking wedge model must be known. To accomplish this, the x, y and z coordinates of the point  $B_p$  (on Figure 143) must be defined at time  $t = 0$  seconds. Additionally the striking wedge length ( $L_{RW}$ ), beam ( $B_{RW}$ ) and half entrance angle (HEA) must also be known. Finally, the angle between the centerline of the striking wedge and a line orthogonal to the plate, where the positive angle is to the positive z-axis, must also be known as shown in Figure 144.

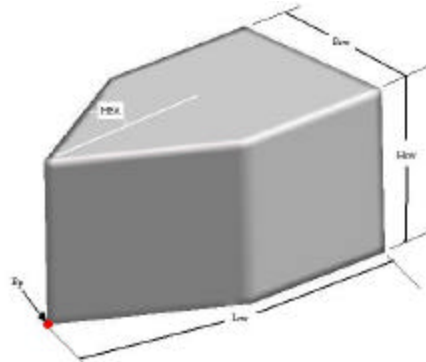


Figure 143 - Striking Wedge Variable Definitions

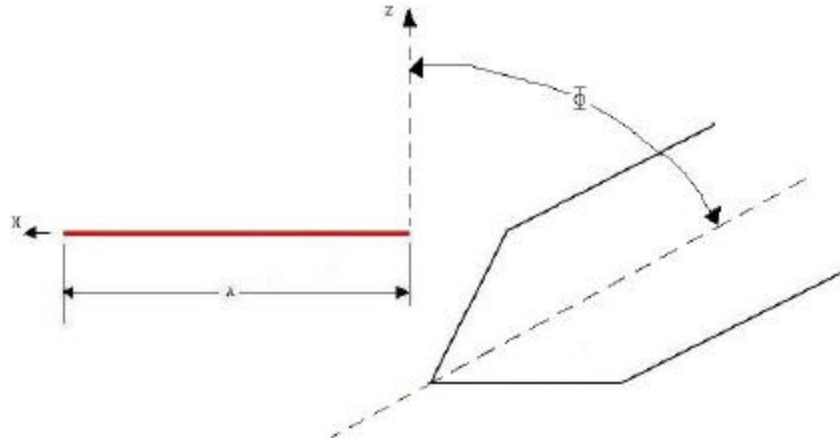


Figure 144 - Collision Angle Definition

Using the definitions prescribed in Figure 143 and Figure 144, then the values of G and F in Figure 132 may be calculated using Equations 5.193 and 5.194, and the contact scenario (CS) may be defined mathematically through the conditional statement of Equation 5.195.

$$G = \max(0, B_{Pv}) \quad (5.193)$$

$$F = H_{RW} + B_{Py} - G \quad (5.194)$$

$$CS = \begin{cases} 1 & \text{if } \left[ \begin{array}{l} B_{PZ} < 0 \wedge P_{XS} < 0 \wedge P_{ZS} > B_{PZ} \\ \text{or } (B_{PZ} > 0 \wedge P_{XP} < 0 \wedge P_{ZP} < B_{PZ}) \end{array} \right. \\ 2 & \text{if } \left[ \begin{array}{l} B_{PZ} > 0 \wedge P_{ZP} \geq B_{PZ} \\ \text{or } (B_{PZ} > 0 \wedge P_{ZS} \leq B_{PZ}) \end{array} \right. \\ 3 & \text{if } \left[ \begin{array}{l} P_{ZP} \geq 0 \wedge P_{XP} \geq 0 \wedge \Phi > 90 \\ \text{or } (P_{ZP} \leq 0 \wedge P_{XS} \geq 0 \wedge \Phi < 90) \end{array} \right. \\ 4 & \text{if } \left[ \begin{array}{l} P_{ZP} \geq 0 \wedge P_{XP} \geq 0 \wedge \Phi \leq 90 \\ \text{or } (P_{ZP} \leq 0 \wedge P_{XS} \geq 0 \wedge \Phi \geq 90) \end{array} \right. \\ \text{unhandled} & \text{otherwise} \end{cases} \quad (5.195)$$

Where the terms ( $P_{XS}$ ,  $P_{XP}$ ,  $P_{ZS}$  and  $P_{ZP}$ ) are defined by Equations 5.196 through 5.200.

$$L = \frac{B_{RW}}{2 \cdot \tan(\text{HEA})} \quad (5.196)$$

$$P_{XS} = B_{PX} - \left( L^2 + \frac{B_{RW}^2}{4} \right)^{\frac{1}{2}} \cdot \sin(\Phi - \text{HEA}) \quad (5.197)$$

$$P_{ZP} = B_{PZ} + \left( L^2 + \frac{B_{RW}^2}{4} \right)^{\frac{1}{2}} \cdot \text{Cos}(\Phi + \text{HEA}) \quad (5.198)$$

$$P_{ZS} = B_{PZ} + \left( L^2 + \frac{B_{RW}^2}{4} \right)^{\frac{1}{2}} \cdot \text{Cos}(\Phi - \text{HEA}) \quad (5.199)$$

$$P_{XP} = B_{PX} - \left( L^2 + \frac{B_{RW}^2}{4} \right)^{\frac{1}{2}} \cdot \text{Sin}(\Phi + \text{HEA}) \quad (5.200)$$

In addition to the mathematical determination of the contact scenario (CS) the variables defined by Figure 143 and Figure 144 allow the determination of the deflections of the points P, Q, R, S, and T over the time step (t) along with the change in the lengths D<sub>1</sub>, D<sub>2</sub>, D<sub>3</sub> and D<sub>4</sub>. As previously discussed, for each contact scenario the deflections may differ and will definitely change depending on the initial step direction. By defining the deflections of P, Q, R, S and T at the initial time (prior to the time step) as WP<sub>0</sub>, WQ<sub>0</sub>, WR<sub>0</sub>, WS<sub>0</sub> and WT<sub>0</sub> respectively, and after the initial step (either x or z) as WP<sub>1</sub>, WQ<sub>1</sub>, WR<sub>1</sub>, WS<sub>1</sub> and WT<sub>1</sub> respectively, and at the end of the time step (after both the x and z motions) as WP<sub>2</sub>, WQ<sub>2</sub>, WR<sub>2</sub>, WS<sub>2</sub> and WT<sub>2</sub> respectively, then for each possible contact formulation the following procedures as outlined in Sections 5.4.5.1 through 5.4.5.8 may be followed. Note that in the following sections the right superscript <sup><0></sup> refers to the value of the variable at time t = 0 zero seconds, odd values of the left superscript (<sup><1></sup>, <sup><3></sup>, <sup><5></sup>...) refer to the variable value after the initial step direction in a time step and even values of the left superscript (<sup><2></sup>, <sup><4></sup>, <sup><6></sup>...) refer to the variable value at the end of the previous time step or at the beginning of the next time step.

#### 5.4.5.1 Determination of Deflections in CS 1 with a Z-Direction Initial Step

Beginning with the initial deflections:

$$WP^{<0>} = WQ^{<0>} = WR^{<0>} = WS^{<0>} = WT^{<0>} = 0$$

$$B_{PZ}^{<0>} = \text{Given}$$

$$B_{PX}^{<0>} = \text{Given}$$

$$\Phi = \text{Given}$$

$$\text{HEA} = \text{Given}$$

$$B_{RW} = \text{Given}$$

$$L_{RW} = \text{Given}$$

$$B_{PY} = \text{Given}$$

(5.201)

$$L = \frac{B_{RW}}{2 \cdot \tan(\text{HEA})} \quad (5.202)$$

$$P_{XS}^{(0)} = B_{PX}^{(0)} - \left( L^2 + \frac{B_{RW}^2}{4} \right)^{\frac{1}{2}} \cdot \sin(\Phi - \text{HEA}) \quad (5.204)$$

$$P_{XP}^{(0)} = B_{PX}^{(0)} - \left( L^2 + \frac{B_{RW}^2}{4} \right)^{\frac{1}{2}} \cdot \sin(\Phi + \text{HEA}) \quad (5.205)$$

$$P_{ZP}^{(0)} = B_{PZ}^{(0)} + \left( L^2 + \frac{B_{RW}^2}{4} \right)^{\frac{1}{2}} \cdot \cos(\Phi + \text{HEA}) \quad (5.206)$$

$$CS = 1 \quad (5.207)$$

$$S_{LP} = \begin{cases} \frac{B_{PZ}^{(0)} - P_{ZP}^{(0)}}{B_{PX}^{(0)} - P_{PX}^{(0)}} & \text{if } \Phi \geq 90 \wedge B_{PZ}^{(0)} > 0 \\ \frac{B_{PZ}^{(0)} - P_{ZS}^{(0)}}{B_{PX}^{(0)} - P_{XS}^{(0)}} & \text{if } \Phi < 90 \wedge B_{PZ}^{(0)} < 0 \\ 0 & \text{otherwise} \end{cases} \quad (5.208)$$

$$B_{PZ}^{(1)} = B_{PZ}^{(0)} + V_Z^{(0)} \cdot \tau \quad (5.209)$$

$$B_{PX}^{(1)} = B_{PX}^{(0)} \quad (5.210)$$

$$P_{XS}^{(1)} = P_{XS}^{(0)} \quad (5.211)$$

$$P_{XP}^{(1)} = P_{XP}^{(0)} \quad (5.212)$$

$$P_{ZS}^{(1)} = P_{ZS}^{(0)} + V_Z^{(0)} \cdot \tau \quad (5.213)$$

$$P_{ZP}^{(1)} = P_{ZP}^{(0)} + V_Z^{(0)} \cdot \tau \quad (5.214)$$

$$D_2 = \max \left( 0, D_3 - V_x^{(0)} \cdot \tau, \frac{D_3}{2} \right) \quad (5.215)$$

$$D_3 = \max \left[ 0, \left( B_{PX}^{(1)} - \frac{B_{PZ}^{(1)}}{S_{LP}} \right) \right] \quad (5.216)$$

$$D_1 = \max \left( 0, D_3 - 2 \cdot V_X^{(0)} \cdot \tau, \frac{D_2}{2} \right) \quad (5.217)$$

$$\text{CONTYPE} = \begin{cases} 0 & \text{if } B_{PZ}^{(0)} > 0 \wedge P_{XP}^{(0)} < 0 \wedge P_{ZP}^{(0)} < B_{PZ}^{(0)} \\ 1 & \text{if } B_{PZ}^{(0)} < 0 \wedge P_{XS}^{(0)} < 0 \wedge P_{ZS}^{(0)} > B_{PZ}^{(0)} \end{cases} \quad (5.218)$$

$$WP^{(1)} = WS^{(1)} - S_{LP} \cdot D_3 \quad (5.219)$$

$$WR^{(1)} = WS^{(1)} - S_{LP} \cdot (D_3 - D_2) \quad (5.220)$$

$$WQ^{(1)} = WS^{(1)} - S_{LP} \cdot (D_3 - D_1) \quad (5.221)$$

$$D_4 = D_3 + V_X^{(0)} \cdot \tau \quad (5.222)$$

$$WS^{(1)} = \begin{cases} \min(0, B_{PZ}^{(1)}) & \text{if } \text{CONTYPE} = 0 \\ \max(0, B_{PZ}^{(1)}) & \text{if } \text{CONTYPE} = 1 \end{cases} \quad (5.223)$$

$$AS_{LP} = \frac{WS^{(1)}}{A - D_3} \quad (5.224)$$

$$WT^{(1)} = AS_{LP} \cdot (A - D_4) \quad (5.225)$$

$$WT^{(2)} = WS^{(1)} \quad (5.226)$$

$$WS^{(2)} = WT^{(2)} - S_{LP} \cdot (D_4 - D_3) \quad (5.227)$$

$$WR^{(2)} = WT^{(2)} - S_{LP} \cdot (D_4 - D_2) \quad (5.228)$$

$$WQ^{(2)} = WT^{(2)} - S_{LP} \cdot (D_4 - D_1) \quad (5.229)$$

$$WP^{(2)} = WT^{(2)} - S_{LP} \cdot D_4 \quad (5.230)$$

The results of Equations 5.201 through 5.230 are used to determine the energies ( $E_{xt}$ ) and ( $E_{zt}$ ) using Equation 5.188. Thus the total energy absorbed by the plate in either the x or z directions is given by Equations 5.231 and 5.232 respectively.

$$TE_{X\tau} = \sum_{i=0}^{\frac{t}{\tau}} \sum_{j=0}^{\frac{t}{\tau}} E_{X\tau} \langle j \rangle \cdot \delta_{ij} \quad (5.231)$$

$$TE_{Z\tau} = \sum_{i=0}^{\frac{t}{\tau}} \sum_{j=0}^{\frac{t}{\tau}} E_{Z\tau} \langle j \rangle \cdot \delta_{ij} \quad (5.232)$$

Using Equations 5.231 and 5.232 the total energy absorbed by the plate at time (T) is given by Equation 5.233 and the updated velocity components for the rigid wedge (assuming for convenience no induced moments) are given by Equations 5.234 and 5.235.

$$TE_{\tau} = TE_{X\tau} + TE_{Z\tau} \quad (5.233)$$

$$V_X \langle 2 \rangle = \sqrt{\max \left[ 0, (V_X^2)^{\langle 0 \rangle} - \frac{2 \cdot TE_{X\tau}}{M} \right]} \quad (5.234)$$

$$V_Z \langle 2 \rangle = \sqrt{\max \left[ 0, (V_Z^2)^{\langle 0 \rangle} - \frac{2 \cdot TE_{Z\tau}}{M} \right]} \quad (5.235)$$

Cycling the system of equations yields:

$$D_1 = D_2 \quad (5.236)$$

$$D_2 = D_3 \quad (5.237)$$

$$D_3 = \max \left( 0, B_{PX} \langle 3 \rangle - \frac{B_{PX} \langle 3 \rangle}{S_{LP}} \right) \quad (5.238)$$

$$D_4 = D_3 + V_X \langle 2 \rangle \cdot \tau \quad (5.239)$$

$$B_{PZ} \langle 2 \rangle = B_{PZ} \langle 1 \rangle \quad (5.240)$$

$$B_{PZ} \langle 3 \rangle = B_{PZ} \langle 2 \rangle + V_Z \langle 2 \rangle \cdot \tau \quad (5.241)$$

$$B_{PX} \langle 2 \rangle = B_{PX} \langle 1 \rangle + V_X \langle 0 \rangle \cdot \tau \quad (5.242)$$

$$B_{PX}^{(3)} = B_{PX}^{(2)} \quad (5.243)$$

$$B_{PX}^{(4)} = B_{PX}^{(3)} + V_X^{(2)} \cdot \tau \quad (5.244)$$

$$B_{PZ}^{(4)} = B_{PZ}^{(3)} \quad (5.245)$$

$$W_P^{(3)} = W_S^{(3)} - S_{LP} \cdot D_3 \quad (5.246)$$

$$W_R^{(3)} = W_S^{(3)} - S_{LP} \cdot (D_3 - D_2) \quad (5.247)$$

$$W_Q^{(3)} = W_S^{(3)} - S_{LP} \cdot (D_3 - D_1) \quad (5.248)$$

$$A_{S_{LP}} = \frac{W_S^{(3)}}{A - D_3} \quad (5.249)$$

$$W_T^{(3)} = A_{S_{LP}} \cdot (A - D_4) \quad (5.250)$$

$$W_T^{(4)} = W_S^{(3)} \quad (5.251)$$

$$W_S^{(4)} = W_T^{(4)} - S_{LP} \cdot (D_4 - D_3) \quad (5.252)$$

$$W_R^{(4)} = W_T^{(4)} - S_{LP} \cdot (D_4 - D_2) \quad (5.253)$$

$$W_Q^{(4)} = W_T^{(4)} - S_{LP} \cdot (D_4 - D_1) \quad (5.254)$$

$$W_P^{(4)} = W_T^{(4)} - S_{LP} \cdot D_4 \quad (5.255)$$

Where the cycle continues to repeat for each time step.

#### 5.4.5.2 Determination of Deflections in CS 1 with a X-Direction Initial Step

Beginning with the initial deflections of Equation 5.201 through 5.206, and making use of Equations 5.208 and 5.218, then:

$$CS = 1 \quad (5.256)$$

$$B_{PX}^{(1)} = B_{PX}^{(0)} + V_X^{(0)} \cdot \tau \quad (5.257)$$

$$B_{PX}^{(2)} = B_{PX}^{(1)} \quad (5.258)$$

$$B_{PZ}^{\langle 1 \rangle} = B_{PZ}^{\langle 0 \rangle} \quad (5.259)$$

$$B_{PZ}^{\langle 2 \rangle} = B_{PZ}^{\langle 1 \rangle} + V_Z^{\langle 0 \rangle} \cdot \tau \quad (5.260)$$

$$D_3 = \max \left[ 0, \left( B_{PX}^{\langle 1 \rangle} - \frac{B_{PZ}^{\langle 1 \rangle}}{S_{LP}} \right) \right] \quad (5.261)$$

$$D_2 = \max \left( 0, D_3 - V_X^{\langle 0 \rangle} \cdot \tau, \frac{D_3}{2} \right) \quad (5.262)$$

$$D_1 = \max \left( 0, D_2 - V_X^{\langle 0 \rangle} \cdot \tau, \frac{D_2}{2} \right) \quad (5.263)$$

$$WS^{\langle 1 \rangle} = \begin{cases} \min(0, B_{PZ}^{\langle 1 \rangle}) & \text{if } \text{CONTYPE} = 0 \\ \max(0, B_{PZ}^{\langle 1 \rangle}) & \text{if } \text{CONTYPE} = 1 \end{cases} \quad (5.264)$$

$$WP^{\langle 1 \rangle} = WS^{\langle 1 \rangle} - S_{LP} \cdot D_3 \quad (5.265)$$

$$WR^{\langle 1 \rangle} = WS^{\langle 1 \rangle} - S_{LP} \cdot (D_3 - D_2) \quad (5.266)$$

$$WQ^{\langle 1 \rangle} = WS^{\langle 1 \rangle} - S_{LP} \cdot (D_3 - D_1) \quad (5.267)$$

$$AS_{LP} = \frac{WS^{\langle 1 \rangle}}{A - D_3} \quad (5.268)$$

$$D_4 = \max \left( 0, B_{PX}^{\langle 2 \rangle} - \frac{B_{PZ}^{\langle 2 \rangle}}{S_{LP}} \right) \quad (5.269)$$

$$WT^{\langle 1 \rangle} = AS_{LP} \cdot (A - D_4) \quad (5.270)$$

$$WT^{\langle 2 \rangle} = \begin{cases} \min(0, B_{PZ}^{\langle 2 \rangle}) & \text{if } \text{CONTYPE} = 0 \\ \max(0, B_{PZ}^{\langle 2 \rangle}) & \text{if } \text{CONTYPE} = 1 \end{cases} \quad (5.271)$$

$$WS^{\langle 2 \rangle} = WT^{\langle 2 \rangle} - S_{LP} \cdot (D_4 - D_3) \quad (5.272)$$

$$WR^{\langle 2 \rangle} = WT^{\langle 2 \rangle} - S_{LP} \cdot (D_4 - D_2) \quad (5.273)$$

$$WQ^{\langle 2 \rangle} = WT^{\langle 2 \rangle} - S_{LP} \cdot (D_4 - D_1) \quad (5.274)$$

$$WP^{(2)} = WT^{(2)} - S_{LP} \cdot D_4 \quad (5.275)$$

Using Equations 5.231 through 5.235 and cycling the system yields:

$$D_1 = D_2 \quad (5.276)$$

$$D_2 = D_3 \quad (5.277)$$

$$B_{PX}^{(3)} = B_{PX}^{(2)} + V_X^{(2)} \cdot \tau \quad (5.278)$$

$$B_{PX}^{(4)} = B_{PX}^{(3)} \quad (5.279)$$

$$B_{PZ}^{(3)} = B_{PZ}^{(2)} \quad (5.280)$$

$$B_{PZ}^{(4)} = B_{PZ}^{(3)} + V_Z^{(2)} \cdot \tau \quad (5.281)$$

$$D_3 = \max \left( 0, B_{PX}^{(3)} - \frac{B_{PZ}^{(3)}}{S_{LP}} \right) \quad (5.282)$$

$$D_4 = \max \left( 0, B_{PX}^{(4)} - \frac{B_{PZ}^{(4)}}{S_{LP}} \right) \quad (5.283)$$

$$WS^{(3)} = \begin{cases} \min(0, B_{PZ}^{(3)}) & \text{if } \text{CONTYPE} = 0 \\ \max(0, B_{PZ}^{(3)}) & \text{if } \text{CONTYPE} = 1 \end{cases} \quad (5.284)$$

$$WP^{(3)} = WS^{(3)} - S_{LP} \cdot D_3 \quad (5.285)$$

$$WR^{(3)} = WS^{(3)} - S_{LP} \cdot (D_3 - D_2) \quad (5.286)$$

$$WQ^{(3)} = WS^{(3)} - S_{LP} \cdot (D_3 - D_1) \quad (5.287)$$

$$AS_{LP} = \frac{WS^{(3)}}{A - D_3} \quad (5.288)$$

$$WT^{(3)} = AS_{LP} \cdot (A - D_4) \quad (5.289)$$

$$WT^{(4)} = \begin{cases} \min(0, B_{PZ}^{(4)}) & \text{if } \text{CONTYPE} = 0 \\ \max(0, B_{PZ}^{(4)}) & \text{if } \text{CONTYPE} = 1 \end{cases} \quad (5.290)$$

$$WS^{(4)} = WT^{(4)} - S_{LP} \cdot (D_4 - D_3) \quad (5.291)$$

$$WR^{(4)} = WT^{(4)} - S_{LP} \cdot (D_4 - D_2) \quad (5.292)$$

$$WQ^{(4)} = WT^{(4)} - S_{LP} \cdot (D_4 - D_1) \quad (5.293)$$

$$WP^{(4)} = WT^{(4)} - S_{LP} \cdot D_4 \quad (5.294)$$

Where the cycle continues to repeat for each time step.

#### 5.4.5.3 Determination of Deflections in CS 2 with a Z-Direction Initial Step

Beginning with the initial deflections of Equations 5.201 through 5.206 then:

$$CS = 2 \quad (5.295)$$

$$CONTYPE = \begin{cases} 0 & \text{if } B_{PZ}^{(0)} > 0 \\ 1 & \text{if } B_{PZ}^{(0)} < 0 \end{cases} \quad (5.296)$$

$$B_{PZ}^{(1)} = B_{PZ}^{(0)} + V_Z^{(0)} \cdot \tau \quad (5.297)$$

$$B_{PX}^{(1)} = B_{PX}^{(0)} \quad (5.298)$$

$$B_{PZ}^{(2)} = B_{PZ}^{(1)} \quad (5.299)$$

$$B_{PX}^{(2)} = B_{PX}^{(1)} + V_X^{(0)} \cdot \tau \quad (5.300)$$

$$D_3 = B_{PX}^{(0)} \quad (5.301)$$

$$D_4 = B_{PX}^{(2)} \quad (5.302)$$

$$D_2 = \max \left( 0, D_3 - V_X^{(0)} \cdot \tau, \frac{D_3}{2} \right) \quad (5.303)$$

$$D_1 = \max \left( 0, D_2 - V_X^{(0)} \cdot \tau, \frac{D_2}{2} \right) \quad (5.304)$$

$$WP^{(1)} = WS^{(1)} = WR^{(1)} = WQ^{(1)} = B_{PZ}^{(1)} \quad (5.305)$$

$$AS_{LP} = \frac{WS^{(1)}}{A - D3} \quad (5.306)$$

$$WT^{(1)} = AS_{LP} \cdot (A - D4) \quad (5.307)$$

$$WT^{(2)} = WS^{(2)} = WR^{(2)} = WQ^{(2)} = WP^{(2)} = WS^{(1)} \quad (5.308)$$

Using Equations 5.231 through 5.235 and cycling the system yields:

$$D_1 = D_2 \quad (5.309)$$

$$D_2 = D_3 \quad (5.310)$$

$$D_3 = D_4 \quad (5.311)$$

$$D_4 = D_3 + V_x^{(2)} \cdot \tau \quad (5.312)$$

$$B_{PX}^{(3)} = B_{PX}^{(2)} \quad (5.313)$$

$$B_{PZ}^{(4)} = B_{PZ}^{(3)} \quad (5.314)$$

$$B_{PZ}^{(3)} = B_{PZ}^{(2)} + V_Z^{(2)} \cdot \tau \quad (5.315)$$

$$WP^{(3)} = WS^{(3)} = WR^{(3)} = WQ^{(3)} = B_{PZ}^{(3)} \quad (5.316)$$

$$AS_{LP} = \frac{WS^{(3)}}{A - D3} \quad (5.317)$$

$$B_{PX}^{(4)} = D_4 \quad (5.318)$$

$$WT^{(3)} = AS_{LP} \cdot (A - D4) \quad (5.319)$$

$$WT^{(4)} = WS^{(4)} = WR^{(4)} = WQ^{(4)} = WP^{(4)} = WS^{(3)} \quad (5.320)$$

Where the cycle continues to repeat for each time step.

#### 5.4.5.4 Determination of Deflections in CS 2 with a X-Direction Initial Step

Beginning with the initial deflections of Equations 5.201 through 5.206, and making use of Equations 5.295 and 5.306, then:

$$B_{PX}^{(1)} = B_{PX}^{(0)} + V_X^{(0)} \cdot \tau \quad (5.321)$$

$$B_{PZ}^{(1)} = B_{PZ}^{(0)} \quad (5.322)$$

$$B_{PX}^{(2)} = B_{PX}^{(1)} \quad (5.324)$$

$$B_{PZ}^{(2)} = B_{PZ}^{(1)} + V_Z^{(0)} \cdot \tau \quad (5.325)$$

$$D_2 = B_{PX}^{(0)} \quad (5.326)$$

$$D_3 = B_{PX}^{(1)} \quad (5.327)$$

$$D_1 = \max\left(0, D_2 - V_X^{(0)} \cdot \tau, \frac{D_2}{2}\right) \quad (5.328)$$

$$D_4 = D_3 + V_X^{(0)} \cdot \tau \quad (5.329)$$

$$W_P^{(1)} = W_S^{(1)} = W_R^{(1)} = W_Q^{(1)} = W_T^{(1)} = 0 \quad (5.330)$$

$$W_S^{(2)} = W_R^{(2)} = W_Q^{(2)} = W_P^{(2)} = B_{PZ}^{(2)} \quad (5.331)$$

$$AS_{LP} = \frac{W_S^{(2)}}{A - D_3} \quad (5.332)$$

$$W_T^{(2)} = AS_{LP} \cdot (A - D_4) \quad (5.333)$$

Using Equations 5.231 through 5.235 and cycling the system yields:

$$D_1 = D_2 \quad (5.334)$$

$$D_2 = D_3 \quad (5.335)$$

$$D_3 = D_4 \quad (5.336)$$

$$D_4 = D_3 + V_X^{(2)} \cdot \tau \quad (5.337)$$

$$B_{PX}^{(3)} = D_3 \quad (5.338)$$

$$B_{PX}^{(4)} = B_{PX}^{(3)} \quad (5.339)$$

$$B_{PZ}^{(3)} = B_{PZ}^{(2)} \quad (5.340)$$

$$B_{PZ}^{(4)} = B_{PZ}^{(3)} + V_Z^{(2)} \cdot \tau \quad (5.341)$$

$$W_S^{(2)} = W_T^{(2)} \quad (5.342)$$

$$W_P^{(3)} = W_S^{(3)} = W_R^{(3)} = W_Q^{(3)} = B_{PZ}^{(2)} \quad (5.343)$$

$$AS_{LP} = \frac{W_S^{(3)}}{A - D3} \quad (5.344)$$

$$W_T^{(3)} = AS_{LP} \cdot (A - D4) \quad (5.345)$$

$$AS_{LP} = \frac{W_S^{(4)}}{A - D3} \quad (5.346)$$

$$W_T^{(4)} = AS_{LP} \cdot (A - D4) \quad (5.347)$$

$$W_S^{(4)} = W_R^{(4)} = W_Q^{(4)} = W_P^{(4)} = B_{PZ}^{(4)} \quad (5.348)$$

Where the cycle continues to repeat for each time step.

#### 5.4.5.5 Determination of Deflections in CS 3 with a Z-Direction Initial Step

Beginning with the initial deflections of Equations 5.201 through 5.206 then:

$$CS = 3 \quad (5.349)$$

$$CONTYPE = \begin{cases} 0 & \text{if } P_{ZP}^{(0)} \geq 0 \wedge P_{XP}^{(0)} \geq 0 \wedge \Phi > 90 \\ 1 & \text{if } P_{ZP}^{(0)} \leq 0 \wedge P_{XP}^{(0)} \geq 0 \wedge \Phi < 90 \end{cases} \quad (5.350)$$

$$B_{PZ}^{(1)} = B_{PZ}^{(0)} + V_Z^{(0)} \cdot \tau \quad (5.351)$$

$$B_{PZ}^{(2)} = B_{PZ}^{(1)} \quad (5.352)$$

$$B_{PX}^{(1)} = B_{PX}^{(0)} \quad (5.353)$$

$$B_{PX}^{(2)} = B_{PX}^{(1)} + V_X^{(0)} \cdot \tau \quad (5.354)$$

$$P_{XS}^{(1)} = P_{XS}^{(0)} \quad (5.355)$$

$$P_{XS}^{(2)} = P_{XS}^{(1)} + V_X^{(0)} \cdot \tau \quad (5.356)$$

$$P_{XP}^{(1)} = P_{XP}^{(0)} \quad (5.357)$$

$$P_{XP}^{(2)} = P_{XP}^{(1)} + V_X^{(0)} \cdot \tau \quad (5.358)$$

$$P_{ZS}^{(2)} = P_{ZS}^{(1)} \quad (5.359)$$

$$P_{ZS}^{(1)} = P_{ZS}^{(0)} + V_Z^{(0)} \cdot \tau \quad (5.360)$$

$$P_{ZP}^{(2)} = P_{ZP}^{(1)} \quad (5.361)$$

$$P_{ZP}^{(1)} = P_{ZP}^{(0)} + V_Z^{(0)} \cdot \tau \quad (5.362)$$

$$AP_{XP}^{(0)} = P_{XP}^{(0)} - (L_{RW} - L)\text{Sin}(\Phi) \quad (5.363)$$

$$AP_{ZP}^{(0)} = P_{ZP}^{(0)} + (L_{RW} - L)\text{Cos}(\Phi) \quad (5.364)$$

$$AP_{ZS}^{(0)} = P_{ZS}^{(0)} + (L_{RW} - L)\text{Cos}(\Phi) \quad (5.365)$$

$$AP_{XS}^{(0)} = P_{XS}^{(0)} - (L_{RW} - L)\text{Sin}(\Phi) \quad (5.366)$$

$$AP_{XP}^{(1)} = AP_{XP}^{(0)} \quad (5.367)$$

$$AP_{XP}^{(2)} = AP_{XP}^{(1)} + V_X^{(0)} \cdot \tau \quad (5.368)$$

$$AP_{XS}^{(1)} = AP_{XS}^{(0)} \quad (5.369)$$

$$AP_{XS}^{(2)} = AP_{XS}^{(1)} + V_X^{(0)} \cdot \tau \quad (5.370)$$

$$AP_{ZP}^{(2)} = AP_{ZP}^{(1)} = AP_{ZP}^{(0)} + V_Z^{(0)} \cdot \tau \quad (5.371)$$

$$AP_{ZS}^{(2)} = AP_{ZS}^{(1)} = AP_{ZS}^{(0)} + V_Z^{(0)} \cdot \tau \quad (5.372)$$

$$S_{LP} = \begin{cases} \frac{B_{PZ}^{(0)} - P_{ZP}^{(0)}}{B_{PX}^{(0)} - P_{XP}^{(0)}} & \text{if } \text{CONTYPE} = 0 \\ \frac{B_{PZ}^{(0)} - P_{ZS}^{(0)}}{B_{PX}^{(0)} - P_{XS}^{(0)}} & \text{if } \text{CONTYPE} = 1 \end{cases} \quad (5.373)$$

$$BS_{LP} = \begin{cases} \frac{P_{ZP}^{(0)} - AP_{ZP}^{(0)}}{P_{XP}^{(0)} - AP_{XP}^{(0)}} & \text{if } CONTYPE = 0 \\ \frac{P_{ZS}^{(0)} - AP_{ZS}^{(0)}}{P_{XS}^{(0)} - AP_{XS}^{(0)}} & \text{if } CONTYPE = 1 \end{cases} \quad (5.374)$$

$$D_2 = \begin{cases} \max\left(0, B_{PX}^{(1)} - \frac{B_{PZ}^{(1)}}{S_{LP}}\right) & \text{if } \left[ \begin{array}{l} CONTYPE = 0 \wedge P_{ZP}^{(1)} \leq 0 \\ \text{or} (CONTYPE = 1 \wedge P_{ZS}^{(1)} \geq 0) \end{array} \right] \\ \max\left(0, P_{XP}^{(1)} - \frac{P_{ZP}^{(1)}}{BS_{LP}}\right) & \text{if } CONTYPE = 0 \wedge P_{ZP}^{(1)} > 0 \\ \max\left(0, P_{XS}^{(1)} - \frac{P_{ZS}^{(1)}}{BS_{LP}}\right) & \text{if } CONTYPE = 1 \wedge P_{ZS}^{(1)} < 0 \end{cases} \quad (5.375)$$

$$D_1 = \begin{cases} P_{XP}^{(1)} & \text{if } CONTYPE = 0 \wedge P_{ZP}^{(1)} \leq 0 \\ P_{XS}^{(1)} & \text{if } CONTYPE = 1 \wedge P_{ZS}^{(1)} \geq 0 \\ \max\left(0, D_2 - V_X^{(0)} \cdot \tau, \frac{D_2}{2}\right) & \text{otherwise} \end{cases} \quad (5.376)$$

$$D_4 = D_2 + V_X^{(0)} \cdot \tau \quad (5.377)$$

$$D_5 = D_1 + V_X^{(0)} \cdot \tau \quad (5.378)$$

$$ORDER = \begin{cases} 0 & \text{if } D_5 \geq D_2 \\ 1 & \text{otherwise} \end{cases} \quad (5.379)$$

$$D_3 = \begin{cases} D_2 & \text{if } ORDER = 1 \\ D_5 & \text{otherwise} \end{cases} \quad (5.380)$$

$$D_2 = \begin{cases} D_2 & \text{if } ORDER = 0 \\ D_5 & \text{otherwise} \end{cases} \quad (5.381)$$

$$W^{(1)} = \begin{cases} \min(0, B_{PZ}^{(1)}) & \text{if } CONTYPE = 0 \\ \max(0, B_{PZ}^{(1)}) & \text{if } CONTYPE = 1 \end{cases} \quad (5.382)$$

$$WR^{(1)} = W^{(1)} \quad \text{if } ORDER = 0 \quad (5.383)$$

$$WS^{(1)} = W^{(1)} \text{ if } ORDER = 1 \quad (5.384)$$

$$WR^{(1)} = \begin{cases} WR^{(1)} & \text{if } ORDER = 0 \\ \left[ WS^{(1)} - S_{LP} \cdot (D_3 - D_2) \right] & \text{if } \begin{cases} CONTYPE = 0 \wedge P_{ZP}^{(1)} \leq 0 \\ \text{or} (CONTYPE = 1 \wedge P_{ZS}^{(1)} \geq 0) \end{cases} \\ \left[ WS^{(1)} - BS_{LP} \cdot (D_3 - D_2) \right] & \text{otherwise} \end{cases} \quad (5.385)$$

$$WS^{(1)} = \begin{cases} WS^{(1)} & \text{if } ORDER = 1 \\ \left[ \frac{WR^{(1)}}{A - D_2} \cdot (A - D_3) \right] & \text{otherwise} \end{cases} \quad (5.386)$$

$$WQ^{(1)} = \begin{cases} P_{ZP}^{(1)} & \text{if } CONTYPE = 0 \wedge P_{ZP}^{(1)} \leq 0 \\ P_{ZS}^{(1)} & \text{if } CONTYPE = 1 \wedge P_{ZS}^{(1)} \geq 0 \\ \left[ WR^{(1)} - BS_{LP} \cdot (D_2 - D_1) \right] & \text{otherwise} \end{cases} \quad (5.387)$$

$$WP^{(1)} = WQ^{(1)} - BS_{LP} \cdot D_1 \quad (5.388)$$

$$AS_{LP} = \frac{WS^{(1)}}{A - D_3} \quad (5.389)$$

$$WT^{(1)} = AS_{LP} \cdot (A - D_4) \quad (5.390)$$

$$WT^{(2)} = WS^{(1)} \quad (5.391)$$

$$WR^{(2)} = \begin{cases} P_{ZP}^{(1)} & \text{if } CONTYPE = 0 \wedge P_{ZP}^{(1)} \leq 0 \\ P_{ZS}^{(1)} & \text{if } CONTYPE = 1 \wedge P_{ZS}^{(1)} \geq 0 \\ WS^{(1)} - BS_{LP} \cdot (D_3 - D_2) & \text{otherwise} \end{cases} \quad (5.392)$$

$$WS^{(2)} = \begin{cases} \left[ WT^{(2)} - S_{LP} \cdot (D_4 - D_3) \right] & \text{if } \begin{cases} CONTYPE = 0 \wedge P_{ZP}^{(1)} \leq 0 \\ \text{or} (CONTYPE = 1 \wedge P_{ZS}^{(1)} \geq 0) \end{cases} \\ \left( WT^{(2)} - BS_{LP} \cdot (D_4 - D_3) \right) & \text{otherwise} \end{cases} \quad (5.393)$$

$$WQ^{(2)} = WR^{(2)} - BS_{LP} \cdot (D_2 - D_1) \quad (5.394)$$

$$WP^{(2)} = WQ^{(2)} - BS_{LP} \cdot D_1 \quad (5.395)$$

Using Equations 5.231 through 5.235 and cycling the system yields:

$$D_1 = D_2 \quad (5.396)$$

$$D_2 = D_3 \quad (5.397)$$

$$D_4 = D_2 + V_x^{(2)} \cdot \tau \quad (5.398)$$

$$\text{ORDER} = \begin{cases} 0 & \text{if } D_5 \geq D_2 \\ 1 & \text{otherwise} \end{cases} \quad (5.399)$$

$$D_3 = \begin{cases} D_2 & \text{if ORDER} = 1 \\ D_5 & \text{otherwise} \end{cases} \quad (5.400)$$

$$D_2 = \begin{cases} D_2 & \text{if ORDER} = 0 \\ D_5 & \text{otherwise} \end{cases} \quad (5.401)$$

$$B_{PZ}^{(3)} = B_{PZ}^{(2)} + V_Z^{(2)} \cdot \tau \quad (5.402)$$

$$B_{PZ}^{(4)} = B_{PZ}^{(3)} \quad (5.403)$$

$$B_{PX}^{(3)} = B_{PX}^{(2)} \quad (5.404)$$

$$B_{PX}^{(4)} = B_{PX}^{(3)} + V_X^{(2)} \cdot \tau \quad (5.405)$$

Where repeating Equations 5.355 through 5.395 with the superscript <sup>1</sup> replaced with <sup>3</sup> and <sup>2</sup> replaced with <sup>4</sup> is sufficient to show how the cycle continues to repeat for each time step.

#### 5.4.5.6 Determination of Deflections in CS 3 with a X-Direction Initial Step

Beginning with the initial deflections of Equations 5.201 through 5.206, and making use of Equations 5.349, 5.350 and 5.363 through 5.366 then:

$$B_{PZ}^{(1)} = B_{PZ}^{(0)} \quad (5.406)$$

$$B_{PZ}^{(2)} = B_{PZ}^{(1)} + V_Z^{(0)} \cdot \tau \quad (5.407)$$

$$B_{PX}^{(1)} = B_{PX}^{(0)} + V_X^{(0)} \cdot \tau \quad (5.408)$$

$$B_{PX}^{(2)} = B_{PX}^{(1)} \quad (5.409)$$

$$P_{XS}^{(2)} = P_{XS}^{(1)} = P_{XS}^{(0)} + V_X^{(0)} \cdot \tau \quad (5.410)$$

$$P_{XP}^{(2)} = P_{XP}^{(1)} = P_{XP}^{(0)} + V_X^{(0)} \cdot \tau \quad (5.411)$$

$$P_{ZP}^{(1)} = P_{ZP}^{(0)} \quad (5.412)$$

$$P_{ZP}^{(2)} = P_{ZP}^{(1)} + V_Z^{(0)} \cdot \tau \quad (5.413)$$

$$P_{ZS}^{(1)} = P_{ZS}^{(0)} \quad (5.414)$$

$$P_{ZS}^{(2)} = P_{ZS}^{(1)} + V_Z^{(0)} \cdot \tau \quad (5.415)$$

$$AP_{ZP}^{(1)} = AP_{ZP}^{(0)} \quad (5.416)$$

$$AP_{ZP}^{(2)} = AP_{ZP}^{(1)} + V_Z^{(0)} \cdot \tau \quad (5.417)$$

$$AP_{ZS}^{(1)} = AP_{ZS}^{(0)} \quad (5.418)$$

$$AP_{ZS}^{(2)} = AP_{ZS}^{(1)} + V_Z^{(0)} \cdot \tau \quad (5.419)$$

$$AP_{XS}^{(2)} = AP_{XS}^{(1)} = AP_{XS}^{(0)} + V_X^{(0)} \cdot \tau \quad (5.420)$$

$$AP_{XP}^{(2)} = AP_{XP}^{(1)} = AP_{XP}^{(0)} + V_X^{(0)} \cdot \tau \quad (5.421)$$

Using Equations 5.373 and 5.374 to define  $S_{LP}$  and  $BS_{LP}$  respectively yields:

$$D_2 = \begin{cases} \max\left(0, P_{XP}^{(1)} - \frac{P_{ZP}^{(1)}}{BS_{LP}}\right) & \text{if } \text{CONTYPE} = 0 \\ \max\left(0, P_{XS}^{(1)} - \frac{P_{ZS}^{(1)}}{BS_{LP}}\right) & \text{if } \text{CONTYPE} = 1 \end{cases} \quad (5.422)$$

$$D_1 = \max\left(0, D_2 - V_X^{(0)} \cdot \tau, \frac{D_2}{2}\right) \quad (5.423)$$

$$D_3 = \begin{cases} \max\left(0, P_{XP}^{(2)} - \frac{P_{ZP}^{(2)}}{BS_{LP}}\right) & \text{if } \text{CONTYPE} = 0 \wedge P_{ZP}^{(2)} > 0 \\ \max\left(0, P_{XS}^{(2)} - \frac{P_{ZS}^{(2)}}{BS_{LP}}\right) & \text{if } \text{CONTYPE} = 1 \wedge P_{ZS}^{(2)} < 0 \\ P_{XP}^{(2)} & \text{if } \text{CONTYPE} = 0 \wedge P_{ZP}^{(2)} \leq 0 \\ P_{XS}^{(2)} & \text{if } \text{CONTYPE} = 1 \wedge P_{ZS}^{(2)} \geq 0 \end{cases} \quad (5.424)$$

$$D_4 = \begin{cases} \max\left(0, B_{PX}^{(2)} - \frac{B_{PZ}^{(2)}}{S_{LP}}\right) & \text{if } \begin{cases} \text{CONTYPE} = 0 \wedge P_{ZP}^{(2)} \leq 0 \\ \text{or } (\text{CONTYPE} = 1 \wedge P_{ZS}^{(2)} \geq 0) \end{cases} \\ D_3 & \text{otherwise} \end{cases} \quad (5.425)$$

$$\text{ORDER} = \begin{cases} 1 & \text{if } D_3 = D_4 \\ 0 & \text{otherwise} \end{cases} \quad (5.426)$$

$$D_3 = \begin{cases} \left(D_2 + \frac{D_4 - D_2}{2}\right) & \text{if } \text{ORDER} = 1 \\ D_3 & \text{otherwise} \end{cases} \quad (5.427)$$

$$WS^{(1)} = WT^{(1)} = WR^{(1)} = 0 \quad (5.428)$$

$$WQ^{(1)} = WR^{(1)} - BS_{LP} \cdot (D_2 - D_1) \quad (5.429)$$

$$WP^{(1)} = WQ^{(1)} - BS_{LP} \cdot D_1 \quad (5.430)$$

$$WS^{(2)} = \begin{cases} P_{ZP}^{(2)} & \text{if } \text{ORDER} = 0 \wedge \text{CONTYPE} = 0 \\ P_{ZS}^{(2)} & \text{if } \text{ORDER} = 0 \wedge \text{CONTYPE} = 1 \\ [-BS_{LP} \cdot (D_4 - D_3)] & \text{otherwise} \end{cases} \quad (5.431)$$

$$WT^{(2)} = 0 \quad (5.432)$$

$$WR^{(2)} = WS^{(2)} - BS_{LP} \cdot (D_3 - D_2) \quad (5.433)$$

$$WQ^{(2)} = WQ^{(1)} + V_Z^{(0)} \cdot \tau \quad (5.434)$$

$$WP^{(2)} = WP^{(1)} + V_Z^{(0)} \cdot \tau \quad (5.435)$$

Using Equations 5.231 through 5.235 and cycling the system yields:

$$B_{PZ}^{(3)} = B_{PZ}^{(2)} \quad (5.436)$$

$$B_{PZ}^{(4)} = B_{PZ}^{(3)} + V_Z^{(2)} \cdot \tau \quad (5.437)$$

$$B_{PX}^{(3)} = B_{PX}^{(2)} + V_X^{(2)} \cdot \tau \quad (5.438)$$

$$B_{PX}^{(4)} = B_{PX}^{(3)} \quad (5.439)$$

$$P_{XS}^{(4)} = P_{XS}^{(3)} = P_{XS}^{(2)} + V_X^{(2)} \cdot \tau \quad (5.440)$$

$$P_{XP}^{(4)} = P_{XP}^{(3)} = P_{XP}^{(2)} + V_X^{(2)} \cdot \tau \quad (5.441)$$

$$P_{ZS}^{(3)} = P_{ZS}^{(2)} \quad (5.442)$$

$$P_{ZS}^{(4)} = P_{ZS}^{(3)} + V_Z^{(2)} \cdot \tau \quad (5.443)$$

$$AP_{ZP}^{(3)} = AP_{ZP}^{(2)} \quad (5.444)$$

$$AP_{ZP}^{(4)} = AP_{ZP}^{(3)} + V_Z^{(2)} \cdot \tau \quad (5.445)$$

$$AP_{ZS}^{(3)} = AP_{ZS}^{(2)} \quad (5.446)$$

$$AP_{ZS}^{(4)} = AP_{ZS}^{(3)} + V_Z^{(2)} \cdot \tau \quad (5.447)$$

$$AP_{XS}^{(4)} = AP_{XS}^{(3)} = AP_{XS}^{(2)} + V_X^{(2)} \cdot \tau \quad (5.448)$$

$$AP_{XP}^{(4)} = AP_{XP}^{(3)} = AP_{XP}^{(2)} + V_X^{(2)} \cdot \tau \quad (5.449)$$

$$P_{ZP}^{(3)} = P_{ZP}^{(2)} \quad (5.450)$$

$$P_{ZP}^{(4)} = P_{ZP}^{(3)} + V_Z^{(2)} \cdot \tau \quad (5.451)$$

$$D_1 = \begin{cases} D_4 & \text{if ORDER} = 1 \\ D_3 & \text{if ORDER} = 0 \end{cases} \quad (5.452)$$

$$D_2 = \begin{cases} (D_1 + V_X^{(2)} \cdot \tau) & \text{if ORDER} = 1 \\ \min(D_4, D_1 + V_X^{(2)} \cdot \tau) & \text{if ORDER} = 0 \end{cases} \quad (5.453)$$

$$D_3 = \begin{cases} \max(D_4, D_1 + V_X^{(2)} \cdot \tau) & \text{if ORDER} = 0 \\ \max\left(0, P_{XP}^{(4)} - \frac{P_{ZP}^{(4)}}{BS_{LP}}\right) & \text{if ORDER} = 1 \wedge \text{CONTYPE} = 0 \wedge P_{ZP}^{(4)} > 0 \\ \max\left(0, P_{XS}^{(4)} - \frac{P_{ZS}^{(4)}}{BS_{LP}}\right) & \text{if ORDER} = 1 \wedge \text{CONTYPE} = 1 \wedge P_{ZS}^{(4)} < 0 \\ P_{XP}^{(4)} & \text{if ORDER} = 1 \wedge \text{CONTYPE} = 0 \wedge P_{ZP}^{(4)} \leq 0 \\ P_{XS}^{(4)} & \text{if ORDER} = 1 \wedge \text{CONTYPE} = 1 \wedge P_{ZS}^{(4)} \geq 0 \end{cases} \quad (5.454)$$

$$\text{ORDER}_A = \begin{cases} 1 & \text{if } D_3 = D_4 \\ 0 & \text{otherwise} \end{cases} \quad (5.455)$$

$$D_3 = \begin{cases} \left(D_2 + \frac{D_4 - D_2}{2}\right) & \text{if ORDER}_A = 1 \\ D_3 & \text{otherwise} \end{cases} \quad (5.456)$$

$$WR^{(3)} = \begin{cases} 0 & \text{if ORDER} = 1 \\ P_{ZP}^{(3)} & \text{if ORDER} = 0 \wedge D_2 = D_1 + V_X^{(2)} \cdot \tau \wedge \text{CONTYPE} = 0 \\ P_{ZS}^{(3)} & \text{if ORDER} = 0 \wedge D_2 = D_1 + V_X^{(2)} \cdot \tau \wedge \text{CONTYPE} = 1 \\ P_{ZP}^{(3)} - BS_{LP} \cdot (D_3 - D_2) & \text{if ORDER} = 0 \wedge D_2 < D_1 + V_X^{(2)} \cdot \tau \wedge \text{CONTYPE} = 0 \\ P_{ZS}^{(3)} - BS_{LP} \cdot (D_3 - D_2) & \text{if ORDER} = 0 \wedge D_2 < D_1 + V_X^{(2)} \cdot \tau \wedge \text{CONTYPE} = 1 \end{cases} \quad (5.457)$$

$$WS^{(3)} = \begin{cases} 0 & \text{if ORDER} = 1 \\ P_{ZP}^{(3)} & \text{if ORDER} = 0 \wedge D_2 < D_1 + V_X^{(2)} \cdot \tau \wedge \text{CONTYPE} = 0 \\ P_{ZS}^{(3)} & \text{if ORDER} = 0 \wedge D_2 < D_1 + V_X^{(2)} \cdot \tau \wedge \text{CONTYPE} = 1 \\ \left[WT^{(3)} - S_{LP} \cdot (D_4 - D_3)\right] & \text{if ORDER} = 0 \wedge D_2 = D_1 + V_X^{(2)} \cdot \tau \end{cases} \quad (5.458)$$

$$WT^{(3)} = \begin{cases} 0 & \text{if ORDER} = 1 \\ \min(B_{PZ}^{(3)}, 0) & \text{if CONTYPE} = 0 \wedge \text{ORDER} = 0 \\ \max(B_{PZ}^{(3)}, 0) & \text{if CONTYPE} = 1 \wedge \text{ORDER} = 0 \end{cases} \quad (5.459)$$

$$WQ^{(3)} = WR^{(3)} - BS_{LP} \cdot (D_2 - D_1) \quad (5.460)$$

$$WP^{(3)} = WQ^{(3)} - BS_{LP} \cdot D_1 \quad (5.461)$$

$$D_1 = \begin{cases} D_1 & \text{if ORDER} = 1 \\ D_2 & \text{if ORDER} = 0 \wedge D_2 = D_1 + V_X^{(2)} \cdot \tau \\ D_3 & \text{if ORDER} = 0 \wedge D_2 < D_1 + V_X^{(2)} \cdot \tau \end{cases} \quad (5.462)$$

$$D_2 = \begin{cases} D_2 & \text{if ORDER} = 1 \\ D_3 & \text{if ORDER} = 0 \wedge D_2 = D_1 + V_X^{(2)} \cdot \tau \\ D_3 + \frac{D_4 - D_3}{2} & \text{if ORDER} = 0 \wedge D_2 < D_1 + V_X^{(2)} \cdot \tau \end{cases} \quad (5.463)$$

$$D_3 = \begin{cases} D_3 & \text{if ORDER} = 1 \\ D_4 & \text{if ORDER} = 0 \end{cases} \quad (5.464)$$

$$D_4 = \begin{cases} D_4 & \text{if ORDER} = 1 \\ \min \left( B_{PX}^{(4)}, B_{PX}^{(4)} - \frac{B_{PZ}^{(4)}}{S_{LP}} \right) & \text{if ORDER} = 0 \end{cases} \quad (5.465)$$

$$WQ^{(3)} = \begin{cases} WQ^{(3)} & \text{if ORDER} = 1 \\ P_{ZP}^{(3)} & \text{if CONTYPE} = 0 \wedge \text{ORDER} = 0 \\ P_{ZS}^{(3)} & \text{if CONTYPE} = 1 \wedge \text{ORDER} = 0 \end{cases} \quad (5.466)$$

$$WS^{(3)} = \begin{cases} WS^{(3)} & \text{if ORDER} = 1 \\ WT^{(3)} & \text{if ORDER} = 0 \end{cases} \quad (5.467)$$

$$WT^{(3)} = \begin{cases} WT^{(3)} & \text{if ORDER} = 1 \\ \left[ \frac{WT^{(3)}}{A - D_3} \cdot (A - D_4) \right] & \text{if ORDER} = 0 \end{cases} \quad (5.468)$$

$$WR^{(3)} = \begin{cases} WR^{(3)} & \text{if ORDER} = 1 \\ \left[ WS^{(3)} - S_{LP} \cdot (D_3 - D_2) \right] & \text{if ORDER} = 0 \end{cases} \quad (5.469)$$

$$WQ^{(4)} = WQ^{(3)} + V_Z^{(2)} \cdot \tau \quad (5.470)$$

$$WP^{(4)} = WP^{(3)} + V_Z^{(2)} \cdot \tau \quad (5.471)$$

$$WT^{(4)} = \begin{cases} 0 & \text{if ORDER} = 1 \\ \min(B_{PZ}^{(4)}, 0) & \text{if CONTYPE} = 0 \wedge \text{ORDER} = 0 \\ \max(B_{PZ}^{(4)}, 0) & \text{if CONTYPE} = 1 \wedge \text{ORDER} = 0 \end{cases} \quad (5.472)$$

$$WS^{(4)} = \begin{cases} P_{ZP}^{(4)} & \text{if ORDER} = 1 \wedge \text{ORDER}_A = 0 \wedge \text{CONTYPE} = 0 \\ P_{ZS}^{(4)} & \text{if ORDER} = 1 \wedge \text{ORDER}_A = 0 \wedge \text{CONTYPE} = 1 \\ [-BS_{LP} \cdot (D_4 - D_3)] & \text{if ORDER} = 1 \wedge \text{ORDER}_A = 1 \\ [WT^{(4)} - S_{LP} \cdot (D_4 - D_3)] & \text{if ORDER} = 0 \end{cases} \quad (5.473)$$

$$WR^{(4)} = \begin{cases} [WS^{(4)} - BS_{LP} \cdot (D_3 - D_2)] & \text{if ORDER} = 1 \\ [WS^{(4)} - S_{LP} \cdot (D_3 - D_2)] & \text{if ORDER} = 0 \end{cases} \quad (5.474)$$

Where the cycle continues to repeat for each time step starting with Equation 5.475.

$$\text{ORDER} = \text{ORDER}_A \quad (5.475)$$

#### 5.4.5.7 Determination of Deflections in CS 4 with a Z-Direction Initial Step

Beginning with the initial deflections of Equations 5.201 through 5.206 and making use of Equations 5.351 through 5.374 then:

$$CS = 4 \quad (5.476)$$

$$\text{CONTYPE} = \begin{cases} 0 & \text{if } P_{ZP}^{(0)} \geq 0 \wedge P_{XP}^{(0)} \geq 0 \wedge \Phi \leq 90 \\ 1 & \text{if } P_{ZP}^{(0)} \leq 0 \wedge P_{XS}^{(0)} \geq 0 \wedge \Phi \geq 90 \end{cases} \quad (5.478)$$

$$D_2 = \min \left( B_{PX}^{(2)}, B_{PX}^{(2)} - \frac{B_{PZ}^{(2)}}{S_{LP}}, D_1 + V_X^{(0)} \cdot \tau \right) \quad (5.479)$$

$$D_3 = \max \left( D_1 + V_X^{(0)} \cdot \tau, \min \left( B_{PX}^{(2)}, B_{PX}^{(2)} - \frac{B_{PZ}^{(2)}}{S_{LP}} \right) \right) \quad (5.480)$$

$$D_4 = D_3 + V_X^{(0)} \cdot \tau \quad (5.481)$$

$$WP^{(1)} = WQ^{(1)} = \begin{cases} P_{ZP}^{(1)} & \text{if CONTYPE} = 0 \\ P_{ZS}^{(1)} & \text{if CONTYPE} = 1 \end{cases} \quad (5.482)$$

$$WR^{(1)} = \begin{cases} \min[0, WQ^{(1)} + S_{LP} \cdot (D_2 - D_1)] & \text{if } CONTYE = 0 \\ \max[0, WQ^{(1)} + S_{LP} \cdot (D_2 - D_1)] & \text{if } CONTYE = 1 \end{cases} \quad (5.483)$$

$$WS^{(1)} = \frac{WR^{(1)}}{A - D_2} \cdot (A - D_3) \quad (5.484)$$

$$WT^{(1)} = \frac{WR^{(1)}}{A - D_2} \cdot (A - D_4) \quad (5.485)$$

$$WP^{(2)} = WQ^{(2)} = WR^{(2)} = WP^{(1)} \quad (5.486)$$

$$WS^{(2)} = \begin{cases} WP^{(1)} & \text{if } D_3 = D_1 + V_X^{(0)} \cdot \tau \\ \min[0, WR^{(2)} + S_{LP} \cdot (D_4 - D_3)] & \text{if } CONTYE = 0 \wedge D_3 > D_1 + V_X^{(0)} \cdot \tau \\ \max[0, WR^{(2)} + S_{LP} \cdot (D_4 - D_3)] & \text{if } CONTYE = 1 \wedge D_3 > D_1 + V_X^{(0)} \cdot \tau \end{cases} \quad (5.487)$$

$$WT^{(2)} = \frac{WS^{(2)}}{A - D_3} \cdot (A - D_4) \quad (5.488)$$

Using Equations 5.231 through 5.235 and cycling the system yields the exact procedure as starting from Equation 5.478 with the superscript <sup>1</sup> replaced with <sup>3</sup> and <sup>2</sup> replaced with <sup>4</sup>.

#### 5.4.5.8 Determination of Deflections in CS 4 with a X-Direction Initial Step

Beginning with the initial deflections of Equations 5.201 through 5.206, and making use of Equations 5.476, 5.477 and 5.406 through 5.420 then:

$$D_1 = \begin{cases} P_{XP}^{(0)} & \text{if } CONTYE = 0 \\ P_{XS}^{(0)} & \text{if } CONTYE = 1 \end{cases} \quad (5.489)$$

$$D_2 = D_1 + V_X^{(0)} \cdot \tau \quad (5.490)$$

$$WP^{(1)} = WQ^{(1)} = WR^{(1)} = WS^{(1)} = WT^{(1)} = 0 \quad (5.491)$$

$$WP^{(2)} = WQ^{(2)} = WR^{(2)} = \begin{cases} P_{ZP}^{(1)} & \text{if } CONTYE = 0 \\ P_{ZS}^{(1)} & \text{if } CONTYE = 1 \end{cases} \quad (5.492)$$

$$WT^{(2)} = \begin{cases} \max(0, B_{PZ}^{(2)}) & \text{if } CONTYE = 1 \\ \min(0, B_{PZ}^{(2)}) & \text{if } CONTYE = 0 \end{cases} \quad (5.493)$$

$$D_4 = \min \left( B_{PX}^{(2)}, B_{PX}^{(2)} - \frac{B_{PZ}^{(2)}}{S_{LP}} \right) \quad (5.494)$$

$$D_3 = D_2 + \frac{D_4 - D_2}{2} \quad (5.495)$$

$$WS = WT - S_{LP} \cdot (D_4 - D_3) \quad (5.496)$$

Using Equations 5.231 through 5.235 then cycling the system yields:

$$D_1 = D_2 \quad (5.497)$$

$$D_2 = \min(D_4, D_1 + V_X^{(2)} \cdot \tau) \quad (5.498)$$

$$D_3 = \max(D_4, D_1 + V_X^{(2)} \cdot \tau) \quad (5.499)$$

$$D_4 = \min \left( B_{PX}^{(3)}, B_{PX}^{(3)} - \frac{B_{PZ}^{(3)}}{S_{LP}} \right) \quad (5.500)$$

$$WP^{(3)} = WQ^{(3)} = WR^{(3)} = WP^{(2)} \quad (5.501)$$

$$WT^{(3)} = WT^{(2)} \quad (5.502)$$

$$WS^{(3)} = WT^{(3)} - S_{LP} \cdot (D_4 - D_3) \quad (5.503)$$

$$D_1 = \begin{cases} D_2 & \text{if } D_2 = D_1 + V_X^{(2)} \cdot \tau \\ D_3 & \text{otherwise} \end{cases} \quad (5.504)$$

$$D_2 = \begin{cases} D_3 & \text{if } D_2 = D_1 + V_X^{(2)} \cdot \tau \\ \left( D_3 + \frac{D_4 - D_3}{2} \right) & \text{otherwise} \end{cases} \quad (5.505)$$

$$D_3 = D_4 \quad (5.506)$$

$$D_4 = \min \left( B_{PX}^{(4)}, B_{PX}^{(4)} - \frac{B_{PZ}^{(4)}}{S_{LP}} \right) \quad (5.507)$$

$$WR^{(3)} = WQ^{(3)} + S_{LP} \cdot (D_2 - D_1) \quad (5.508)$$

$$WS^{(3)} = WT^{(3)} \quad (5.509)$$

$$WT^{(3)} = \frac{WS^{(3)}}{A - D_3} \cdot (A - D_4) \quad (5.510)$$

$$WT^{(4)} = WT^{(3)} + V_Z^{(2)} \cdot \tau \quad (5.511)$$

$$WS^{(4)} = WS^{(3)} + V_Z^{(2)} \cdot \tau \quad (5.512)$$

$$WR^{(4)} = WR^{(3)} + V_Z^{(2)} \cdot \tau \quad (5.513)$$

$$WQ^{(4)} = WP^{(4)} = WP^{(3)} + V_Z^{(2)} \cdot \tau \quad (5.514)$$

Using Equations 5.232 and 5.235 the cycle continues to repeat for each time step starting with Equation 5.515.

$$D_1 = D_1 \quad (5.515)$$

$$D_2 = \min(D_4, D_1 + V_X^{(4)} \cdot \tau) \quad (5.516)$$

$$D_3 = \max(D_4, D_1 + V_X^{(4)} \cdot \tau) \quad (5.517)$$

$$WP^{(4)} = WQ^{(4)} = WR^{(4)} = \begin{cases} P_{ZP}^{(4)} & \text{if CONTYPE} = 0 \\ P_{ZS}^{(4)} & \text{if CONTYPE} = 1 \end{cases} \quad (5.518)$$

$$D_4 = D_4 + V_X^{(4)} \cdot \tau \quad (5.519)$$

$$WT^{(4)} = WT^{(4)} \quad (5.520)$$

$$WS^{(4)} = WT^{(4)} - S_{LP} \cdot (D_4 - D_3) \quad (5.521)$$

Where the cycle continues to repeat for each time step.

The complexity of the equations of Sections 5.4.5.1 through 5.4.5.8 is simplified as much as possible by the flow chart of Appendix J detailing the energy absorption procedure from a plate of Figure 142.

#### 5.4.6 Validation of Energy Absorption of Twenty-Five-Region Plate

To validate the proposed twenty-five-region plate plastic membrane theory for the determination of the energy absorbed through the non-uniform longitudinal deflection of transverse bulkheads and webs, the method is compared to finite element analysis for 20 separate cases as outlined by Table 17. For each case the initial conditions are provided in Table 16.

Table 16 - Constant Parameters for Twenty-Five Region Plate Test Cases

<b>Case Costants</b>		
<b>Variable</b>	<b>Value</b>	<b>Units</b>
Rigid Wedge Mass	50228.4	Kg
Failure Strain	0.1	--
HEA	23.2	Degrees
A	7.5	m
B	10	m
Analysis Time Step	0.001	s
Plate Yield Stress	2.35E+08	Pa
Rigid Wedge Height	5.5	m
Rigid Wedge Beam	3	m
Rigid Wedge Length	10	m

Table 17 - Twenty-Five Region Plate Test Case Variable Values

<b>Case</b>	<b>Variable</b>							
	<b>CS</b>	<b>Collision Angle (degrees)</b>	<b>Initial X Component Velocity (m/s)</b>	<b>Initial Z Component Velocity (m/s)</b>	<b>Plate Thickness (mm)</b>	<b>Bpx (m)</b>	<b>Bpy (m)</b>	<b>Bpz (m)</b>
1	1	90	3	5	20	0	1.5	0.5
2	1	75	5	3	20	0	1.5	0.5
3	1-4	90	3	3	20	3	-0.5	1.5
4	1-3	105	4	5	20	2	-0.5	2.5
5	2	66.8	2	4	20	2	0.75	0.5
6	2	66.8	4	1	20	2	0.75	0.5
7	2	66.8	2	4	20	2	-0.75	0.5
8	2	66.8	5	3	20	2	-0.75	0.5
9	3	105	4	2	20	4	-0.5	3
10	3	105	2	4	20	4	-0.5	3
11	3	115	5	2	20	4	1	4
12	3	115	2	5	20	4	1	4
13	4	75	5	1	20	4	1.5	1
14	4	75	1	5	20	4	1.5	1
15	4	90	5	2	20	5	-2	1.75
16	4	75	2	5	20	5	-2	2.75
17	1	90	3	5	8	0	1.5	0.5
18	1	90	3	5	31	0	1.5	0.5
19	3	115	2	5	16	4	1	4
20	3	115	2	5	25	4	1	4

Figure 145 through Figure 153 show a comparison of the resultant deformation from both the finite element analysis and twenty-five-region plate theory for case 4 of Table 17.

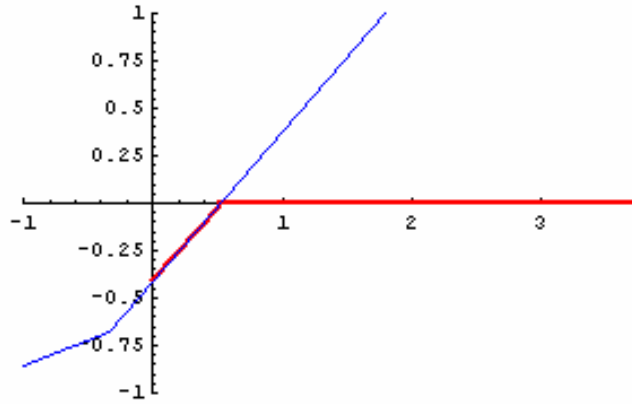


Figure 145 - Test Case 4 Twenty-Five Region Plate Deflection at 0.1 Seconds

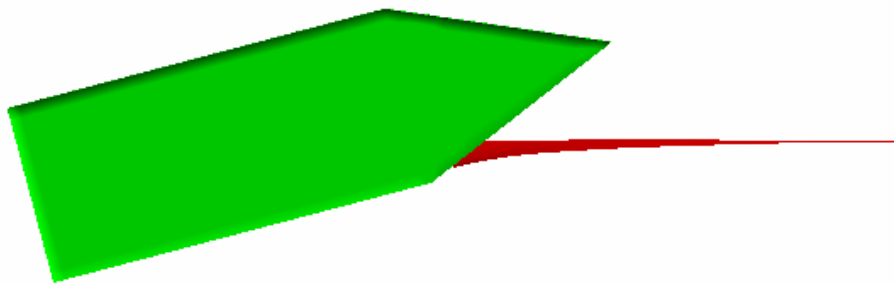


Figure 146 - Test Case 4 FEA Deflection at 0.1 Seconds

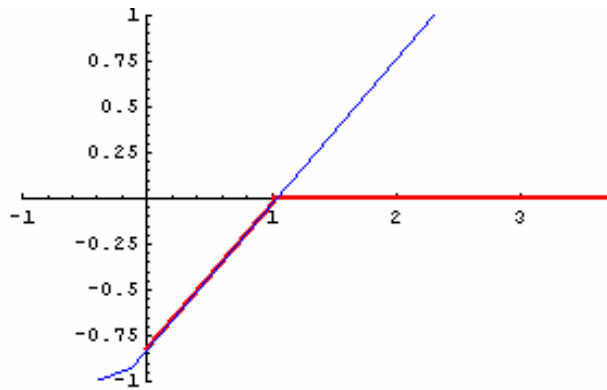


Figure 147 - Test Case 4 Twenty-Five Region Plate Deflection at 0.2 Seconds

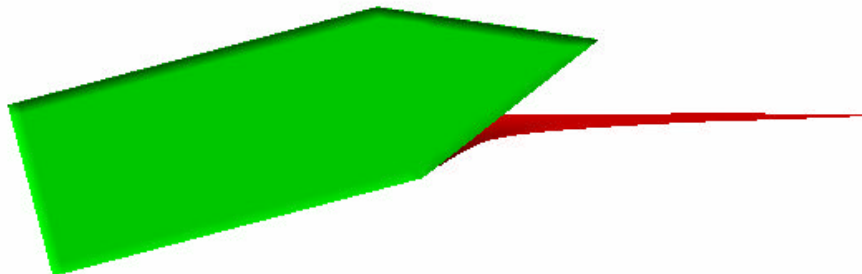


Figure 148 - Test Case 4 FEA Deflection at 0.2 Seconds

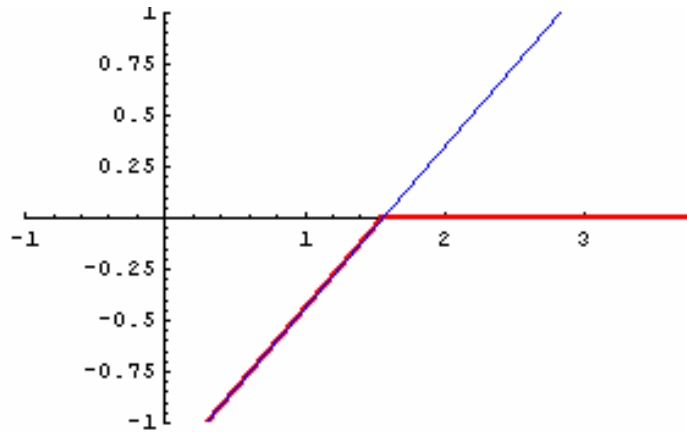


Figure 149 - Test Case 4 Twenty-Five Region Plate Deflection at 0.3 Seconds

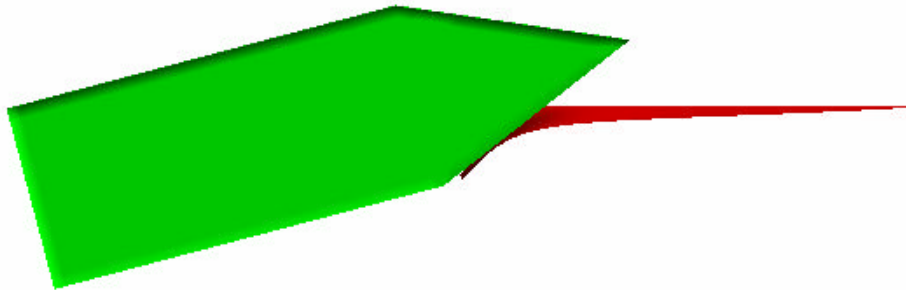


Figure 150 - Test Case 4 FEA Deflection at 0.3 Seconds

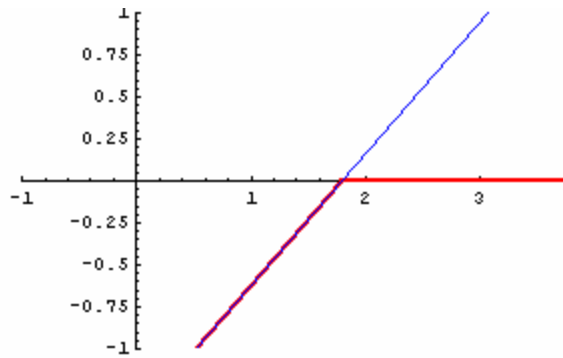


Figure 151 - Test Case 4 Twenty-Five Region Plate Deflection at 0.35 Seconds

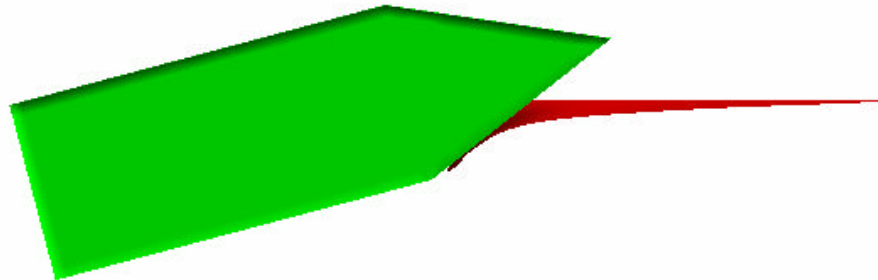


Figure 152 - Test Case 4 FEA Deflection at 0.35 Seconds



Figure 153 - Test Case 4 FEA Plate Mesh Deflection at 0.35 Seconds

Figure 154 through Figure 173 provide the comparison of the energy verses time response for each case of Table 17.

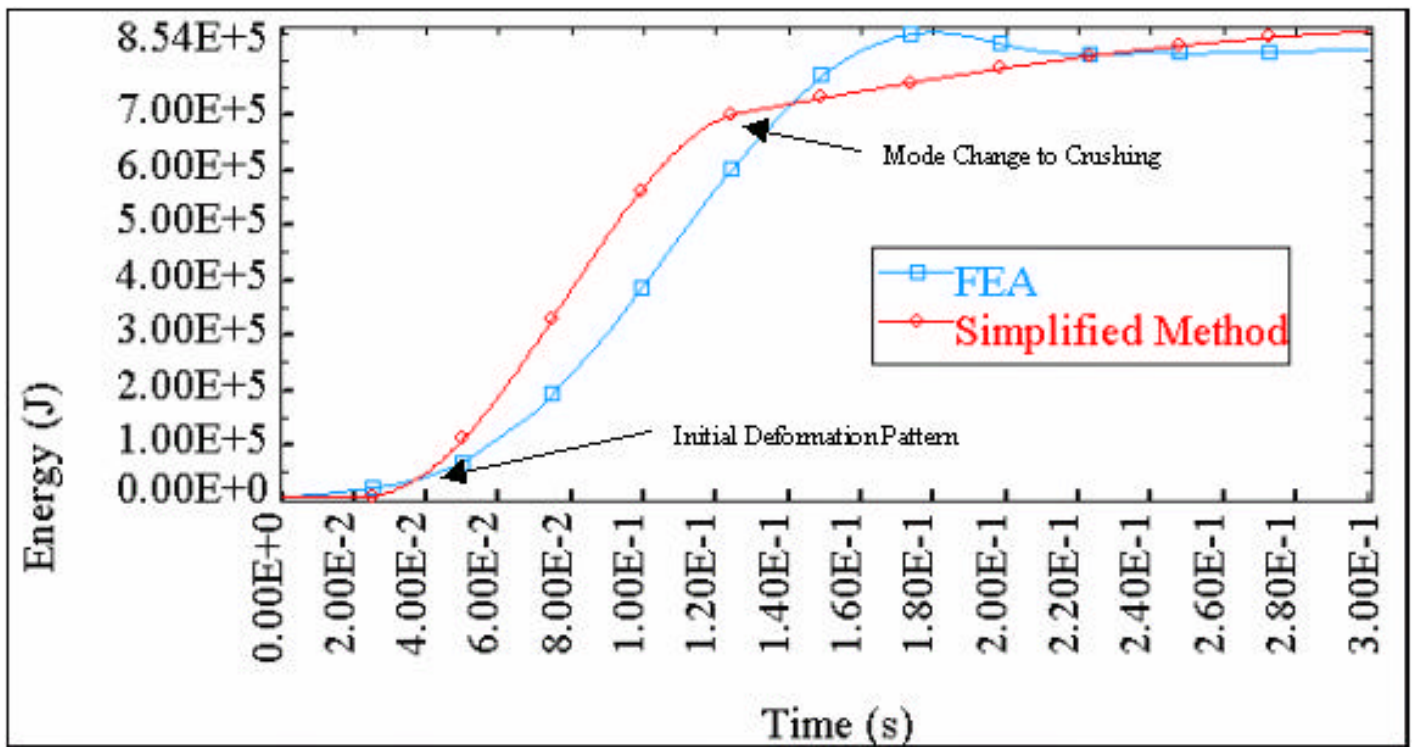


Figure 154 - Case 1 Simplified Method and FEA Absorbed Energy vs. Time Comparison

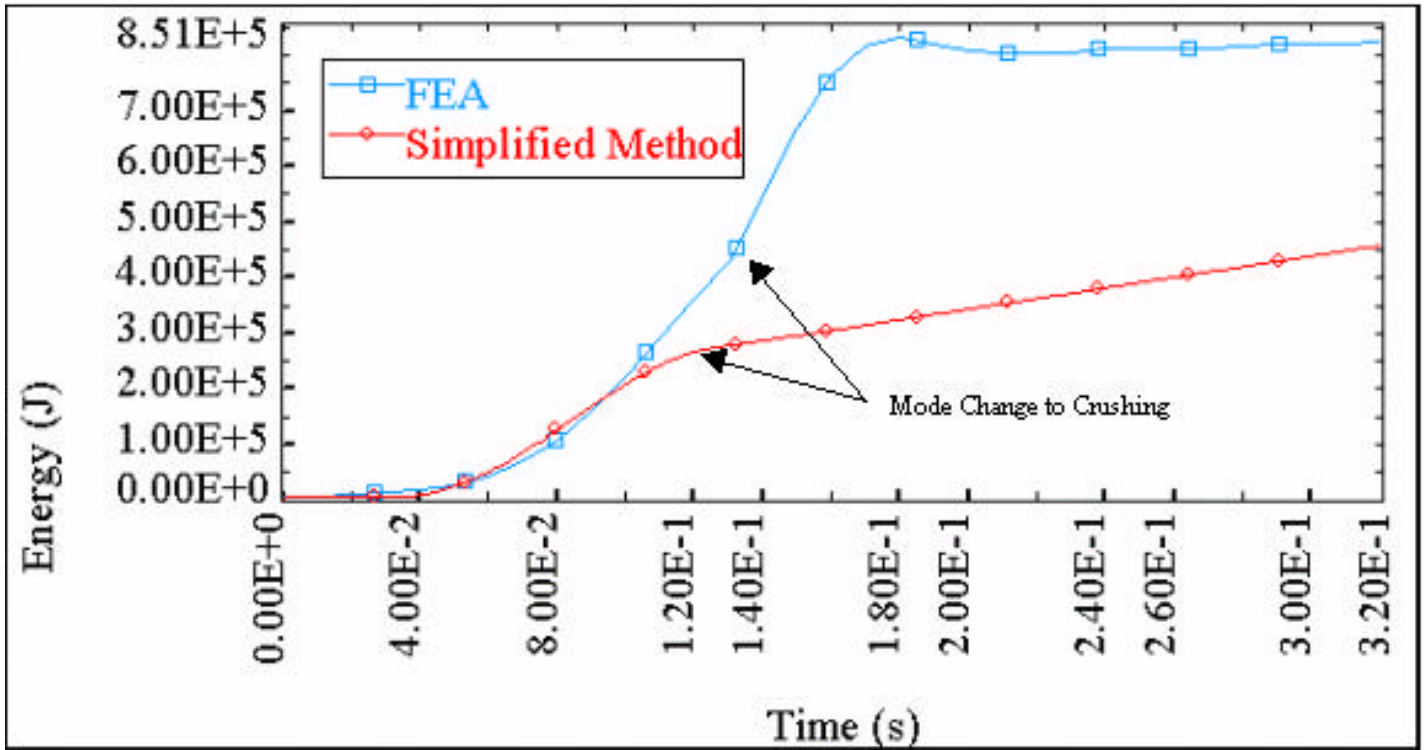


Figure 155 - Case 2 Simplified Method and FEA Absorbed Energy vs. Time Comparison

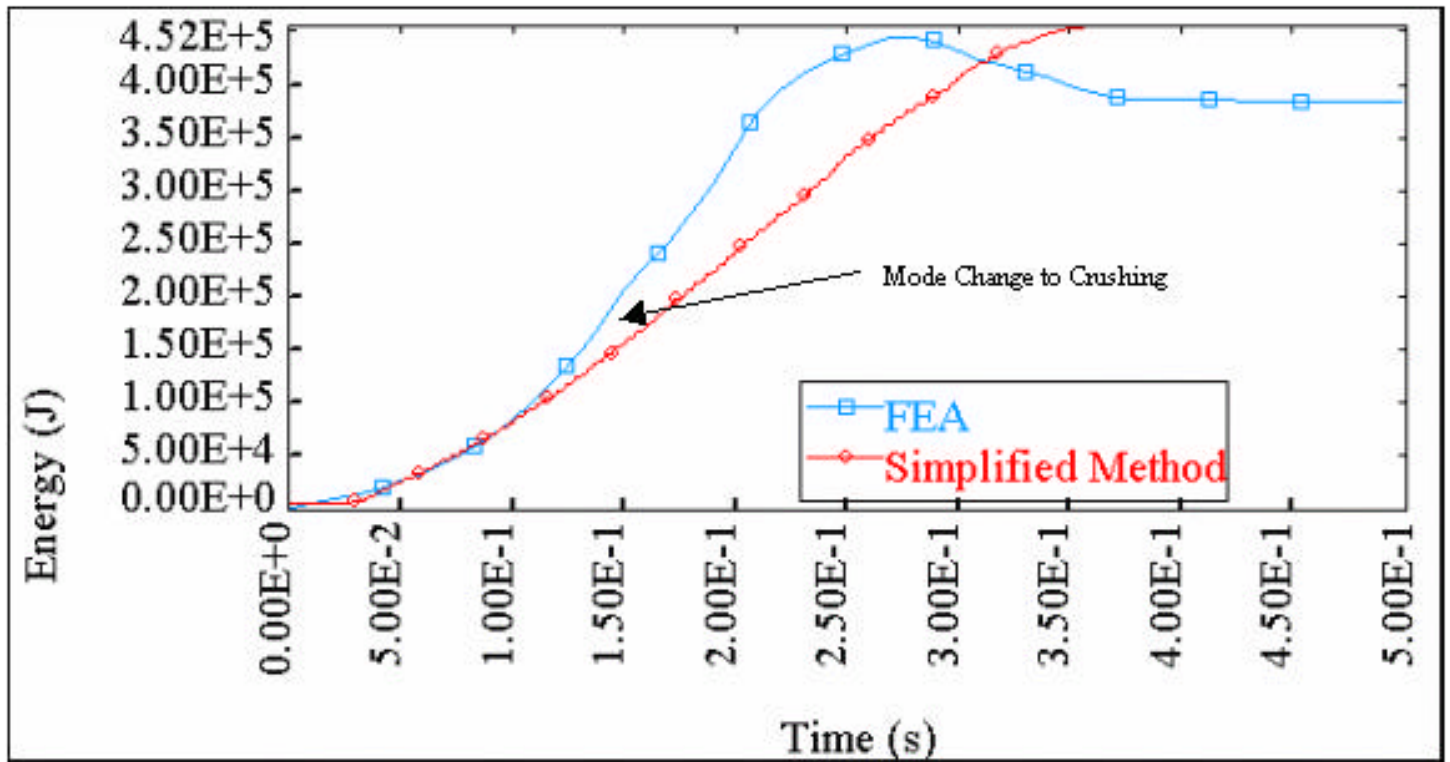


Figure 156 - Case 3 Simplified Method and FEA Absorbed Energy vs. Time Comparison

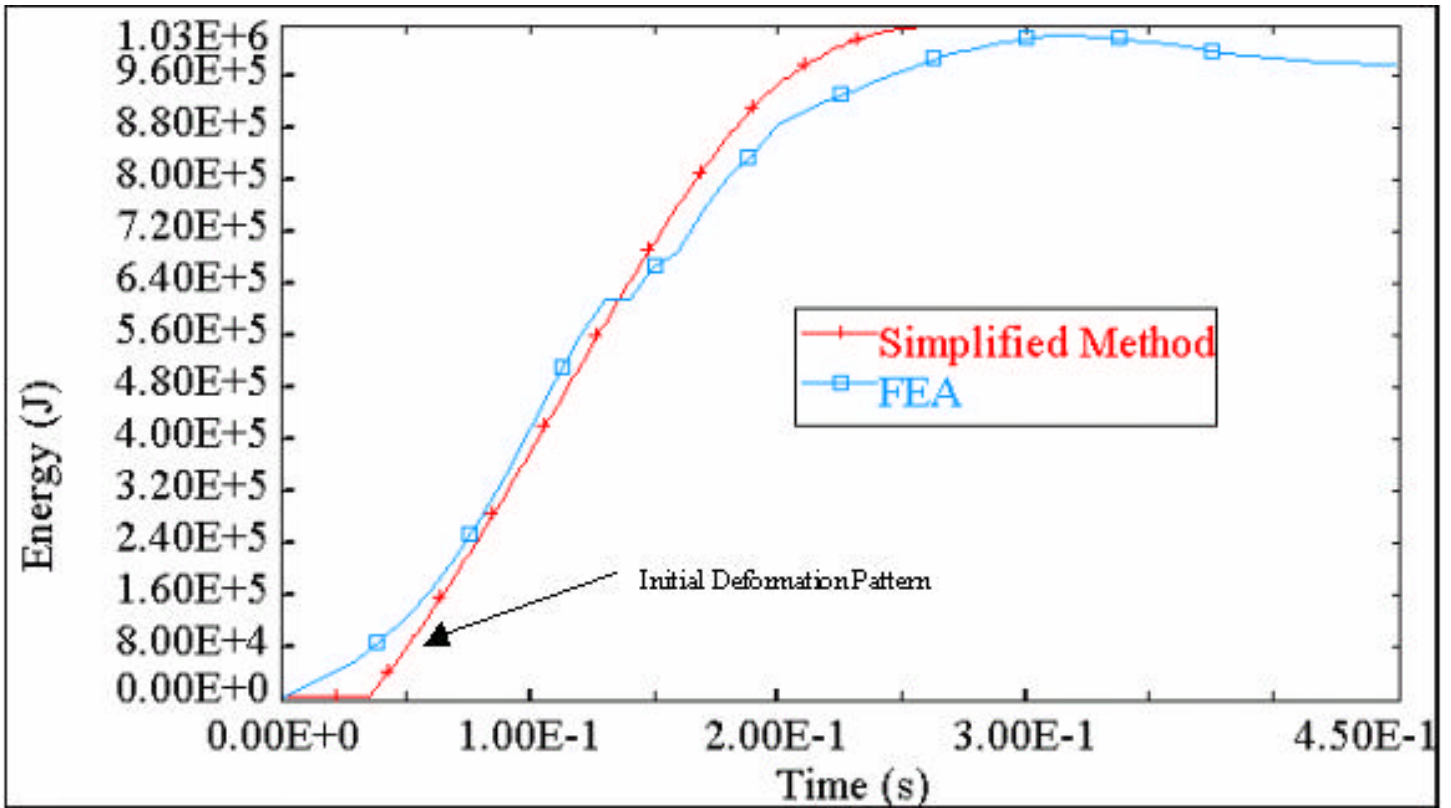


Figure 157 - Case 4 Simplified Method and FEA Absorbed Energy vs. Time Comparison

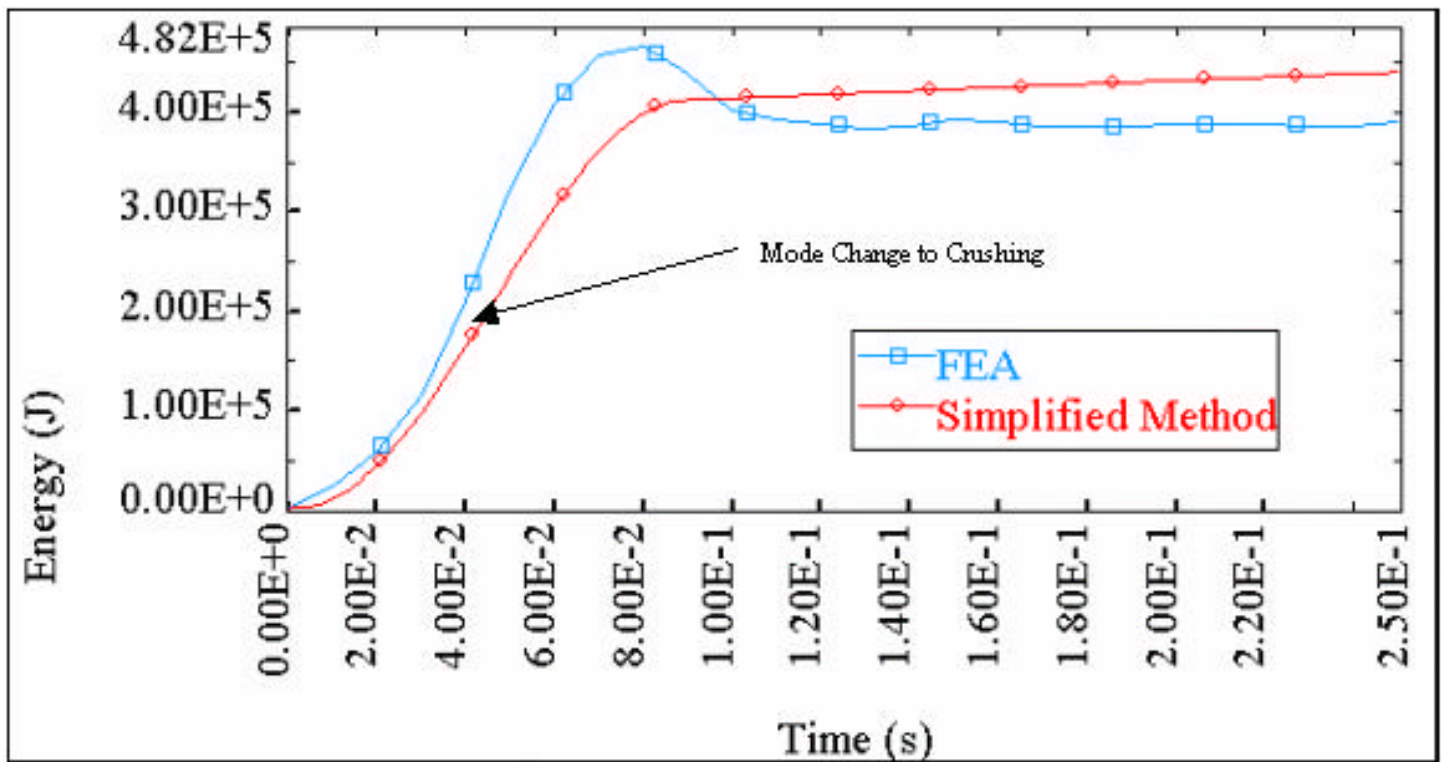


Figure 158 - Case 5 Simplified Method and FEA Absorbed Energy vs. Time Comparison

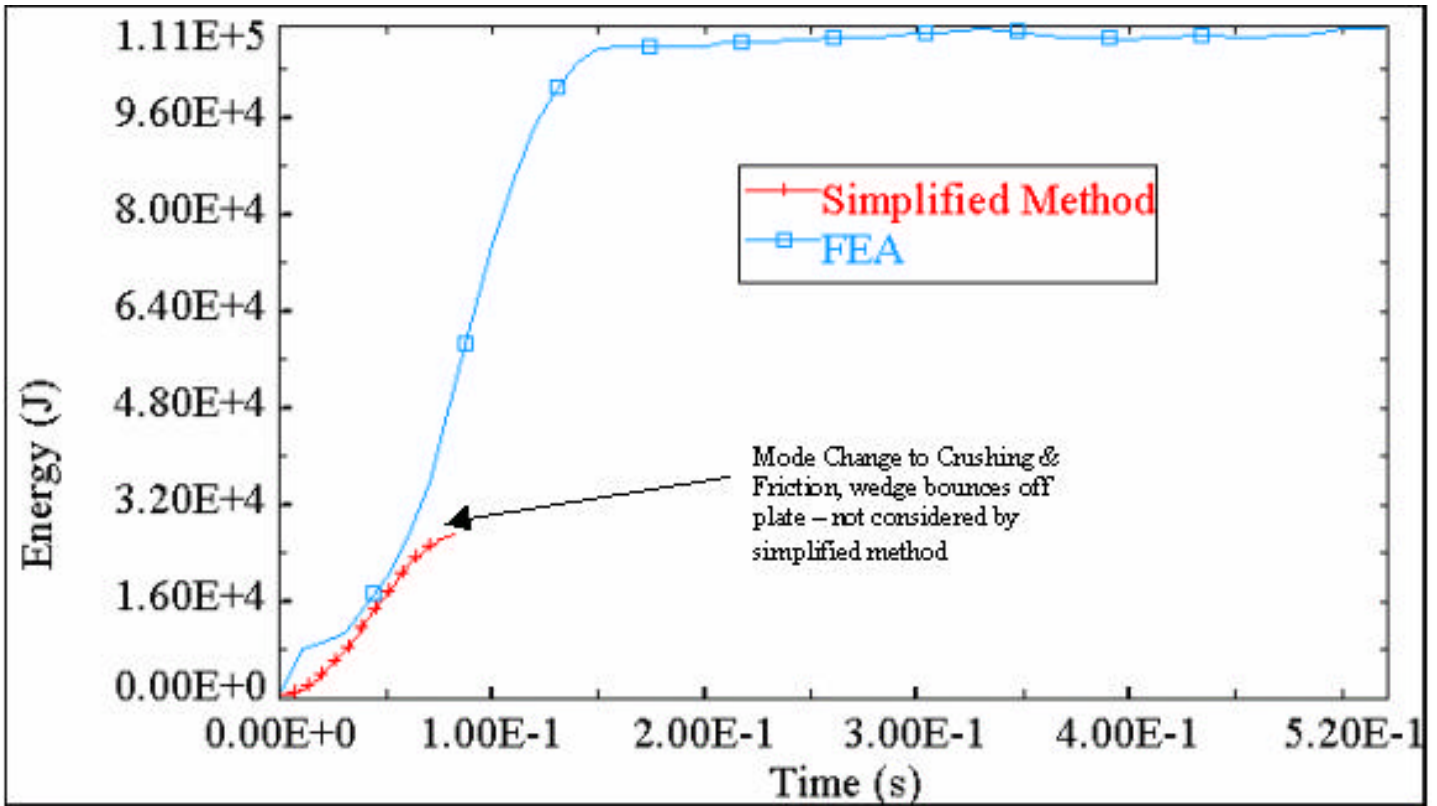


Figure 159 - Case 6 Simplified Method and FEA Absorbed Energy vs. Time Comparison

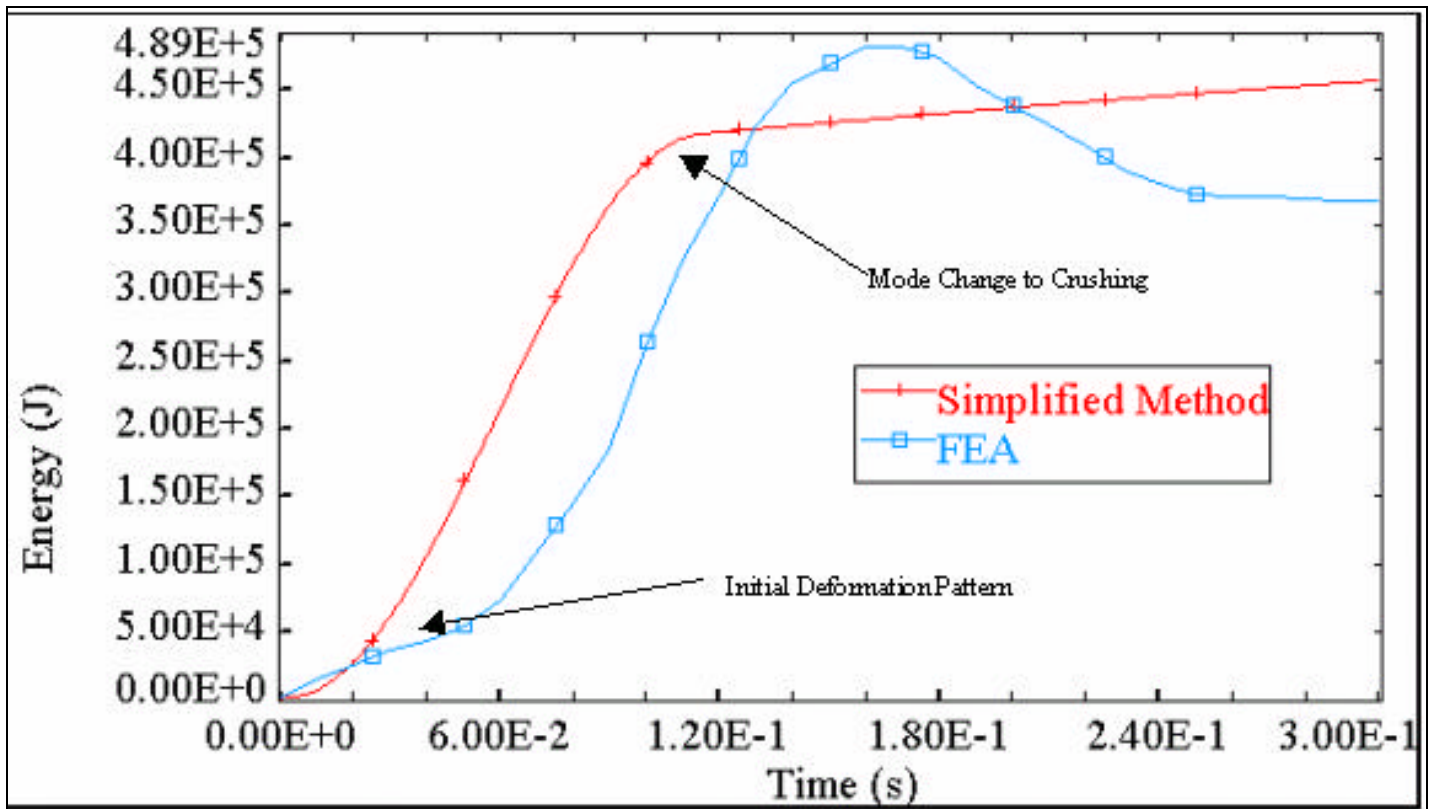


Figure 160 - Case 7 Simplified Method and FEA Absorbed Energy vs. Time Comparison

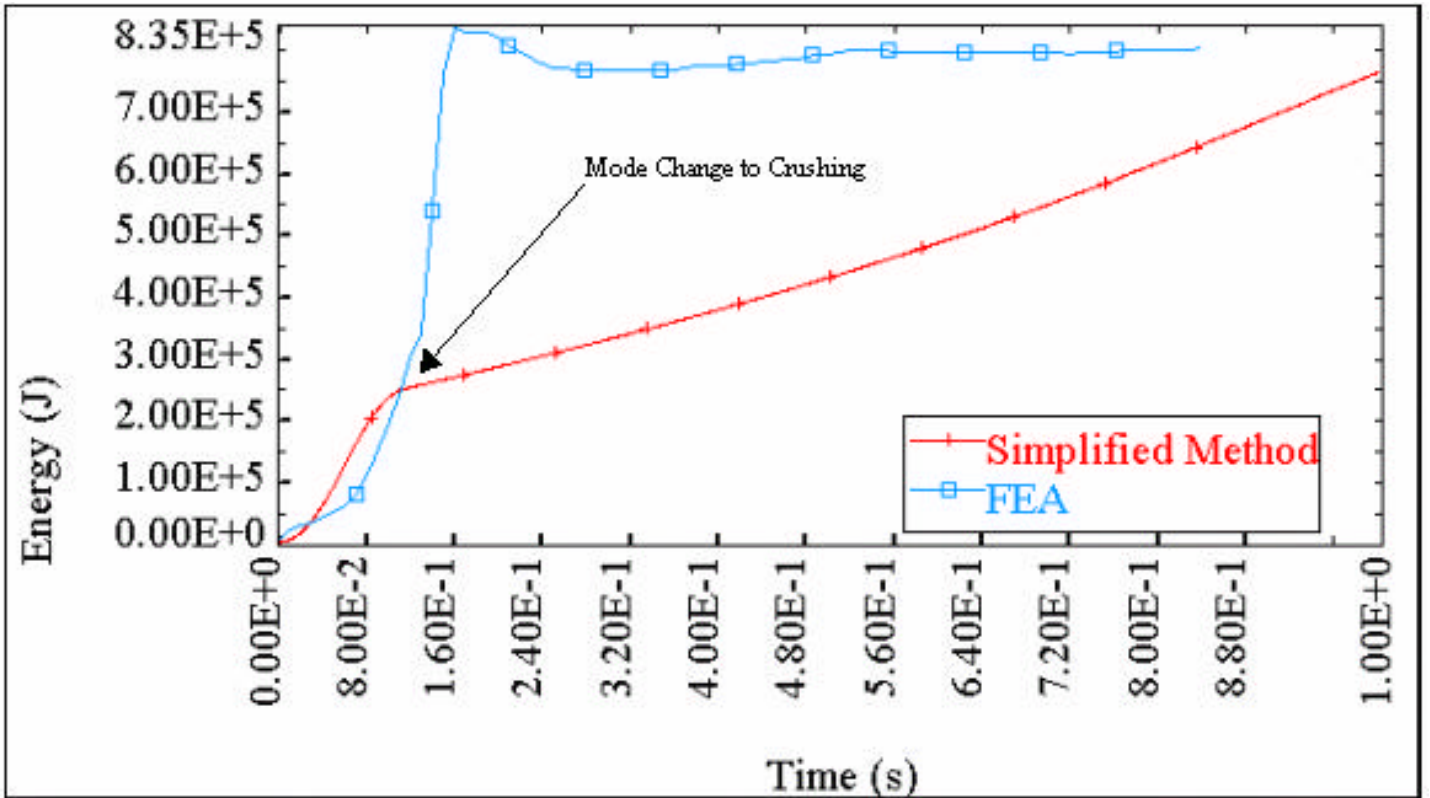


Figure 161 - Case 8 Simplified Method and FEA Absorbed Energy vs. Time Comparison

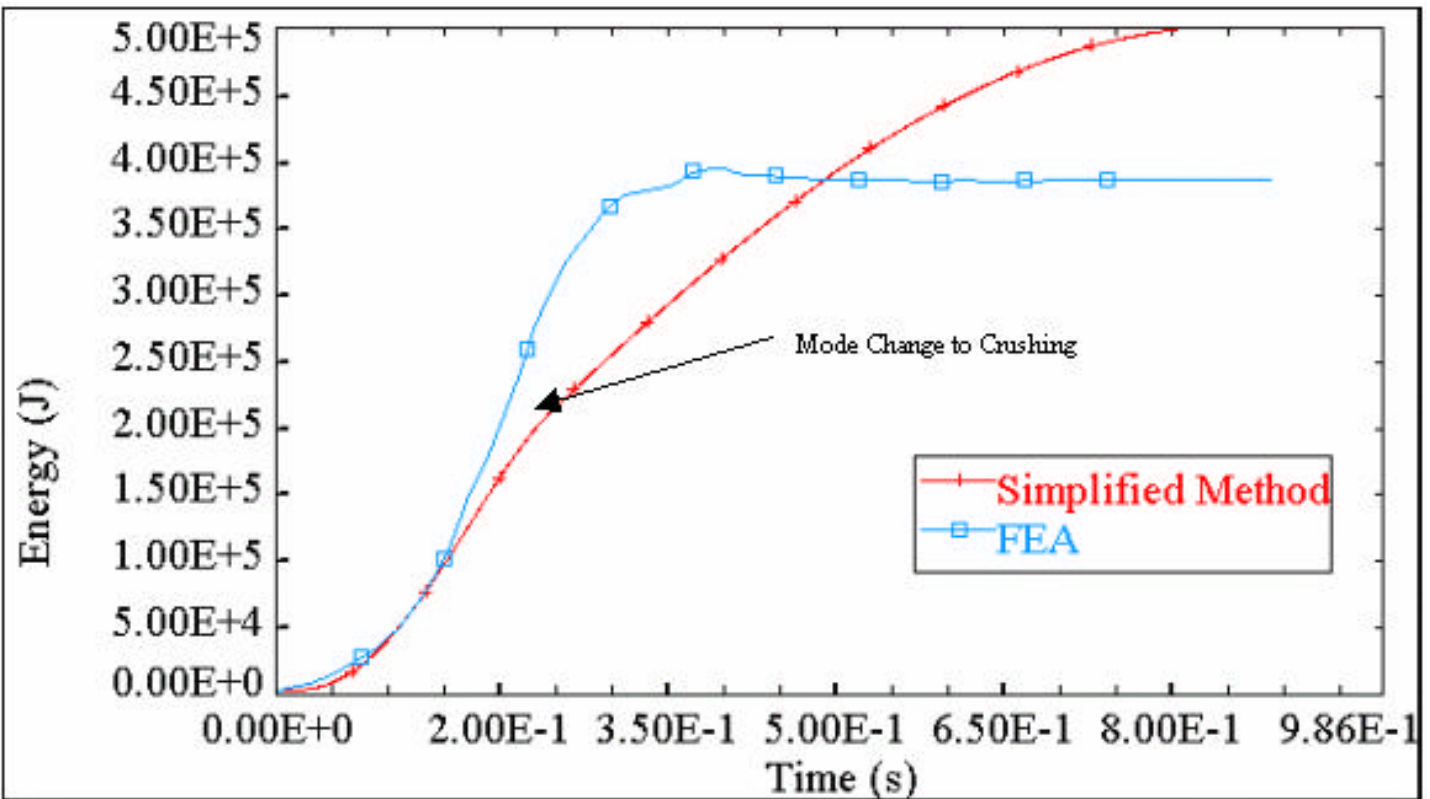


Figure 162 - Case 9 Simplified Method and FEA Absorbed Energy vs. Time

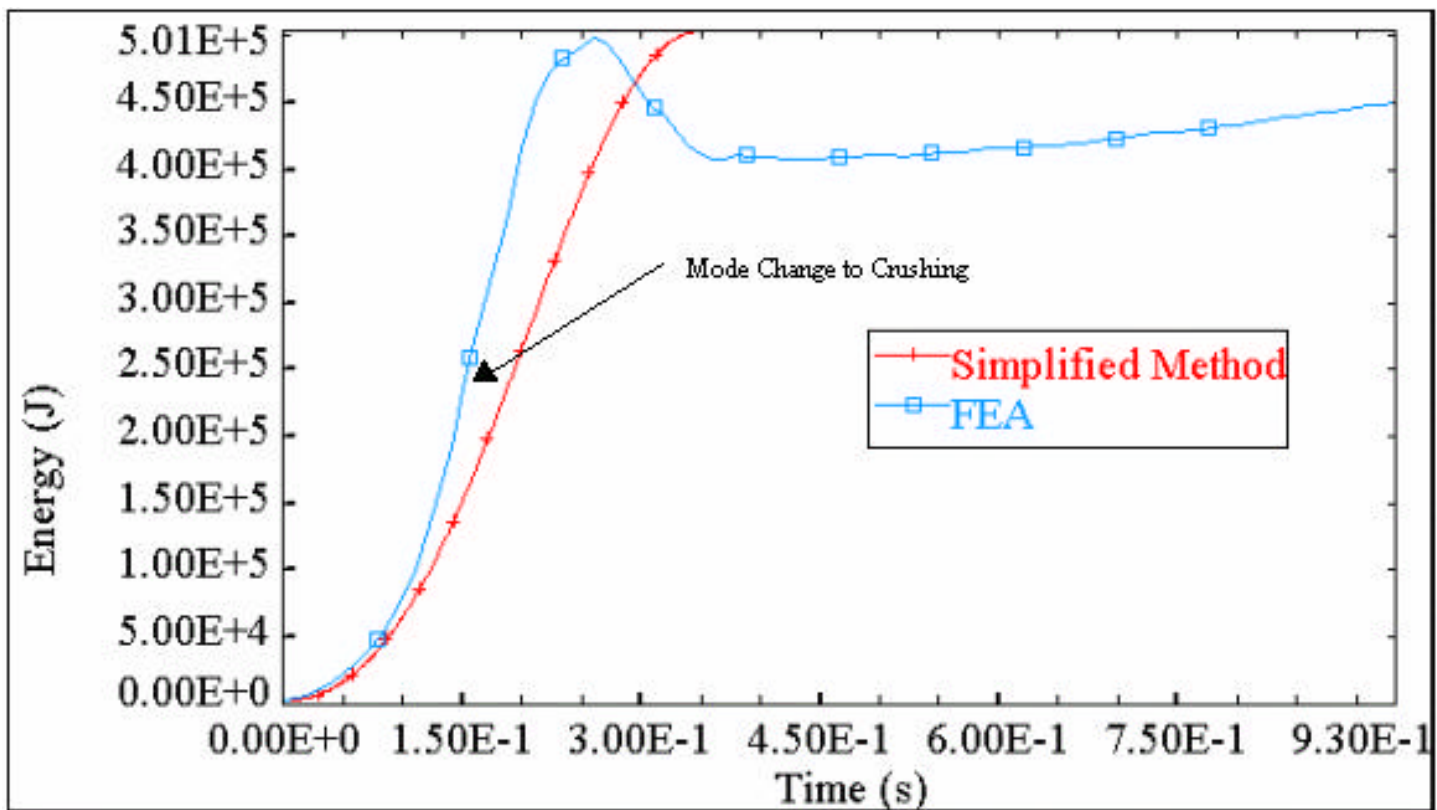


Figure 163 - Case 10 Simplified Method and FEA Absorbed Energy vs. Time

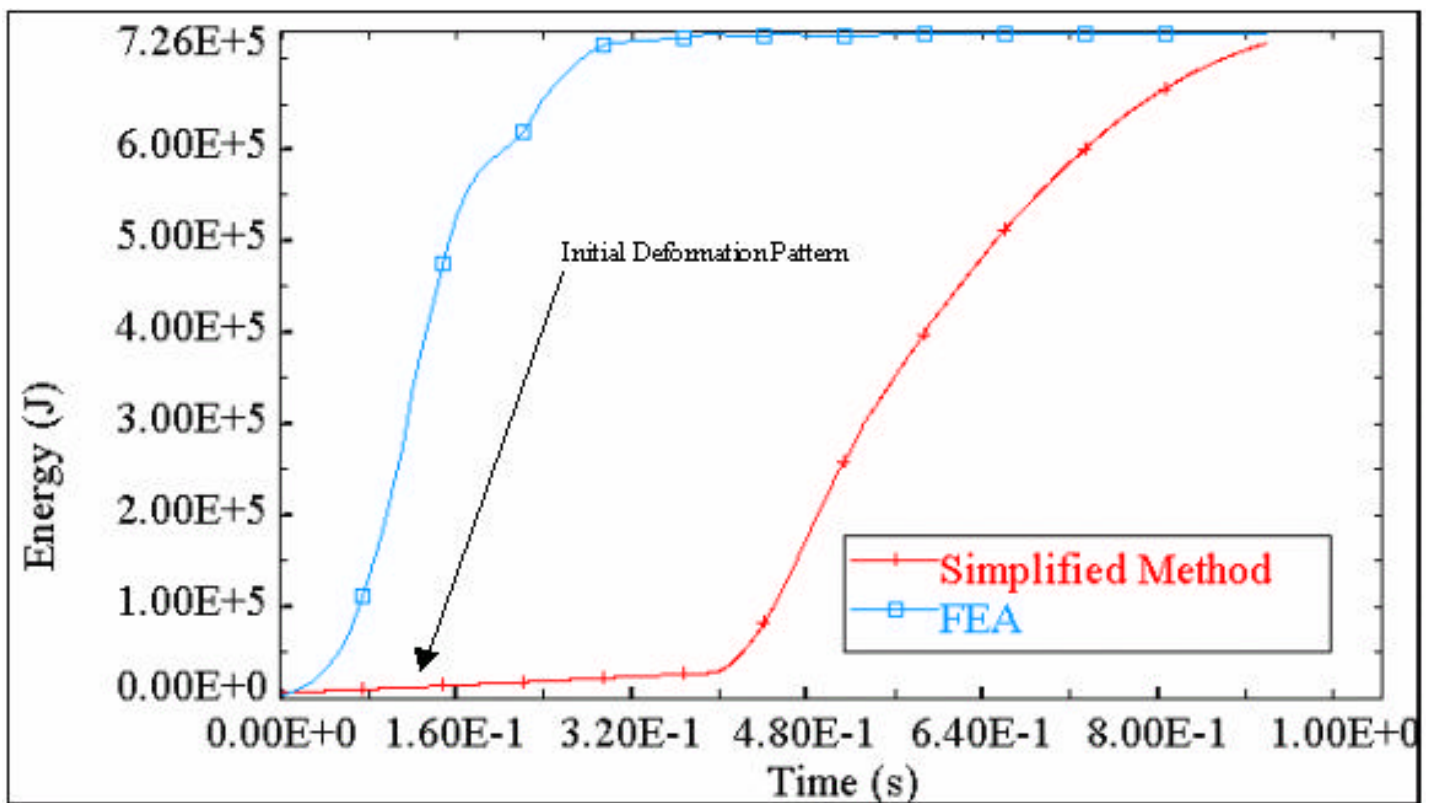


Figure 164 - Case 11 Simplified Method and FEA Absorbed Energy vs. Time

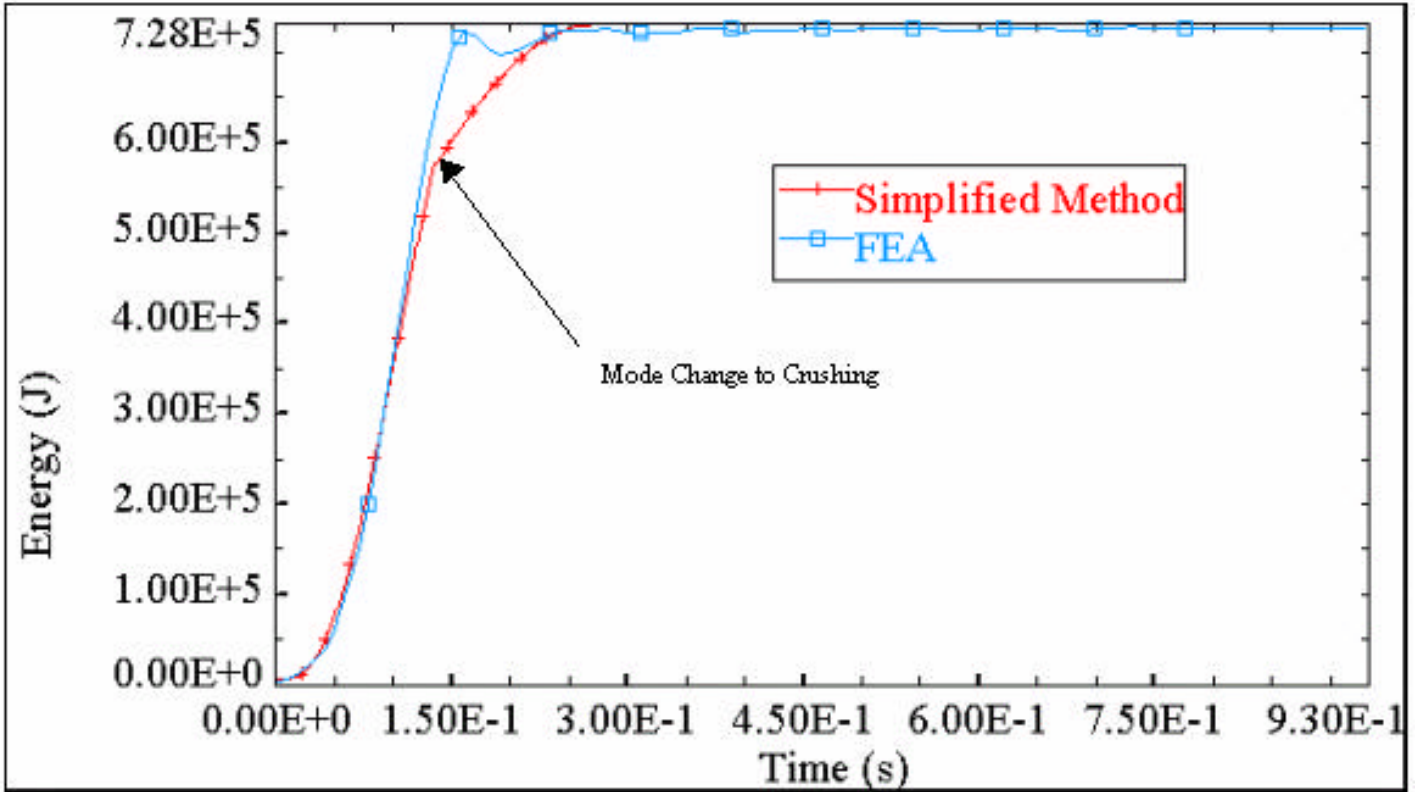


Figure 165 - Case 12 Simplified Method and FEA Absorbed Energy vs. Time

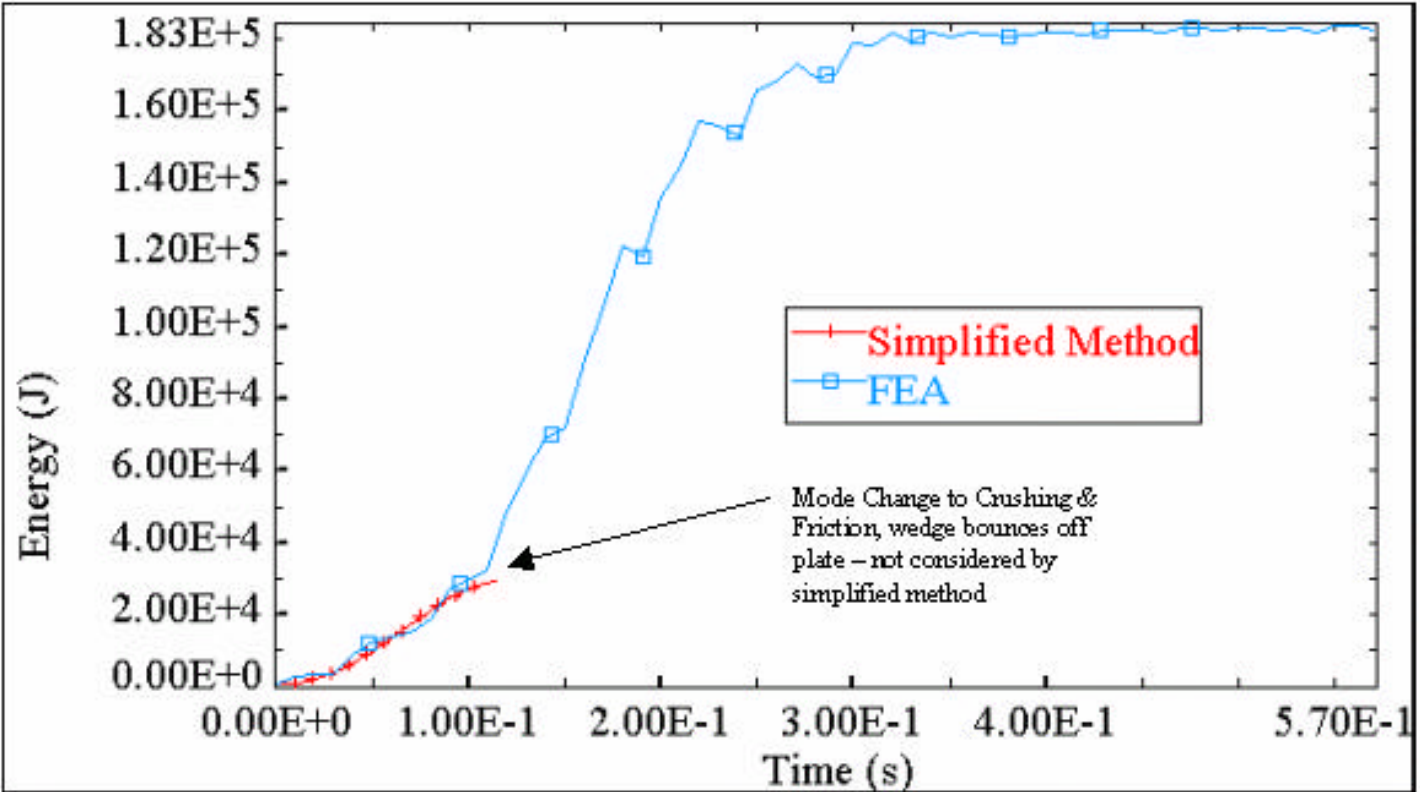


Figure 166 - Case 13 Simplified Method and FEA Absorbed Energy vs. Time

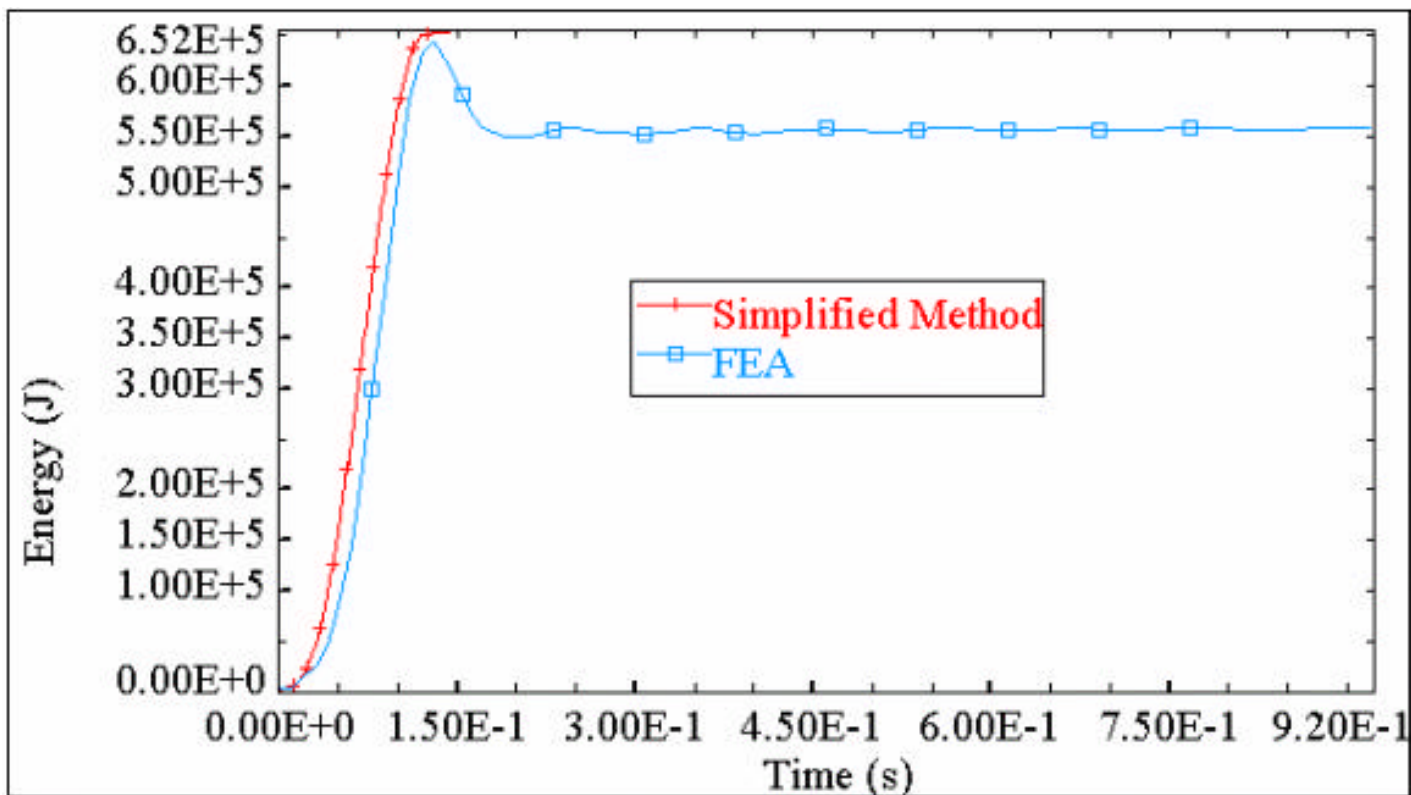


Figure 167 - Case 14 Simplified Method and FEA Absorbed Energy vs. Time

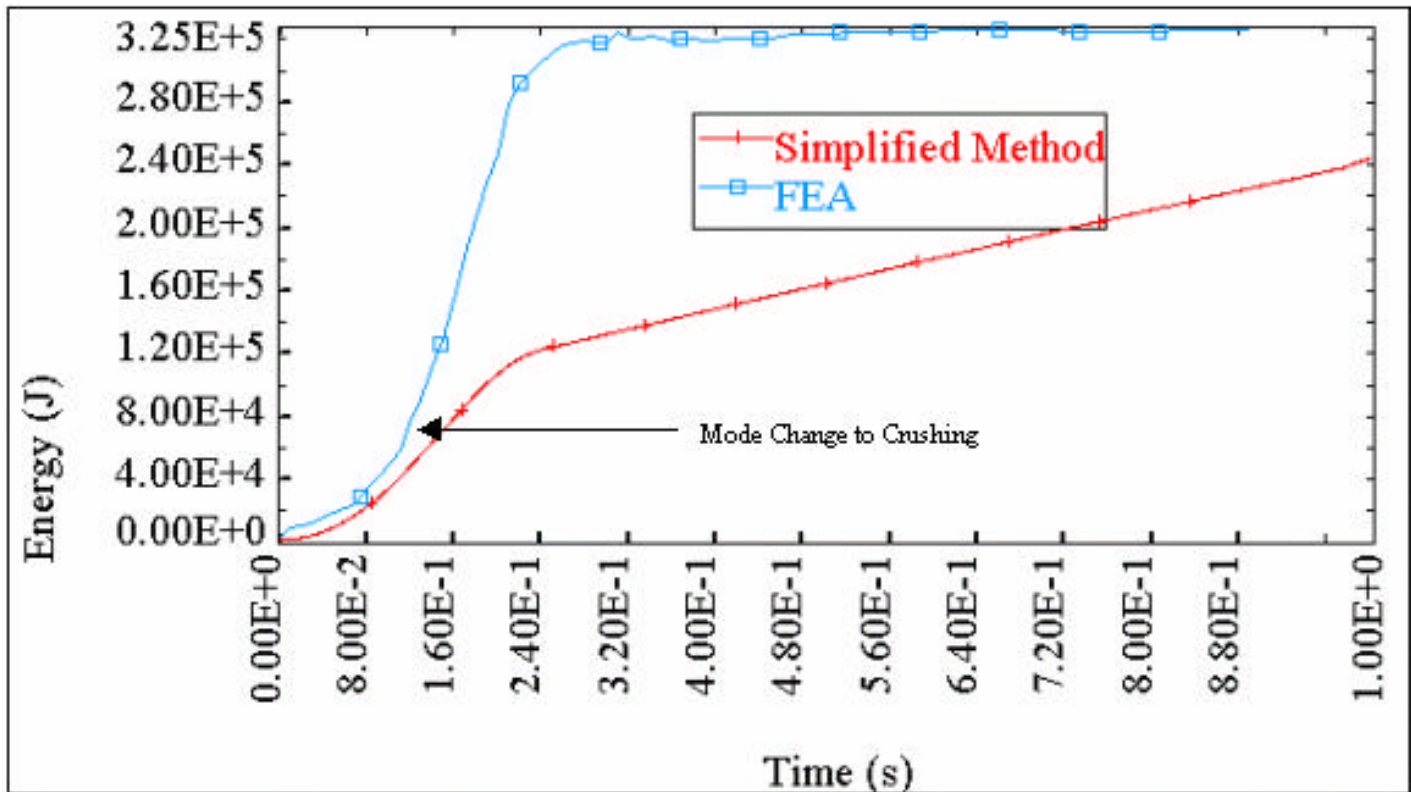


Figure 168 - Case 15 Simplified Method and FEA Absorbed Energy vs. Time

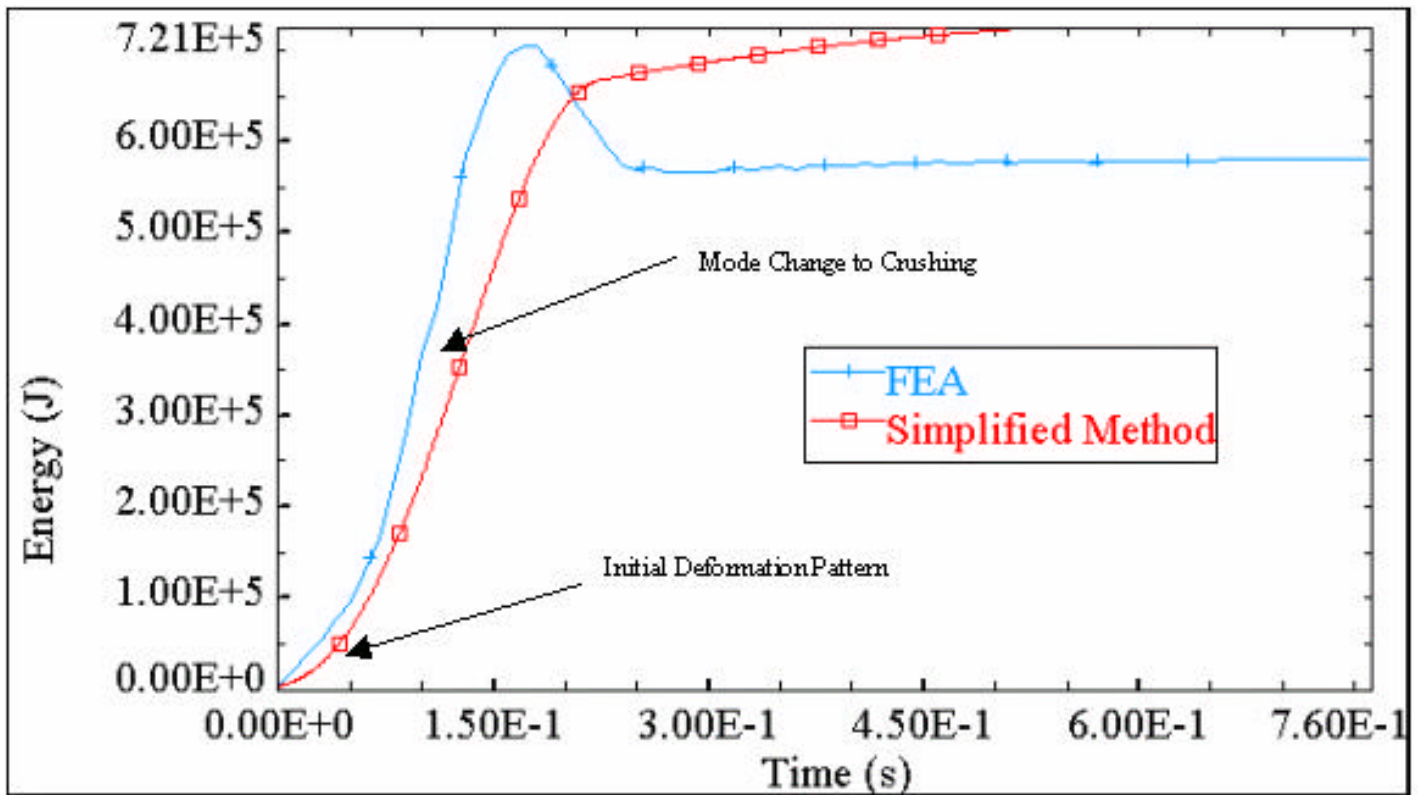


Figure 169 - Case 16 Simplified Method and FEA Absorbed Energy vs. Time

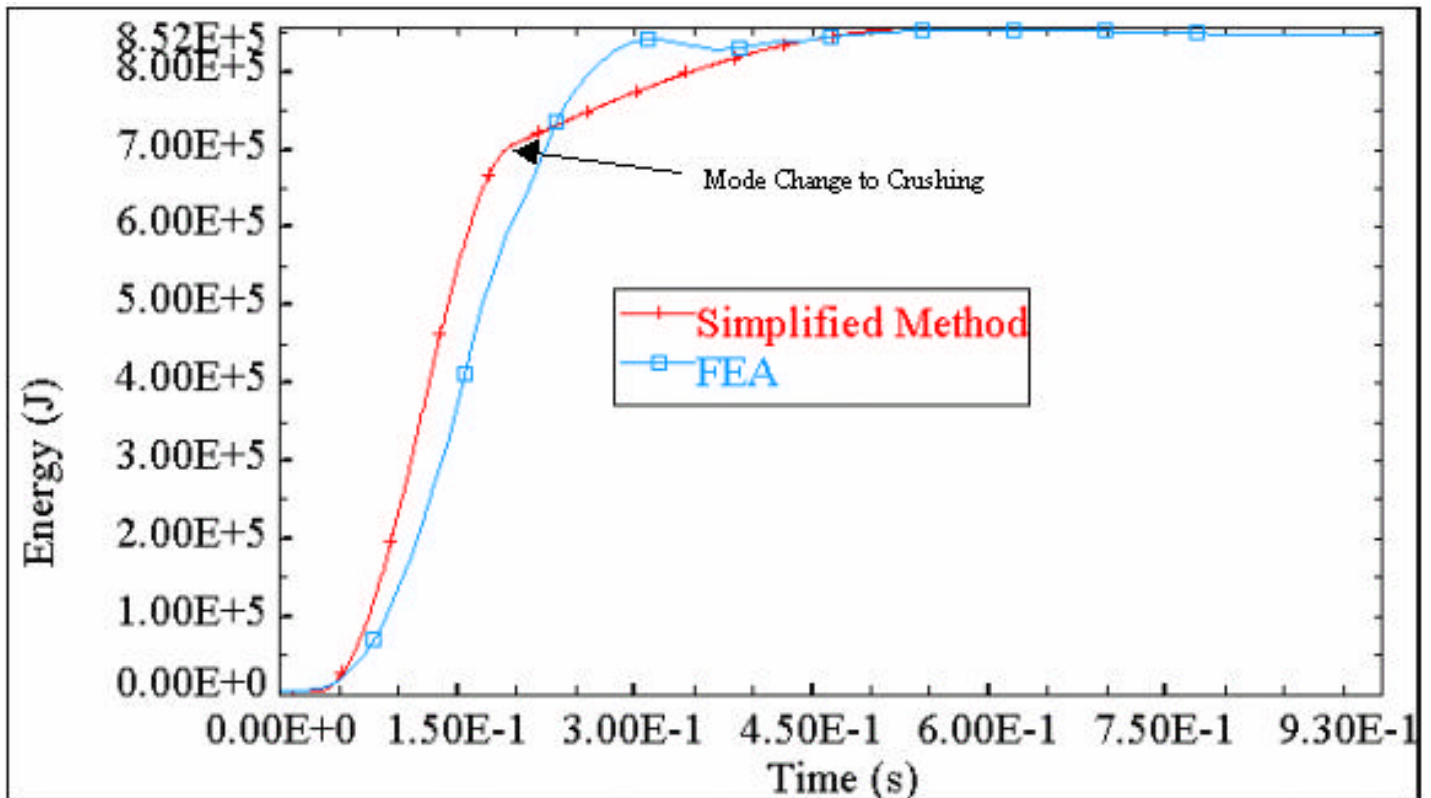


Figure 170 - Case 17 Simplified Method and FEA Absorbed Energy vs. Time

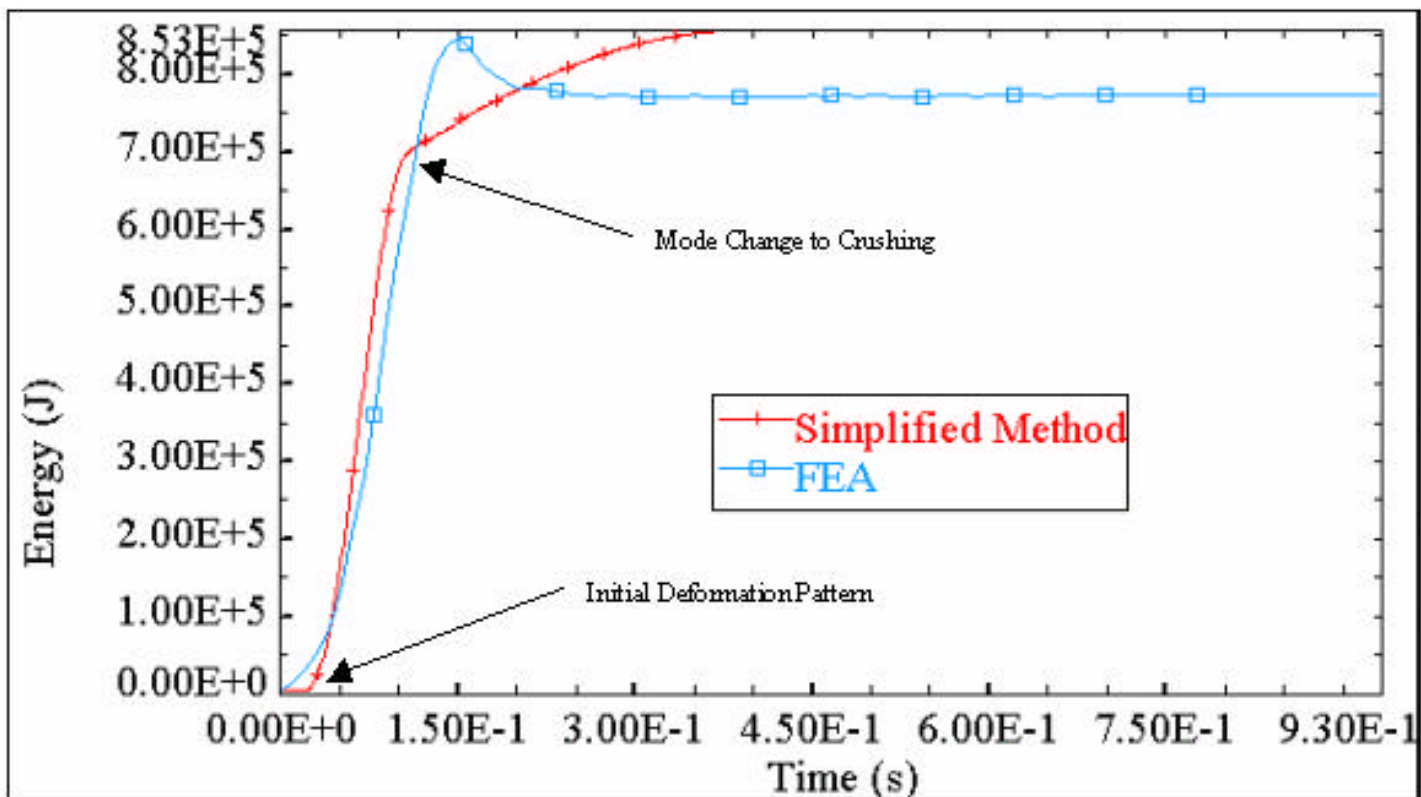


Figure 171 - Case 18 Simplified Method and FEA Absorbed Energy vs. Time

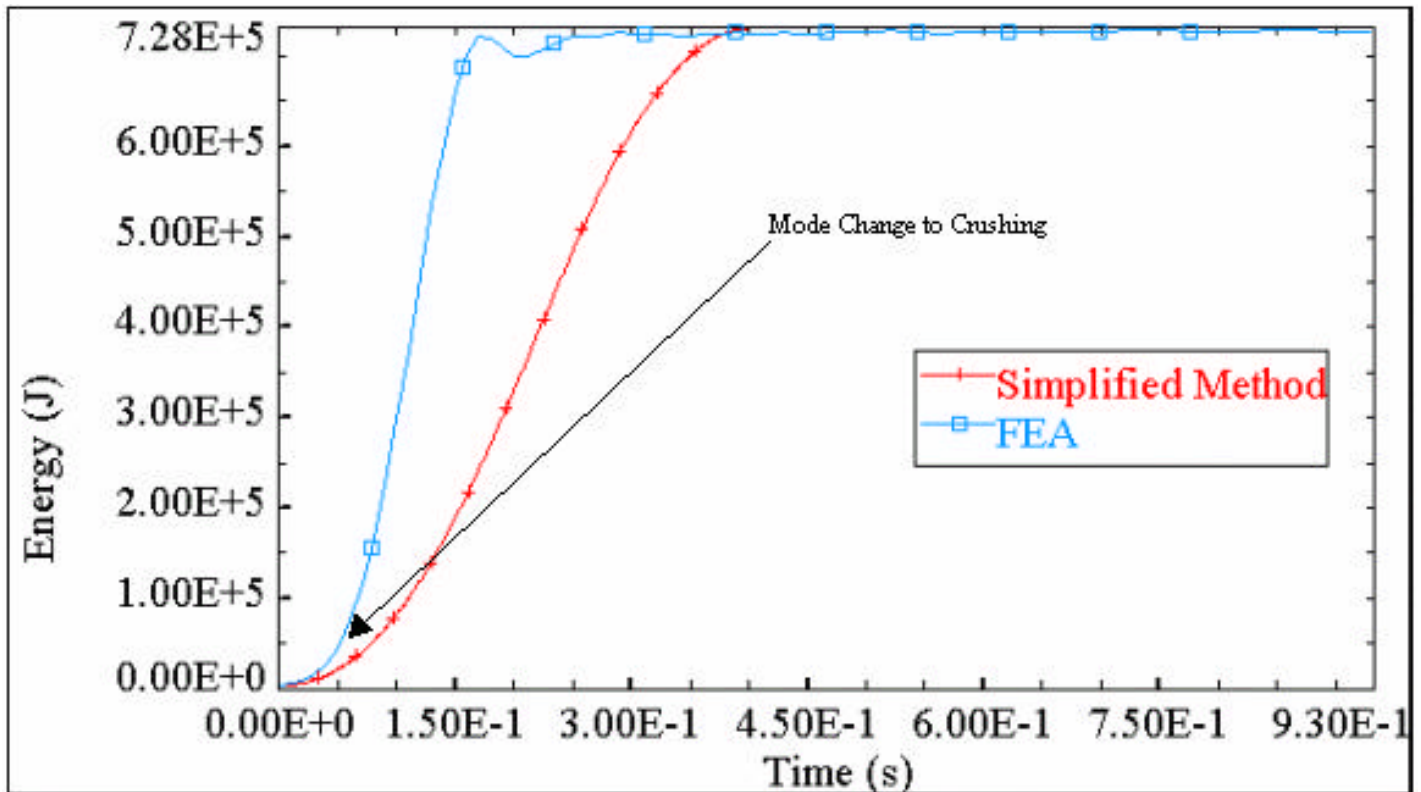


Figure 172 - Case 19 Simplified Method and FEA Absorbed Energy vs. Time

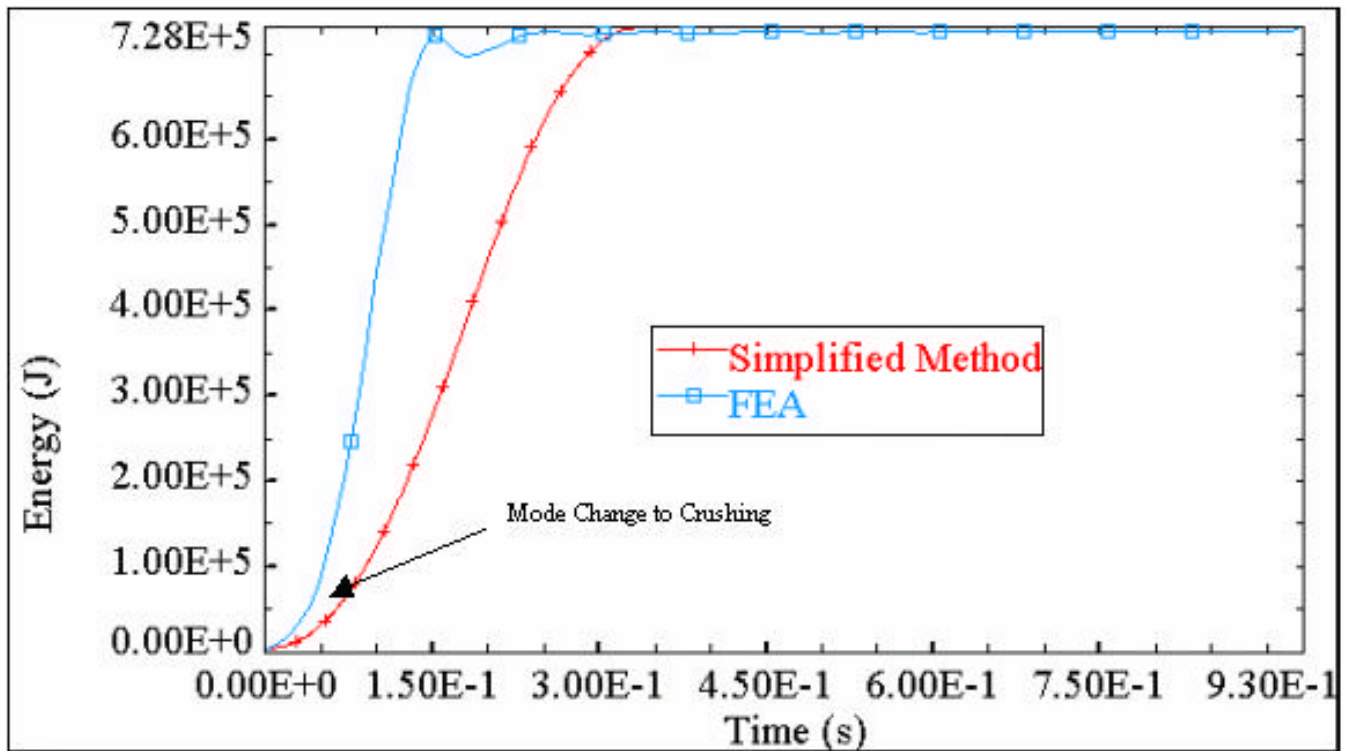


Figure 173 - Case 20 Simplified Method and FEA Absorbed Energy vs. Time

As shown in Figure 154 through Figure 173, there are two differences between the theoretical prediction and the finite element results. These are 1) elastic/plastic bending as indicated by the notation of “Initial Deformation Pattern” and 2) combination deflection and crushing or pure crushing as indicated by the notation “Mode Change to Crushing”. Figure 174 shows crushing in the finite element analysis of Case 6 in Table 17 while the same case analyzed by the twenty-five-region simplified method does not consider this crushing.

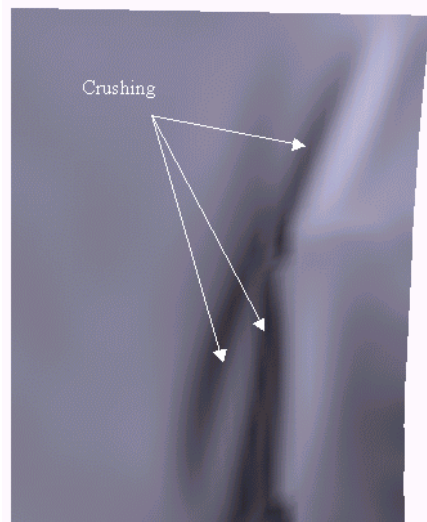


Figure 174 - FEA Plate Crushing

As discussed in Section 5.4.1 the theory for the energy absorbed by the plate using the flow theory of plasticity is limited to a perfectly plastic material law that does not account for the

energy absorbed in initial elastic bending. Additionally, the simplified method strictly assumes that the deformation of the plate is exactly the shape of the impinging rigid wedge, consequently, plastic bending occurring in the finite element model is not accounted for in the simplified method. The difference between the initial bending deformation in the finite element model and the simplified method is highlighted in Figure 175 and the effects of this difference are seen in Cases 4 and 11 (Figure 157 and Figure 164) where for Case 11 the component of the velocity in the x direction is greater than the component in the z direction and the collision angle is highly oblique forcing more energy to be absorbed in the initial bending of the plate in the finite element model.

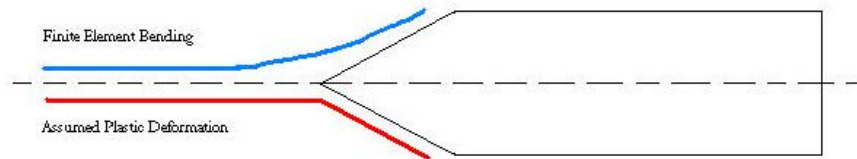


Figure 175 - FEA Bending vs. Simplified Method Deformation

The second difference in Figure 154 through Figure 173 is due to the change in the deformation mode of the plate from lateral deflection to that of crushing as treated by the method of Section 5.2 but not shown in these figures. As the plate is laterally deformed, a velocity in the x direction will tend to push against the plate instigating an axial stress on the plate and causing a change in the deformation mode to crushing. To overcome this variation in the above test cases, the theory of Section 5.2 is incorporated into the flow theory such that if the energy to crush the plate is less than the energy required to laterally deform the plate then the method of Section 5.2 is used to determine the energy absorbed during the time step, if however the energy to laterally deform the plate is the lesser then that energy and deformation mode is used for the time step. Figure 176 through Figure 182 present the results of this combination of method analysis for Cases 2, 7, 8, 12, 15, 18 and 19 of Table 17.

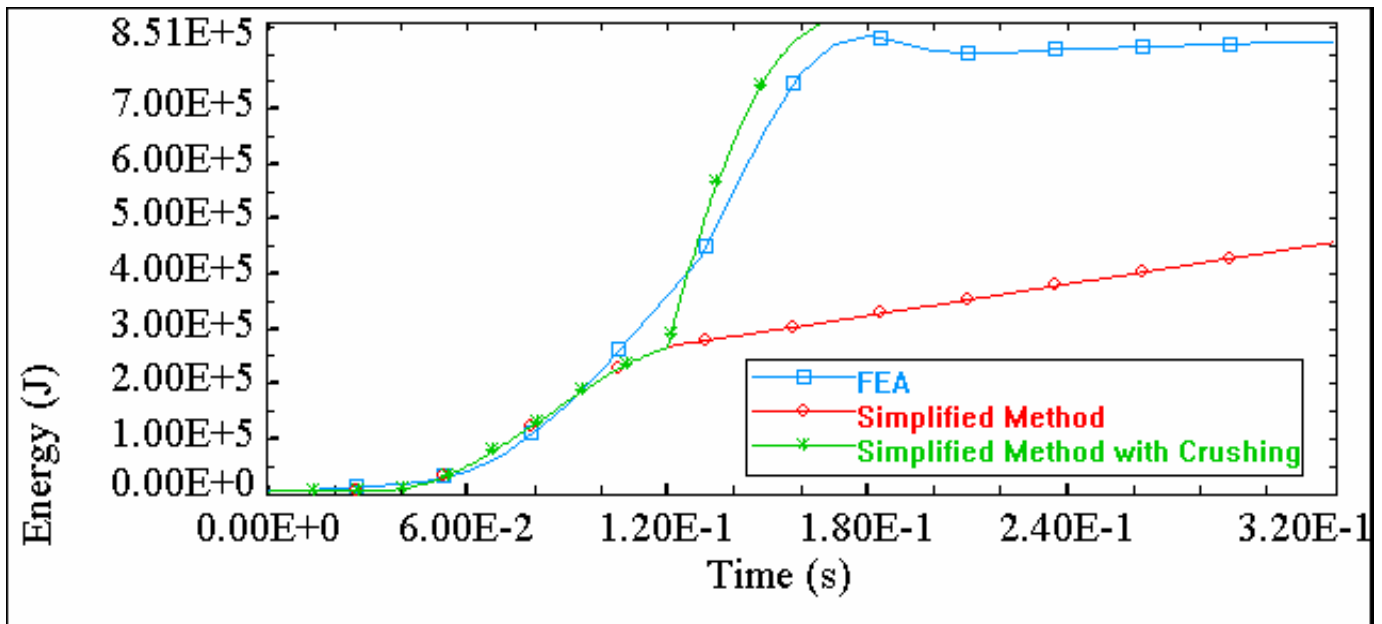


Figure 176 - Case 2 Simplified Method (With and Without Crushing) and FEA

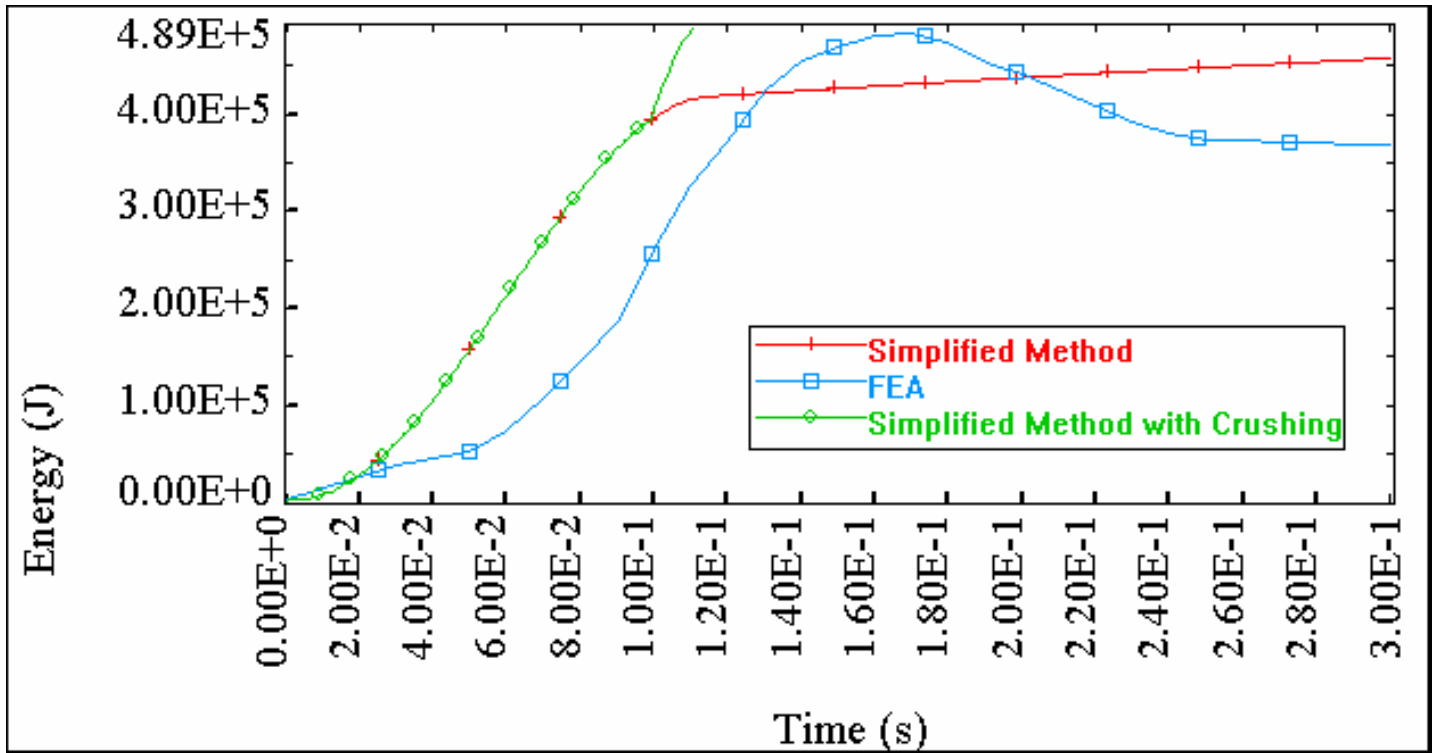


Figure 177 - Case 7 Simplified Method (With and Without Crushing) and FEA

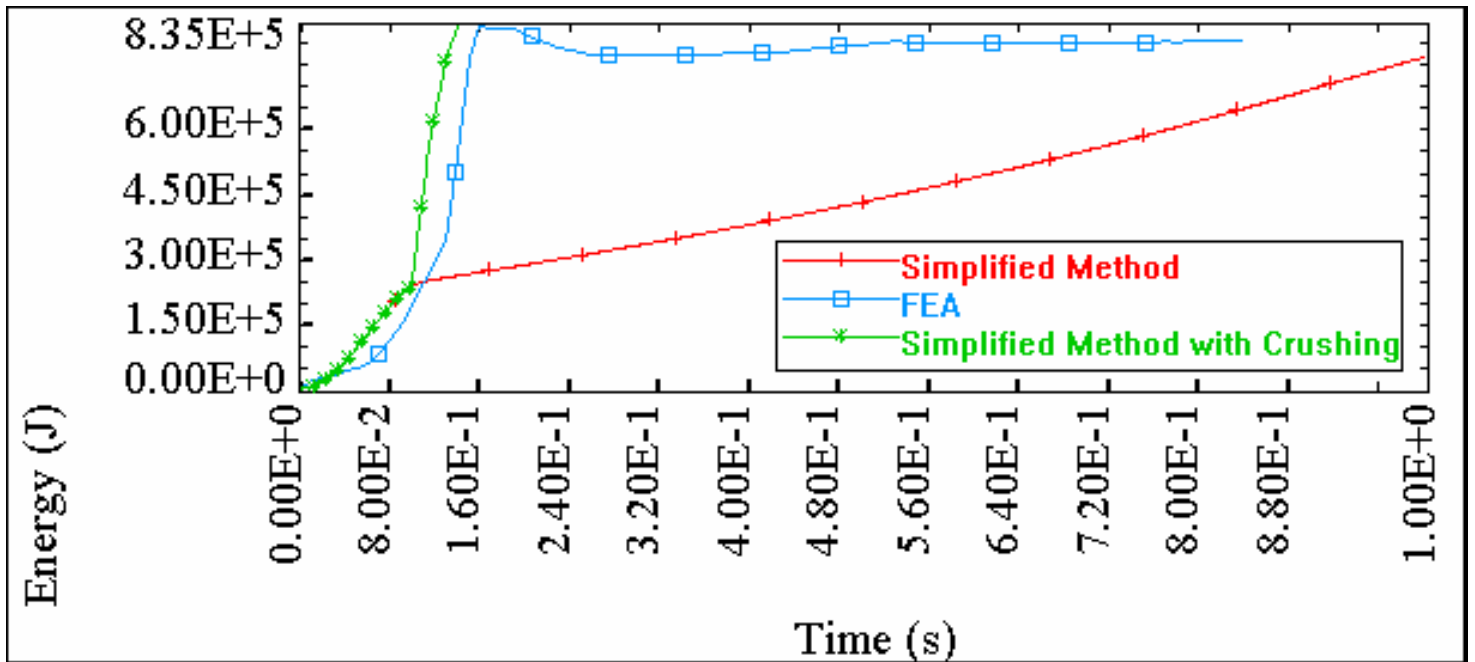


Figure 178 - Case 8 Simplified Method (With and Without Crushing) and FEA

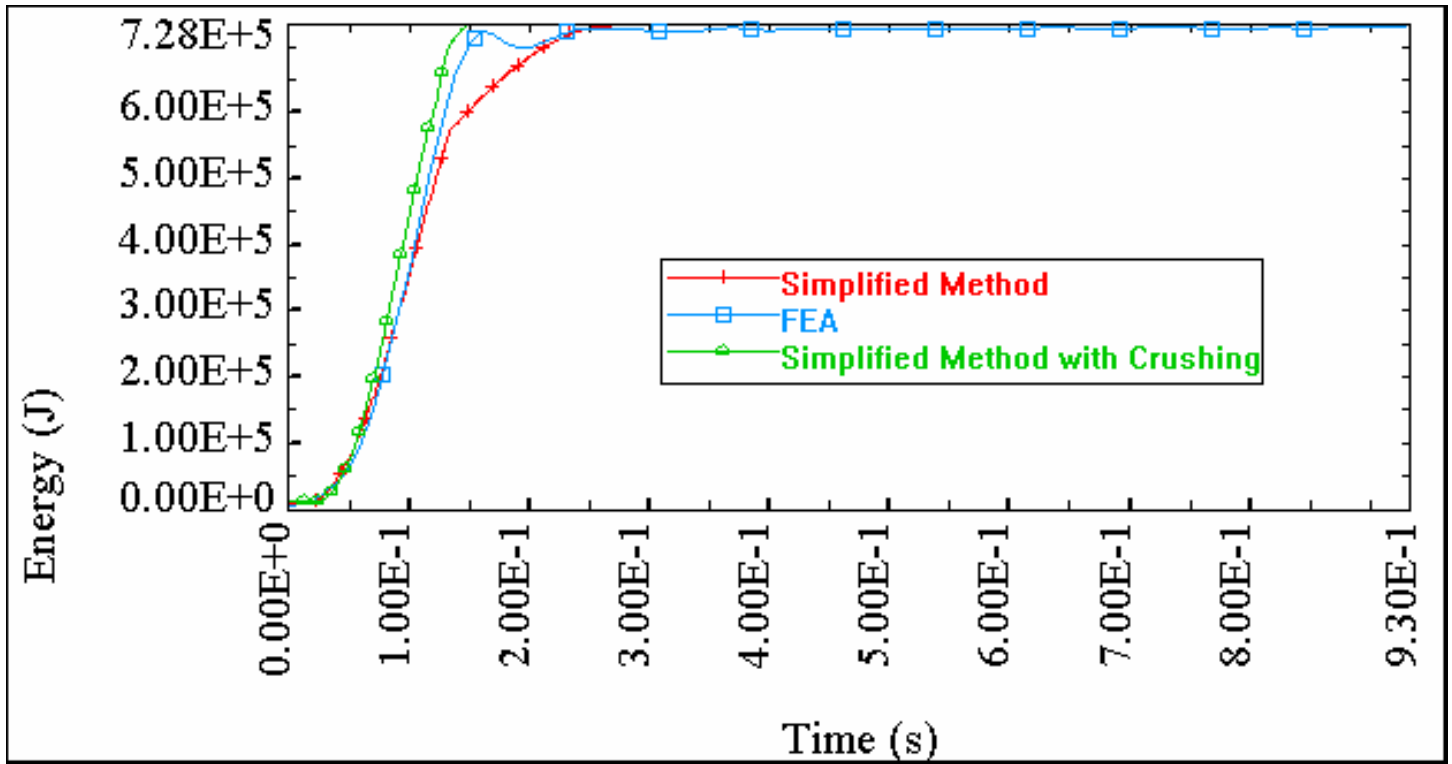


Figure 179 - Case 12 Simplified Method (With and Without Crushing) and FEA

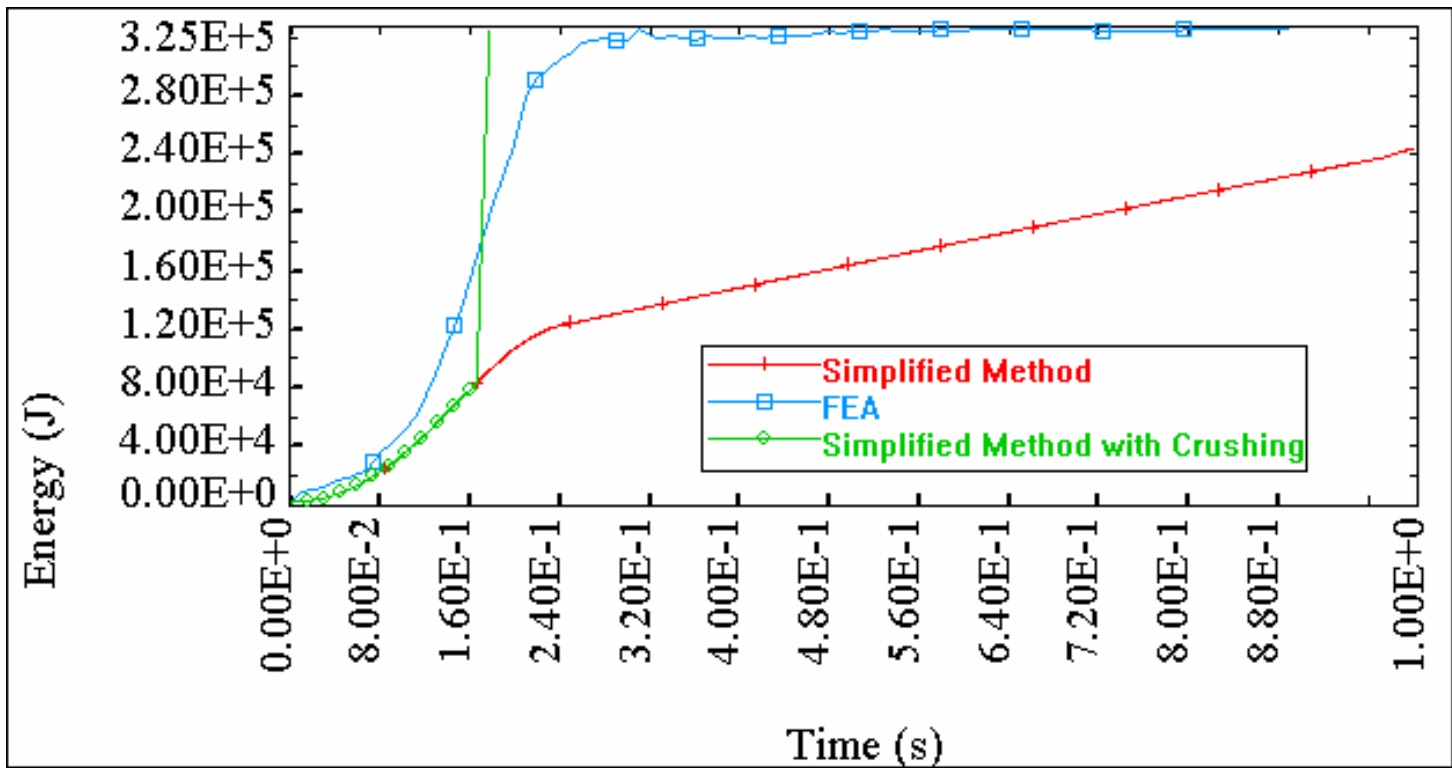


Figure 180 - Case 15 Simplified Method (With and Without Crushing) and FEA

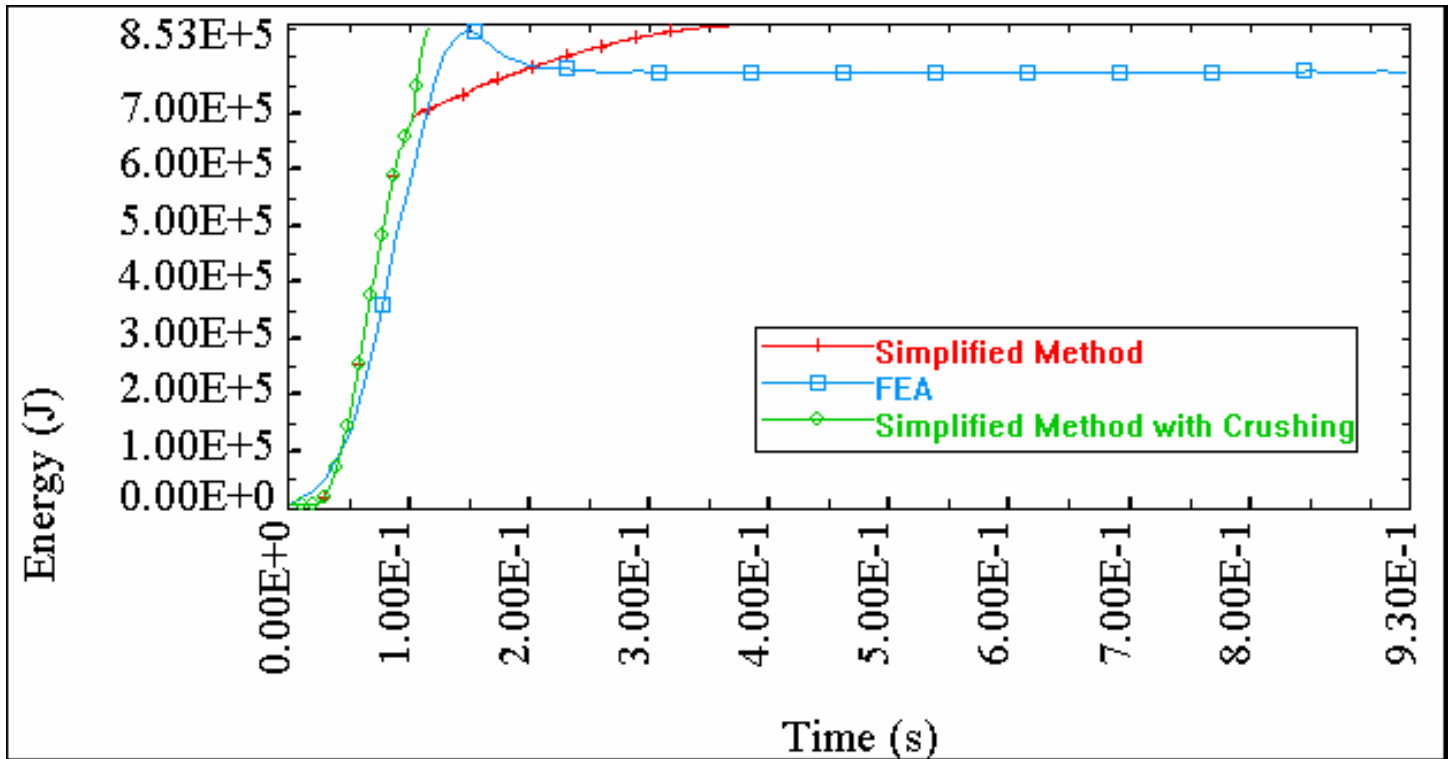


Figure 181 - Case 18 Simplified Method (With and Without Crushing) and FEA

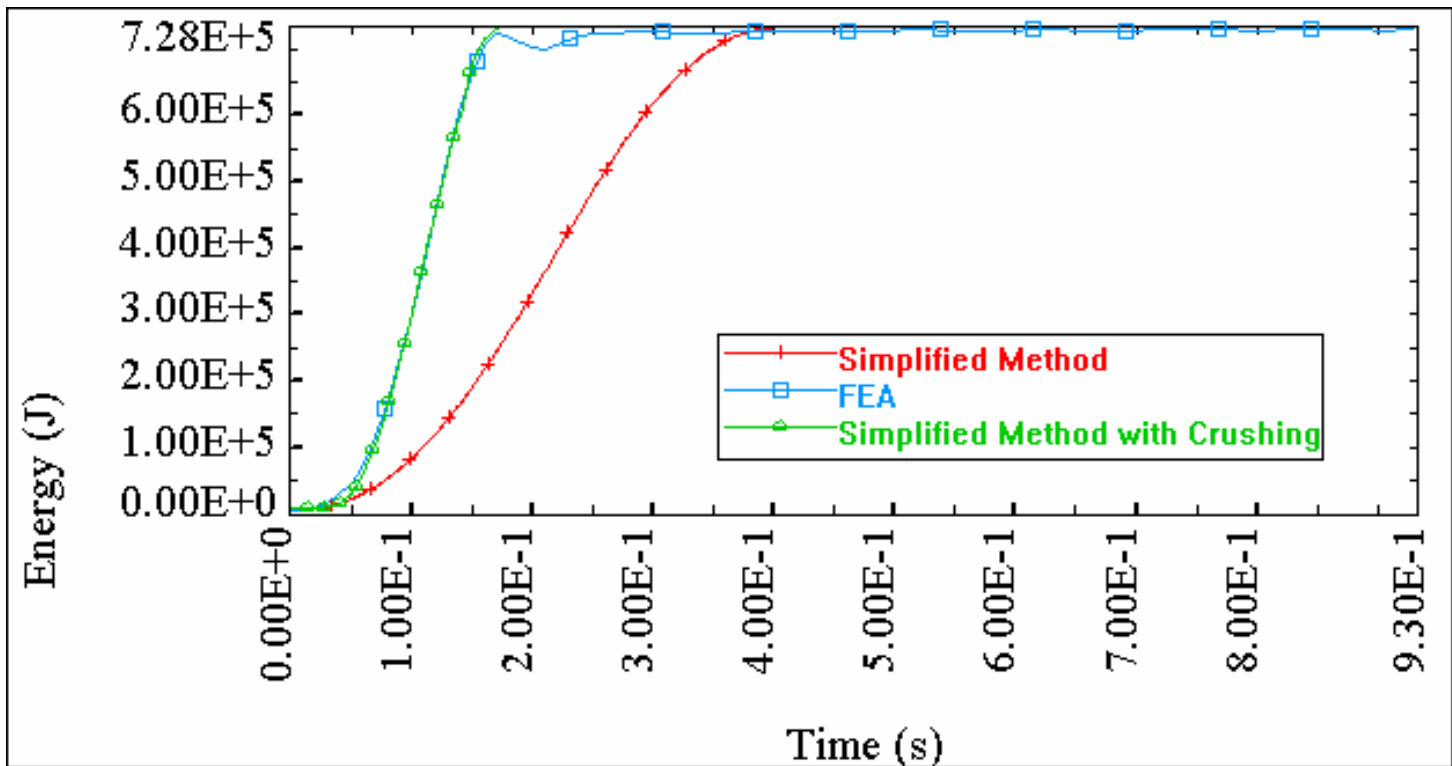


Figure 182 - Case 19 Simplified Method (With and Without Crushing) and FEA

As shown in Figure 176 through Figure 182 the combination mode provides a better representation of the energy absorbed by the plate when subjected to a lateral and axial load. The

correlation coefficients for these cases are provided in Table 18 as calculated using Equation 5.1. SIMCOL Version 3.0 is adapted to use this combination mode for the energy absorbed by transverse bulkheads and webs.

Table 18 - Correlation Coefficient of Simplified Method to FEA Energy vs. Time Curves

<b><u>Case #</u></b>	<b><u>Correlation Coefficient</u></b>
2	0.744
7	0.623
8	0.648
12	0.875
15	0.571
18	0.71
19	0.903

## CHAPTER 6 SIMCOL Version 3.0 Validation

Collisions are high consequence, low probability events. Because of this high consequence, most collisions involve litigation and sometimes years of legal proceedings. The focus of these proceedings is frequently on human error vice a precise technical analysis of what happened and what resulted. For these reasons, complete technical data describing the struck and striking ship, the collision event, and the resulting damage is very difficult to obtain.

Data required to validate SIMCOL 3.0 to describe a collision event include:

- Struck ship design parameters
- Struck ship variables – speed, trim, draft or displacement
- Event variables - collision angle ( $\phi$ ), strike location (l)
- Striking ship variables – type, dwt, speed, displacement, length, beam, bow half-entrance angle (HEA), draft at bow

In this project, SIMCOL is validated using two collision events described by Minorsky's [9] original data updated by additional library research, and using IMO probabilistic data. The first validation case is the collision between the David E. Day and the Marine Flier in the Pacific Ocean on May 17, 1952. The second validation case is the collision between the P&T Adventurer and the Tullahoma in the North Pacific on August 4, 1951.

### 6.1 *David E. Day Marine Flier Collision*

On May 17, 1952 the C4 cargo vessel “Marine Flier” struck the T2 tanker “David E. Day” at a reported 55-degree collision angle between frames 59 and 62 of the David E. Day, approximately 9 meters forward of amidships. The reported vessel speeds at the time of the collision were 16.3 knots for the David E. Day and 16.5 knots for the Marine Flier causing a reported 17 ft of penetration and 35 ft of damage length. Extensive examination of documents related to the collision indicates that the actual speeds of the Marine Flier and David E. Day at the time of the collision were closer to 5 to 7 knots and the collision angle was in actuality between 50 and 55 degrees. In part, these changes were due to last minute “Full Astern” and “Hard Right Rudder” orders given by the masters of each vessel in the effort to avoid the collision.

Structural drawings for both ships were obtained through the National Archives and Records Administration and this data was used to model the collision in SIMCOL Version 3.0. Appendix C provides information on the “Marine Flier”. Appendix F provides information on the “David E. Day”. In the SIMCOL analysis the collision angle was set at 51 degrees with a collision location 10 meters forward of amidships. The initial striking vessel speed was set at 5.5 knots, and the struck vessel speed was retained at 7 knots. The SIMCOL results indicate 5.289 meters or 17.35 ft of penetration and 10.787 meters or 35.39 ft of damage length. The SIMCOL results are conservative by approximately 2% in penetration and 1% in damage length compared to Minorsky's (1959) reported penetration and damage length values.

This case was also modeled using LSDYNA. Differences between SIMCOL Version 3.0 results, actual and finite element analysis results are shown in Table 19.

Table 19 – FEA/SIMCOL/Actual Damage Comparison

<b>Validation with Marine Flier - David E. Day Collision</b>		
Method	Penetration (ft)	L.E.D. (ft)
SIMCOL	17.35	35.39
FEA	16.7	32.8
% Difference	3.75%	7.32%
Reported	17	35
% Difference	2.06%	1.11%

## 6.2 P&T Adventurer Tullahoma Collision

On August 4, 1951 the Victory cargo vessel “P&T Adventurer” struck the T2 tanker “Tullahoma” at a reported 90-degree collision angle between frames 41 and 45 on the Tullahoma, approximately 44.5 meters aft of amidships. The reported vessel speeds at the time of the collision were 10 knots for the Tullahoma and 14 knots for the Adventurer causing a reported 25 ft of penetration and 20 ft of damage length. However, extensive examination of documents related to the collision indicates that the actual speed of the Adventurer at the time of the collision was closer to 9.5 knots and the actual speed of the Tullahoma was approximately 8 knots. Again, these changes were due to last minute orders given by the masters of each vessel in the effort to avoid the collision.

Structural drawings for both ships were obtained through the National Archives and Records Administration and this data was used to model the collision in SIMCOL Version 3.0. Appendix D provides information on the “P&T Adventurer”. Appendix F provides information on the “Tullahoma”. In the SIMCOL analysis, the collision angle was set at 90 degrees with a collision location of 44.5 meters aft of amidships. The initial striking vessel speed was set at 9.5 knots, with the struck vessel speed set at 8 knots. The SIMCOL results indicate 7.694 meters or 25.24 ft of penetration and 6.34 meters or 20.8 ft of damage length. The SIMCOL results are conservative by approximately 1% in penetration and 4% in damage length compared to Minorsky’s (1959) reported penetration and damage length values.

This case was also modeled using LSDYNA. Differences between SIMCOL Version 3.0 results, actual and finite element analysis results are shown in Table 20.

Table 20 - SIMCOL Validation Percent Difference

<b>Validation with Tullahoma - P&amp;T Adventurer Collision</b>		
Method	Penetration (ft)	L.E.D. (ft)
SIMCOL	25.24	20.8
Reported	25	20
% Difference	0.96%	4.00%

### 6.3 SIMCOL Probabilistic Validation

Data required by SIMCOL to describe a collision event includes:

- Struck ship design parameters
- Struck ship variables – speed, trim, draft or displacement
- Event variables - collision angle ( $\phi$ ), strike location (l)
- Striking ship variables – type, displacement, speed, length, beam, bow half-entrance angle (HEA), draft at bow

Except for the struck ship design parameters, for a random collision these are all random variables with varying degrees of dependency, some discrete and some continuous.

Two primary data sources are used in this study to determine the probabilities and probability density functions necessary to define these random variables:

- 1998 Sandia Report [78].
- 1993 Lloyd's Worldwide Ship data [79].

The Sandia Report [78] considers collision data from 4 sources:

1. Lloyd's Casualty Data for 1973 to 1993 – contains 30,000 incident reports of which 1947 were ship to ship collision events, 702 of which occurred in ports. This data was used primarily to estimate the probability and geographical location of collisions and fires that could harm nuclear flasks. It did not include specific scenario and technical data. It is not directly applicable to collision scenarios.
2. ORI Analysis, 1980 [80] – includes a summary of data from cargo vessel accidents in 1974 and 1975 for 78000 transits of ships over 5000 gross tons. Most of this data is from the USCG Commercial Vessel Casualty File. It includes 216 collisions for ships in US waters or US ships in international waters. 8 collisions of tankers and cargo ships and other tanker accidents from the ECO World Tanker Accident file are also included. This totals 1122 cargo ship accidents. 115 are struck cargo ship collisions with more than 90 percent of these in inland and coastal waters. The study addresses the probability of various accident types.
3. ORI Analysis, 1981 [81] – Includes the probability of striking ship displacement, speed, collision angle and collision location for struck cargo ship collisions.
4. Engineering Computer Optecnomics, Inc (ECO) World Fleet Data.

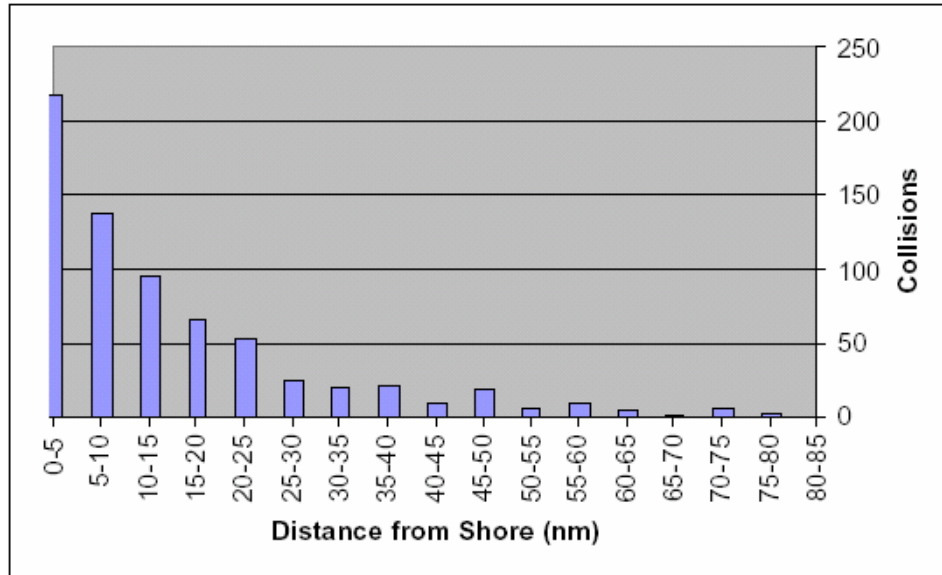


Figure 183 - Collisions, 1973-1993 All Ships Worldwide [78]

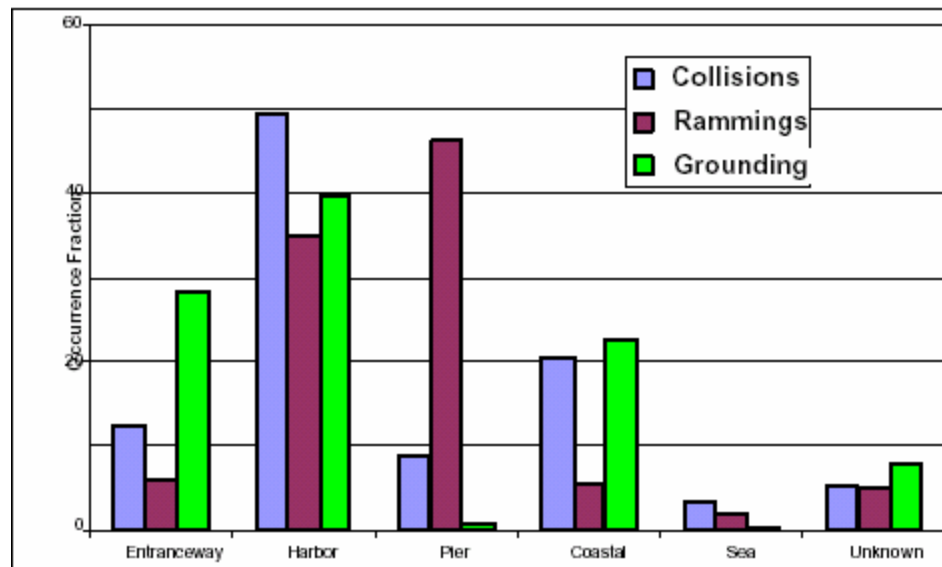


Figure 184 - Accident Location [78] – Worldwide Tanker Data, 1969-1974

### 6.3.1 Collision Probability

The Lloyd's accident data referenced in the Sandia Report [78] is extensive. Although it provides little detail on the collision scenario and damage, the statistics on geographical location and probability of occurrence are informative. Figure 183 and Figure 184 show that collisions occur primarily in near-shore areas where there is a high concentration of ships approaching ports. This is not surprising. Collision probabilities per nautical mile sailed are approximately  $2 \times 10^{-7}$ . Collision frequency per port call is approximately  $4 \times 10^{-5}$ .

### 6.3.2 Collision Event Random Variables

Collision event random variables are not expected to be fully independent, but their interdependence is difficult to quantify because of limited collision data. Figure 185 provides a framework for defining the relationship of scenario variables. Available data are incomplete to fully quantify this relationship. Strike location must often be inferred from the damage description because a reliable record of the precise location is not available. Ship heading and speed prior to the collision are often included in accident reports, but collision angle and ship speed at the moment of collision are frequently not included or only estimated and described imprecisely. Expected dependencies, labeled Numbers 1 through 4 in Figure 185, are:

1. Striking ship type and displacement. This data may come from actual collision events or from ship encounter data. Worldwide ship characteristics may also be used if it is assumed that a given struck ship encounters a representative sample of all worldwide ships. Actual collision data is very limited and encounter data is difficult to obtain. This report develops the striking ship type probability and the corresponding striking ship displacement probability density functions from worldwide data. The striking ship type is treated as an independent random variable, and a unique striking ship displacement probability density function is developed for each type. It is expected that there should be some degree of bias for striking ships to be similar in size and type to struck ships. Similar ships operate on similar routes. This bias would not be reflected in worldwide data. Data required to access the extent of this bias is very limited. The striking ship collision speed is also treated as an independent random variable. Its probability density function is developed from actual collision data. Collision speed is the striking ship speed at the moment of collision, and is not strongly dependent on service speed. It depends primarily on actions taken just prior to collision and its probability density function is assumed to be the same for all ships.
2. Striking ship principal characteristics. Other striking ship principal characteristics are treated as dependent variables, and they are derived from striking ship displacement and type based on regression analysis of worldwide ship data. Given a specific type and displacement of striking ship, other principal characteristics are strongly related. Principal characteristics include length, beam, draft, bow half entrance angle, bow height, and bow stiffness or structural design.
3. Struck ship draft, trim and speed. A specific struck ship with known design characteristics in a specific trade will have specific distributions for draft, trim and speed. In this report, full load draft and zero trim are assumed. Struck ship speed is treated as an independent random variable. The probability density function for struck ship speed is developed from actual collision data.
4. Collision angle and strike location. When two ships are maneuvering to avoid a collision (in-extremis), it is expected that the resulting collision angle and strike locations are related, but there is insufficient data to quantify this relationship. In this report, they are treated as independent random variables. The probability density functions for collision angle and strike location are developed from actual collision data.

### 6.3.2.1 Striking Ship Type and Displacement

Figure 186 provides probabilities of the struck ship encountering specific ship types. These probabilities are based on the fraction of each ship type in the worldwide population in 1993 [79]. Each of the general types includes a number of more specific types:

- Tankers – includes crude and product tankers, ore/oil carriers, LPG tankers, chemical tankers, LNG tankers, and oil/bulk/ore carriers
- Bulk carriers - includes dry bulkers, ore carriers, fish carriers, coal carriers, bulk/timber carriers, cement carriers and wood chip carriers
- Freighters – includes general freighters and refrigerated freighters
- Passenger – includes passenger and combo passenger/cargo ships

Containerships – includes containerships, car carriers, container/RO-ROs, ROROs, bulk/car carriers, and bulk/containerships.

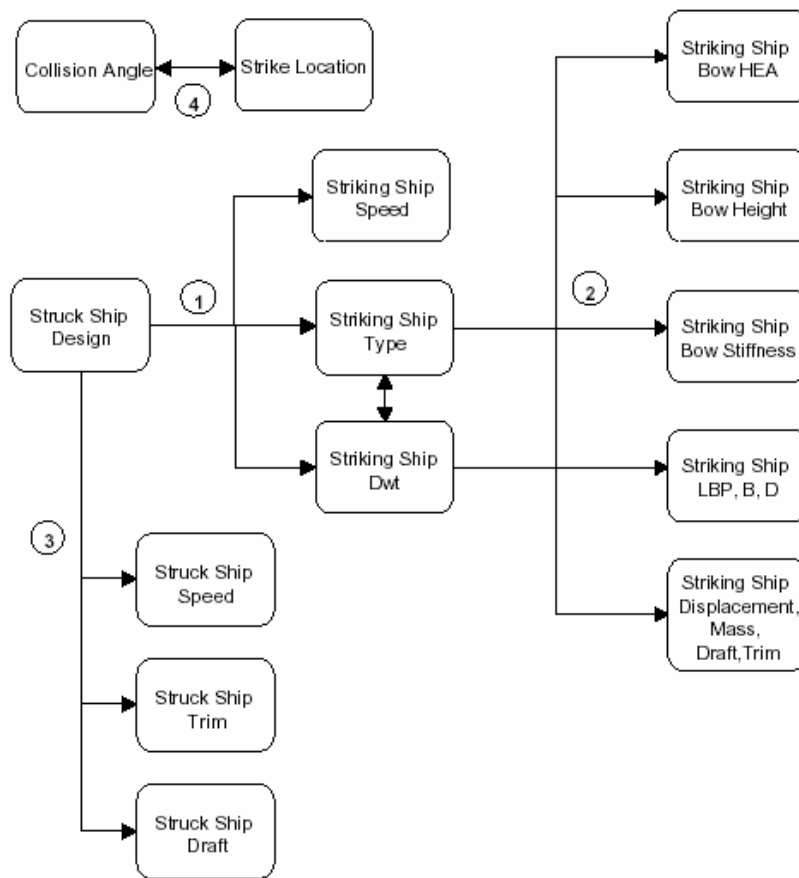


Figure 185 – Collision Event Variables

It is likely that particular ships are more likely to meet ships of the same type since they travel the same routes, but this relationship could not be established with available data. Additional collision data must be obtained to establish this relationship.

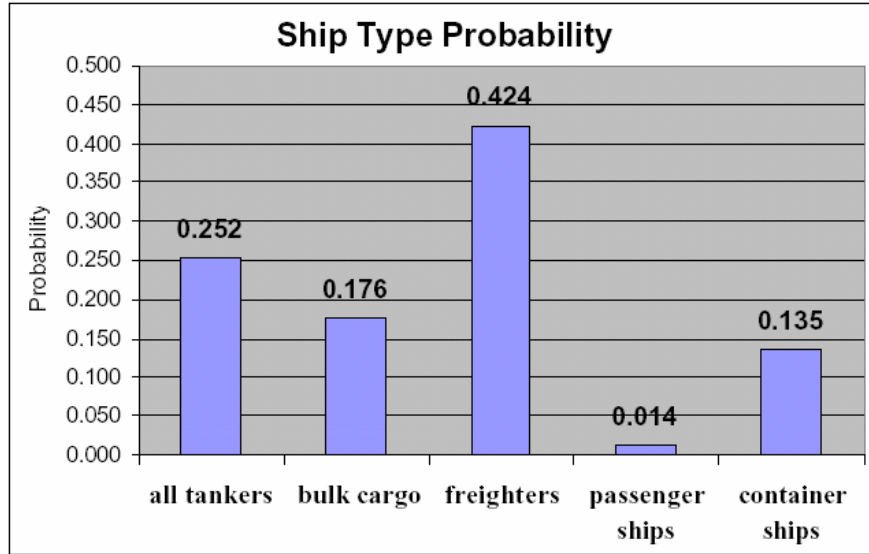


Figure 186 – Ship Type Probability [79]

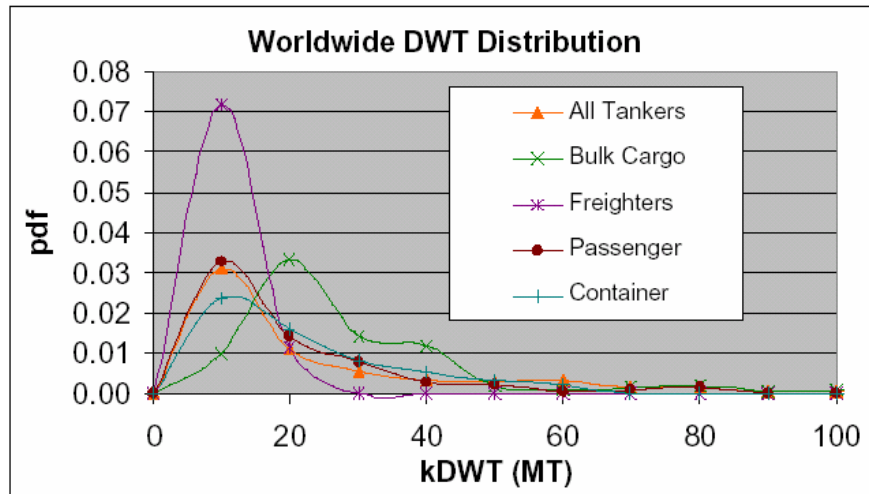


Figure 187 - Striking Ship Displacement, Worldwide Distribution

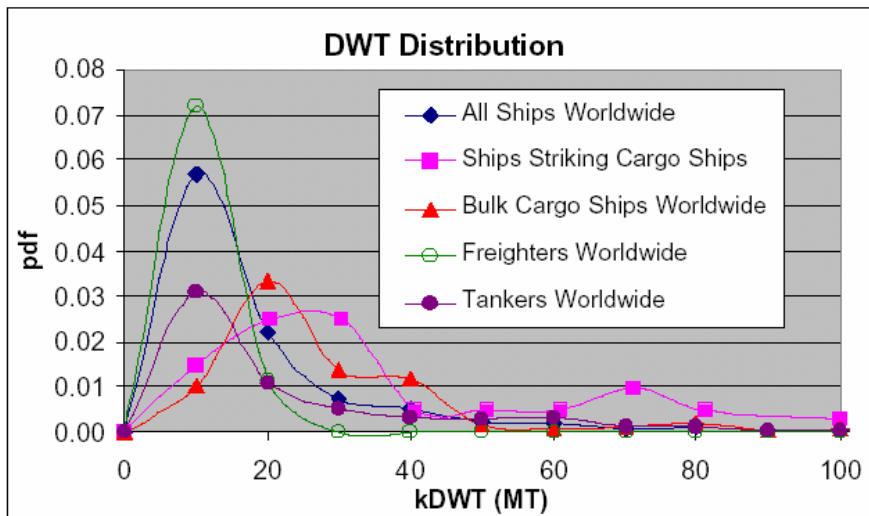


Figure 188 – Displacement of Ships Striking Bulk Carriers [78]

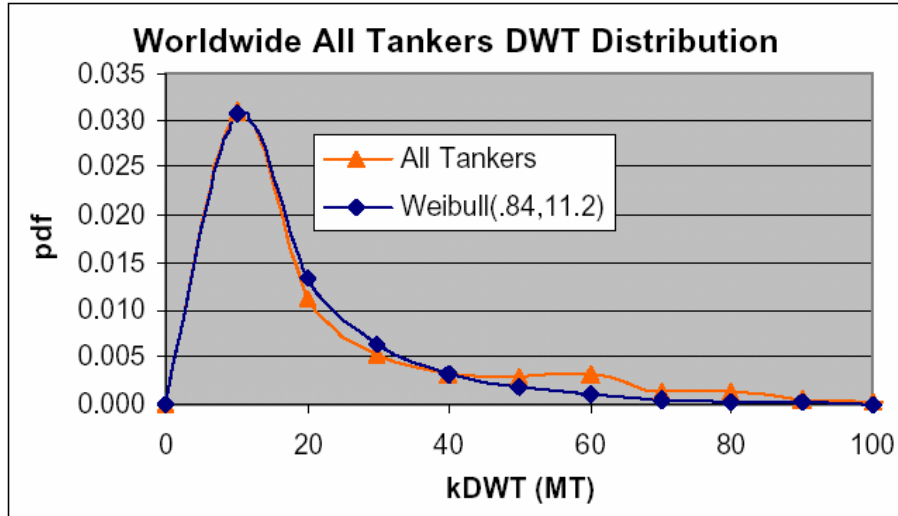


Figure 189 - Striking Ship Displacement - All Tankers

Figure 187 shows the worldwide distributions of displacement for each of these ship types and all ships [79]. The distributions are significantly different and must be applied individually to each ship type. Figure 188 shows the displacement distribution for ships striking bulk cargo ships obtained from the Sandia collision data [78]. This is actual collision data. There is a significant difference between the all-ships worldwide distribution and the striking ship distributions. The cargo ship striking ship distribution is similar to the cargo ship distribution with a bias to larger ships. Unfortunately, the Sandia data is not sufficient to establish a general rule or striking ship displacement pdf for all ship types. The worldwide displacement distributions are used in the study.

Figure 189 through Figure 193 show the displacement distributions and a best-fit distribution for each type. Table 21 provides a summary of parameter values for these distributions.

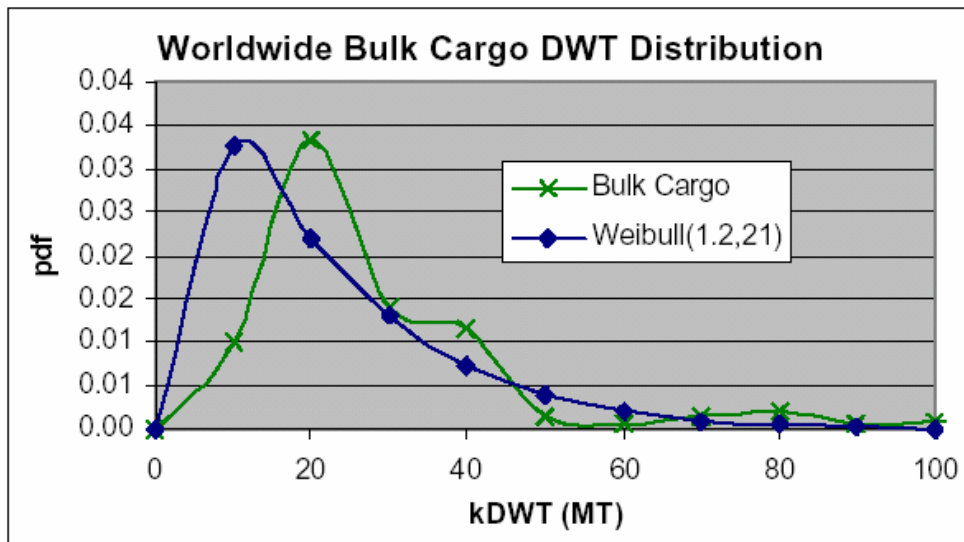


Figure 190 - Striking Ship Displacement - Bulk Cargo Ships

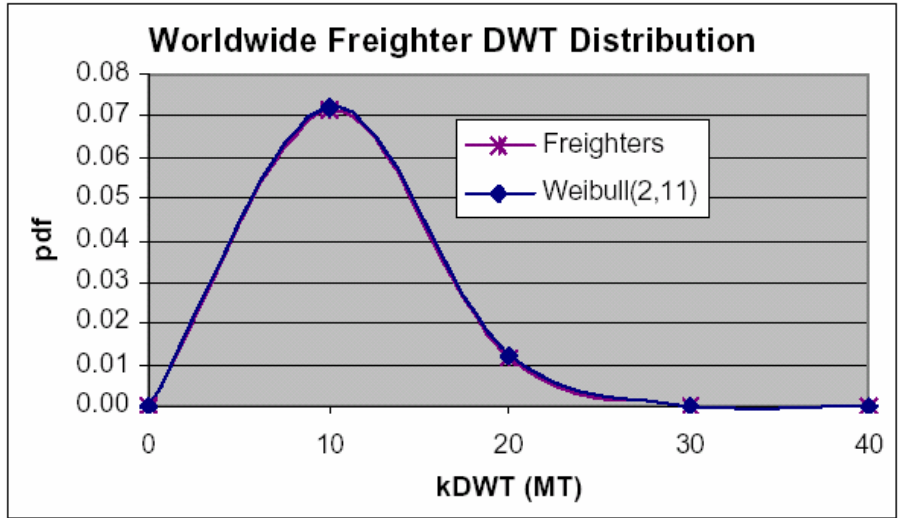


Figure 191 - Striking Ship Displacement - Freighters

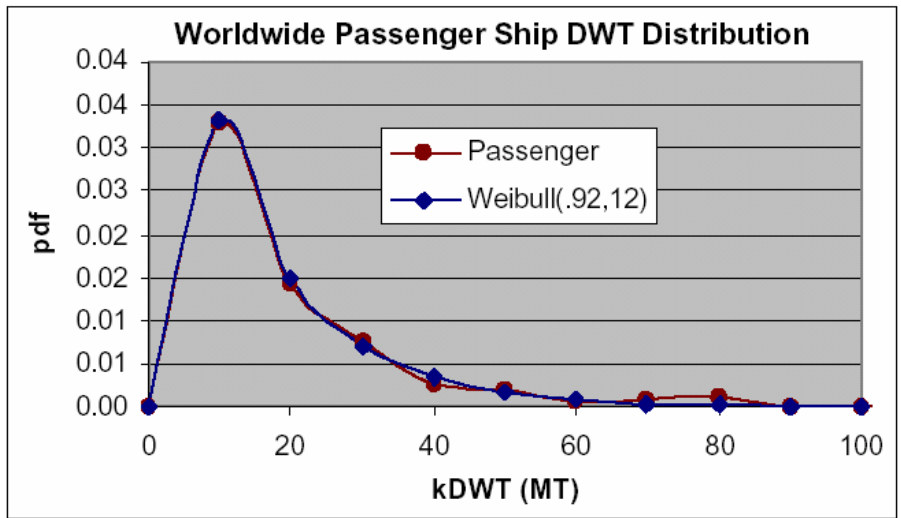


Figure 192 - Striking Ship Displacement - Passenger Ships

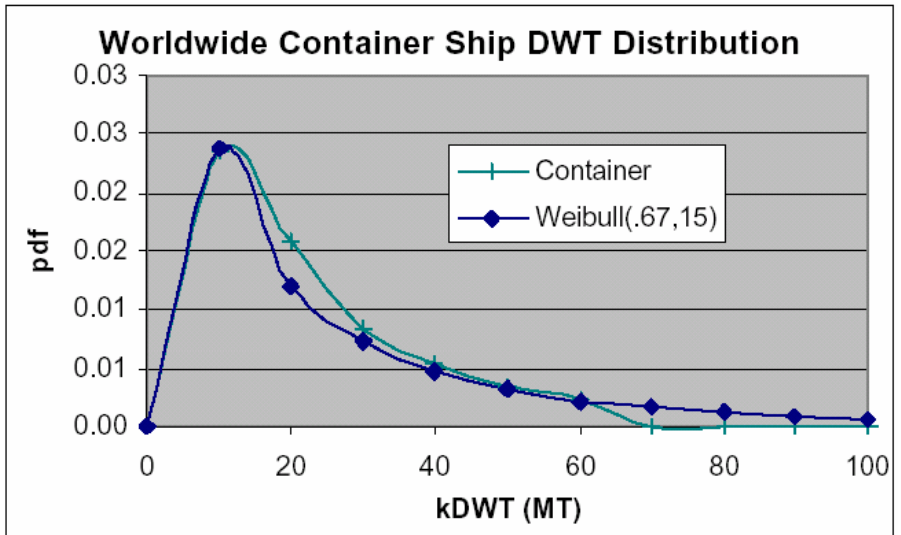


Figure 193 - Striking Ship Displacement - Container Ships

Table 21 - Striking Ship Type and Displacement

Ship Type	Probability of Encounter	Displacement pdf	Weibull a	Weibull b	Mean (kMT)	s (kMT)	Displacement Range (MT)
Tanker	0.252	Weibull	0.84	11.2	12.277	14.688	699-273550
Bulk carrier	0.176	Weibull	1.20	21.0	19.754	16.532	1082-129325
Freighter	0.424	Weibull	2.00	11.0	9.748	5.096	500-41600
Passenger ship	0.014	Weibull	0.92	12.0	12.479	13.579	997-76049
Container ship	0.135	Weibull	0.67	15.0	19.836	30.52	1137-58889

Collision speed is the striking ship speed at the moment of collision, and is not strongly related to service speed. It depends primarily on actions taken just prior to collision. Collision speed data must be collected from actual collision events. Figure 194 is a plot of data derived from the Sandia Report [80] and limited USCG tanker collision data [82]. An approximate Weibull distribution ( $\alpha = 2.2, \beta = 6.5$ ) is fit to this data. The mean of this distribution is substantially less than service speed(s), and indicates significant adjustment in speed prior to the actual collision event.

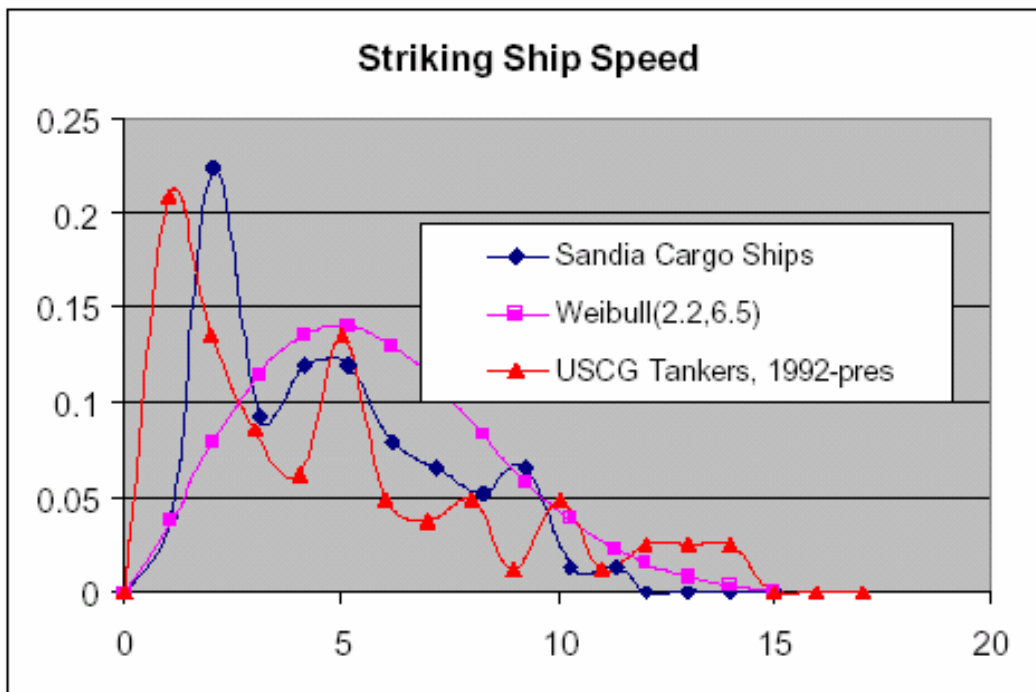


Figure 194 – Striking Ship Speed [80,82]

### 6.3.2.2 Striking Ship Characteristics

In this section, data and regression curves are presented for deriving striking ship half-entrance angle, length, beam, draft, and bow height from striking ship type and displacement.

Bow half-entrance angle is not a standard ship principal characteristic. A limited number of drawings were reviewed in the Sandia Study [78]. Table 22 and Figure 195 present the results of this analysis. The trends in this data are difficult to explain and the data is insufficient to derive

pdfs. Table 23 provides single values derived from Table 22 for each type of ship. These values are used in this study.

Table 22 - Bow Half Entrance Angle (all ships)

Displacement (tonne)	Bow Half Entrance Angle, (Degrees)			
	Tanker	Cargo	Container	Passenger
0-10160	28	29	17	17
10160-20320	30	20	17	17
20320-30480	30	20	17	17
30480-40640	38	20	17	17
40640-50800	38	20	17	17
50800-60960	38	20	17	17
60960-71120	38	20	17	17
71120-81280	38	20	17	17
81280-above	38	20	17	17

Lloyd’s worldwide data [79] is used to specify the remaining principal characteristics as a function of ship type and displacement. This data is plotted in Figure 196 through Figure 216 and summarized in Table 23. A simple power function is used to fit this data.

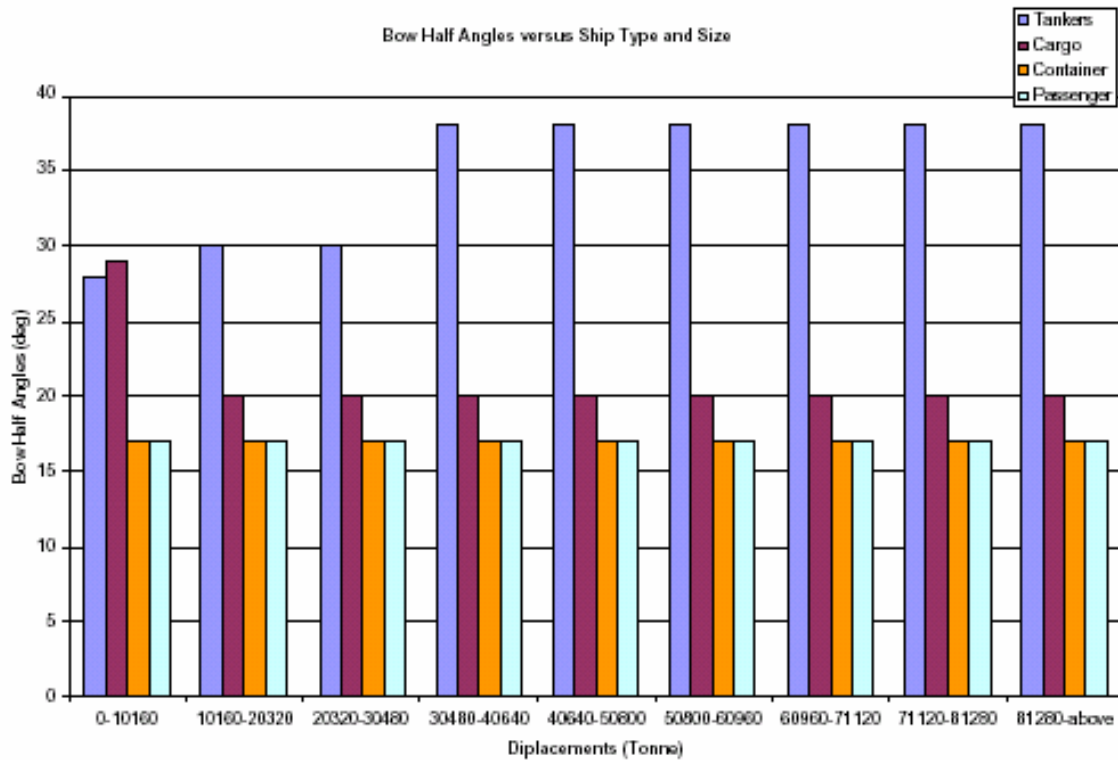


Figure 195 - Bow Half Entrance Angle (all ships by type, design practice) [78]

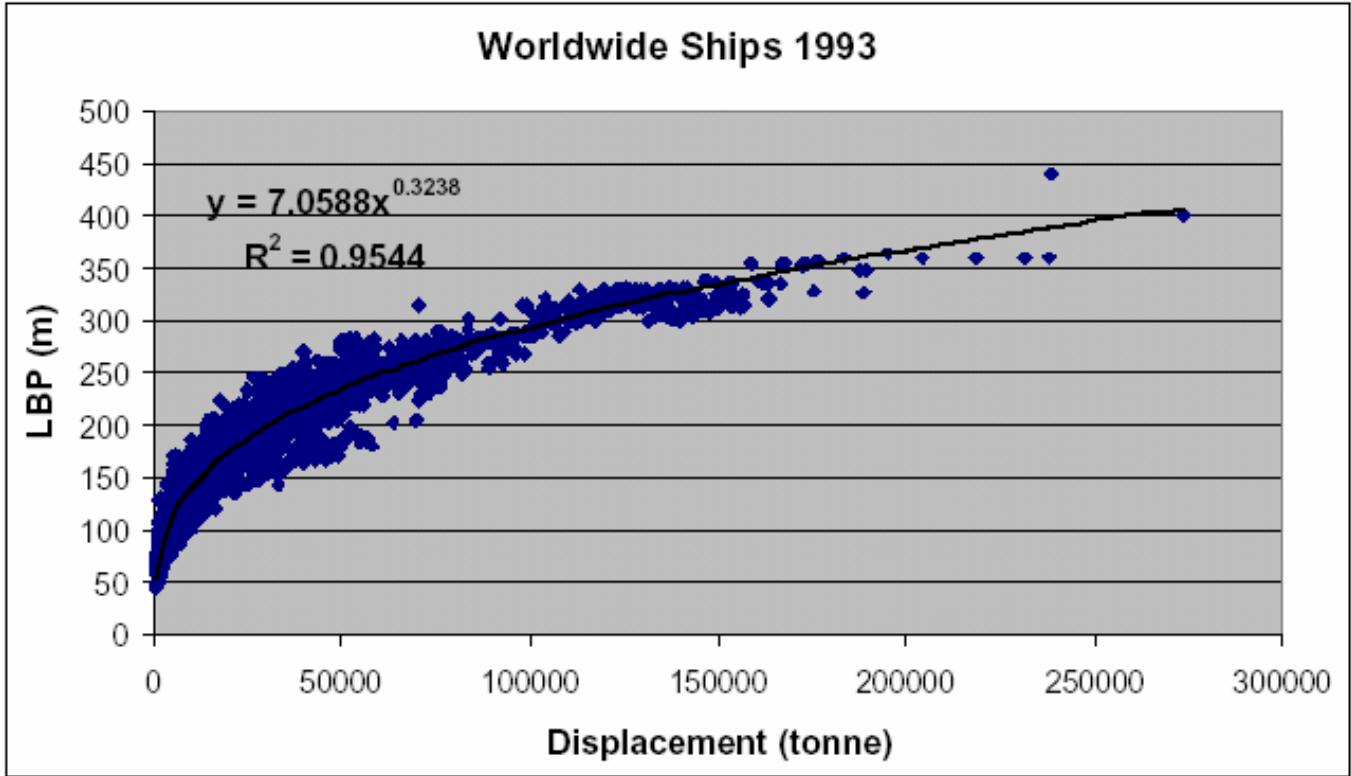


Figure 196 – All Ships Length vs. Displacement [79]

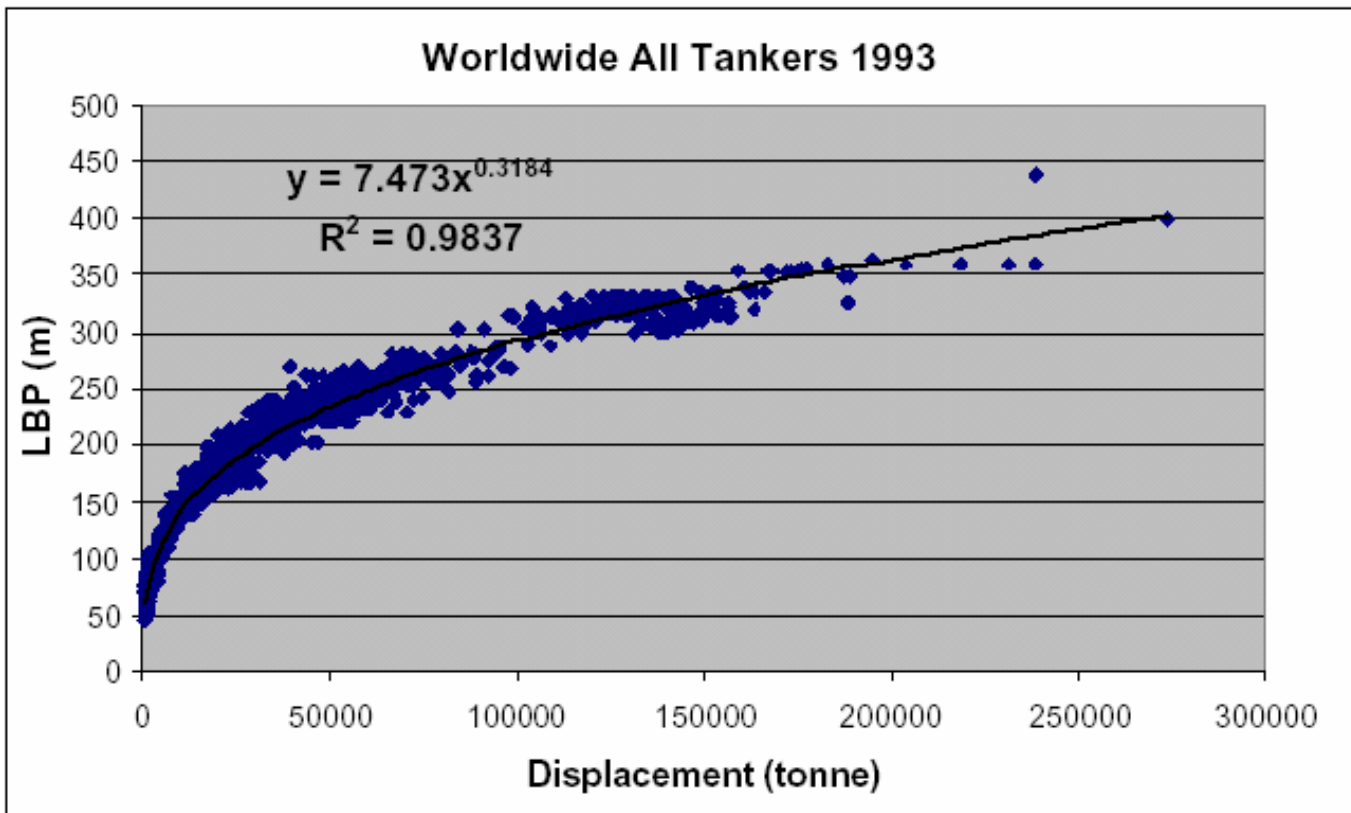


Figure 197 – All Tankers Length vs. Displacement [79]

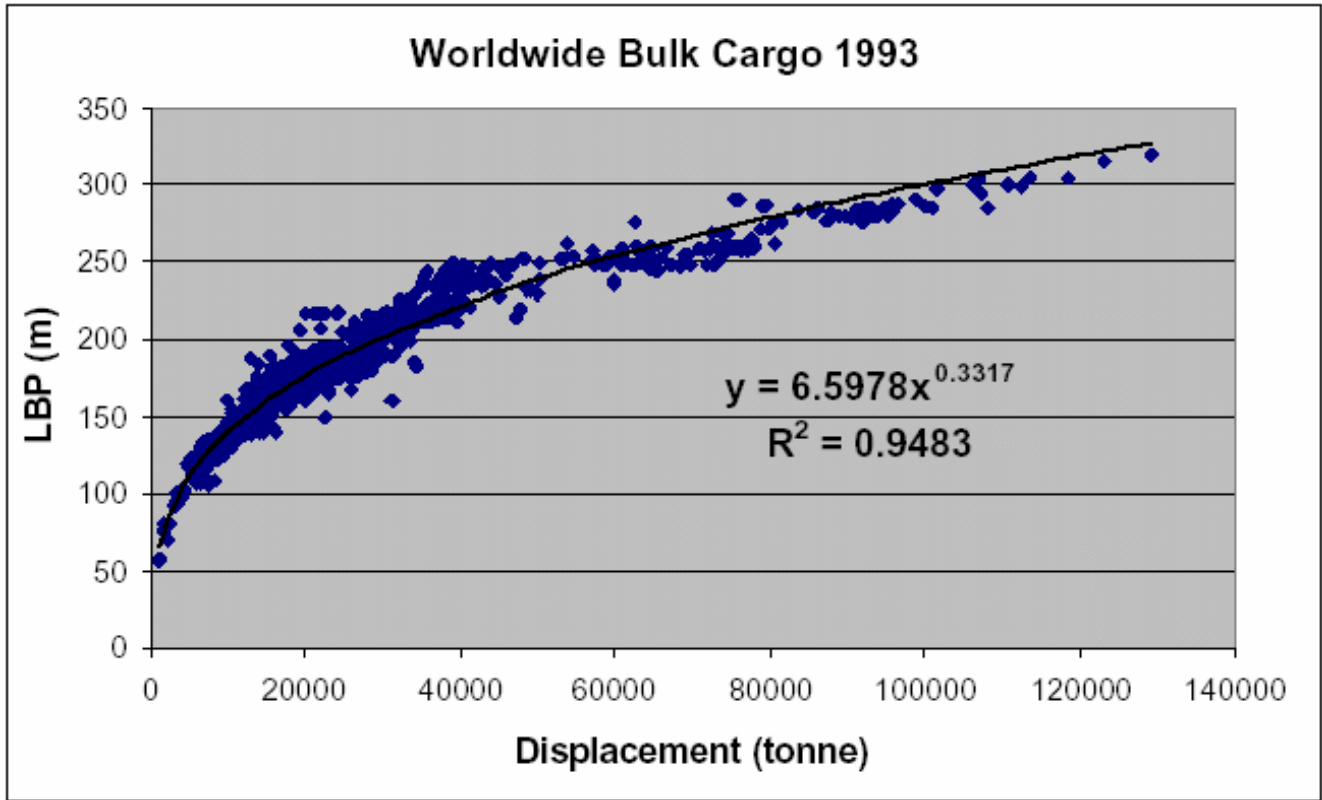


Figure 198 – Bulk Cargo Ships Length vs. Displacement [79]

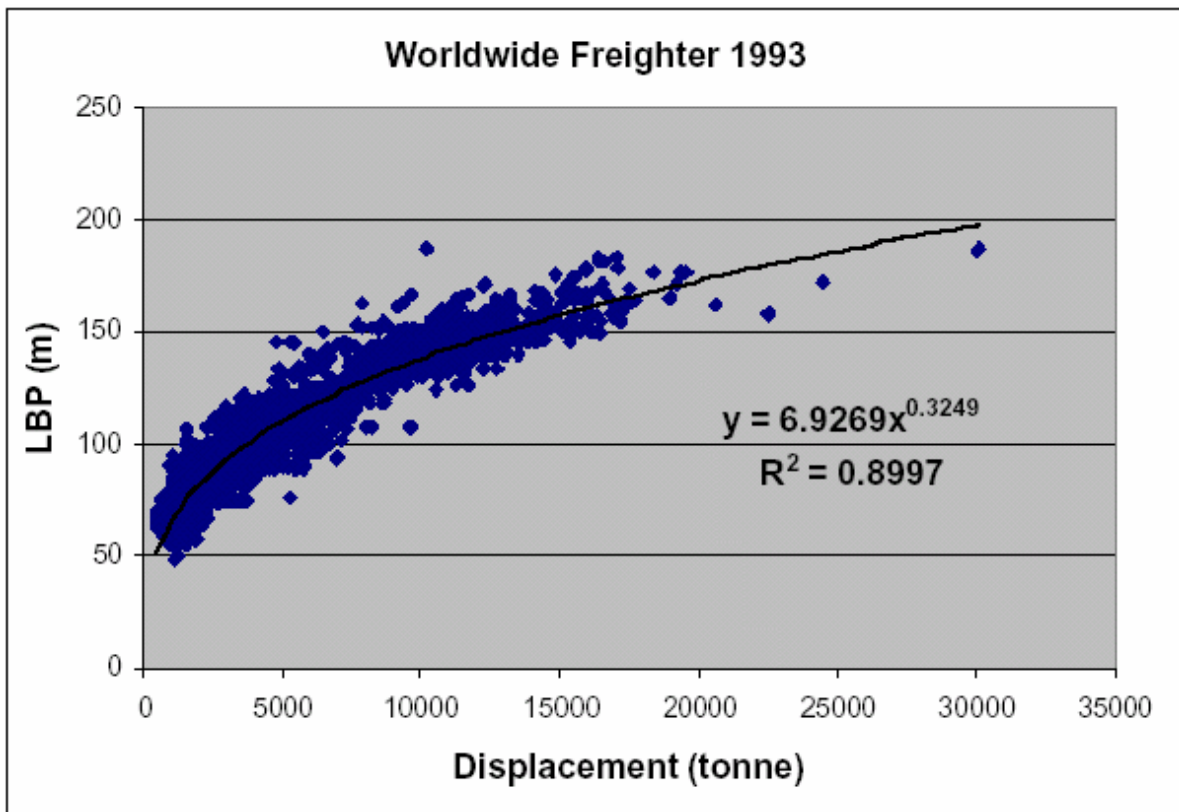


Figure 199 – Freighter Length vs. Displacement

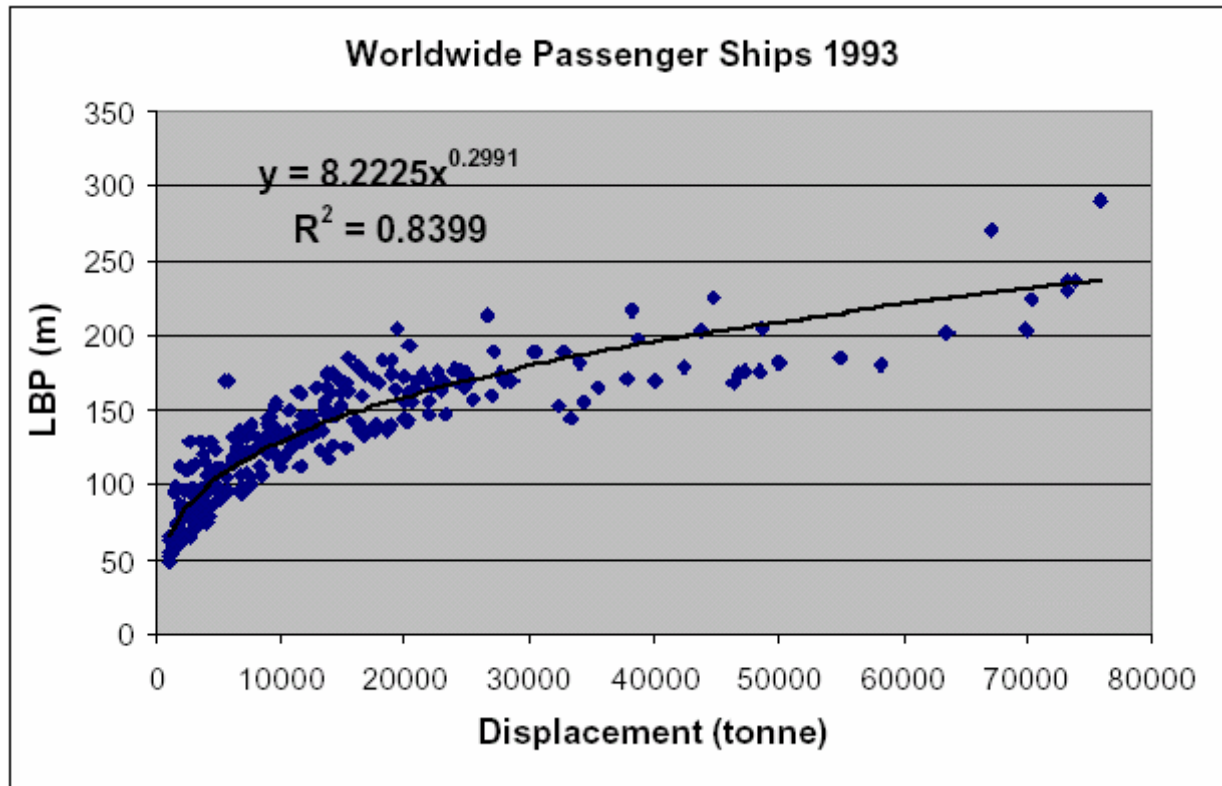


Figure 200 – Passenger Ship Length vs. Displacement [79]

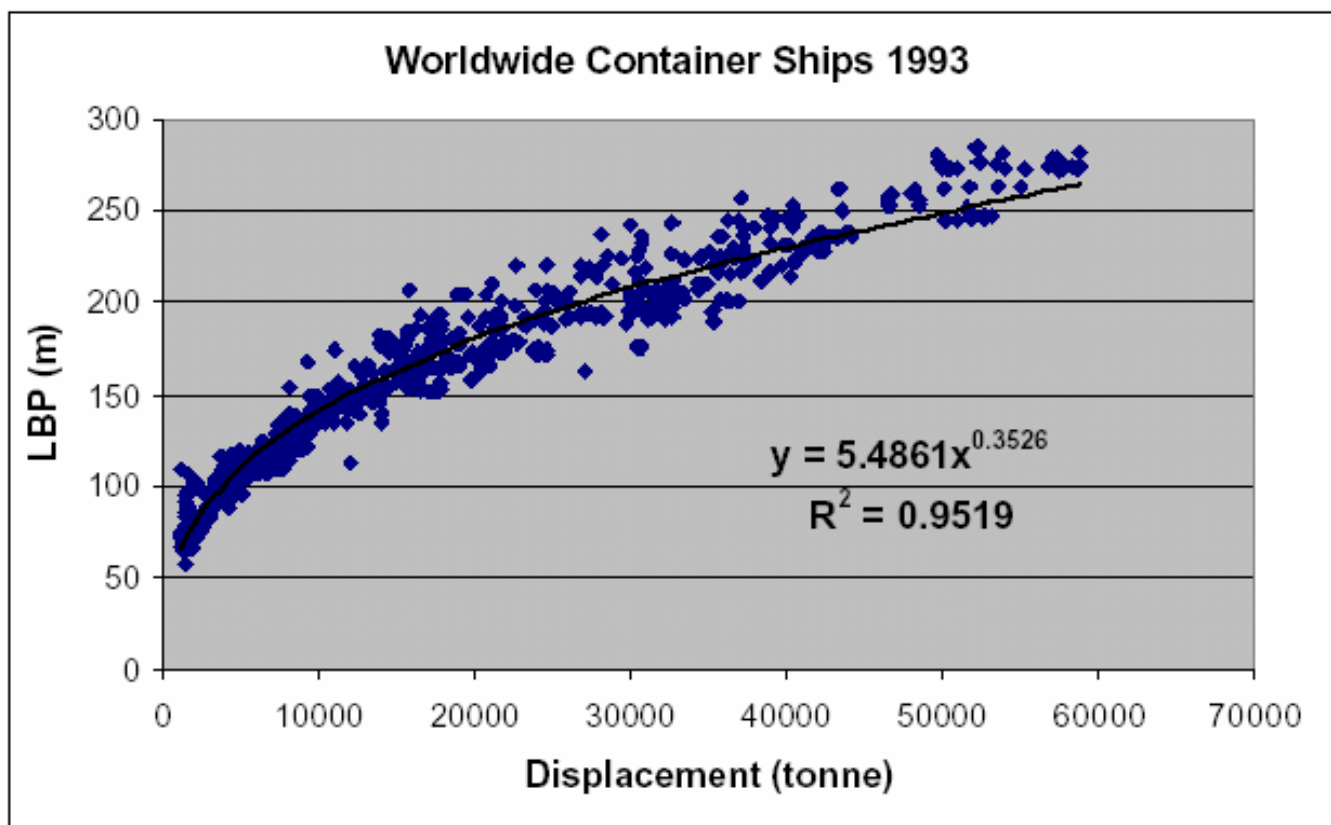


Figure 201 – Container Ship Length vs. Displacement [79]

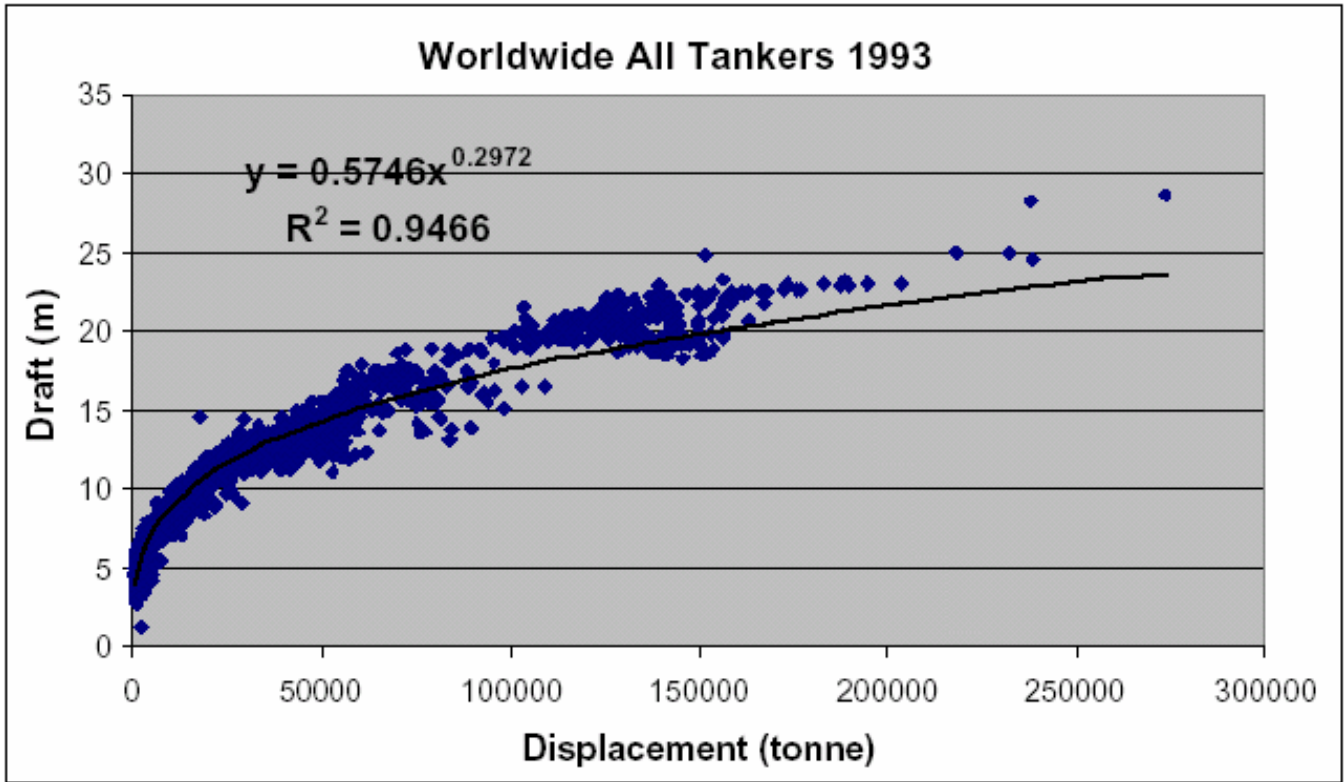


Figure 202 – All-Tankers Full Load Draft vs. Displacement [79]

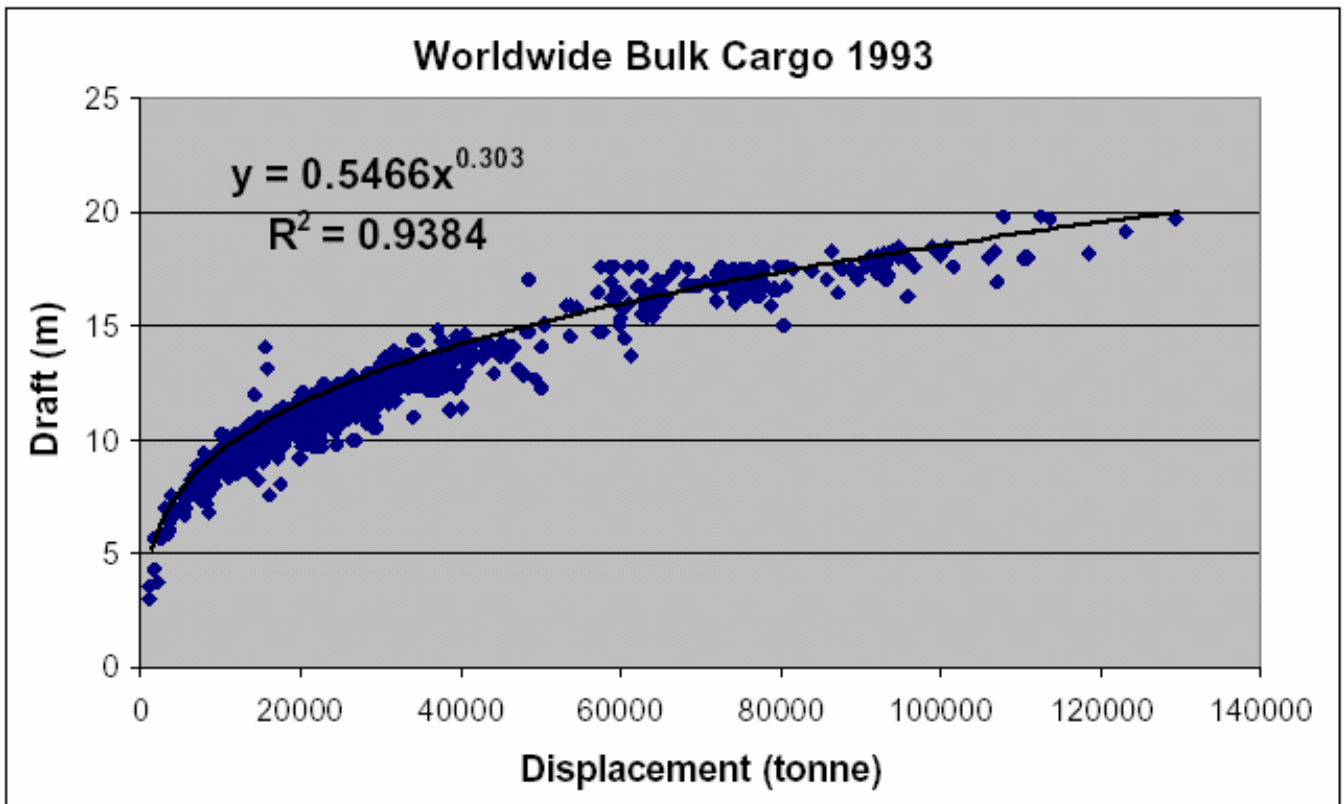


Figure 203 – Bulk Cargo Ship Full Load Draft vs. Displacement [79]

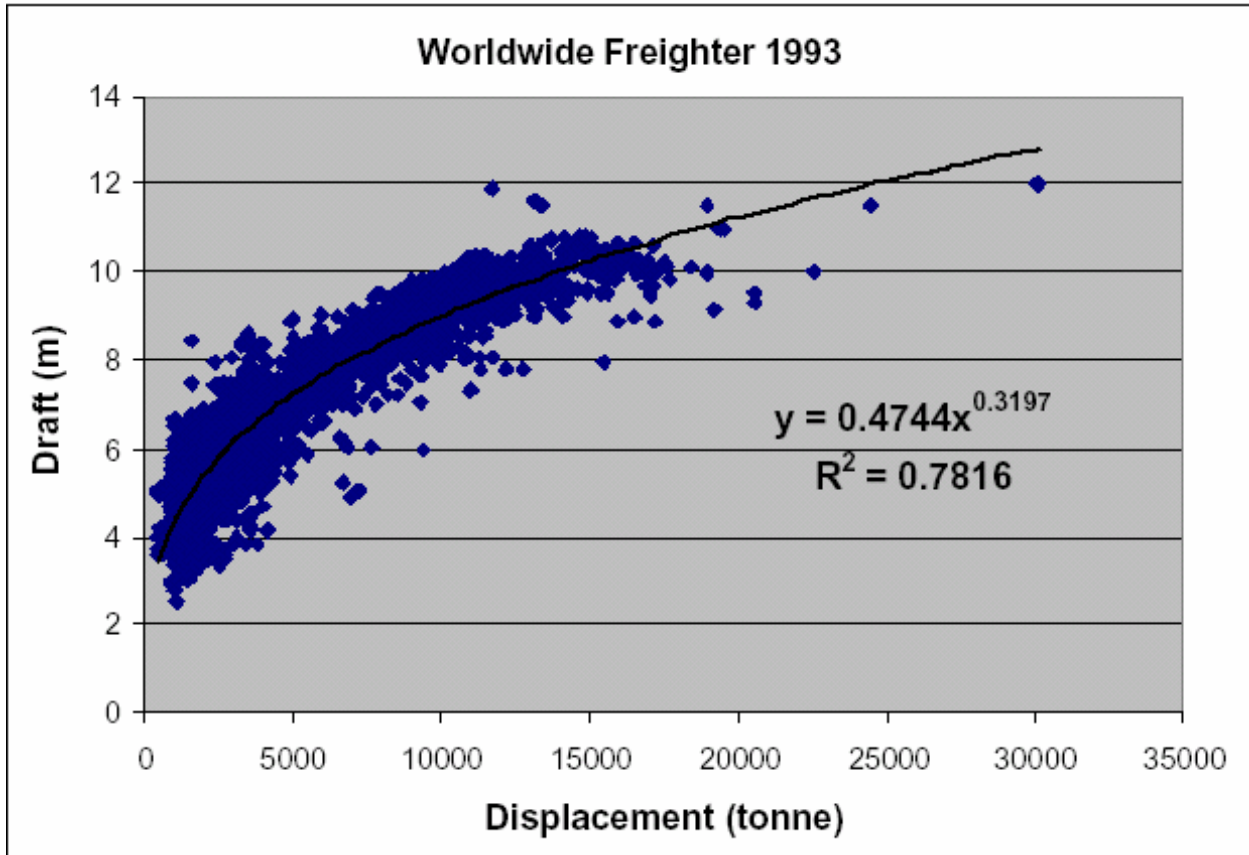


Figure 204 – Freighter Full Load Draft vs. Displacement [79]

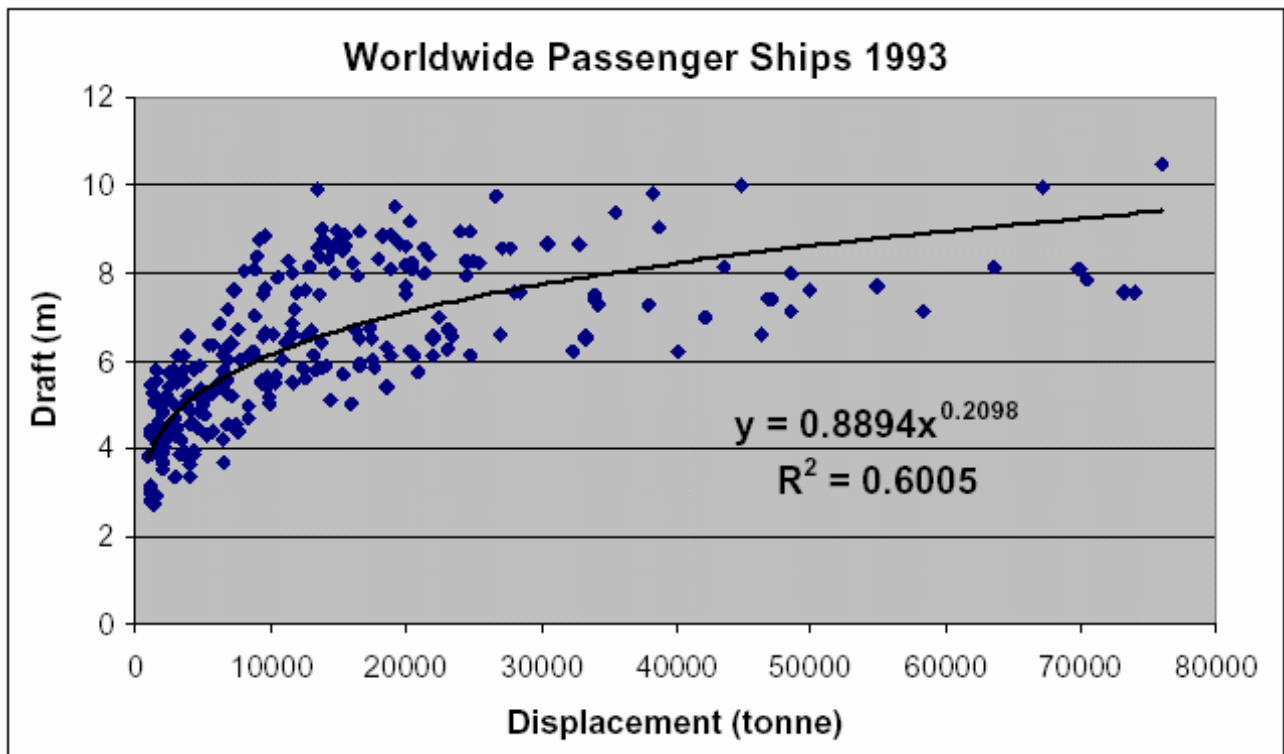


Figure 205 – Passenger Ship Full Load Draft vs. Displacement [79]

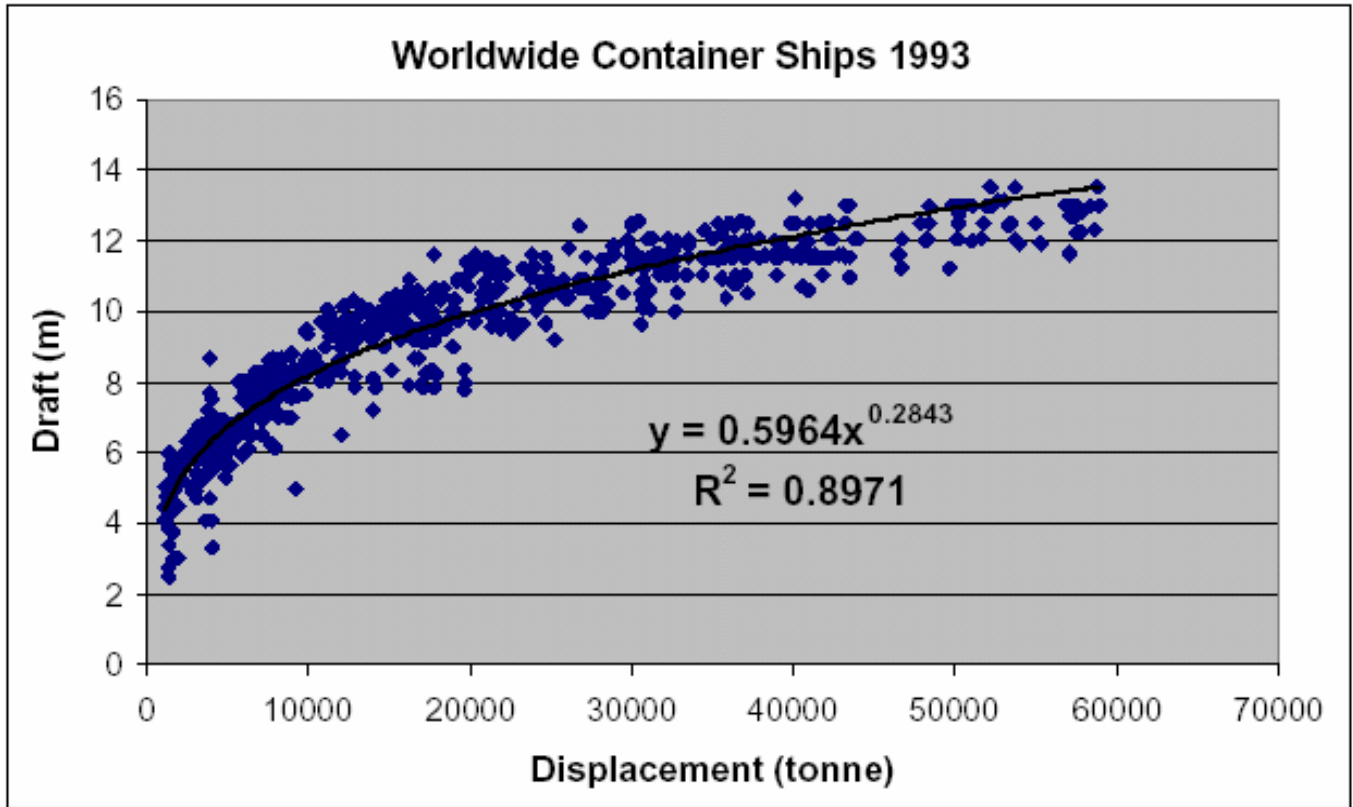


Figure 206 – Container Ship Full Load Draft vs. Displacement [79]

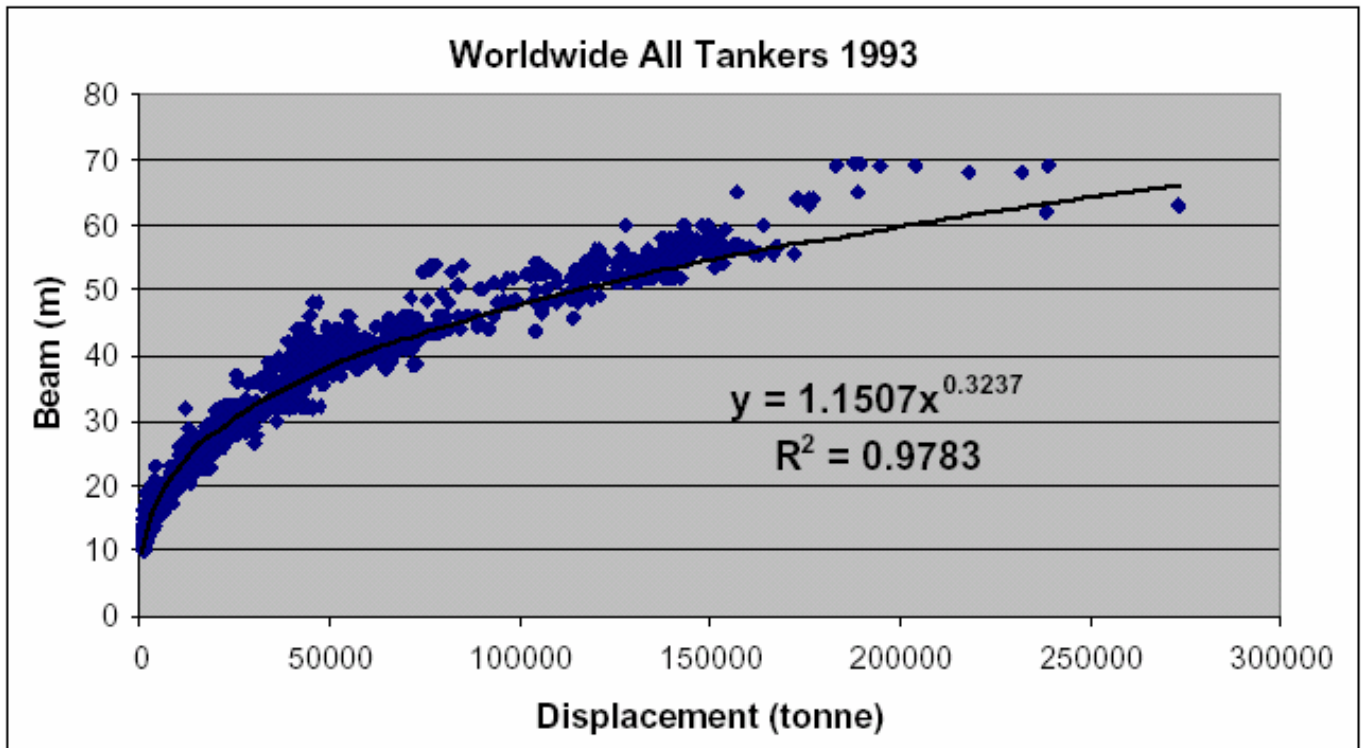


Figure 207 – All Tankers Beam vs. Displacement [79]

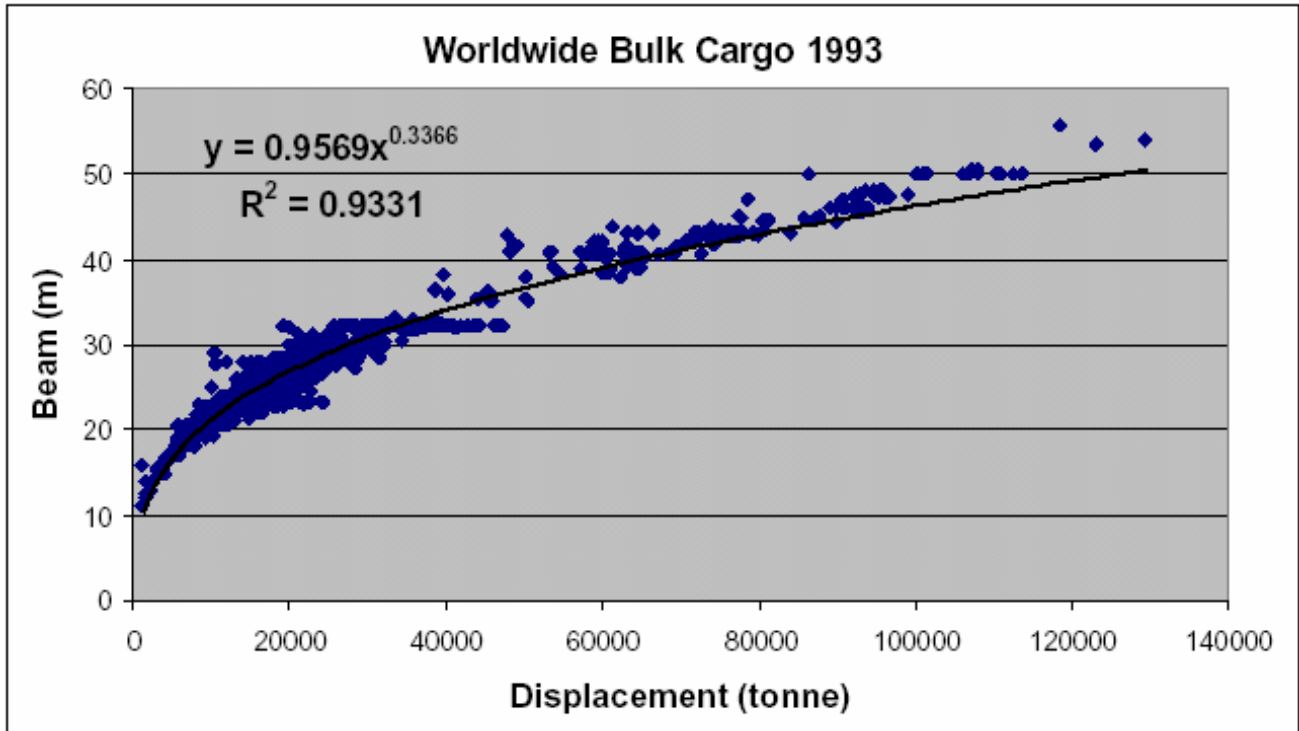


Figure 208 – Bulk Cargo Ship Beam vs. Displacement [79]

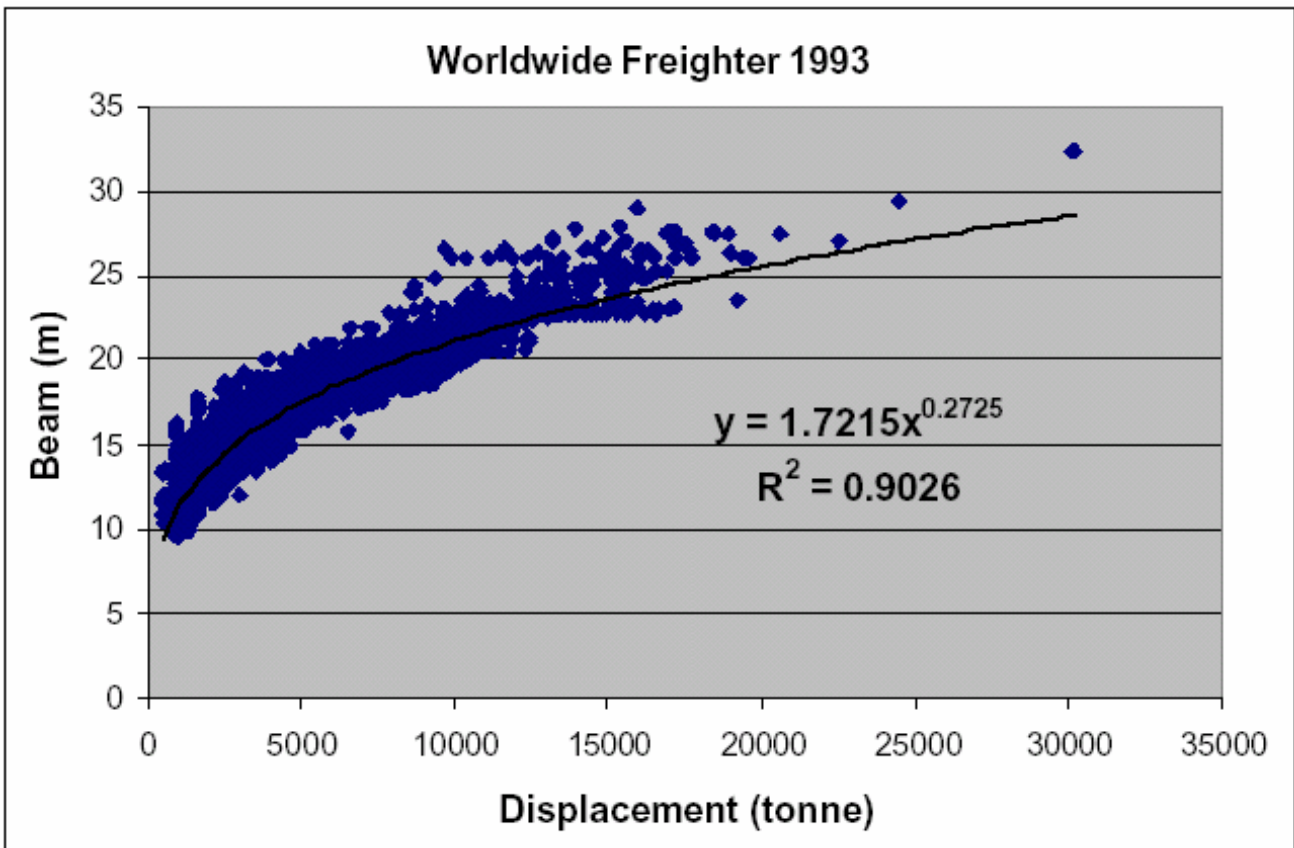


Figure 209 – Freighter Beam vs. Displacement [79]

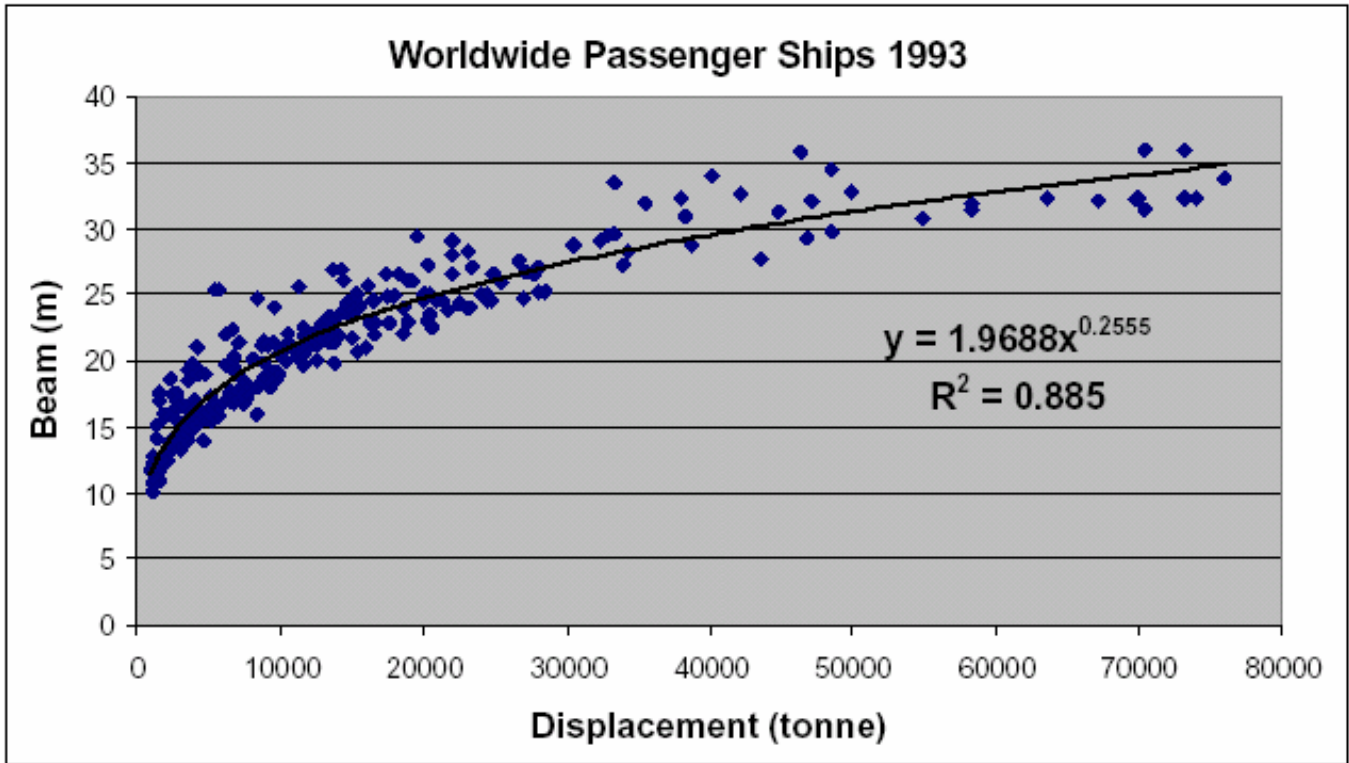


Figure 210 – Passenger Ship Beam vs. Displacement [79]

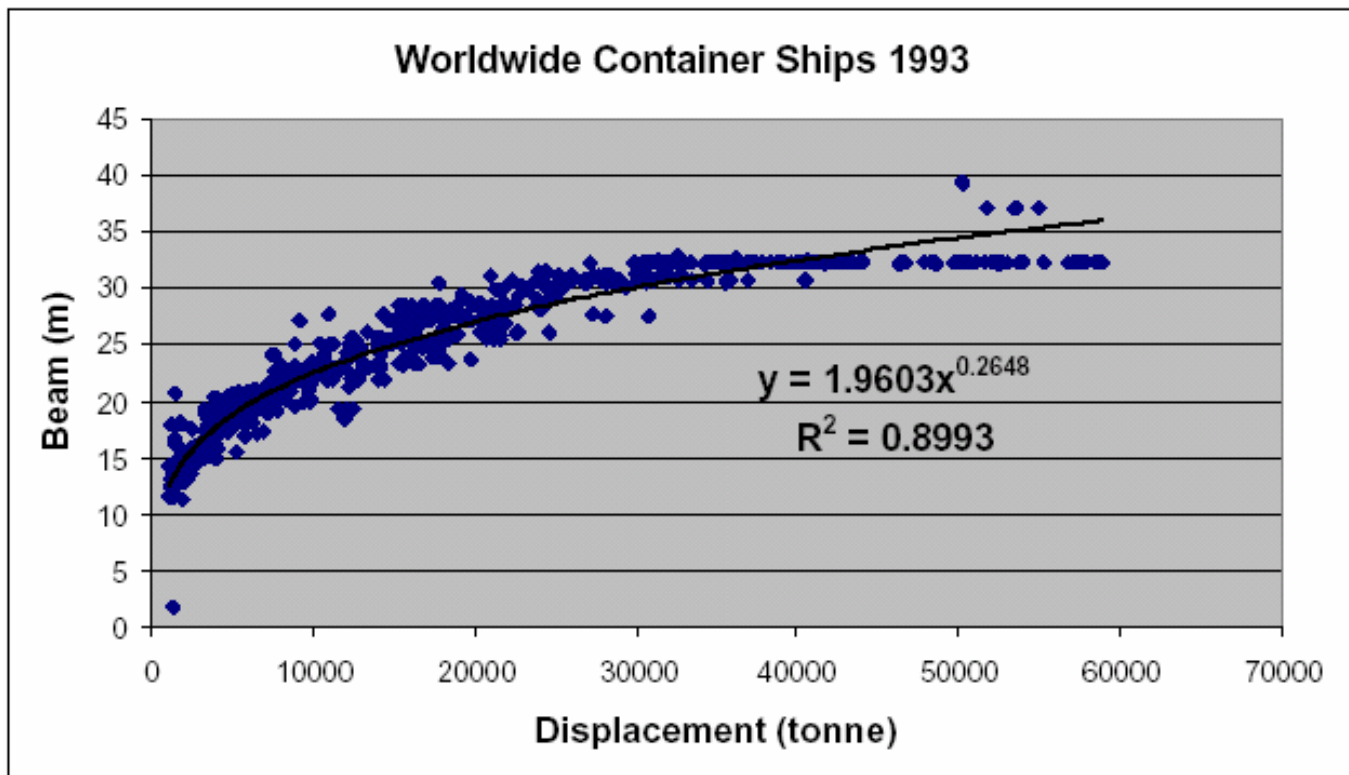


Figure 211 – Container Ship Beam vs. Displacement [79]

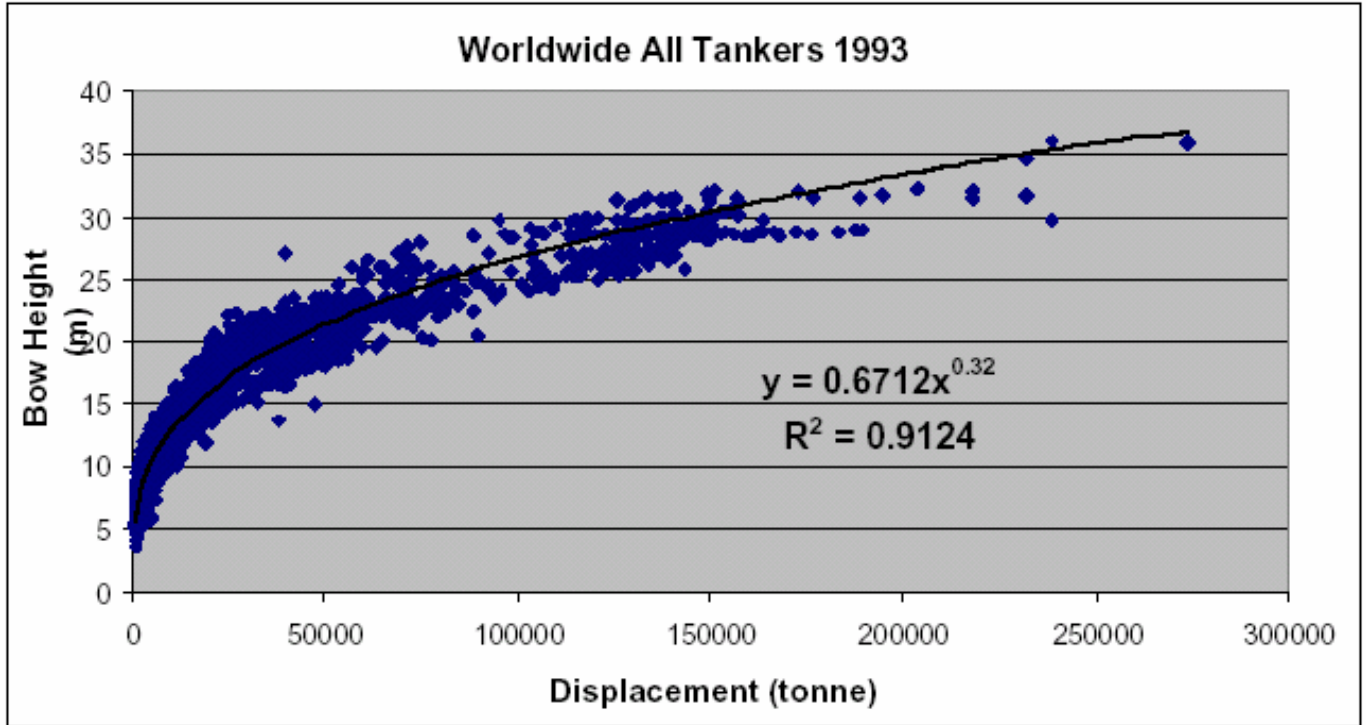


Figure 212 – All Tankers Bow Height vs. Displacement [79]

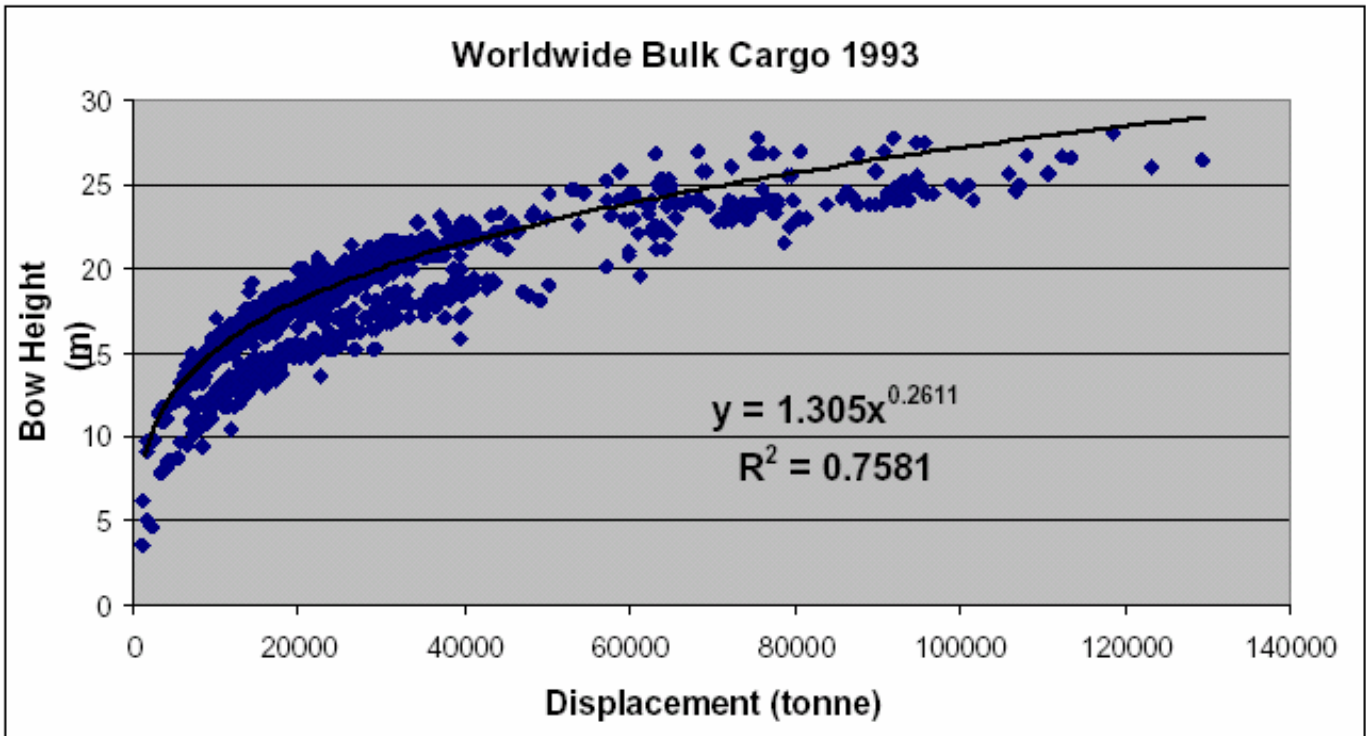


Figure 213 – Bulk Cargo Ship Bow Height vs. Displacement [79]

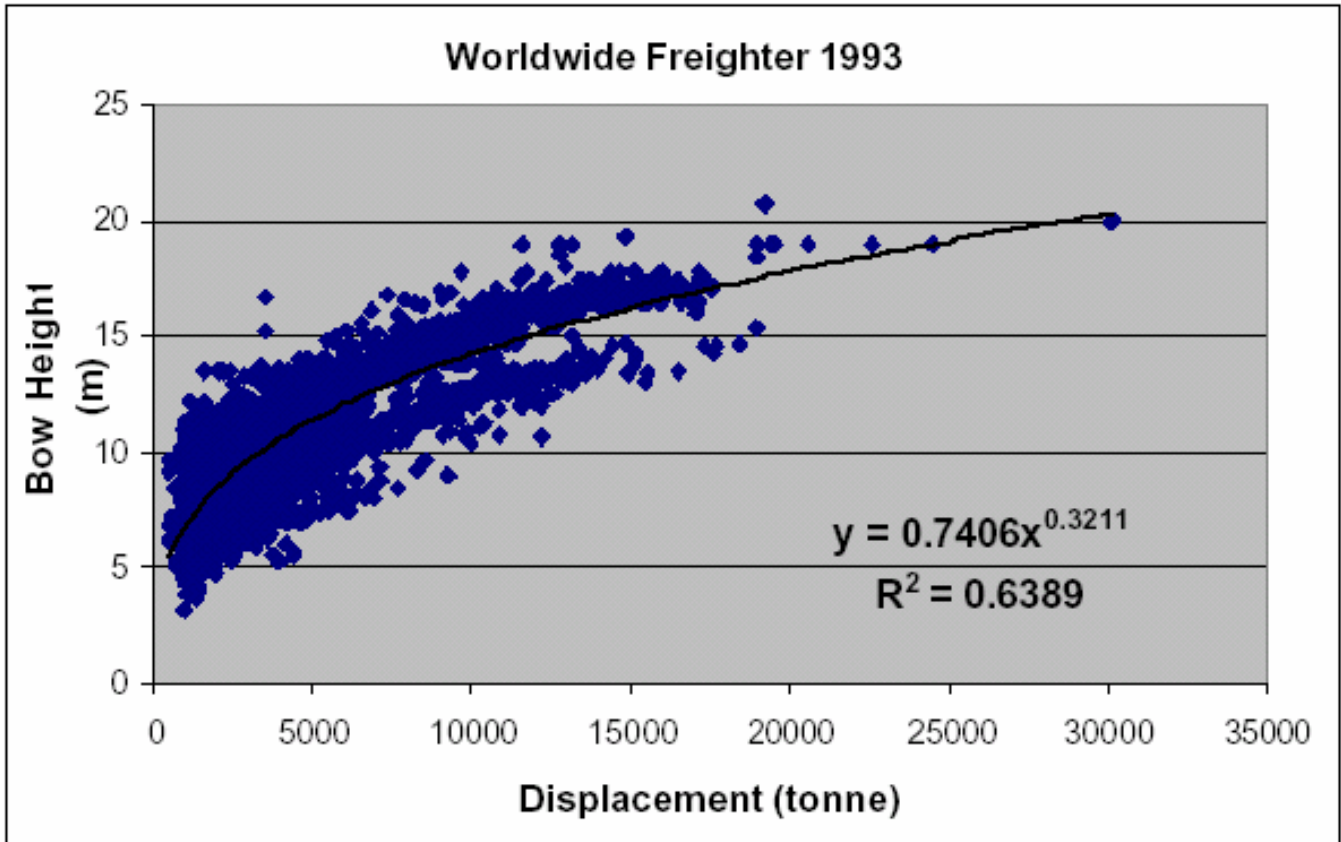


Figure 214 – Freighter Bow Height vs. Displacement [70]

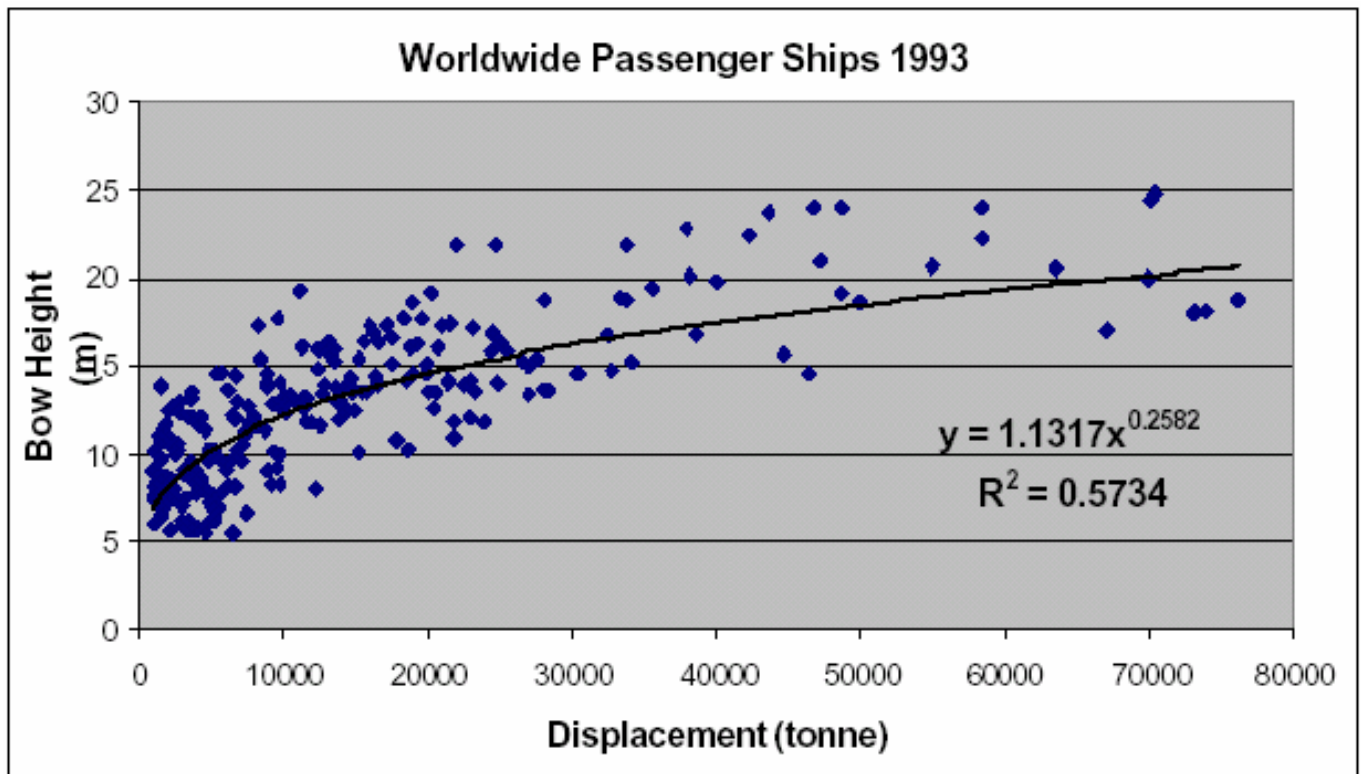


Figure 215 – Passenger Ship Bow Height vs. Displacement [79]

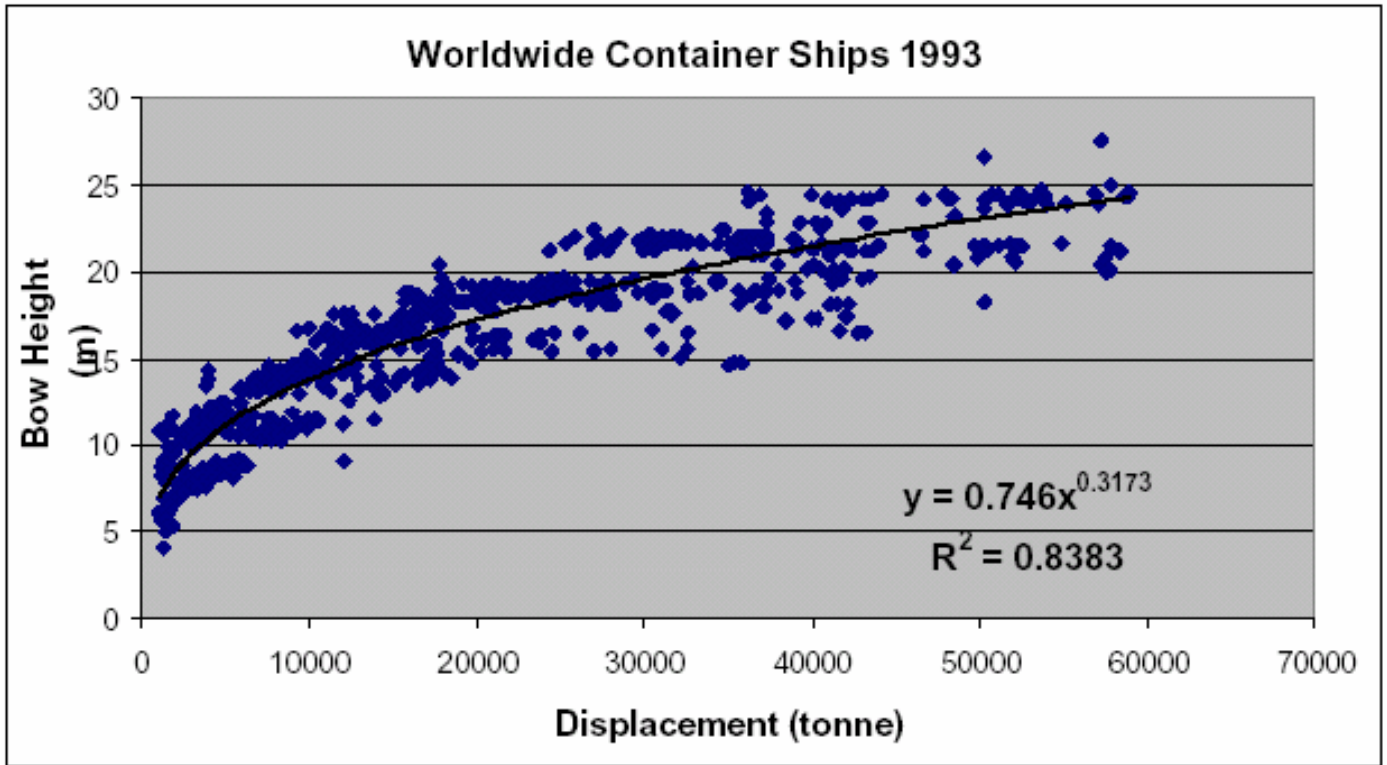


Figure 216 – Container Ship Bow Height vs. Displacement [79]

Table 23 - Striking Ship Characteristics

Ship Type	LBP		Beam		Draft		Bow Height		HEA
	Coef	Power	Coef	Power	Coef	Power	Coef	Power	
Tanker	7.473	.3184	1.1507	.3237	.5746	.2972	.6712	.3200	38
Bulk carrier	6.598	.3317	.9569	.3366	.5466	.3030	1.305	.2611	20
Freighter	6.927	.3249	1.7215	.2725	.4744	.3197	.7406	.3211	20
Passenger ship	8.223	.2991	1.9688	.2555	.8894	.2098	1.1317	.2582	17
Container ship	5.486	.3526	1.9603	.2648	.5964	.2843	.7460	.3173	17

### 6.3.2.3 Struck Ship Variables

Figure 217 is a plot of struck ship speed data derived from USCG tanker collision data [82]. The struck ship collision speed distribution is also very different from service speed. Struck ships are frequently moored or at anchor as is indicated by the significant pdf value at zero speed. An exponential distribution ( $\alpha = 0.584$ ) is fit to this data.

Full load displacement and draft with zero trim are assumed for the struck ship.

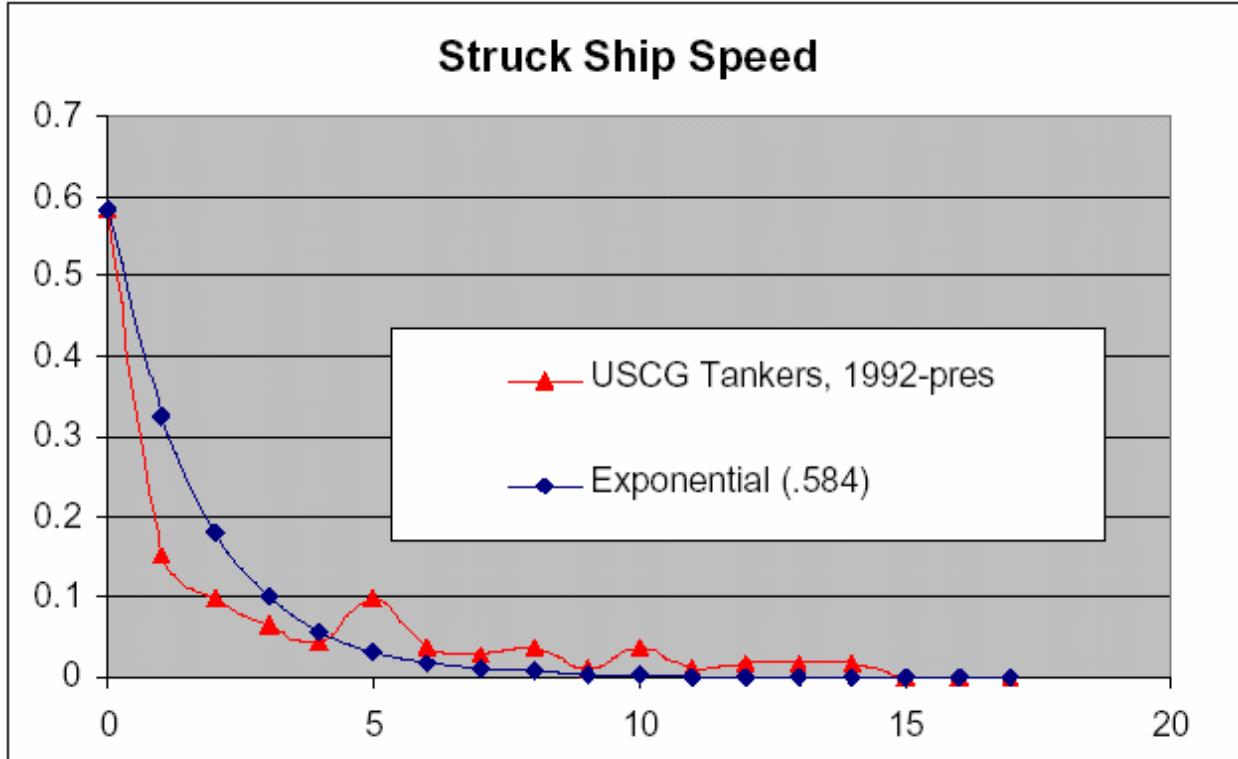


Figure 217 - Struck Ship Speed [82]

#### 6.3.2.4 Collision Scenario Variables

Figure 218 is a plot of collision angle data derived from the Sandia Report [78]. An approximate Normal distribution ( $\mu = 90$  degrees,  $\sigma = 28.97$  degrees) is fit to this data and is used to select collision angle in the Monte Carlo simulation. At more oblique angles, there is a higher probability of ships passing each other or only striking a glancing blow. These cases are frequently not reported.

The current IMO pdf for longitudinal strike location specifies a constant value over the entire length of the struck ship [4]. The constant pdf was chosen for convenience and because of the limited available data. Figure 219 shows a bar chart of the actual data used to develop the IMO pdf and data gathered for cargo ships in the Sandia Study [78]. This data does not indicate a constant pdf. The IMO data is from 56 of 200 significant collision events for which the strike location was known. The Sandia data indicates a somewhat higher probability of midship and forward strike compared to the IMO data.

### 6.3.3 Probabilistic Validation

The probabilistic validation of SIMCOL Version 3.0 is performed by comparison of IMO probabilistic damage extents reported in Annex 1 [4] and the HARDER Project [133] reported damage extent database to SIMCOL analysis of a 100k dwt single hull reference tanker (SH100) and a 150k dwt double hull reference tanker (DH150) using 10000 probabilistic striking ship contact scenarios developed as discussed above and [100]. The structure and design of both the SH100 and DH150 are provided in Appendix G and Appendix E respectively.

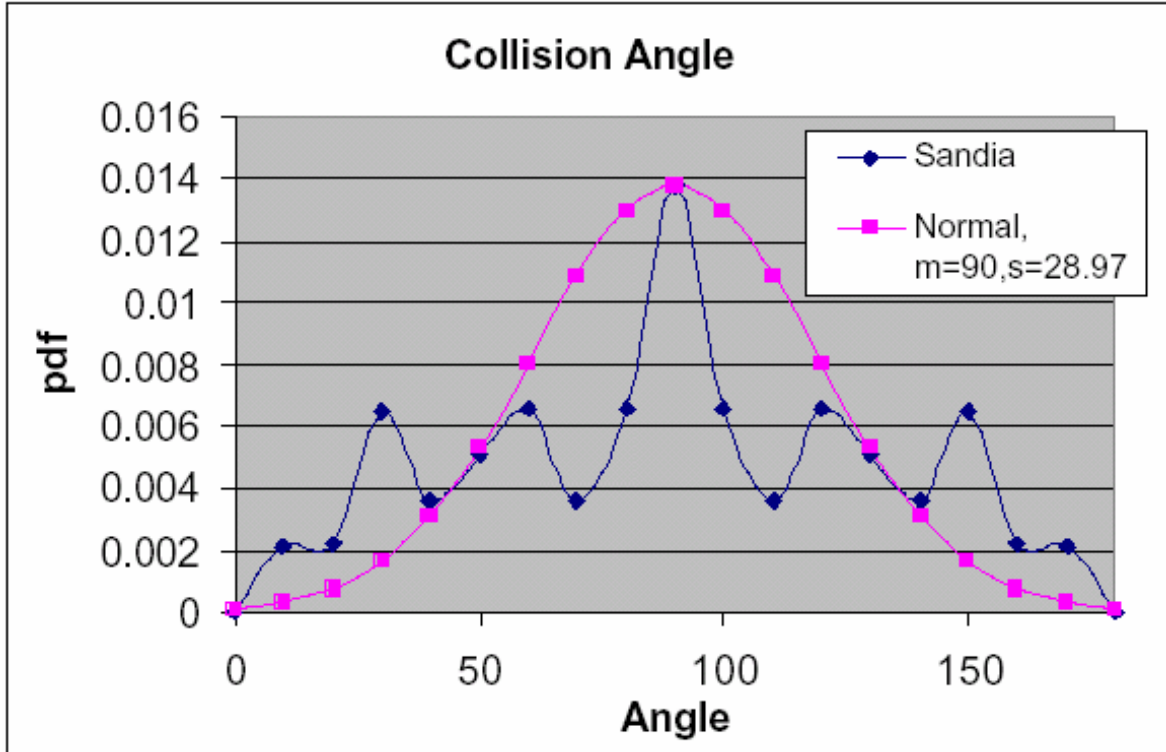


Figure 218 – Collision Angle pdf

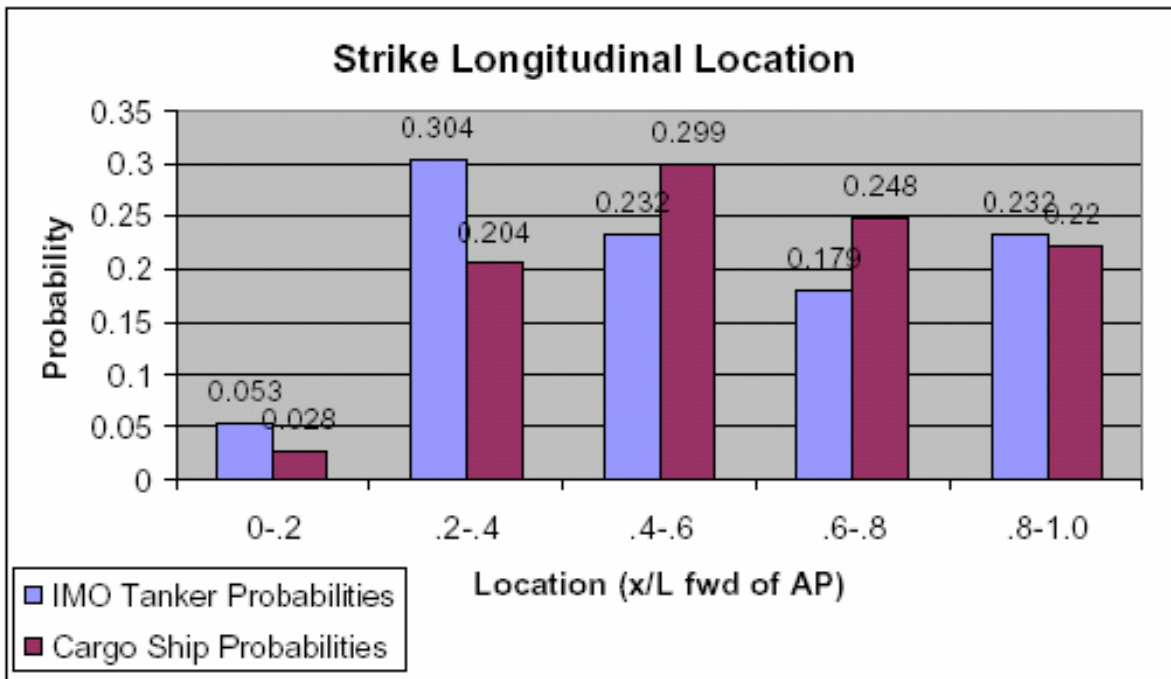


Figure 219 - Longitudinal Side Damage Probabilities [78]

Figure 220 and Figure 221 show the comparison of the non-dimensional results of the penetration for the SH100 and DH150 respectively.

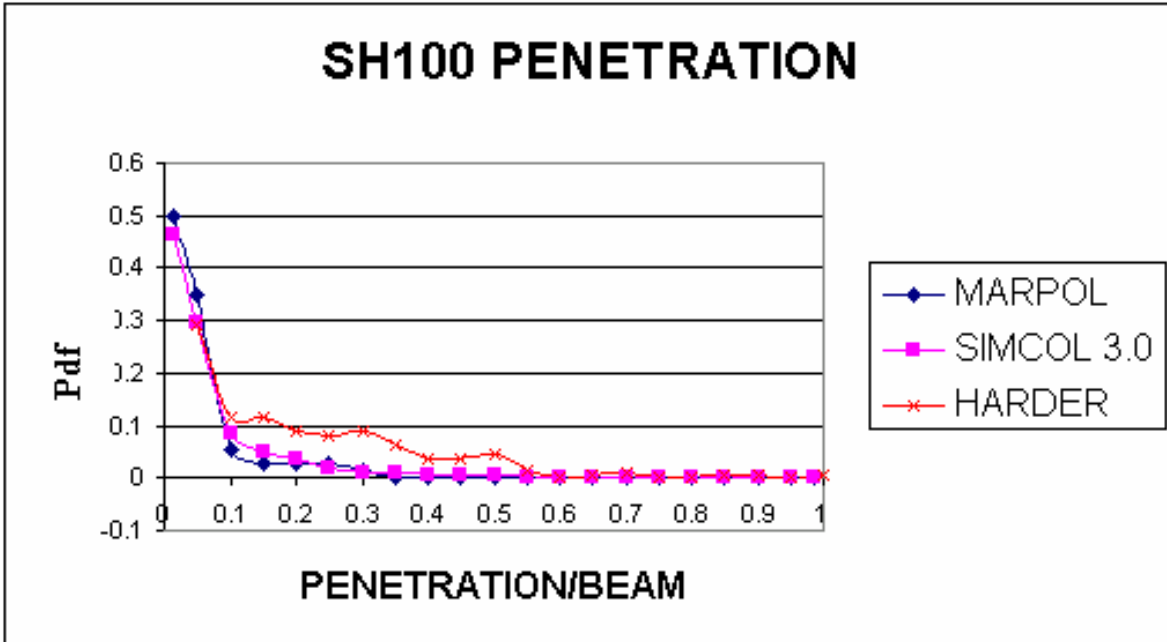


Figure 220 - SIMCOL, MARPOL & HARDER SH100 Penetration Comparison

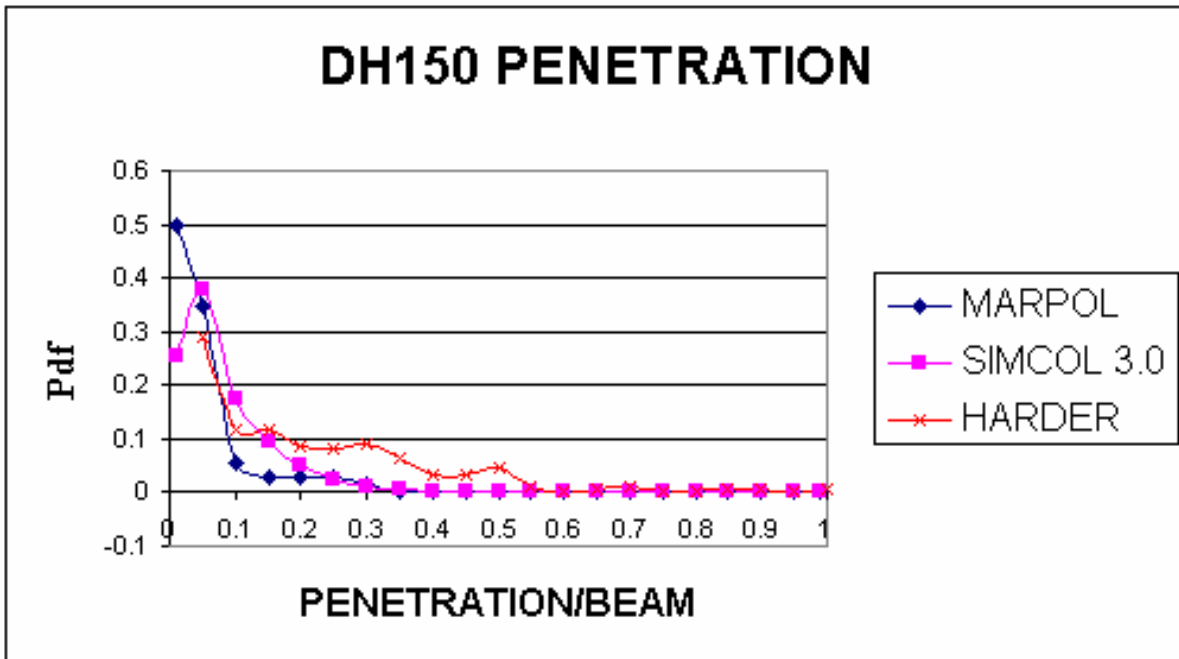


Figure 221 - SIMCOL, MARPOL & HARDER DH150 Penetration Comparison

The SIMCOL Version 3.0 results compare well to the trends of both the MARPOL and HARDER data where the SH100 SIMCOL analysis results better match the MARPOL data, which was compiled using older single hull vessels [100]. The DH150 results fall between the MARPOL and HARDER data where the HARDER data contains the original MARPOL data and a collection of more recent collision events involving both single and double hull vessels.

Figure 222 and Figure 223 show the comparison of the non-dimensional results of the longitudinal extent of damage (LED) for the SH100 and DH150 respectively.

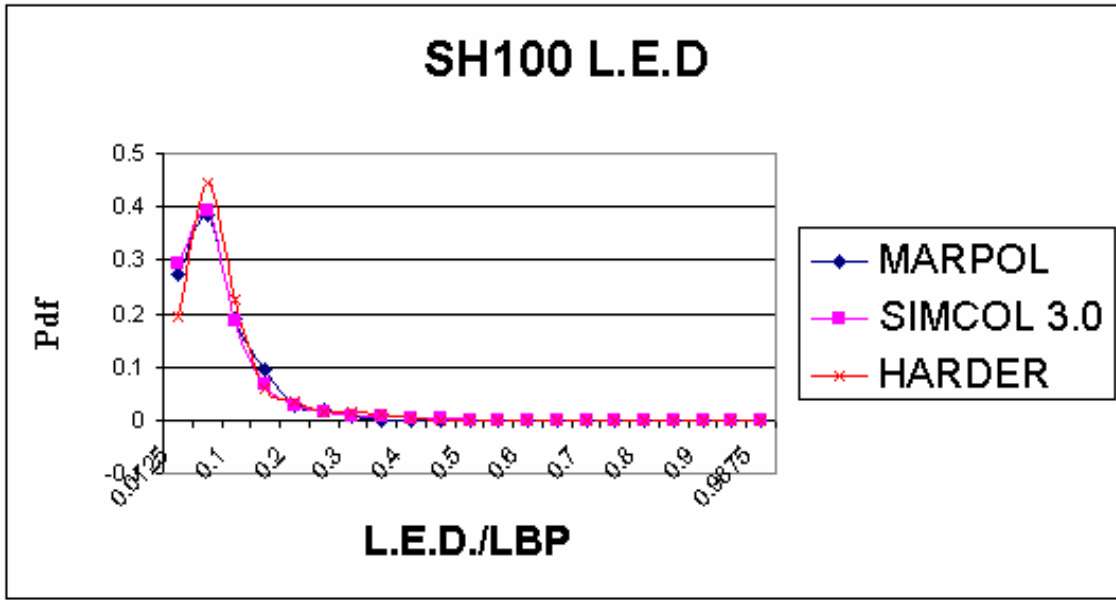


Figure 222 - SIMCOL, MARPOL & HARDER SH100 LED Comparison

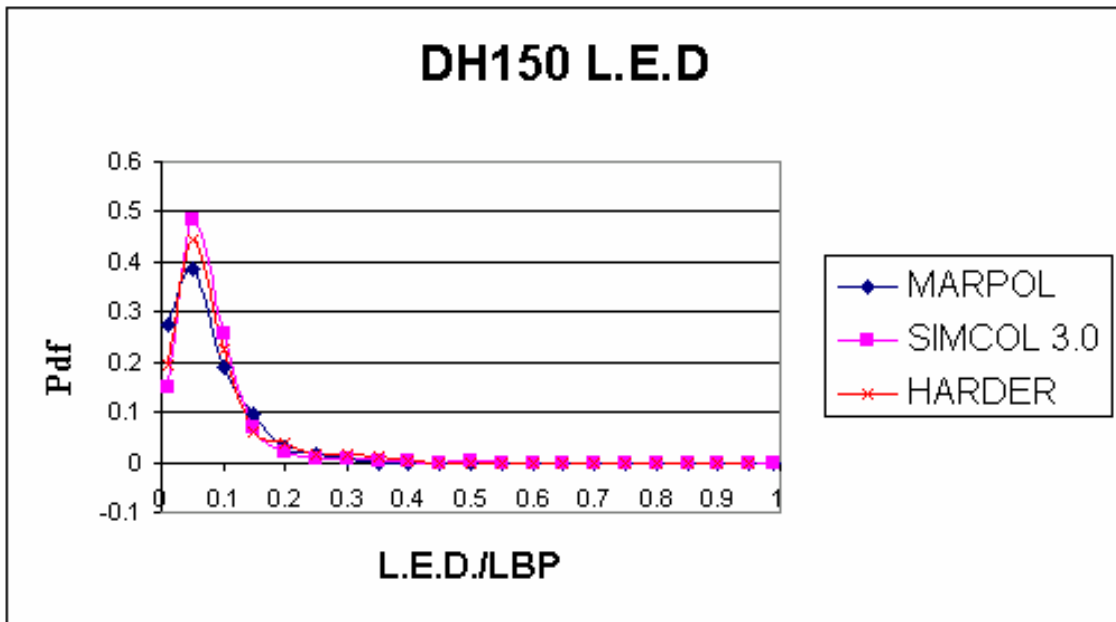


Figure 223 - SIMCOL, MARPOL & HARDER DH150 LED Comparison

Because of the geometry of the striking ship used in SIMCOL as shown in Figure 112, the standard calculation of LED using the distance between the forward most and aft most contact of the striking ship to the struck ship hull will be low compared to the actual results for collisions where the collision angle is less oblique and penetration is low. This is because the LED is determined on the geometry of the striking ship; specifically for less oblique low penetration collisions the LED is most sensitive to the half entrance angle (HEA). However, the defined SIMCOL HEA input is for the striking ship waterline but in actual less oblique low penetration collisions the LED is predominantly a function of the HEA at the forecastle deck or the at the bulb, both of which are often greater than the HEA at the waterline. To overcome the deficiency in the LED calculation SIMCOL Version 3.0 uses the following calculation of LED.

$$\frac{LED}{LBP1} = \begin{cases} \frac{LOC\_AFT - LOC\_FOR}{LBP1} & \text{if } PEN < B2 \wedge \frac{LOC\_AFT - LOC\_FOR}{LBP1} < B4 \\ \left[ \frac{LOC\_AFT - LOC\_FOR}{LBP1} \cdot \frac{B1}{B2} \cdot (B3 - PEN) \right] & \text{otherwise} \end{cases} \quad (6.1)$$

Where:

**PEN** penetration of striking ship into the struck ship divided by the struck ship beam

**LBP1** struck ship length between perpendiculars

**LOC\_FOR** forward most point on struck ship that striking ship hull contacts

**LOC\_AFT** aft most point on struck ship that striking ship hull contacts

**B1** = 1/B2

**B2** = 0.25 or other fitted value

**B3** = 0.3125 or other fitted value

**B4** = 0.2

A restriction on B1, B2, B3 and B4 is required such that  $B4=B2/(B3 \times B1)$ . Additionally, a second restriction on B2 is required such that  $B2=0.25$ . This method considers only the less oblique cases where penetration and longitudinal extent of damage are minimal as occurs in all less oblique low penetration collisions.

As with the penetration results of Figure 220 and Figure 221 the SIMCOL LED results of Figure 222 and Figure 223 compare well to the data of both MARPOL and HARDER where the maximum variation between any of the data is less than 10%.

## CHAPTER 7 Conclusions and Future Work

This study takes the second step in predicting side damage and oil outflow in ship collisions. It provides a rational probabilistic method for defining collision cases, provides a validation of a simplified collision model both deterministically and probabilistically, and provides results comparing damage for single hull and double hull tankers.

The most significant products of this study are the demonstration of a rational process and the development of a method for determining longitudinal extent of damage through transverse structure. There will certainly be future improvements to the collision statistical description and to collision and outflow models, but this process works as is shown through various validation cases. It provides an important piece of the overall framework for assessing the environmental performance of tankers. The proposed methodology provides a practical means of considering structural design in a regulatory framework, and when implemented will improve the safety and environmental performance of ships.

The following specific tasks were completed using SIMCOL in support of this project:

1. Completed the development of SIMCOL Version 3.0.
2. Developed the capability to model collision events using LSDYNA.
3. Validated SIMCOL Version 3.0.
4. Defined probabilistic oil tanker collision events. Probabilities and probability density functions were developed for important collision event parameters.
5. Predicted probabilistic structural damage for two notional oil tankers. Collision damage was calculated for ten thousand collision events and results were compared to probability density functions.
6. Developed and included a simplified deformable bow model in SIMCOL.
7. Developed a simplified model for the structural response of transverse structure in collision and incorporated the model into SIMCOL.

This work continues. Significant future work planned includes:

1. Continue to collect collision case data that may be used to validate LSDYNA and SIMCOL collision models. Perform additional validation.
2. Apply this methodology to the structural optimization of a tanker design for crashworthiness. Analyze the effect of various structural design parameters on crashworthiness.
3. Develop a raked bow (with and without bulb) model for SIMCOL to enable a higher degree of accuracy in capturing the striking vessel bow geometry.
4. Apply SIMCOL in a probabilistic optimization framework such as Model Center or ISIGHT and develop response surface models relating probabilistic collision damage extents to design characteristics.
5. Develop SIMCOL user-friendly front-end interface.

## References

- [1] Sirkar, J., Ameer, P., Brown, A.J., Goss, P., Michel, K., Willis, W., "A Framework for Assessing the Environmental Performance of Tankers in Accidental Grounding and Collision", *SNAME Transactions* **105**, 253-295, 1997.
- [2] Rawson, C., Crake, K. and Brown, A.J., "Assessing the Environmental Performance of Tankers in Accidental Grounding and Collision", *SNAME Transactions* **106**, 41-58, 1998.
- [3] Brown, A.J. and Amrozowicz, M., "Tanker Environmental Risk - Putting the Pieces Together", SNAME/SNAJ International Conference on Designs and Methodologies for Collision and Grounding Protection of Ships, August 1996.
- [4] IMO, "Interim Guidelines for Approval of Alternative Methods of Design and Construction of Oil Tankers under Regulation 13F(5) of Annex I of MARPOL 73/78", Resolution MEPC.66 (37), Adopted September 14, 1995.
- [5] Jones, N., "A Literature Survey on the Collision and grounding Protection of Ships", Ship Structure Committee Report No. SSC-283, 1979.
- [6] Giannotti, J.G., Jones, N., Genalis, P. and Van Mater, P.R., "Critical Evaluations of Low-Energy Ship Collision - Damage Theories and Design Methodologies, Volume I: Evaluation and Recommendations", Ship Structure Committee Report No. SSC-284, 1979.
- [7] Giannotti, J.G., Jones, N., Genalis, P. and Van Mater, P.R., "Critical Evaluations of Low-Energy Ship Collision - Damage Theories and Design Methodologies, Volume II: Literature Search and Review", Ship Structure Committee Report No. SSC-285, 1979.
- [8] ISSC, Report by Specialist Panel V.4 – Structural Design Against Collision and Grounding, Proceedings of the 13<sup>th</sup> International Ship and Offshore Structures Congress 1997, Trondheim, Norway, 1997.
- [9] Minorsky, V.V., "An Analysis of Ship Collisions with Reference to Protection of Nuclear Power Plants," *Journal of Ship Research*, 1959.
- [10] Simonsen, B.C., "Theory and Validation for the DAMAGE Collision Module", Joint MIT-Industry Program on Tanker Safety, Report No. 67, June 1999.
- [11] Crake, K., "Probabilistic Evaluations of Tanker Ship Damage in Grounding Events", Naval Engineer Thesis, MIT, 1995.
- [12] Hutchison, B.L., "Barge Collisions, Rammings and Groundings - an Engineering Assessment of the Potential for Damage to Radioactive Material Transport Casks", Report No. SAND85-7165 TTC-05212, 1986.
- [13] Zhang, S., "The Mechanics of Ship Collisions", Ph.D. Thesis, Department of Naval Architecture and Offshore Engineering, technical University of Denmark, Lyngby, 1999.
- [14] Pedersen, P.T. and Zhang, S., 1998. "On Impact Mechanics in Ship Collisions", *Marine Structures*, Vol. 11, pp. 429-449.

- [15] Reardon, P. and Sprung, J.L., "Validation of Minorsky's Ship Collision Model and Use of the Model to Estimate the Probability of Damaging a Radioactive Material Transportation Cask During a Ship Collision", *Proceedings of the International Conference on Design and Methodologies for Collision and Grounding Protection of Ships*, San Francisco, August 1996.
- [16] McDermott, J.F., Kline, R.G., Jones, E.L., Maniar, N.M., Chiang, W.P., "Tanker Structural Analysis for Minor Collisions", *SNAME Transactions*, Vol. 82, pp. 382-414, 1974.
- [17] Woisin, G., "Design Against Collision", *International Symposium on Advances in Marine Technology*, Trondheim, Norway, June 1979.
- [18] Rosenblatt & Son, Inc, "Tanker Structural Analysis for Minor Collision", USCG Report, CG-D-72-76, 1975.
- [19] Reckling, K.A., "Mechanics of Minor Ship Collisions", *International Journal of Impact Engineering*, Vol. 1, No. 3, pp. 281-299, 1983.
- [20] Wierzbicki, T., "Crushing Behavior of Plate Intersections", *Structural Crashworthiness*, edited by A. Jones and T. Wierzbicki, Chapter 3, Butterworth and Co., London, 1983.
- [21] Paik, J. and Wierzbicki, T., "A Benchmark Study on Crushing and Cutting of Plated Structures", *Journal of Ship Research*, p. 147, June, 1997.
- [22] Pedersen, P.T., et al, "Ship Impacts: Bow Collisions", *International Journal of Impact Engineering*, Vol. 13, No. 2, pp. 163-187, 1993.
- [23] Amdahl, J., "Energy Absorption in Ship-Platform Impacts", Dr. Ing. Thesis, Report No. UR-83-84, The Norwegian Institute of Technology, Trondheim, 1983.
- [24] Yang, P.D.C. and Caldwell, J.B., "Collision Energy Absorption in Ships Bow Structures", *International Journal of Impact Engineering*, Vol. 7, No. 2, 1988.
- [25] Ito, H., et al, "A Simplified Method to Analyze the Strength of Double Hulled Structures in Collision", *Journal of Society of Naval Architects of Japan*, Vol. 156, pp. 283-295, 1984.
- [26] Ito, H., et al, "A Simplified Method to Analyze the Strength of Double Hulled Structures in Collision, 2<sup>nd</sup> Report", *Journal of Society of Naval Architects of Japan*, Vol. 158, pp. 420-434, 1985.
- [27] Ito, H., et al, "A Simplified Method to Analyze the Strength of Double Hulled Structures in Collision, 3<sup>rd</sup> Report", *Journal of Society of Naval Architects of Japan*, Vol. 160, pp. 401-409, 1986.
- [28] Paik, J.K., et al, "On Rational Design of Double Hull Tanker Structures against Collision", *1999 SNAME Annual Meeting*, 1999.
- [29] Paik, J.K. and Pedersen, P.T., "Modeling of the Internal Mechanics in Ship Collisions", *Ocean Engineering*, Vol. 23, No. 2, pp. 107-142, 1996.
- [30] Hallquist, J.O (1998), "LSDYNA Examples Manual", Livermore Software Technology Corporation (LSTC), March 1998.
- [31] Hallquist, J.O (1998), "LSDYNA Theoretical Manual", Livermore Software Technology Corporation (LSTC), May 1998.

- [32] Hallquist, J.O (1999), “LSDYNA Keyword Users Manual – Nonlinear Dynamic Structural Analysis of Structures”, Livermore Software Technology Corporation (LSTC), May 1999.
- [33] Lenselink, H., and Thung, K.G., “Numerical Simulations of the Dutch-Japanese Full Scale Ship Collision Tests”, Proceedings of Conference on Prediction Methodology of Tanker Structural Failure, ASIS, Tokyo, July 1992.
- [34] Wevers, L.J. and Vredeveltdt, A.W., "Full Scale Ship Collision Experiments", TNO Report 98-CMC-R0359, 1999.
- [35] Chen, D., “Simplified Collision Model (SIMCOL)”, Dept. of Ocean Engineering, Virginia Tech, Master of Science Thesis, May 2000.
- [36] Gibbs and Cox, Inc., "Design Criteria and Guide for Design of Nuclear-Powered Merchant Ships", for the US Department of Commerce, MARAD Nuclear Projects Office, January 1960.
- [37] Kierkegaard, H., “Ship Collisions with Icebergs”, PhD Thesis, DTU, April 1993.
- [38] Kitamura, K. and Akita, M., “A Study on Collision by an Elastic Stem to the Side Structure of Ships”, Trans. SNAJ, 131, 307-317, 1972.
- [39] Hagiwara, K., Takanabe, H. and Kawano, H., “A Proposed Method of Predicting Ship Collision Damage”, International Journal of Impact Engineering, No. 1, International Journal of Impact Engineering, No. 1, 1983.
- [40] Kim, J.Y., “Crushing of a Bow: Theory vs. Scale Model Tests”, Joint MIT-Industry Program on Tanker Safety, Report No. 69, June 1999.
- [41] Kim, J.Y., “Analysis of a Dropped Bow Collision Model”, Joint MIT-Industry Program on Tanker Safety, Report No. 72, May 2000.
- [42] Gooding, Peter W. (1999), “Collision with a Crushable Bow”, MIT Thesis, 1999
- [43] Gerard, G., ""The Crippling Strength of Compression Elements", *Journal of Aeronautical Science*, 1958.
- [44] Amdahl, J. and Kavlie, D., “Experimental and Numerical Simulation of Double Hull Stranding”, Proceedings of the DNV-MIT Workshop on “Mechanics of Ship Collision and Grounding”, Oslo, 1992.
- [45] Amdahl, J. and Kavlie, D., “Design of Tankers for Grounding and Collision”, MARIENV ’95, 1995.
- [46] Lehmann, E. and Yu, X., “Progressive Folding of Bulbous Bows”, The Sixth International Symposium on Practical Design of Ships and Mobile Units (PRADS), September, 1995.
- [47] Lutzen, M., Simonsen, B.C. and Pedersen, P.T., "Rapid Prediction of Damage to Struck and Striking Vessels in a Collision Event", Ship Structure Symposium 2000, Washington D.C., 2000.
- [48] Kierkegaard, H., Ship Bow Response in High Energy Collision", *Marine Structures*, Vol. 6, pp. 359-376, 1993.
- [49] Arita, K., “A Probabilistic Assessment on Protective Structures in Ship Collisions”, 63 General Meeting of Ship Research Institute, 1994.

- [50] Valsgard, S. and Pettersen, E., "Simplified Non-Linear Analysis of Ship/Ship Collisions", Norwegian Maritime Research, No. 3, pp. 2-17, 1982.
- [51] Bach-Gansmo, O. and Valsgard S., "Simplified stiffness evaluation of a bulbous ship bow", Progress report No. 1, DnV, Report No. 81-0437 (Rev. no. 1 of 17.02.82), 1981.
- [52] Chang, P.Y., Seibold, F. and Thasantorn, C., "A Rational Methodology for the Prediction of Structural Response due to Collision of Ships.", Paper No. 6, SNAME Annual Meeting, New York, NY, Nov. 13-15, 1980.
- [53] Wang, G., Katsuyuki, S., Ohtsubo, H. (1995), "Predicting Collision Strength of Bow Structure", Marienv 95
- [54] Suzuki, K., Ohtsubo, H. (1995), "Crushing Strength of Ship Bow Structure - Calculation of Absorbed Energy and Optimal Design", Marienv95
- [55] Vakkalanka, Suryanarayana, "Simplified Bow Model for a Striking Ship in Collision", Dept. of Ocean Engineering, Virginia Tech, Master of Science Thesis, July 2000.
- [56] Xia, Jianjun, "Finite Element Analysis of Ship Collisions", Department of Ocean Engineering, Virginia Tech, Master of Science Thesis, May 2001.
- [57] Kitamura, O., "FEM Approach to the Simulation of Collision and Grounding Damage", 2<sup>nd</sup> International Conference on Collision and Grounding of Ships, Copenhagen, Denmark, July, 2001.
- [58] Gu, Y. and Wang, Z.L., "An Inertia Equivalent Model for Numerical Simulation of Ship-Ship Collisions", 2<sup>nd</sup> International Conference on Collision and Grounding of Ships, Copenhagen, Denmark, July, 2001.
- [59] Lemmen, P.P.M. and Vredeveldt, A.W., "Application of Explicit Finite Element Method in Ship Collision Analysis", TNO Report 93-CMC-R1153, 1 December 1993.
- [60] Servis, D. et. al., "The Implementation of Finite Element Codes for the Simulation of Ship-Ship Collision", 2<sup>nd</sup> International Conference on Collision and Grounding of Ships, Copenhagen, Denmark, July, 2001.
- [61] Naar, H. et. al., "Comparison of the Crashworthiness of Various Bottom and Side Structures", 2<sup>nd</sup> International Conference on Collision and Grounding of Ships, Copenhagen, Denmark, July, 2001.
- [62] Sinmao, M. & Abramowicz, W. "Joint MIT-Industry Report #66." MIT Department of Ocean Engineering, 1999.
- [63] Tikka, K.K. & Chen, Y.J. "Prediction of Structural Response in Grounding", Ship Structure Symposium 2000, Washington D.C., 2000.
- [64] Simonsen, B.C. "Ship Grounding on Rock – I.", Marine Structures, 10, pp. 519-562, 1997.
- [65] Kitamura, O. "Buffer Bow Design for the Improved Safety of Ships", Ship Structure Symposium 2000, Washington D.C., 2000.
- [66] "Machinery's Handbook 25, Twenty Fifth Edition." Industrial Press Inc., 1996.
- [67] Simonsen, B.C. & Wierzbicki, T. "Joint MIT-Industry Report #59." MIT Department of Ocean Engineering, 1999.

- [68] Shibue, T., Abe, A. and Fujita, K. "The Effect of the Strut Arrangement on the Energy Absorption of Side Structure in Collision", 2<sup>nd</sup> International Conference on Collision and Grounding of Ships, Copenhagen, Denmark, July, 2001.
- [69] Lehmann, E. & Peschmann, J. "Energy Absorption by the Steel Structure of Ships in the Event of Collisions", 2<sup>nd</sup> International Conference on Collision and Grounding of Ships, Copenhagen, Denmark, July, 2001.
- [70] Wisniewski, K., Kolakowski, P., Rozmarynowski, B. & Gierlinski, J.T. "Dynamic FE simulation of damage in ships collision", 2<sup>nd</sup> International Conference on Collision and Grounding of Ships, Copenhagen, Denmark, July, 2001.
- [71] "LSDYNA USER'S MANUAL", Livermore Software Technology Corporation, 2001.
- [72] Lemmen, P.M., Vredeveltdt, A.W., and Pinkster, J.A., "Design Analysis for Grounding Experiments", SNAME/SNAJ International Conference on Designs and Methodologies for Collision and Grounding Protection of Ships, San Francisco, August 1996.
- [73] Simonsen and Lauridsen. "Energy Absorption and Ductile Failure in Metal Sheets Under Lateral Indentation by a Sphere", 2003.
- [74] Kitamura, O., "Comparative Study on Collision Resistance of Side Structure", Marine Technology, Vol. 34, No. 4, pp.293-308, October 1997.
- [75] Servis, D.P., and Samuelides, M., "Ship Collision Analysis Using Finite Elements", Safer Euro Spring Meeting, Nantes Greece, 28 April 1999.
- [76] Francis, P.H., Cook, T.S., and Nagy, A., Ship Structure Committee Report Number 276 (SSC-276), 1978.
- [77] R.L. Rothman & R.E. Monroe, Ship Structure Committee Report Number 235 (SSC-235), 1973.
- [78] Sandia National Laboratories, *Data and Methods for the Assessment of the Risks Associated with the Maritime Transport of Radioactive Materials Results of the SeaRAM Program Studies*, SAND98-1171/2, Albuquerque, NM, May 1998.
- [79] Lloyds Worldwide Ship data, provided by MARAD, 1993.
- [80] ORI, *Hazardous Environment Experienced by Radioactive Material Packages Transported by Water*, Silver Spring, MD, October 1980.
- [81] ORI, *Accident Severities Experienced by Radioactive Material Packages Transported by Water*, Silver Spring, MD, November 1981.
- [82] USCG Ship Casualty Data, 1982-1990.
- [83] Brown, A.J., *Modeling Structural Damage in Ship Collisions*, Ship Structure Committee, SSC No. 442, 164 pages, 2002.
- [84] MVI, *SS P&T ADVENTURER-SS TULLAHOMA Collision Off Destruction Island*, Chief, Merchant Vessel Inspection Division, March 1952
- [85] Hughes, Ship Structural Design, SNAME, 1988
- [86] Sanford, Principles of Fracture Mechanics, Prentice Hall, 2003

- [87] Wierzbicki and Abromowicz, *On the Crushing Mechanics of Thin-Walled Structures*, ASME Winter Annual Meeting, Presented 1983
- [88] Lutzen, Marie, "Ship Collision Damages", Department of Mechanical Engineering, Technical University of Denmark, Doctoral Thesis, December 2001.
- [89] ASIS, *Research on the Methodology for the Prediction of Accidental Damage to Tanker Structure in Case of Collision and Grounding and Development of New Hull Design with Improved Crashworthiness*, March 1998
- [90] Bower, A.F., 1999, Lecture Notes – Advanced Mechanics of Solids
- [91] USCG, *Decision and Final Order of the Commandant in the Matter of License No. 124294*, May 1952
- [92] Brown, A.J., Sajdak, J.A.W., *Floating Production, Storage and Offloading Vessel Collision Study*, Report for Herbert Engineering SSSE 01-4, April 2002
- [93] Brown, A.J., Chen, D., *Probabilistic Method for Predicting Ship Collision Damage*, Oceanic Engineering International, V.6 No. 1, 2002
- [94] Glykas, Das & Barltrop, *Application of Failure and Fracture Criteria During a Tanker Head-on Collision*, Ocean Engineering V.28, 2001
- [95] Paik & Thayamballi, *A Concise Introduction to the Idealized Structural Unit Method for Nonlinear Analysis of Large Plated Structures and its Application*, Thin Walled Structures, V.41, 2003
- [96] Glykas & Das, *Energy Conservation During a Tanker Collision*, Ocean Engineering, V.28, 2001
- [97] Egge & Bckenhauer, *Calculation of the Collisin Resistance of Ships and its Assessment for Classification Purposes*, Nuclear Engineering and Design, V.150, 1994
- [98] Carlebur, *Full-Scale Collision Tests*, Safety Science, V.19, 1995
- [99] Ishiyama, Nishimura & Tsuchiya, *Impact Response of Thin Walled Plane Frame Strucures*, Journal of Impact Engineering, V.1, No. 3, 1983
- [100] Brown, A.J., "Collision Scenarios and Probabilistic Collision Damage", *Marine Structures*, 15 (2002), pp.335-364, 2002
- [101] Wang, G., *Some Recent Studies on Plastic Behavior of Plates Subjected to Large Impact Loads*, Journal of Offshore Mechanics and Arctic Engineering, V.124, August 2002
- [102] Zhu & Faulkner, *Dynamic Inelastic Behavior of Plates in Minor Ship Collisions*, Journal of Impact Engineering, V.15, No. 2, 1994
- [103] Ziliotto et al., *Comparison of Different Finite Element Analyses of the Transverse Frame of a 350000 TDW Tanker*, Marine Structures, V.4, 1991
- [104] Zheng & Wierzbicki, *A Theoretical Study of Steady-State Wedge Cutting Through Metal Plates*, International Journal of Fracture, V.78, 1996
- [105] Wierzbicki, Bao and Werner, *Ductile Fracture: Theory, Calibration and Applications*, EuroPAM, 2002

- [106] Wierzbicki & Driscoll, *Crushing Damage of Web Girders Under Localized Static Loads*, Journal of Construction Steel Research, V.33, 1995
- [107] Ueda, Rashed & Paik, *Buckling and Ultimate Strength Interaction in Plates and Stiffened Panels Under Combined Inplane Biaxial and Shearing Forces*, Marine Structures, V.8, 1995
- [108] Hu & Jiang, *A Finite Element Simulation of the test Procedure of Stiffened Panels*, Marine Structures, V.11, 1998
- [109] Jones & Jouri, *A Study of Plate Tearing for Ship Collision and Grounding Damage*, Journal of Ship Research, V.31, No. 4, December 1987
- [110] Johnson & Katcharian, *Several Recent Rammings Investigated by the National Transportation Safety Board*, Marine Technology, V.28, No. 6, November 1991
- [111] Huang, Chen & Zhang, *Pseudo-Shakedown in the Collision Mechanics of Ships*, International Journal of Impact Engineering, V.24, 2000
- [112] Kuroiwa, Kawamoto, Kusuba & Stillman, (1995), *Numerical Simulation of Collision and Grounding of Ships*, Marienv95
- [113] Daidola, *Tanker Structure Behavior During Collision and Grounding*, Marine Technology, V.32, No. 1, January 1995
- [114] Paik & Pedersen, *Ultimate and Crushing Strength of Plated Structures*, Journal of Ship Research, V.39, No. 3, September 1995
- [115] Paik, Chung & Chun, *On Quasi-Static Crushing of a Stiffened Square Tube*, Journal of Ship Research, V.40, No. 3, September 1996
- [116] Pedersen, (1995), *Collision and Grounding Mechanics*, WEMT 95 – Ship Safety and the Protection of the Environment
- [117] Paik & Pedersen, *On Design of Double Hull Tankers Against Collisions*, Sixth International Symposium on Practical Design of Ships and Mobile Units, PRADS95, September 1995
- [118] Hayduk & Wierzbicki, *Extensional Collapse Modes of Structural Members*, Computers & Structures, V.18, No. 3, 1984
- [119] Dand, *Hydrodynamic Aspects of Shallow Water Collisions*, RINA Meeting, London, April 1976
- [120] Paik & Wierzbicki, *A Benchmark Study on Crushing and Cutting of Plate Structures*, Journal of Ship Research, V.41, No. 2, June 1997
- [121] Paik, Thayamballi & Yang, *Residual Strength Assessment of Ships after Collision and Grounding*, Marine Technology, January 1998
- [122] Pedersen & Zhang, *Collision Analysis for MS DEXTRA*, SAFER EURORO Spring Meeting, April 1999
- [123] Pedersen & Zhang, *Effect of Ship Structure and Size on Grounding and Collision Damage Distributions*, Ocean Engineering, V.27, 2000
- [124] Pedersen & Zhang, *Absorbed Energy in Ship Collisions and Grounding – Revising Minorsky's Empirical Method*, Journal of Ship Research, June 2000

- [125] Petersen, *Dynamics of Ship Collisions*, Ocean Engineering, V.9, No. 4, 1982
- [126] Paik, Choe & Thayamballi, *Predicting Resistance of Spherical-Type LNG Carrier Structures to Ship Collisions*, Marine Technology, V.39, No. 2, April 2002
- [127] Sano, et al., *A Study on the Strength of Double Hull Side Structure of VLCC in Collision*, Marienv95, 1995
- [128] Sano, et al., *Strength Analysis of a New Double Hull Structure for VLCC in Collision*, SNAME/SNAJ Conference, August 1996
- [129] Simonsen & Ocakli, *Experiments and Theory on Deck and Girder Crushing*, Thin-Walled Structures, V.34, 1999
- [130] Simonsen & Wierzbicki, *Plasticity, Fracture and Friction in Steady-State Plate Cutting*, International Journal of Impact Engineering, V.19, No. 8, 1997
- [131] Arita & Shoji, (1995), *Expected Effectiveness of Double Side Structures in Ship Collisions*, Marienv95
- [132] Akita, Ando, Fujita & Kitamura, *Studies on Collision-Protective Structures in Nuclear Powered Ships*, Nuclear Engineering and Design, V.19, 1972
- [133] Mains, C., *Updated Damage Statistics on Collision and Grounding*, Germanischer Lloyd, 1-11-D-2001-01-1, July 2001
- [134] Sajdak, J.A.W., "Analyses of Ship Collisions: Determination of Longitudinal Extent of Damage and Penetration", Dr. Eng. Thesis, Virginia Polytechnic Institute and State University, Blacksburg, 2004.
- [135] Brown, A.J., "Oil Tanker Design Methodology Considering Probabilistic Accident Damage", *International Journal of Advanced Manufacturing Systems*, Vol. 4, Issue 1, pp. 25-34, September 2001.
- [136] Brown, A.J., Tikka, K., Daidola, J., Lutzen, M., Choe, I., "Structural Design and Response in Collision and Grounding", *SNAME Transactions* **108**, pp. 447-473, 2000.
- [137] Brown, A.J., "Collision Scenarios and Probabilistic Collision Damage", 2nd International Conference on Collision and Grounding, Copenhagen, Denmark, pp. 259-272, July 1-3, 2001.
- [138] Brown, A.J., "Optimum Risk Tanker (ORT): A Systematic Approach to a TAPS Tanker Design", Ship Structure Committee (SSC) Symposium 2000, Arlington, VA, July, 2000.

## Appendix A: 150K dwt Bulk Carrier Bow Structural Data

### 150,000 DWT Bulk Carrier

#### Ship Particulars

LBP	: 274 m
Breadth moulded	: 47.0 m
Depth molded	: 21.6 m
Depth to forecastle deck	: 26.0 m
Max. Draft	: 15.96 m
Displacement	: 174850 tons
Max. service speed	: 7.7 m/s ( 15.00 knots )

*The bow is stiffened longitudinally. The transverse frames supporting the longitudinals have a spacing of 3.2 m. The most important structural data for the bow are:*

#### Material

Yield Stress for plates and stiffeners ( $\sigma_Y$ )	: 315 Mpa
Ratio between ultimate and Yield stress ( $\sigma_u/\sigma_Y$ )	: 1.6

#### Bottom

plate thickness	: 18.0 mm
longitudinals, spacing	: L450 x 150 x 12/16
CL-Girder	: L2500 x 400 x 15/25

#### Side shell

Plate thickness, side shell up to 8.1 m abl	: 18.0 mm
Plate thickness, side shell between 8.1 and 17.0 m abl	: 33.0 mm
Plate thickness, side shell between 17.0 and 26.0 m abl	: 16.0 mm
Longitudinals between 1.2 and 6.8 m abl, spacing 0.8 m	: L450 x 150 x 12/16
Longitudinals between 8.4 and 16.2 m abl, spacing 0.6 m	: L400 x 100 x 19/19

Longitudinals between 17.4 and 24.8 m abl, spacing 0.8 m : L350 x 100 x 12/17

Forecastle deck, 26.0 m abl

Plate thickness : 13.0 mm  
Longitudinals, spacing : L250 x 90 x 12/16  
CL-girder : L1400 x 250 x 12/25

Tank top, 20.0 m abl

Plate thickness : 13.0 mm  
Longitudinals, spacing : L250 x 90 x 12/16  
CL-girder : L1400 x 250 x 12/25

Deck (not water-tight), 7.7 m abl

Plate thickness : 13.0 mm  
Longitudinals, spacing : L250 x 90 x 12/16  
CL-girder : L1400 x 250 x 12/25

Breast hooks

Number of breast hooks : 32  
Cross-section : 1200 x 15  
Length : 3000 mm  
CL-girder along stem line cross-section : T1400 x 250 x 12/25  
CL-bulkhead in bulb fwd F.P (plate thickness) : 12mm  
Vertical stiffening spacing : 0.8 m

## Appendix B: 40K dwt Container Ship Bow Structural Data

### 40,000 DWT Containership

#### Principal dimensions:

<b>LBP</b>	: 211.50 m
<b>Breadth moulded</b>	: 32.20 m
<b>Depth mld to main deck</b>	: 21.00 m
<b>Depth to shelter deck</b>	: 24.00 m
<b>Max. Draft</b>	: 11.90 m
<b>Displacement (Loaded)</b>	: 54,000 tons
<b>Max. Service Speed</b>	: 11.3 m/s (21.97 knots)

*The bulbous bow is stiffened longitudinally. The transverse frames supporting the longitudinals have a spacing of 2.4 m. The most important structural data for the bow are:*

#### Bottom:

<b>Plate thickness</b>	: 19.0
<b>Longitudinals, spacing 0.8 m</b>	: L 250 X 90 X 12 / 16
<b>CL-Girder</b>	: L 1900 X 250 X 15 / 25

#### Side shell

<b>Plate thickness, side shell up to 6.1 m abl</b>	: 17.0 mm
<b>Plate thickness, side shell between 6.1 and 12.3 m abl</b>	: 35.0 mm
<b>Plate thickness, side shell between 12.3 and 21.0 m abl</b>	: 16.0 mm
<b>Plate thickness, side shell above 21.0 m abl</b>	: 14.0 mm
<b>Longitudinals below 5.2 m abl and above 13.6 m abl (spacing 0.8 m)</b>	: L250 x 90 x 10/15
<b>Longitudinals between 6.6 and 12.0 m abl, spacing 0.6 m</b>	: L250 x 90 x 12/16

#### Forecastle deck, 24.0 m at

Plate thickness : 15.0 mm  
Longitudinals, spacing 0.8 m : L150 x 100 x 9  
CL-girder : L700 x 150 x 12/12

Main deck, 21.0 m abl

Plate thickness : 11.0 mm  
Longitudinals, spacing 0.8 m : L150 x 100 x 9  
CL-girder : L700 x 150 x 12/12

Deck 17.6 m abl

Plate thickness : 11.0 mm  
Longitudinals, spacing 0.8 m : L150 x 100 x 9  
CL-girder : L700 x 150 x 12/12

Deck 12.8 m abl

Plate thickness : 15.0 mm  
Longitudinals, spacing 0.8 m : L200 x 90 x 9/14  
CL-girder : L700 x 150 x 12/12

Deck (not water-tight), 6 m abl

Plate thickness : 11.0 mm  
Longitudinals, spacing 0.8 m : Fl. 150 x 12

## **Appendix C: C4 Cargo Ship Bow Structural Data**

The scantlings and dimensions of the C4 cargo vessel used are the same as the Victory Cargo ship of appendix D multiplied by a factor of 1.149. All thicknesses used are exactly those of the VC2-S-AP3 of Appendix D.

## Appendix D: Victory Cargo Ship Bow Structural Data

### VC2-S-AP3 (Victory Cargo)

#### Ship Particulars:

LBP	: 436.5 ft
LWL	: 444.0 ft
Length Overall	: 455.25 ft
Moulded beam	: 62.0 ft
Moulded depth	: 38.0 ft
Moulded Draft at DWL	: 28.0 ft
Displacement (loaded)	: 14,832 tons
Max. Service Speed	: 16.0 knots

*The bow is stiffened transversely. The transverse stiffener spacing is 2.0 ft. The most important structural data for the bow are:*

#### Material:

Yield Stress for plates and stiffeners	: 235 Mpa
Ratio between ultimate and Yield stress	: 1.4

Bottom:

Plate thickness : 27.0 mm

CL-Girder : 19.5 mm

Sideshell:

Plate thickness, side shell up to 18 ft abl : 27.0 mm

Plate thickness, side shell between 18 ft and 51 ft abl : 21.25 mm

Forecastle deck, 51 ft abl:

Plate thickness : 10.5 mm

CL-Girder : 27 in x 19.5 mm

Main deck, 42 ft abl:

Plate thickness : 10.5 mm

CL-Girder : 28 in x 19.5 mm

Second deck, 28 ft abl:

Plate thickness : 10.5 mm

CL-Girder : 24 in x 19.5 mm

Stringer deck 3 (not watertight), 35 ft abl:

Plate thickness : 10.5 mm

Stringer deck 2 (not watertight), 23 ft abl:

Plate thickness : 10.5 mm

Stringer deck 1 (not watertight), 18 ft abl:

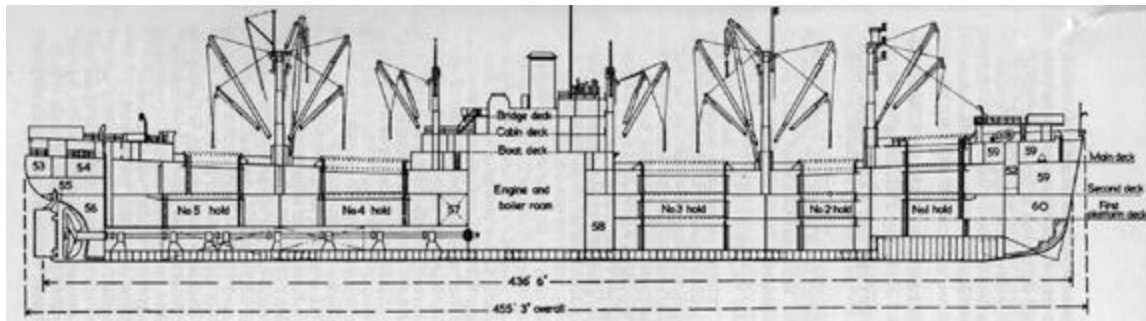
Plate thickness : 10.5 mm

Breast hooks:

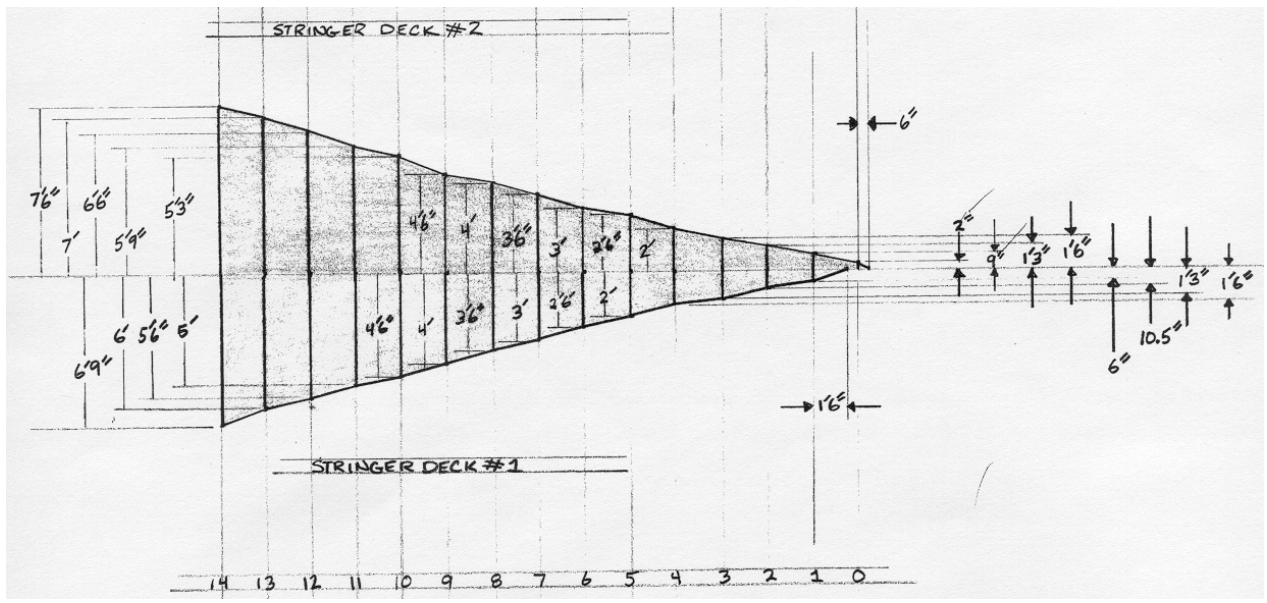
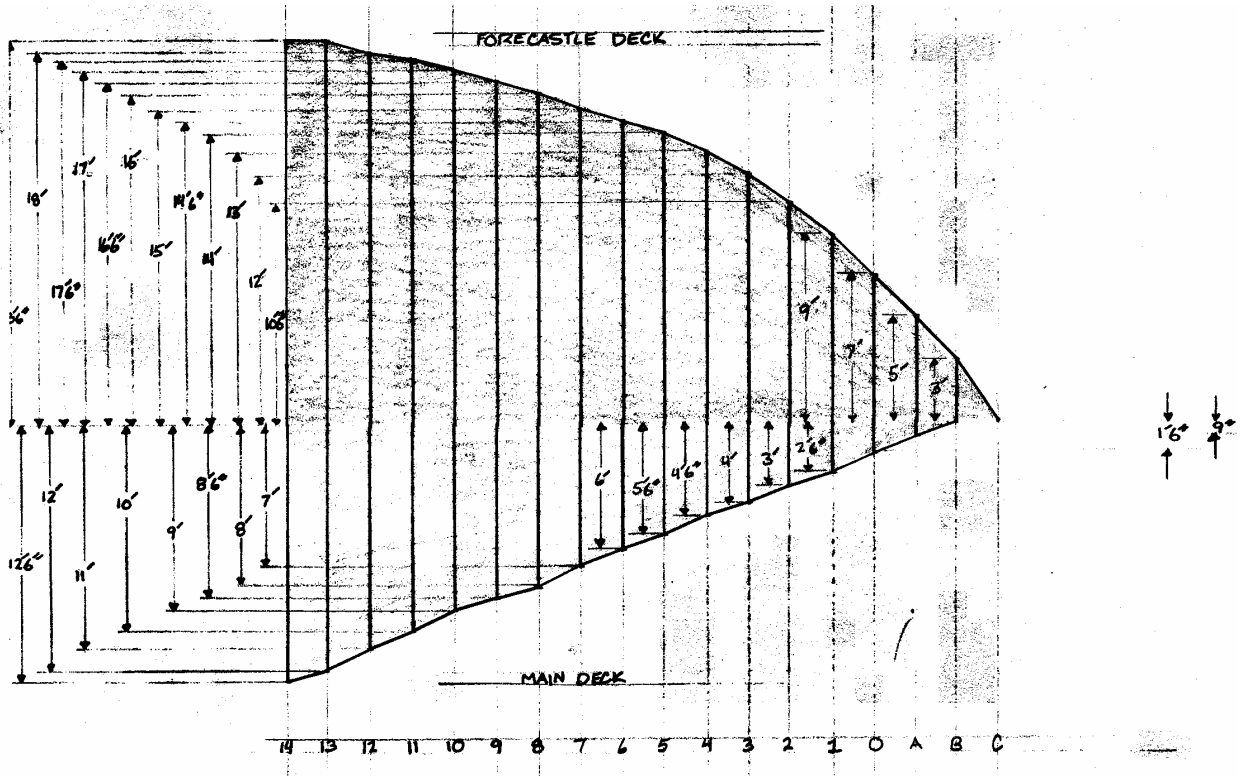
Number of breast hooks : 14

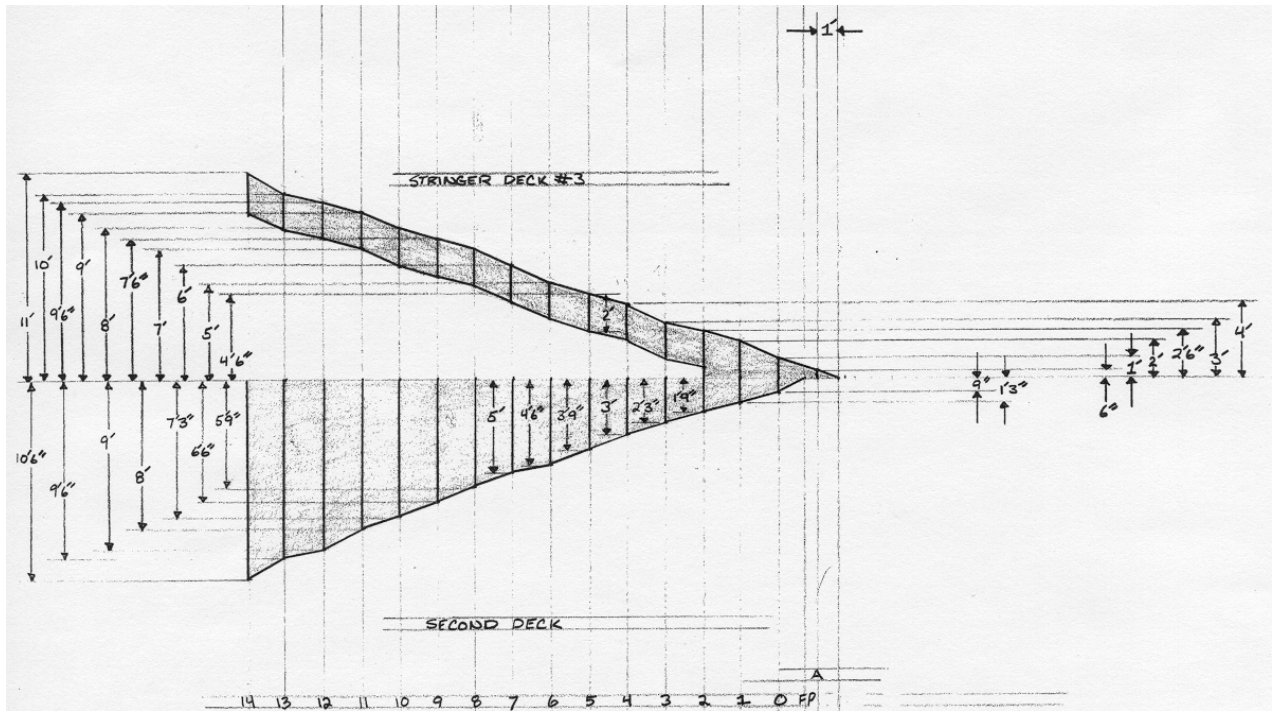
Thickness : 10.0 mm

*The following are graphical representations of the VC2-S-AP3 bow:*







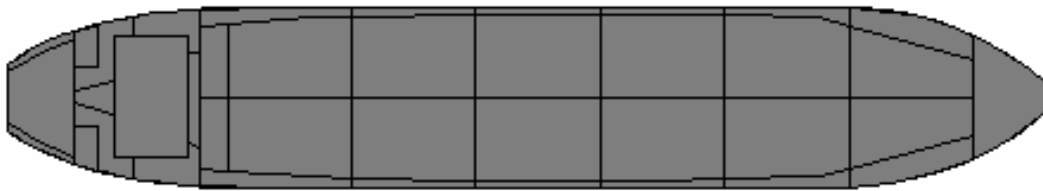


## Appendix E: 150K dwt Double Hull Tanker Cargo Section Structural Data

Naval Architecture

**L = 264 m    B = 48 m    D = 24 m    T = 16.8 m    D = 178867 MT**

Profile and Plan



Weights and Stability

→ Full Load Departure					
Item	Weight MT	VCG m	LCG m-MS	TCG m-CL	FSMom m-MT
Light Ship	22,849	12.960	1.380F	0.000	----
Constant	673	20.740	10.013A	0.000	----
Cargo Oil	150,056	13.523	12.767F	0.000S	254,794
Fuel Oil	4,328	17.069	93.920A	0.004S	3,395
Diesel Oil	334	17.986	106.941A	0.392P	88
Lube Oil	129	16.661	101.003A	7.355P	41
Fresh Water	498	22.596	116.193A	0.000	0
SW Ballast	0	----	----	----	----
Misc.	0	----	----	----	----
Misc. Weights	0	----	----	----	----
Displacement	178,867	13.600	7.980F	0.006P	258,318
Stability Calculation		Trim Calculation			
KMt	19.676 m		LCF Draft	16.800 m	
VCG	13.600 m		LCB (even keel)	7.981F m-MS	
GMt (Solid)	6.076 m		LCF	0.217A m-MS	
FSc	1.444 m		MT1cm	2,111 m-MT	
GMt (Corrected)	4.632 m		Trim	0.000 m	
			List	0.15 deg	

Primary Subdivision

Double Bottom:  $h_{DB} = 2.32$  meters

Double Side:  $w = 2$  meters

Compartment	Mir	# Sta	Aft m-MS	Fwd m-MS
<b>1 FOREPEAK</b>	<b>N</b>	<b>7</b>	<b>119.000F</b>	<b>139.400F</b>
2 FOCSLE DECK	N	5	119.000F	139.000F
3 NO.1 WBT S	Y	13	86.000F	119.000F
4 NO.1 COT S	N	13	86.000F	119.000F
5 NO.1 WBT P	N	13	86.000F	119.000F
6 NO.1 COT P	N	13	86.000F	119.000F
7 NO.2 WBT S	Y	9	53.000F	86.000F
8 NO.2 COT S	Y	9	53.000F	86.000F
9 NO.2 WBT P	N	9	53.000F	86.000F
10 NO.2 COT P	N	9	53.000F	86.000F
11 NO.3 WBT S	Y	7	20.000F	53.000F
12 NO.3 COT S	Y	7	20.000F	53.000F
13 NO.3 WBT P	N	7	20.000F	53.000F
14 NO.3 COT P	N	7	20.000F	53.000F
15 NO.4 WBT S	Y	9	13.000A	20.000F
16 NO.4 COT S	Y	9	13.000A	20.000F
17 NO.4 WBT P	N	9	13.000A	20.000F
18 NO.4 COT P	N	9	13.000A	20.000F
19 NO.5 WBT S	Y	7	46.000A	13.000A
20 NO.5 COT S	Y	7	46.000A	13.000A
21 NO.5 WBT P	N	7	46.000A	13.000A
22 NO.5 COT P	N	7	46.000A	13.000A
23 NO.6 WBT S	Y	11	86.500A	46.000A
24 NO.6 COT S	Y	9	79.000A	46.000A
25 NO.6 WBT P	N	11	86.500A	46.000A
26 NO.6 COT P	N	9	79.000A	46.000A
27 SLOP TANK S	Y	5	86.500A	79.000A
<b>28 SLOP TANK P</b>	<b>N</b>	<b>5</b>	<b>86.500A</b>	<b>79.000A</b>

Full Load cargo

→ Full Load Departure									
Cargo Oil	Weight	%	Capacity	VCG	LCG	TCG	FSmom	Density	Volume
Tank Name	MT	Full	MT	m-BL	m-MS	m-CL	m-MT	MT/m3	m3
NO.1 COT P	8,462	98.0	8,635	13.876	100.607F	7.268P	8,506	0.8550	9,897
NO.1 COT S	8,462	98.0	8,635	13.876	100.607F	7.268S	8,506	0.8550	9,897
NO.2 COT P	12,677	98.0	12,935	13.418	69.217F	10.388P	21,834	0.8550	14,827
NO.2 COT S	12,677	98.0	12,935	13.418	69.217F	10.388S	21,835	0.8550	14,827
NO.3 COT P	13,309	98.0	13,580	13.316	36.449F	10.891P	24,454	0.8550	15,566
NO.3 COT S	13,309	98.0	13,580	13.316	36.449F	10.891S	24,454	0.8550	15,566
NO.4 COT P	13,382	98.0	13,655	13.302	3.504F	10.950P	24,757	0.8550	15,652
NO.4 COT S	13,382	98.0	13,655	13.302	3.504F	10.950S	24,757	0.8550	15,652
NO.5 COT P	13,105	98.0	13,373	13.357	29.387A	10.727P	23,627	0.8550	15,328
NO.5 COT S	13,105	98.0	13,373	13.357	29.387A	10.727S	23,627	0.8550	15,328
NO.6 COT P	11,875	98.0	12,117	13.802	61.844A	9.877P	20,440	0.8550	13,889
NO.6 COT S	11,875	98.0	12,117	13.802	61.844A	9.877S	20,440	0.8550	13,889
SLOP TANK P	2,218	98.0	2,263	14.826	82.680A	8.458P	3,778	0.8550	2,594
SLOP TANK S	2,218	98.0	2,263	14.826	82.680A	8.458S	3,778	0.8550	2,594
<b>Totals</b>	<b>150,056</b>	<b>98.0</b>	<b>153,118</b>	<b>13.523</b>	<b>12.767F</b>	<b>0.000S</b>	<b>254,794</b>		<b>175,504</b>

## Structural Design

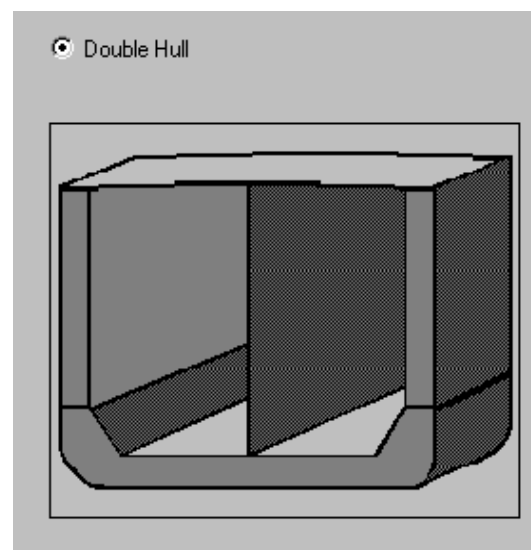
### Ship Dimensions

Title : <input type="text" value="IMO 150 dwt DH Reference Tanker"/>		
Block Coefficient : <input type="text" value="0.83"/>	Design Ship Speed (Knots) : <input type="text" value="13"/>	
Transverse Metacentric Height		Roll Radius Of Gyration
<input checked="" type="radio"/> Rules <input type="radio"/> User Defined		<input checked="" type="radio"/> Rules <input type="radio"/> User Defined
LBP (m) : <input type="text" value="264"/>	Length (m) : <input type="text" value="264"/>	
Breadth (m) : <input type="text" value="48"/>	Depth (m) : <input type="text" value="24"/>	Draft (m) : <input type="text" value="16.8"/>

The diagram illustrates the hull geometry of the ship. The side view shows the ship's profile with the After Perpendicular (A.P.) and Fore Perpendicular (F.P.) marked. The dimensions shown are Length, LBP (Length Between Perpendiculars), and Length of Waterline, LWL. The cross-section shows the hull's Breadth, Depth, and Draft. The coordinate systems are defined with X and Y axes for the side view, and Y and Z axes for the cross-section.

### HULL TYPE



## MIDSHIP GEOMETRY

Camber (m)	<input type="text" value="0.5"/>
Bilge Radius (m)	<input type="text" value="2.5"/>
Gunwale Radius (m)	<input type="text" value="1"/>
Web Spacing (m)	<input type="text" value="3.3"/>
Floor Spacing (m)	<input type="text" value="3.3"/>
Double Bottom Height (m)	<input type="text" value="2.3"/>

**Note:**

1. Camber	4. Bilge Radius
2. Gunwale Radius	5. Floor Spacing
3. Web Spacing	6. Double Bottom Height

## TANK DEFINITION

Definition		
No.	Type	Length (m)
1	Wing Cargo Tank	33.000
2	J Shape Ballast Tank	33.000
3		
4		
5		

**Tank**

Help for defining tank

Characteristics		
No.	Width (m)	Height (m)
1	22.000	22.200
2	24.000	24.023
3		
4		
5		

Press./Vacuum (Kgf/cm<sup>2</sup>) Relief Valve

Cargo Density (tf/m<sup>3</sup>)

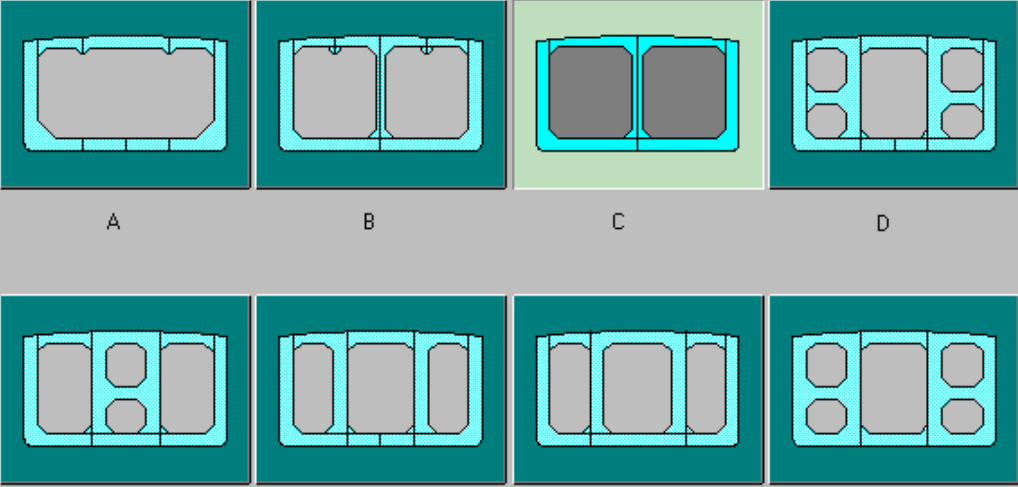
Height of VentPipe (mm)

**Graphics**

# TRANSVERSE MEMBERS

## Web Configuration

**Web Config.** | General Data | Main Supporting Member | Transverse Bulkhead | Corrugated Bulkhead



A B C D

E F G H  
Single Hull Configuration

Spacing

Side Transverse (m) :       Deck Transverse (m) :

Vertical Web On Longitudinal Bulkhead (m) :

### Main Supporting Members – Side Transverse (Web)

Transverse Member Description :

Side Transverse

No.	Bw(m)	Bh(m)	Mat.	Lib.ID	Cont
1L	1.600	2.150	MILD	25	
1U	2.500	2.500	MILD	24	

Web thickness upper = 12 mm

Web thickness lower = 18 mm

### Main Supporting Members – Deck Transverse

Transverse Member Description :

Deck Transverse

No.	Bw(m)	Bh(m)	Mat.	Lib.ID	Width(mm)	Thick(mm)	Cont
20	2.500	2.500	MILD	26	500.000	24.000	✘
2I	2.500	2.500	MILD	26	500.000	24.000	✘

Deck Transverse Web thickness = 15 mm; Depth = 2.5 m

## Main Supporting Members – Vertical Web on Longitudinal Bulkhead

Transverse Member Description :  
 Vertical Web on Longitudinal Bulkhead

No.	Bw(m)	Bh(m)	Mat.	Lib.ID	Width(mm)	Thick(mm)	Cont
3L	2.500	2.500	MILD	27	500.000	24.000	✕
3U	2.500	2.500	MILD	27	500.000	24.000	✕

No.	Other Bh(m)	Other Bw(m)	Depth(m)
3L	2.500	2.500	
3U	2.500	2.500	2.500

CL Bulkhead Vertical Web thickness = 14 mm; Depth = 2.0 m

## Double Bottom Floor / Girder Properties

**Floor/Girder** | Exception

GROUP 1 | Tank Type: Wing Cargo Tank

Desc. Floors | Ls (m) 33

Bs (m) 20.4 | BsM (m) 10.2 | PDBZ (m) 16.5

No. of Floors 9 | No. of Girders 3 | No. of Segments 0

Distances		
No.	Girder	Floor
1	5.100	3.300
2	10.200	6.600
3	15.300	9.900
4		13.200
5		16.500

Girder Material: HT32  
 Floor Material: HT32  
 Girder Thickness (mm): 12  
 Floor Thickness (mm): 15

# Transverse Bulkhead

**Horz Girder On Trn BHD.**
Transverse BHD Plate/Stiffener
Vert Web On Trn BHD.

Group No.

Group

Position Description

L(m)     Lb(m)     Lib.ID

Mat.     Xp(m)     Yp(m)

he(m)     S(m)     Tp(mm)

**Horz Girder On Trn BHD.**
Transverse BHD Plate/Stiffener
Vert Web On Trn BHD.

Group No.

Group

Position Description

L(m)     Lb(m)     Lib.ID

Mat.     Xp(m)     Yp(m)

he(m)     S(m)     Tp(mm)

Horz Girder On Trn BHD.      Transverse BHD Plate/Stiffener      Vert Web On Trn BHD.

Group No.

Group

Position Description

L(m)       Lb(m)       Lib.ID

Mat.       Xp(m)       Yp(m)

he(m)       S(m)       Tp(mm)

Horz Girder On Trn BHD.      Transverse BHD Plate/Stiffener      Vert Web On Trn BHD.

Group No.

Group

Position Description

L(m)       Lb(m)       Lib.ID

Mat.       Xp(m)       Yp(m)

he(m)       S(m)       Tp(mm)

Horz Girder On Trn BHD. **Transverse BHD Plate/Stiffener** Vert Web On Trn BHD.

TB Group 1 Tank Type Wing Cargo Tank

Description Upper Xap (m) 152

Plate

Group Plate 1 Zp (m) 11 SMax (mm) 850 Yp (m) 18.9

Description TB Upper Thick.(mm) 12 Mat MILD

Stiffener

No.	Type	Sp(mm)	Sl(m)	ZStfp(m)	YStfp(m)	Lib.ID	Mat.
1	1	850.00	5.100	11.000	21.450	11	MILD
2							
3							
4							
5							

Horz Girder On Trn BHD. **Transverse BHD Plate/Stiffener** Vert Web On Trn BHD.

TB Group 2 Tank Type Wing Cargo Tank

Description Middle Xap (m) 152

Plate

Group Plate 1 Zp (m) 11 SMax (mm) 850 Yp (m) 13.8

Description TB Middle Thick.(mm) 14 Mat MILD

Stiffener

No.	Type	Sp(mm)	Sl(m)	ZStfp(m)	YStfp(m)	Lib.ID	Mat.
1	1	850.00	5.100	11.000	16.350	16	MILD
2							
3							
4							
5							

Horz Girder On Trn BHD. **Transverse BHD Plate/Stiffener** Vert Web On Trn BHD.

TB Group 3 Tank Type Wing Cargo Tank

Description Lower Xap (m) 152

Plate

Group Plate 1 Zp (m) 11 SMax (mm) 850 Yp (m) 8.7

Description TB Lower Thick.(mm) 16 Mat MILD

Stiffener

No.	Type	Sp(mm)	Sl(m)	ZStfp(m)	YStfp(m)	Lib.ID	Mat.
1	1	850.00	5.100	11.000	11.250	20	MILD
2							
3							
4							
5							

Horz Girder On Trn BHD. **Transverse BHD Plate/Stiffener** Vert Web On Trn BHD.

TB Group 4 Tank Type Wing Cargo Tank

Description Stool Xap (m) 152

Plate

Group Plate 1 Zp (m) 11 SMax (mm) 850 Yp (m) 4.45

Description TB Stool Thick.(mm) 18 Mat MILD

Stiffener

No.	Type	Sp(mm)	Sl(m)	ZStfp(m)	YStfp(m)	Lib.ID	Mat.
1	1	850.00	4.250	11.000	6.575	18	MILD
2							
3							
4							
5							

Horz Girder On Trm BHD.      **Transverse BHD Plate/Stiffener**      Vert Web On Trm BHD.

TB Group 8      Tank Type Wing Cargo Tank

Description Bottom      Xap (m) 152

Plate

Group Plate 1      Zp (m) 11      SMax (mm) 850      Yp (m) 2.3

Description TB Bottom      Thick.(mm) 18      Mat MILD

Stiffener

No.	Type	Sp(mm)	Sl(m)	ZStfp(m)	YStfp(m)	Lib.ID	Mat.
1	1	850.00	2.150	11.000	3.375	8	MILD
2							
3							
4							
5							

Horz Girder On Trm BHD.      **Transverse BHD Plate/Stiffener**      Vert Web On Trm BHD.

TB Group 5      Tank Type J Shape Ballast Tank

Description Upper      Xap (m) 152

Plate

Group Plate 1      Zp (m) 23      SMax (mm) 668      Yp (m) 18.9

Description J Tank TB Upper      Thick.(mm) 12      Mat MILD

Stiffener

No.	Type	Sp(mm)	Sl(m)	ZStfp(m)	YStfp(m)	Lib.ID	Mat.
1	1	668.00	5.100	23.000	21.450	10	MILD
2							
3							
4							
5							

Horz Girder On Trn BHD. **Transverse BHD Plate/Stiffener** Vert Web On Trn BHD.

TB Group 6 Tank Type J Shape Ballast Tank

Description Middle Xap (m) 152

Plate  
Group Plate 1 Zp (m) 23 SMax (mm) 668 Yp (m) 13.8

Description J Tank TB Middle Thick.(mm) 12 Mat MILD

Stiffener

No.	Type	Sp(mm)	Sl(m)	ZStfp(m)	YStfp(m)	Lib.ID	Mat.
1	1	668.00	5.100	11.000	16.350	14	MILD
2							
3							
4							
5							

Horz Girder On Trn BHD. **Transverse BHD Plate/Stiffener** Vert Web On Trn BHD.

TB Group 7 Tank Type J Shape Ballast Tank

Description Lower Xap (m) 152

Plate  
Group Plate 1 Zp (m) 23 SMax (mm) 668 Yp (m) 8.7

Description J Tank TB Lower Thick.(mm) 14 Mat MILD

Stiffener

No.	Type	Sp(mm)	Sl(m)	ZStfp(m)	YStfp(m)	Lib.ID	Mat.
1	1	668.00	5.100	23.000	11.250	17	MILD
2							
3							
4							
5							

Horz Girder On Trm BHD. **Transverse BHD Plate/Stiffener** Vert Web On Trm BHD.

TB Group 9 Tank Type J Shape Ballast Tank

Description Stool Xap (m) 152

Plate

Group Plate 1 Zp (m) 23 SMax (mm) 668 Yp (m) 4.45

Description J tank TB Stool Thick.(mm) 14 Mat MILD

Stiffener

No.	Type	Sp(mm)	Sl(m)	ZStfp(m)	YStfp(m)	Lib.ID	Mat.
1	1	668.00	4.250	23.000	6.575	16	MILD
2							
3							
4							
5							

Horz Girder On Trm BHD. **Transverse BHD Plate/Stiffener** Vert Web On Trm BHD.

TB Group 10 Tank Type J Shape Ballast Tank

Description IB Xap (m) 152

Plate

Group Plate 1 Zp (m) 12 SMax (mm) 850 Yp (m) 0

Description TB IB Thick.(mm) 20 Mat MILD

Stiffener

No.	Type	Sp(mm)	Sl(m)	ZStfp(m)	YStfp(m)	Lib.ID	Mat.
1	1	850.00	2.300	12.000	1.150	9	MILD
2							
3							
4							
5							

Material

**Material Zones:**

Bottom			
Mat.	Yield (kg/cm <sup>2</sup> )	Ultimate (kg/cm <sup>2</sup> )	Q
HT32	3200.0	4500.0	0.78

Side			
Mat.	Yield (kg/cm <sup>2</sup> )	Ultimate (kg/cm <sup>2</sup> )	Q
MILD	2400.0	4100.0	1.00

Deck			
Mat.	Yield (kg/cm <sup>2</sup> )	Ultimate (kg/cm <sup>2</sup> )	Q
HT32	3200.0	4500.0	0.78

Note:  
1. Bottom Zone  
2. Side Zone  
3. Deck Zone

**MATERIAL TABLE**

MAT # (kgf/cm <sup>2</sup> )	MAT ID (kgf/cm <sup>2</sup> )	YIELD STRESS	ULT STRESS	Q-FAC	Sm
1	MILD	2400.	4100.	1.000	1.0
2	HT32	3200.	4500.	.780	.950
3	HT36	3600.	5000.	.720	.908
4	HT40	4000.	5200.	.680	.875

## Stiffener Library:

#ID#	TYPE	ABS ID	DESCRIPTION	VAR 1 (mm)	VAR 2 (mm)	VAR 3 (mm)	VAR 4 (mm)	VAR 5 (mm)	VAR 6 (mm)
1	LANG	ILA200A	200x90x9x12 LIA	200.00	90.00	9.00	12.00	7.50	15.00
2	LANG	ILA225A	225x90x9x12 LIA	225.00	90.00	9.00	12.00	7.50	15.00
3	LANG	ILA250A	250x90x9x13 LIA	250.00	90.00	9.00	13.00	7.50	15.00
4	LANG	ILA250B	250x90x10.5x15 LIA	250.00	90.00	10.50	15.00	7.50	15.00
5	LANG	ILA250C	250x90x11.5x16 LIA	250.00	90.00	11.50	16.00	7.50	15.00
6	LANG	ILA275A	250x100x10.5x14 LIA	275.00	100.00	10.50	14.00	7.50	15.00
7	LANG	ILA300A	300x100x10.5x15 LIA	300.00	100.00	10.50	15.00	7.50	15.00
8	LANG	ILA300B	300x100x11.5x16 LIA	300.00	100.00	11.50	16.00	7.50	15.00
9	LANG	ILA325A	325x120x10.5x14 LIA	325.00	120.00	10.50	14.00	10.00	20.00
10	LANG	ILA325B	325x120x11.5x15 LIA	325.00	120.00	11.50	15.00	10.00	20.00
11	LANG	ILA350A	350x120x10.5x16 LIA	350.00	120.00	10.50	16.00	10.00	20.00
12	LANG	ILA350B	350x120x11.5x18 LIA	350.00	120.00	11.50	18.00	10.00	20.00
13	LANG	ILA375A	375x120x10.5x18 LIA	375.00	120.00	10.50	18.00	10.00	20.00
14	LANG	ILA375B	375x120x11.5x20 LIA	375.00	120.00	11.50	20.00	10.00	20.00
15	LANG	ILA400A	400x120x11.5x23 LIA	400.00	120.00	11.50	23.00	10.00	20.00
16	LANG	ILA425A	425x120x11.5x24 LIA	425.00	120.00	11.50	24.00	10.00	20.00
17	LANG	ILA450A	450x120x11.5x25 LIA	450.00	120.00	11.50	25.00	10.00	20.00
18	LANG	ILA475A	475x120x11.5x28 LIA	475.00	120.00	11.50	28.00	10.00	20.00
19	LANG	ILA475B	475x120x12.5x30 LIA	475.00	120.00	12.50	30.00	10.00	20.00
20	LANG	ILA500A	500x120x12.5x33 LIA	500.00	120.00	12.50	33.00	10.00	20.00
21	LANG	ILA500B	500x120x13.5x35 LIA	500.00	120.00	13.50	35.00	10.00	20.00
22	FLAT	USER-DEF	FB 400x28	400.00	28.00				
23	UANG	IUA150G	150X90X15 UIA	150.00	90.00	15.00	15.00	6.00	12.00
24	FLAT	USER-DEF	FB2000X12	2000.00	12.00				
25	FLAT	USER-DEF	FB2000X18	2000.00	18.00				
26	MSTF	USER-DEF	DECK WEB		3				
27	MSTF	USER-DEF	LBHD WEB		7				
28	MSTF	USER-DEF	BHD L STR		4				
29	MSTF	USER-DEF	BHD U STR		4				

## User-Defined Shapes / Webs:

**Built-up Multi-Stiffener**

ID#	Type	ABSID	Description
26	MSTF	USER-DEF	DECK WEB

Attach Point		Plate DIM's		Stiffener	
X(mm)	Y(mm)	Theta	t(mm)	l(mm)	STF ID FAC
1	0.00	0.00	15.00	2500.00	
2	250.00	2512.00	90.00	24.00	500.00
3	-7.50	2000.00	90.00	20.00	200.00
4					
5					

Stiffener Properties

Area: 535.000 cm<sup>2</sup> Web-area: 375.000 cm<sup>2</sup>  
 Depth: 252.400 cm AS<sub>stiff</sub>: 535.000 cm<sup>2</sup>

Stiffener Centroids:  $\bar{y} = 158.914$  cm,  $\bar{x} = -0.804$  cm

Stiffener Moments of Inertia:  $I_{xx} = 3474032.750$  cm<sup>4</sup>,  $I_{yy} = 30680.539$  cm<sup>4</sup>,  $I_{xy} = -17666.973$  cm<sup>4</sup>

Stiffener Section Moduli:  $SM_{x,t} = 37161.004$  cm<sup>3</sup>,  $SM_{x,b} = 21861.084$  cm<sup>3</sup>,  $SM_{yy} = 1188.996$  cm<sup>3</sup>

Corrosion margins (mm): Plate: 0.00, Web: 0.00, Flange: 0.00

Attached Plate (mm): Breadth: 0.00, Thickness: 0.00

Plate Offset: X (mm): 0, Angle (deg): 0

Buttons: Save, Graphics, Copy Multistiffener, OK, Cancel

**Graphics**

All dimensions are in m

Close

**Built-up Multi-Stiffener**

ID#	Type	ABSID	Description
27	MSTF	USER-DEF	LBHD WEB

Attach Point		Plate DIM's		Stiffener	
X(mm)	Y(mm)	Theta	t(mm)	l(mm)	STF ID FAC
1	0.00	8.00	0.00	14.00	2000.00
2	250.00	2018.00	90.00	18.00	450.00
3	-8.00	1508.00	90.00	16.00	200.00
4	1650.00	0.00	90.00	16.00	3300.00
5	0.00	-8.00	180.00	14.00	2000.00

Stiffener Properties

Area: 1314.000 cm<sup>2</sup> Web-area: 560.000 cm<sup>2</sup>  
 Depth: 405.400 cm AS<sub>stiff</sub>: 1314.000 cm<sup>2</sup>

Stiffener Centroids:  $\bar{y} = -0.000$  cm,  $\bar{x} = -0.218$  cm

Stiffener Moments of Inertia:  $I_{xx} = 15609361.000$  cm<sup>4</sup>,  $I_{yy} = 4829577.500$  cm<sup>4</sup>,  $I_{xy} = -0.001$  cm<sup>4</sup>

Stiffener Section Moduli:  $SM_{x,t} = 77007.211$  cm<sup>3</sup>,  $SM_{x,b} = 77007.211$  cm<sup>3</sup>,  $SM_{yy} = 29231.578$  cm<sup>3</sup>

Corrosion margins (mm): Plate: 0.00, Web: 0.00, Flange: 0.00

Attached Plate (mm): Breadth: 0.00, Thickness: 0.00

Plate Offset: X (mm): 0, Angle (deg): 0

Buttons: Save, Graphics, Copy Multistiffener, OK, Cancel

**Graphics**

All dimensions are in m

Close

**Built-up Multi-Stiffener**

ID#	Type	ABSID	Description
28	MSTF	USER-DEF	BHD L STR

Attach Point		Plate DIM's		Stiffener	
X(mm)	Y(mm)	Theta	t(mm)	l(mm)	STF
1	0.00	0.00	18.00	3500.00	
2	350.00	3512.00	90.00	24.00	700.00
3	8.00	2000.00	90.00	20.00	200.00
4	8.00	2800.00	90.00	20.00	200.00
5					

Stiffener Properties

Area: 878.000 cm<sup>2</sup> Web-area: 630.000 cm<sup>2</sup>  
 Depth: 352.400 cm ASstiff: 878.000 cm<sup>2</sup>

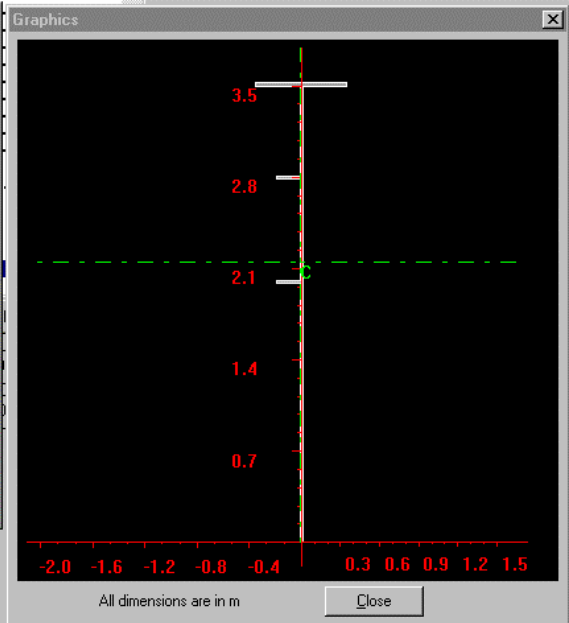
Centroid: 214.637 cm X̄, -0.838 cm ȳ

SMx,t: 77914.563 cm<sup>3</sup> SMx,b: 50008.609 cm<sup>3</sup>  
 SMyy: 2185.032 cm<sup>3</sup>

Corrosion margins (mm): Plate: 0.00, Web: 0.00, Flange: 0.00  
 Attached Plate (mm): Breadth: 0.00, Thickness: 0.00

Plate Offset: X (mm): 0, Angle (deg): 0

Buttons: Save, Graphics, Copy Multistiffener, OK, Cancel



**Built-up Multi-Stiffener**

ID#	Type	ABSID	Description
29	MSTF	USER-DEF	BHD U STR

Attach Point		Plate DIM's		Stiffener	
X(mm)	Y(mm)	Theta	t(mm)	l(mm)	STF
1	0.00	0.00	14.00	3500.00	
2	350.00	3512.00	90.00	24.00	700.00
3	7.00	2000.00	90.00	20.00	200.00
4	7.00	2800.00	90.00	20.00	200.00
5					

Stiffener Properties

Area: 738.000 cm<sup>2</sup> Web-area: 490.000 cm<sup>2</sup>  
 Depth: 352.400 cm ASstiff: 738.000 cm<sup>2</sup>

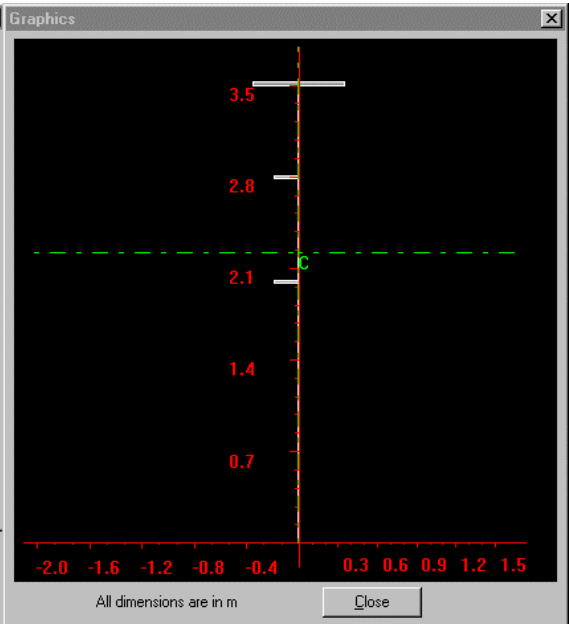
Centroid: 222.157 cm X̄, -1.008 cm ȳ

SMx,t: 69430.539 cm<sup>3</sup> SMx,b: 40704.910 cm<sup>3</sup>  
 SMyy: 2152.732 cm<sup>3</sup>

Corrosion margins (mm): Plate: 0.00, Web: 0.00, Flange: 0.00  
 Attached Plate (mm): Breadth: 0.00, Thickness: 0.00

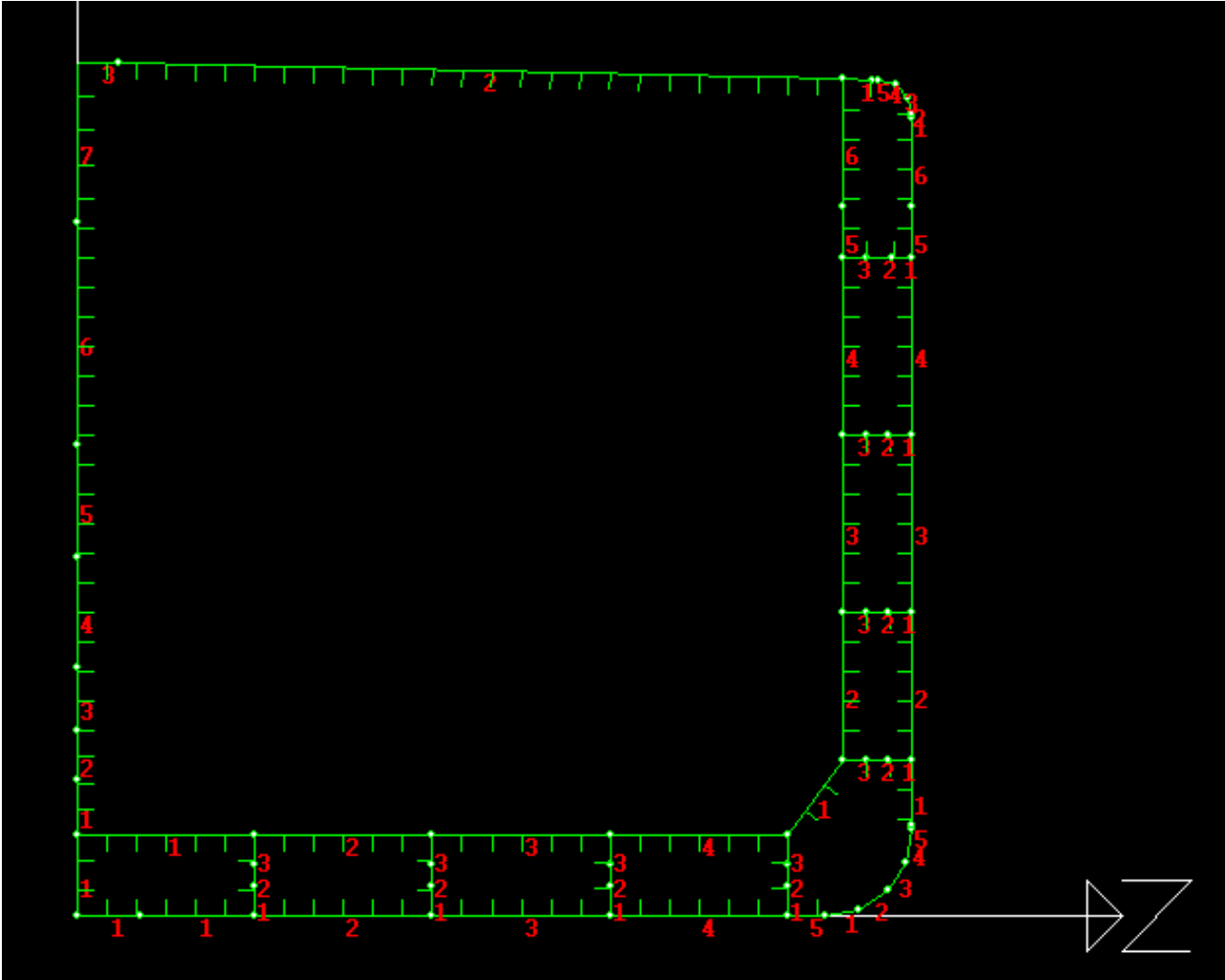
Plate Offset: X (mm): 0, Angle (deg): 0

Buttons: Save, Graphics, Copy Multistiffener, OK, Cancel



Longitudinal Plate and Stiffener Elements

Local Plate IDs:



Global Plate Ids:

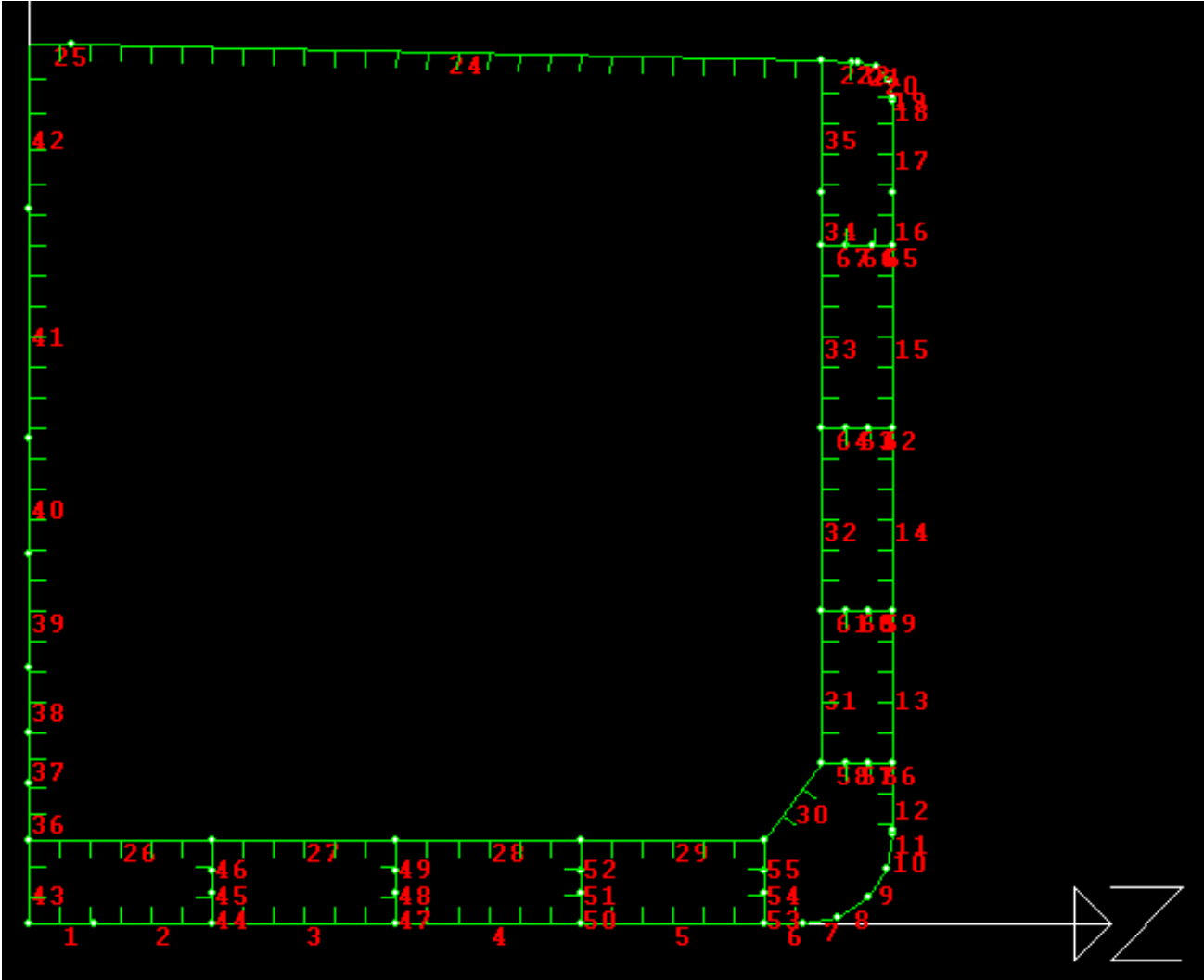
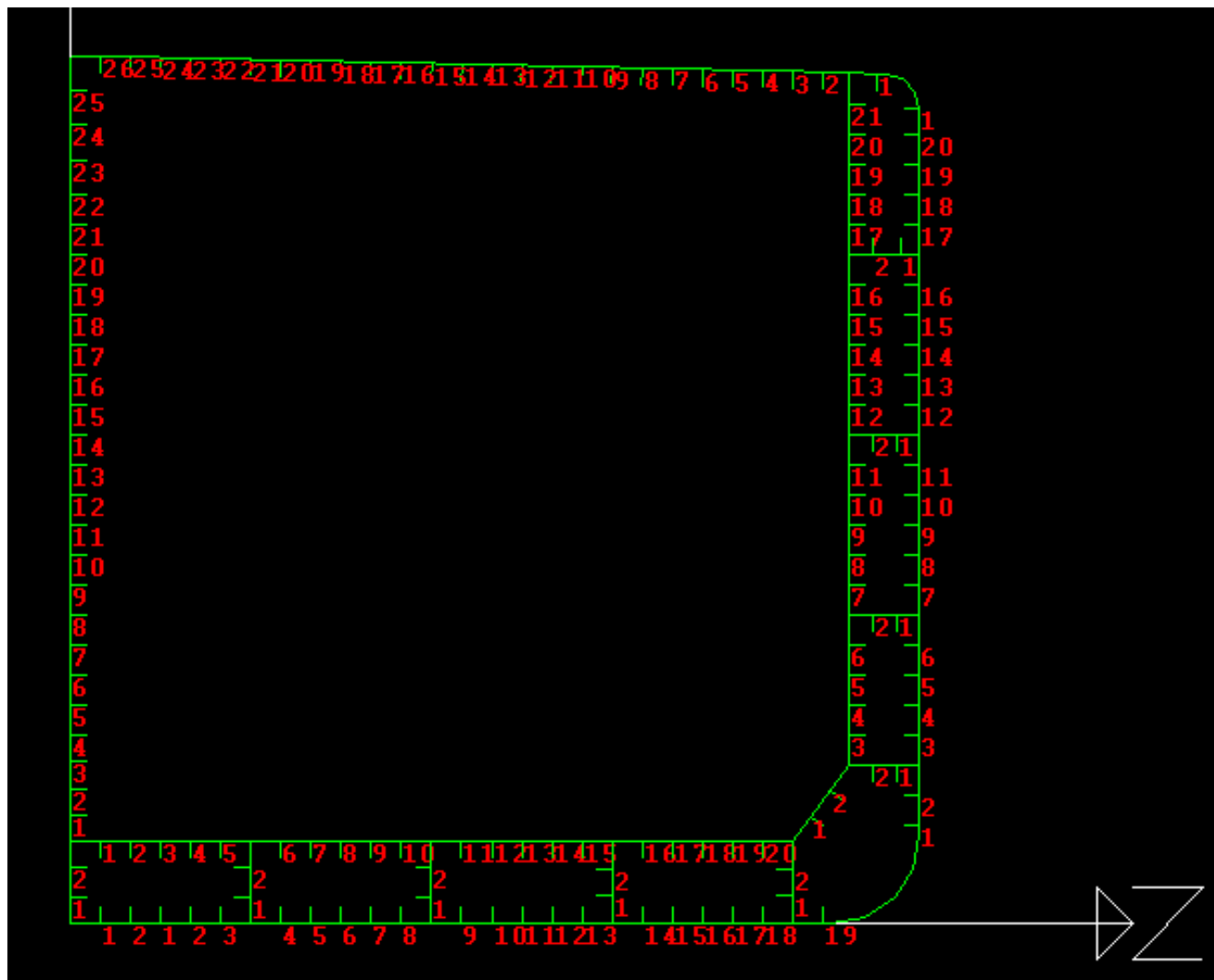


Plate:

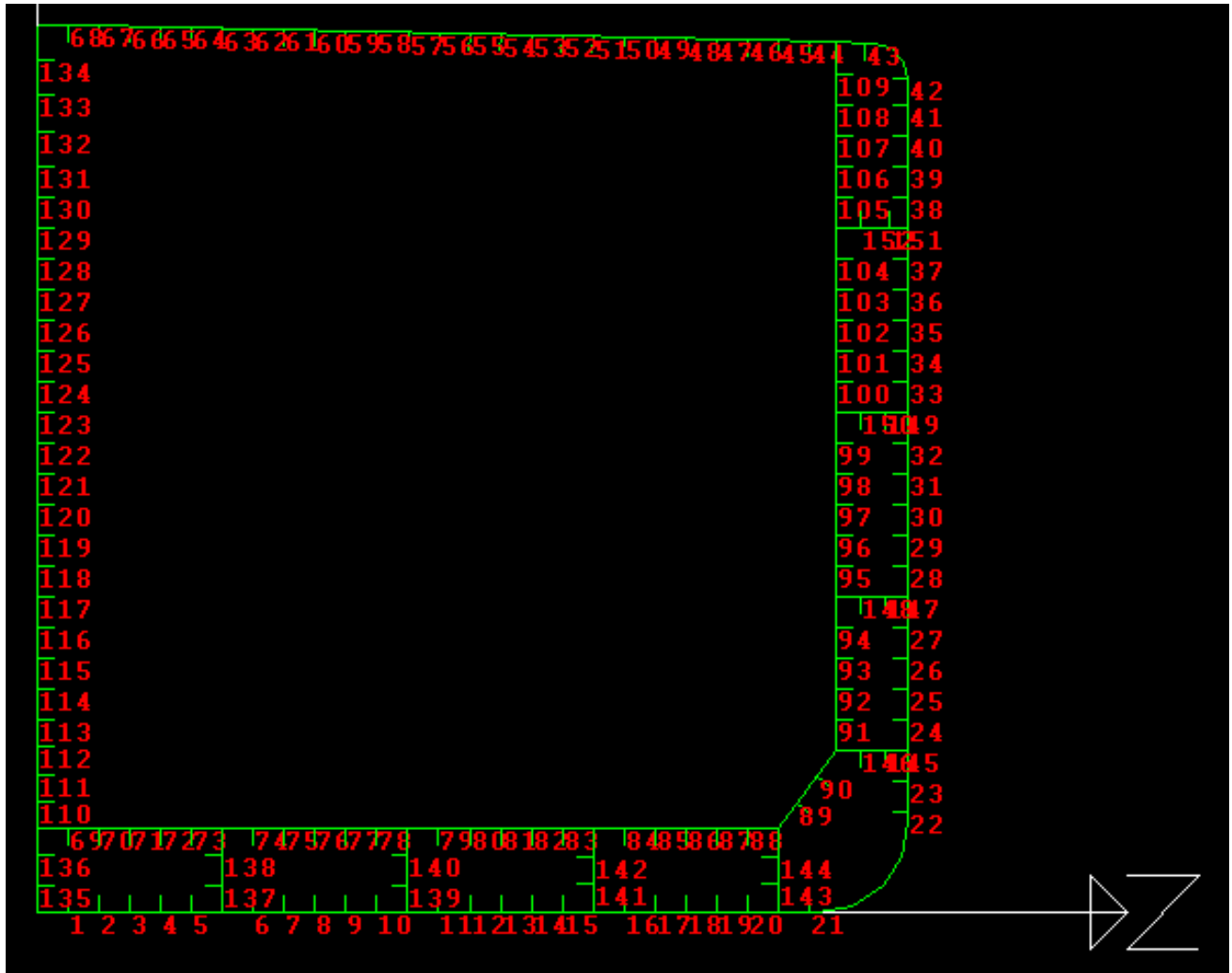
SEQ	ID	DESCRIPTION	B	THK	CORROSION	A	SPACING	MATID	START	NODE	END NODE	
NO			m	cm	(mm)	cm2	(m)		X-COORD	Y-COORD	X-COORD	Y-COORD
									(METER)	(METER)	(METER)	(METER)
1	KPL-01	KEEL PLATE	1.8	1.9	1	342	0.85	2	0	0	1.8	0
2	BTM-01	BOTTOM	3.3	1.7	1	561	0.85	2	1.8	0	5.1	0
3	BTM-02	BOTTOM	5.1	1.7	1	867	0.85	2	5.1	0	10.2	0
4	BTM-03	BOTTOM	5.1	1.7	1	867	0.85	2	10.2	0	15.3	0
5	BTM-04	BOTTOM	5.1	1.7	1	867	0.85	2	15.3	0	20.4	0
6	BTM-05	BOTTOM	1.1	1.7	1	187	0.85	2	20.4	0	21.5	0
7	BLG-01	BILGE	0.976	1.7	1	165.87	2.201	2	21.5	0	22.457	0.19
8	BLG-02	BILGE	0.975	1.7	1	165.82	2.927	2	22.457	0.19	23.268	0.732
9	BLG-03	BILGE	0.975	1.7	1	165.82	2.927	2	23.268	0.732	23.81	1.543
10	BLG-04	BILGE	0.976	1.7	1	165.87	2.201	2	23.81	1.543	24	2.5
11	BLG-05	BILGE	0.1	1.7	1	17	1.226	2	24	2.5	24	2.6
12	SHL-01	SIDE	1.85	1.7	1.5	314.5	0.85	2	24	2.6	24	4.45
13	SHL-02	SIDE	4.25	1.8	1.5	765	0.85	1	24	4.45	24	8.7
14	SHL-03	SIDE	5.1	1.8	1.5	918	0.85	1	24	8.7	24	13.8
15	SHL-04	SIDE	5.1	1.8	1.5	918	0.85	1	24	13.8	24	18.9
16	SHL-05	SIDE	1.45	1.8	1.5	261	0.85	1	24	18.9	24	20.35
17	SHL-06	SIDE	2.55	2	1.5	510	0.85	2	24	20.35	24	22.9
18	GWR-01	GUNWALE	0.1	2	2	20	0.7	2	24	22.9	24	23
19	GWR-02	GUNWALE	0.518	2	2	103.53	0.518	2	24	23	23.866	23.5
20	GWR-03	GUNWALE	0.518	2	2	103.52	0.518	2	23.866	23.5	23.5	23.866
21	GWR-04	GUNWALE	0.518	2	2	103.53	0.718	2	23.5	23.866	23	24
22	GWR-05	GUNWALE	0.15	2	2	30.01	0.718	2	23	24	22.85	24.003
23	DEC-01	UPPER DECK	0.85	2	2	170.05	0.8	2	22.85	24.003	22	24.023
24	DEC-02	UPPER DECK	20.805	1.9	1	3953.04	0.855	2	22	24.023	1.2	24.5
25	DEC-03	UPPER DECK	1.2	1.9	1	228	0.855	2	1.2	24.5	0	24.5
26	INB-01	INNER BOTTOM	5.1	1.7	1.5	867	0.85	2	0	2.3	5.1	2.3
27	INB-02	INNER BOTTOM	5.1	1.7	1.5	867	0.85	2	5.1	2.3	10.2	2.3
28	INB-03	INNER BOTTOM	5.1	1.7	1.5	867	0.85	2	10.2	2.3	15.3	2.3
29	INB-04	INNER BOTTOM	5.1	1.7	1.5	867	0.85	2	15.3	2.3	20.4	2.3
30	INS-01	I.S. BULKHEAD	2.68	2	1.5	536	0.9	2	20.4	2.3	22	4.45
31	INS-02	I.S. BULKHEAD	4.25	1.8	1.5	765	0.85	2	22	4.45	22	8.7
32	INS-03	I.S. BULKHEAD	5.1	1.9	1.5	969	0.85	1	22	8.7	22	13.8
33	INS-04	I.S. BULKHEAD	5.1	1.6	1.5	816	0.85	1	22	13.8	22	18.9
34	INS-05	I.S. BULKHEAD	1.45	1.65	1.5	239.25	0.85	1	22	18.9	22	20.35
35	INS-06	I.S. BULKHEAD	3.673	1.8	1.5	661.14	0.873	2	22	20.35	22	24.023
36	CTR-01	C.L. BULKHEAD	1.6	1.6	1	128	0.75	2	0	2.3	0	3.9
37	CTR-02	C.L. BULKHEAD	1.4	1.65	1	115.5	0.75	1	0	3.9	0	5.3
38	CTR-03	C.L. BULKHEAD	1.8	1.65	1	148.5	0.85	1	0	5.3	0	7.1

SEQ	ID		B	THK	CORROSION	A	SPACING	MATID	START	NODE	END NODE	
39	CTR-04	C.L. BULKHEAD	3.2	1.6	1	256	0.85	1	0	7.1	0	10.3
40	CTR-05	C.L. BULKHEAD	3.2	1.5	1	240	0.85	1	0	10.3	0	13.5
41	CTR-06	C.L. BULKHEAD	6.4	1.5	1	480	0.85	1	0	13.5	0	19.9
42	CTR-07	C.L. BULKHEAD	4.6	1.8	1	414	0.975	2	0	19.9	0	24.5
43	BGR-01	W.T.BTM.GIRDER	2.3	1.8	2	207	0.8	2	0	0	0	2.3
44	NBG-01	N-TIGHT B. GDR	0.85	1.4	2	119	0.8	2	5.1	0	5.1	0.85
45	NBG-02	N-TIGHT B. GDR	0.6	0	2	0	0.8	2	5.1	0.85	5.1	1.45
46	NBG-03	N-TIGHT B. GDR	0.85	1.4	2	119	0.8	2	5.1	1.45	5.1	2.3
47	NBG-04	N-TIGHT B. GDR	0.85	1.4	2	119	0.8	2	10.2	0	10.2	0.85
48	NBG-05	N-TIGHT B. GDR	0.6	0	2	0	0.8	2	10.2	0.85	10.2	1.45
49	NBG-06	N-TIGHT B. GDR	0.85	1.4	2	119	0.8	2	10.2	1.45	10.2	2.3
50	NBG-07	N-TIGHT B. GDR	0.85	1.5	2	127.5	0.8	2	15.3	0	15.3	0.85
51	NBG-08	N-TIGHT B. GDR	0.6	0	2	0	0.7	2	15.3	0.85	15.3	1.45
52	NBG-09	N-TIGHT B. GDR	0.85	1.5	2	127.5	0.8	2	15.3	1.45	15.3	2.3
53	NBG-10	N-TIGHT B. GDR	0.85	1.5	2	127.5	0.8	2	20.4	0	20.4	0.85
54	NBG-11	N-TIGHT B. GDR	0.6	0	2	0	0.7	2	20.4	0.85	20.4	1.45
55	NBG-12	N-TIGHT B. GDR	0.85	1.5	2	127.5	0.8	2	20.4	1.45	20.4	2.3
56	NTS-01	NON-TIGHT STR	0.7	1.2	2	84	0.7	1	24	4.45	23.3	4.45
57	NTS-02	NON-TIGHT STR	0.6	0	2	0	0.7	1	23.3	4.45	22.7	4.45
58	NTS-03	NON-TIGHT STR	0.7	1.2	2	84	0.7	1	22.7	4.45	22	4.45
59	NTS-04	NON-TIGHT STR	0.7	1.2	2	84	0.7	1	24	8.7	23.3	8.7
60	NTS-05	NON-TIGHT STR	0.6	0	2	0	0.7	1	23.3	8.7	22.7	8.7
61	NTS-06	NON-TIGHT STR	0.7	1.2	2	84	0.7	1	22.7	8.7	22	8.7
62	NTS-07	NON-TIGHT STR	0.7	1.2	2	84	0.7	1	24	13.8	23.3	13.8
63	NTS-08	NON-TIGHT STR	0.6	0	2	0	0.7	1	23.3	13.8	22.7	13.8
64	NTS-09	NON-TIGHT STR	0.7	1.2	2	84	0.7	1	22.7	13.8	22	13.8
65	NTS-10	NON-TIGHT STR	0.6	1.2	2	72	0.8	1	24	18.9	23.4	18.9
66	NTS-11	NON-TIGHT STR	0.7	0	2	0	0.8	1	23.4	18.9	22.7	18.9
67	NTS-12	NON-TIGHT STR	0.7	1.2	2	84	0.8	1	22.7	18.9	22	18.9

Local Stiffener Ids:



Global Stiffener IDs:



**Stiffeners:**

ID	SID	XLB	A	STFSP	MATID
			cm2	(m)	
KPL- 101	15	400x120x11.5x23 LIA	71.6	0.85	2
KPL- 102	15	400x120x11.5x23 LIA	71.6	0.85	2
BTM- 101	15	400x120x11.5x23 LIA	71.6	0.85	2
BTM- 102	15	400x120x11.5x23 LIA	71.6	0.85	2
BTM- 103	15	400x120x11.5x23 LIA	71.6	0.85	2
BTM- 204	15	400x120x11.5x23 LIA	71.6	0.85	2
BTM- 205	15	400x120x11.5x23 LIA	71.6	0.85	2
BTM- 206	15	400x120x11.5x23 LIA	71.6	0.85	2
BTM- 207	15	400x120x11.5x23 LIA	71.6	0.85	2
BTM- 208	15	400x120x11.5x23 LIA	71.6	0.85	2
BTM- 309	15	400x120x11.5x23 LIA	71.6	0.85	2
BTM- 310	15	400x120x11.5x23 LIA	71.6	0.85	2
BTM- 311	15	400x120x11.5x23 LIA	71.6	0.85	2
BTM- 312	15	400x120x11.5x23 LIA	71.6	0.85	2
BTM- 313	15	400x120x11.5x23 LIA	71.6	0.85	2
BTM- 414	15	400x120x11.5x23 LIA	71.6	0.85	2
BTM- 415	15	400x120x11.5x23 LIA	71.6	0.85	2
BTM- 416	15	400x120x11.5x23 LIA	71.6	0.85	2
BTM- 417	15	400x120x11.5x23 LIA	71.6	0.85	2
BTM- 418	15	400x120x11.5x23 LIA	71.6	0.85	2
BTM- 519	15	400x120x11.5x23 LIA	71.6	0.85	2
SHL- 101	12	350x120x11.5x18 LIA	60.42	0.85	2
SHL- 102	12	350x120x11.5x18 LIA	60.42	0.85	2
SHL- 203	12	350x120x11.5x18 LIA	60.42	0.85	2
SHL- 204	12	350x120x11.5x18 LIA	60.42	0.85	2
SHL- 205	12	350x120x11.5x18 LIA	60.42	0.85	1
SHL- 206	11	350x120x10.5x16 LIA	54.91	0.85	1
SHL- 307	11	350x120x10.5x16 LIA	54.91	0.85	1
SHL- 308	9	325x120x10.5x14 LIA	50.1	0.85	1
SHL- 309	9	325x120x10.5x14 LIA	50.1	0.85	1
SHL- 310	9	325x120x10.5x14 LIA	50.1	0.85	1
SHL- 311	9	325x120x10.5x14 LIA	50.1	0.85	1
SHL- 412	7	300x100x10.5x15 LIA	45.29	0.85	1
SHL- 413	7	300x100x10.5x15 LIA	45.29	0.85	1
SHL- 414	7	300x100x10.5x15 LIA	45.29	0.85	1
SHL- 415	7	300x100x10.5x15 LIA	45.29	0.85	1
SHL- 416	7	300x100x10.5x15 LIA	45.29	0.85	1
SHL- 517	7	300x100x10.5x15 LIA	45.29	0.85	1
SHL- 618	7	300x100x10.5x15 LIA	45.29	0.85	1

ID	SID	XLB	A	STFSP	MATID
SHL- 619	5	250x90x11.5x16 LIA	41.67	0.85	2
SHL- 620	5	250x90x11.5x16 LIA	41.67	0.85	2
GWR- 101	5	250x90x11.5x16 LIA	41.67	0.05	2
DEC- 101	22	FB 400x28	112	0.425	2
DEC- 202	22	FB 400x28	112	0.8	2
DEC- 203	22	FB 400x28	112	0.85	2
DEC- 204	22	FB 400x28	112	0.85	2
DEC- 205	22	FB 400x28	112	0.85	2
DEC- 206	22	FB 400x28	112	0.85	2
DEC- 207	22	FB 400x28	112	0.85	2
DEC- 208	22	FB 400x28	112	0.85	2
DEC- 209	22	FB 400x28	112	0.85	2
DEC- 210	22	FB 400x28	112	0.85	2
DEC- 211	22	FB 400x28	112	0.85	2
DEC- 212	22	FB 400x28	112	0.85	2
DEC- 213	22	FB 400x28	112	0.85	2
DEC- 214	22	FB 400x28	112	0.85	2
DEC- 215	22	FB 400x28	112	0.85	2
DEC- 216	22	FB 400x28	112	0.85	2
DEC- 217	22	FB 400x28	112	0.85	2
DEC- 218	22	FB 400x28	112	0.85	2
DEC- 219	22	FB 400x28	112	0.85	2
DEC- 220	22	FB 400x28	112	0.85	2
DEC- 221	22	FB 400x28	112	0.85	2
DEC- 222	22	FB 400x28	112	0.85	2
DEC- 223	22	FB 400x28	112	0.85	2
DEC- 224	22	FB 400x28	112	0.85	2
DEC- 225	22	FB 400x28	112	1.103	2
DEC- 326	22	FB 400x28	112	0.6	2
INB- 101	15	400x120x11.5x23 LIA	71.6	0.85	2
INB- 102	15	400x120x11.5x23 LIA	71.6	0.85	2
INB- 103	15	400x120x11.5x23 LIA	71.6	0.85	2
INB- 104	15	400x120x11.5x23 LIA	71.6	0.85	2
INB- 105	15	400x120x11.5x23 LIA	71.6	0.85	2
INB- 206	15	400x120x11.5x23 LIA	71.6	0.85	2
INB- 207	15	400x120x11.5x23 LIA	71.6	0.85	2
INB- 208	15	400x120x11.5x23 LIA	71.6	0.85	2
INB- 209	15	400x120x11.5x23 LIA	71.6	0.85	2
INB- 210	15	400x120x11.5x23 LIA	71.6	0.85	2
INB- 311	15	400x120x11.5x23 LIA	71.6	0.85	2
INB- 312	15	400x120x11.5x23 LIA	71.6	0.85	2
INB- 313	15	400x120x11.5x23 LIA	71.6	0.85	2

ID	SID	XLB	A	STFSP	MATID
INB- 314	15	400x120x11.5x23 LIA	71.6	0.85	2
INB- 315	15	400x120x11.5x23 LIA	71.6	0.85	2
INB- 416	15	400x120x11.5x23 LIA	71.6	0.85	2
INB- 417	15	400x120x11.5x23 LIA	71.6	0.85	2
INB- 418	15	400x120x11.5x23 LIA	71.6	0.85	2
INB- 419	15	400x120x11.5x23 LIA	71.6	0.85	2
INB- 420	15	400x120x11.5x23 LIA	71.6	0.85	2
INS- 101	13	375x120x10.5x18 LIA	59.73	0.895	2
INS- 102	13	375x120x10.5x18 LIA	59.73	0.895	2
INS- 203	13	375x120x10.5x18 LIA	59.73	0.85	2
INS- 204	13	375x120x10.5x18 LIA	59.73	0.85	2
INS- 205	12	350x120x11.5x18 LIA	60.42	0.85	1
INS- 206	12	350x120x11.5x18 LIA	60.42	0.85	1
INS- 307	11	350x120x10.5x16 LIA	54.91	0.85	1
INS- 308	11	350x120x10.5x16 LIA	54.91	0.85	1
INS- 309	11	350x120x10.5x16 LIA	54.91	0.85	1
INS- 310	11	350x120x10.5x16 LIA	54.91	0.85	1
INS- 311	11	350x120x10.5x16 LIA	54.91	0.85	1
INS- 412	11	350x120x10.5x16 LIA	54.91	0.85	1
INS- 413	11	350x120x10.5x16 LIA	54.91	0.85	1
INS- 414	7	300x100x10.5x15 LIA	45.29	0.85	1
INS- 415	7	300x100x10.5x15 LIA	45.29	0.85	1
INS- 416	7	300x100x10.5x15 LIA	45.29	0.85	1
INS- 517	7	300x100x10.5x15 LIA	45.29	0.85	1
INS- 618	7	300x100x10.5x15 LIA	45.29	0.85	1
INS- 619	7	300x100x10.5x15 LIA	45.29	0.85	1
INS- 620	7	300x100x10.5x15 LIA	45.29	0.85	1
INS- 621	7	300x100x10.5x15 LIA	45.29	0.862	1
CTR- 101	11	350x120x10.5x16 LIA	27.46	0.75	2
CTR- 102	11	350x120x10.5x16 LIA	27.46	0.75	2
CTR- 203	11	350x120x10.5x16 LIA	27.46	0.75	1
CTR- 204	11	350x120x10.5x16 LIA	27.46	0.8	1
CTR- 305	11	350x120x10.5x16 LIA	27.46	0.85	1
CTR- 306	11	350x120x10.5x16 LIA	27.46	0.85	1
CTR- 407	11	350x120x10.5x16 LIA	27.46	0.85	1
CTR- 408	11	350x120x10.5x16 LIA	27.46	0.85	1
CTR- 409	11	350x120x10.5x16 LIA	27.46	0.85	1
CTR- 510	11	350x120x10.5x16 LIA	27.46	0.85	1
CTR- 511	9	325x120x10.5x14 LIA	25.05	0.85	1
CTR- 512	9	325x120x10.5x14 LIA	25.05	0.85	1
CTR- 513	9	325x120x10.5x14 LIA	25.05	0.85	1
CTR- 614	9	325x120x10.5x14 LIA	25.05	0.85	1

ID	SID	XLB	A	STFSP	MATID
CTR- 615	9	325x120x10.5x14 LIA	25.05	0.85	1
CTR- 616	9	325x120x10.5x14 LIA	25.05	0.85	1
CTR- 617	9	325x120x10.5x14 LIA	25.05	0.85	1
CTR- 618	9	325x120x10.5x14 LIA	25.05	0.85	1
CTR- 619	9	325x120x10.5x14 LIA	25.05	0.85	1
CTR- 620	5	250x90x11.5x16 LIA	20.84	0.85	1
CTR- 621	5	250x90x11.5x16 LIA	20.84	0.85	1
CTR- 722	5	250x90x11.5x16 LIA	20.84	0.912	1
CTR- 723	5	250x90x11.5x16 LIA	20.84	0.975	2
CTR- 724	5	250x90x11.5x16 LIA	20.84	0.975	2
CTR- 725	5	250x90x11.5x16 LIA	20.84	0.975	2
BGR- 101	13	375x120x10.5x18 LIA	29.86	0.775	2
BGR- 102	12	350x120x11.5x18 LIA	30.21	0.775	2
NBG- 101	3	250x90x9x13 LIA	33.39	1.1	2
NBG- 302	3	250x90x9x13 LIA	33.39	0.425	2
NBG- 403	3	250x90x9x13 LIA	33.39	1.1	2
NBG- 604	3	250x90x9x13 LIA	33.39	0.425	2
NBG- 705	3	250x90x9x13 LIA	33.39	0.75	2
NBG- 906	3	250x90x9x13 LIA	33.39	0.75	2
NBG-1007	3	250x90x9x13 LIA	33.39	0.75	2
NBG-1208	3	250x90x9x13 LIA	33.39	0.75	2
NTS- 101	3	250x90x9x13 LIA	33.39	0.975	1
NTS- 302	3	250x90x9x13 LIA	33.39	0.35	1
NTS- 403	3	250x90x9x13 LIA	33.39	0.975	1
NTS- 604	3	250x90x9x13 LIA	33.39	0.35	1
NTS- 705	3	250x90x9x13 LIA	33.39	0.975	1
NTS- 906	3	250x90x9x13 LIA	33.39	0.35	1
NTS-1007	0	250x90x9x13 LIA	33.39	0.975	1
NTS-1208	0	250x90x9x13 LIA	33.39	0.35	1

## Appendix F: T2 Tanker Cargo Section Structural Data

T2-SE-A1 Single Hull Tanker

### Ship Dimensions:

Length Overall	: 523.5 ft
LBP	: 503.0 ft
Moulded beam	: 68.0 ft
Moulded depth	: 39.25 ft
Draft loaded	: 30.25 ft
Displacement (loaded)	: 16,613 tons
Max. Service Speed	: 14.5 knots

### Material:

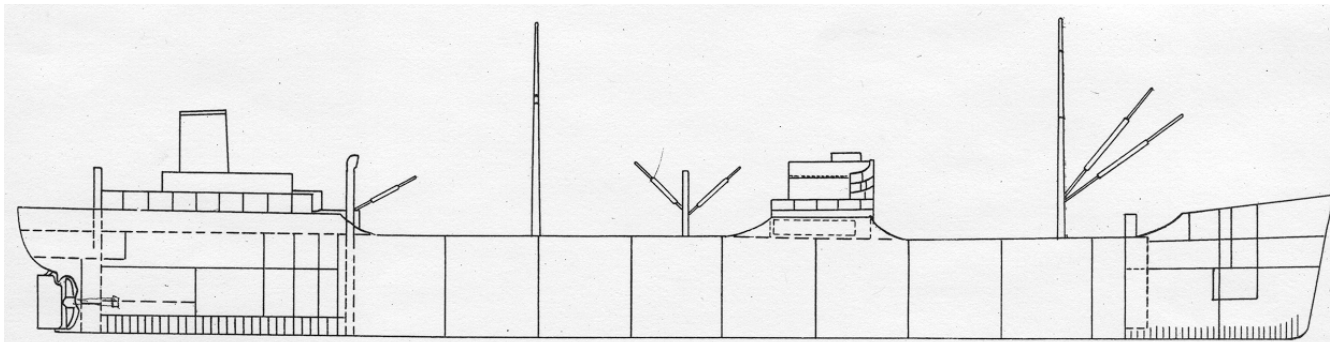
Yield Stress for plates and stiffeners	: 235 MPa
Ratio between ultimate and Yield stress	: 1.4

Hull Type: Single Hull

### Midship Geometry:

Camber	: 1.5 ft
Bilge Radius	: 6.0 ft
Web Spacing	: 12.167 ft

The following are graphical representations of the T2-SE-A1:



### TYPICAL T2 TANKER

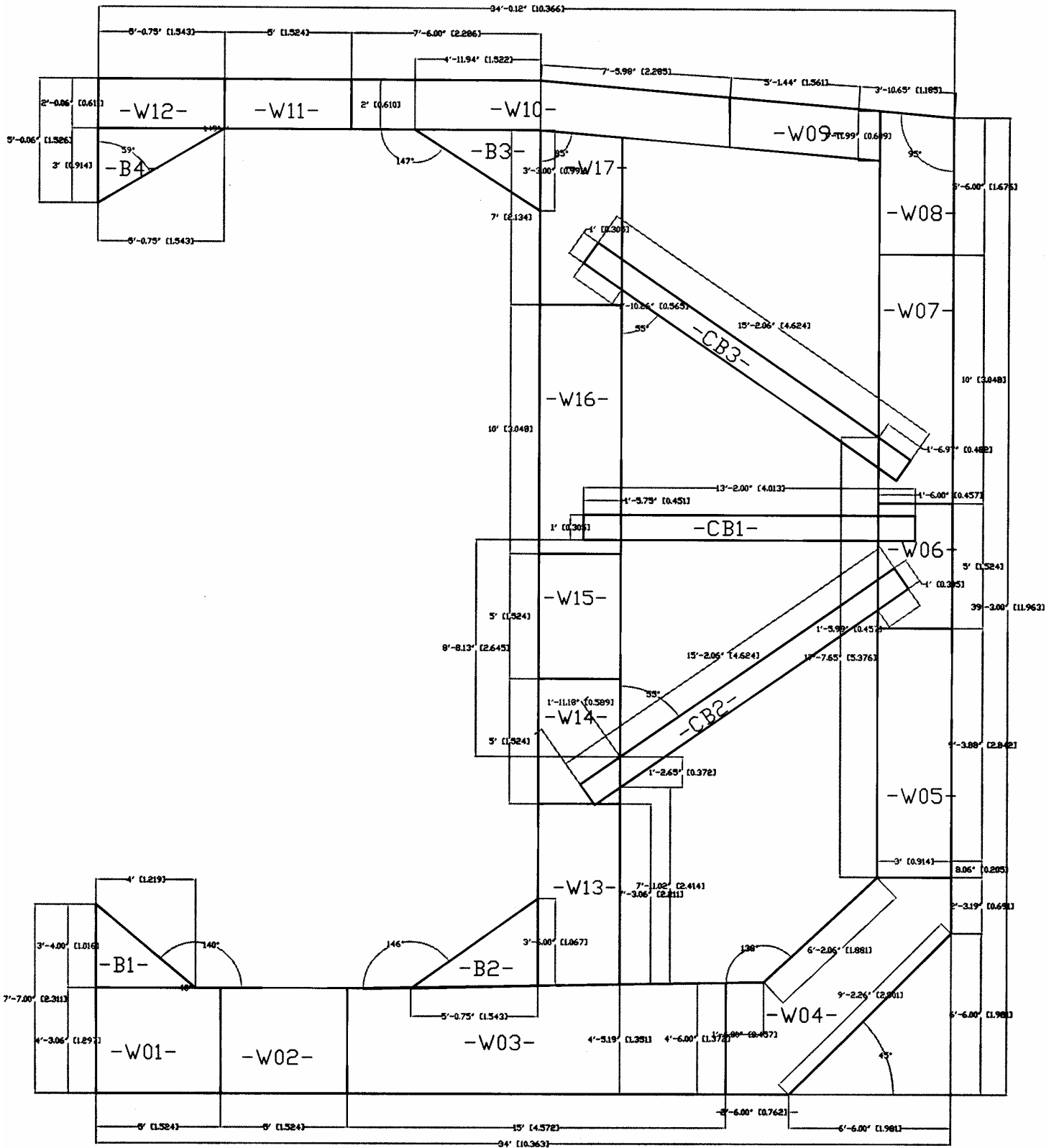
GENERAL CHARACTERISTICS OF STEAMSHIP LAKE CHAMPLAIN (T2-SE-A1 DESIGN)

Length, overall	523' 6"
Beam, moulded	68'
Draft, loaded	30' $\frac{1}{4}$ "
Gross tonnage	10,448
Deadweight tonnage	16,613

Machinery	TURBO-ELECTRIC
Horsepower, shaft	6000
Speed, knots	14.5
Cruising range, miles	12,600
Crew, approximately	44

LIQUID CARGO	BARRELS
TANK NO. 1 (Side)	5,077
TANK NO. 2 (Side and Center)	15,549
TANK NO. 3 "	17,128
TANK NO. 4 "	17,402
TANK NO. 5 "	17,416
TANK NO. 6 "	17,422
TANK NO. 7 "	17,408
TANK NO. 8 "	17,305
TANK NO. 9 "	16,451
TOTAL	141,158
DRY CARGO	BALE CU. FT.
SECOND DECK FRAME NO. 76-89	15,203

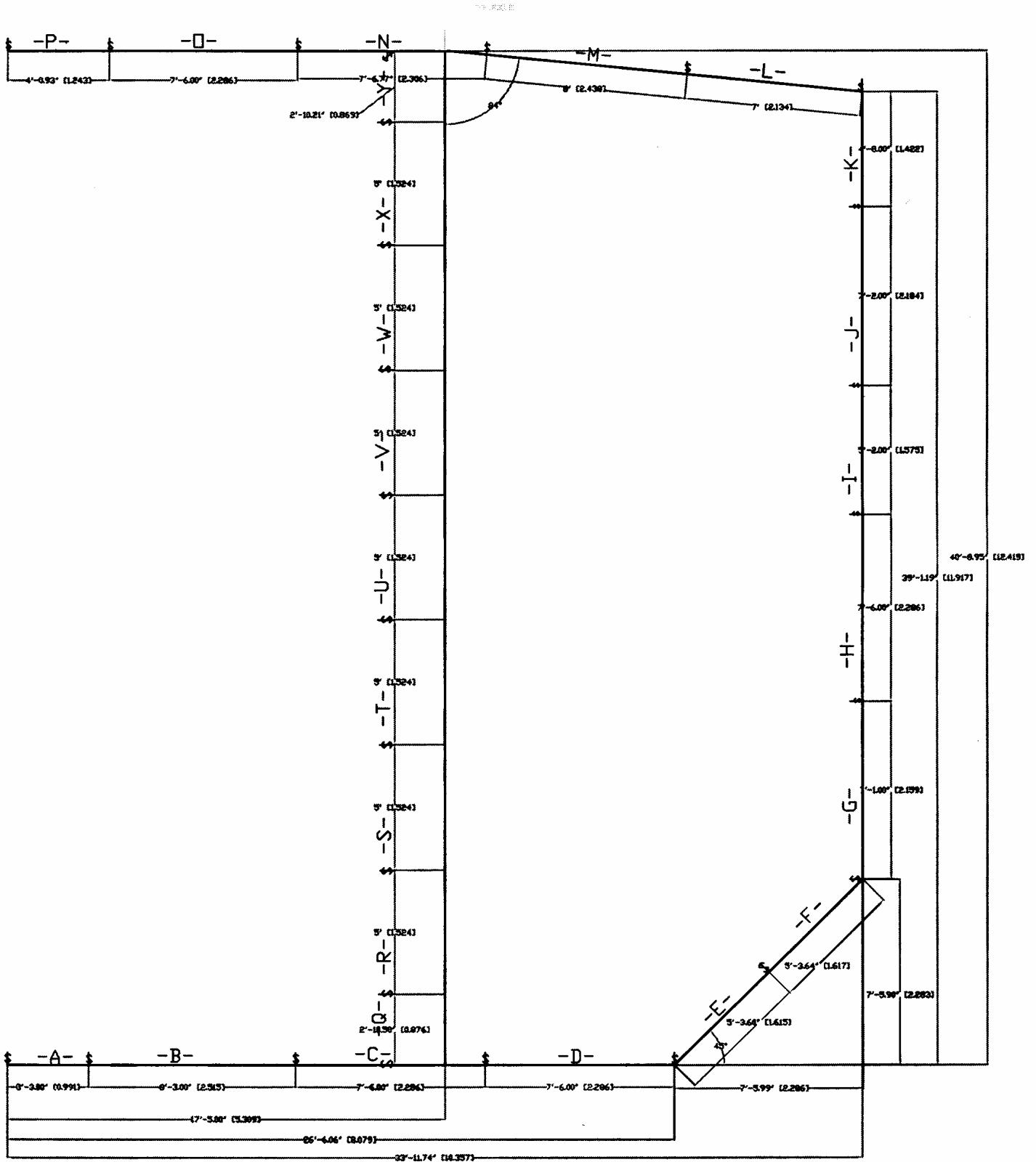
Typical T2 Tanker Profile



Midship Section Web and Bracket Drawing  
 (note: all dimensions are: feet-inches [meters])

<b><u>WEB</u></b>	<b>FLANGE DEPTH (m)</b>	<b>FLANGE THICKNESS (m)</b>	<b>PLATE THICKNESS (#)</b>
W01	0.1778	0.0127	20
W02	0.1778	0.0127	20
W03	0.1778	0.0127	20
W04	0.1778	0.0127	20
W05	0.127	0.0127	20
W06	0.127	0.0127	20
W07	0.127	0.0127	20
W08	0.127	0.0127	20
W09	0.127	0.0127	20
W10	0.127	0.0127	20
W11	0.127	0.0127	20
W12	0.127	0.0127	20
W13	0.127	0.0127	20
W14	0.127	0.0127	20
W15	0.127	0.0127	20
W16	0.127	0.0127	20
W17	0.127	0.0127	20
<b><u>BRACKET</u></b>			
B1	0.1778	0.0127	20
B2	0.1778	0.0127	20
B3	0.127	0.0127	20
B4	0.127	0.0127	20
<b><u>CENTER BRACE</u></b>			
CB1	N/A	N/A	64
CB2	N/A	N/A	53
CB3	N/A	N/A	53

Flange Details and Plate Weight for Midship Section Web and Bracket Drawing



Midship Section Shell Plating Drawing

Plate	location	thickness (m)
A	bottom shell	0.015748
B	bottom shell	0.019304
C	bottom shell	0.019304
D	bottom shell	0.019304
E	bilge shell	0.016764
F	bilge shell	0.016764
G	side shell	0.014478
H	side shell	0.014478
I	side shell	0.014478
J	side shell	0.014478
K	side shell	0.022098
L	upper deck shell	0.023876
M	upper deck shell	0.020828
N	upper deck shell	0.020828
O	upper deck shell	0.020828
P	upper deck shell	0.020828
Q	vertical web shell	0.015748
R	vertical web shell	0.014732
S	vertical web shell	0.013716
T	vertical web shell	0.012192
U	vertical web shell	0.011176
V	vertical web shell	0.010668
W	vertical web shell	0.010668
X	vertical web shell	0.0127
Y	vertical web shell	0.0127

(Plate Thickness Table)

Plate	Stiffener	Stiffener Spacing (m)	Stiffener Dimensions (m)
A	L26	0.762 from CL	0.4826 x 0.1524 x 0.0127
B	L25	0.762	0.4826 x 0.1524 x 0.0128
	L24	0.762	0.4826 x 0.1524 x 0.0129
	L23	0.762	0.4826 x 0.1524 x 0.0130
C	L22	0.762	0.4826 x 0.1524 x 0.0131
	L21	0.762	0.4826 x 0.1524 x 0.0132
	L20	0.762	0.4826 x 0.1524 x 0.0133
D	L19	0.762	0.4826 x 0.1524 x 0.0134
	L18	0.762	0.4826 x 0.1524 x 0.0135
	L17	0.762	0.4826 x 0.1524 x 0.0136
E	L16	0.762	0.4826 x 0.1524 x 0.0137
	L15	0.9144	0.4826 x 0.1524 x 0.0138
F	L14	0.9144	0.4826 x 0.1524 x 0.0139
	L13	0.9144	0.4826 x 0.1524 x 0.0140
G	L12	0.9144	0.391 x 0.1524 x 0.0127
	L11	0.762	0.391 x 0.1524 x 0.0128
	L10	0.762	0.391 x 0.1524 x 0.0129
H	L9	0.762	0.391 x 0.1524 x 0.0130
	L8	0.762	0.391 x 0.1524 x 0.0131
	L7	0.762	0.254 x 0.1016 x 0.0127
I	L6	0.762	0.254 x 0.1016 x 0.0128
	L5	0.762	0.254 x 0.1016 x 0.0129
J	L4	0.762	0.254 x 0.1016 x 0.0130
	L3	0.762	0.254 x 0.1016 x 0.0131
	L2	0.762	0.254 x 0.1016 x 0.0132
K	L1	0.762	0.254 x 0.1016 x 0.0133
		0.9144 to mid line of upper deck	
L	L27	0.9144 from side	0.2032 x 0.1016 x 0.0112
	L28	0.9144	0.2032 x 0.1016 x 0.0113
M	L25	0.9144	0.2032 x 0.1016 x 0.0114
	L30	0.762	0.2032 x 0.1016 x 0.0115
	L31	0.762	0.2032 x 0.1016 x 0.0116
N	L32	0.762	0.2032 x 0.1016 x 0.0117
	L33	0.762	0.2032 x 0.1016 x 0.0118
O	L34	0.762	0.2032 x 0.1016 x 0.0119
	L35	0.762	0.2032 x 0.1016 x 0.0120
	L36	0.762	0.2032 x 0.1016 x 0.0121
P	L37	0.762	0.2032 x 0.1016 x 0.0122

Stiffener Detail Table

(note: Longitudinal L26 spacing measured from center line)

(note: all other longitudinals measured from previous longitudinal position)

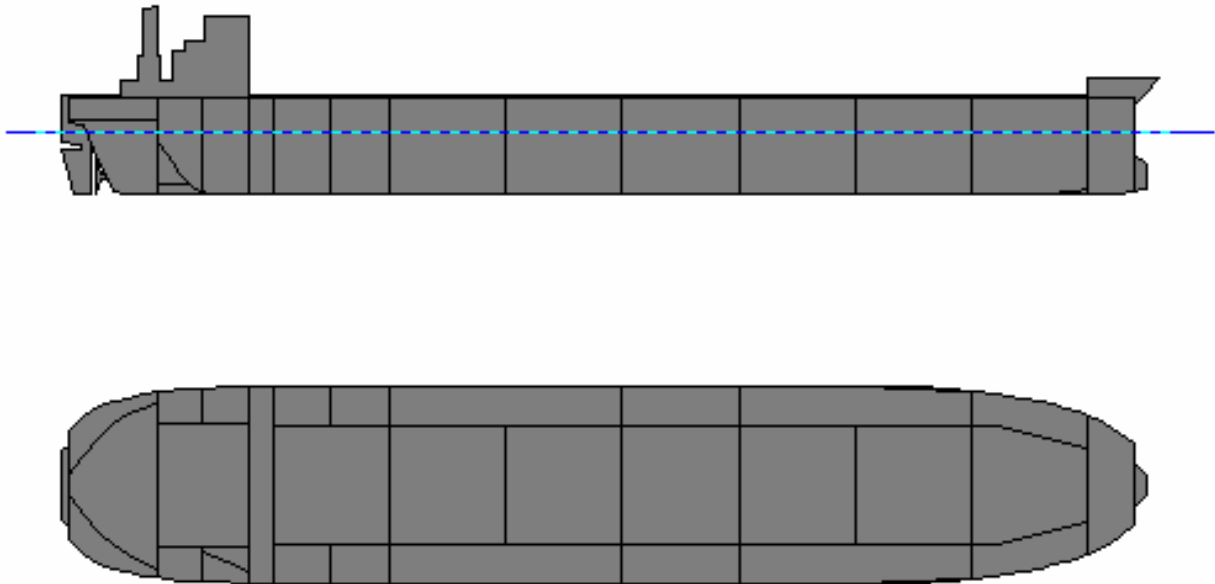
## Appendix G: 100k dwt Single Hull Tanker Cargo Section Structural Data

100k dwt Single Hull Tanker from Kuroiwa (1996)

Naval Architecture:

**L = 222 m    B = 42 m    D = 20.3 m    T = 13.35 m    D = 111015 MT**

Profile and Plan:



Weights and Stability:

FullLoadDepart					
Item	Weight MT	VCG m	LCG m-MS	TCG m-CL	FSMom m-MT
Light Ship	14,723	12.000	10.817A	0.000	---
Constant	300	14.000	80.000A	0.000	---
Cargo Oil	92,537	10.323	9.935F	0.000P	128,072
Fuel Oil	2,196	11.770	79.691A	0.000	778
Fresh Water	1,258	14.797	89.229A	0.000	0
SW Ballast	0	---	---	---	---
Misc. Weights	0	---	---	---	---
Displacement	111,015	10.635	4.042F	0.000S	128,850
<b>Stability Calculation</b>			<b>Trim Calculation</b>		
KMt	17.125	m	LCF Draft	13.350	m
VCG	10.635	m	LCB (even keel)	4.042F	m-MS
GMt (Solid)	6.490	m	LCF	2.261F	m-MS
FSc	1.161	m	MT1cm	1.335	m-MT
GMt (Corrected)	5.330	m	Trim	0.000	m
			List	0.0	deg
<b>Drafts</b>			<b>Strength Calculations</b>		
Draft at A.P.	13.350	m	Shear	0	MT at 0.000 m-MS
Draft at M.S.	13.350	m	Bending Moment	0	m-MT at 0.000 m-MS

Primary Subdivision

Cargo Block Longitudinal Bulkheads – 12.5 m from CL (CO-CUB-S and P):

Compartment	Mir	# Sta	Aft m-MS	Fwd m-MS	Port m	Stbd m	Lower m	Upper m
<b>1 FOREPEAK</b>	<b>N</b>	<b>7</b>	<b>105.000F</b>	<b>115.000F</b>	<b>HULL</b>	<b>HULL</b>	<b>HULL</b>	<b>HULL</b>
2 NO.1 WBT S	N	11	80.000F	105.000F	CO-CUB-S	HULL	HULL	HULL
3 NO.1 COT C	N	11	80.000F	105.000F	CO-CUB-P	CO-CUB-S	HULL	HULL
4 NO.1 WBT P	N	11	80.000F	105.000F	HULL	CO-CUB-P	HULL	HULL
5 NO.2 WBT S	N	11	30.000F	80.000F	CO-CUB-S	HULL	HULL	HULL
6 NO.2 COT C	N	11	55.000F	80.000F	CO-CUB-P	CO-CUB-S	HULL	HULL
7 NO.2 WBT P	N	11	30.000F	80.000F	HULL	CO-CUB-P	HULL	HULL
8 NO.3 COT C	N	3	30.000F	55.000F	CO-CUB-P	CO-CUB-S	HULL	HULL
9 NO.4 COT S	N	3	5.000F	30.000F	CO-CUB-S	HULL	HULL	HULL
10 NO.4 COT C	N	3	5.000F	30.000F	CO-CUB-P	CO-CUB-S	HULL	HULL
11 NO.4 COT P	N	3	5.000F	30.000F	HULL	CO-CUB-P	HULL	HULL
12 NO.5 COT C	N	3	20.000A	5.000F	CO-CUB-P	CO-CUB-S	HULL	HULL
13 NO.4 WBT S	N	3	45.000A	5.000F	CO-CUB-S	HULL	HULL	HULL
14 NO.6 COT C	N	3	45.000A	20.000A	CO-CUB-P	CO-CUB-S	HULL	HULL
15 NO.4 WBT P	N	3	45.000A	5.000F	HULL	CO-CUB-P	HULL	HULL
16 NO.7 COT S	N	5	57.500A	45.000A	CO-CUB-S	HULL	HULL	HULL
17 NO.7 COT C	N	5	70.000A	45.000A	CO-CUB-P	CO-CUB-S	HULL	HULL
18 NO.7 COT P	N	5	57.500A	45.000A	HULL	CO-CUB-P	HULL	HULL
19 SLOP TANK S	N	3	70.000A	57.500A	CO-CUB-S	HULL	HULL	HULL
20 SLOP TANK P	N	3	70.000A	57.500A	HULL	CO-CUB-P	HULL	HULL
21 COFFERDAM	N	5	75.000A	70.000A	HULL	HULL	HULL	HULL
22 FO S	N	7	85.000A	75.000A	13.000S	HULL	HULL	HULL
23 ENGINE ROOM	N	7	95.000A	75.000A	13.000P	13.000S	2.000	HULL
24 ENG ROOM DB	N	5	95.000A	75.000A	HULL	HULL	HULL	2.000
25 FO P	N	7	85.000A	75.000A	HULL	13.000P	HULL	HULL
26 FRESH WTR S	N	5	95.000A	85.000A	13.000S	HULL	HULL	HULL
27 FRESH WTR P	N	5	95.000A	85.000A	HULL	13.000P	HULL	HULL
<b>28 STRNG GEAR</b>	<b>N</b>	<b>7</b>	<b>114.000A</b>	<b>95.000A</b>	<b>HULL</b>	<b>HULL</b>	<b>16.000</b>	<b>HULL</b>

Full Load cargo:

→ FullLoadDepart									
Cargo Oil	Weight	%	Capacity	VCG	LCG	TCG	FSmom	Density	Volume
Tank Name	MT	Full	MT	m-BL	m-MS	m-CL	m-MT	MT/m3	m3
NO.1 COT C	9,582	98.0	9,777	10.354	91.439F	0.000	13,010	0.9130	10,495
NO.2 COT C	11,316	98.0	11,547	10.330	67.500F	0.000	18,398	0.9130	12,394
NO.3 COT C	11,317	98.0	11,548	10.328	42.500F	0.000	18,394	0.9130	12,395
NO.4 COT S	3,789	98.0	3,867	10.230	17.500F	16.731S	1,173	0.9130	4,151
NO.4 COT C	11,318	98.0	11,549	10.328	17.500F	0.000	18,395	0.9130	12,396
NO.4 COT P	3,789	98.0	3,867	10.230	17.500F	16.731P	1,172	0.9130	4,151
NO.5 COT C	11,318	98.0	11,549	10.327	7.500A	0.000	18,396	0.9130	12,397
NO.6 COT C	11,318	98.0	11,549	10.328	32.500A	0.000	18,395	0.9130	12,397
NO.7 COT S	1,891	98.0	1,929	10.248	51.243A	16.722S	586	0.9130	2,071
NO.7 COT C	11,317	98.0	11,548	10.328	57.500A	0.000	18,395	0.9130	12,396
NO.7 COT P	1,891	98.0	1,929	10.248	51.243A	16.722P	586	0.9130	2,071
SLOP TANK S	1,845	98.0	1,883	10.424	63.690A	16.635S	586	0.9130	2,021
SLOP TANK P	1,845	98.0	1,883	10.424	63.690A	16.635P	586	0.9130	2,021
<b>Totals</b>	<b>92,537</b>	<b>98.0</b>	<b>94,425</b>	<b>10.323</b>	<b>9.935F</b>	<b>0.000S</b>	<b>128,072</b>		<b>101,355</b>

Structural Design  
Ship Dimensions

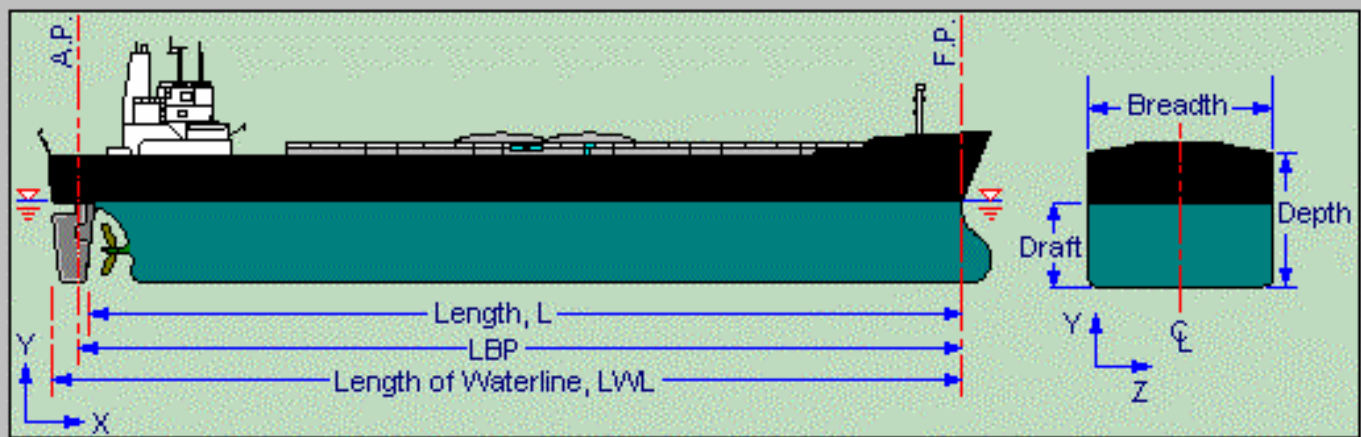
Title : 100K DWT SH Tanker

Block Coefficient : 0.89      Design Ship Speed (Knots) : 13

Transverse Metacentric Height \_\_\_\_\_      Roll Radius Of Gyration \_\_\_\_\_  
 Rules    User Defined       Rules    User Defined

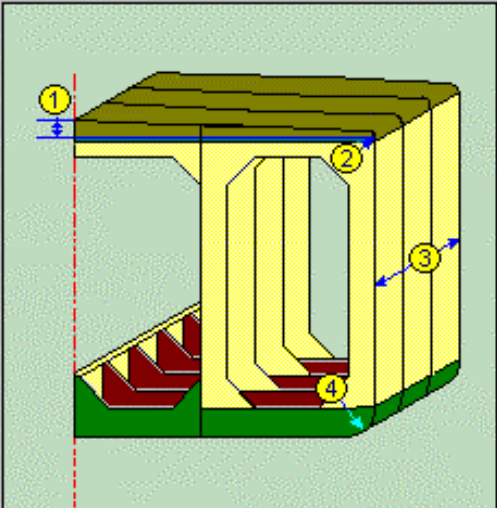
LBP (m) : 222      Length (m) : 222

Breadth (m) : 42      Depth (m) : 20.3      Draft (m) : 13.35



## MIDSHIP GEOMETRY

Camber (m)	0.5
Bilge Radius (m)	2.5
Gunwale Radius (m)	1
Web Spacing (m)	5.015



**Note:**

1. Camber
2. Gunwale Radius
3. Web Spacing
4. Bilge Radius

## TANK DEFINITION

**Definition**

No.	Type	Length (m)
1	Center Cargo Tank	25.000
2	Wing Cargo Tank	25.000
3		
4		
5		

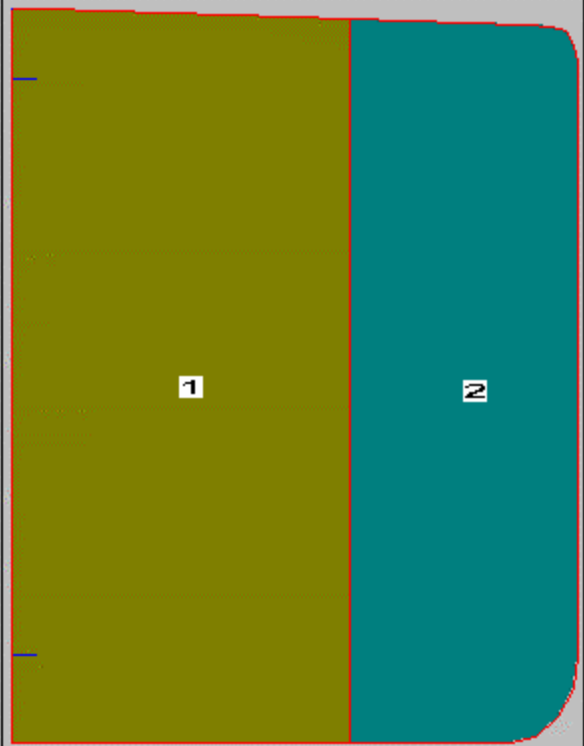
**Tank**

Define

Help for defining tank

Erase

**Graphics**



**Characteristics**

No.	Width (m)	Height (m)
1	25.000	20.800
2	8.500	20.502
3		
4		
5		

**Press./Vacuum (Kgf/cm<sup>2</sup>)**

Relief Valve Wing Cargo:

Center Cargo:

**Density (tf/m<sup>3</sup>)**

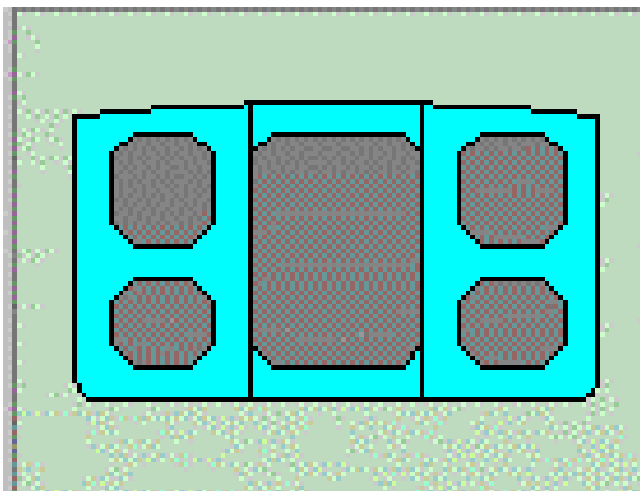
Wing Cargo:

Center Cargo:

Height of VentPipe (mm):

# TRANSVERSE MEMBERS

## Web Configuration



Spacing

Side Transverse (m) :       Deck Transverse (m) :

Vertical Web On Longitudinal Bulkhead (m) :

Strut

Number of Strut :

Span for main supporting member

User Defined       Tank Configuration

### Main Supporting Members – Side Transverse (Web)

Transverse Member Description :

Side Transverse

No.	Bw(m)	Bh(m)	Mat.	Lib.ID	Cont
1L	1.600	2.150	MILD	26	<input type="checkbox"/>
1U	2.500	2.500	MILD	26	<input type="checkbox"/>

Web thickness: 15 mm

### Main Supporting Members – Deck Transverse

Transverse Member Description :

Deck Transverse

No.	Bw(m)	Bh(m)	Mat.	Lib.ID	Width(mm)	Thick(mm)	Cont
20	2.500	2.500	MILD	26	500.000	24.000	<input checked="" type="checkbox"/>
2I	2.500	2.500	MILD	26	500.000	24.000	<input checked="" type="checkbox"/>

Deck Transverse web thickness: 15 mm

## Main Supporting Members – Vertical Web on Longitudinal Bulkhead

Transverse Member Description :

Vertical Web on Longitudinal Bulkhead

No.	Bw(m)	Bh(m)	Mat.	Lib.ID	Width(mm)	Thick(mm)	Cont
3L	2.500	2.500	MILD	26	500.000	24.000	✕
3U	2.500	2.500	MILD	26	500.000	24.000	✕

No.	Other Bh(m)	Other Bw(m)	Depth(m)
3L	2.500	2.500	
3U	2.500	2.500	2.500

Vertical Web thickness: 15mm

## Transverse Bulkhead

Wing Cargo Tank       Center Cargo Tank

Group No. Group 1

Group

Position Description Lower Stringer

L(m) 22      Lb(m) 17      Lib.ID 28

Mat. MILD      Xp(m) 11      Yp(m) 8.7

he(m) 2.5      S(m) 4.675      Tp(mm) 18

Horz Girder On Trn BHD.	Transverse BHD Plate/Stiffener	Vert Web On Trn BHD.
<input checked="" type="radio"/> Wing Cargo Tank <input type="radio"/> Center Cargo Tank		
Group No. <input type="text" value="Group 2"/>		
Group <input type="text" value="Upper Stringer"/>		
L(m) <input type="text" value="22"/>	Lb(m) <input type="text" value="17"/>	Lib.ID <input type="text" value="29"/>
Mat. <input type="text" value="MILD"/>	Xp(m) <input type="text" value="11"/>	Yp(m) <input type="text" value="18.9"/>
he(m) <input type="text" value="2.5"/>	S(m) <input type="text" value="5.1"/>	Tp(mm) <input type="text" value="12"/>

Horz Girder On Trn BHD.	Transverse BHD Plate/Stiffener	Vert Web On Trn BHD.
<input checked="" type="radio"/> Wing Cargo Tank <input type="radio"/> Center Cargo Tank		
Group No. <input type="text" value="Group 3"/>		
Group <input type="text" value="Stool Level"/>		
L(m) <input type="text" value="22"/>	Lb(m) <input type="text" value="17"/>	Lib.ID <input type="text" value="28"/>
Mat. <input type="text" value="MILD"/>	Xp(m) <input type="text" value="11"/>	Yp(m) <input type="text" value="4.45"/>
he(m) <input type="text" value="2.5"/>	S(m) <input type="text" value="3.2"/>	Tp(mm) <input type="text" value="18"/>

Horz Girder On Trn BHD.

Transverse BHD Plate/Stiffener

Vert Web On Trn BHD.

Wing Cargo Tank

Center Cargo Tank

Group No.

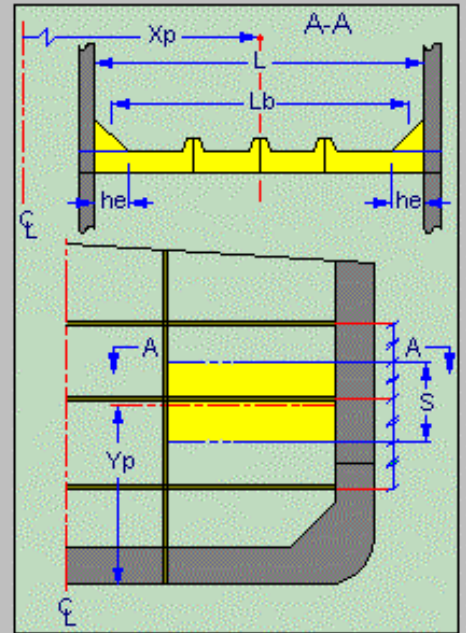
Group

Position Description

L(m)  Lb(m)  Lib.ID

Mat.  Xp(m)  Yp(m)

he(m)  S(m)  Tp(mm)



Horz Girder On Trn BHD.

Transverse BHD Plate/Stiffener

Vert Web On Trn BHD.

TB Group 1 Tank Type

Description  Xap (m)

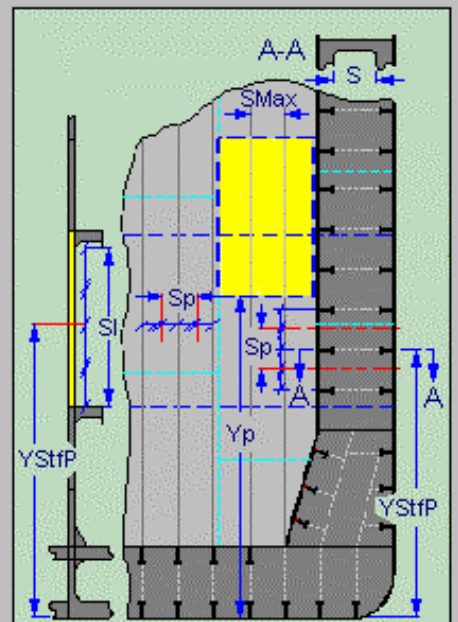
Plate

Group  Zp (m)  SMax (mm)  Yp (m)

Description  Thick.(mm)  Mat

Stiffener

No.	Type	Sp(mm)	Sl(m)	ZStfp(m)	YStfp(m)	Lib.ID	Mat.
1	1	850.00	5.100	11.000	21.450	11	MILD
2							
3							
4							
5							



Horz Girder On Trn BHD. **Transverse BHD Plate/Stiffener** Vert Web On Trn BHD.

TB Group 2 Tank Type Wing Cargo Tank

Description Middle Xap (m) 152

Plate

Group Plate 1 Zp (m) 11 SMax (mm) 850 Yp (m) 13.8

Description TB Middle Thick.(mm) 14 Mat MILD

Stiffener

No.	Type	Sp(mm)	Sl(m)	ZStfp(m)	YStfp(m)	Lib.ID	Mat.
1	1	850.00	5.100	11.000	16.350	16	MILD
2							
3							
4							
5							

Horz Girder On Trn BHD. **Transverse BHD Plate/Stiffener** Vert Web On Trn BHD.

TB Group 3 Tank Type Wing Cargo Tank

Description Lower Xap (m) 152

Plate

Group Plate 1 Zp (m) 11 SMax (mm) 850 Yp (m) 8.7

Description TB Lower Thick.(mm) 16 Mat MILD

Stiffener

No.	Type	Sp(mm)	Sl(m)	ZStfp(m)	YStfp(m)	Lib.ID	Mat.
1	1	850.00	5.100	11.000	11.250	20	MILD
2							
3							
4							
5							

Horz Girder On Trm BHD.      **Transverse BHD Plate/Stiffener**      Vert Web On Trm BHD.

TB Group 4      Tank Type Wing Cargo Tank

Description Stool      Xap (m) 152

Plate

Group Plate 1      Zp (m) 11      SMax (mm) 850      Yp (m) 4.45

Description TB Stool      Thick.(mm) 18      Mat MILD

Stiffener

No.	Type	Sp(mm)	Sl(m)	ZStfp(m)	YStfp(m)	Lib.ID	Mat.
1	1	850.00	4.250	11.000	6.575	18	MILD
2							
3							
4							
5							

### Struts

HStrut (m) 10.150      Mat. HT32      Lib.ID 30 MSTF USER

Material

Material Zones:

Bottom			
Mat.	Yield (kg/cm <sup>2</sup> )	Ultimate (kg/cm <sup>2</sup> )	Q
HT32	3200.0	4500.0	0.78
Side			
Mat.	Yield (kg/cm <sup>2</sup> )	Ultimate (kg/cm <sup>2</sup> )	Q
MILD	2400.0	4100.0	1.00
Deck			
Mat.	Yield (kg/cm <sup>2</sup> )	Ultimate (kg/cm <sup>2</sup> )	Q
HT32	3200.0	4500.0	0.78

Note:  
1.Bottom Zone  
2.Side Zone  
3.Deck Zone

MATERIAL TABLE

MAT #	MAT ID	YIELD STRESS	ULT STRESS	Q-FAC	Sm
(kgf/cm2)	(kgf/cm2)				
1	MILD	2400.	4100.	1.000	1.0
2	HT32	3200.	4500.	.780	.950
3	HT36	3600.	5000.	.720	.908
4	HT40	4000.	5200.	.680	.875

Stiffener Library:

#---- STIFFENER PROPERTIES; FILE:C:\SH\_50\SH100\SH100.slb ; RECORDS: 29

#ID#	TYPE	ABS ID	DESCRIPTION	VAR 1	VAR 2	VAR 3	VAR 4	VAR 5	VAR 6
#(dimensions)			(mm)	(mm)	(mm)	(mm)	(mm)	(mm)	(mm)
1	LANG	ILA200A	200x90x9x12 LIA	200.00	90.00	9.00	12.00	7.50	15.00
2	LANG	ILA225A	225x90x9x12 LIA	225.00	90.00	9.00	12.00	7.50	15.00
3	LANG	ILA250A	250x90x9x13 LIA	250.00	90.00	9.00	13.00	7.50	15.00
4	LANG	ILA250B	250x90x10.5x15 LIA	250.00	90.00	10.50	15.00	7.50	15.00
5	LANG	ILA250C	250x90x11.5x16 LIA	250.00	90.00	11.50	16.00	7.50	15.00
6	LANG	ILA275A	250x100x10.5x14 LIA	275.00	100.00	10.50	14.00	7.50	15.00
7	LANG	ILA300A	300x100x10.5x15 LIA	300.00	100.00	10.50	15.00	7.50	15.00
8	LANG	ILA300B	300x100x11.5x16 LIA	300.00	100.00	11.50	16.00	7.50	15.00
9	LANG	ILA325A	325x120x10.5x14 LIA	325.00	120.00	10.50	14.00	10.00	20.00
10	LANG	ILA325B	325x120x11.5x15 LIA	325.00	120.00	11.50	15.00	10.00	20.00
11	LANG	ILA350A	350x120x10.5x16 LIA	350.00	120.00	10.50	16.00	10.00	20.00

12	LANG ILA350B	350x120x11.5x18 LIA	350.00	120.00	11.50	18.00	10.00	20.00
13	LANG ILA375A	375x120x10.5x18 LIA	375.00	120.00	10.50	18.00	10.00	20.00
14	LANG ILA375B	375x120x11.5x20 LIA	375.00	120.00	11.50	20.00	10.00	20.00
15	LANG ILA400A	400x120x11.5x23 LIA	400.00	120.00	11.50	23.00	10.00	20.00
16	LANG ILA425A	425x120x11.5x24 LIA	425.00	120.00	11.50	24.00	10.00	20.00
17	LANG ILA450A	450x120x11.5x25 LIA	450.00	120.00	11.50	25.00	10.00	20.00
18	LANG ILA475A	475x120x11.5x28 LIA	475.00	120.00	11.50	28.00	10.00	20.00
19	LANG ILA475B	475x120x12.5x30 LIA	475.00	120.00	12.50	30.00	10.00	20.00
20	LANG ILA500A	500x120x12.5x33 LIA	500.00	120.00	12.50	33.00	10.00	20.00
21	LANG ILA500B	500x120x13.5x35 LIA	500.00	120.00	13.50	35.00	10.00	20.00
22	FLAT USER-DEF FB	400x28	400.00	28.00				
23	UANG IUA150G	150X90X15 UIA	150.00	90.00	15.00	15.00	6.00	12.00
24	FLAT USER-DEF FB	2000X12	2000.00	12.00				
25	FLAT USER-DEF FB	2000X18	2000.00	18.00				
26	MSTF USER-DEF DECK	WEB	3					
27	MSTF USER-DEF LBHD	WEB	7					
28	MSTF USER-DEF BHD	L STR	4					
29	MSTF USER-DEF BHD	U STR	4					

# User-Defined Shapes / Webs:

**Built-up Multi-Stiffener**

ID#	Type	ABSID	Description
26	MSTF	USER-DEF	DECK WEB

Attach Point		Plate DIM's		Stiffener			
X(mm)	Y(mm)	Theta	t(mm)	l(mm)	STF	ID	FAC
1	0.00	0.00	15.00	2500.00	<input type="checkbox"/>	<input type="checkbox"/>	<input type="checkbox"/>
2	250.00	2512.00	90.00	24.00	500.00	<input type="checkbox"/>	<input type="checkbox"/>
3	-7.50	2000.00	90.00	20.00	200.00	<input type="checkbox"/>	<input type="checkbox"/>
4						<input type="checkbox"/>	<input type="checkbox"/>
5						<input type="checkbox"/>	<input type="checkbox"/>

Transformation in Reference Frame of Attached Plate

Offset Angle Definition

Stiffener Properties

Area: 535.000 cm<sup>2</sup> Web-area: 375.000 cm<sup>2</sup>

Depth: 252.400 cm ASStiff: 535.000 cm<sup>2</sup>

Corrosion margins (mm)

Plate: 0.00 Web: 0.00 Flange: 0.00

Attached Plate (mm)

Breadth: 0.00 Thickness: 0.00

Plate Offset

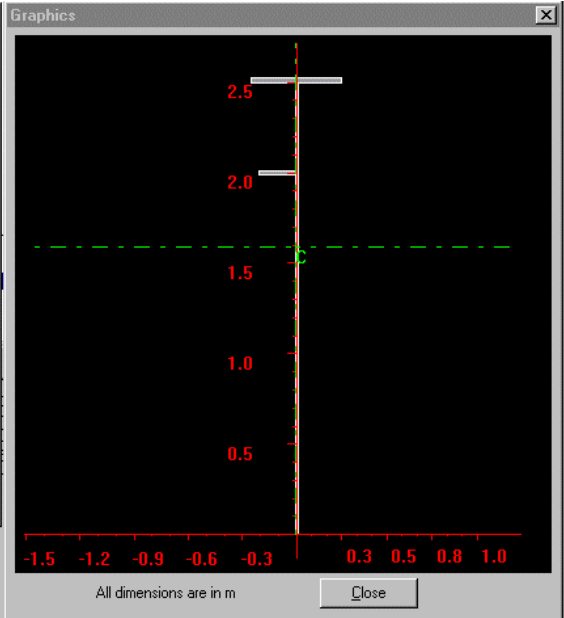
X (mm): 0 Angle (deg): 0

SMx,t: 37161.004 cm<sup>3</sup> SMx,b: 21861.084 cm<sup>3</sup>

SMyy: 1188.996 cm<sup>3</sup>

Save Graphics

Copy Multistiffener OK Cancel



**Built-up Multi-Stiffener**

ID#	Type	ABSID	Description
27	MSTF	USER-DEF	LBHD WEB

Attach Point		Plate DIM's		Stiffener			
X(mm)	Y(mm)	Theta	t(mm)	l(mm)	STF	ID	FAC
1	0.00	8.00	0.00	14.00	2000.00	<input type="checkbox"/>	<input type="checkbox"/>
2	250.00	2018.00	90.00	18.00	450.00	<input type="checkbox"/>	<input type="checkbox"/>
3	-8.00	1508.00	90.00	16.00	200.00	<input type="checkbox"/>	<input type="checkbox"/>
4	1650.00	0.00	90.00	16.00	3300.00	<input type="checkbox"/>	<input type="checkbox"/>
5	0.00	-8.00	180.00	14.00	2000.00	<input type="checkbox"/>	<input type="checkbox"/>

Transformation in Reference Frame of Attached Plate

Offset Angle Definition

Stiffener Properties

Area: 1314.000 cm<sup>2</sup> Web-area: 560.000 cm<sup>2</sup>

Depth: 405.400 cm ASStiff: 1314.000 cm<sup>2</sup>

Corrosion margins (mm)

Plate: 0.00 Web: 0.00 Flange: 0.00

Attached Plate (mm)

Breadth: 0.00 Thickness: 0.00

Plate Offset

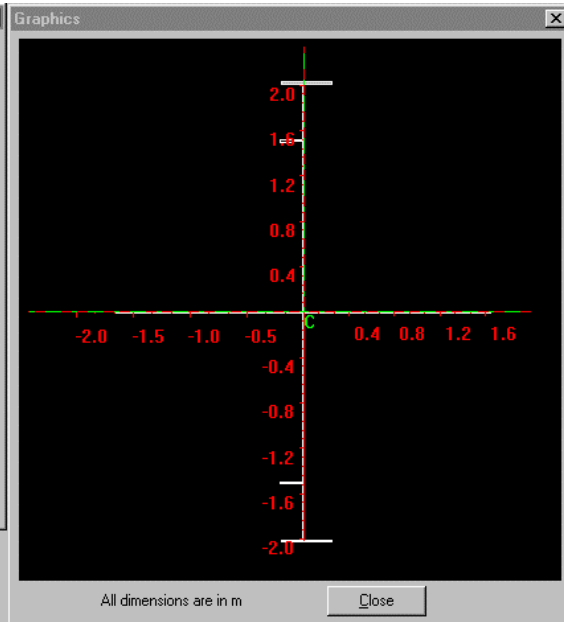
X (mm): 0 Angle (deg): 0

SMx,t: 77007.211 cm<sup>3</sup> SMx,b: 77007.211 cm<sup>3</sup>

SMyy: 29231.578 cm<sup>3</sup>

Save Graphics

Copy Multistiffener OK Cancel



**Built-up Multi-Stiffener**

ID#	Type	ABSID	Description
28	MSTF	USER-DEF	BHD L STR

Attach Point	Plate DIM's	Stiffener					
X(mm)	Y(mm)	Theta	t(mm)	l(mm)	STF	ID	FAC
1	0.00	0.00	18.00	3500.00			
2	350.00	3512.00	90.00	24.00	700.00		
3	8.00	2000.00	90.00	20.00	200.00		
4	8.00	2800.00	90.00	20.00	200.00		
5							

Transformation in Reference Frame of Attached Plate

Offset Angle Definition

Stiffener Properties

Area: 878.000 cm<sup>2</sup> Web-area: 630.000 cm<sup>2</sup>  
 Depth: 352.400 cm AStiff: 878.000 cm<sup>2</sup>

Corrosion margins (mm)

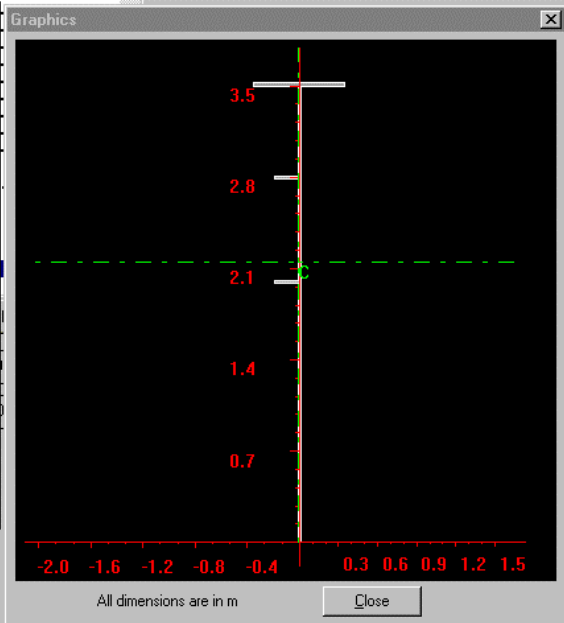
Plate	Web	Flange	Attached Plate (mm)
Breadth	Thickness		
0.00	0.00	0.00	0.00

Plate Offset

X (mm): 0 Angle (deg): 0

SMx,t: 77914.563 cm<sup>3</sup> SMx,b: 50008.609 cm<sup>3</sup>  
 SMyy: 2165.032 cm<sup>3</sup>

Save Graphics  
 Copy Multistiffener OK Cancel



**Built-up Multi-Stiffener**

ID#	Type	ABSID	Description
29	MSTF	USER-DEF	BHD U STR

Attach Point	Plate DIM's	Stiffener					
X(mm)	Y(mm)	Theta	t(mm)	l(mm)	STF	ID	FAC
1	0.00	0.00	14.00	3500.00			
2	350.00	3512.00	90.00	24.00	700.00		
3	7.00	2000.00	90.00	20.00	200.00		
4	7.00	2800.00	90.00	20.00	200.00		
5							

Transformation in Reference Frame of Attached Plate

Offset Angle Definition

Stiffener Properties

Area: 738.000 cm<sup>2</sup> Web-area: 490.000 cm<sup>2</sup>  
 Depth: 352.400 cm AStiff: 738.000 cm<sup>2</sup>

Corrosion margins (mm)

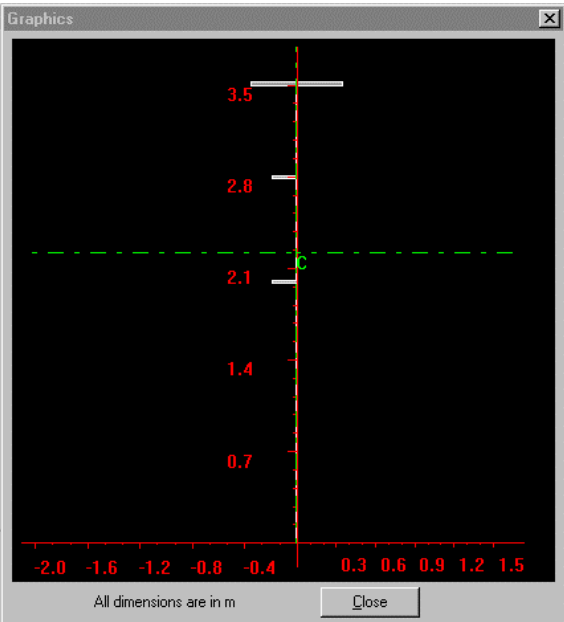
Plate	Web	Flange	Attached Plate (mm)
Breadth	Thickness		
0.00	0.00	0.00	0.00

Plate Offset

X (mm): 0 Angle (deg): 0

SMx,t: 69430.539 cm<sup>3</sup> SMx,b: 40704.910 cm<sup>3</sup>  
 SMyy: 2152.732 cm<sup>3</sup>

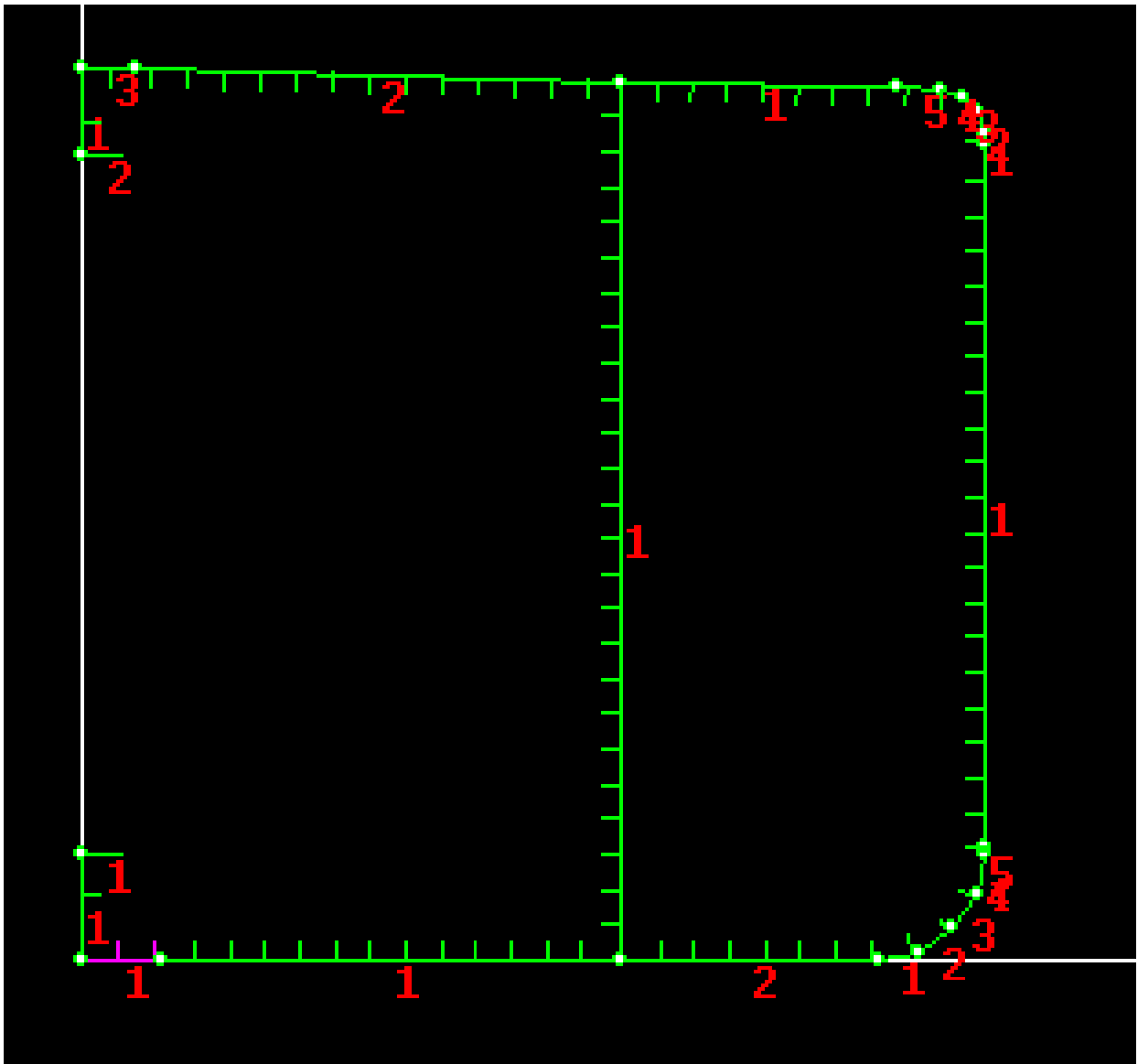
Save Graphics  
 Copy Multistiffener OK Cancel





# Longitudinal Plate and Stiffener Elements

Local Plate IDs:



Global Plate Ids:

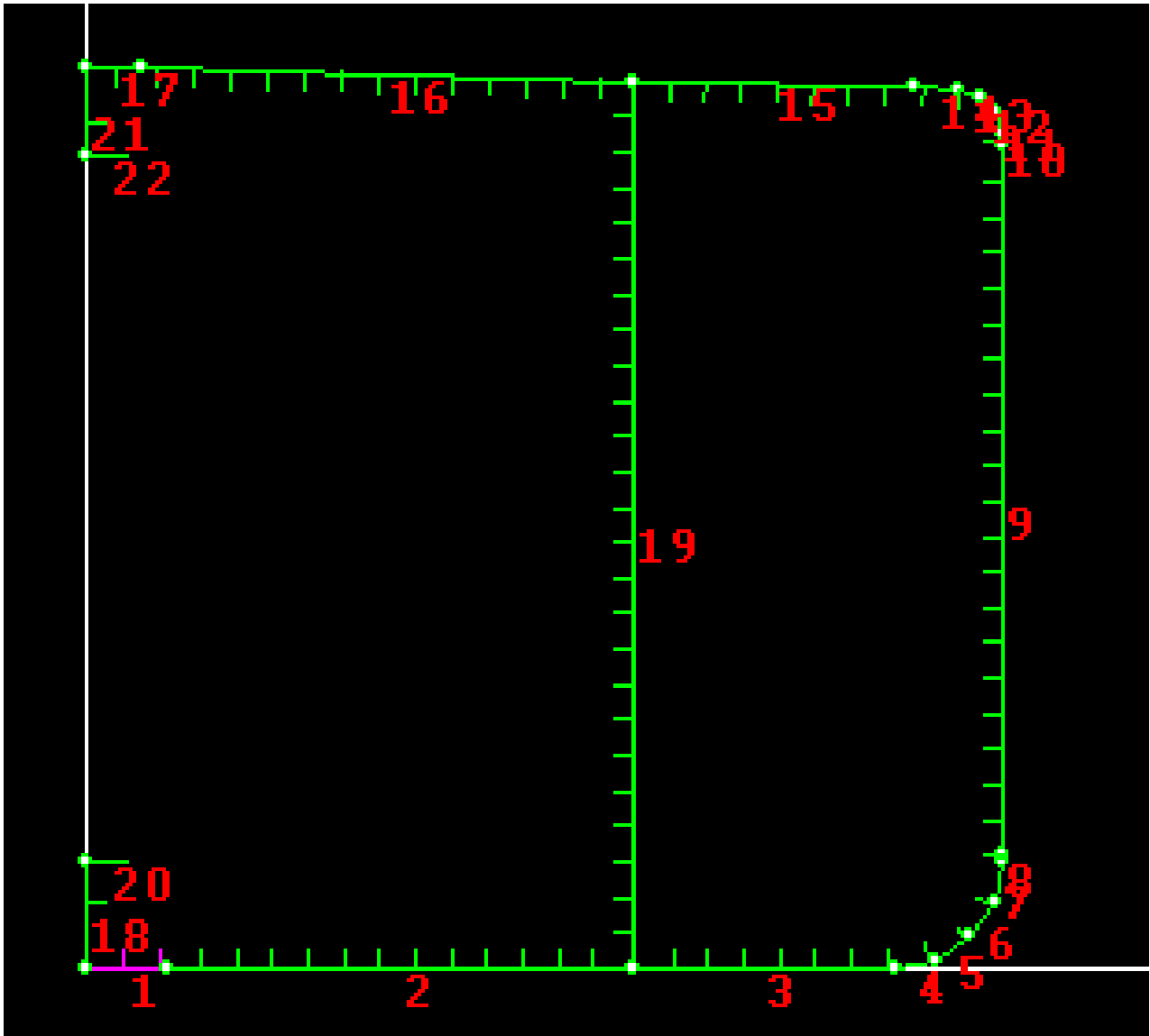
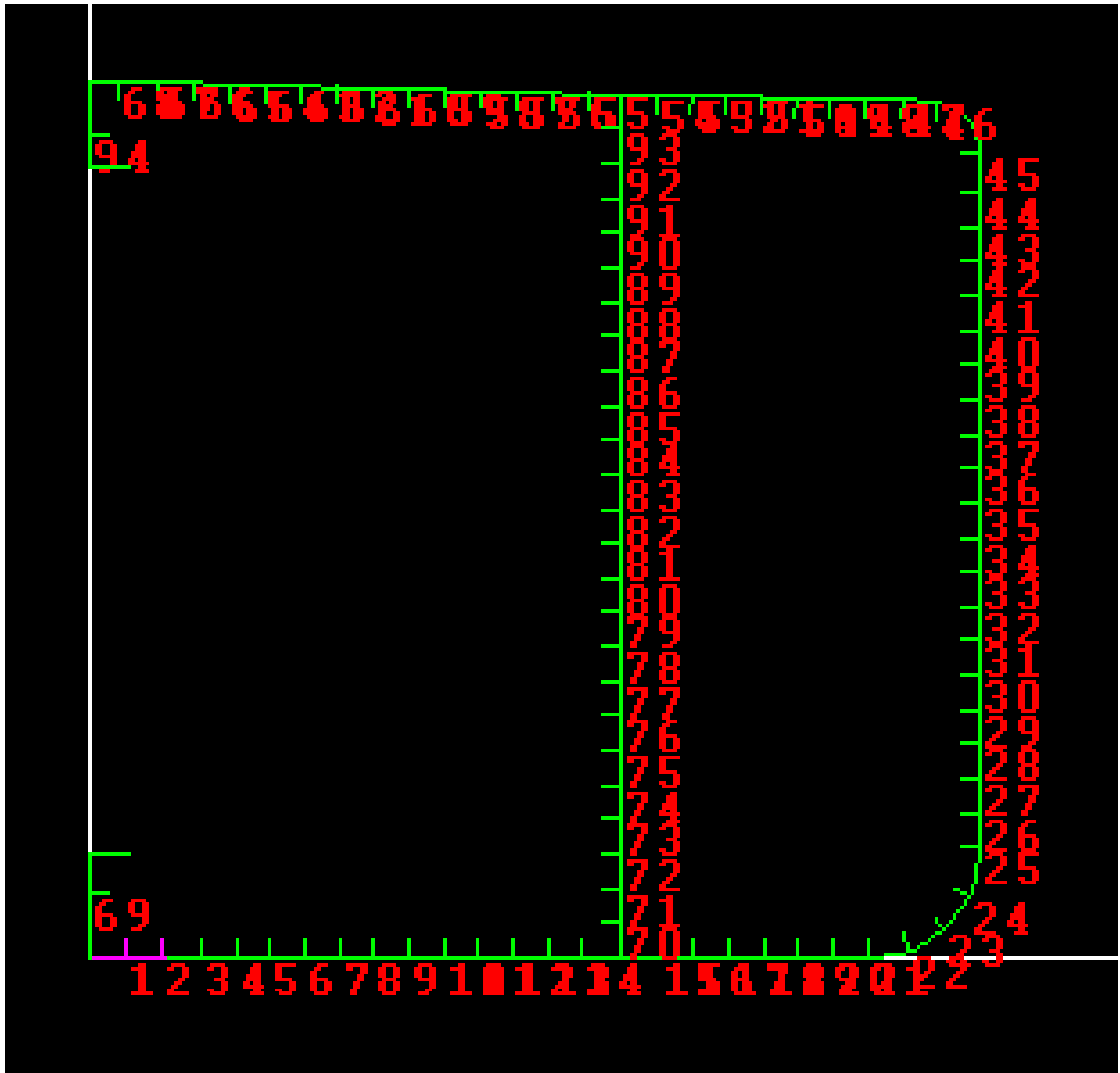


Plate:

DESCRIPTION	ID	B	TP	A	SPACING	MATID	START		END	
		m	cm	cm2	(m)		X-COORD	Y-COORD	X-COORD	Y-COORD
KEEL PLATE	KPL-01	1.8	2	360	0.96	3	0	0	1.8	0
BOTTOM	BTM-01	10.7	1.7	1819	0.96	3	1.8	0	12.5	0
BOTTOM	BTM-02	6	1.7	1020	0.92	3	12.5	0	18.5	0
BILGE	BLG-01	0.976	1.7	165.87	0.98	3	18.5	0	19.457	0.19
BILGE	BLG-02	0.975	1.7	165.82	0.976	3	19.457	0.19	20.268	0.732
BILGE	BLG-03	0.975	1.7	165.82	1.131	3	20.268	0.732	20.81	1.543
BILGE	BLG-04	0.976	1.7	165.87	1.231	3	20.81	1.543	21	2.5
BILGE	BLG-05	0.1	1.7	17	1.076	3	21	2.5	21	2.6
SIDE	SHL-01	16.4	1.6	2624	0.92	2	21	2.6	21	19
GUNWALE	GWR-01	0.3	1.7	51	0.92	2	21	19	21	19.3
GUNWALE	GWR-02	0.518	1.7	88	0.718	2	21	19.3	20.866	19.8
GUNWALE	GWR-03	0.518	1.7	87.99	0.518	2	20.866	19.8	20.5	20.166
GUNWALE	GWR-04	0.518	1.7	88	0.518	2	20.5	20.166	20	20.3
GUNWALE	GWR-05	1.001	1.7	170.2	0.901	2	20	20.3	19	20.348
UPPER DECK	DEC-01	6.502	1.7	1105.31	0.901	2	19	20.348	12.5	20.502
UPPER DECK	DEC-02	11.304	1.7	1921.67	0.904	2	12.5	20.502	1.2	20.8
UPPER DECK	DEC-03	1.2	1.7	204	0.904	2	1.2	20.8	0	20.8
N-TIGHT B. GDR	NBG-01	2.5	2.2	275	1.5	2	0	0	0	2.5
Other BULKHEAD	OTH-01	20.502	1.6	3280.32	0.822	2	12.5	0	12.5	20.502
MISC.	MSC-01	1	2	200	1	2	0	2.5	1	2.5
MISC.	MSC-02	2	1.7	170	1.25	2	0	20.8	0	18.8
MISC.	MSC-03	1	1.7	170	1	2	0	18.8	1	18.8

Local Stiffener Ids:





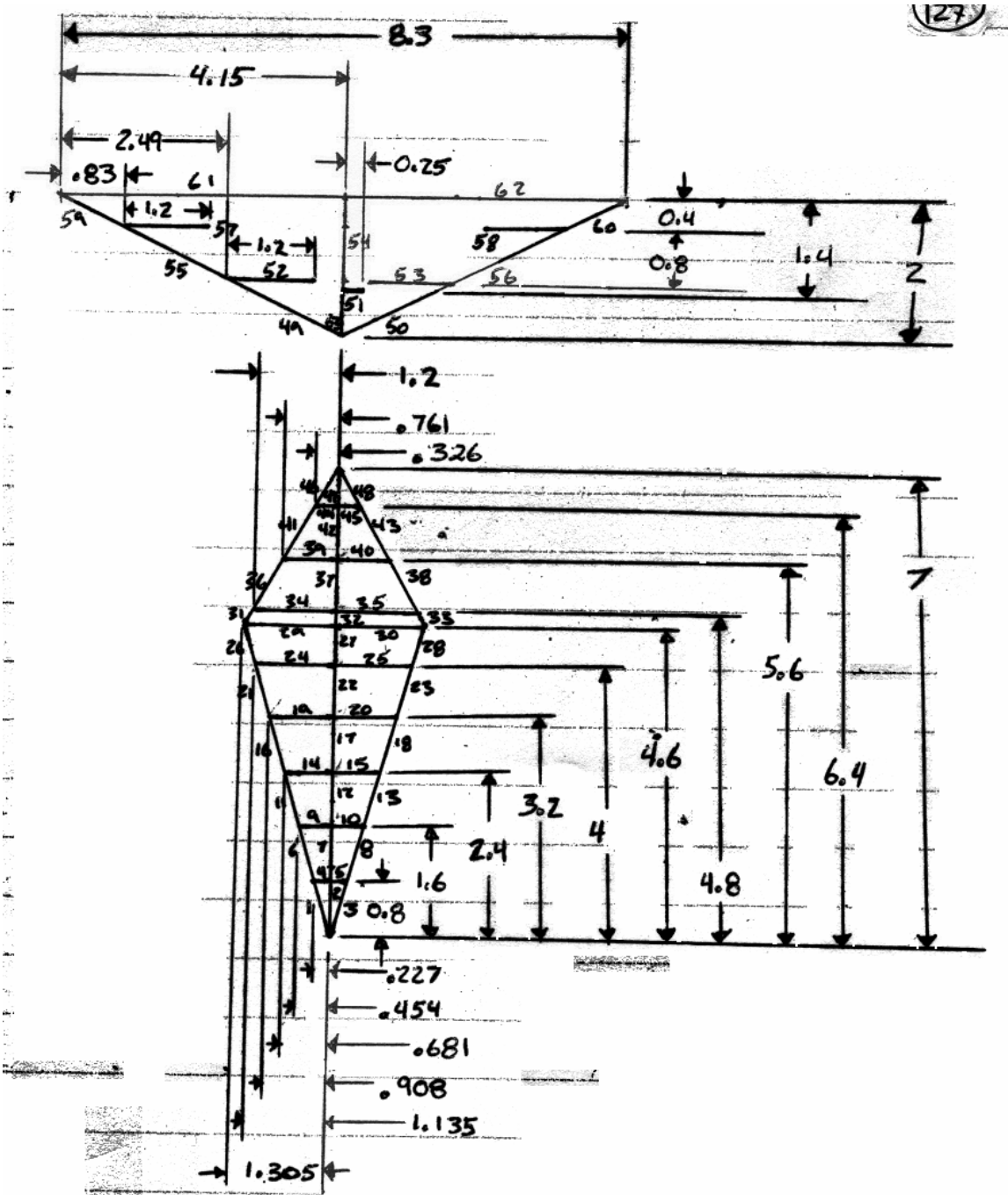
**Stiffeners:**

<i>ID</i>	<i>MSID</i>	<i>XLB</i>	<i>A</i>	<i>STFSP</i>	<i>UNSPAN</i>	<i>MATID</i>
			cm2	(m)	(m)	
KPL- 101	21	500x120x13.5x35 LIA	105.42	0.82	3.815	2
KPL- 102	21	500x120x13.5x35 LIA	105.42	0.89	3.815	2
BTM- 101	21	500x120x13.5x35 LIA	105.42	0.89	3.815	2
BTM- 102	21	500x120x13.5x35 LIA	105.42	0.82	3.815	2
BTM- 103	21	500x120x13.5x35 LIA	105.42	0.82	3.815	2
BTM- 104	21	500x120x13.5x35 LIA	105.42	0.82	3.815	2
BTM- 105	21	500x120x13.5x35 LIA	105.42	0.82	3.815	2
BTM- 106	21	500x120x13.5x35 LIA	105.42	0.82	3.815	2
BTM- 107	21	500x120x13.5x35 LIA	105.42	0.82	3.815	2
BTM- 108	21	500x120x13.5x35 LIA	105.42	0.82	3.815	2
BTM- 109	21	500x120x13.5x35 LIA	105.42	0.82	3.815	2
BTM- 110	21	500x120x13.5x35 LIA	105.42	0.82	3.815	2
BTM- 111	21	500x120x13.5x35 LIA	105.42	0.82	3.815	2
BTM- 112	21	500x120x13.5x35 LIA	105.42	0.85	3.815	2
BTM- 213	21	500x120x13.5x35 LIA	105.42	0.87	3.815	2
BTM- 214	21	500x120x13.5x35 LIA	105.42	0.82	3.815	2
BTM- 215	21	500x120x13.5x35 LIA	105.42	0.82	3.815	2
BTM- 216	21	500x120x13.5x35 LIA	105.42	0.82	3.815	2
BTM- 217	21	500x120x13.5x35 LIA	105.42	0.82	3.815	2
BTM- 218	21	500x120x13.5x35 LIA	105.42	0.82	3.815	2
BTM- 219	21	500x120x13.5x35 LIA	105.42	1.053	3.815	2
BLG- 101	0	500x120x13.5x35 LIA	105.42	0.488	3.815	2
BLG- 202	0	500x120x13.5x35 LIA	105.42	0.488	3.815	2
BLG- 303	0	500x120x13.5x35 LIA	105.42	0.488	3.815	2
SHL- 101	20	500x120x12.5x33 LIA	98.62	0.82	4.515	2
SHL- 102	20	500x120x12.5x33 LIA	98.62	0.82	4.515	2
SHL- 103	20	500x120x12.5x33 LIA	98.62	0.82	4.515	2
SHL- 104	20	500x120x12.5x33 LIA	98.62	0.82	4.515	2
SHL- 105	20	500x120x12.5x33 LIA	98.62	0.82	4.515	2
SHL- 106	20	500x120x12.5x33 LIA	98.62	0.82	4.515	2
SHL- 107	20	500x120x12.5x33 LIA	98.62	0.82	4.515	2
SHL- 108	20	500x120x12.5x33 LIA	98.62	0.82	4.515	2
SHL- 109	20	500x120x12.5x33 LIA	98.62	0.82	4.515	2
SHL- 110	20	500x120x12.5x33 LIA	98.62	0.82	4.515	2
SHL- 111	20	500x120x12.5x33 LIA	98.62	0.82	4.515	2
SHL- 112	20	500x120x12.5x33 LIA	98.62	0.82	4.515	2
SHL- 113	20	500x120x12.5x33 LIA	98.62	0.82	4.515	2
SHL- 114	20	500x120x12.5x33 LIA	98.62	0.82	4.515	2
SHL- 115	20	500x120x12.5x33 LIA	98.62	0.82	4.515	2
SHL- 116	20	500x120x12.5x33 LIA	98.62	0.82	4.515	2

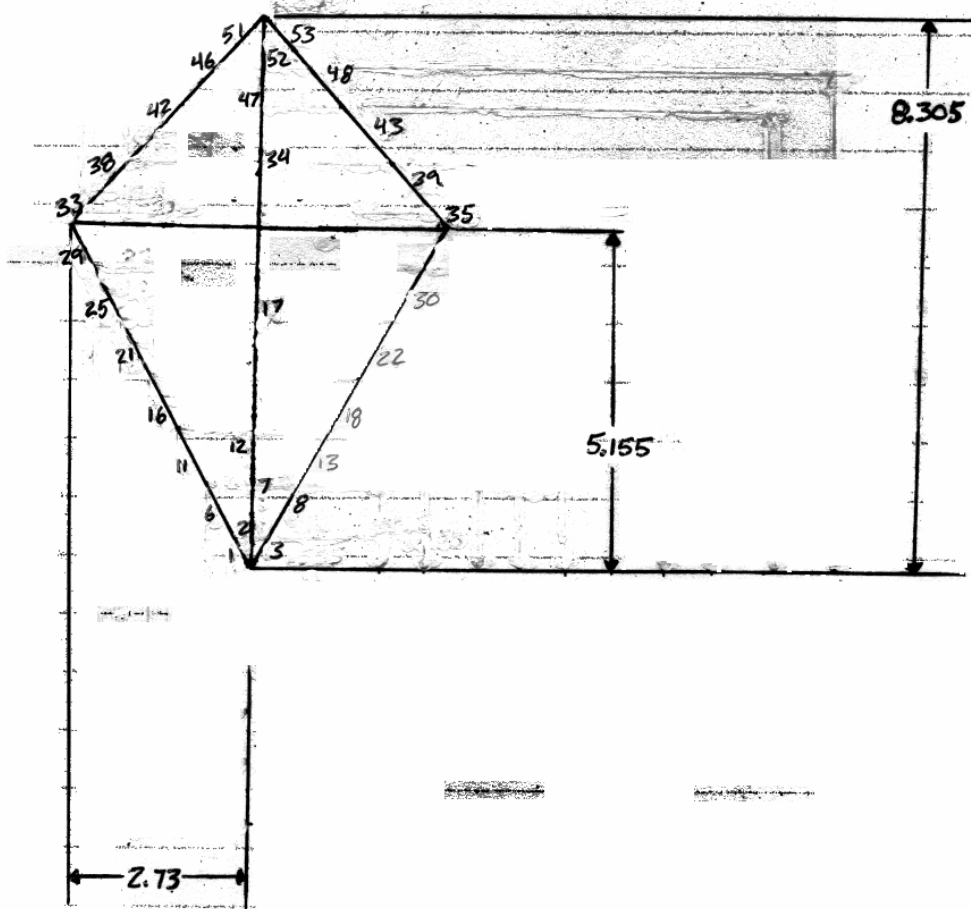
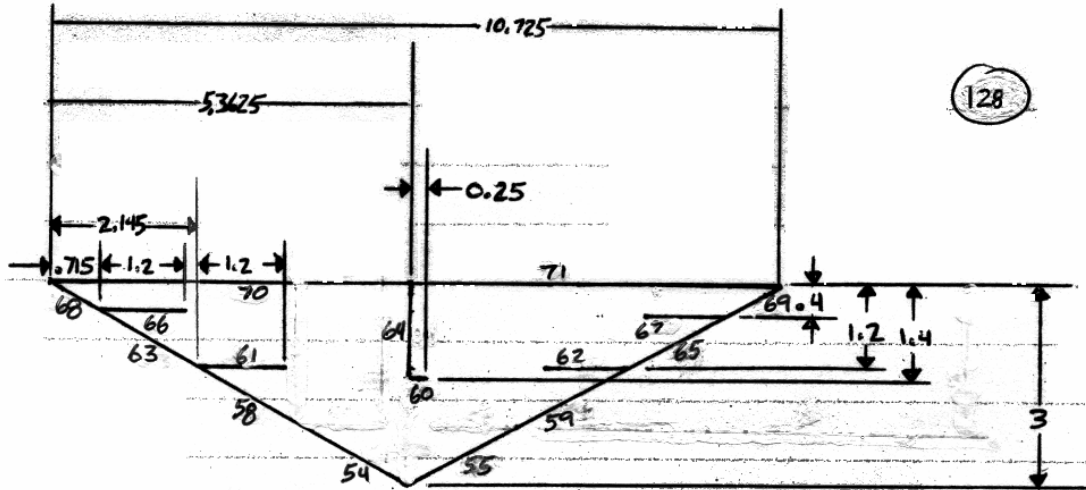
<i>ID</i>	<i>MSID</i>	<i>XLB</i>	<i>A</i>	<i>STFSP</i>	<i>UNSPAN</i>	<i>MATID</i>
			cm2	(m)	(m)	
SHL- 117	20	500x120x12.5x33 LIA	98.62	0.82	4.515	2
SHL- 118	20	500x120x12.5x33 LIA	98.62	0.82	4.515	2
SHL- 119	20	500x120x12.5x33 LIA	98.62	0.82	4.515	2
SHL- 120	20	500x120x12.5x33 LIA	98.62	0.82	4.515	2
GWR- 101	14	375x120x11.5x20 LIA	65.47	0.15	4.515	2
GWR- 502	14	375x120x11.5x20 LIA	65.47	0.82	4.515	2
GWR- 503	14	375x120x11.5x20 LIA	65.47	0.861	4.515	2
DEC- 101	18	475x120x11.5x28 LIA	85.65	0.861	4.515	2
DEC- 102	18	475x120x11.5x28 LIA	85.65	0.82	4.515	2
DEC- 103	18	475x120x11.5x28 LIA	85.65	0.82	4.515	2
DEC- 104	18	475x120x11.5x28 LIA	85.65	0.82	4.515	2
DEC- 105	18	475x120x11.5x28 LIA	85.65	0.82	4.515	2
DEC- 106	18	475x120x11.5x28 LIA	85.65	0.82	4.515	2
DEC- 107	18	475x120x11.5x28 LIA	85.65	0.841	4.515	2
DEC- 208	18	475x120x11.5x28 LIA	85.65	0.8	4.515	2
DEC- 209	18	475x120x11.5x28 LIA	85.65	0.85	4.515	2
DEC- 210	18	475x120x11.5x28 LIA	85.65	0.85	4.515	2
DEC- 211	18	475x120x11.5x28 LIA	85.65	0.85	4.515	2
DEC- 212	18	475x120x11.5x28 LIA	85.65	0.85	4.515	2
DEC- 213	18	475x120x11.5x28 LIA	85.65	0.85	4.515	2
DEC- 214	18	475x120x11.5x28 LIA	85.65	0.85	4.515	2
DEC- 215	18	475x120x11.5x28 LIA	85.65	0.85	4.515	2
DEC- 216	18	475x120x11.5x28 LIA	85.65	0.85	4.515	2
DEC- 217	18	475x120x11.5x28 LIA	85.65	0.85	4.515	2
DEC- 218	18	475x120x11.5x28 LIA	85.65	0.85	4.515	2
DEC- 219	18	475x120x11.5x28 LIA	85.65	0.85	4.515	2
DEC- 220	18	475x120x11.5x28 LIA	85.65	0.927	4.515	2
DEC- 321	18	475x120x11.5x28 LIA	85.65	0.6	4.515	2
NBG- 101	14	375x120x11.5x20 LIA	32.73	1.25	4.515	2
OTH 101	20	500x120x12.5x33 LIA	98.62	0.82	4.515	2
OTH 102	20	500x120x12.5x33 LIA	98.62	0.82	4.515	2
OTH 103	20	500x120x12.5x33 LIA	98.62	0.82	4.515	2
OTH 104	20	500x120x12.5x33 LIA	98.62	0.82	4.515	2
OTH 105	20	500x120x12.5x33 LIA	98.62	0.82	4.515	2
OTH 106	20	500x120x12.5x33 LIA	98.62	0.82	4.515	2
OTH 107	20	500x120x12.5x33 LIA	98.62	0.82	4.515	2
OTH 108	20	500x120x12.5x33 LIA	98.62	0.82	4.515	2
OTH 109	20	500x120x12.5x33 LIA	98.62	0.82	4.515	2
OTH 110	20	500x120x12.5x33 LIA	98.62	0.82	4.515	2
OTH 111	20	500x120x12.5x33 LIA	98.62	0.82	4.515	2
OTH 112	20	500x120x12.5x33 LIA	98.62	0.82	4.515	2

<i>ID</i>	<i>MSID</i>	<i>XLB</i>	<i>A</i>	<i>STFSP</i>	<i>UNSPAN</i>	<i>MATID</i>
			cm2	(m)	(m)	
OTH 113	20	500x120x12.5x33 LIA	98.62	0.82	4.515	2
OTH 114	20	500x120x12.5x33 LIA	98.62	0.82	4.515	2
OTH 115	20	500x120x12.5x33 LIA	98.62	0.82	4.515	2
OTH 116	20	500x120x12.5x33 LIA	98.62	0.82	4.515	2
OTH 117	20	500x120x12.5x33 LIA	98.62	0.82	4.515	2
OTH 118	20	500x120x12.5x33 LIA	98.62	0.82	4.515	2
OTH 119	20	500x120x12.5x33 LIA	98.62	0.82	4.515	2
OTH 120	20	500x120x12.5x33 LIA	98.62	0.82	4.515	2
OTH 121	20	500x120x12.5x33 LIA	98.62	0.82	4.515	2
OTH 122	20	500x120x12.5x33 LIA	98.62	0.82	4.515	2
OTH 123	20	500x120x12.5x33 LIA	98.62	0.82	4.515	2
OTH 124	20	500x120x12.5x33 LIA	98.62	0.821	4.515	2
MSC- 201	14	375x120x11.5x20 LIA	32.73	1.5	5.015	2



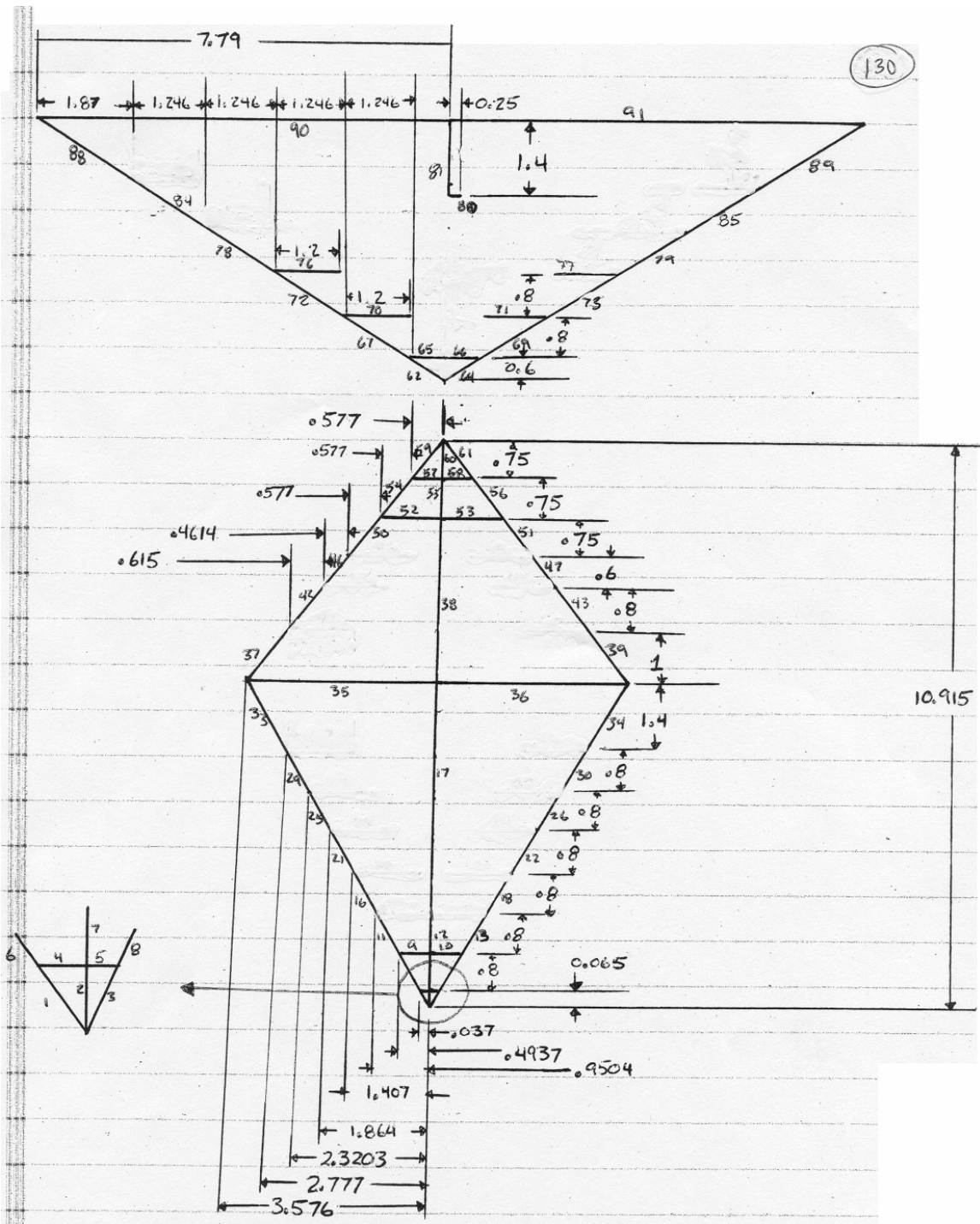


SECTION 2 150K DWT BULK CARRIER SCALE 1:100

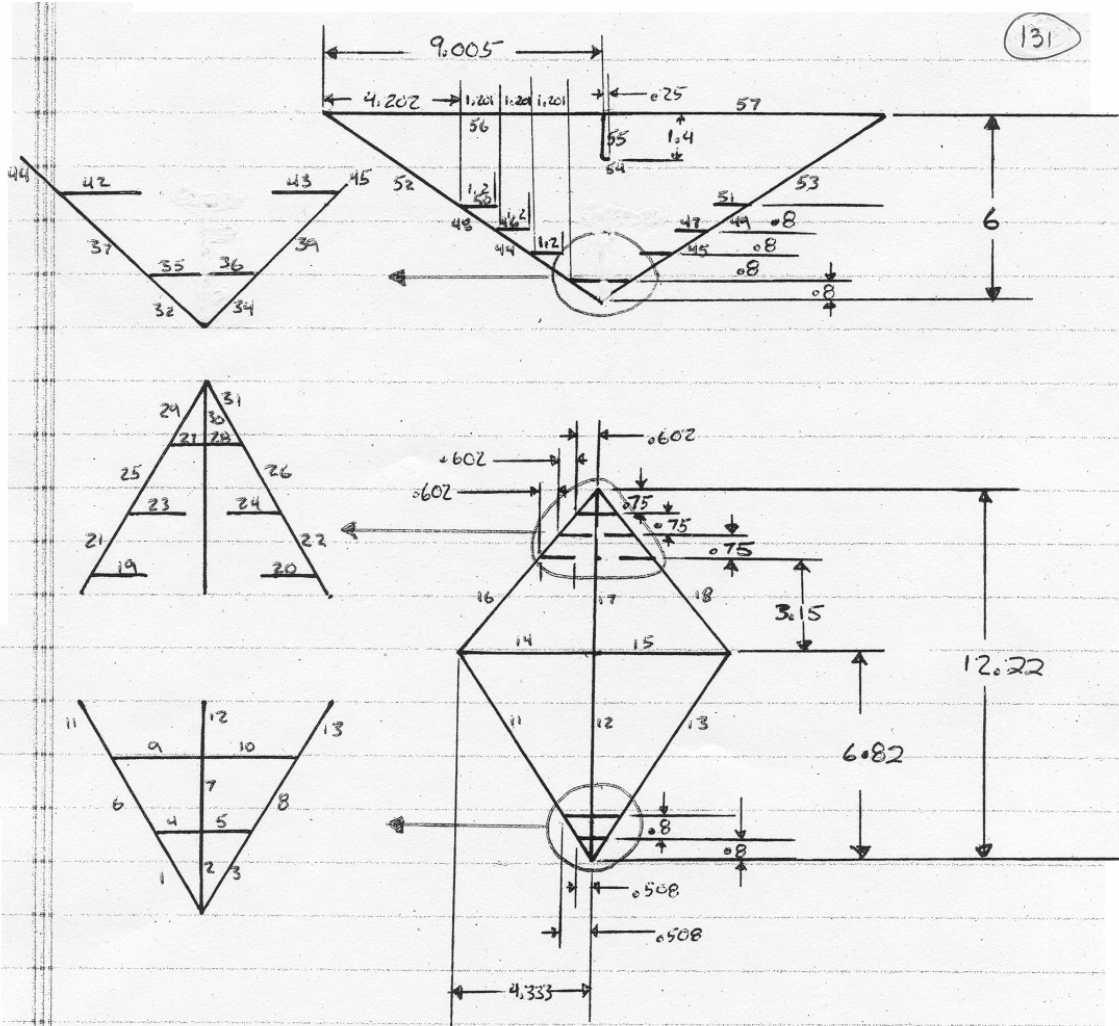


SECTION 3 150K DWT BULK CARRIER SCALE 1:100





SECTION 5 150K DWT BULK CARRIER SCALE 1:100



SECTION 6 150K DWT BULK CARRIER SCALE 1:200

Following are the properties for each element used in the Amdahl analysis with the smeared thickness, average thickness, and damaged area calculations for each illustrated section above.

The necessary units and functions for the analysis of the 150k dwt Bulk Carrier using Amdahls method with Pedersons Modifications are given as follows, the below calculation considers no longitudinal stiffener intersections, does not include the stem and only considers those breasthooks which span the complete distance between frames (not sections):

MPa := 10<sup>6</sup>Pa      Mega Pascal Definition

$$t_s(h_w, t_w, h_f, t_f, s_s, E_t) := \left[ \frac{(h_w \cdot t_w + h_f \cdot t_f)}{s_s} + E_t \right] \quad \text{Smeared Plate Thickness Formula}$$

MN := 10<sup>6</sup>N      Mega Newton Definition

Crushing Stress Formula:

$$\sigma_c(\sigma_0, n_{AT}, \tau, DA, n_C, n_T) := 2.42 \cdot \sigma_0 \cdot \left( \frac{n_{AT} \tau^2}{DA} \right)^{\frac{2}{3}} \cdot 0.87 + 1.27 \cdot \frac{n_C + 0.31 \cdot n_T}{\left[ (n_C + 0.31 \cdot n_T) \cdot \tau^2 \right]^{\frac{1}{4}}} \cdot DA^{\frac{2}{3}}$$

P<sub>AV</sub>(DA, σ<sub>c</sub>) := DA · σ<sub>c</sub>      Average Crushing Load Formula

The necessary 150k dwt Bulk Carrier Ship Particulars are defined as shown below.

Δ := 174850000kg      Displacement

V<sub>s</sub> := 9.3  $\frac{m}{s}$       Maximum Service Speed

The material properties for the 150k dwt Bulk Carrier are defined as shown below.

σ<sub>y</sub> := 315MPa      Mild Steel Yield Stress

σ<sub>u</sub> := 1.6 · σ<sub>y</sub>      σ<sub>u</sub> = 504 MPa      Mild Steel Ultimate Stress

Therefor the Distance between transverse frames is defined as follows:

D<sub>T</sub> := 0.8m      Distance Between Transverse "Sections" equals 1/4 the distance between transverse frames.

Properties for Section 1 are given as follows:

n<sub>T<sub>1</sub></sub> := 4      Number of "T" intersections for section 1

n<sub>L<sub>1</sub></sub> := 0      Number of Angle Intersections for section 1

n<sub>C<sub>1</sub></sub> := 2      Number of Cruciform Intersections for section 1

n<sub>F<sub>1</sub></sub> := 10      Number of Elements within Section 1

n<sub>AT<sub>1</sub></sub> := n<sub>T<sub>1</sub></sub> + n<sub>L<sub>1</sub></sub>      n<sub>AT<sub>1</sub></sub> = 4      Number of "T" and Angle Intersections for section 1

$s1b :=$ 

1.3956
.6
1.3956
1.26
1.26
.9304
.4
.9304
2.1
2.1

 m

Element Spans within section 1 for elements 1 through 10

$s1E_t :=$ 

16
12
16
15
15
16
12
16
13
13

 mm

Element Plate Thicknesses within section 1 for elements 1 through 10

$s1h_w :=$ 

0
0
0
0
0
0
0
0
0
0
250
250

 mm

Element Web heights within section 1 on elements 1 through 10

$s1t_w :=$ 

0
0
0
0
0
0
0
0
0
0
12
12

 mm

Element Web Thicknesses within section 1 on elements 1 through 10

$s1h_f :=$ 

0
0
0
0
0
0
0
0
0
0
90
90

 mm

Element Flange Span within Section 1 on elements 1 through 10

$s1t_f :=$ 

0
0
0
0
0
0
0
0
0
0
16
16

 mm

Element Flange Thickness within section 1 elements 1 through 10

$$s1s := \begin{pmatrix} 1 \\ 1 \\ 1 \\ 1 \\ 1 \\ 1 \\ 800 \\ 800 \end{pmatrix} \text{ mm} \quad \text{Element Stiffener Spacing within section 1 elements 1 through 10} \quad := 1..n_F \quad \text{Iteration Counter}$$

$$s1t_s := t_s(s1h_w, s1t_w, s1h_f, s1t_f, s1s, s1E_t)$$

$$s1t_s = \begin{pmatrix} 0.016 \\ 0.012 \\ 0.016 \\ 0.015 \\ 0.015 \\ 0.016 \\ 0.012 \\ 0.016 \\ 0.019 \\ 0.019 \end{pmatrix} \text{ m} \quad \text{Element Smeared thicknesses in section 1 for elements 1 through 14}$$

$$\tau_1 := \frac{1}{n_{F1}} \left( \sum_{i=1}^{n_{F1}} s1t_{s_i} \right) \quad \tau_1 = 0.016 \text{ m} \quad \text{Section 1 Average Thickness}$$

$$DA_1 := \tau_1 \cdot \sum_{i=1}^{n_{F1}} s1b_i \quad DA_1 = 0.192 \text{ m}^2 \quad \text{Section 1 Damaged Cross Sectional Area}$$

$$DA_{E1} := \sum_{i=1}^{n_{F1}} s1b_i \cdot s1t_{s_i} \quad DA_{E1} = 0.202 \text{ m}^2 \quad \text{Section 1 Exact Damaged Cross Sectional Area}$$

Properties for **Section 2** are given as follows:

$n_{T2} := 27$	Number of "T" intersections for section 2		
$n_{L2} := 0$	Number of Angle Intersections for section 2		
$n_{C2} := 10$	Number of Cruciform Intersections for section 2		
$n_{F2} := 63$	Number of Elements within Section 2		
$n_{AT2} := n_{T2} + n_{L2}$	$n_{AT2} = 27$	Number of "T" and Angle Intersections for section 2	

Element Spans within section 2 for elements 1 through 63

$s2b_1 := .8316\text{m}$	$s2b_2 := 0.8\text{m}$	$s2b_3 := .8316\text{m}$	$s2b_4 := .227\text{m}$
$s2b_5 := .227\text{m}$	$s2b_6 := .8316\text{m}$	$s2b_7 := .8\text{m}$	$s2b_8 := .8316\text{m}$
$s2b_9 := .454\text{m}$	$s2b_{10} := .454\text{m}$	$s2b_{11} := .8316\text{m}$	$s2b_{12} := .8\text{m}$

s2b <sub>13</sub> := .8316m	s2b <sub>14</sub> := .681m	s2b <sub>15</sub> := .681m	s2b <sub>16</sub> := .8316m
s2b <sub>17</sub> := 0.8m	s2b <sub>18</sub> := .8316m	s2b <sub>19</sub> := .908m	s2b <sub>20</sub> := .908m
s2b <sub>21</sub> := .8316m	s2b <sub>22</sub> := .8m	s2b <sub>23</sub> := .8316m	s2b <sub>24</sub> := 1.135m
s2b <sub>25</sub> := 1.135m	s2b <sub>26</sub> := .6236m	s2b <sub>27</sub> := 0.6m	s2b <sub>28</sub> := .6236m
s2b <sub>29</sub> := 1.305m	s2b <sub>30</sub> := 1.305m	s2b <sub>31</sub> := .2259m	s2b <sub>32</sub> := .2m
s2b <sub>33</sub> := .2259m	s2b <sub>34</sub> := 1.2m	s2b <sub>35</sub> := 1.2m	s2b <sub>36</sub> := .9125m
s2b <sub>37</sub> := .8m	s2b <sub>38</sub> := .9125m	s2b <sub>39</sub> := .761m	s2b <sub>40</sub> := .761m
s2b <sub>41</sub> := .9106m	s2b <sub>42</sub> := .8m	s2b <sub>43</sub> := .9106m	s2b <sub>44</sub> := .326m
s2b <sub>45</sub> := .326m	s2b <sub>46</sub> := .6828m	s2b <sub>47</sub> := .6m	s2b <sub>48</sub> := .6828m
s2b <sub>49</sub> := 1.8427m	s2b <sub>50</sub> := 1.8427m	s2b <sub>51</sub> := .25m	s2b <sub>52</sub> := 1.2m
s2b <sub>53</sub> := 1.2m	s2b <sub>54</sub> := 1.4m	s2b <sub>55</sub> := 1.8427m	s2b <sub>56</sub> := 1.8427m
s2b <sub>57</sub> := 1.2m	s2b <sub>58</sub> := 1.2m	s2b <sub>59</sub> := .9214m	s2b <sub>60</sub> := .9214m
s2b <sub>61</sub> := 4.15m	s2b <sub>62</sub> := 4.15m	s2b <sub>63</sub> := .6m	

Element Plate Thicknesses within section 2 for elements 1 through 63

s2E <sub>t1</sub> := 18mm	s2E <sub>t2</sub> := 12mm	s2E <sub>t3</sub> := 18mm	s2E <sub>t4</sub> := 15mm
s2E <sub>t5</sub> := 15mm	s2E <sub>t6</sub> := 18mm	s2E <sub>t7</sub> := 12mm	s2E <sub>t8</sub> := 18mm
s2E <sub>t9</sub> := 15mm	s2E <sub>t10</sub> := 15mm	s2E <sub>t11</sub> := 18mm	s2E <sub>t12</sub> := 12mm
s2E <sub>t13</sub> := 18mm	s2E <sub>t14</sub> := 15mm	s2E <sub>t15</sub> := 15mm	s2E <sub>t16</sub> := 18mm
s2E <sub>t17</sub> := 12mm	s2E <sub>t18</sub> := 18mm	s2E <sub>t19</sub> := 15mm	s2E <sub>t20</sub> := 15mm
s2E <sub>t21</sub> := 18mm	s2E <sub>t22</sub> := 12mm	s2E <sub>t23</sub> := 18mm	s2E <sub>t24</sub> := 15mm
s2E <sub>t25</sub> := 15mm	s2E <sub>t26</sub> := 18mm	s2E <sub>t27</sub> := 12mm	s2E <sub>t28</sub> := 18mm
s2E <sub>t29</sub> := 13mm	s2E <sub>t30</sub> := 13mm	s2E <sub>t31</sub> := 18mm	s2E <sub>t32</sub> := 12mm
s2E <sub>t33</sub> := 18mm	s2E <sub>t34</sub> := 15mm	s2E <sub>t35</sub> := 15mm	s2E <sub>t36</sub> := 33mm
s2E <sub>t37</sub> := 12mm	s2E <sub>t38</sub> := 33mm	s2E <sub>t39</sub> := 15mm	s2E <sub>t40</sub> := 15mm
s2E <sub>t41</sub> := 33mm	s2E <sub>t42</sub> := 12mm	s2E <sub>t43</sub> := 33mm	s2E <sub>t44</sub> := 15mm
s2E <sub>t45</sub> := 15mm	s2E <sub>t46</sub> := 33mm	s2E <sub>t47</sub> := 12mm	s2E <sub>t48</sub> := 33mm
s2E <sub>t49</sub> := 16mm	s2E <sub>t50</sub> := 16mm	s2E <sub>t51</sub> := 25mm	s2E <sub>t52</sub> := 15mm
s2E <sub>t53</sub> := 15mm	s2E <sub>t54</sub> := 12mm	s2E <sub>t55</sub> := 16mm	s2E <sub>t56</sub> := 16mm
s2E <sub>t57</sub> := 15mm	s2E <sub>t58</sub> := 15mm	s2E <sub>t59</sub> := 16mm	s2E <sub>t60</sub> := 16mm
s2E <sub>t61</sub> := 13mm	s2E <sub>t62</sub> := 13mm	s2E <sub>t63</sub> := 12mm	

Element Web heights within section 2 on elements 1 through 63

s2h <sub>w1</sub> := 450mm	s2h <sub>w2</sub> := 0mm	s2h <sub>w3</sub> := 450mm	s2h <sub>w4</sub> := 0mm
s2h <sub>w5</sub> := 0mm	s2h <sub>w6</sub> := 450mm	s2h <sub>w7</sub> := 0mm	s2h <sub>w8</sub> := 450mm

$s2h_{w_9} := 0\text{mm}$	$s2h_{w_{10}} := 0\text{mm}$	$s2h_{w_{11}} := 450\text{mm}$	$s2h_{w_{12}} := 0\text{mm}$
$s2h_{w_{13}} := 450\text{mm}$	$s2h_{w_{14}} := 0\text{mm}$	$s2h_{w_{15}} := 0\text{mm}$	$s2h_{w_{16}} := 450\text{mm}$
$s2h_{w_{17}} := 0\text{mm}$	$s2h_{w_{18}} := 450\text{mm}$	$s2h_{w_{19}} := 0\text{mm}$	$s2h_{w_{20}} := 0\text{mm}$
$s2h_{w_{21}} := 450\text{mm}$	$s2h_{w_{22}} := 0\text{mm}$	$s2h_{w_{23}} := 450\text{mm}$	$s2h_{w_{24}} := 0\text{mm}$
$s2h_{w_{25}} := 0\text{mm}$	$s2h_{w_{26}} := 450\text{mm}$	$s2h_{w_{27}} := 0\text{mm}$	$s2h_{w_{28}} := 450\text{mm}$
$s2h_{w_{29}} := 250\text{mm}$	$s2h_{w_{30}} := 250\text{mm}$	$s2h_{w_{31}} := 400\text{mm}$	$s2h_{w_{32}} := 0\text{mm}$
$s2h_{w_{33}} := 400\text{mm}$	$s2h_{w_{34}} := 0\text{mm}$	$s2h_{w_{35}} := 0\text{mm}$	$s2h_{w_{36}} := 400\text{mm}$
$s2h_{w_{37}} := 0\text{mm}$	$s2h_{w_{38}} := 400\text{mm}$	$s2h_{w_{39}} := 0\text{mm}$	$s2h_{w_{40}} := 0\text{mm}$
$s2h_{w_{41}} := 400\text{mm}$	$s2h_{w_{42}} := 0\text{mm}$	$s2h_{w_{43}} := 400\text{mm}$	$s2h_{w_{44}} := 0\text{mm}$
$s2h_{w_{45}} := 0\text{mm}$	$s2h_{w_{46}} := 400\text{mm}$	$s2h_{w_{47}} := 0\text{mm}$	$s2h_{w_{48}} := 400\text{mm}$
$s2h_{w_{49}} := 350\text{mm}$	$s2h_{w_{50}} := 350\text{mm}$	$s2h_{w_{51}} := 0\text{mm}$	$s2h_{w_{52}} := 0\text{mm}$
$s2h_{w_{53}} := 0\text{mm}$	$s2h_{w_{54}} := 0\text{mm}$	$s2h_{w_{55}} := 350\text{mm}$	$s2h_{w_{56}} := 350\text{mm}$
$s2h_{w_{57}} := 0\text{mm}$	$s2h_{w_{58}} := 0\text{mm}$	$s2h_{w_{59}} := 350\text{mm}$	$s2h_{w_{60}} := 350\text{mm}$
$s2h_{w_{61}} := 250\text{mm}$	$s2h_{w_{62}} := 250\text{mm}$	$s2h_{w_{63}} := 0\text{mm}$	

Element Web heights within section 2 on elements 1 through 63

$s2t_{w_1} := 12\text{mm}$	$s2t_{w_2} := 0\text{mm}$	$s2t_{w_3} := 12\text{mm}$	$s2t_{w_4} := 0\text{mm}$
$s2t_{w_5} := 0\text{mm}$	$s2t_{w_6} := 12\text{mm}$	$s2t_{w_7} := 0\text{mm}$	$s2t_{w_8} := 12\text{mm}$
$s2t_{w_9} := 0\text{mm}$	$s2t_{w_{10}} := 0\text{mm}$	$s2t_{w_{11}} := 12\text{mm}$	$s2t_{w_{12}} := 0\text{mm}$
$s2t_{w_{13}} := 12\text{mm}$	$s2t_{w_{14}} := 0\text{mm}$	$s2t_{w_{15}} := 0\text{mm}$	$s2t_{w_{16}} := 12\text{mm}$
$s2t_{w_{17}} := 0\text{mm}$	$s2t_{w_{18}} := 12\text{mm}$	$s2t_{w_{19}} := 0\text{mm}$	$s2t_{w_{20}} := 0\text{mm}$
$s2t_{w_{21}} := 12\text{mm}$	$s2t_{w_{22}} := 0\text{mm}$	$s2t_{w_{23}} := 12\text{mm}$	$s2t_{w_{24}} := 0\text{mm}$
$s2t_{w_{25}} := 0\text{mm}$	$s2t_{w_{26}} := 12\text{mm}$	$s2t_{w_{27}} := 0\text{mm}$	$s2t_{w_{28}} := 12\text{mm}$
$s2t_{w_{29}} := 12\text{mm}$	$s2t_{w_{30}} := 12\text{mm}$	$s2t_{w_{31}} := 19\text{mm}$	$s2t_{w_{32}} := 0\text{mm}$
$s2t_{w_{33}} := 19\text{mm}$	$s2t_{w_{34}} := 0\text{mm}$	$s2t_{w_{35}} := 0\text{mm}$	$s2t_{w_{36}} := 19\text{mm}$
$s2t_{w_{37}} := 0\text{mm}$	$s2t_{w_{38}} := 19\text{mm}$	$s2t_{w_{39}} := 0\text{mm}$	$s2t_{w_{40}} := 0\text{mm}$
$s2t_{w_{41}} := 19\text{mm}$	$s2t_{w_{42}} := 0\text{mm}$	$s2t_{w_{43}} := 19\text{mm}$	$s2t_{w_{44}} := 0\text{mm}$
$s2t_{w_{45}} := 0\text{mm}$	$s2t_{w_{46}} := 19\text{mm}$	$s2t_{w_{47}} := 0\text{mm}$	$s2t_{w_{48}} := 19\text{mm}$
$s2t_{w_{49}} := 12\text{mm}$	$s2t_{w_{50}} := 12\text{mm}$	$s2t_{w_{51}} := 0\text{mm}$	$s2t_{w_{52}} := 0\text{mm}$
$s2t_{w_{53}} := 0\text{mm}$	$s2t_{w_{54}} := 0\text{mm}$	$s2t_{w_{55}} := 12\text{mm}$	$s2t_{w_{56}} := 12\text{mm}$
$s2t_{w_{57}} := 0\text{mm}$	$s2t_{w_{58}} := 0\text{mm}$	$s2t_{w_{59}} := 12\text{mm}$	$s2t_{w_{60}} := 12\text{mm}$
$s2t_{w_{61}} := 12\text{mm}$	$s2t_{w_{62}} := 12\text{mm}$	$s2t_{w_{63}} := 0\text{mm}$	

Element Flange Span within Section 2 on elements 1 through 63

$s2h_f := 150\text{mm}$	$s2h_f := 0\text{mm}$	$s2h_f := 150\text{mm}$	$s2h_f := 0\text{mm}$
-------------------------	-----------------------	-------------------------	-----------------------



s2s <sub>1</sub> := 800mm	s2s <sub>2</sub> := 0mm	s2s <sub>3</sub> := 800mm	s2s <sub>4</sub> := 0mm
s2s <sub>5</sub> := 0mm	s2s <sub>6</sub> := 800mm	s2s <sub>7</sub> := 0mm	s2s <sub>8</sub> := 800mm
s2s <sub>9</sub> := 0mm	s2s <sub>10</sub> := 0mm	s2s <sub>11</sub> := 800mm	s2s <sub>12</sub> := 0mm
s2s <sub>13</sub> := 800mm	s2s <sub>14</sub> := 0mm	s2s <sub>15</sub> := 0mm	s2s <sub>16</sub> := 800mm
s2s <sub>17</sub> := 0mm	s2s <sub>18</sub> := 800mm	s2s <sub>19</sub> := 0mm	s2s <sub>20</sub> := 0mm
s2s <sub>21</sub> := 800mm	s2s <sub>22</sub> := 0mm	s2s <sub>23</sub> := 800mm	s2s <sub>24</sub> := 0mm
s2s <sub>25</sub> := 0mm	s2s <sub>26</sub> := 800mm	s2s <sub>27</sub> := 0mm	s2s <sub>28</sub> := 800mm
s2s <sub>29</sub> := 800mm	s2s <sub>30</sub> := 800mm	s2s <sub>31</sub> := 600mm	s2s <sub>32</sub> := 0mm
s2s <sub>33</sub> := 600mm	s2s <sub>34</sub> := 0mm	s2s <sub>35</sub> := 0mm	s2s <sub>36</sub> := 600mm
s2s <sub>37</sub> := 0mm	s2s <sub>38</sub> := 600mm	s2s <sub>39</sub> := 0mm	s2s <sub>40</sub> := 0mm
s2s <sub>41</sub> := 600mm	s2s <sub>42</sub> := 0mm	s2s <sub>43</sub> := 600mm	s2s <sub>44</sub> := 0mm
s2s <sub>45</sub> := 0mm	s2s <sub>46</sub> := 600mm	s2s <sub>47</sub> := 0mm	s2s <sub>48</sub> := 600mm
s2s <sub>49</sub> := 800mm	s2s <sub>50</sub> := 800mm	s2s <sub>51</sub> := 0mm	s2s <sub>52</sub> := 0mm
s2s <sub>53</sub> := 0mm	s2s <sub>54</sub> := 0mm	s2s <sub>55</sub> := 800mm	s2s <sub>56</sub> := 800mm
s2s <sub>57</sub> := 0mm	s2s <sub>58</sub> := 0mm	s2s <sub>59</sub> := 800mm	s2s <sub>60</sub> := 800mm
s2s <sub>61</sub> := 800mm	s2s <sub>62</sub> := 800mm	s2s <sub>63</sub> := 0mm	

i := 1..n<sub>F2</sub>      Iteration Counter

s2t<sub>s<sub>i</sub></sub> := t<sub>s</sub>(s2h<sub>w<sub>i</sub></sub>, s2t<sub>w<sub>i</sub></sub>, s2h<sub>f<sub>i</sub></sub>, s2t<sub>f<sub>i</sub></sub>, s2s<sub>i</sub>, s2E<sub>t<sub>i</sub></sub>)      Smeared Thickness Calculation

$\tau_2 := \frac{1}{n_{F_2}} \left( \sum_{i=1}^{n_{F_2}} s2t_{s_i} \right)$        $\tau_2 = 0.022 \text{ m}$       Section 2 Average Thickness

$DA_2 := \tau_2 \cdot \sum_{i=1}^{n_{F_2}} s2b_i$        $DA_2 = 1.278 \text{ m}^2$       Section 2 Damaged Cross Sectional Area

$DA_{E_2} := \sum_{i=1}^{n_{F_2}} s2b_i \cdot s2t_{s_i}$        $DA_{E_2} = 1.249 \text{ m}^2$       Section 2 Exact Damaged Cross Sectional Area

Properties for **Section 3** are given as follows:

n <sub>T<sub>3</sub></sub> := 31	Number of "T" intersections for section 3	
n <sub>L<sub>3</sub></sub> := 4	Number of Angle Intersections for section 3	
n <sub>C<sub>3</sub></sub> := 4	Number of Cruciform Intersections for section 3	
n <sub>F<sub>3</sub></sub> := 72	Number of Elements within Section 3	
n <sub>AT<sub>3</sub></sub> := n <sub>T<sub>3</sub></sub> + n <sub>L<sub>3</sub></sub>	n <sub>AT<sub>3</sub></sub> = 35	Number of "T" and Angle Intersections for section 3

Element Spans within section 3 for elements 1 through 72

s3b <sub>1</sub> := .6281m	s3b <sub>2</sub> := .555m	s3b <sub>3</sub> := .6281m	s3b <sub>4</sub> := .294m
s3b <sub>5</sub> := .294m	s3b <sub>6</sub> := .9054m	s3b <sub>7</sub> := .8m	s3b <sub>8</sub> := .9054m
s3b <sub>9</sub> := .718m	s3b <sub>10</sub> := .718m	s3b <sub>11</sub> := .9054m	s3b <sub>12</sub> := .8m
s3b <sub>13</sub> := .9054m	s3b <sub>14</sub> := 1.2m	s3b <sub>15</sub> := 1.2m	s3b <sub>16</sub> := .9054m
s3b <sub>17</sub> := 3m	s3b <sub>18</sub> := .9054m	s3b <sub>19</sub> := 1.2m	s3b <sub>20</sub> := 1.2m
s3b <sub>21</sub> := .9054m	s3b <sub>22</sub> := .9054m	s3b <sub>23</sub> := 1.2m	s3b <sub>24</sub> := 1.2m
s3b <sub>25</sub> := .9054m	s3b <sub>26</sub> := .9054m	s3b <sub>27</sub> := 1.2m	s3b <sub>28</sub> := 1.2m
s3b <sub>29</sub> := .679m	s3b <sub>30</sub> := .679m	s3b <sub>31</sub> := 2.73m	s3b <sub>32</sub> := 2.73m
s3b <sub>33</sub> := .2625m	s3b <sub>34</sub> := 1.8m	s3b <sub>35</sub> := .2625m	s3b <sub>36</sub> := 1.2m
s3b <sub>37</sub> := 1.2m	s3b <sub>38</sub> := 1.063m	s3b <sub>39</sub> := 1.063m	s3b <sub>40</sub> := 1.2m
s3b <sub>41</sub> := 1.2m	s3b <sub>42</sub> := 1.056m	s3b <sub>43</sub> := 1.056m	s3b <sub>44</sub> := 1.2m
s3b <sub>45</sub> := 1.2m	s3b <sub>46</sub> := .794m	s3b <sub>47</sub> := .6m	s3b <sub>48</sub> := .794m
s3b <sub>49</sub> := .65m	s3b <sub>50</sub> := .65m	s3b <sub>51</sub> := .9925m	s3b <sub>52</sub> := .75m
s3b <sub>53</sub> := .9925m	s3b <sub>54</sub> := 2.05m	s3b <sub>55</sub> := 2.05m	s3b <sub>56</sub> := 1.2m
s3b <sub>57</sub> := 1.2m	s3b <sub>58</sub> := 1.6385m	s3b <sub>59</sub> := 1.6385m	s3b <sub>60</sub> := .25m
s3b <sub>61</sub> := 1.2m	s3b <sub>62</sub> := 1.2m	s3b <sub>63</sub> := 1.6385m	s3b <sub>64</sub> := 1.4m
s3b <sub>65</sub> := 1.6385m	s3b <sub>66</sub> := 1.2m	s3b <sub>67</sub> := 1.2m	s3b <sub>68</sub> := .82m
s3b <sub>69</sub> := .82m	s3b <sub>70</sub> := 5.3625m	s3b <sub>71</sub> := 5.3625m	s3b <sub>72</sub> := 0m

Element Plate Thicknesses within section 3 for elements 1 through 72

s3E <sub>t1</sub> := 18mm	s3E <sub>t2</sub> := 12mm	s3E <sub>t3</sub> := 18mm	s3E <sub>t4</sub> := 15mm
s3E <sub>t5</sub> := 15mm	s3E <sub>t6</sub> := 18mm	s3E <sub>t7</sub> := 12mm	s3E <sub>t8</sub> := 18mm
s3E <sub>t9</sub> := 15mm	s3E <sub>t10</sub> := 15mm	s3E <sub>t11</sub> := 18mm	s3E <sub>t12</sub> := 12mm
s3E <sub>t13</sub> := 18mm	s3E <sub>t14</sub> := 15mm	s3E <sub>t15</sub> := 15mm	s3E <sub>t16</sub> := 18mm
s3E <sub>t17</sub> := 12mm	s3E <sub>t18</sub> := 18mm	s3E <sub>t19</sub> := 15mm	s3E <sub>t20</sub> := 15mm
s3E <sub>t21</sub> := 18mm	s3E <sub>t22</sub> := 18mm	s3E <sub>t23</sub> := 15mm	s3E <sub>t24</sub> := 15mm
s3E <sub>t25</sub> := 18mm	s3E <sub>t26</sub> := 18mm	s3E <sub>t27</sub> := 15mm	s3E <sub>t28</sub> := 15mm
s3E <sub>t29</sub> := 18mm	s3E <sub>t30</sub> := 18mm	s3E <sub>t31</sub> := 13mm	s3E <sub>t32</sub> := 13mm
s3E <sub>t33</sub> := 18mm	s3E <sub>t34</sub> := 12mm	s3E <sub>t35</sub> := 18mm	s3E <sub>t36</sub> := 15mm
s3E <sub>t37</sub> := 15mm	s3E <sub>t38</sub> := 33mm	s3E <sub>t39</sub> := 33mm	s3E <sub>t40</sub> := 15mm
s3E <sub>t41</sub> := 15mm	s3E <sub>t42</sub> := 33mm	s3E <sub>t43</sub> := 33mm	s3E <sub>t44</sub> := 15mm
s3E <sub>t45</sub> := 15mm	s3E <sub>t46</sub> := 33mm	s3E <sub>t47</sub> := 12mm	s3E <sub>t48</sub> := 33mm
s3E <sub>t49</sub> := 15mm	s3E <sub>t50</sub> := 15mm	s3E <sub>t51</sub> := 33mm	s3E <sub>t52</sub> := 12mm
s3E <sub>t53</sub> := 33mm	s3E <sub>t54</sub> := 16mm	s3E <sub>t55</sub> := 16mm	s3E <sub>t56</sub> := 15mm
s3E <sub>t57</sub> := 15mm	s3E <sub>t58</sub> := 16mm	s3E <sub>t59</sub> := 16mm	s3E <sub>t60</sub> := 25mm

$s3E_{t_{61}} := 15\text{mm}$	$s3E_{t_{62}} := 15\text{mm}$	$s3E_{t_{63}} := 16\text{mm}$	$s3E_{t_{64}} := 12\text{mm}$
$s3E_{t_{65}} := 16\text{mm}$	$s3E_{t_{66}} := 15\text{mm}$	$s3E_{t_{67}} := 15\text{mm}$	$s3E_{t_{68}} := 16\text{mm}$
$s3E_{t_{69}} := 16\text{mm}$	$s3E_{t_{70}} := 13\text{mm}$	$s3E_{t_{71}} := 13\text{mm}$	$s3E_{t_{72}} := 12\text{mm}$

**Element Web heights within section 3 on elements 1 through 72**

$s3h_w := 450\text{mm}$	$s3h_w := 0\text{mm}$	$s3h_w := 450\text{mm}$	$s3h_w := 0\text{mm}$
$s3h_w := 0\text{mm}$	$s3h_w := 450\text{mm}$	$s3h_w := 0\text{mm}$	$s3h_w := 450\text{mm}$
$s3h_w := 0\text{mm}$	$s3h_w := 0\text{mm}$	$s3h_w := 450\text{mm}$	$s3h_w := 0\text{mm}$
$s3h_w := 450\text{mm}$	$s3h_w := 0\text{mm}$	$s3h_w := 0\text{mm}$	$s3h_w := 450\text{mm}$
$s3h_w := 0\text{mm}$	$s3h_w := 450\text{mm}$	$s3h_w := 0\text{mm}$	$s3h_w := 0\text{mm}$
$s3h_w := 450\text{mm}$	$s3h_w := 450\text{mm}$	$s3h_w := 0\text{mm}$	$s3h_w := 0\text{mm}$
$s3h_w := 450\text{mm}$	$s3h_w := 450\text{mm}$	$s3h_w := 0\text{mm}$	$s3h_w := 0\text{mm}$
$s3h_w := 450\text{mm}$	$s3h_w := 450\text{mm}$	$s3h_w := 250\text{mm}$	$s3h_w := 250\text{mm}$
$s3h_w := 400\text{mm}$	$s3h_w := 0\text{mm}$	$s3h_w := 400\text{mm}$	$s3h_w := 0\text{mm}$
$s3h_w := 0\text{mm}$	$s3h_w := 400\text{mm}$	$s3h_w := 400\text{mm}$	$s3h_w := 0\text{mm}$
$s3h_w := 0\text{mm}$	$s3h_w := 400\text{mm}$	$s3h_w := 400\text{mm}$	$s3h_w := 0\text{mm}$
$s3h_w := 0\text{mm}$	$s3h_w := 400\text{mm}$	$s3h_w := 0\text{mm}$	$s3h_w := 400\text{mm}$
$s3h_w := 0\text{mm}$	$s3h_w := 0\text{mm}$	$s3h_w := 400\text{mm}$	$s3h_w := 0\text{mm}$
$s3h_w := 400\text{mm}$	$s3h_w := 350\text{mm}$	$s3h_w := 350\text{mm}$	$s3h_w := 0\text{mm}$
$s3h_w := 0\text{mm}$	$s3h_w := 350\text{mm}$	$s3h_w := 350\text{mm}$	$s3h_w := 0\text{mm}$
$s3h_w := 0\text{mm}$	$s3h_w := 0\text{mm}$	$s3h_w := 350\text{mm}$	$s3h_w := 0\text{mm}$
$s3h_w := 350\text{mm}$	$s3h_w := 0\text{mm}$	$s3h_w := 0\text{mm}$	$s3h_w := 350\text{mm}$
$s3h_w := 350\text{mm}$	$s3h_w := 250\text{mm}$	$s3h_w := 250\text{mm}$	$s3h_w := 0\text{mm}$

**Element Web heights within section 3 on elements 1 through 72**

$s3t_w := 12\text{mm}$	$s3t_w := 0\text{mm}$	$s3t_w := 12\text{mm}$	$s3t_w := 0\text{mm}$
$s3t_w := 0\text{mm}$	$s3t_w := 12\text{mm}$	$s3t_w := 0\text{mm}$	$s3t_w := 12\text{mm}$
$s3t_w := 0\text{mm}$	$s3t_w := 0\text{mm}$	$s3t_w := 12\text{mm}$	$s3t_w := 0\text{mm}$
$s3t_w := 12\text{mm}$	$s3t_w := 0\text{mm}$	$s3t_w := 0\text{mm}$	$s3t_w := 12\text{mm}$
$s3t_w := 0\text{mm}$	$s3t_w := 12\text{mm}$	$s3t_w := 0\text{mm}$	$s3t_w := 0\text{mm}$
$s3t_w := 12\text{mm}$	$s3t_w := 12\text{mm}$	$s3t_w := 0\text{mm}$	$s3t_w := 0\text{mm}$
$s3t_w := 12\text{mm}$	$s3t_w := 12\text{mm}$	$s3t_w := 0\text{mm}$	$s3t_w := 0\text{mm}$
$s3t_w := 12\text{mm}$	$s3t_w := 12\text{mm}$	$s3t_w := 12\text{mm}$	$s3t_w := 12\text{mm}$
$s3t_w := 19\text{mm}$	$s3t_w := 0\text{mm}$	$s3t_w := 19\text{mm}$	$s3t_w := 0\text{mm}$
$s3t_w := 0\text{mm}$	$s3t_w := 19\text{mm}$	$s3t_w := 19\text{mm}$	$s3t_w := 0\text{mm}$

$s3t_w_{41} := 0\text{mm}$	$s3t_w_{42} := 19\text{mm}$	$s3t_w_{43} := 19\text{mm}$	$s3t_w_{44} := 0\text{mm}$
$s3t_w_{45} := 0\text{mm}$	$s3t_w_{46} := 19\text{mm}$	$s3t_w_{47} := 0\text{mm}$	$s3t_w_{48} := 19\text{mm}$
$s3t_w_{49} := 0\text{mm}$	$s3t_w_{50} := 0\text{mm}$	$s3t_w_{51} := 19\text{mm}$	$s3t_w_{52} := 0\text{mm}$
$s3t_w_{53} := 19\text{mm}$	$s3t_w_{54} := 12\text{mm}$	$s3t_w_{55} := 12\text{mm}$	$s3t_w_{56} := 0\text{mm}$
$s3t_w_{57} := 0\text{mm}$	$s3t_w_{58} := 12\text{mm}$	$s3t_w_{59} := 12\text{mm}$	$s3t_w_{60} := 0\text{mm}$
$s3t_w_{61} := 0\text{mm}$	$s3t_w_{62} := 0\text{mm}$	$s3t_w_{63} := 12\text{mm}$	$s3t_w_{64} := 0\text{mm}$
$s3t_w_{65} := 12\text{mm}$	$s3t_w_{66} := 0\text{mm}$	$s3t_w_{67} := 0\text{mm}$	$s3t_w_{68} := 12\text{mm}$
$s3t_w_{69} := 12\text{mm}$	$s3t_w_{70} := 12\text{mm}$	$s3t_w_{71} := 12\text{mm}$	$s3t_w_{72} := 0\text{mm}$

Element Flange Span within Section 3 on elements 1 through 72

$s3h_f_1 := 150\text{mm}$	$s3h_f_2 := 0\text{mm}$	$s3h_f_3 := 150\text{mm}$	$s3h_f_4 := 0\text{mm}$
$s3h_f_5 := 0\text{mm}$	$s3h_f_6 := 150\text{mm}$	$s3h_f_7 := 0\text{mm}$	$s3h_f_8 := 150\text{mm}$
$s3h_f_9 := 0\text{mm}$	$s3h_f_{10} := 0\text{mm}$	$s3h_f_{11} := 150\text{mm}$	$s3h_f_{12} := 0\text{mm}$
$s3h_f_{13} := 150\text{mm}$	$s3h_f_{14} := 0\text{mm}$	$s3h_f_{15} := 0\text{mm}$	$s3h_f_{16} := 150\text{mm}$
$s3h_f_{17} := 0\text{mm}$	$s3h_f_{18} := 150\text{mm}$	$s3h_f_{19} := 0\text{mm}$	$s3h_f_{20} := 0\text{mm}$
$s3h_f_{21} := 150\text{mm}$	$s3h_f_{22} := 150\text{mm}$	$s3h_f_{23} := 0\text{mm}$	$s3h_f_{24} := 0\text{mm}$
$s3h_f_{25} := 150\text{mm}$	$s3h_f_{26} := 150\text{mm}$	$s3h_f_{27} := 0\text{mm}$	$s3h_f_{28} := 0\text{mm}$
$s3h_f_{29} := 150\text{mm}$	$s3h_f_{30} := 150\text{mm}$	$s3h_f_{31} := 90\text{mm}$	$s3h_f_{32} := 90\text{mm}$
$s3h_f_{33} := 100\text{mm}$	$s3h_f_{34} := 0\text{mm}$	$s3h_f_{35} := 100\text{mm}$	$s3h_f_{36} := 0\text{mm}$
$s3h_f_{37} := 0\text{mm}$	$s3h_f_{38} := 100\text{mm}$	$s3h_f_{39} := 100\text{mm}$	$s3h_f_{40} := 0\text{mm}$
$s3h_f_{41} := 0\text{mm}$	$s3h_f_{42} := 100\text{mm}$	$s3h_f_{43} := 100\text{mm}$	$s3h_f_{44} := 0\text{mm}$
$s3h_f_{45} := 0\text{mm}$	$s3h_f_{46} := 100\text{mm}$	$s3h_f_{47} := 0\text{mm}$	$s3h_f_{48} := 100\text{mm}$
$s3h_f_{49} := 0\text{mm}$	$s3h_f_{50} := 0\text{mm}$	$s3h_f_{51} := 100\text{mm}$	$s3h_f_{52} := 0\text{mm}$
$s3h_f_{53} := 100\text{mm}$	$s3h_f_{54} := 100\text{mm}$	$s3h_f_{55} := 100\text{mm}$	$s3h_f_{56} := 0\text{mm}$
$s3h_f_{57} := 0\text{mm}$	$s3h_f_{58} := 100\text{mm}$	$s3h_f_{59} := 100\text{mm}$	$s3h_f_{60} := 0\text{mm}$
$s3h_f_{61} := 0\text{mm}$	$s3h_f_{62} := 0\text{mm}$	$s3h_f_{63} := 100\text{mm}$	$s3h_f_{64} := 0\text{mm}$
$s3h_f_{65} := 100\text{mm}$	$s3h_f_{66} := 0\text{mm}$	$s3h_f_{67} := 0\text{mm}$	$s3h_f_{68} := 100\text{mm}$
$s3h_f_{69} := 100\text{mm}$	$s3h_f_{70} := 90\text{mm}$	$s3h_f_{71} := 90\text{mm}$	$s3h_f_{72} := 0\text{mm}$

Element Flange Thickness within section 3 elements 1 through 72

$s3t_f_1 := 16\text{mm}$	$s3t_f_2 := 0\text{mm}$	$s3t_f_3 := 16\text{mm}$	$s3t_f_4 := 0\text{mm}$
$s3t_f_5 := 0\text{mm}$	$s3t_f_6 := 16\text{mm}$	$s3t_f_7 := 0\text{mm}$	$s3t_f_8 := 16\text{mm}$
$s3t_f_9 := 0\text{mm}$	$s3t_f_{10} := 0\text{mm}$	$s3t_f_{11} := 16\text{mm}$	$s3t_f_{12} := 0\text{mm}$
$s3t_f_{13} := 16\text{mm}$	$s3t_f_{14} := 0\text{mm}$	$s3t_f_{15} := 0\text{mm}$	$s3t_f_{16} := 16\text{mm}$
$s3t_f_{17} := 0\text{mm}$	$s3t_f_{18} := 16\text{mm}$	$s3t_f_{19} := 0\text{mm}$	$s3t_f_{20} := 0\text{mm}$

$s3t_{21} := 16\text{mm}$	$s3t_{22} := 16\text{mm}$	$s3t_{23} := 0\text{mm}$	$s3t_{24} := 0\text{mm}$
$s3t_{25} := 16\text{mm}$	$s3t_{26} := 16\text{mm}$	$s3t_{27} := 0\text{mm}$	$s3t_{28} := 0\text{mm}$
$s3t_{29} := 16\text{mm}$	$s3t_{30} := 16\text{mm}$	$s3t_{31} := 16\text{mm}$	$s3t_{32} := 16\text{mm}$
$s3t_{33} := 19\text{mm}$	$s3t_{34} := 0\text{mm}$	$s3t_{35} := 19\text{mm}$	$s3t_{36} := 0\text{mm}$
$s3t_{37} := 0\text{mm}$	$s3t_{38} := 19\text{mm}$	$s3t_{39} := 19\text{mm}$	$s3t_{40} := 0\text{mm}$
$s3t_{41} := 0\text{mm}$	$s3t_{42} := 19\text{mm}$	$s3t_{43} := 19\text{mm}$	$s3t_{44} := 0\text{mm}$
$s3t_{45} := 0\text{mm}$	$s3t_{46} := 19\text{mm}$	$s3t_{47} := 0\text{mm}$	$s3t_{48} := 19\text{mm}$
$s3t_{49} := 0\text{mm}$	$s3t_{50} := 0\text{mm}$	$s3t_{51} := 19\text{mm}$	$s3t_{52} := 0\text{mm}$
$s3t_{53} := 19\text{mm}$	$s3t_{54} := 17\text{mm}$	$s3t_{55} := 17\text{mm}$	$s3t_{56} := 0\text{mm}$
$s3t_{57} := 0\text{mm}$	$s3t_{58} := 17\text{mm}$	$s3t_{59} := 17\text{mm}$	$s3t_{60} := 0\text{mm}$
$s3t_{61} := 0\text{mm}$	$s3t_{62} := 0\text{mm}$	$s3t_{63} := 17\text{mm}$	$s3t_{64} := 0\text{mm}$
$s3t_{65} := 17\text{mm}$	$s3t_{66} := 0\text{mm}$	$s3t_{67} := 0\text{mm}$	$s3t_{68} := 17\text{mm}$
$s3t_{69} := 17\text{mm}$	$s3t_{70} := 16\text{mm}$	$s3t_{71} := 16\text{mm}$	$s3t_{72} := 0\text{mm}$

Element Stiffener Spacing within section 3 elements 1 through 72

$s3s_1 := 800\text{mm}$	$s3s_2 := 1\text{mm}$	$s3s_3 := 800\text{mm}$	$s3s_4 := 1\text{mm}$
$s3s_5 := 1\text{mm}$	$s3s_6 := 800\text{mm}$	$s3s_7 := 1\text{mm}$	$s3s_8 := 800\text{mm}$
$s3s_9 := 1\text{mm}$	$s3s_{10} := 1\text{mm}$	$s3s_{11} := 800\text{mm}$	$s3s_{12} := 1\text{mm}$
$s3s_{13} := 800\text{mm}$	$s3s_{14} := 1\text{mm}$	$s3s_{15} := 1\text{mm}$	$s3s_{16} := 800\text{mm}$
$s3s_{17} := 1\text{mm}$	$s3s_{18} := 800\text{mm}$	$s3s_{19} := 1\text{mm}$	$s3s_{20} := 1\text{mm}$
$s3s_{21} := 800\text{mm}$	$s3s_{22} := 800\text{mm}$	$s3s_{23} := 1\text{mm}$	$s3s_{24} := 1\text{mm}$
$s3s_{25} := 800\text{mm}$	$s3s_{26} := 800\text{mm}$	$s3s_{27} := 1\text{mm}$	$s3s_{28} := 1\text{mm}$
$s3s_{29} := 800\text{mm}$	$s3s_{30} := 800\text{mm}$	$s3s_{31} := 800\text{mm}$	$s3s_{32} := 800\text{mm}$
$s3s_{33} := 600\text{mm}$	$s3s_{34} := 1\text{mm}$	$s3s_{35} := 600\text{mm}$	$s3s_{36} := 1\text{mm}$
$s3s_{37} := 1\text{mm}$	$s3s_{38} := 600\text{mm}$	$s3s_{39} := 600\text{mm}$	$s3s_{40} := 1\text{mm}$
$s3s_{41} := 1\text{mm}$	$s3s_{42} := 600\text{mm}$	$s3s_{43} := 600\text{mm}$	$s3s_{44} := 1\text{mm}$
$s3s_{45} := 1\text{mm}$	$s3s_{46} := 600\text{mm}$	$s3s_{47} := 1\text{mm}$	$s3s_{48} := 600\text{mm}$
$s3s_{49} := 1\text{mm}$	$s3s_{50} := 1\text{mm}$	$s3s_{51} := 600\text{mm}$	$s3s_{52} := 1\text{mm}$
$s3s_{53} := 600\text{mm}$	$s3s_{54} := 800\text{mm}$	$s3s_{55} := 800\text{mm}$	$s3s_{56} := 1\text{mm}$
$s3s_{57} := 1\text{mm}$	$s3s_{58} := 800\text{mm}$	$s3s_{59} := 800\text{mm}$	$s3s_{60} := 1\text{mm}$
$s3s_{61} := 1\text{mm}$	$s3s_{62} := 1\text{mm}$	$s3s_{63} := 800\text{mm}$	$s3s_{64} := 1\text{mm}$
$s3s_{65} := 800\text{mm}$	$s3s_{66} := 1\text{mm}$	$s3s_{67} := 1\text{mm}$	$s3s_{68} := 800\text{mm}$
$s3s_{69} := 800\text{mm}$	$s3s_{70} := 800\text{mm}$	$s3s_{71} := 800\text{mm}$	$s3s_{72} := 1\text{mm}$

$i := n_F$       Iteration Counter

$$s3t_{s_i} := t_s(s3h_{w_i}, s3t_{w_i}, s3h_{f_i}, s3t_{f_i}, s3s_i, s3E_{t_i}) \quad \text{Smearred Thickness Calculation}$$

$$\tau_3 := \frac{1}{n_{F_3}} \sum_{i=1}^{n_{F_3}} s3t_{s_i} \quad \tau_3 = 0.023 \text{ m} \quad \text{Section 3 Average Thickness}$$

$$DA_3 := \tau_3 \sum_{i=1}^{n_{F_3}} s3b_i \quad DA_3 = 1.902 \text{ m}^2 \quad \text{Section 3 Damaged Cross Sectional Area}$$

$$DA_{E_3} := \sum_{i=1}^{n_{F_3}} s3b_i \cdot s3t_{s_i} \quad DA_{E_3} = .793 \text{ m}^2 \quad \text{Section 3 Exact Damaged Cross Sectional Area}$$

Properties for Section 4 are given as follows:

$n_{T_4} := 39$	Number of "T" intersections for section 4
$n_{L_4} := 4$	Number of Angle Intersections for section 4
$n_{C_4} := 6$	Number of Cruciform Intersections for section 4
$n_{F_4} := 91$	Number of Elements within Section 4
$n_{AT_4} := n_{T_4} + n_{L_4}$	$n_{AT_4} = 43$ Number of "T" and Angle Intersections for section 4

Element Spans within section 4 for elements 1 through 91

$s4b_1 := .3457\text{m}$	$s4b_2 := .31\text{m}$	$s4b_3 := .3457\text{m}$	$s4b_4 := .1531\text{m}$
$s4b_5 := .1531\text{m}$	$s4b_6 := .7975\text{m}$	$s4b_7 := .8\text{m}$	$s4b_8 := .7975\text{m}$
$s4b_9 := .55\text{m}$	$s4b_{10} := .55\text{m}$	$s4b_{11} := .7975\text{m}$	$s4b_{12} := .8\text{m}$
$s4b_{13} := .7975\text{m}$	$s4b_{14} := .943\text{m}$	$s4b_{15} := .943\text{m}$	$s4b_{16} := .7975\text{m}$
$s4b_{17} := 3.8\text{m}$	$s4b_{18} := .7975\text{m}$	$s4b_{19} := 1.2\text{m}$	$s4b_{20} := 1.2\text{m}$
$s4b_{21} := .7975\text{m}$	$s4b_{22} := .7975\text{m}$	$s4b_{23} := 1.2\text{m}$	$s4b_{24} := 1.2\text{m}$
$s4b_{25} := .7975\text{m}$	$s4b_{26} := .7975\text{m}$	$s4b_{27} := 1.2\text{m}$	$s4b_{28} := 1.2\text{m}$
$s4b_{29} := .7975\text{m}$	$s4b_{30} := .7975\text{m}$	$s4b_{31} := 1.2\text{m}$	$s4b_{32} := 1.2\text{m}$
$s4b_{33} := .669\text{m}$	$s4b_{34} := .669\text{m}$	$s4b_{35} := 2.82\text{m}$	$s4b_{36} := 2.82\text{m}$
$s4b_{37} := .247\text{m}$	$s4b_{38} := 2.4\text{m}$	$s4b_{39} := .247\text{m}$	$s4b_{40} := 1.2\text{m}$
$s4b_{41} := 1.2\text{m}$	$s4b_{42} := .9852\text{m}$	$s4b_{43} := .9852\text{m}$	$s4b_{44} := 1.2\text{m}$
$s4b_{45} := 1.2\text{m}$	$s4b_{46} := .9881\text{m}$	$s4b_{47} := .9881\text{m}$	$s4b_{48} := 1.2\text{m}$
$s4b_{49} := 1.2\text{m}$	$s4b_{50} := .7411\text{m}$	$s4b_{51} := .7411\text{m}$	$s4b_{52} := 1.085\text{m}$
$s4b_{53} := 1.085\text{m}$	$s4b_{54} := .9259\text{m}$	$s4b_{55} := .75\text{m}$	$s4b_{56} := .9259\text{m}$
$s4b_{57} := .542\text{m}$	$s4b_{58} := .542\text{m}$	$s4b_{59} := .9253\text{m}$	$s4b_{60} := .75\text{m}$
$s4b_{61} := .9253\text{m}$	$s4b_{62} := .7692\text{m}$	$s4b_{63} := 0\text{m}$	$s4b_{64} := .7692\text{m}$

s4b <sub>65</sub> := .657m	s4b <sub>66</sub> := .657m	s4b <sub>67</sub> := 1.538m	s4b <sub>68</sub> := 0m
s4b <sub>69</sub> := 1.538m	s4b <sub>70</sub> := 1.2m	s4b <sub>71</sub> := 1.2m	s4b <sub>72</sub> := 1.538m
s4b <sub>73</sub> := 1.538m	s4b <sub>74</sub> := 0m	s4b <sub>75</sub> := 0m	s4b <sub>76</sub> := 1.2m
s4b <sub>77</sub> := 1.2m	s4b <sub>78</sub> := 1.538m	s4b <sub>79</sub> := 1.538m	s4b <sub>80</sub> := .25m
s4b <sub>81</sub> := 1.4m	s4b <sub>82</sub> := 1.2m	s4b <sub>83</sub> := 1.2m	s4b <sub>84</sub> := 1.538m
s4b <sub>85</sub> := 1.538m	s4b <sub>86</sub> := 1.2m	s4b <sub>87</sub> := 1.2m	s4b <sub>88</sub> := .7692m
s4b <sub>89</sub> := .7692m	s4b <sub>90</sub> := 6.57m	s4b <sub>91</sub> := 6.57m	

**Element Plate Thicknesses within section 4 for elements 1 through 91**

s4E <sub>t1</sub> := 18mm	s4E <sub>t2</sub> := 12mm	s4E <sub>t3</sub> := 18mm	s4E <sub>t4</sub> := 15mm
s4E <sub>t5</sub> := 15mm	s4E <sub>t6</sub> := 18mm	s4E <sub>t7</sub> := 12mm	s4E <sub>t8</sub> := 18mm
s4E <sub>t9</sub> := 15mm	s4E <sub>t10</sub> := 15mm	s4E <sub>t11</sub> := 18mm	s4E <sub>t12</sub> := 12mm
s4E <sub>t13</sub> := 18mm	s4E <sub>t14</sub> := 15mm	s4E <sub>t15</sub> := 15mm	s4E <sub>t16</sub> := 18mm
s4E <sub>t17</sub> := 12mm	s4E <sub>t18</sub> := 18mm	s4E <sub>t19</sub> := 15mm	s4E <sub>t20</sub> := 15mm
s4E <sub>t21</sub> := 18mm	s4E <sub>t22</sub> := 18mm	s4E <sub>t23</sub> := 15mm	s4E <sub>t24</sub> := 15mm
s4E <sub>t25</sub> := 18mm	s4E <sub>t26</sub> := 18mm	s4E <sub>t27</sub> := 15mm	s4E <sub>t28</sub> := 15mm
s4E <sub>t29</sub> := 18mm	s4E <sub>t30</sub> := 18mm	s4E <sub>t31</sub> := 15mm	s4E <sub>t32</sub> := 15mm
s4E <sub>t33</sub> := 18mm	s4E <sub>t34</sub> := 18mm	s4E <sub>t35</sub> := 13mm	s4E <sub>t36</sub> := 13mm
s4E <sub>t37</sub> := 18mm	s4E <sub>t38</sub> := 12mm	s4E <sub>t39</sub> := 18mm	s4E <sub>t40</sub> := 15mm
s4E <sub>t41</sub> := 15mm	s4E <sub>t42</sub> := 33mm	s4E <sub>t43</sub> := 33mm	s4E <sub>t44</sub> := 15mm
s4E <sub>t45</sub> := 15mm	s4E <sub>t46</sub> := 33mm	s4E <sub>t47</sub> := 33mm	s4E <sub>t48</sub> := 15mm
s4E <sub>t49</sub> := 15mm	s4E <sub>t50</sub> := 33mm	s4E <sub>t51</sub> := 33mm	s4E <sub>t52</sub> := 15mm
s4E <sub>t53</sub> := 15mm	s4E <sub>t54</sub> := 33mm	s4E <sub>t55</sub> := 12mm	s4E <sub>t56</sub> := 33mm
s4E <sub>t57</sub> := 15mm	s4E <sub>t58</sub> := 15mm	s4E <sub>t59</sub> := 33mm	s4E <sub>t60</sub> := 12mm
s4E <sub>t61</sub> := 33mm	s4E <sub>t62</sub> := 16mm	s4E <sub>t63</sub> := 12mm	s4E <sub>t64</sub> := 16mm
s4E <sub>t65</sub> := 15mm	s4E <sub>t66</sub> := 15mm	s4E <sub>t67</sub> := 16mm	s4E <sub>t68</sub> := 12mm
s4E <sub>t69</sub> := 16mm	s4E <sub>t70</sub> := 15mm	s4E <sub>t71</sub> := 15mm	s4E <sub>t72</sub> := 16mm
s4E <sub>t73</sub> := 16mm	s4E <sub>t74</sub> := 25mm	s4E <sub>t75</sub> := 25mm	s4E <sub>t76</sub> := 15mm
s4E <sub>t77</sub> := 15mm	s4E <sub>t78</sub> := 16mm	s4E <sub>t79</sub> := 16mm	s4E <sub>t80</sub> := 25mm
s4E <sub>t81</sub> := 12mm	s4E <sub>t82</sub> := 15mm	s4E <sub>t83</sub> := 15mm	s4E <sub>t84</sub> := 16mm
s4E <sub>t85</sub> := 16mm	s4E <sub>t86</sub> := 15mm	s4E <sub>t87</sub> := 15mm	s4E <sub>t88</sub> := 16mm
s4E <sub>t89</sub> := 16mm	s4E <sub>t90</sub> := 13mm	s4E <sub>t91</sub> := 13mm	

**Element Web heights within section 4 on elements 1 through 91**

s4h <sub>w1</sub> := 450mm	s4h <sub>w2</sub> := 0mm	s4h <sub>w3</sub> := 450mm	s4h <sub>w4</sub> := 0mm
----------------------------	--------------------------	----------------------------	--------------------------

$s4h_{w_5} := 0\text{mm}$	$s4h_{w_6} := 450\text{mm}$	$s4h_{w_7} := 0\text{mm}$	$s4h_{w_8} := 450\text{mm}$
$s4h_{w_9} := 0\text{mm}$	$s4h_{w_{10}} := 0\text{mm}$	$s4h_{w_{11}} := 450\text{mm}$	$s4h_{w_{12}} := 0\text{mm}$
$s4h_{w_{13}} := 450\text{mm}$	$s4h_{w_{14}} := 0\text{mm}$	$s4h_{w_{15}} := 0\text{mm}$	$s4h_{w_{16}} := 450\text{mm}$
$s4h_{w_{17}} := 0\text{mm}$	$s4h_{w_{18}} := 450\text{mm}$	$s4h_{w_{19}} := 0\text{mm}$	$s4h_{w_{20}} := 0\text{mm}$
$s4h_{w_{21}} := 450\text{mm}$	$s4h_{w_{22}} := 450\text{mm}$	$s4h_{w_{23}} := 0\text{mm}$	$s4h_{w_{24}} := 0\text{mm}$
$s4h_{w_{25}} := 450\text{mm}$	$s4h_{w_{26}} := 450\text{mm}$	$s4h_{w_{27}} := 0\text{mm}$	$s4h_{w_{28}} := 0\text{mm}$
$s4h_{w_{29}} := 450\text{mm}$	$s4h_{w_{30}} := 450\text{mm}$	$s4h_{w_{31}} := 0\text{mm}$	$s4h_{w_{32}} := 0\text{mm}$
$s4h_{w_{33}} := 450\text{mm}$	$s4h_{w_{34}} := 450\text{mm}$	$s4h_{w_{35}} := 250\text{mm}$	$s4h_{w_{36}} := 250\text{mm}$
$s4h_{w_{37}} := 400\text{mm}$	$s4h_{w_{38}} := 0\text{mm}$	$s4h_{w_{39}} := 400\text{mm}$	$s4h_{w_{40}} := 0\text{mm}$
$s4h_{w_{41}} := 0\text{mm}$	$s4h_{w_{42}} := 400\text{mm}$	$s4h_{w_{43}} := 400\text{mm}$	$s4h_{w_{44}} := 0\text{mm}$
$s4h_{w_{45}} := 0\text{mm}$	$s4h_{w_{46}} := 400\text{mm}$	$s4h_{w_{47}} := 400\text{mm}$	$s4h_{w_{48}} := 0\text{mm}$
$s4h_{w_{49}} := 0\text{mm}$	$s4h_{w_{50}} := 400\text{mm}$	$s4h_{w_{51}} := 400\text{mm}$	$s4h_{w_{52}} := 0\text{mm}$
$s4h_{w_{53}} := 0\text{mm}$	$s4h_{w_{54}} := 400\text{mm}$	$s4h_{w_{55}} := 0\text{mm}$	$s4h_{w_{56}} := 400\text{mm}$
$s4h_{w_{57}} := 0\text{mm}$	$s4h_{w_{58}} := 0\text{mm}$	$s4h_{w_{59}} := 400\text{mm}$	$s4h_{w_{60}} := 0\text{mm}$
$s4h_{w_{61}} := 400\text{mm}$	$s4h_{w_{62}} := 350\text{mm}$	$s4h_{w_{63}} := 0\text{mm}$	$s4h_{w_{64}} := 350\text{mm}$
$s4h_{w_{65}} := 0\text{mm}$	$s4h_{w_{66}} := 0\text{mm}$	$s4h_{w_{67}} := 350\text{mm}$	$s4h_{w_{68}} := 0\text{mm}$
$s4h_{w_{69}} := 350\text{mm}$	$s4h_{w_{70}} := 0\text{mm}$	$s4h_{w_{71}} := 0\text{mm}$	$s4h_{w_{72}} := 350\text{mm}$
$s4h_{w_{73}} := 350\text{mm}$	$s4h_{w_{74}} := 0\text{mm}$	$s4h_{w_{75}} := 0\text{mm}$	$s4h_{w_{76}} := 0\text{mm}$
$s4h_{w_{77}} := 0\text{mm}$	$s4h_{w_{78}} := 350\text{mm}$	$s4h_{w_{79}} := 350\text{mm}$	$s4h_{w_{80}} := 0\text{mm}$
$s4h_{w_{81}} := 0\text{mm}$	$s4h_{w_{82}} := 0\text{mm}$	$s4h_{w_{83}} := 0\text{mm}$	$s4h_{w_{84}} := 350\text{mm}$
$s4h_{w_{85}} := 350\text{mm}$	$s4h_{w_{86}} := 0\text{mm}$	$s4h_{w_{87}} := 0\text{mm}$	$s4h_{w_{88}} := 350\text{mm}$
$s4h_{w_{89}} := 350\text{mm}$	$s4h_{w_{90}} := 250\text{mm}$	$s4h_{w_{91}} := 250\text{mm}$	

Element Web thickness within section 4 on elements 1 through 91

$s4t_w := 12\text{mm}$	$s4t_w := 0\text{mm}$	$s4t_w := 12\text{mm}$	$s4t_w := 0\text{mm}$
$s4t_w := 0\text{mm}$	$s4t_w := 12\text{mm}$	$s4t_w := 0\text{mm}$	$s4t_w := 12\text{mm}$
$s4t_w := 0\text{mm}$	$s4t_w := 0\text{mm}$	$s4t_w := 12\text{mm}$	$s4t_w := 0\text{mm}$
$s4t_w := 12\text{mm}$	$s4t_w := 0\text{mm}$	$s4t_w := 0\text{mm}$	$s4t_w := 12\text{mm}$
$s4t_w := 0\text{mm}$	$s4t_w := 12\text{mm}$	$s4t_w := 0\text{mm}$	$s4t_w := 0\text{mm}$
$s4t_w := 12\text{mm}$	$s4t_w := 12\text{mm}$	$s4t_w := 0\text{mm}$	$s4t_w := 0\text{mm}$
$s4t_w := 12\text{mm}$	$s4t_w := 12\text{mm}$	$s4t_w := 0\text{mm}$	$s4t_w := 0\text{mm}$
$s4t_w := 12\text{mm}$	$s4t_w := 12\text{mm}$	$s4t_w := 0\text{mm}$	$s4t_w := 0\text{mm}$
$s4t_w := 12\text{mm}$	$s4t_w := 12\text{mm}$	$s4t_w := 12\text{mm}$	$s4t_w := 12\text{mm}$
$s4t_w := 12\text{mm}$	$s4t_w := 0\text{mm}$	$s4t_w := 19\text{mm}$	$s4t_w := 0\text{mm}$
$s4t_w := 19\text{mm}$			

$s4t_w_{41} := 0\text{mm}$	$s4t_w_{42} := 19\text{mm}$	$s4t_w_{43} := 19\text{mm}$	$s4t_w_{44} := 0\text{mm}$
$s4t_w_{45} := 0\text{mm}$	$s4t_w_{46} := 19\text{mm}$	$s4t_w_{47} := 19\text{mm}$	$s4t_w_{48} := 0\text{mm}$
$s4t_w_{49} := 0\text{mm}$	$s4t_w_{50} := 19\text{mm}$	$s4t_w_{51} := 19\text{mm}$	$s4t_w_{52} := 0\text{mm}$
$s4t_w_{53} := 0\text{mm}$	$s4t_w_{54} := 19\text{mm}$	$s4t_w_{55} := 0\text{mm}$	$s4t_w_{56} := 19\text{mm}$
$s4t_w_{57} := 0\text{mm}$	$s4t_w_{58} := 0\text{mm}$	$s4t_w_{59} := 19\text{mm}$	$s4t_w_{60} := 0\text{mm}$
$s4t_w_{61} := 19\text{mm}$	$s4t_w_{62} := 12\text{mm}$	$s4t_w_{63} := 0\text{mm}$	$s4t_w_{64} := 12\text{mm}$
$s4t_w_{65} := 0\text{mm}$	$s4t_w_{66} := 0\text{mm}$	$s4t_w_{67} := 12\text{mm}$	$s4t_w_{68} := 0\text{mm}$
$s4t_w_{69} := 12\text{mm}$	$s4t_w_{70} := 0\text{mm}$	$s4t_w_{71} := 0\text{mm}$	$s4t_w_{72} := 12\text{mm}$
$s4t_w_{73} := 12\text{mm}$	$s4t_w_{74} := 0\text{mm}$	$s4t_w_{75} := 0\text{mm}$	$s4t_w_{76} := 0\text{mm}$
$s4t_w_{77} := 0\text{mm}$	$s4t_w_{78} := 12\text{mm}$	$s4t_w_{79} := 12\text{mm}$	$s4t_w_{80} := 0\text{mm}$
$s4t_w_{81} := 0\text{mm}$	$s4t_w_{82} := 0\text{mm}$	$s4t_w_{83} := 0\text{mm}$	$s4t_w_{84} := 12\text{mm}$
$s4t_w_{85} := 12\text{mm}$	$s4t_w_{86} := 0\text{mm}$	$s4t_w_{87} := 0\text{mm}$	$s4t_w_{88} := 12\text{mm}$
$s4t_w_{89} := 12\text{mm}$	$s4t_w_{90} := 12\text{mm}$	$s4t_w_{91} := 12\text{mm}$	

**Element Flange Span within Section 4 on elements 1 through 91**

$s4h_f_1 := 150\text{mm}$	$s4h_f_2 := 0\text{mm}$	$s4h_f_3 := 150\text{mm}$	$s4h_f_4 := 0\text{mm}$
$s4h_f_5 := 0\text{mm}$	$s4h_f_6 := 150\text{mm}$	$s4h_f_7 := 0\text{mm}$	$s4h_f_8 := 150\text{mm}$
$s4h_f_9 := 0\text{mm}$	$s4h_f_{10} := 0\text{mm}$	$s4h_f_{11} := 150\text{mm}$	$s4h_f_{12} := 0\text{mm}$
$s4h_f_{13} := 150\text{mm}$	$s4h_f_{14} := 0\text{mm}$	$s4h_f_{15} := 0\text{mm}$	$s4h_f_{16} := 150\text{mm}$
$s4h_f_{17} := 0\text{mm}$	$s4h_f_{18} := 150\text{mm}$	$s4h_f_{19} := 0\text{mm}$	$s4h_f_{20} := 0\text{mm}$
$s4h_f_{21} := 150\text{mm}$	$s4h_f_{22} := 150\text{mm}$	$s4h_f_{23} := 0\text{mm}$	$s4h_f_{24} := 0\text{mm}$
$s4h_f_{25} := 150\text{mm}$	$s4h_f_{26} := 150\text{mm}$	$s4h_f_{27} := 0\text{mm}$	$s4h_f_{28} := 0\text{mm}$
$s4h_f_{29} := 150\text{mm}$	$s4h_f_{30} := 150\text{mm}$	$s4h_f_{31} := 0\text{mm}$	$s4h_f_{32} := 0\text{mm}$
$s4h_f_{33} := 150\text{mm}$	$s4h_f_{34} := 150\text{mm}$	$s4h_f_{35} := 90\text{mm}$	$s4h_f_{36} := 90\text{mm}$
$s4h_f_{37} := 100\text{mm}$	$s4h_f_{38} := 0\text{mm}$	$s4h_f_{39} := 100\text{mm}$	$s4h_f_{40} := 0\text{mm}$
$s4h_f_{41} := 0\text{mm}$	$s4h_f_{42} := 100\text{mm}$	$s4h_f_{43} := 100\text{mm}$	$s4h_f_{44} := 0\text{mm}$
$s4h_f_{45} := 0\text{mm}$	$s4h_f_{46} := 100\text{mm}$	$s4h_f_{47} := 100\text{mm}$	$s4h_f_{48} := 0\text{mm}$
$s4h_f_{49} := 0\text{mm}$	$s4h_f_{50} := 100\text{mm}$	$s4h_f_{51} := 100\text{mm}$	$s4h_f_{52} := 0\text{mm}$
$s4h_f_{53} := 0\text{mm}$	$s4h_f_{54} := 100\text{mm}$	$s4h_f_{55} := 0\text{mm}$	$s4h_f_{56} := 100\text{mm}$
$s4h_f_{57} := 0\text{mm}$	$s4h_f_{58} := 0\text{mm}$	$s4h_f_{59} := 100\text{mm}$	$s4h_f_{60} := 0\text{mm}$
$s4h_f_{61} := 100\text{mm}$	$s4h_f_{62} := 100\text{mm}$	$s4h_f_{63} := 0\text{mm}$	$s4h_f_{64} := 100\text{mm}$
$s4h_f_{65} := 0\text{mm}$	$s4h_f_{66} := 0\text{mm}$	$s4h_f_{67} := 100\text{mm}$	$s4h_f_{68} := 0\text{mm}$
$s4h_f_{69} := 100\text{mm}$	$s4h_f_{70} := 0\text{mm}$	$s4h_f_{71} := 0\text{mm}$	$s4h_f_{72} := 100\text{mm}$
$s4h_f_{74} := 100\text{mm}$	$s4h_f_{74} := 0\text{mm}$	$s4h_f_{75} := 0\text{mm}$	$s4h_f_{76} := 0\text{mm}$

$s4h_{f77} := 0\text{mm}$	$s4h_{f78} := 100\text{mm}$	$s4h_{f79} := 100\text{mm}$	$s4h_{f80} := 0\text{mm}$
$s4h_{f81} := 0\text{mm}$	$s4h_{f82} := 0\text{mm}$	$s4h_{f83} := 0\text{mm}$	$s4h_{f84} := 100\text{mm}$
$s4h_{f85} := 100\text{mm}$	$s4h_{f86} := 0\text{mm}$	$s4h_{f87} := 0\text{mm}$	$s4h_{f88} := 100\text{mm}$
$s4h_{f89} := 100\text{mm}$	$s4h_{f90} := 90\text{mm}$	$s4h_{f91} := 90\text{mm}$	

Element Flange Thickness within section 4 elements 1 through 91

$s4t_{f1} := 16\text{mm}$	$s4t_{f2} := 0\text{mm}$	$s4t_{f3} := 16\text{mm}$	$s4t_{f4} := 0\text{mm}$
$s4t_{f5} := 0\text{mm}$	$s4t_{f6} := 16\text{mm}$	$s4t_{f7} := 0\text{mm}$	$s4t_{f8} := 16\text{mm}$
$s4t_{f9} := 0\text{mm}$	$s4t_{f10} := 0\text{mm}$	$s4t_{f11} := 16\text{mm}$	$s4t_{f12} := 0\text{mm}$
$s4t_{f13} := 16\text{mm}$	$s4t_{f14} := 0\text{mm}$	$s4t_{f15} := 0\text{mm}$	$s4t_{f16} := 16\text{mm}$
$s4t_{f17} := 0\text{mm}$	$s4t_{f18} := 16\text{mm}$	$s4t_{f19} := 0\text{mm}$	$s4t_{f20} := 0\text{mm}$
$s4t_{f21} := 16\text{mm}$	$s4t_{f22} := 16\text{mm}$	$s4t_{f23} := 0\text{mm}$	$s4t_{f24} := 0\text{mm}$
$s4t_{f25} := 16\text{mm}$	$s4t_{f26} := 16\text{mm}$	$s4t_{f27} := 0\text{mm}$	$s4t_{f28} := 0\text{mm}$
$s4t_{f29} := 16\text{mm}$	$s4t_{f30} := 16\text{mm}$	$s4t_{f31} := 0\text{mm}$	$s4t_{f32} := 0\text{mm}$
$s4t_{f33} := 16\text{mm}$	$s4t_{f34} := 16\text{mm}$	$s4t_{f35} := 16\text{mm}$	$s4t_{f36} := 16\text{mm}$
$s4t_{f37} := 19\text{mm}$	$s4t_{f38} := 0\text{mm}$	$s4t_{f39} := 19\text{mm}$	$s4t_{f40} := 0\text{mm}$
$s4t_{f41} := 0\text{mm}$	$s4t_{f42} := 19\text{mm}$	$s4t_{f43} := 19\text{mm}$	$s4t_{f44} := 0\text{mm}$
$s4t_{f45} := 0\text{mm}$	$s4t_{f46} := 19\text{mm}$	$s4t_{f47} := 19\text{mm}$	$s4t_{f48} := 0\text{mm}$
$s4t_{f49} := 0\text{mm}$	$s4t_{f50} := 19\text{mm}$	$s4t_{f51} := 19\text{mm}$	$s4t_{f52} := 0\text{mm}$
$s4t_{f53} := 0\text{mm}$	$s4t_{f54} := 19\text{mm}$	$s4t_{f55} := 0\text{mm}$	$s4t_{f56} := 19\text{mm}$
$s4t_{f57} := 0\text{mm}$	$s4t_{f58} := 0\text{mm}$	$s4t_{f59} := 19\text{mm}$	$s4t_{f60} := 0\text{mm}$
$s4t_{f61} := 19\text{mm}$	$s4t_{f62} := 17\text{mm}$	$s4t_{f63} := 0\text{mm}$	$s4t_{f64} := 17\text{mm}$
$s4t_{f65} := 0\text{mm}$	$s4t_{f66} := 0\text{mm}$	$s4t_{f67} := 17\text{mm}$	$s4t_{f68} := 0\text{mm}$
$s4t_{f69} := 17\text{mm}$	$s4t_{f70} := 0\text{mm}$	$s4t_{f71} := 0\text{mm}$	$s4t_{f72} := 17\text{mm}$
$s4t_{f73} := 17\text{mm}$	$s4t_{f74} := 0\text{mm}$	$s4t_{f75} := 0\text{mm}$	$s4t_{f76} := 0\text{mm}$
$s4t_{f77} := 0\text{mm}$	$s4t_{f78} := 17\text{mm}$	$s4t_{f79} := 17\text{mm}$	$s4t_{f80} := 0\text{mm}$
$s4t_{f81} := 0\text{mm}$	$s4t_{f82} := 0\text{mm}$	$s4t_{f83} := 0\text{mm}$	$s4t_{f84} := 17\text{mm}$
$s4t_{f85} := 17\text{mm}$	$s4t_{f86} := 0\text{mm}$	$s4t_{f87} := 0\text{mm}$	$s4t_{f88} := 17\text{mm}$
$s4t_{f89} := 17\text{mm}$	$s4t_{f90} := 16\text{mm}$	$s4t_{f91} := 16\text{mm}$	

Element Stiffener Spacing within section 4 elements 1 through 91

$s4s_1 := 800\text{mm}$	$s4s_2 := 1\text{mm}$	$s4s_3 := 800\text{mm}$	$s4s_4 := 1\text{mm}$
$s4s_5 := 1\text{mm}$	$s4s_6 := 800\text{mm}$	$s4s_7 := 1\text{mm}$	$s4s_8 := 800\text{mm}$
$s4s_9 := 1\text{mm}$	$s4s_{10} := 1\text{mm}$	$s4s_{11} := 800\text{mm}$	$s4s_{12} := 1\text{mm}$
$s4s_{13} := 800\text{mm}$	$s4s_{14} := 1\text{mm}$	$s4s_{15} := 1\text{mm}$	$s4s_{16} := 800\text{mm}$

s4s <sub>17</sub> := 1mm	s4s <sub>18</sub> := 800mm	s4s <sub>19</sub> := 1mm	s4s <sub>20</sub> := 1mm
s4s <sub>21</sub> := 800mm	s4s <sub>22</sub> := 800mm	s4s <sub>23</sub> := 1mm	s4s <sub>24</sub> := 1mm
s4s <sub>25</sub> := 800mm	s4s <sub>26</sub> := 800mm	s4s <sub>27</sub> := 1mm	s4s <sub>28</sub> := 1mm
s4s <sub>29</sub> := 800mm	s4s <sub>30</sub> := 800mm	s4s <sub>31</sub> := 1mm	s4s <sub>32</sub> := 1mm
s4s <sub>33</sub> := 800mm	s4s <sub>34</sub> := 800mm	s4s <sub>35</sub> := 800mm	s4s <sub>36</sub> := 800mm
s4s <sub>37</sub> := 600mm	s4s <sub>38</sub> := 1mm	s4s <sub>39</sub> := 600mm	s4s <sub>40</sub> := 1mm
s4s <sub>41</sub> := 1mm	s4s <sub>42</sub> := 600mm	s4s <sub>43</sub> := 600mm	s4s <sub>44</sub> := 1mm
s4s <sub>45</sub> := 1mm	s4s <sub>46</sub> := 600mm	s4s <sub>47</sub> := 600mm	s4s <sub>48</sub> := 1mm
s4s <sub>49</sub> := 1mm	s4s <sub>50</sub> := 600mm	s4s <sub>51</sub> := 600mm	s4s <sub>52</sub> := 1mm
s4s <sub>53</sub> := 1mm	s4s <sub>54</sub> := 600mm	s4s <sub>55</sub> := 1mm	s4s <sub>56</sub> := 600mm
s4s <sub>57</sub> := 1mm	s4s <sub>58</sub> := 1mm	s4s <sub>59</sub> := 600mm	s4s <sub>60</sub> := 1mm
s4s <sub>61</sub> := 600mm	s4s <sub>62</sub> := 800mm	s4s <sub>63</sub> := 1mm	s4s <sub>64</sub> := 800mm
s4s <sub>65</sub> := 1mm	s4s <sub>66</sub> := 1mm	s4s <sub>67</sub> := 800mm	s4s <sub>68</sub> := 1mm
s4s <sub>69</sub> := 800mm	s4s <sub>70</sub> := 1mm	s4s <sub>71</sub> := 1mm	s4s <sub>72</sub> := 800mm
s4s <sub>73</sub> := 800mm	s4s <sub>74</sub> := 1mm	s4s <sub>75</sub> := 1mm	s4s <sub>76</sub> := 1mm
s4s <sub>77</sub> := 1mm	s4s <sub>78</sub> := 800mm	s4s <sub>79</sub> := 800mm	s4s <sub>80</sub> := 1mm
s4s <sub>81</sub> := 1mm	s4s <sub>82</sub> := 1mm	s4s <sub>83</sub> := 1mm	s4s <sub>84</sub> := 800mm
s4s <sub>85</sub> := 800mm	s4s <sub>86</sub> := 1mm	s4s <sub>87</sub> := 1mm	s4s <sub>88</sub> := 800mm
s4s <sub>89</sub> := 800mm	s4s <sub>90</sub> := 800mm	s4s <sub>91</sub> := 800mm	

i := 1 .. n<sub>F4</sub>      Iteration Counter

s4t<sub>s<sub>i</sub></sub> := t<sub>s</sub>(s4h<sub>w<sub>i</sub></sub>, s4t<sub>w<sub>i</sub></sub>, s4h<sub>f<sub>i</sub></sub>, s4t<sub>f<sub>i</sub></sub>, s4s<sub>i</sub>, s4E<sub>t<sub>i</sub></sub>)      Smearred Thickness Calculation

$$\tau_4 := \frac{1}{n_{F_4}} \left( \sum_{i=1}^{n_{F_4}} s4t_{s_i} \right) \quad \tau_4 = 0.023 \text{ m} \quad \text{Section 4 Average Thickness}$$

$$DA_4 := \tau_4 \cdot \sum_{i=1}^{n_{F_4}} s4b_i \quad DA_4 = 2.248 \text{ m}^2 \quad \text{Section 4 Damaged Cross Sectional Area}$$

$$DA_{E_4} := \sum_{i=1}^{n_{F_4}} s4b_i \cdot s4t_{s_i} \quad DA_{E_4} = 2.1 \text{ m}^2 \quad \text{Section 4 Exact Damaged Cross Sectional Area}$$

Properties for Section 5 are given as follows:

n <sub>T5</sub> := 41	Number of "T" intersections for section 5
n <sub>L5</sub> := 4	Number of Angle Intersections for section 5
n <sub>Cz</sub> := 3	Number of Cruciform Intersections for section 5

$n_{F_5} := 91$                       Number of Elements within Section 5  
 $n_{AT_5} := n_{T_5} + n_{L_5}$                        $n_{AT_5} = 45$                       Number of "T" and Angle Intersections for section 5

Element Spans within section 5 for elements 1 through 91

$s5b_1 := .0748m$	$s5b_2 := .065m$	$s5b_3 := .0748m$	$s5b_4 := 0m$
$s5b_5 := 0m$	$s5b_6 := .9212m$	$s5b_7 := .8m$	$s5b_8 := .9212m$
$s5b_9 := .4937m$	$s5b_{10} := .4937m$	$s5b_{11} := .9212m$	$s5b_{12} := .8m$
$s5b_{13} := .9212m$	$s5b_{14} := 1.2m$	$s5b_{15} := 1.2m$	$s5b_{16} := .9212m$
$s5b_{17} := 4.6m$	$s5b_{18} := .9212m$	$s5b_{19} := 1.2m$	$s5b_{20} := 1.2m$
$s5b_{21} := .9212m$	$s5b_{22} := .9212m$	$s5b_{23} := 1.2m$	$s5b_{24} := 1.2m$
$s5b_{25} := .9212m$	$s5b_{26} := .9212m$	$s5b_{27} := 1.2m$	$s5b_{28} := 1.2m$
$s5b_{29} := .9212m$	$s5b_{30} := .9212m$	$s5b_{31} := 0m$	$s5b_{32} := 0m$
$s5b_{33} := 1.612m$	$s5b_{34} := 1.612m$	$s5b_{35} := 3.567m$	$s5b_{36} := 3.567m$
$s5b_{37} := 1.2612m$	$s5b_{38} := 3.15m$	$s5b_{39} := 1.2612m$	$s5b_{40} := 0m$
$s5b_{41} := 0m$	$s5b_{42} := 1.009m$	$s5b_{43} := 1.009m$	$s5b_{44} := 0m$
$s5b_{45} := 0m$	$s5b_{46} := .7569m$	$s5b_{47} := .7569m$	$s5b_{48} := 1.2m$
$s5b_{49} := 1.2m$	$s5b_{50} := .9463m$	$s5b_{51} := .9463m$	$s5b_{52} := 1.2m$
$s5b_{53} := 1.2m$	$s5b_{54} := .9463m$	$s5b_{55} := .75m$	$s5b_{56} := .9463m$
$s5b_{57} := .577m$	$s5b_{58} := .577m$	$s5b_{59} := .9463m$	$s5b_{60} := .75m$
$s5b_{61} := .9463m$	$s5b_{62} := 1.1118m$	$s5b_{63} := 0m$	$s5b_{64} := 1.1118m$
$s5b_{65} := .936m$	$s5b_{66} := .936m$	$s5b_{67} := 1.4807m$	$s5b_{68} := 0m$
$s5b_{69} := 1.4807m$	$s5b_{70} := 1.2m$	$s5b_{71} := 1.2m$	$s5b_{72} := 1.4807m$
$s5b_{73} := 1.4807m$	$s5b_{74} := 0m$	$s5b_{75} := 0m$	$s5b_{76} := 1.2m$
$s5b_{77} := 1.2m$	$s5b_{78} := 1.4807m$	$s5b_{79} := 1.4807m$	$s5b_{80} := .25m$
$s5b_{81} := 1.4m$	$s5b_{82} := 1.2m$	$s5b_{83} := 1.2m$	$s5b_{84} := 1.4807m$
$s5b_{85} := 1.4807m$	$s5b_{86} := 0m$	$s5b_{87} := 0m$	$s5b_{88} := 2.2219m$
$s5b_{89} := 2.2219m$	$s5b_{90} := 7.79m$	$s5b_{91} := 7.79m$	

$i := 1..n_{F_5}$                       Iteration Counter

Element Plate Thicknesses within section 5 for elements 1 through 91

$s5E_t := s4E_t$

Element Web heights within section 5 on elements 1 through 91

$s5h_w := s4h_w$

Element Web thickness within section 5 on elements 1 through 91

$$s5t_w := s4t_w$$

Element Flange Span within Section 5 on elements 1 through 91

$$s5h_f := s4h_f$$

Element Flange Thickness within section 5 elements 1 through 91

$$s5t_f := s4t_f$$

Element Stiffener Spacing within section 4 elements 1 through 91

$$s5s_i := s4s_i$$

$$s5t_s := t_s(s5h_w, s5t_w, s5h_f, s5t_f, s5s_i, s5E_t) \quad \text{Smearred Thickness Calculation}$$

$$\tau_5 := \frac{1}{n_{F_5}} \left( \sum_{i=1}^{n_{F_5}} s5t_{s_i} \right) \quad \tau_5 = 0.023 \text{ m} \quad \text{Section 5 Average Thickness}$$

$$DA_5 := \tau_5 \cdot \sum_{i=1}^{n_{F_5}} s5b_i \quad DA_5 = 2.348 \text{ m}^2 \quad \text{Section 5 Damaged Cross Sectional Area}$$

$$DA_{E_5} := \sum_{i=1}^{n_{F_5}} s5b_i \cdot s5t_{s_i} \quad DA_{E_5} = 2.277 \text{ m}^2 \quad \text{Section 5 Exact Damaged Cross Sectional Area}$$

Properties for Section 6 are given as follows:

$n_{T_6} := 51$	Number of "T" intersections for section 6
$n_{L_6} := 4$	Number of Angle Intersections for section 6
$n_{C_6} := 3$	Number of Cruciform Intersections for section 6
$n_{F_6} := 57$	Number of Elements within Section 6
$n_{AT_6} := n_{T_6} + n_{L_6}$	$n_{AT_6} = 55$ Number of "T" and Angle Intersections for section 6

Element Spans within section 6 for elements 1 through 57

$s6b_1 := .9477\text{m}$	$s6b_2 := 0.8\text{m}$	$s6b_3 := .9477\text{m}$	$s6b_4 := .508\text{m}$
$s6b_5 := .508\text{m}$	$s6b_6 := .9477\text{m}$	$s6b_7 := .8\text{m}$	$s6b_8 := .9477\text{m}$
$s6b_9 := 1.2\text{m}$	$s6b_{10} := 1.2\text{m}$	$s6b_{11} := 6.185\text{m}$	$s6b_{12} := 5.22\text{m}$
$s6b_{13} := 6.185\text{m}$	$s6b_{14} := 4.333\text{m}$	$s6b_{15} := 4.333\text{m}$	$s6b_{16} := 4.038\text{m}$
$s6b_{17} := 3.15\text{m}$	$s6b_{18} := 4.038\text{m}$	$s6b_{19} := 1.2\text{m}$	$s6b_{20} := 1.2\text{m}$
$s6b_{21} := .9617\text{m}$	$s6b_{22} := .9617\text{m}$	$s6b_{23} := 1.2\text{m}$	$s6b_{24} := 1.2\text{m}$
$s6b_{25} := .9617\text{m}$	$s6b_{26} := .9617\text{m}$	$s6b_{27} := .602\text{m}$	$s6b_{28} := .602\text{m}$

s6b <sub>29</sub> := .9617m	s6b <sub>30</sub> := .75m	s6b <sub>31</sub> := .9617m	s6b <sub>32</sub> := 1.4422m
s6b <sub>33</sub> := 0m	s6b <sub>34</sub> := 1.4422m	s6b <sub>35</sub> := 1.2m	s6b <sub>36</sub> := 1.2m
s6b <sub>37</sub> := 1.4422m	s6b <sub>38</sub> := 0m	s6b <sub>39</sub> := 1.4422m	s6b <sub>40</sub> := 0m
s6b <sub>41</sub> := 0m	s6b <sub>42</sub> := 1.2m	s6b <sub>43</sub> := 1.2m	s6b <sub>44</sub> := 1.4422m
s6b <sub>45</sub> := 1.4422m	s6b <sub>46</sub> := 1.2m	s6b <sub>47</sub> := 1.2m	s6b <sub>48</sub> := 1.4422m
s6b <sub>49</sub> := 1.4422m	s6b <sub>50</sub> := 2.4m	s6b <sub>51</sub> := 2.4m	s6b <sub>52</sub> := 5.05m
s6b <sub>53</sub> := 5.05m	s6b <sub>54</sub> := .25m	s6b <sub>55</sub> := 1.4m	s6b <sub>56</sub> := 9.005m
s6b <sub>57</sub> := 9.005m			

Element Plate Thicknesses within section 6 for elements 1 through 57

s6E <sub>t1</sub> := 18mm	s6E <sub>t2</sub> := 12mm	s6E <sub>t3</sub> := 18mm	s6E <sub>t4</sub> := 15mm
s6E <sub>t5</sub> := 15mm	s6E <sub>t6</sub> := 18mm	s6E <sub>t7</sub> := 12mm	s6E <sub>t8</sub> := 18mm
s6E <sub>t9</sub> := 15mm	s6E <sub>t10</sub> := 15mm	s6E <sub>t11</sub> := 18mm	s6E <sub>t12</sub> := 12mm
s6E <sub>t13</sub> := 18mm	s6E <sub>t14</sub> := 13mm	s6E <sub>t15</sub> := 13mm	s6E <sub>t16</sub> := 33mm
s6E <sub>t17</sub> := 12mm	s6E <sub>t18</sub> := 33mm	s6E <sub>t19</sub> := 15mm	s6E <sub>t20</sub> := 15mm
s6E <sub>t21</sub> := 33mm	s6E <sub>t22</sub> := 33mm	s6E <sub>t23</sub> := 15mm	s6E <sub>t24</sub> := 15mm
s6E <sub>t25</sub> := 33mm	s6E <sub>t26</sub> := 33mm	s6E <sub>t27</sub> := 15mm	s6E <sub>t28</sub> := 15mm
s6E <sub>t29</sub> := 33mm	s6E <sub>t30</sub> := 12mm	s6E <sub>t31</sub> := 33mm	s6E <sub>t32</sub> := 16mm
s6E <sub>t33</sub> := 12mm	s6E <sub>t34</sub> := 16mm	s6E <sub>t35</sub> := 15mm	s6E <sub>t36</sub> := 15mm
s6E <sub>t37</sub> := 16mm	s6E <sub>t38</sub> := 12mm	s6E <sub>t39</sub> := 16mm	s6E <sub>t40</sub> := 25mm
s6E <sub>t41</sub> := 25mm	s6E <sub>t42</sub> := 15mm	s6E <sub>t43</sub> := 15mm	s6E <sub>t44</sub> := 16mm
s6E <sub>t45</sub> := 16mm	s6E <sub>t46</sub> := 15mm	s6E <sub>t47</sub> := 15mm	s6E <sub>t48</sub> := 16mm
s6E <sub>t49</sub> := 16mm	s6E <sub>t50</sub> := 15mm	s6E <sub>t51</sub> := 15mm	s6E <sub>t52</sub> := 16mm
s6E <sub>t53</sub> := 16mm	s6E <sub>t54</sub> := 25mm	s6E <sub>t55</sub> := 12mm	s6E <sub>t56</sub> := 13mm
s6E <sub>t57</sub> := 13mm			

Element Web heights within section 6 on elements 1 through 57

s6h <sub>w1</sub> := 450mm	s6h <sub>w2</sub> := 0mm	s6h <sub>w3</sub> := 450mm	s6h <sub>w4</sub> := 0mm
s6h <sub>w5</sub> := 0mm	s6h <sub>w6</sub> := 450mm	s6h <sub>w7</sub> := 0mm	s6h <sub>w8</sub> := 450mm
s6h <sub>w9</sub> := 0mm	s6h <sub>w10</sub> := 0mm	s6h <sub>w11</sub> := 450mm	s6h <sub>w12</sub> := 0mm
s6h <sub>w13</sub> := 450mm	s6h <sub>w14</sub> := 250mm	s6h <sub>w15</sub> := 250mm	s6h <sub>w16</sub> := 400mm
s6h <sub>w17</sub> := 0mm	s6h <sub>w18</sub> := 400mm	s6h <sub>w19</sub> := 0mm	s6h <sub>w20</sub> := 0mm
s6h <sub>w21</sub> := 400mm	s6h <sub>w22</sub> := 400mm	s6h <sub>w23</sub> := 0mm	s6h <sub>w24</sub> := 0mm
s6h <sub>w25</sub> := 400mm	s6h <sub>w26</sub> := 400mm	s6h <sub>w27</sub> := 0mm	s6h <sub>w28</sub> := 0mm
s6h <sub>w29</sub> := 400mm	s6h <sub>w30</sub> := 0mm	s6h <sub>w31</sub> := 400mm	s6h <sub>w32</sub> := 350mm

$s6h_w_{33} := 0\text{mm}$	$s6h_w_{34} := 350\text{mm}$	$s6h_w_{35} := 0\text{mm}$	$s6h_w_{36} := 0\text{mm}$
$s6h_w_{37} := 350\text{mm}$	$s6h_w_{38} := 0\text{mm}$	$s6h_w_{39} := 350\text{mm}$	$s6h_w_{40} := 0\text{mm}$
$s6h_w_{41} := 0\text{mm}$	$s6h_w_{42} := 0\text{mm}$	$s6h_w_{43} := 0\text{mm}$	$s6h_w_{44} := 350\text{mm}$
$s6h_w_{45} := 350\text{mm}$	$s6h_w_{46} := 0\text{mm}$	$s6h_w_{47} := 0\text{mm}$	$s6h_w_{48} := 350\text{mm}$
$s6h_w_{49} := 350\text{mm}$	$s6h_w_{50} := 0\text{mm}$	$s6h_w_{51} := 0\text{mm}$	$s6h_w_{52} := 350\text{mm}$
$s6h_w_{53} := 350\text{mm}$	$s6h_w_{54} := 0\text{mm}$	$s6h_w_{55} := 0\text{mm}$	$s6h_w_{56} := 250\text{mm}$
$s6h_w_{57} := 250\text{mm}$			

Element Web heights within section 6 on elements 1 through 57

$s6t_w_1 := 12\text{mm}$	$s6t_w_2 := 0\text{mm}$	$s6t_w_3 := 12\text{mm}$	$s6t_w_4 := 0\text{mm}$
$s6t_w_5 := 0\text{mm}$	$s6t_w_6 := 12\text{mm}$	$s6t_w_7 := 0\text{mm}$	$s6t_w_8 := 12\text{mm}$
$s6t_w_9 := 0\text{mm}$	$s6t_w_{10} := 0\text{mm}$	$s6t_w_{11} := 12\text{mm}$	$s6t_w_{12} := 0\text{mm}$
$s6t_w_{13} := 12\text{mm}$	$s6t_w_{14} := 12\text{mm}$	$s6t_w_{15} := 12\text{mm}$	$s6t_w_{16} := 19\text{mm}$
$s6t_w_{17} := 0\text{mm}$	$s6t_w_{18} := 19\text{mm}$	$s6t_w_{19} := 0\text{mm}$	$s6t_w_{20} := 0\text{mm}$
$s6t_w_{21} := 19\text{mm}$	$s6t_w_{22} := 19\text{mm}$	$s6t_w_{23} := 0\text{mm}$	$s6t_w_{24} := 0\text{mm}$
$s6t_w_{25} := 19\text{mm}$	$s6t_w_{26} := 19\text{mm}$	$s6t_w_{27} := 0\text{mm}$	$s6t_w_{28} := 0\text{mm}$
$s6t_w_{29} := 19\text{mm}$	$s6t_w_{30} := 0\text{mm}$	$s6t_w_{31} := 19\text{mm}$	$s6t_w_{32} := 12\text{mm}$
$s6t_w_{33} := 0\text{mm}$	$s6t_w_{34} := 12\text{mm}$	$s6t_w_{35} := 0\text{mm}$	$s6t_w_{36} := 0\text{mm}$
$s6t_w_{37} := 12\text{mm}$	$s6t_w_{38} := 0\text{mm}$	$s6t_w_{39} := 12\text{mm}$	$s6t_w_{40} := 0\text{mm}$
$s6t_w_{41} := 0\text{mm}$	$s6t_w_{42} := 0\text{mm}$	$s6t_w_{43} := 0\text{mm}$	$s6t_w_{44} := 12\text{mm}$
$s6t_w_{45} := 12\text{mm}$	$s6t_w_{46} := 0\text{mm}$	$s6t_w_{47} := 0\text{mm}$	$s6t_w_{48} := 12\text{mm}$
$s6t_w_{49} := 12\text{mm}$	$s6t_w_{50} := 0\text{mm}$	$s6t_w_{51} := 0\text{mm}$	$s6t_w_{52} := 12\text{mm}$
$s6t_w_{53} := 12\text{mm}$	$s6t_w_{54} := 0\text{mm}$	$s6t_w_{55} := 0\text{mm}$	$s6t_w_{56} := 12\text{mm}$
$s6t_w_{57} := 12\text{mm}$			

Element Flange Span within Section 6 on elements 1 through 57

$s6h_f_1 := 150\text{mm}$	$s6h_f_2 := 0\text{mm}$	$s6h_f_3 := 150\text{mm}$	$s6h_f_4 := 0\text{mm}$
$s6h_f_5 := 0\text{mm}$	$s6h_f_6 := 150\text{mm}$	$s6h_f_7 := 0\text{mm}$	$s6h_f_8 := 150\text{mm}$
$s6h_f_9 := 0\text{mm}$	$s6h_f_{10} := 0\text{mm}$	$s6h_f_{11} := 150\text{mm}$	$s6h_f_{12} := 0\text{mm}$
$s6h_f_{13} := 150\text{mm}$	$s6h_f_{14} := 90\text{mm}$	$s6h_f_{15} := 90\text{mm}$	$s6h_f_{16} := 100\text{mm}$
$s6h_f_{17} := 0\text{mm}$	$s6h_f_{18} := 100\text{mm}$	$s6h_f_{19} := 0\text{mm}$	$s6h_f_{20} := 0\text{mm}$
$s6h_f_{21} := 100\text{mm}$	$s6h_f_{22} := 100\text{mm}$	$s6h_f_{23} := 0\text{mm}$	$s6h_f_{24} := 0\text{mm}$
$s6h_f_{25} := 100\text{mm}$	$s6h_f_{26} := 100\text{mm}$	$s6h_f_{27} := 0\text{mm}$	$s6h_f_{28} := 0\text{mm}$
$s6h_f_{30} := 100\text{mm}$	$s6h_f_{30} := 0\text{mm}$	$s6h_f_{31} := 100\text{mm}$	$s6h_f_{32} := 100\text{mm}$
$s6h_f_{33} := 0\text{mm}$	$s6h_f_{34} := 100\text{mm}$	$s6h_f_{35} := 0\text{mm}$	$s6h_f_{36} := 0\text{mm}$

$s6h_{f_{37}} := 100\text{mm}$	$s6h_{f_{38}} := 0\text{mm}$	$s6h_{f_{39}} := 100\text{mm}$	$s6h_{f_{40}} := 0\text{mm}$
$s6h_{f_{41}} := 0\text{mm}$	$s6h_{f_{42}} := 0\text{mm}$	$s6h_{f_{43}} := 0\text{mm}$	$s6h_{f_{44}} := 100\text{mm}$
$s6h_{f_{45}} := 100\text{mm}$	$s6h_{f_{46}} := 0\text{mm}$	$s6h_{f_{47}} := 0\text{mm}$	$s6h_{f_{48}} := 100\text{mm}$
$s6h_{f_{49}} := 100\text{mm}$	$s6h_{f_{50}} := 0\text{mm}$	$s6h_{f_{51}} := 0\text{mm}$	$s6h_{f_{52}} := 100\text{mm}$
$s6h_{f_{53}} := 100\text{mm}$	$s6h_{f_{54}} := 0\text{mm}$	$s6h_{f_{55}} := 0\text{mm}$	$s6h_{f_{56}} := 90\text{mm}$
$s6h_{f_{57}} := 90\text{mm}$			

Element Flange Thickness within section 6 elements 1 through 57

$s6t_{f_1} := 16\text{mm}$	$s6t_{f_2} := 0\text{mm}$	$s6t_{f_3} := 16\text{mm}$	$s6t_{f_4} := 0\text{mm}$
$s6t_{f_5} := 0\text{mm}$	$s6t_{f_6} := 16\text{mm}$	$s6t_{f_7} := 0\text{mm}$	$s6t_{f_8} := 16\text{mm}$
$s6t_{f_9} := 0\text{mm}$	$s6t_{f_{10}} := 0\text{mm}$	$s6t_{f_{11}} := 16\text{mm}$	$s6t_{f_{12}} := 0\text{mm}$
$s6t_{f_{13}} := 16\text{mm}$	$s6t_{f_{14}} := 16\text{mm}$	$s6t_{f_{15}} := 16\text{mm}$	$s6t_{f_{16}} := 19\text{mm}$
$s6t_{f_{17}} := 0\text{mm}$	$s6t_{f_{18}} := 19\text{mm}$	$s6t_{f_{19}} := 0\text{mm}$	$s6t_{f_{20}} := 0\text{mm}$
$s6t_{f_{21}} := 19\text{mm}$	$s6t_{f_{22}} := 19\text{mm}$	$s6t_{f_{23}} := 0\text{mm}$	$s6t_{f_{24}} := 0\text{mm}$
$s6t_{f_{25}} := 19\text{mm}$	$s6t_{f_{26}} := 19\text{mm}$	$s6t_{f_{27}} := 0\text{mm}$	$s6t_{f_{28}} := 0\text{mm}$
$s6t_{f_{29}} := 19\text{mm}$	$s6t_{f_{30}} := 0\text{mm}$	$s6t_{f_{31}} := 19\text{mm}$	$s6t_{f_{32}} := 17\text{mm}$
$s6t_{f_{33}} := 0\text{mm}$	$s6t_{f_{34}} := 17\text{mm}$	$s6t_{f_{35}} := 0\text{mm}$	$s6t_{f_{36}} := 0\text{mm}$
$s6t_{f_{37}} := 17\text{mm}$	$s6t_{f_{38}} := 0\text{mm}$	$s6t_{f_{39}} := 17\text{mm}$	$s6t_{f_{40}} := 0\text{mm}$
$s6t_{f_{41}} := 0\text{mm}$	$s6t_{f_{42}} := 0\text{mm}$	$s6t_{f_{43}} := 0\text{mm}$	$s6t_{f_{44}} := 17\text{mm}$
$s6t_{f_{45}} := 17\text{mm}$	$s6t_{f_{46}} := 0\text{mm}$	$s6t_{f_{47}} := 0\text{mm}$	$s6t_{f_{48}} := 17\text{mm}$
$s6t_{f_{49}} := 17\text{mm}$	$s6t_{f_{50}} := 0\text{mm}$	$s6t_{f_{51}} := 0\text{mm}$	$s6t_{f_{52}} := 17\text{mm}$
$s6t_{f_{53}} := 17\text{mm}$	$s6t_{f_{54}} := 0\text{mm}$	$s6t_{f_{55}} := 0\text{mm}$	$s6t_{f_{56}} := 16\text{mm}$
$s6t_{f_{57}} := 16\text{mm}$			

Element Stiffener Spacing within section 6 elements 1 through 57

$s6s_1 := 800\text{mm}$	$s6s_2 := 1\text{mm}$	$s6s_3 := 800\text{mm}$	$s6s_4 := 1\text{mm}$
$s6s_5 := 1\text{mm}$	$s6s_6 := 800\text{mm}$	$s6s_7 := 1\text{mm}$	$s6s_8 := 800\text{mm}$
$s6s_9 := 1\text{mm}$	$s6s_{10} := 1\text{mm}$	$s6s_{11} := 800\text{mm}$	$s6s_{12} := 1\text{mm}$
$s6s_{13} := 800\text{mm}$	$s6s_{14} := 800\text{mm}$	$s6s_{15} := 800\text{mm}$	$s6s_{16} := 600\text{mm}$
$s6s_{17} := 1\text{mm}$	$s6s_{18} := 600\text{mm}$	$s6s_{19} := 1\text{mm}$	$s6s_{20} := 1\text{mm}$
$s6s_{21} := 600\text{mm}$	$s6s_{22} := 600\text{mm}$	$s6s_{23} := 1\text{mm}$	$s6s_{24} := 1\text{mm}$
$s6s_{25} := 600\text{mm}$	$s6s_{26} := 600\text{mm}$	$s6s_{27} := 1\text{mm}$	$s6s_{28} := 1\text{mm}$
$s6s_{29} := 600\text{mm}$	$s6s_{30} := 1\text{mm}$	$s6s_{31} := 600\text{mm}$	$s6s_{32} := 800\text{mm}$
$s6s_{33} := 1\text{mm}$	$s6s_{34} := 800\text{mm}$	$s6s_{35} := 1\text{mm}$	$s6s_{36} := 1\text{mm}$
$s6s_{37} := 800\text{mm}$	$s6s_{38} := 1\text{mm}$	$s6s_{39} := 800\text{mm}$	$s6s_{40} := 1\text{mm}$

$$\begin{array}{llll}
s6s_{41} := 1 \text{ mm} & s6s_{42} := 1 \text{ mm} & s6s_{43} := 1 \text{ mm} & s6s_{44} := 800 \text{ mm} \\
s6s_{45} := 800 \text{ mm} & s6s_{46} := 1 \text{ mm} & s6s_{47} := 1 \text{ mm} & s6s_{48} := 800 \text{ mm} \\
s6s_{49} := 800 \text{ mm} & s6s_{50} := 1 \text{ mm} & s6s_{51} := 1 \text{ mm} & s6s_{52} := 800 \text{ mm} \\
s6s_{53} := 800 \text{ mm} & s6s_{54} := 1 \text{ mm} & s6s_{55} := 1 \text{ mm} & s6s_{56} := 800 \text{ mm} \\
s6s_{57} := 800 \text{ mm} & & & 
\end{array}$$

$$i := 1 .. n_{F_6} \quad \text{Iteration Counter}$$

$$s6t_{s_i} := t_s(s6h_{w_i}, s6t_{w_i}, s6h_f, s6t_f, s6s_i, s6E_i) \quad \text{Smearred Thickness Calculation}$$

$$\tau_6 := \frac{1}{n_{F_6}} \left( \sum_{i=1}^{n_{F_6}} s6t_{s_i} \right) \quad \tau_6 = 0.023 \text{ m} \quad \text{Section 6 Average Thickness}$$

$$DA_6 := \tau_6 \cdot \sum_{i=1}^{n_{F_6}} s6b_i \quad DA_6 = 2.405 \text{ m}^2 \quad \text{Section 6 Damaged Cross Sectional Area}$$

$$DA_{E_6} := \sum_{i=1}^{n_{F_6}} s6b_i \cdot s6t_{s_i} \quad DA_{E_6} = 2.4 \text{ m}^2 \quad \text{Section 6 Exact Damaged Cross Sectional Area}$$

Determining the crush force for each indentation step of 0.8 meters is done by the following calculations.

$$m_x := \Delta \cdot 1.05 \quad m_x = 1.836 \times 10^8 \text{ kg}$$

$$E_0 := \frac{1}{2} \cdot m_x \cdot V_s^2 \quad E_0 = 7.939 \times 10^9 \text{ J}$$

Section 1, from  $x = 0$  to  $x = 0.8$  meters has the following properties

$$V_0 := V_s \quad V_0 = 9.3 \frac{\text{m}}{\text{s}} \quad \text{Ship forward Velocity}$$

$$\epsilon_{r0} := \frac{V_0 \cdot s}{0.8 \text{ m}} \quad \epsilon_{r0} = 11.625 \quad \text{Strain Rate}$$

$$\sigma_0 := 1.29 \cdot \sigma_u \cdot \epsilon_{r0}^{0.037} \quad \sigma_0 = 7.119 \times 10^8 \text{ Pa} \quad \text{Dynamic Flow Stress}$$

$$s\sigma_{c_1} := \sigma_d(\sigma_0, n_{AT_1}, \tau_1, DA_{E_1}, n_{C_1}, n_{T_1}) \quad s\sigma_{c_1} = 1.316 \times 10^8 \text{ Pa} \quad \text{Crushing Stress}$$

$$P_{c_1} := P_{AV}(DA_{E_1}, s\sigma_{c_1}) \quad P_{c_1} = 26.603 \text{ MN} \quad \text{Crushing Force}$$

$$E_1 := \int_{0 \text{ m}}^{(0.8-0.75) \text{ m}} P_{c_1} dx \quad E_1 = 1.596 \times 10^7 \text{ J} \quad \text{Crushing Energy for } x = 0 \text{ to } 0.8 \text{ m}$$

$$E_{R_1} := E_0 - E_1 \quad E_{R_1} = 7.923 \times 10^9 \text{ J} \quad \text{Remaining Kinetic Energy}$$

Point Velocity at x = 0.8 meters is given below.

$$V_1 := \left( \frac{E_{R_1}}{\frac{1}{2} \cdot m_x} \right)^{\frac{1}{2}} \quad V_1 = 9.291 \frac{\text{m}}{\text{s}}$$

Section 2, from x = 0.8 to x = 1.6 meters has the following properties

$$\epsilon r_1 := \frac{V_1 \cdot s}{0.8 \text{ m}} \quad \epsilon r_1 = 11.613$$

$$\sigma_0 := 1.29 \cdot \sigma_u \cdot (\epsilon r_1)^{0.037} \quad \sigma_0 = 7.119 \times 10^8 \text{ Pa}$$

$$s\sigma_{c_2} := \sigma_c(\sigma_0, n_{AT_2}, \tau_2, DA_{E_2}, n_{C_2}, n_{T_2}) \quad s\sigma_{c_2} = 1.872 \times 10^8 \text{ Pa}$$

$$P_{c_2} := P_{AV}(DA_{E_2}, s\sigma_{c_2}) \quad P_{c_2} = 233.71 \text{ MN}$$

$$E_2 := \int_{(0.8-0.75)\text{m}}^{(1.6-0.75)\text{m}} P_{c_2} dx \quad E_2 = 1.402 \times 10^8 \text{ J} \quad \text{Crushing Energy for x = 0.8 to 1.6 m}$$

$$E_{R_2} := E_{R_1} - E_2 \quad E_{R_2} = 7.783 \times 10^9 \text{ J} \quad \text{Remaining Kinetic Energy}$$

Point Velocity at x = 1.6 meters is given below.

$$V_2 := \left( \frac{E_{R_2}}{\frac{1}{2} \cdot m_x} \right)^{\frac{1}{2}} \quad V_2 = 9.208 \frac{\text{m}}{\text{s}}$$

Section 3, from x = 1.6 to x = 2.4 meters has the following properties

$$\epsilon r_2 := \frac{V_2 \cdot s}{0.8 \text{ m}} \quad \epsilon r_2 = 11.51$$

$$\sigma_0 := 1.29 \cdot \sigma_u \cdot (\epsilon r_2)^{0.037} \quad \sigma_0 = 7.117 \times 10^8 \text{ Pa}$$

$$s\sigma_{c_3} := \sigma_c(\sigma_0, n_{AT_3}, \tau_3, DA_{E_3}, n_{C_3}, n_{T_3}) \quad s\sigma_{c_3} = 1.608 \times 10^8 \text{ Pa}$$

$$P_{c_3} := P_{AV}(DA_{E_3}, s\sigma_{c_3}) \quad P_{c_3} = 288.227 \text{ MN}$$

$$E_3 := \int_{(1.6-0.75)m}^{(2.4-0.75)m} P_{c_3} dx \quad E_3 = 1.729 \times 10^8 \text{ J} \quad \text{Crushing Energy for } x = 1.6 \text{ to } 2.4 \text{ m}$$

$$E_{R_3} := E_{R_2} - E_3 \quad E_{R_3} = 7.61 \times 10^9 \text{ J} \quad \text{Remaining Kinetic Energy}$$

Point Velocity at  $x = 2.4$  meters is given below.

$$V_3 := \frac{E_{R_3}^{\frac{1}{2}}}{\frac{1}{2} \cdot m_x} \quad V_3 = 9.105 \frac{\text{m}}{\text{s}}$$

Section 4, from  $x = 2.4$  to  $x = 3.2$  meters has the following properties

$$\epsilon r_3 := \frac{V_3 \cdot s}{0.8m} \quad \epsilon r_3 = 11.381$$

$$\sigma_0 := 1.29 \cdot \sigma_u \cdot (\epsilon r_3)^{0.037} \quad \sigma_0 = 7.114 \times 10^8 \text{ Pa}$$

$$s\sigma_{c_4} := \sigma_c(\sigma_0, n_{AT_4}, \tau_4, DA_{E_4}, n_{C_4}, n_{T_4}) \quad s\sigma_{c_4} = 1.694 \times 10^8 \text{ Pa}$$

$$P_{c_4} := P_{AV}(DA_{E_4}, s\sigma_{c_4}) \quad P_{c_4} = 355.803 \text{ MN}$$

$$E_4 := \int_{(2.4-0.75)m}^{(3.2-0.75)m} P_{c_4} dx \quad E_4 = 2.135 \times 10^8 \text{ J} \quad \text{Crushing Energy for } x = 2.4 \text{ to } 3.2 \text{ m}$$

$$E_{R_4} := E_{R_3} - E_4 \quad E_{R_4} = 7.397 \times 10^9 \text{ J} \quad \text{Remaining Kinetic Energy}$$

Point Velocity at  $x = 3.2$  meters is given below.

$$V_4 := \frac{E_{R_4}^{\frac{1}{2}}}{\frac{1}{2} \cdot m_x} \quad V_4 = 8.977 \frac{\text{m}}{\text{s}}$$

Section 5, from  $x = 3.2$  to  $x = 4$  meters has the following properties

$$\epsilon r_4 := \frac{V_4 \cdot s}{0.8m} \quad \epsilon r_4 = 11.221$$

$$\sigma_0 := 1.29 \cdot \sigma_u \cdot (\epsilon r_4)^{0.037} \quad \sigma_0 = 7.11 \times 10^8 \text{ Pa}$$

$$s\sigma_{c_5} := \sigma_c(\sigma_0, n_{AT_5}, \tau_5, DA_{E_5}, n_{C_5}, n_{T_5}) \quad s\sigma_{c_5} = 1.557 \times 10^8 \text{ Pa}$$

$$P_{c_5} := P_{AV}(DA_{E_5}, s\sigma_{c_5}) \quad P_{c_5} = 354.483 \text{ MN}$$

$$E_5 := \int_{(3.2-0.75)m}^{(4-0.75)m} P_{c_5} dx \quad E_5 = 2.127 \times 10^8 \text{ J} \quad \text{Crushing Energy for } x = 3.2 \text{ to } 4 \text{ m}$$

$$E_{R_5} := E_{R_4} - E_5 \quad E_{R_5} = 7.184 \times 10^9 \text{ J} \quad \text{Remaining Kinetic Energy}$$

Point Velocity at  $x = 4$  meters is given below.

$$V_5 := \left( \frac{E_{R_5}}{\frac{1}{2} \cdot m_x} \right)^{\frac{1}{2}} \quad V_5 = 8.847 \frac{\text{m}}{\text{s}}$$

Section 6, from  $x = 4$  to  $x = 4.8$  meters has the following properties

$$\epsilon r_5 := \frac{V_5 \cdot s}{0.8m} \quad \epsilon r_5 = 11.058$$

$$\sigma_0 := 1.29 \cdot \sigma_u \cdot (\epsilon r_5)^{0.037} \quad \sigma_0 = 7.106 \times 10^8 \text{ Pa}$$

$$s\sigma_{c_6} := \sigma_c(\sigma_0, n_{AT_6}, \tau_6, DA_{E_6}, n_{C_6}, n_{T_6}) \quad s\sigma_{c_6} = 1.701 \times 10^8 \text{ Pa}$$

$$P_{c_6} := P_{AV}(DA_{E_6}, s\sigma_{c_6}) \quad P_{c_6} = 408.216 \text{ MN}$$

$$E_6 := \int_{(4-0.75)m}^{(4.8-0.75)m} P_{c_6} dx \quad E_6 = 2.449 \times 10^8 \text{ J} \quad \text{Crushing Energy for } x = 4 \text{ to } 4.8 \text{ m}$$

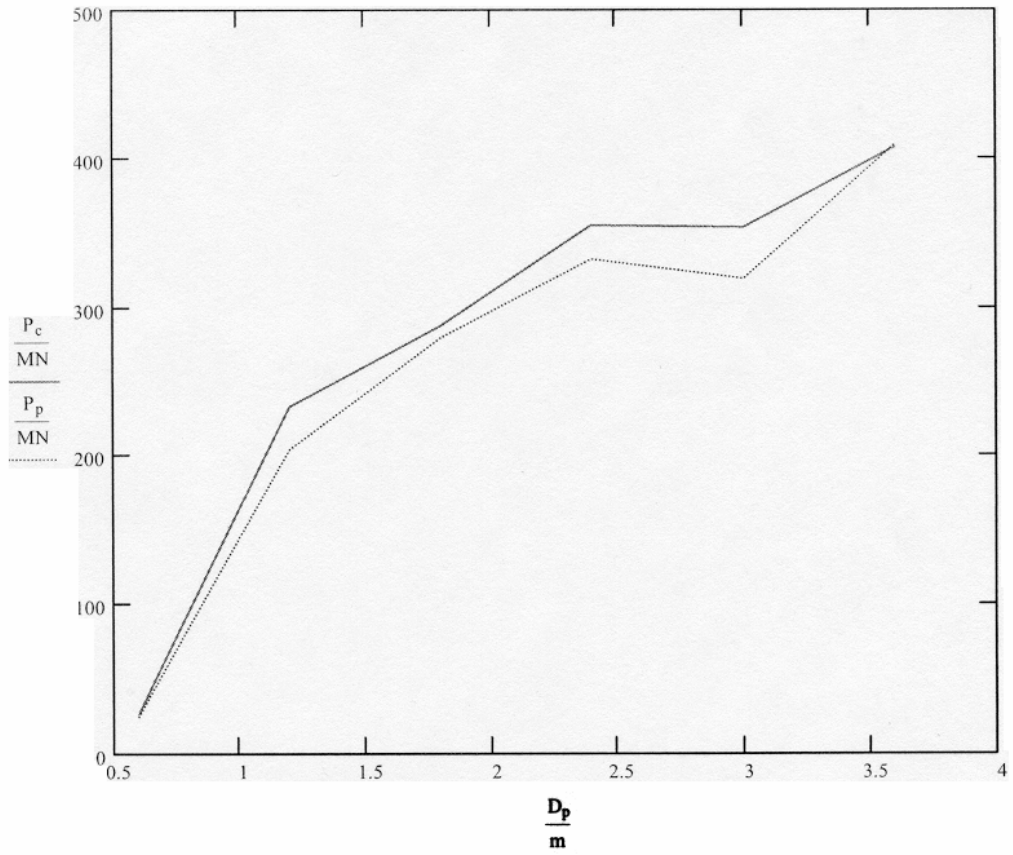
$$E_{R_6} := E_{R_5} - E_6 \quad E_{R_6} = 6.939 \times 10^9 \text{ J} \quad \text{Remaining Kinetic Energy}$$

Point Velocity at  $x = 4.8$  meters is given below.

$$V_6 := \left( \frac{E_{R_6}}{\frac{1}{2} \cdot m_x} \right)^{\frac{1}{2}} \quad V_6 = 8.694 \frac{\text{m}}{\text{s}}$$

The following figure provides a comparison of the above results for sections 1 through 6 to those numerical results extracted from the graph presented by pederson for the 150k dwt Bulk Carrier.

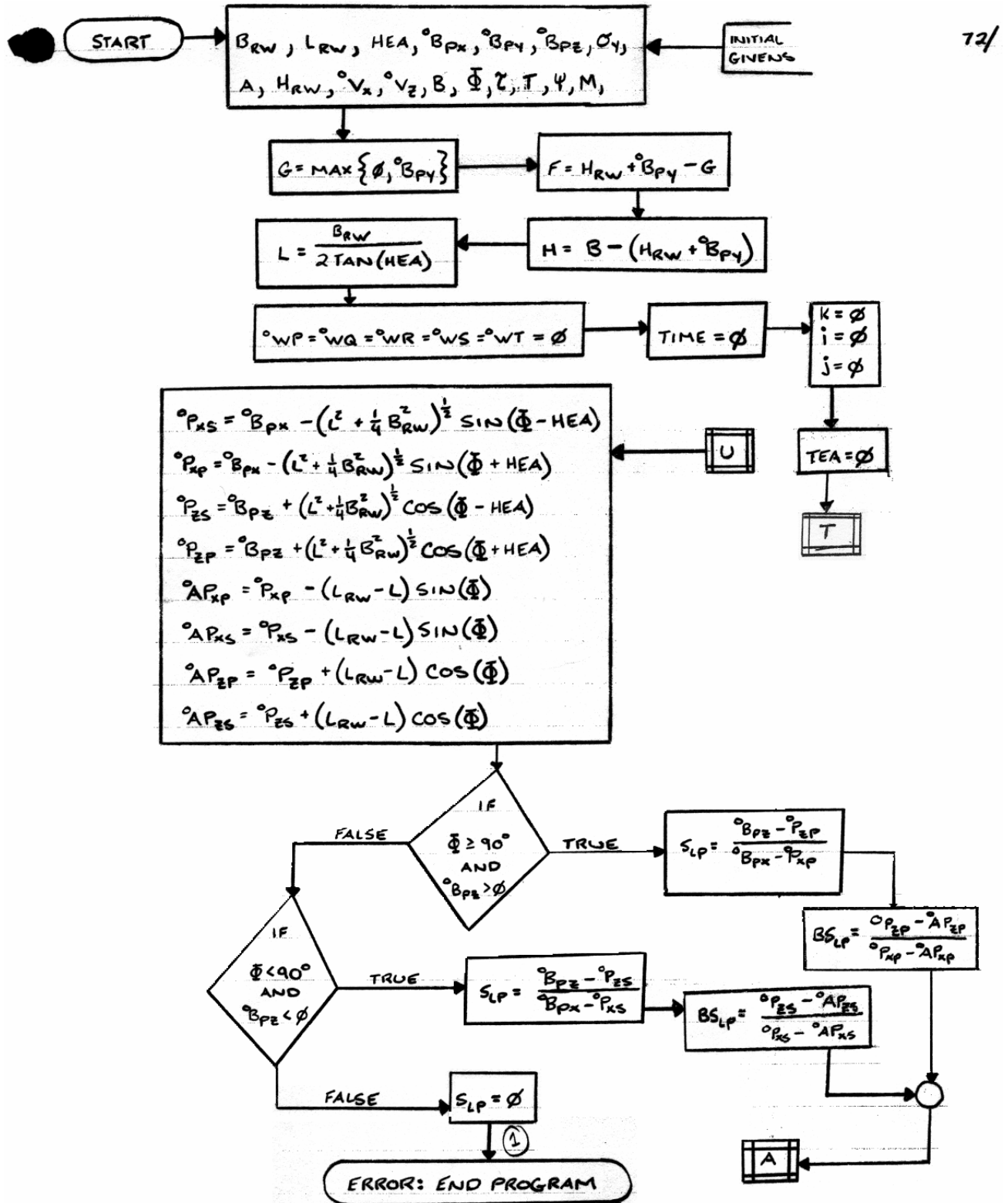
$$P_c = \begin{pmatrix} 26.603 \\ 233.71 \\ 288.227 \\ 355.803 \\ 354.483 \\ 408.216 \end{pmatrix} \text{ MN} \quad P_p = \begin{pmatrix} 25 \\ 205 \\ 280 \\ 333 \\ 320 \\ 410 \end{pmatrix} \text{ MN} \quad D_c = \begin{pmatrix} 0.8 \\ 1.6 \\ 2.4 \\ 3.2 \\ 4 \\ 4.8 \end{pmatrix} \text{ m} \quad D_p := 0.75 \cdot D_c \quad D_p = \begin{pmatrix} 0.6 \\ 1.2 \\ 1.8 \\ 2.4 \\ 3 \\ 3.6 \end{pmatrix} \text{ m}$$

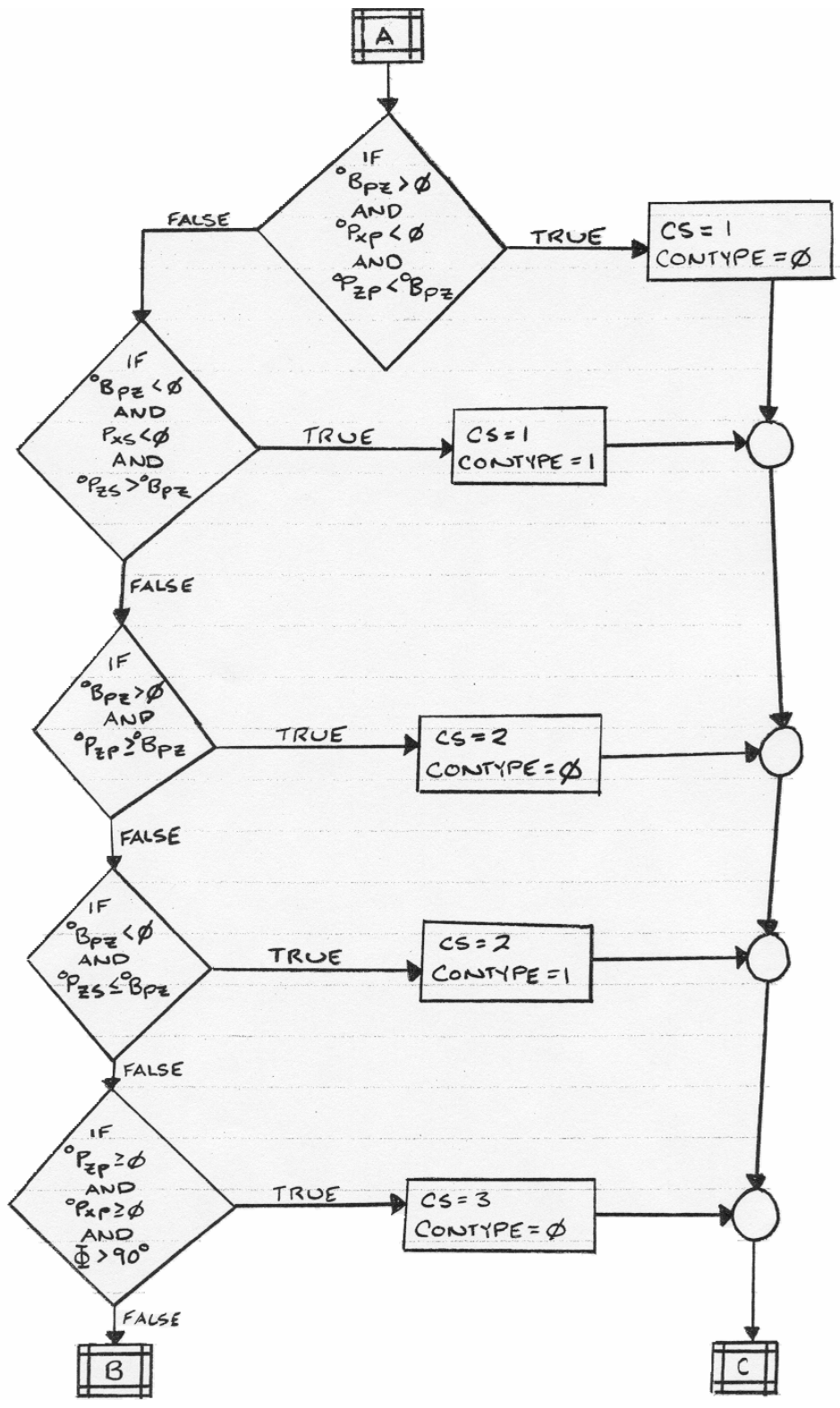


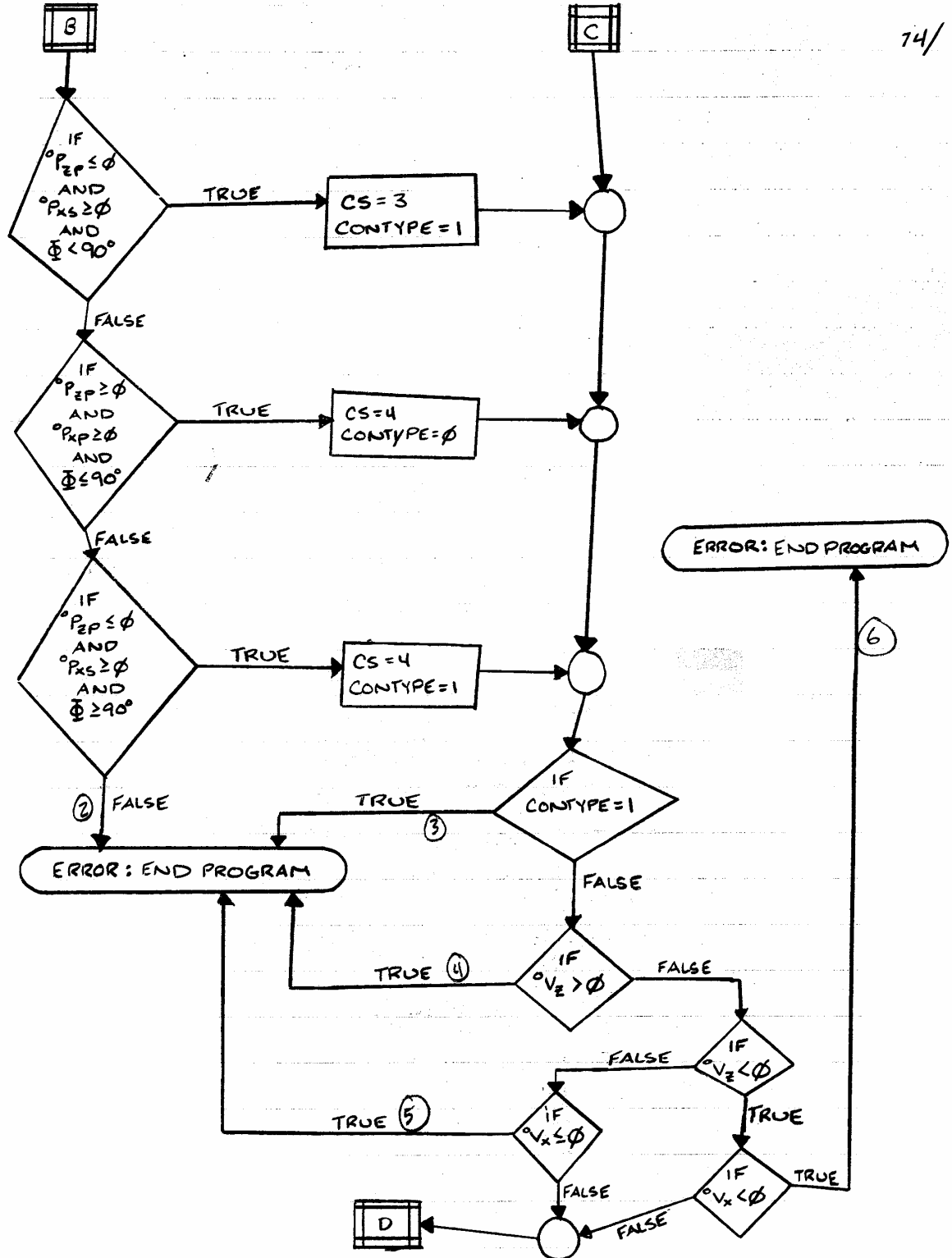
**Pp is Pedersons reported results as extracted.**

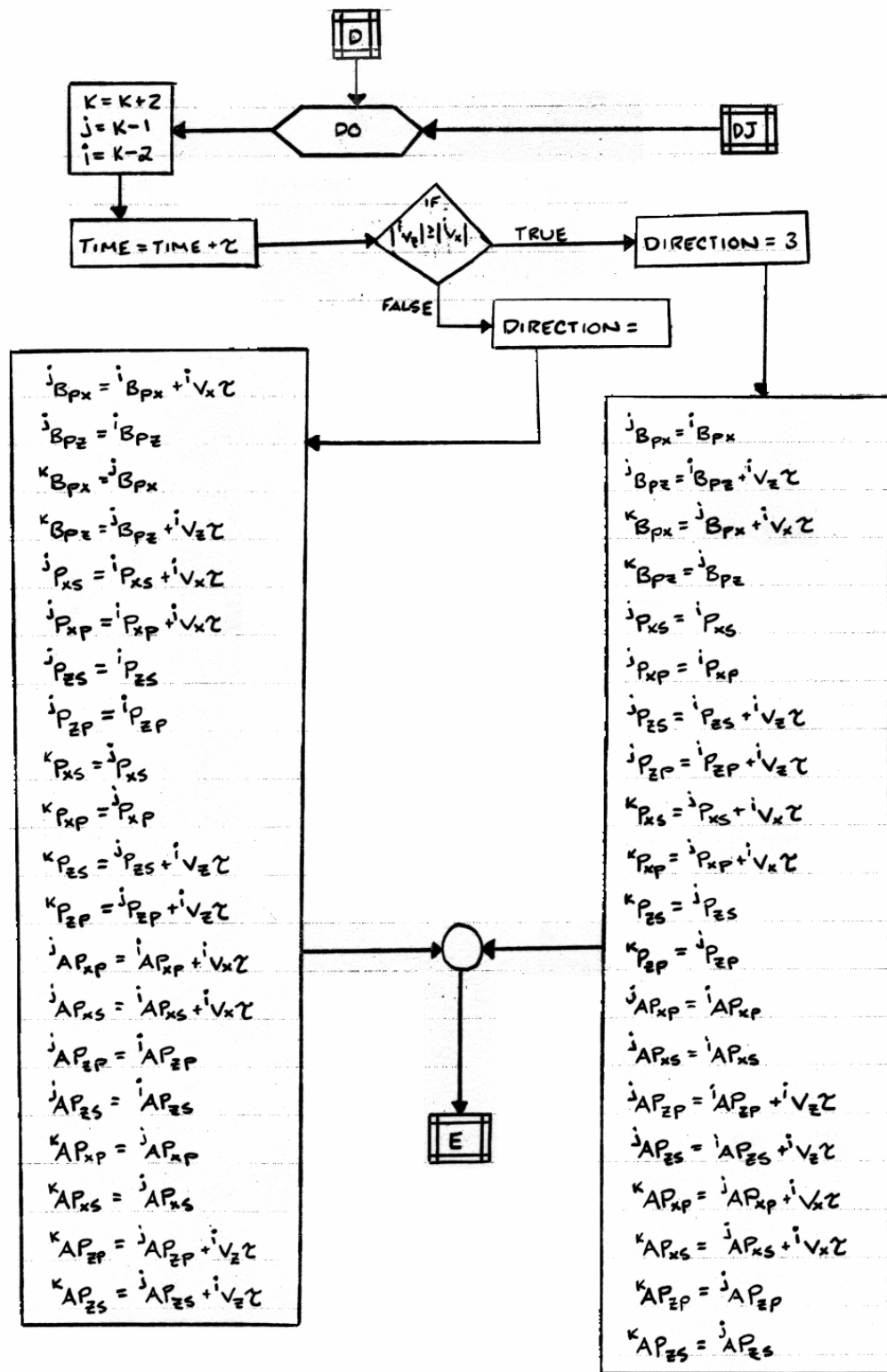
**Pc is reanalysis of Amdahls method neglecting Pedersen's cruciform assumption, including stiffener T's formed from longitudinals and side shell.**

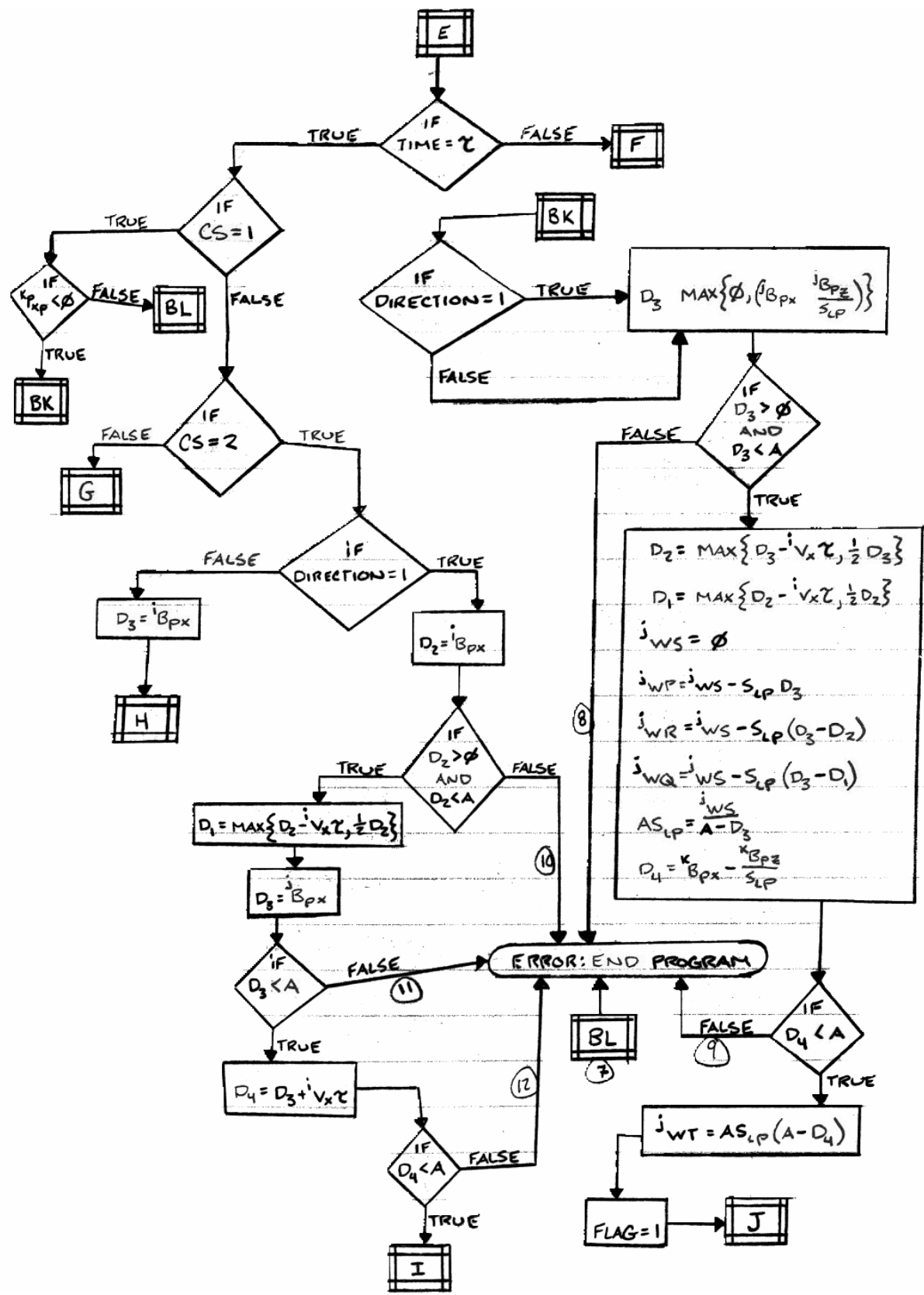
## Appendix J: Flowchart of Method of Lateral Deformation of Webs and Transverse Bulkheads

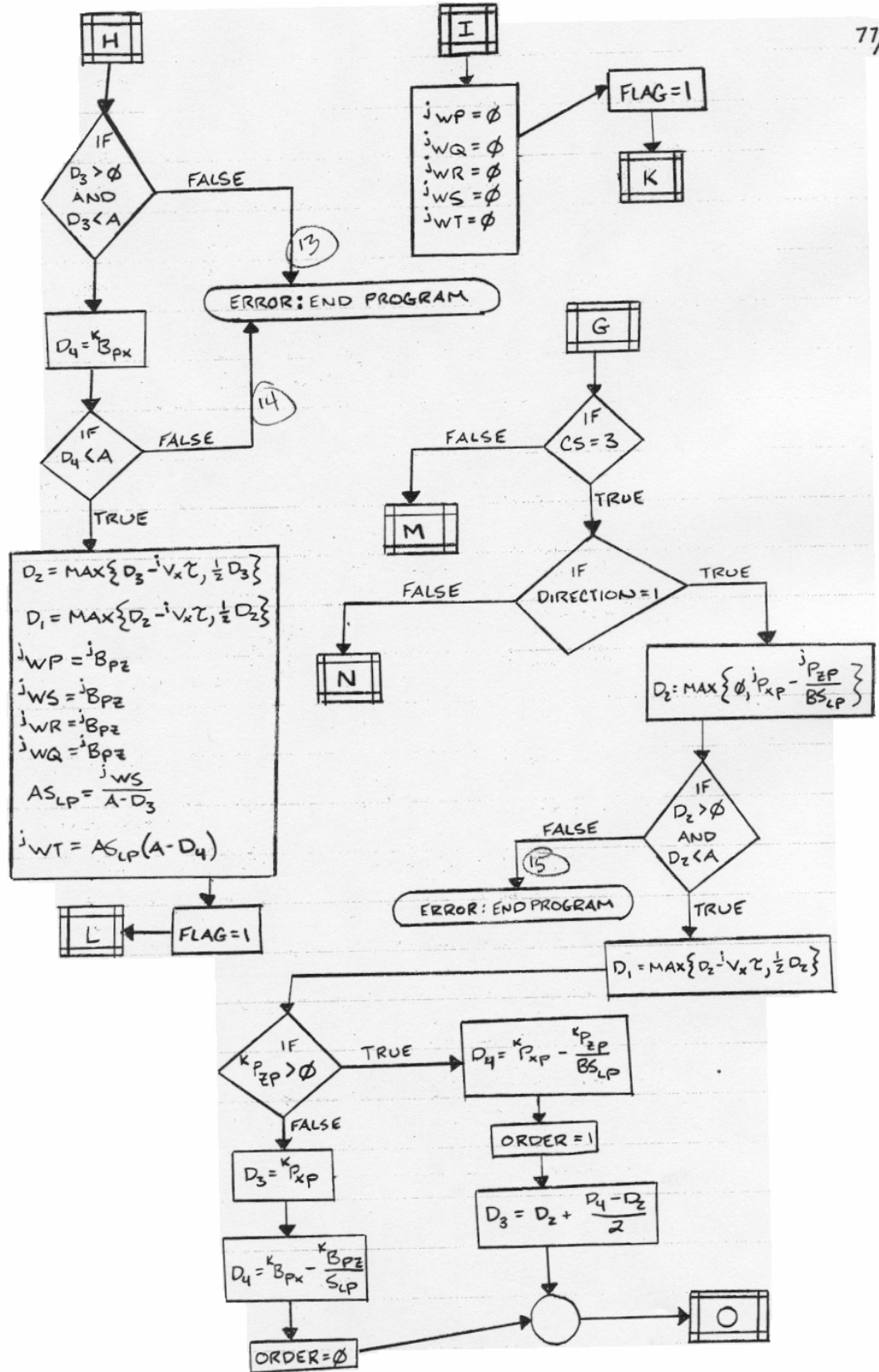


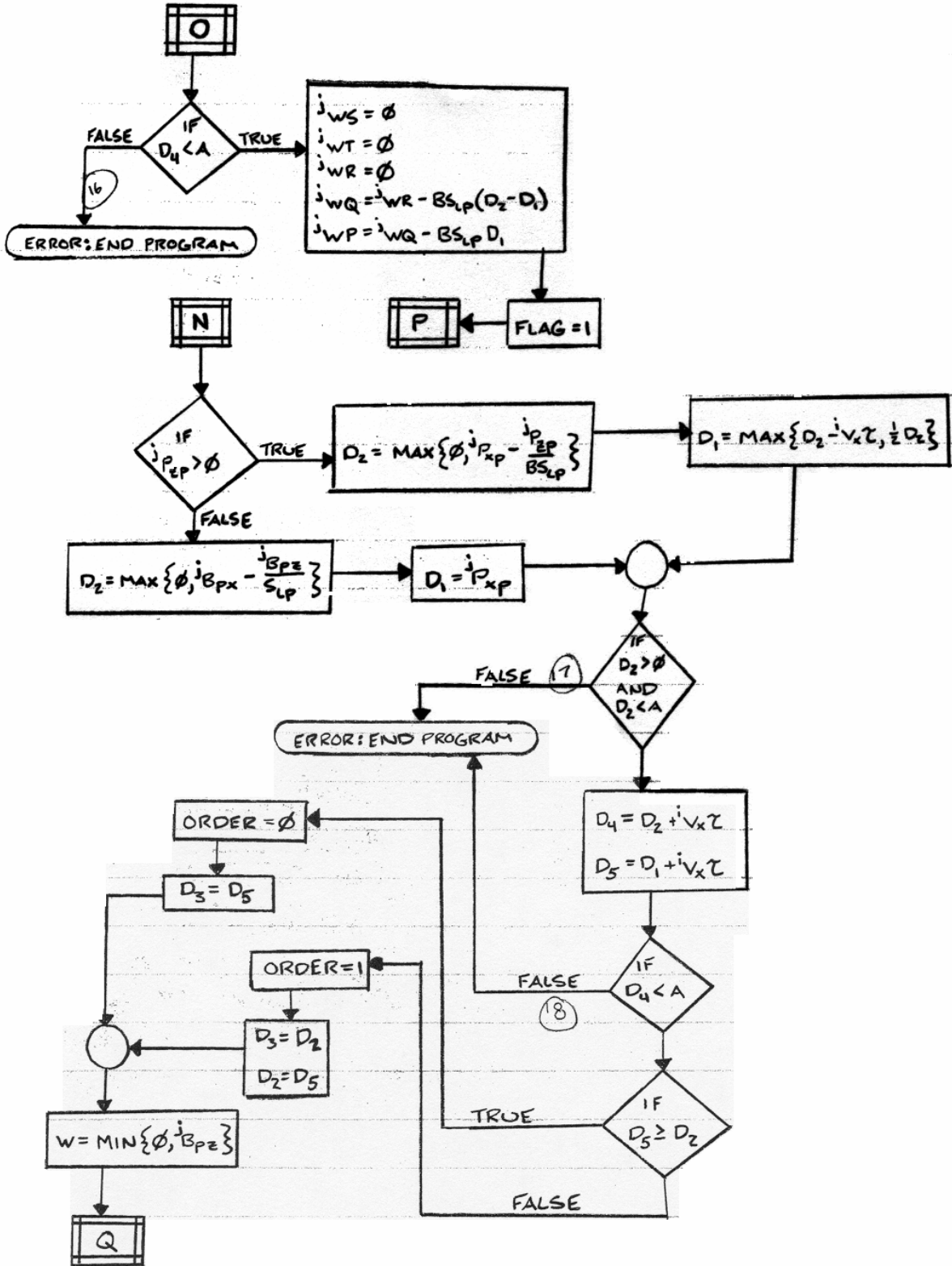




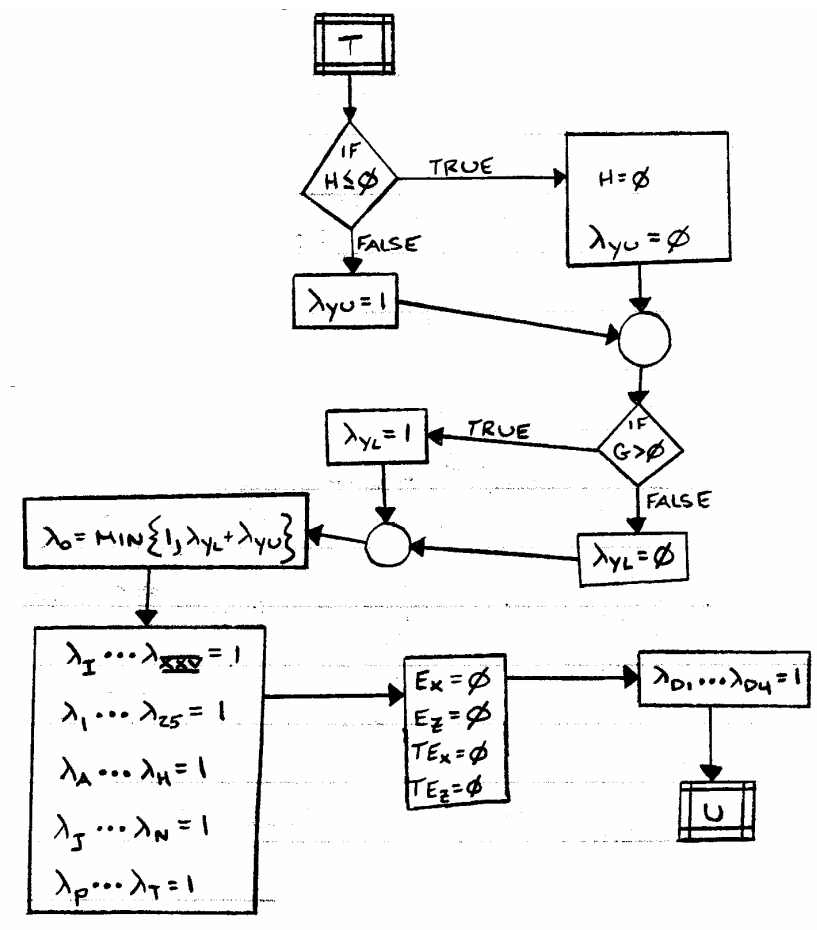










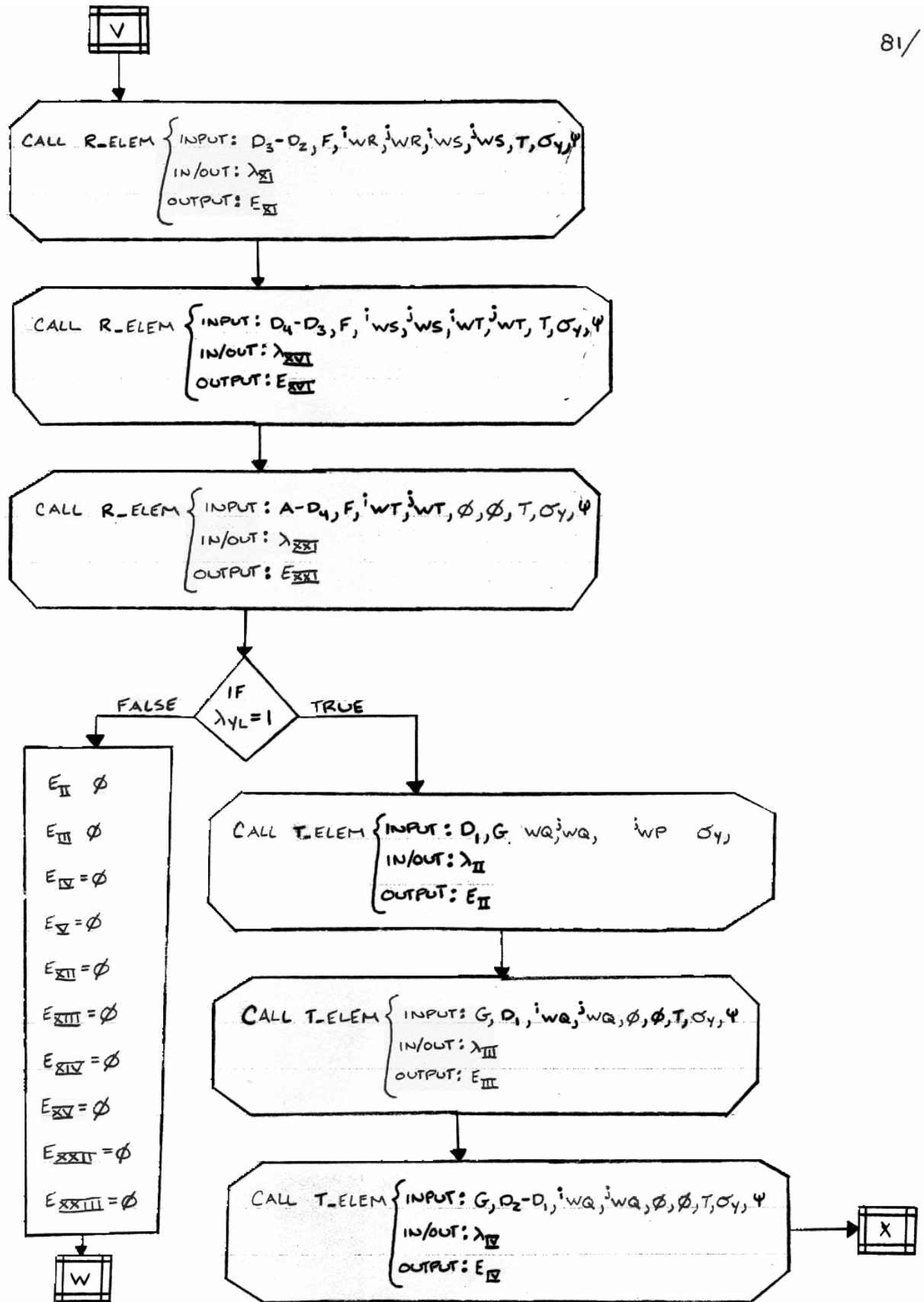


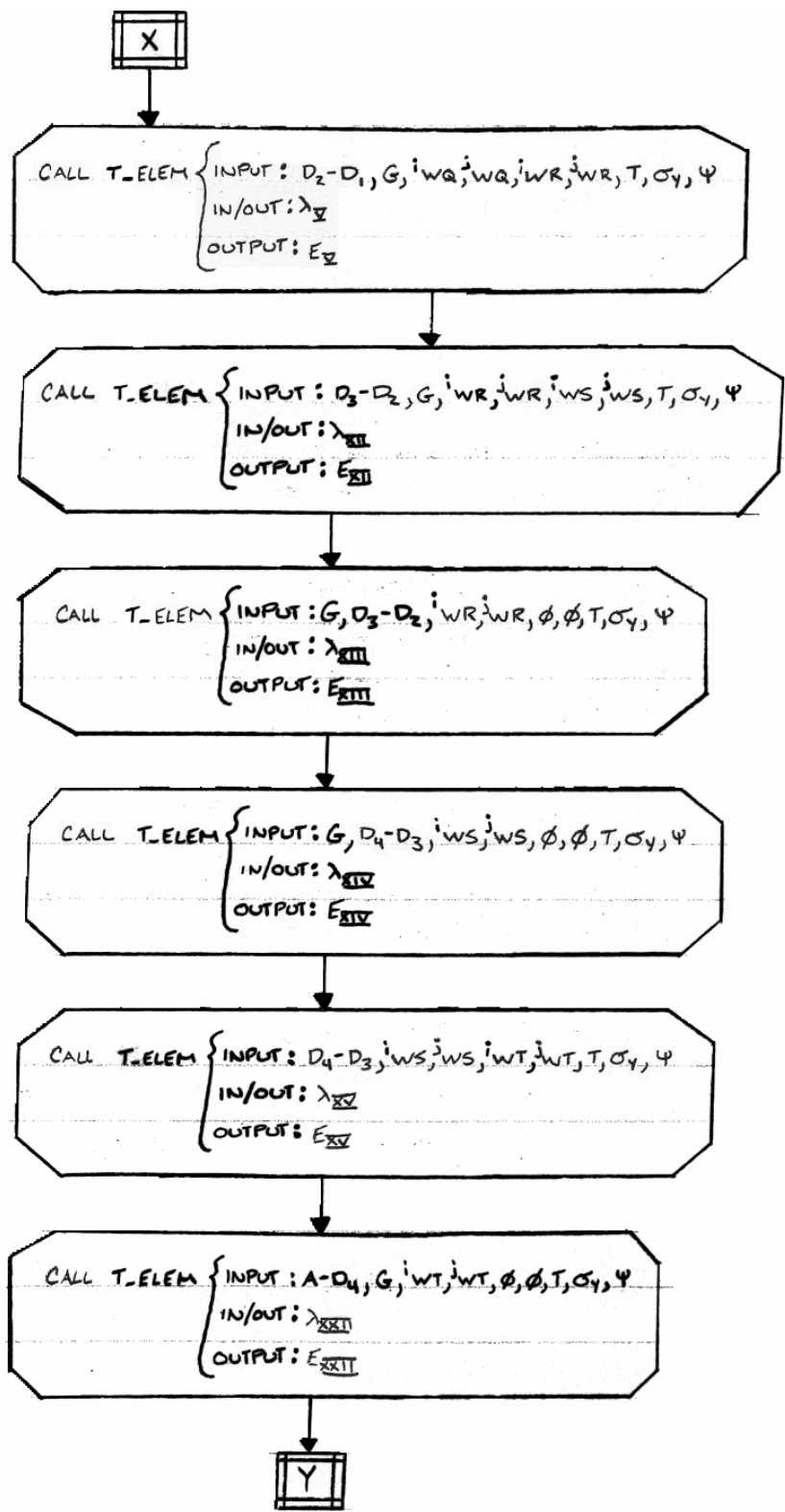
J, K, L, P, R, S, BZ, CA, CE,  
CI, CL, CN, CR,

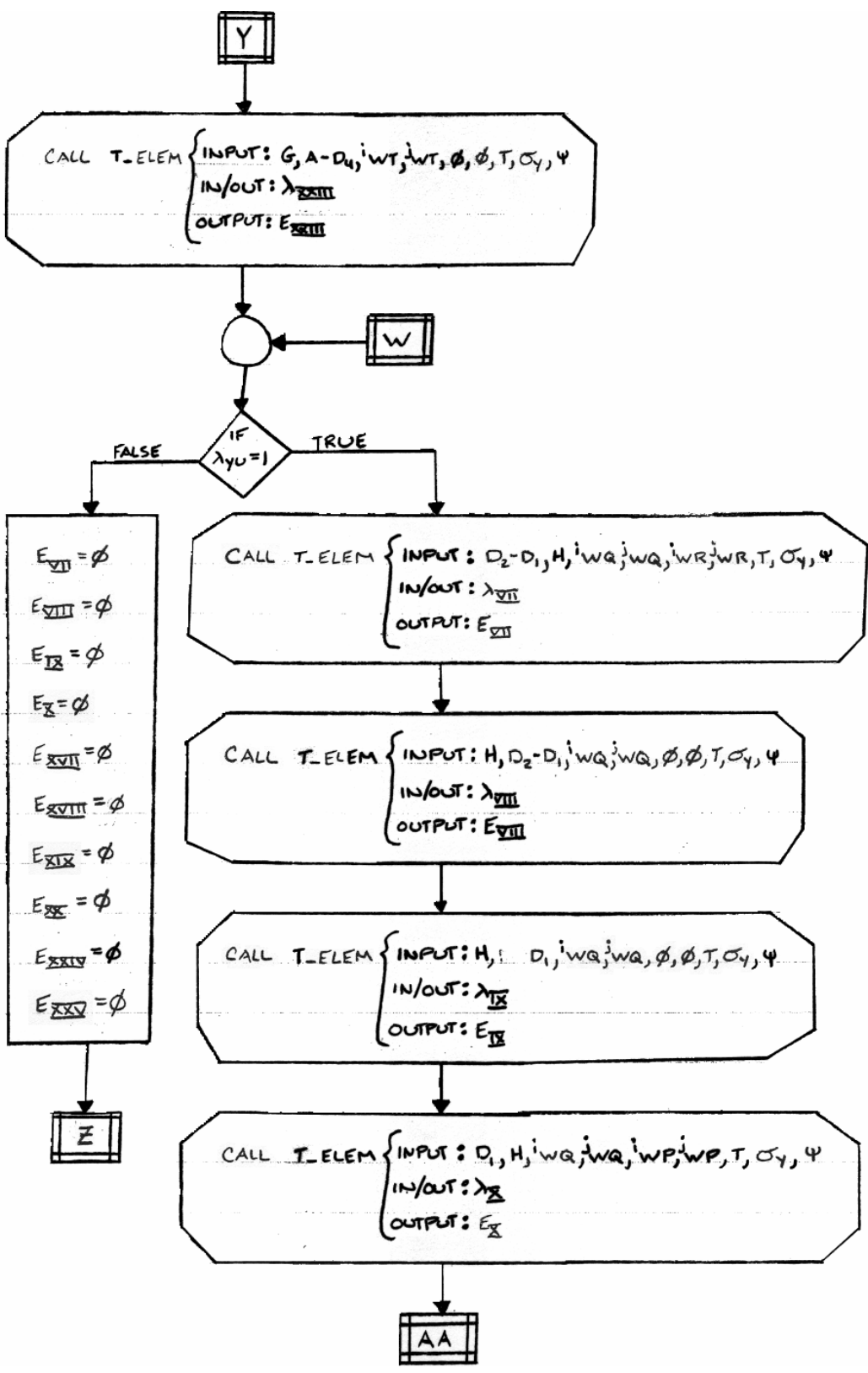
CALL R-ELEM { INPUT: D<sub>1</sub>, F, i<sub>WP</sub>, j<sub>WP</sub>, i<sub>WQ</sub>, j<sub>WQ</sub>, T, σ<sub>y</sub>, ψ  
IN/OUT: λ<sub>x</sub>  
OUTPUT: E<sub>x</sub>

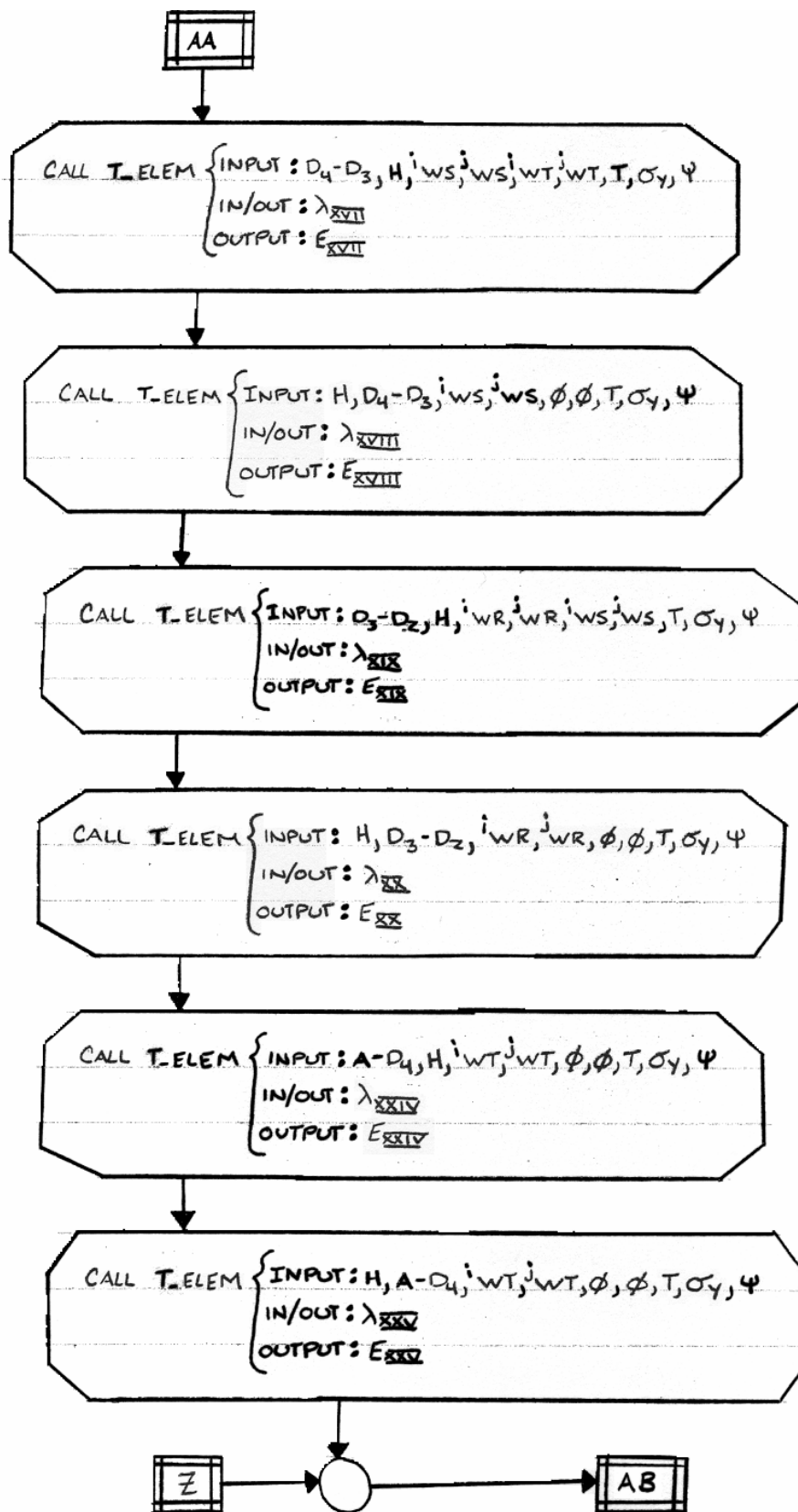
CALL R-ELEM { INPUT: D<sub>2</sub>-D<sub>1</sub>, F, i<sub>WQ</sub>, j<sub>WQ</sub>, i<sub>WR</sub>, j<sub>WR</sub>, T, σ<sub>y</sub>, ψ  
IN/OUT: λ<sub>z</sub>  
OUTPUT: E<sub>z</sub>

V









$$\lambda_A^{\text{MIN}} = [(\lambda_{II} + \lambda_{III} + \lambda_{IV} + \xi_1 - \lambda_{XIII}) (\lambda_{V} + \lambda_{VI} + \lambda_{VII} + \xi_1 - \lambda_{XX}) (\lambda_{II} + \dots \\ \dots + \lambda_{III} + \lambda_{XIII} + \lambda_{XIV} + \xi_1 - \lambda_{XIV}) (\lambda_{V} + \lambda_{VI} + \lambda_{XX} + \lambda_{XIX} + \dots \\ \dots + \xi_1 - \lambda_{XVII}) (\lambda_{II} + \lambda_{III} + \lambda_{XIII} + \lambda_{XIV} + \lambda_{XV} + \xi_1 - \lambda_{XVII}) (\lambda_{V} + \dots \\ \dots + \lambda_{VI} + \lambda_{XX} + \lambda_{XVII} + \lambda_{XVIII} + \xi_1 - \lambda_{XVIII}), 1]$$

$$\lambda_1 = \lambda_A \left( \frac{\lambda_{II} + \lambda_{IV}}{2} \right) \text{MIN} \{1, \lambda_I [(\lambda_{II} + \lambda_{III} + \lambda_{VI}) (\lambda_{V} + \lambda_{VI} + \lambda_{IX}) (\lambda_{II} + \dots \\ \dots + \lambda_{III} + \lambda_{XIII} + \lambda_{XIV}) (\lambda_{V} + \lambda_{IX} + \lambda_{XX} + \lambda_{XI}) (\lambda_{II} + \lambda_{III} + \lambda_{XIII} + \dots \\ \dots + \lambda_{XIV} + \lambda_{XVI}) (\lambda_{V} + \lambda_{IX} + \lambda_{XX} + \lambda_{XVII} + \lambda_{XVIII}) (\lambda_{II} + \lambda_{III} + \dots \\ \dots + \lambda_{XIII} + \lambda_{XIV} + \lambda_{XVIII} + \lambda_{XIX}) (\lambda_{V} + \lambda_{IX} + \lambda_{XX} + \lambda_{XVIII} + \dots \\ \dots + \lambda_{XXV} + \lambda_{XXVI})]\}$$

$$\lambda_2 = \lambda_I \lambda_{II} \rightarrow \lambda_3 = \lambda_{III} \lambda_{IV} \rightarrow \lambda_4 = \lambda_3 \rightarrow \lambda_5 = \lambda_{V} \lambda_{VI} \lambda_{XIII}$$

$$\lambda_C^{\text{MIN}} = [(\lambda_{V} + \xi_1 - \lambda_{XIII}) (\lambda_{XIII} + \xi_1 - \lambda_{XX}) (\lambda_{II} + \lambda_{III} + \lambda_{XIII} + \lambda_{XIV} + \dots \\ \dots + \xi_1 - \lambda_{XIV}) (\lambda_{V} + \lambda_{IX} + \lambda_{XX} + \lambda_{XIX} + \xi_1 - \lambda_{XVII}) (\lambda_{II} + \lambda_{III} + \dots \\ \dots + \lambda_{XIII} + \lambda_{XIV} + \lambda_{XV} + \xi_1 - \lambda_{XVII}) (\lambda_{V} + \lambda_{IX} + \lambda_{XX} + \lambda_{XVIII} + \dots \\ \dots + \lambda_{XVIII} + \xi_1 - \lambda_{XVIII}), 1]$$

$$\lambda_D = \text{MIN} \{1, (\lambda_I + \lambda_{III} + \lambda_{XIII})\} \rightarrow \lambda_E = \text{MIN} \{1, (\lambda_I + \lambda_{IX} + \lambda_{XX})\}$$

$$\lambda_G = \text{MIN} \{1, (\lambda_{XIII} + \lambda_{XIV})\} \leftarrow \lambda_F = \text{MIN} \{1, (\lambda_{XX} + \lambda_{XIX})\}$$

$$\lambda_B = \frac{1}{2} (\lambda_D + \lambda_E \lambda_F \lambda_G) (\lambda_E + \lambda_D \lambda_F \lambda_G) (\lambda_F + \lambda_D \lambda_E \lambda_G) (\lambda_G + \lambda_D \lambda_E \lambda_F)$$

AC

86/

$$\lambda_6 = \lambda_8 \lambda_c \text{ MIN} \{1, \lambda_{VI} [(\lambda_{II} + \lambda_{III} + \lambda_{VIII} + \lambda_{XI})(\lambda_X + \lambda_{IX} + \lambda_{XX} + \lambda_{XI})(\lambda_{II} + \dots \\ \dots + \lambda_{III} + \lambda_{VIII} + \lambda_{XIV} + \lambda_{XVI})(\lambda_X + \lambda_{IX} + \lambda_{XX} + \lambda_{XVIII} + \lambda_{XVI})(\lambda_{II} + \dots \\ \dots + \lambda_{III} + \lambda_{VIII} + \lambda_{XIV} + \lambda_{XVIII} + \lambda_{XXI})(\lambda_X + \lambda_{IX} + \lambda_{XX} + \lambda_{XVIII} + \lambda_{XXV} + \dots \\ \dots + \lambda_{XXI})]\}$$

$$\lambda_7 = \lambda_{VII} \lambda_{XX} \lambda_{VI} \rightarrow \lambda_8 = \lambda_{VII} \lambda_{IX} \rightarrow \lambda_9 = \lambda_8 \rightarrow \lambda_{10} = \lambda_I \lambda_X$$

$$\lambda_J = [(\lambda_{III} + \xi_1 - \lambda_{XIV}) (\lambda_{XIX} + \xi_1 - \lambda_{XVIII}) (\lambda_{II} + \lambda_{III} + \lambda_{VIII} + \lambda_{XIV} + \lambda_{XV} + \dots \\ \dots + \xi_1 - \lambda_{XXIII}) (\lambda_X + \lambda_{IX} + \lambda_{XX} + \lambda_{XVIII} + \lambda_{XXII} + \xi_1 - \lambda_{XXV})]^{-1}$$

$$\lambda_K = \text{MIN} \{1, (\lambda_I + \lambda_{III} + \lambda_{VI} + \lambda_{VIII} + \lambda_{XIV})\} \rightarrow \lambda_M = \text{MIN} \{1, (\lambda_{XVIII} + \lambda_{XXI})\}$$

$$\lambda_L = \text{MIN} \{1, (\lambda_I + \lambda_{IX} + \lambda_{VI} + \lambda_{XX} + \lambda_{XXIII})\} \leftarrow \lambda_N = \text{MIN} \{1, (\lambda_{XIV} + \lambda_{XVI})\}$$

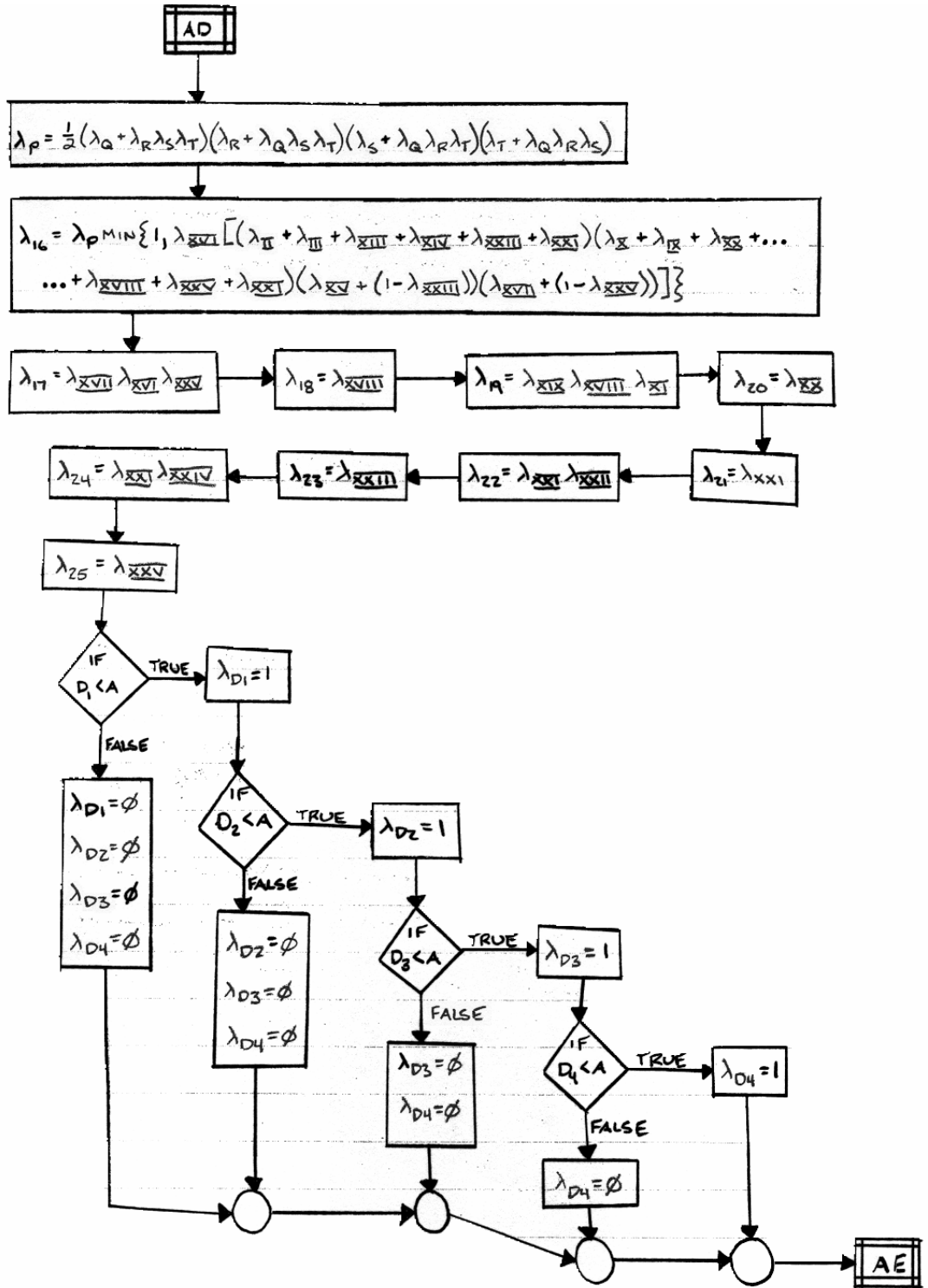
$$\lambda_H = \frac{1}{2} (\lambda_K + \lambda_L \lambda_M \lambda_N) (\lambda_L + \lambda_K \lambda_M \lambda_N) (\lambda_M + \lambda_K \lambda_L \lambda_N) (\lambda_N + \lambda_K \lambda_L \lambda_M)$$

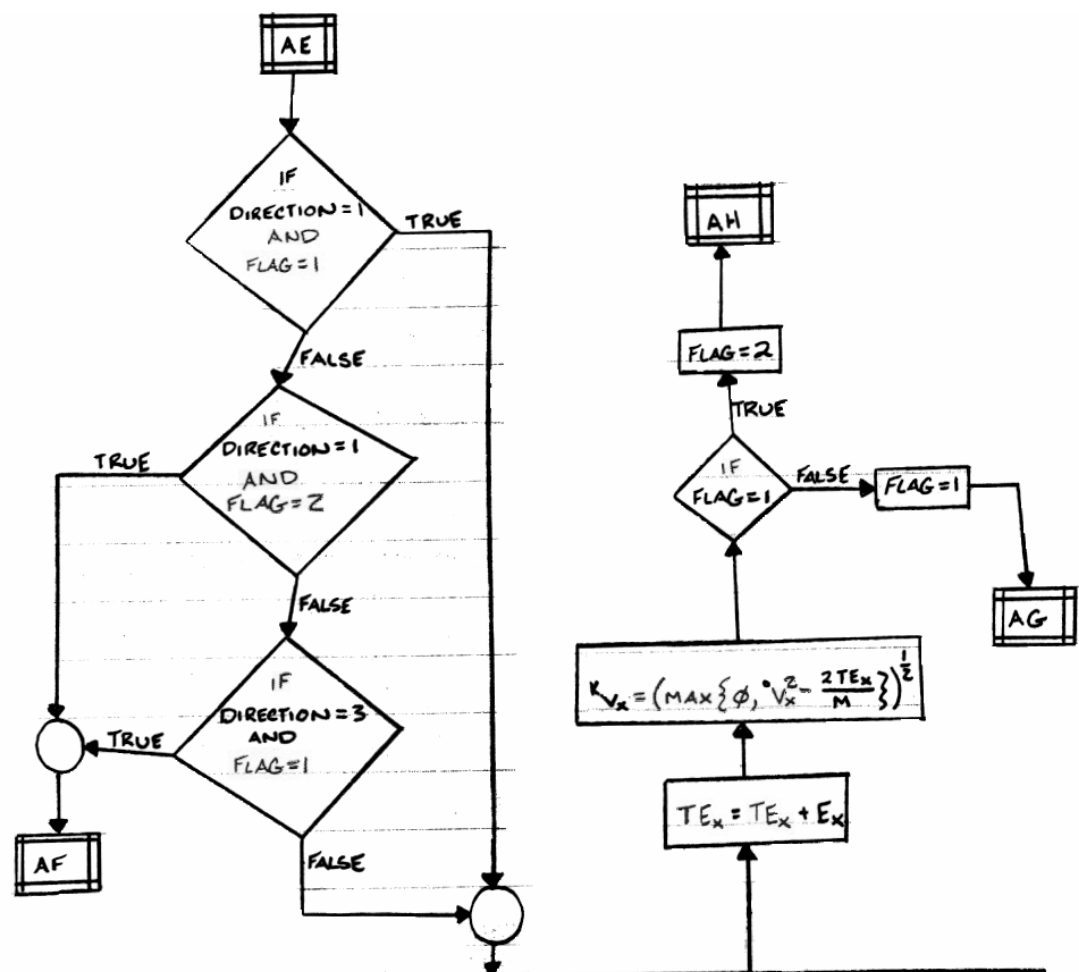
$$\lambda_H = \lambda_J \lambda_H \text{ MIN} \{1, \lambda_{XI} [(\lambda_{II} + \lambda_{III} + \lambda_{VIII} + \lambda_{XIV} + \lambda_{XVI})(\lambda_X + \lambda_{IX} + \lambda_{XX} + \dots \\ \dots + \lambda_{XVIII} + \lambda_{XXI})(\lambda_{II} + \lambda_{III} + \lambda_{VIII} + \lambda_{XIV} + \lambda_{XVIII} + \lambda_{XXI})(\lambda_X + \lambda_{IX} + \dots \\ \dots + \lambda_{XX} + \lambda_{XVIII} + \lambda_{XXV} + \lambda_{XXI})]\}$$

$$\lambda_{12} = \lambda_{XII} \lambda_{XI} \lambda_{XIV} \rightarrow \lambda_{13} = \lambda_{XIII} \rightarrow \lambda_{14} = \lambda_{XIV} \rightarrow \lambda_{15} = \lambda_{XV} \lambda_{XXIII} \lambda_{XVI}$$

$$\lambda_Q = \text{MIN} \{1, (\lambda_I + \lambda_{III} + \lambda_{VI} + \lambda_{XI} + \lambda_{XIV} + \lambda_{XXIII})\} \leftarrow \lambda_S = \text{MIN} \{1, (\lambda_{XXI} + \lambda_{XXV})\}$$

$$\lambda_R = \text{MIN} \{1, (\lambda_I + \lambda_{IX} + \lambda_{VI} + \lambda_{XI} + \lambda_{XVIII} + \lambda_{XXV})\} \rightarrow \lambda_T = \text{MIN} \{1, (\lambda_{XXI} + \lambda_{XXIII})\} \rightarrow \text{AD}$$

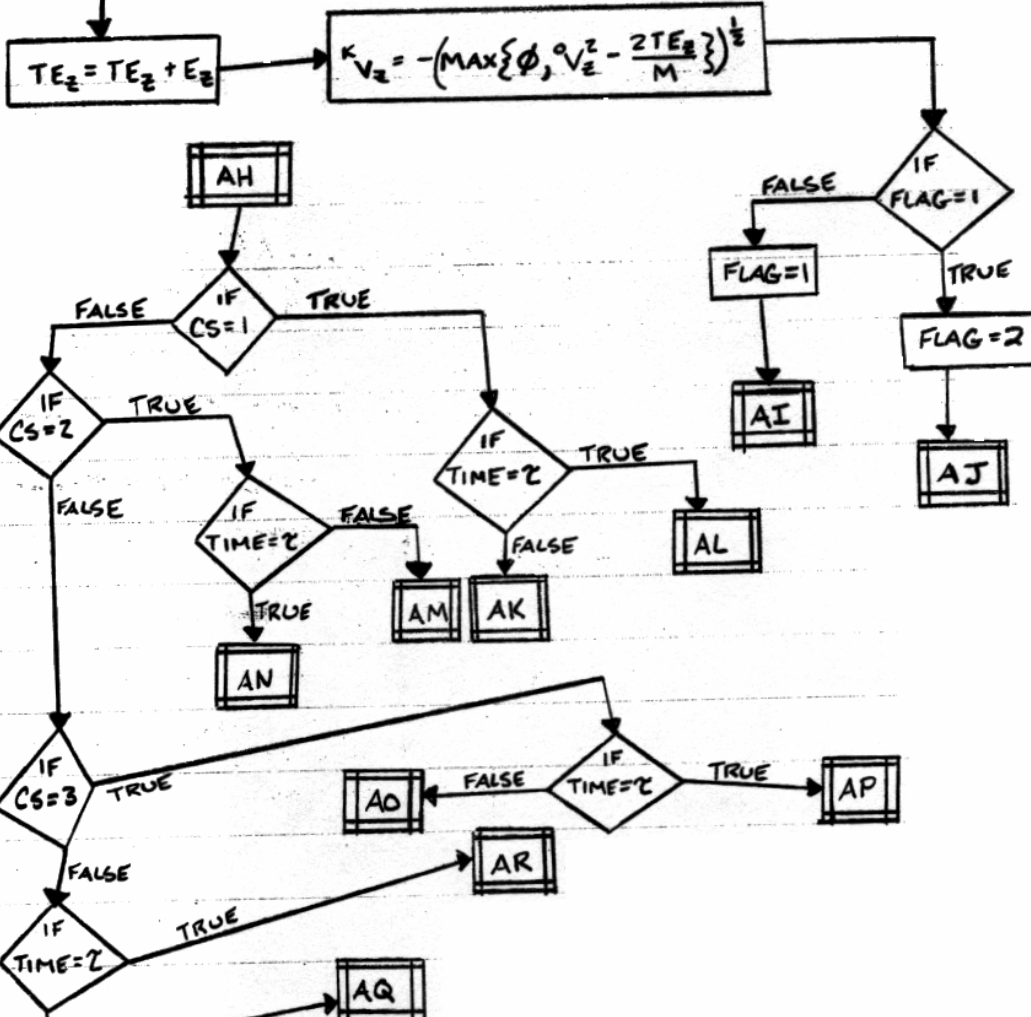


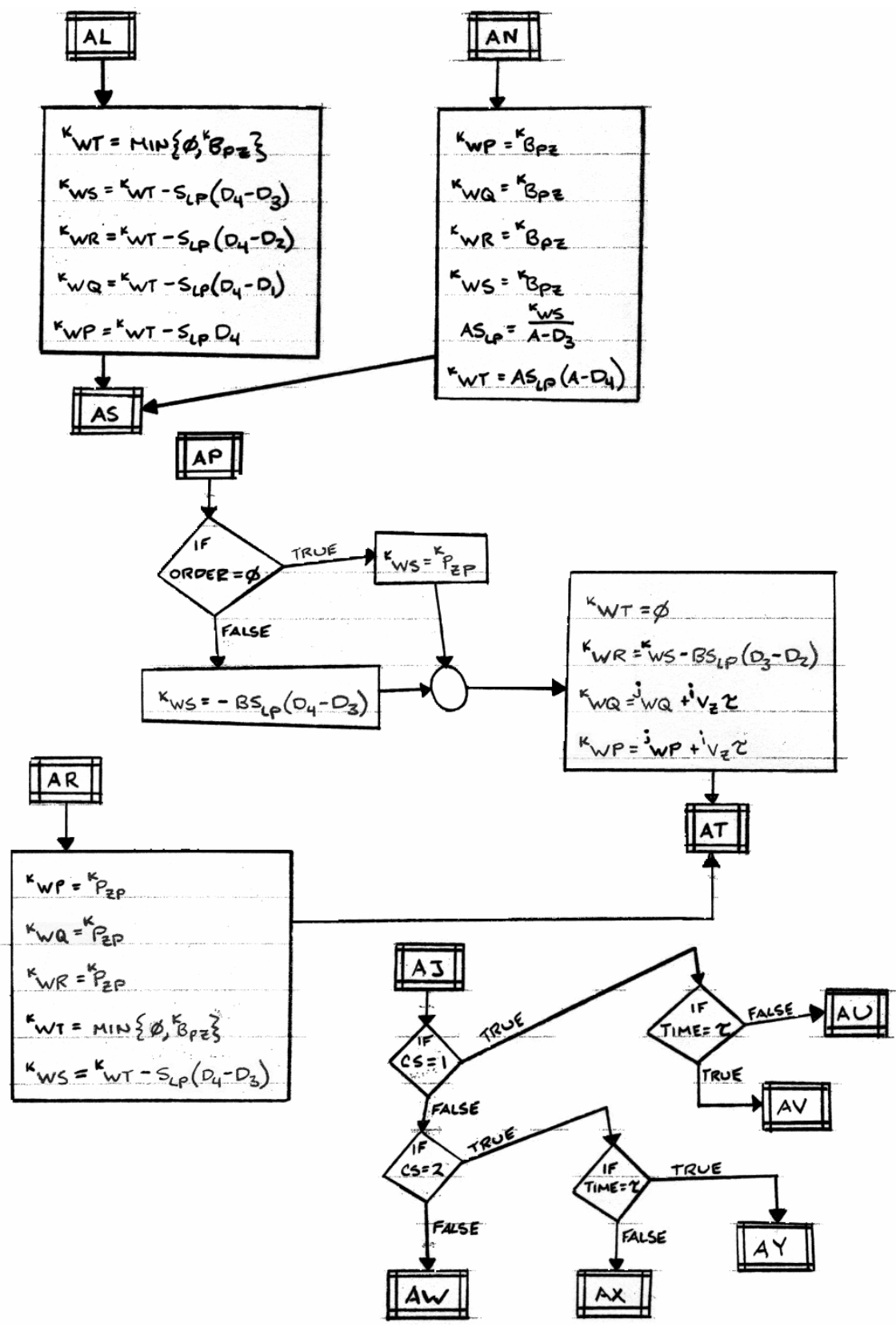


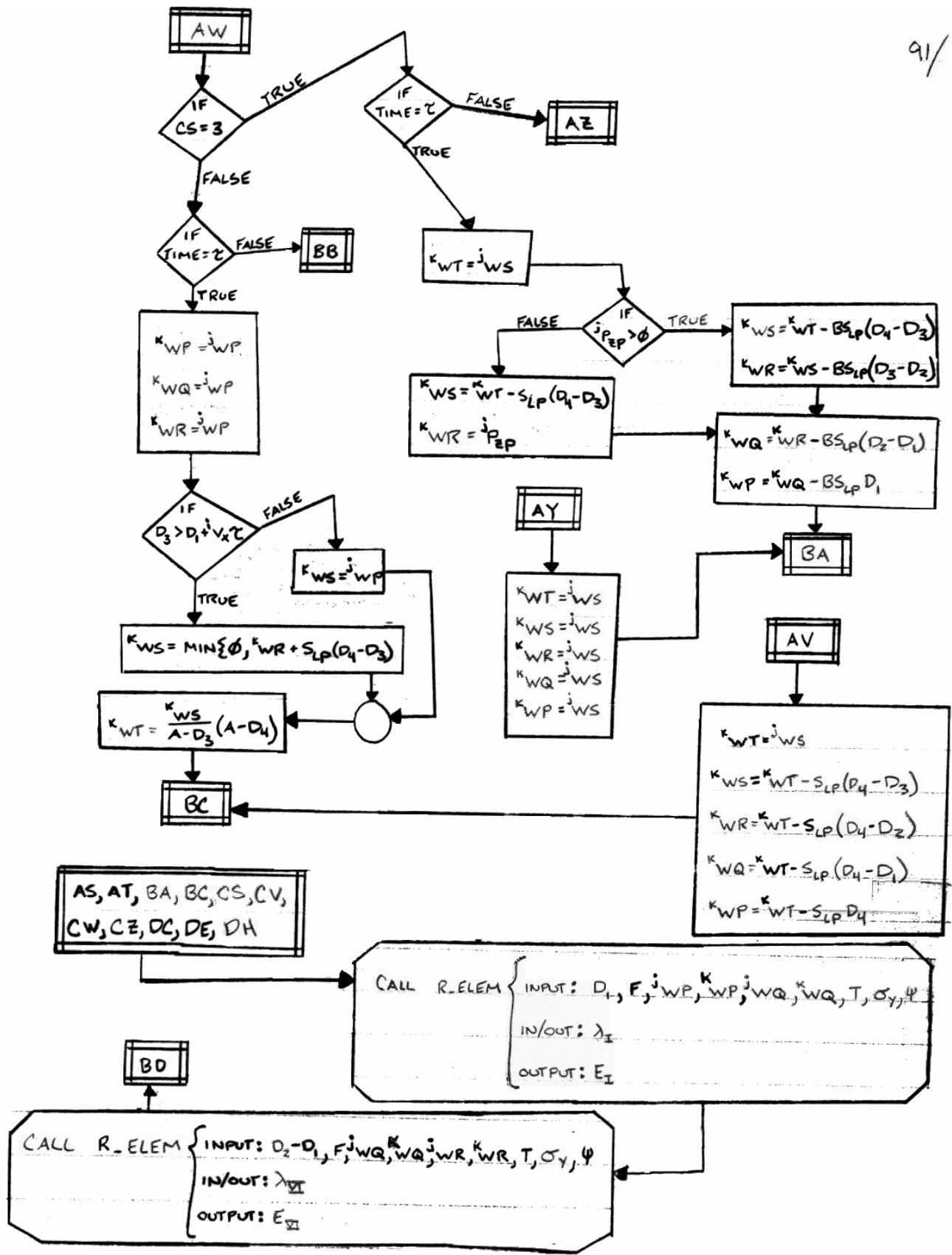
$$\begin{aligned}
 E_x = \lambda_0 [ & \lambda_1 E_I + \lambda_{D1} \lambda_6 E_{VI} + \lambda_{D2} \lambda_{11} E_{XI} + \lambda_{D3} \lambda_{16} E_{XVI} + \dots \\
 & \dots + \lambda_{D4} \lambda_{21} E_{XXI} + \lambda_{D5} (\lambda_2 E_{II} + \lambda_3 E_{III} + \lambda_{D1} \{ \lambda_4 E_{IV} + \dots \\
 & \dots + \lambda_5 E_V \} + \lambda_{D2} \{ \lambda_{12} E_{XII} + \lambda_{13} E_{XIII} \} + \lambda_{D3} \{ \lambda_{14} E_{XIV} + \dots \\
 & \dots + \lambda_{15} E_{XV} \} + \lambda_{D4} \{ \lambda_{22} E_{XXII} + \lambda_{23} E_{XXIII} \} + \lambda_{D5} (\lambda_9 E_{IX} + \dots \\
 & \dots + \lambda_{10} E_X + \lambda_{D1} \{ \lambda_7 E_{VII} + \lambda_8 E_{VIII} \} + \lambda_{D2} \{ \lambda_{19} E_{XIX} + \dots \\
 & \dots + \lambda_{20} E_{XX} \} + \lambda_{D3} \{ \lambda_{17} E_{XXVII} + \lambda_{18} E_{XXVIII} \} + \lambda_{D4} \{ \lambda_{25} E_{XXV} + \dots \\
 & \dots + \lambda_{24} E_{XXIV} \} ) ]
 \end{aligned}$$

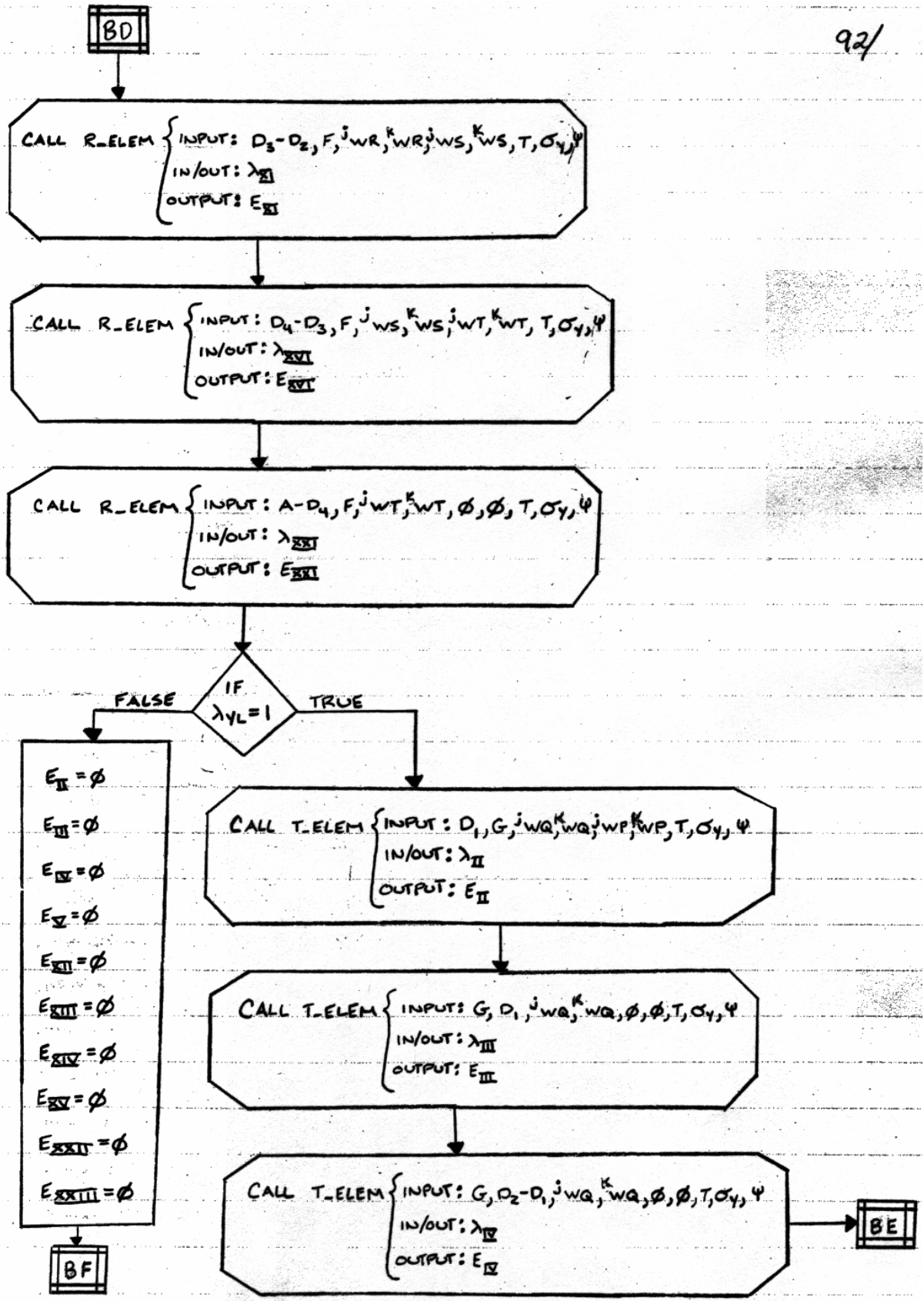
AF

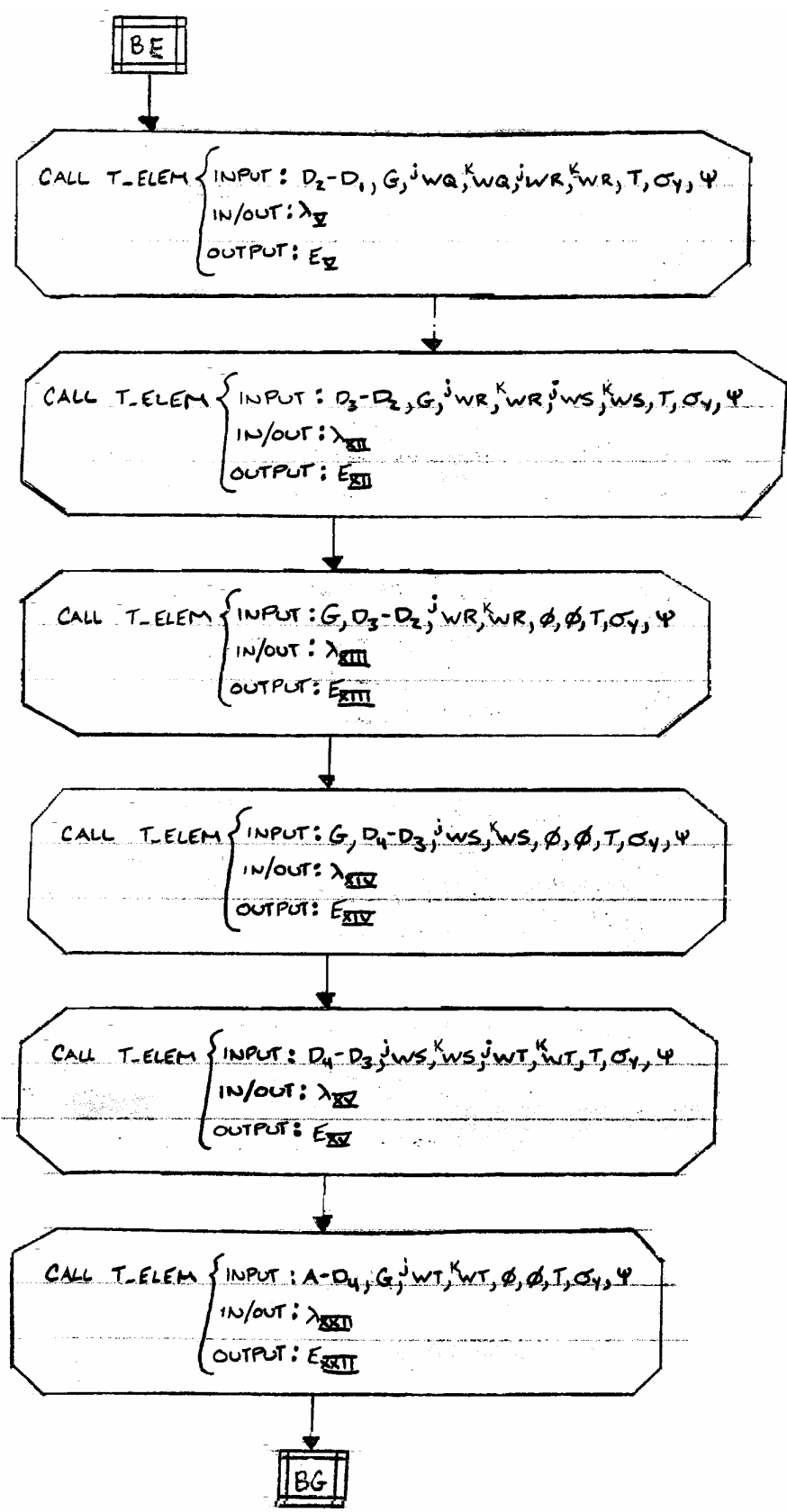
$$E_z = \lambda_0 \left[ \lambda_1 E_I + \lambda_{D1} \lambda_6 E_{VI} + \lambda_{D2} \lambda_{11} E_{VII} + \lambda_{D3} \lambda_{16} E_{XVI} + \dots \right. \\
 \dots + \lambda_{D4} \lambda_{21} E_{XXI} + \lambda_{YL} (\lambda_2 E_{II} + \lambda_3 E_{III} + \lambda_{D1} \{ \lambda_4 E_{IV} + \dots \\
 \dots + \lambda_5 E_{V} \} + \lambda_{D2} \{ \lambda_{12} E_{XII} + \lambda_{13} E_{XIII} \} + \lambda_{D3} \{ \lambda_{14} E_{XIV} + \dots \\
 \dots + \lambda_{15} E_{XV} \} + \lambda_{D4} \{ \lambda_{22} E_{XXII} + \lambda_{23} E_{XXIII} \} + \lambda_{YU} (\lambda_9 E_{IX} + \dots \\
 \dots + \lambda_{10} E_{X} + \lambda_{D1} \{ \lambda_7 E_{VII} + \lambda_8 E_{VIII} \} + \lambda_{D2} \{ \lambda_{19} E_{XIX} + \dots \\
 \dots + \lambda_{20} E_{XX} \} + \lambda_{D3} \{ \lambda_{17} E_{XVII} + \lambda_{18} E_{XVIII} \} + \lambda_{D4} \{ \lambda_{25} E_{XXV} + \dots \\
 \dots + \lambda_{24} E_{XXIV} \} \left. \right]$$

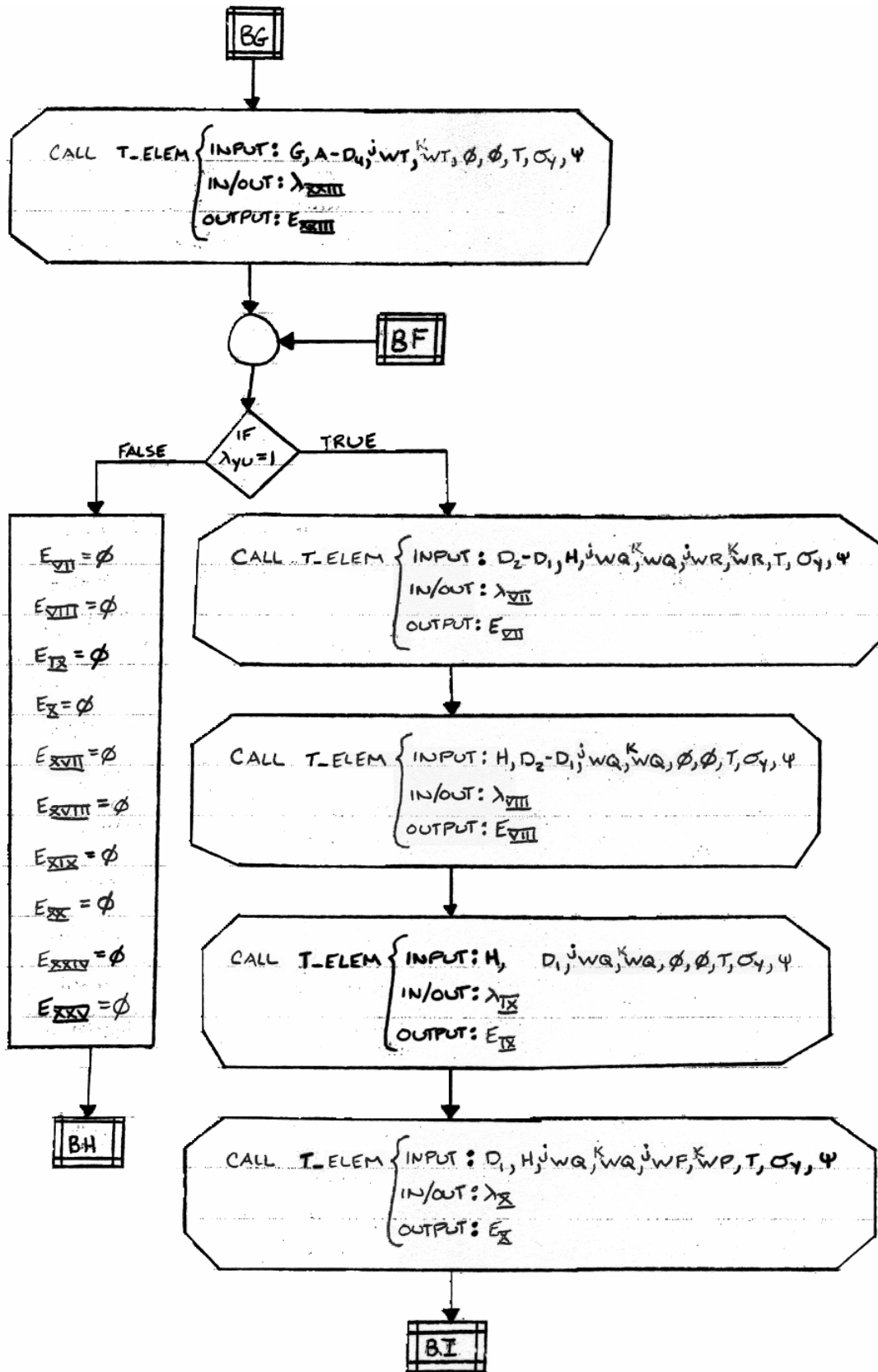


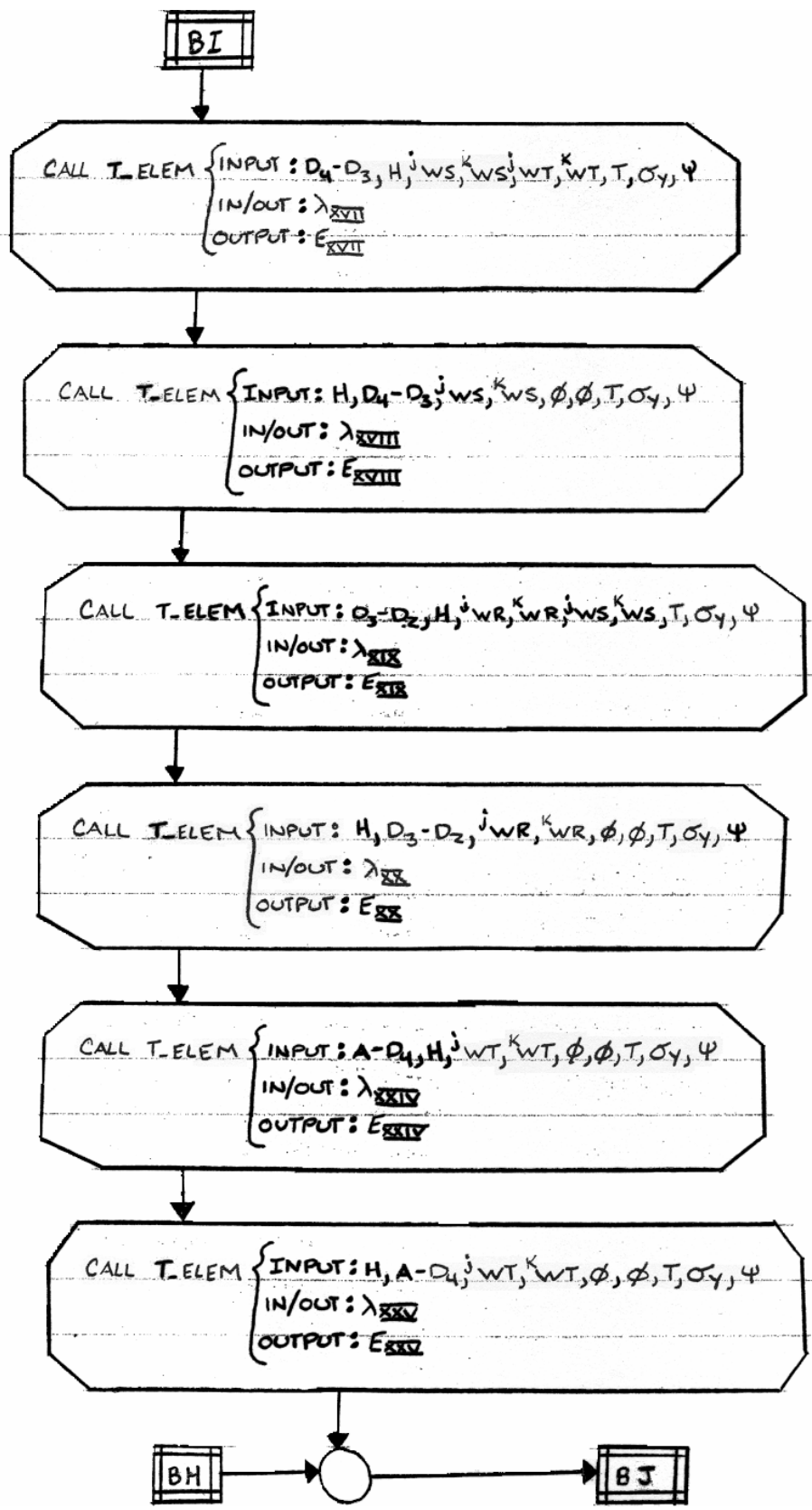




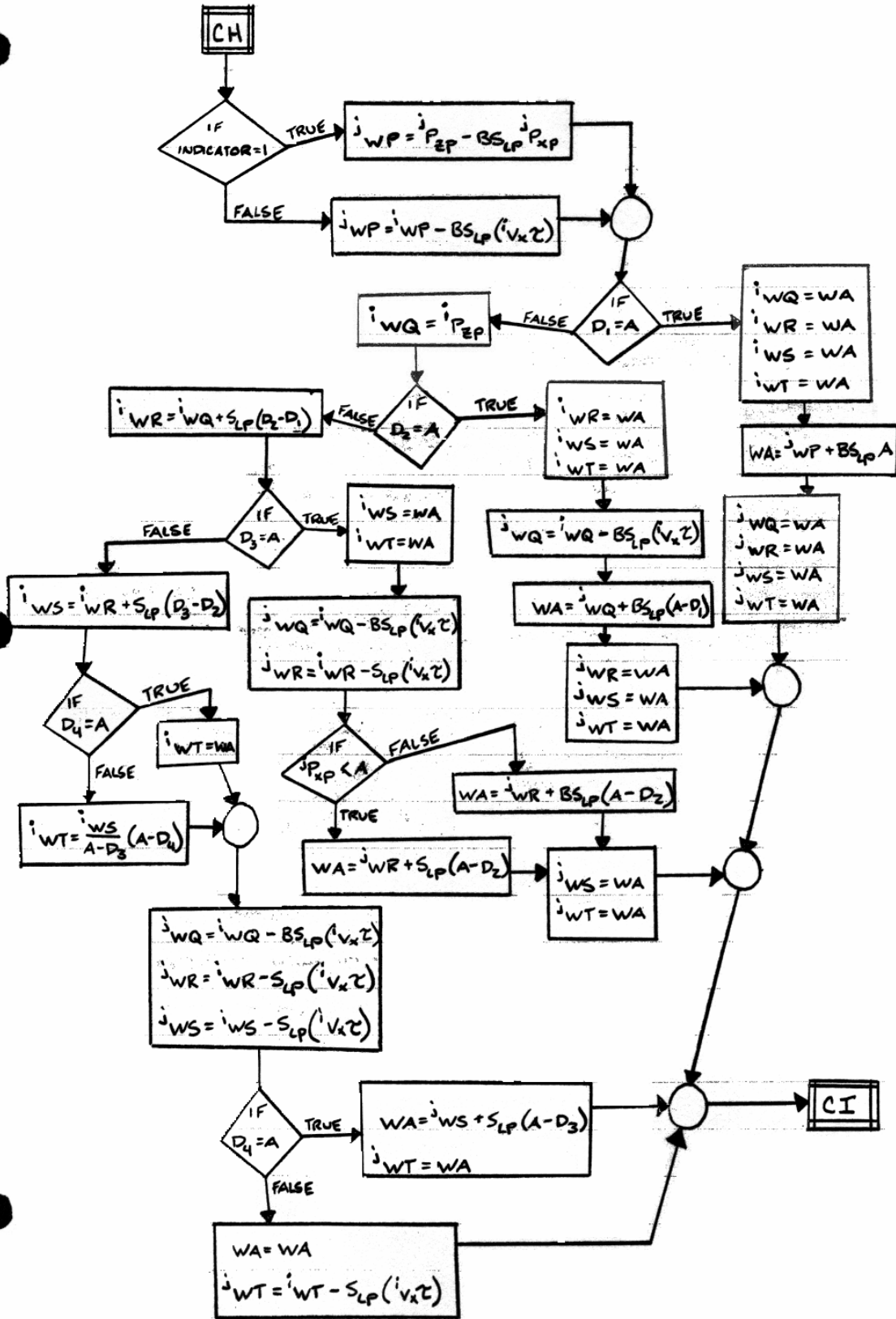




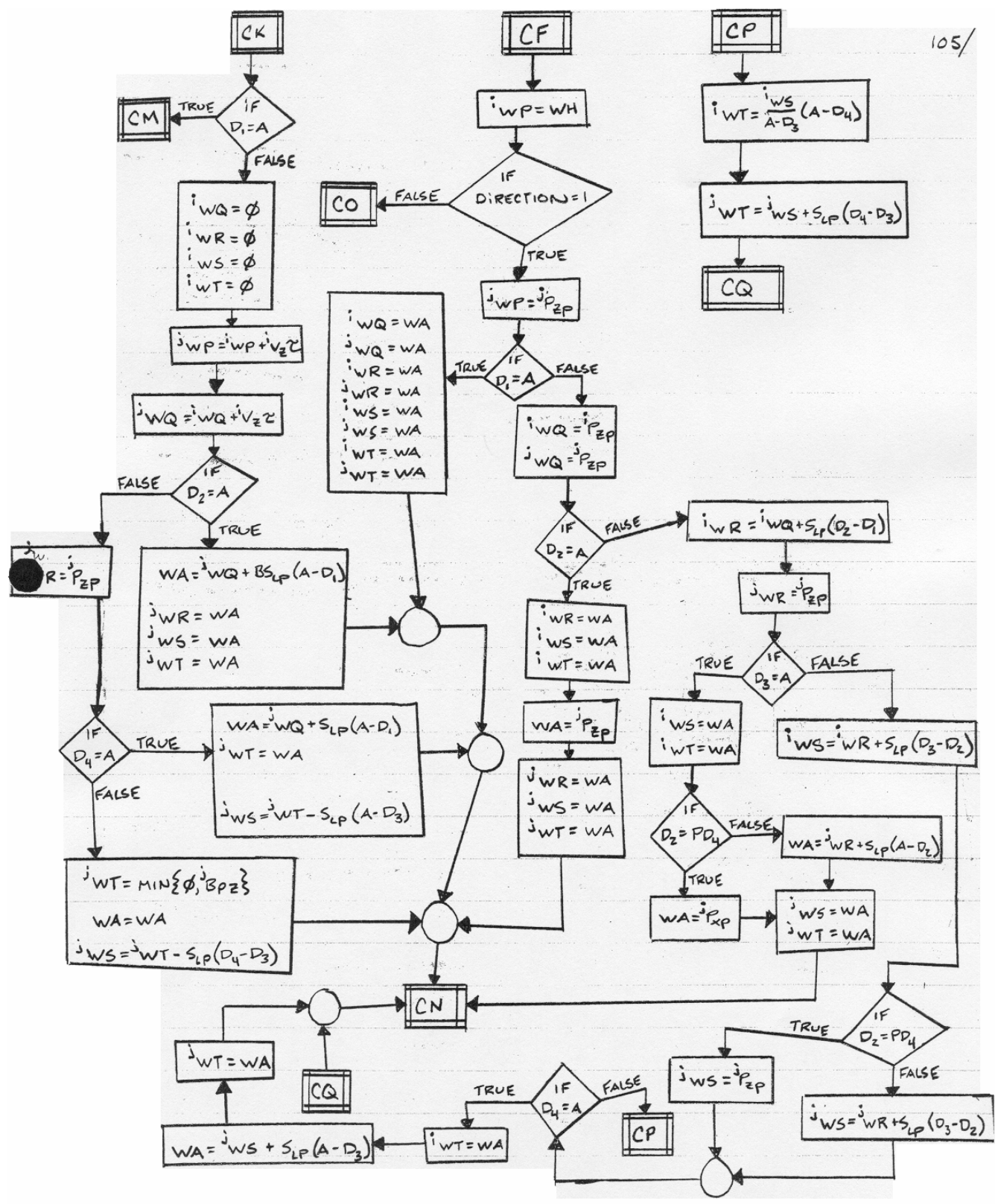


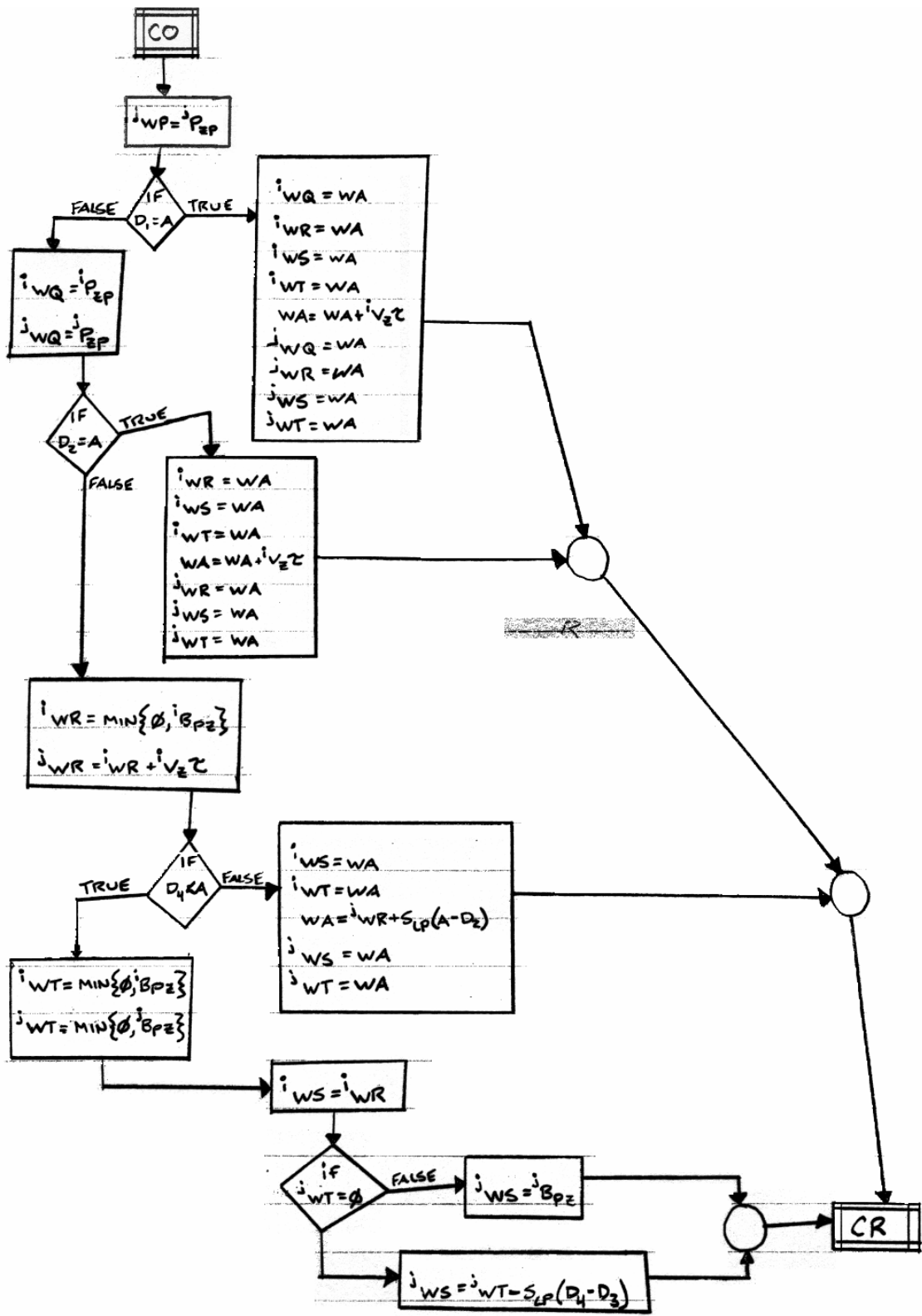


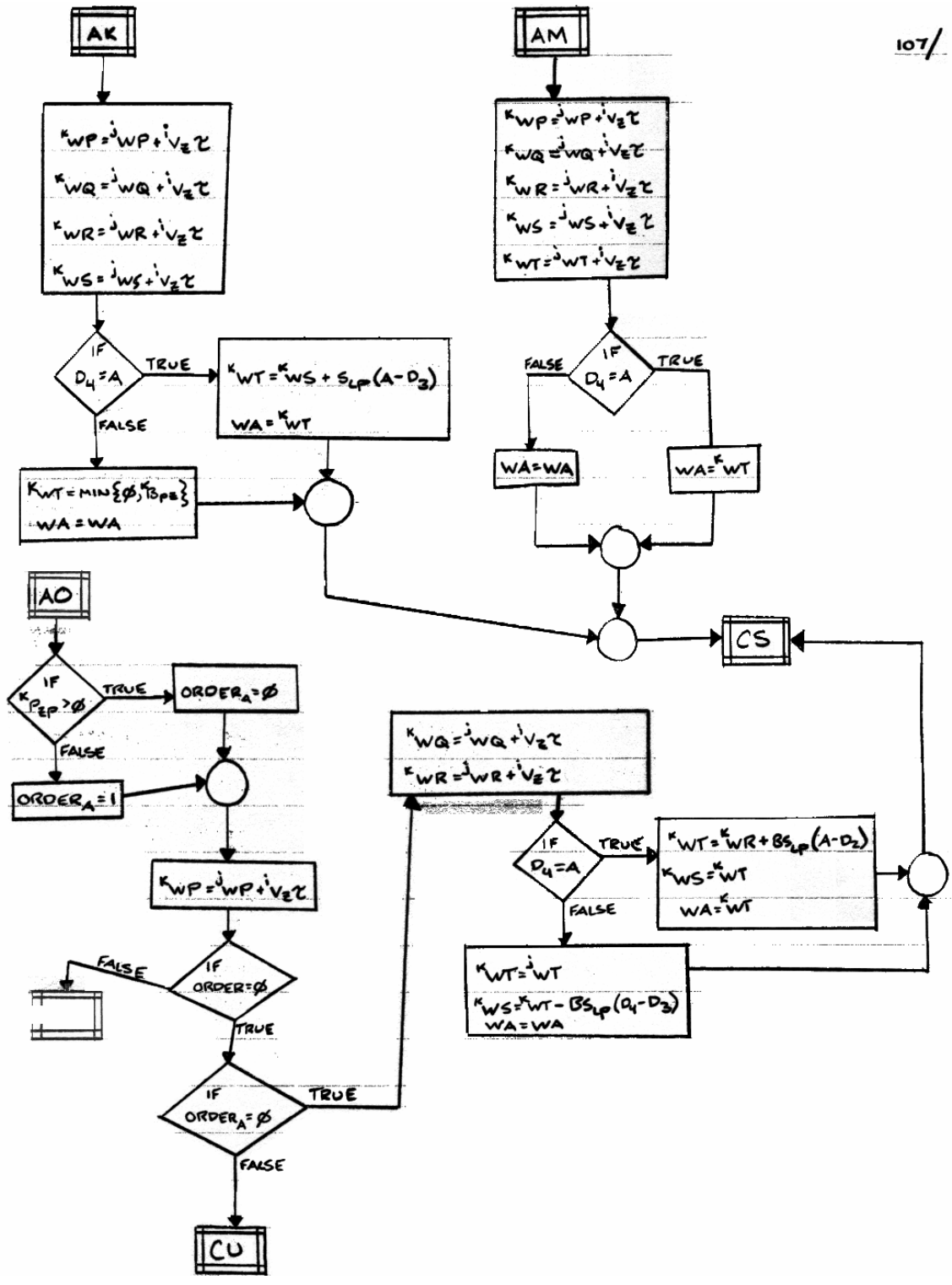


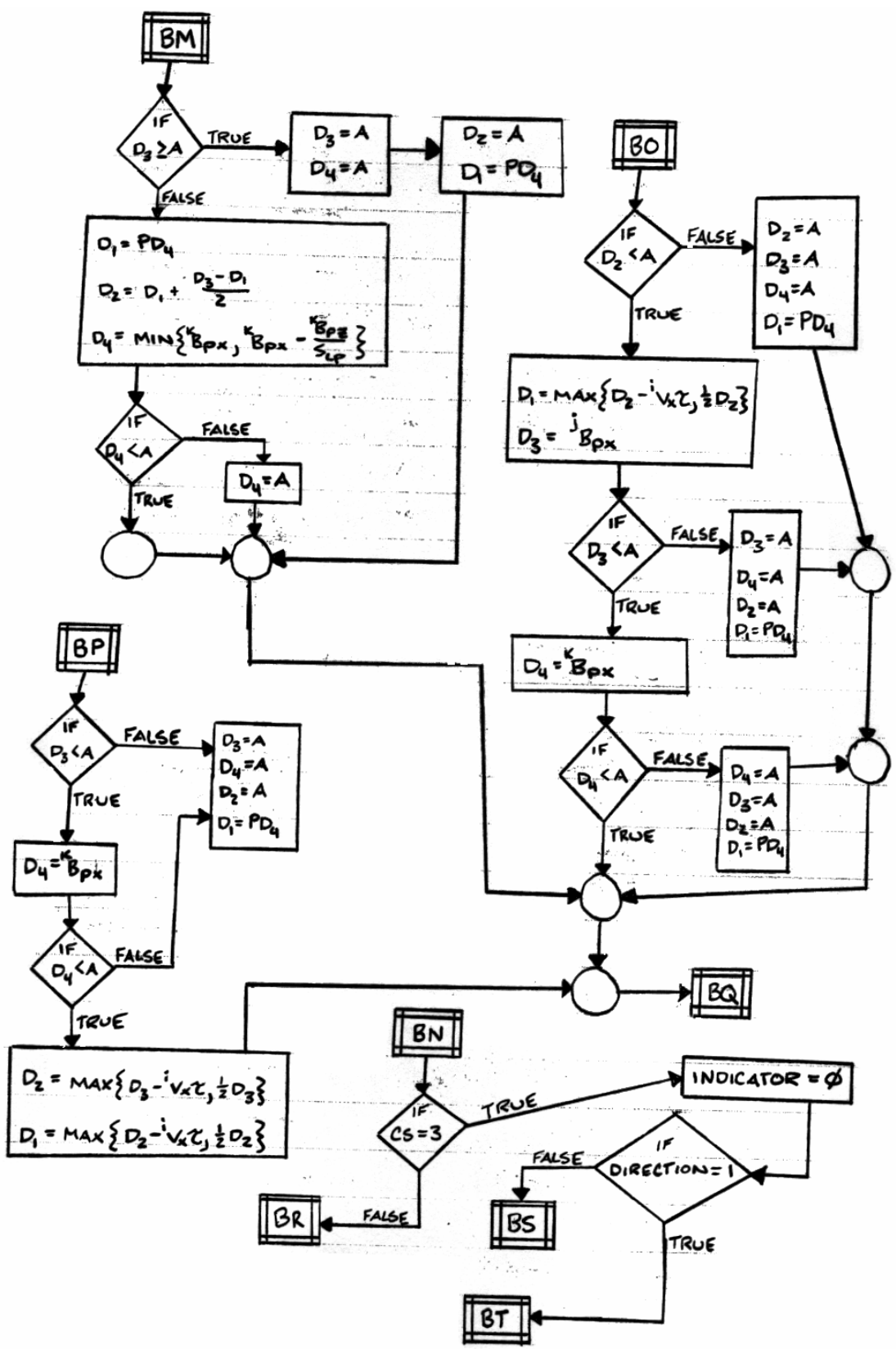


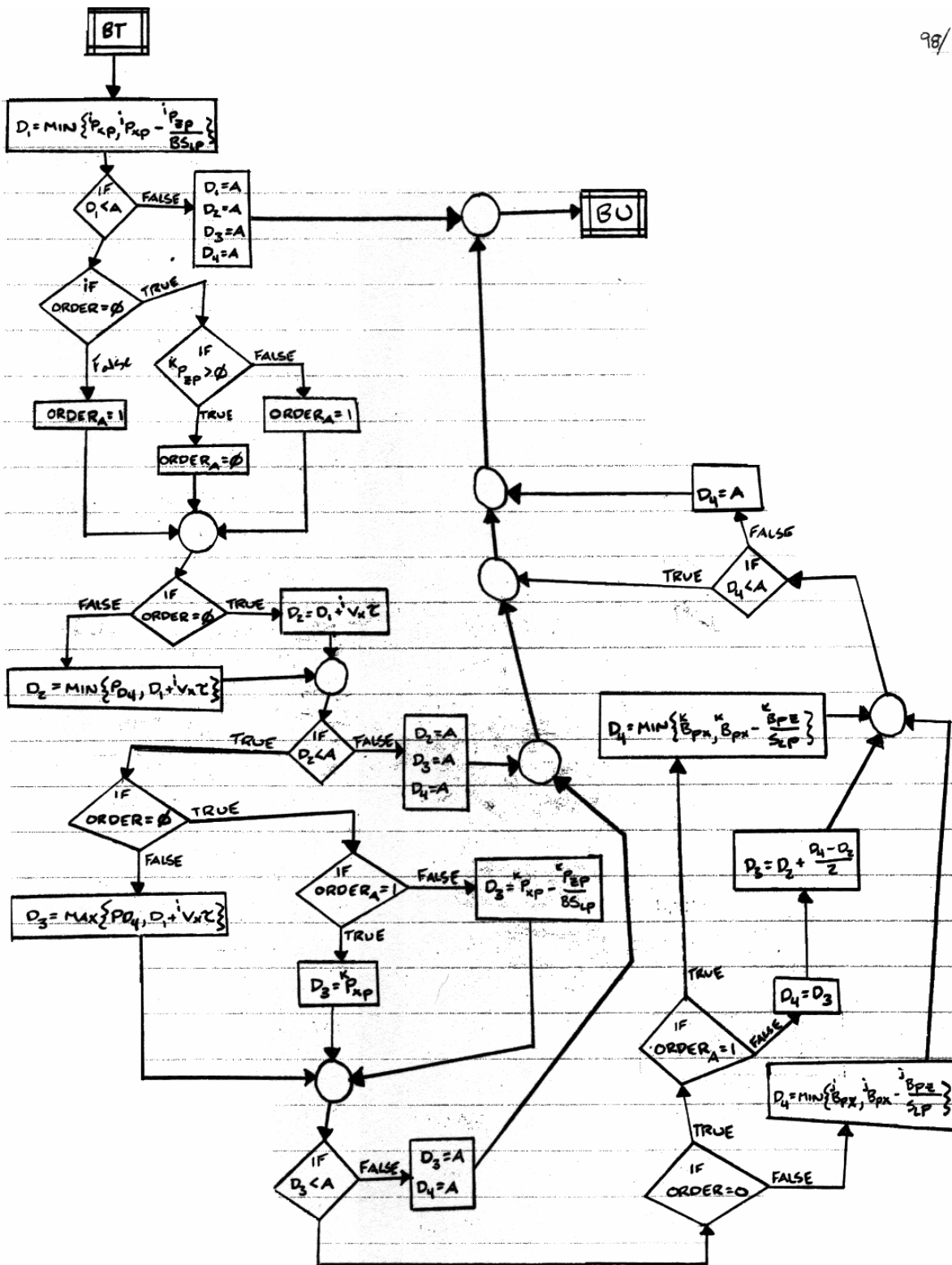


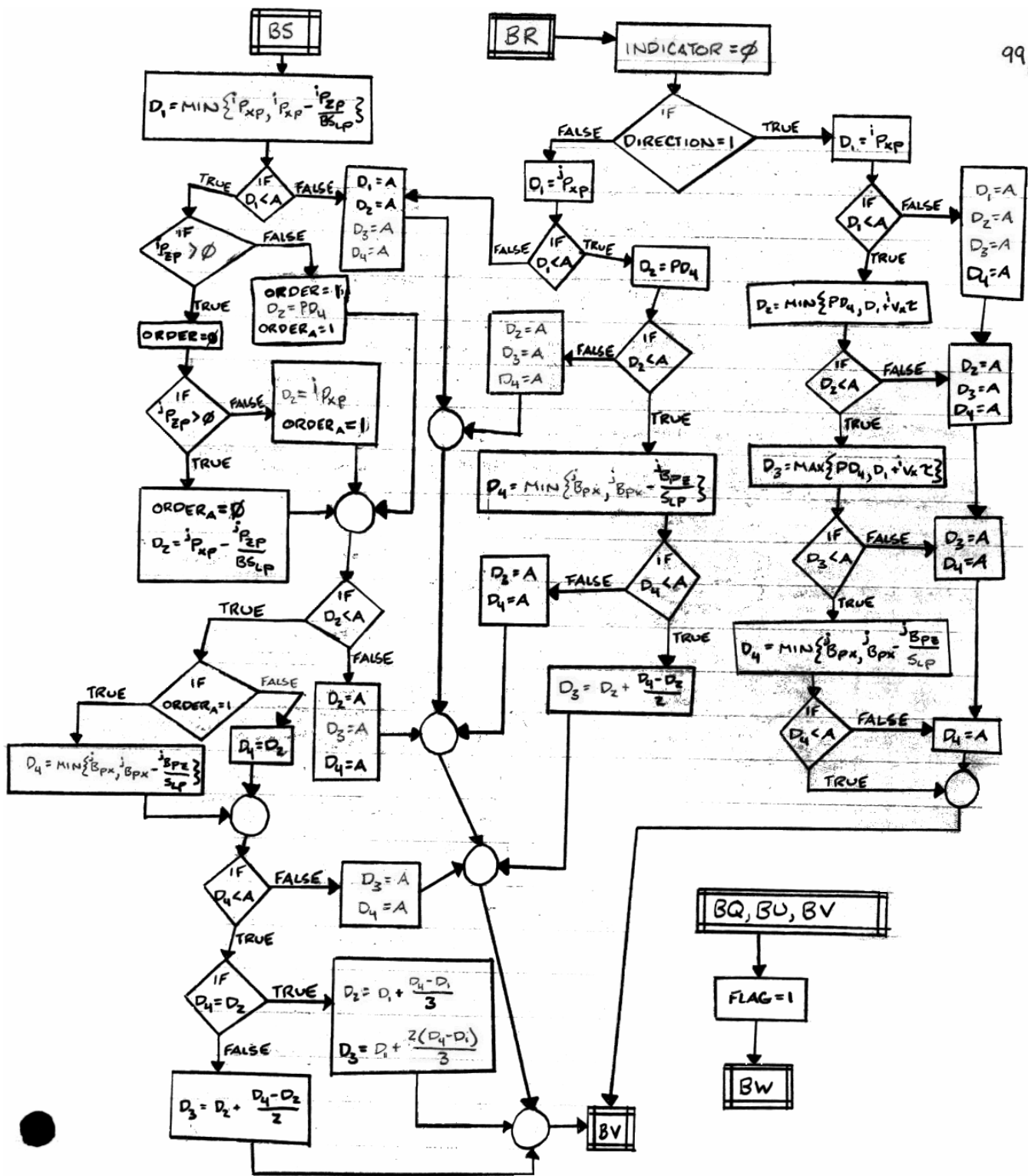


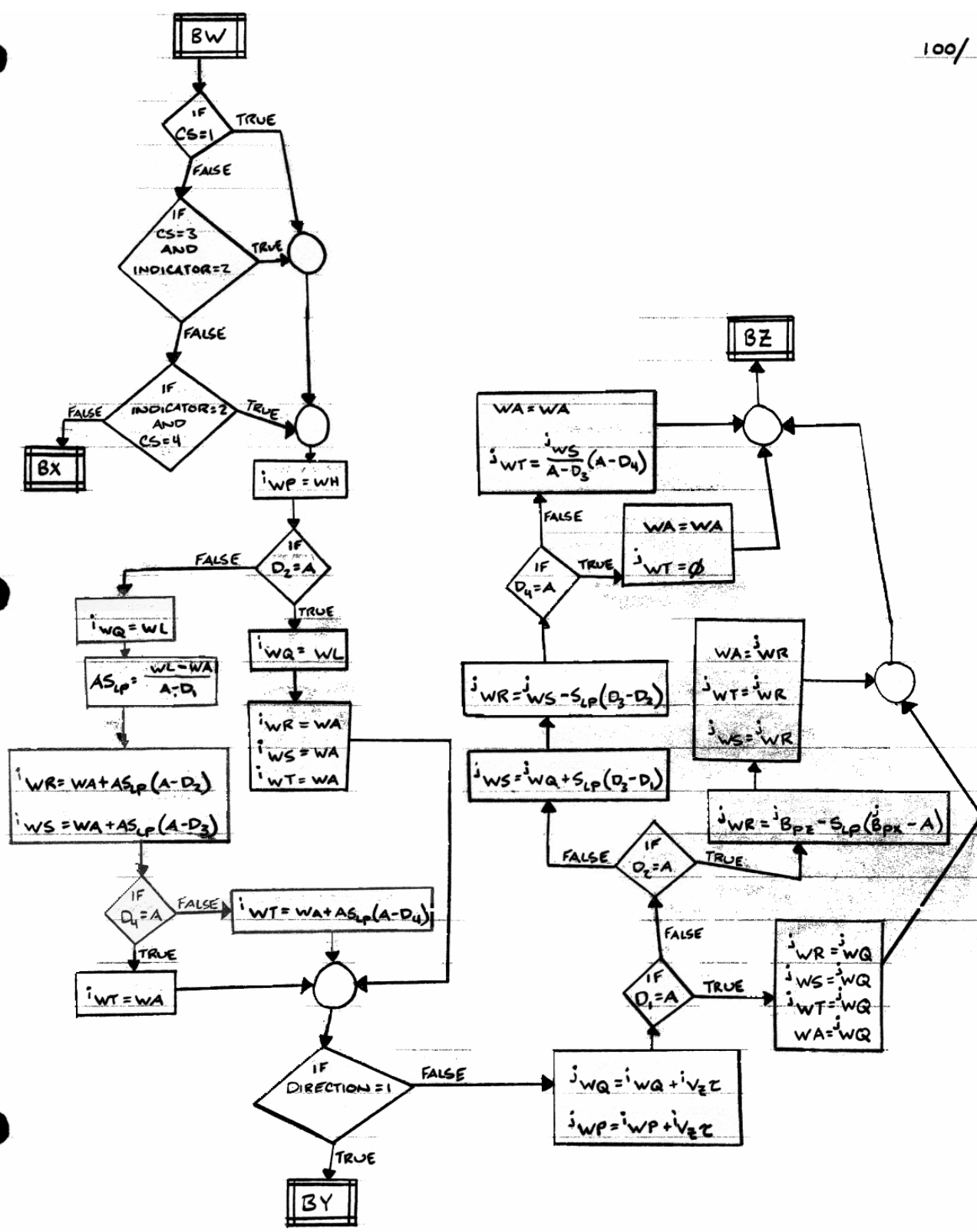






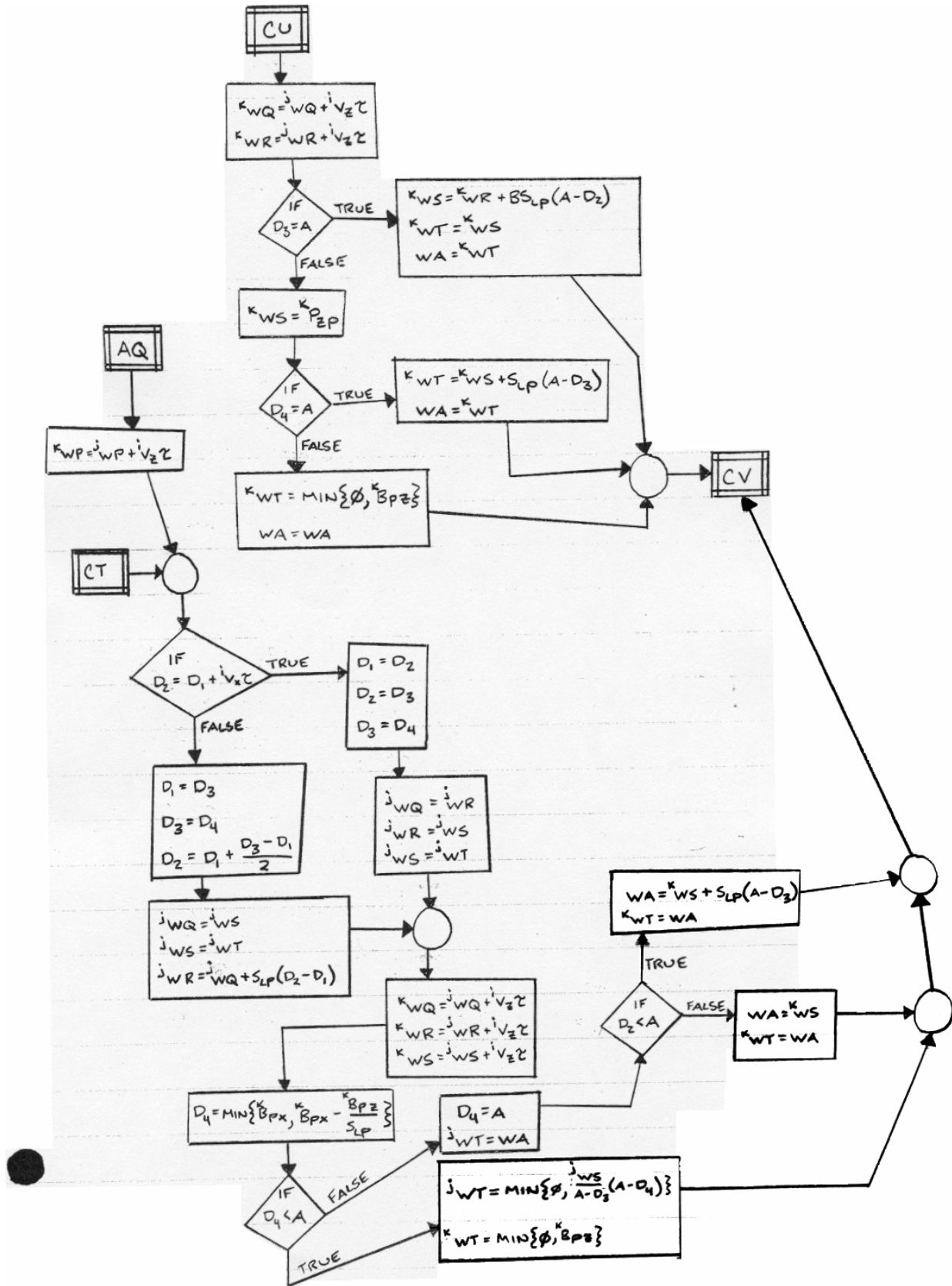


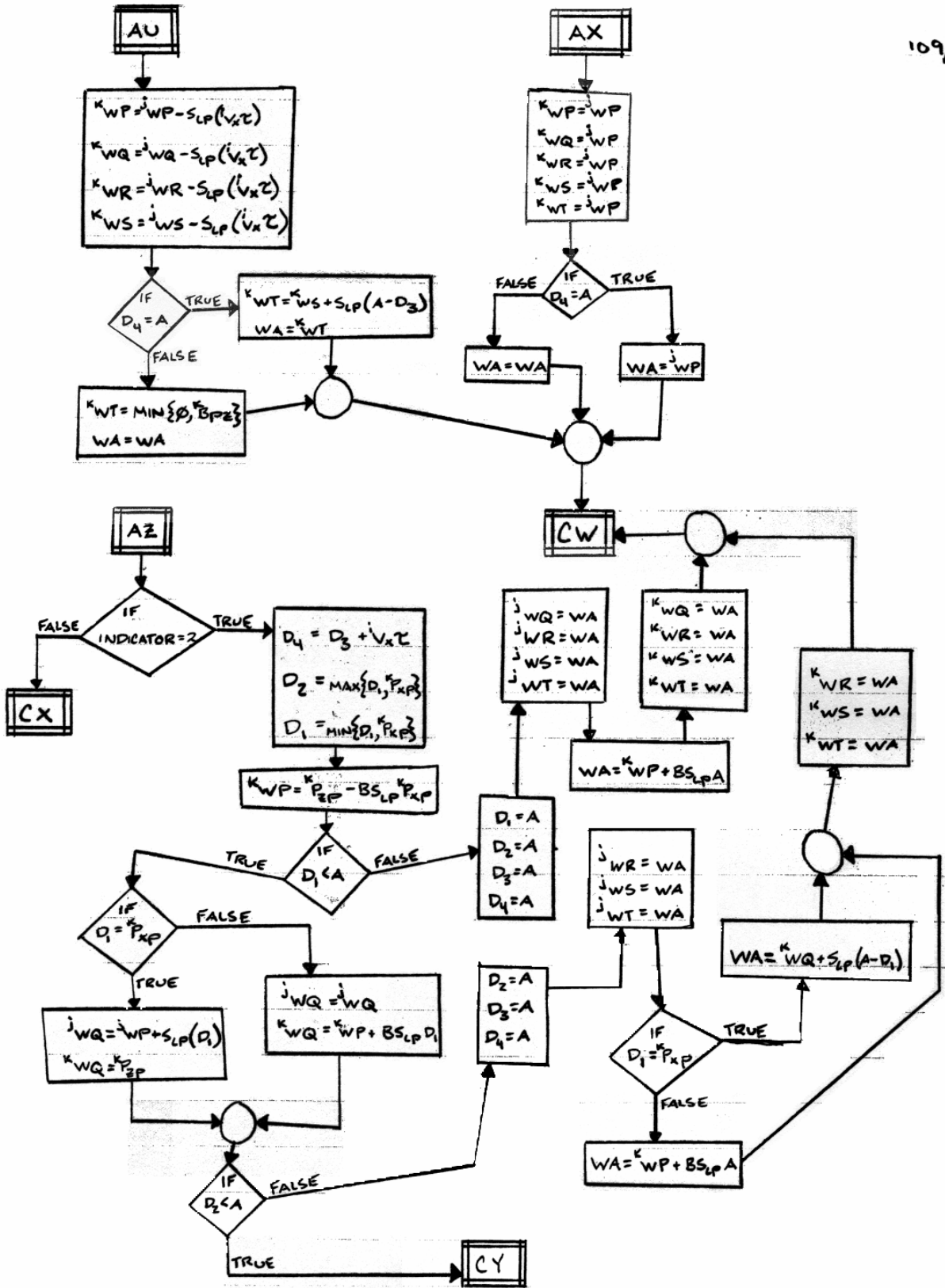


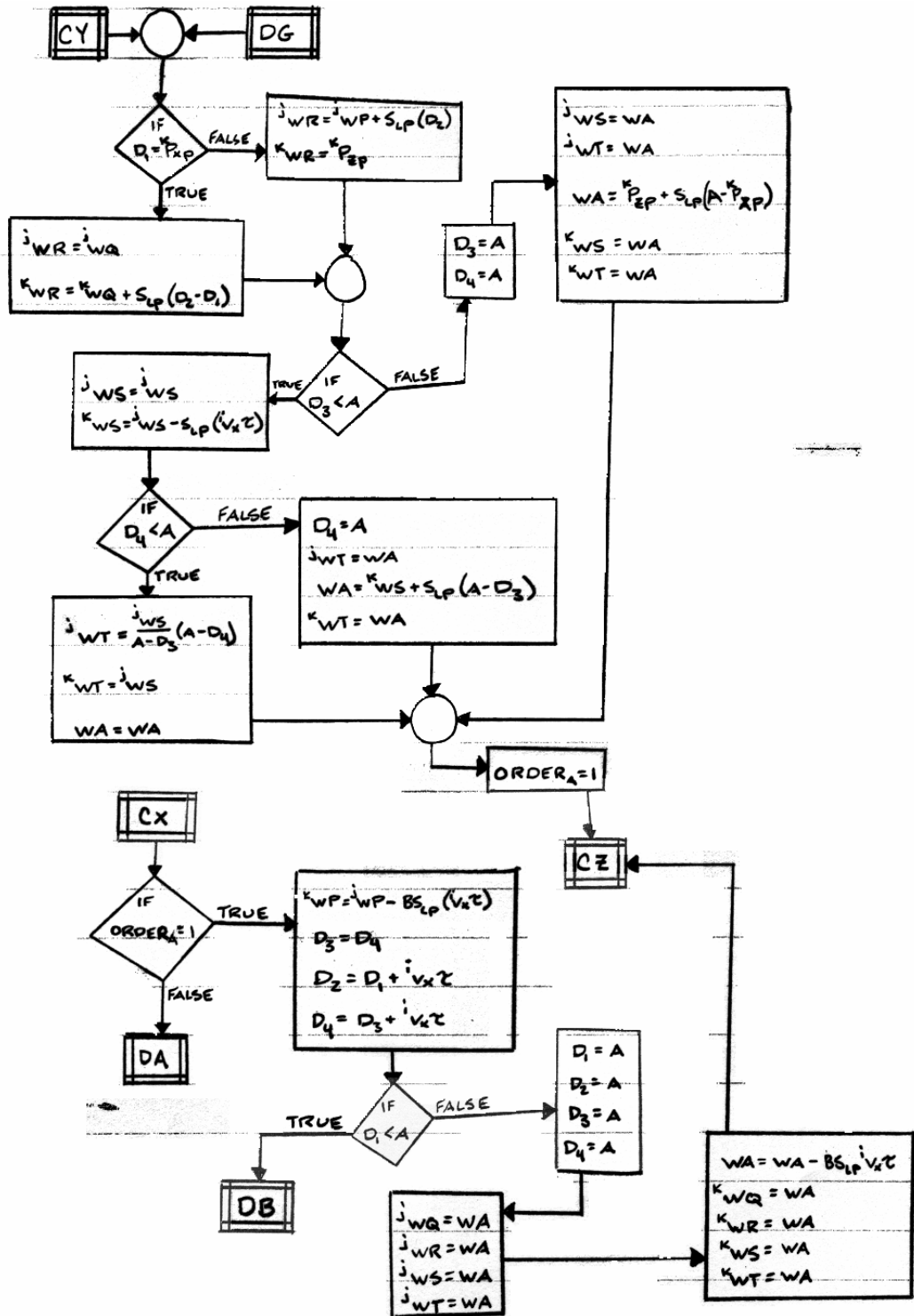




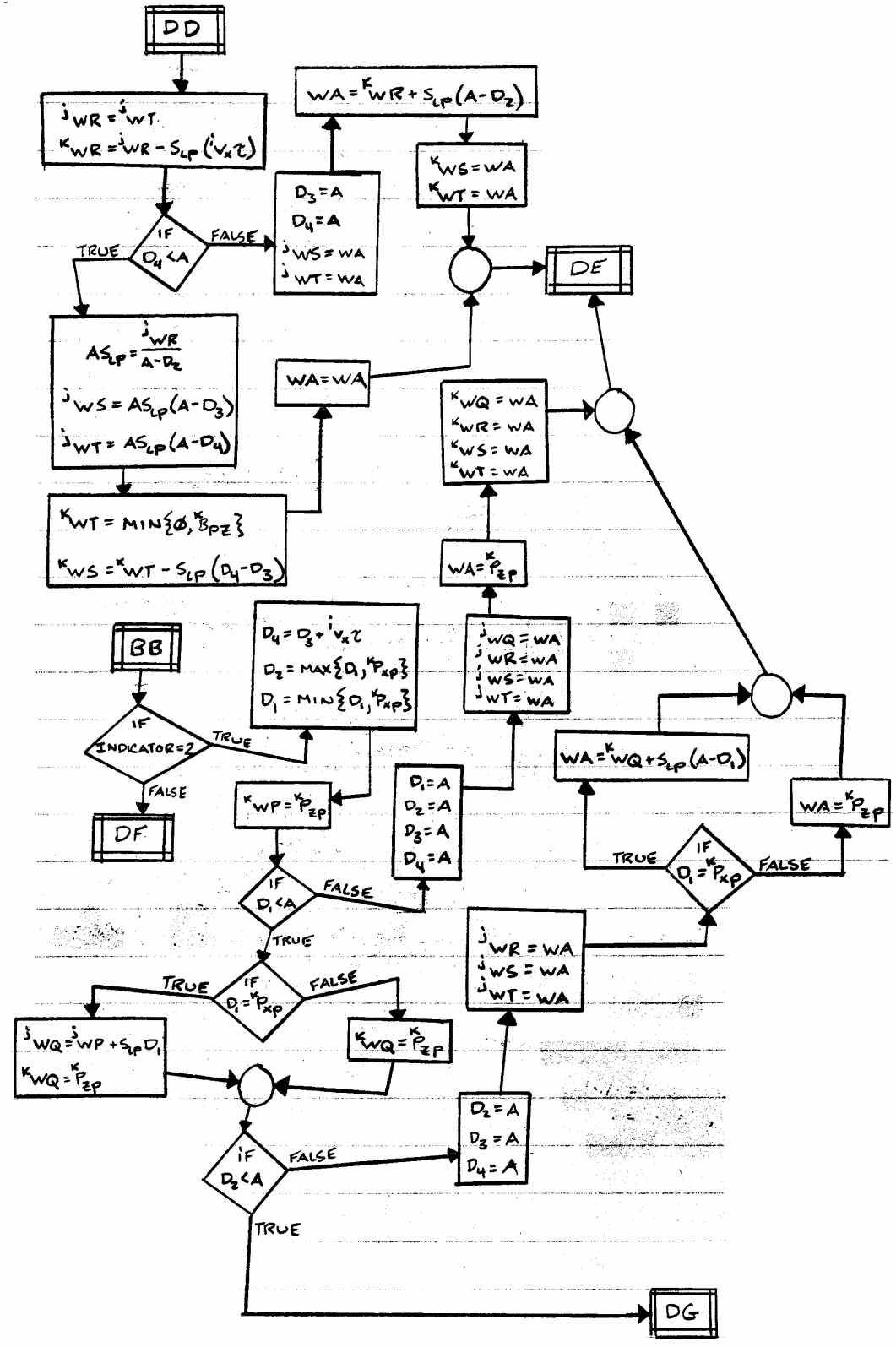


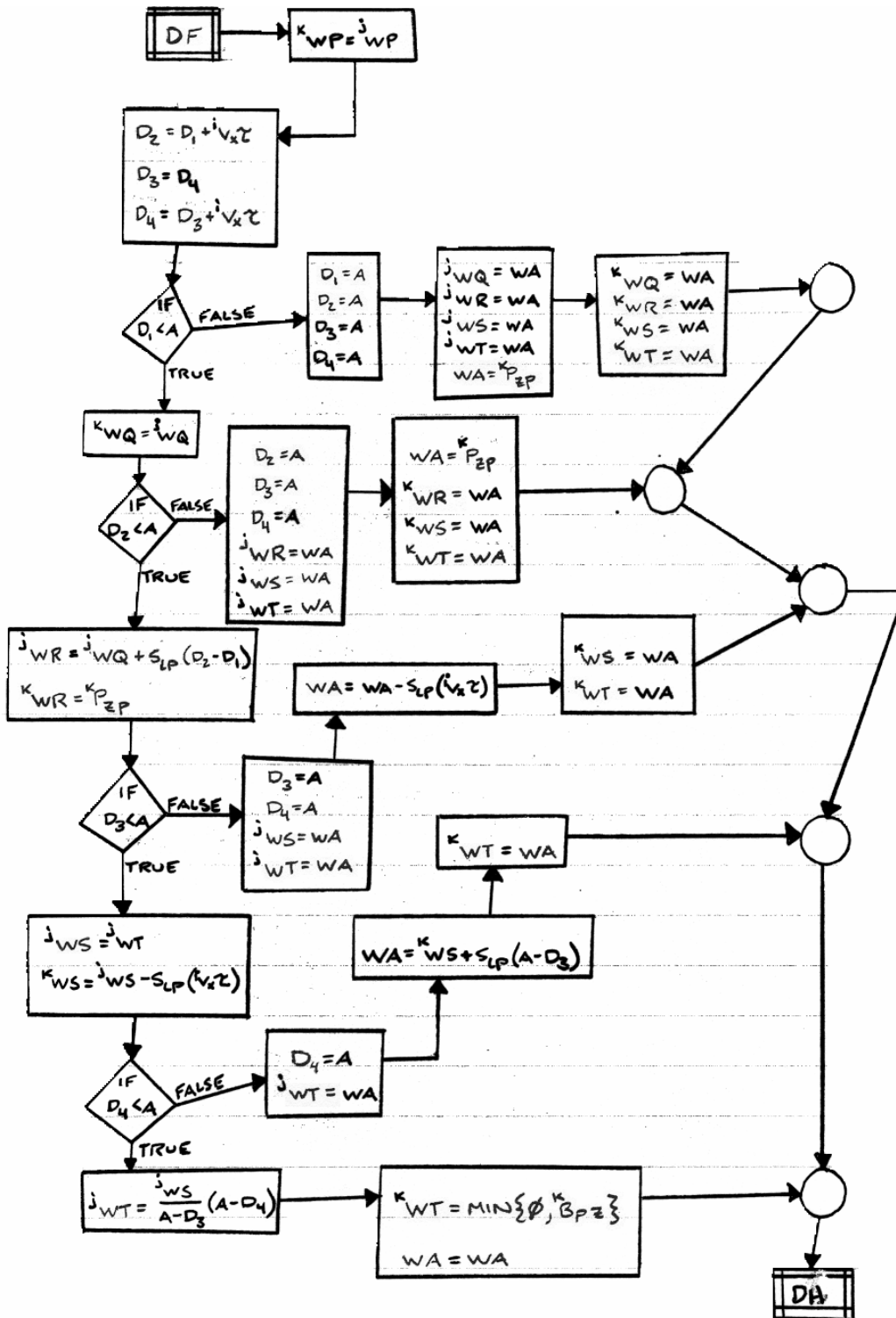


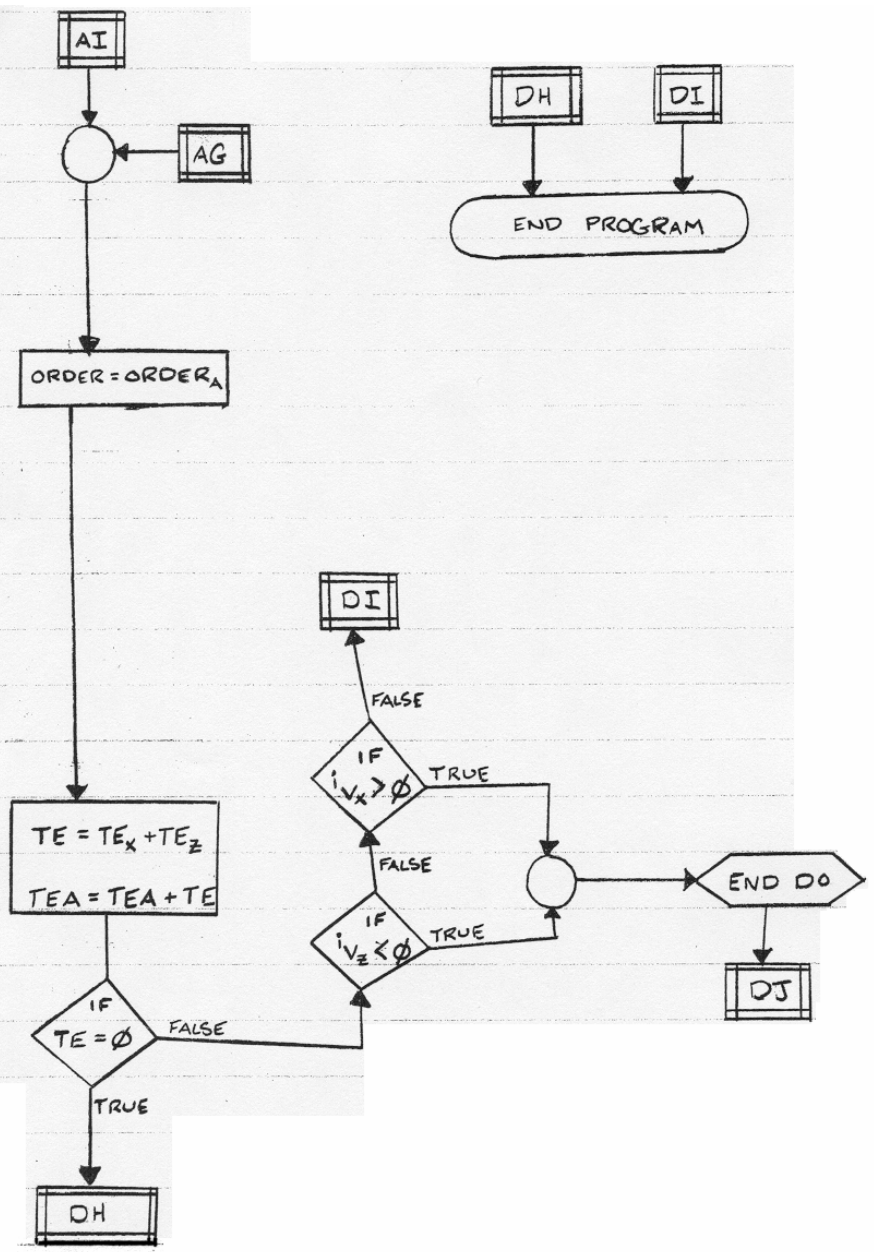






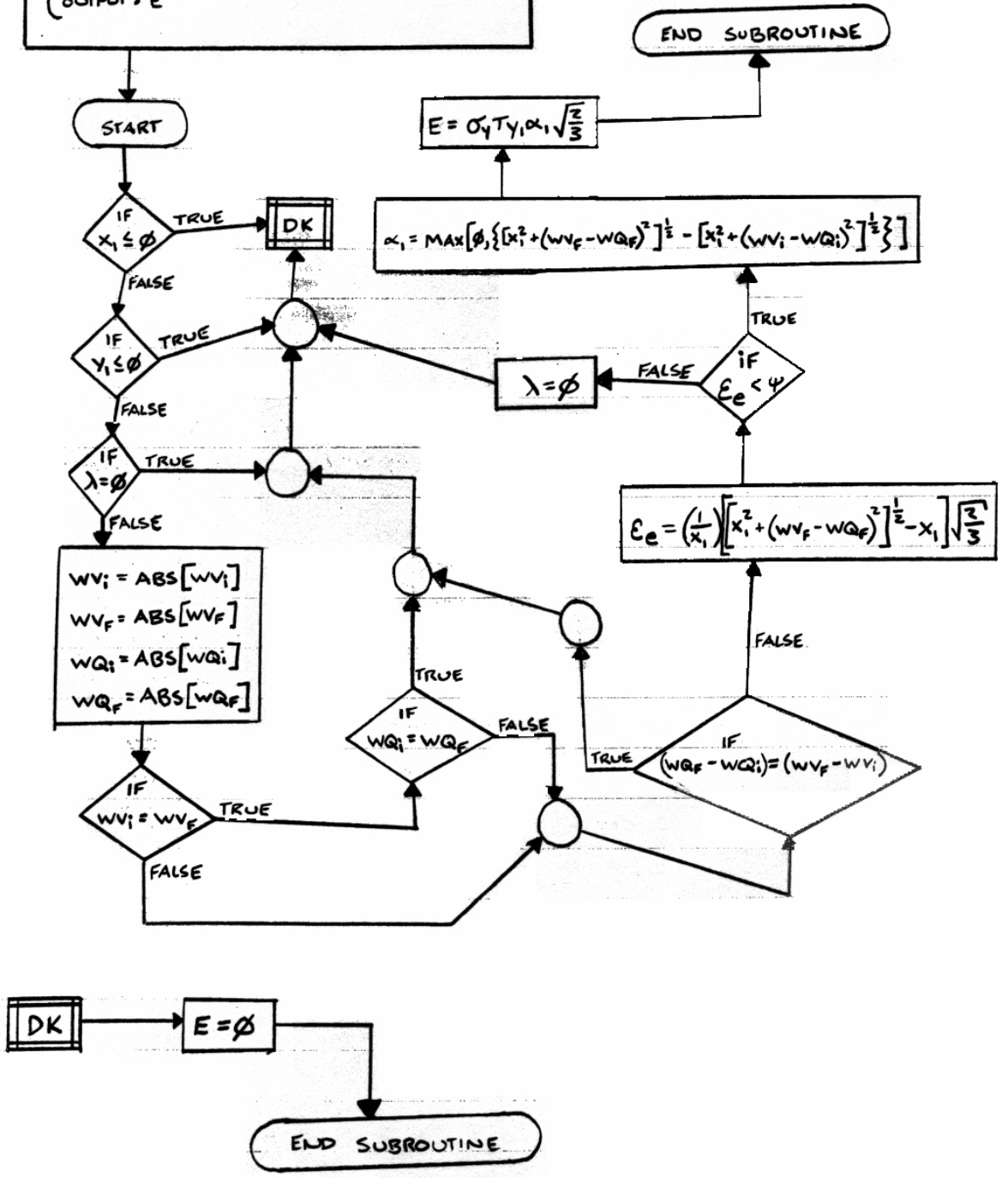




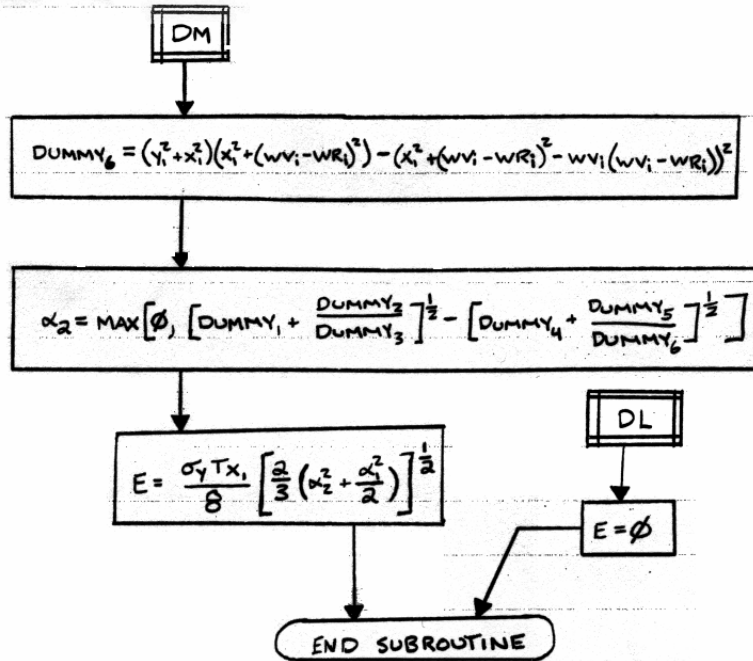


SUBROUTINE R-ELEM

INPUT :  $x_1, y_1, wv_i, wv_f, wq_i, wq_f, T, \sigma_y, \psi$   
 IN/OUT :  $\lambda$   
 OUTPUT :  $E$







# SHIP STRUCTURE COMMITTEE PARTNERS AND LIAISON MEMBERS

## PARTNERS

### The Society of Naval Architects and Marine Engineers

Mr. Bruce S. Rosenblatt  
President,  
Society of Naval Architects and Marine Engineers

Dr. John Daidola  
Chairman,  
SNAME Technical & Research Steering  
Committee

### The Gulf Coast Region Maritime Technology Center

Dr. John Crisp  
Executive Director,  
Gulf Coast Maritime Technology Center

Dr. Bill Vorus  
Site Director,  
Gulf Coast Maritime Technology Center

## LIAISON MEMBERS

American Iron and Steel Institute  
American Society for Testing & Materials  
American Society of Naval Engineers  
American Welding Society  
Bethlehem Steel Corporation  
Canada Center for Minerals & Energy Technology  
Colorado School of Mines  
Edison Welding Institute  
International Maritime Organization  
Int'l Ship and Offshore Structure Congress  
INTERTANKO  
Massachusetts Institute of Technology  
Memorial University of Newfoundland  
National Cargo Bureau  
Office of Naval Research  
Oil Companies International Maritime Forum  
Tanker Structure Cooperative Forum  
Technical University of Nova Scotia  
United States Coast Guard Academy  
United States Merchant Marine Academy  
United States Naval Academy  
University of British Columbia  
University of California Berkeley  
University of Houston - Composites Eng & Appl.  
University of Maryland  
University of Michigan  
University of Waterloo  
Virginia Polytechnic and State Institute  
Webb Institute  
Welding Research Council  
Worcester Polytechnic Institute  
World Maritime Consulting, INC

Mr. Alexander Wilson  
Captain Charles Piersall (Ret.)  
Captain Dennis K. Kruse (USN Ret.)  
Mr. Richard Frank  
Dr. Harold Reemsnyder  
Dr. William R. Tyson  
Dr. Stephen Liu  
Mr. Dave Edmonds  
Mr. Tom Allen  
Dr. Alaa Mansour  
Mr. Dragos Rauta  
Mr. Dave Burke / Captain Chip McCord  
Dr. M. R. Haddara  
Captain Jim McNamara  
Dr. Yapa Rajapaksie  
Mr. Phillip Murphy  
Mr. Rong Huang  
Dr. C. Hsiung  
Commander Kurt Colella  
Dr. C. B. Kim  
Dr. Ramswar Bhattacharyya  
Dr. S. Calisal  
Dr. Robert Bea  
Dr. Jerry Williams  
Dr. Bilal Ayyub  
Dr. Michael Bernitsas  
Dr. J. Roorda  
Dr. Alan Brown  
Dr. Kirsi Tikka  
Dr. Martin Prager  
Dr. Nick Dembsey  
VADM Gene Henn, USCG Ret.

## RECENT SHIP STRUCTURE COMMITTEE PUBLICATIONS

Ship Structure Committee Publications on the Web - All reports from SSC 392 and forward are available to be downloaded from the Ship Structure Committee Web Site at URL:

<http://www.shipstructure.org>

SSC 391 and below are available on the SSC CD-ROM Library. Visit the National Technical Information Service (NTIS) Web Site for ordering information at URL:

<http://www.ntis.gov/fcpc/cpn7833.htm>

SSC Report Number	Report Bibliography
SSC 436	Effect of Fabrication Tolerances on Fatigue Life of Welded Joints
SSC 435	Predicting Stable Fatigue Crack Propagation in Stiffened Panels R.J. Dexter, H.N. Mahmoud 2004
SSC 434	Predicting Motion and Structural Loads in Stranded Ships Phase 1 A.J. Brown, M. Simbulan, J. McQuillan, M. Gutierrez 2004
SSC 433	Interactive Buckling Testing of Stiffened Steel Plate Panels Q. Chen, R.S. Hanson, G.Y. Grondin 2004
SSC 432	Adaptation of Commercial Structural Criteria to Military Needs R.Vara, C.M. Potter, R.A. Sielski, J.P. Sikora, L.R. Hill, J.C. Adamchak, D.P. Kihl, J. Hebert, R.I. Basu, L. Ferreiro, J. Watts, P.D. Herrington 2003
SSC 431	Retention of Weld Metal Properties and Prevention of Hydrogen Cracking R.J. Wong 2003
SSC 430	Fracture Toughness of a Ship Structure A.Dinovitzer, N. Pussegoda, 2003
SSC 429	Rapid Stress Intensity Factor Solution Estimation for Ship Structures Applications L. Blair Carroll, S. Tiku, A.S. Dinovitzer 2003
SSC 428	In-Service Non-Destructive Evaluation of Fatigue and Fracture Properties for Ship Structure S. Tiku 2003
SSC 427	Life Expectancy Assessment of Ship Structures A. Dinovitzer 2003
SSC 426	Post Yield Stability of Framing J. DesRochers, C. Pothier, E. Crocker 2003